RECEIVED - 10/17/67
MS-DV-SE000 1480R
C01

MISSILE AND SPACE DIVISION

FINAL REPORT

VOYAGER SPACECRAFT

PHASE B, TASK D

VOLUME II (BOOK 1 OF 5)

SYSTEM DESCRIPTION

VOYAGER

GENERAL ELECTRIC

GPO PRICE $ _____

CFSTI PRICE(S) $ _____

Hard copy (HC) 8.00

Microfiche (MF) .65

ff 653 July 65

MAR 1968
RECEIVED
NASA STI FACILITY
INPUT BRANCH

N68-19101

(ACCESSION NUMBER) (THRU)

411 (PAGES) 1 (CODE)

CR-93550 (NASA CR OR TMX OR AD NUMBER) 31 (CATEGORY)

FACILITY FORM 602

GENERAL ELECTRIC

DIN 67SD4379
16 OCTOBER 1967

FINAL REPORT
VOYAGER SPACECRAFT
PHASE B, TASK D

VOLUME II (BOOK 1 OF 5)

SYSTEM DESCRIPTION

PREPARED FOR

GEORGE C. MARSHALL SPACE FLIGHT CENTER

UNDER MSFC CONTRACT NO. NAS8-22603

GENERAL ELECTRIC
MISSILE AND SPACE DIVISION
Valley Forge Space Technology Center
P.O. Box 8555 • Philadelphia 1, Penna.

PRECEDING PAGE BLANK NOT FILMED.

VOLUME SUMMARY

The Voyager Phase B, Task D Final Report is contained in four volumes. The volume numbers and titles are as follows:

Volume I	Summary
Volume II	System Description
Book 1	Guidelines and Study Approach, System Functional Description
Book 2	Telecommunication
Book 3	Guidance and Control Computer and Sequencer Power Subsystem Electrical System
Book 4	Engineering Mechanics Propulsion Planet Scan Platform
Book 5	Design Standards Operational Support Equipment Mission Dependent Equipment
Volume III	Implementation Plan
Volume IV	Engineering Tasks
Book 1	Effect of Capsule RTG's on Spacecraft
Book 2	Applicability of Apollo Checkout Equipment
Book 3	Central Computer
Book 4	Mars Atmosphere Definition
Book 5	Photo-Imaging

VOYAGER TASK D
VOLUME II
SYSTEM DESCRIPTION

Section		VOY-D No.
I	GUIDELINES AND STUDY APPROACH	100
II	SYSTEM FUNCTIONAL DESCRIPTION AND ANALYSIS	200
	Spacecraft Description	210
	Spacecraft Configuration	220
	Functional System Integration	230
	Baseline Science Definition	240
	Interface Requirements	250
	Trajectory and Guidance Analysis	260
	System Analyses and Trade Studies	270
	Power Gain Product Study	271
	Spacecraft Propulsion Fourth Staging	272
	Planetary Quarantine	273
	Auxiliary Thruster Considerations	274
	Reliability Analyses	275
III	SUBSYSTEM FUNCTIONAL DESCRIPTION AND ANALYSIS	300
	Telecommunication Subsystem	310
	Radio Subsystem	311
	Command Subsystem	312
	Telemetry Subsystem	313
	Data Storage Subsystem	314
	Data Automation Subsystem	315
	Guidance and Control	320
	Attitude Control System	321
	Reaction Control Subsystem	322
	Autopilot	323
	Computer and Sequencer	330
	Power Subsystem	340
	Electrical System	350
	Engineering Mechanics	360
	Structure	361
	Thermal Control Subsystem	362
	Mechanism Subsystem	363
	Pyrotechnics and Planetary Vehicle Separation	364
	Propulsion Subsystem	370
	Planet Scan Platform Subsystem	380
IV	DESIGN STANDARDS	400
V	OPERATIONAL SUPPORT EQUIPMENT	500
VI	MISSION DEPENDENT EQUIPMENT	600

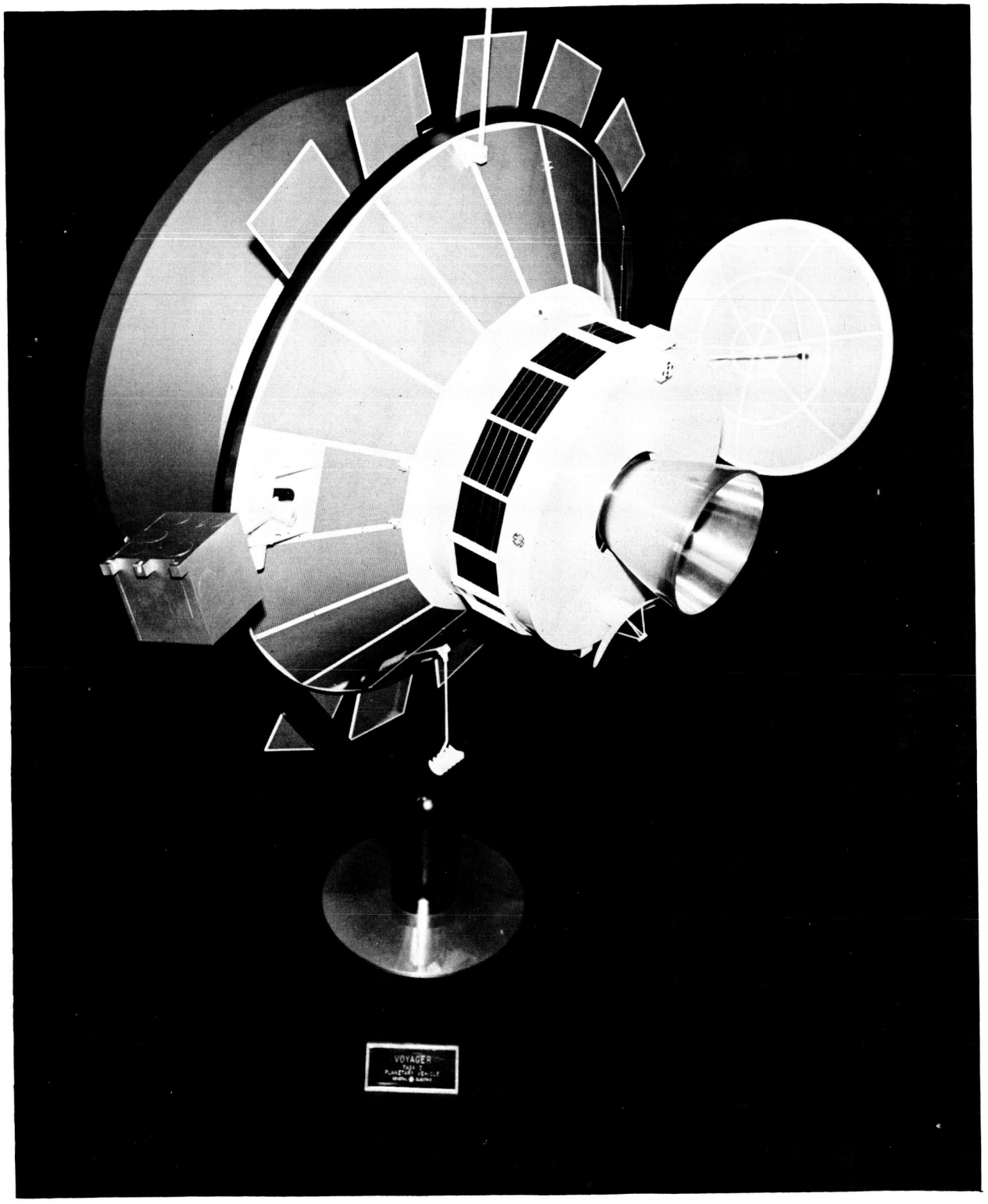

Voyage Planetary Vehicle

VOYAGER TASK D
Volume II
PREFACE

This volume describes the design of the Voyager Spacecraft System, the Operational Support Equipment requirements, and the Mission Dependent Equipment requirements resulting from the system update study.

The mission concept for Voyager has not changed substantially since the previous Phase B, Task B study in late 1965. The Saturn V Launch Vehicle is used to inject two identical planetary vehicles on a Mars trajectory. Each planetary vehicle consists of a flight spacecraft and a flight capsule and, after separation from the Saturn V, the two vehicles provide complete mission redundancy. The flight spacecraft serves as a bus to deliver the flight capsule into Mars orbit from which it subsequently descends and soft lands to carry out surface experiments. The flight spacecraft then carries out an orbiting science mission for periods ranging from six months for early missions to two years for subsequent missions.

The flight spacecraft developed in this system update is shown in the illustration on the page opposite. This design is described in detail in this volume which is organized in the following major sections:

Section	Subject	Identification No.
I	Guidelines and Study Approach	VOY-D-100
II	System Functional Description and Analysis	VOY-D-200
III	Subsystem Functional Description and Analysis	VOY-D-300
IV	Design Standards	VOY-D-400
V	Operational Support Equipment	VOY-D-500
VI	Mission Dependent Equipment	VOY-D-600

Section I describes the study approach and discusses major constraints and guidelines that were imposed, with emphasis on requirements or guidelines which have changed since the last Voyager System design study.

Section II is a system level description of the resulting spacecraft design and its interfaces with other systems. Major system analyses and trade studies, such as trajectory and orbit selection, are covered.

Section III describes the baseline design of each subsystem, with discussion of alternates that were considered in arriving at the selected design.

Section IV covers some limited areas of design standards to be applied to the Voyager spacecraft.

Section V is an analysis of Operational Support Equipment (OSE) requirements and an evaluation of a number of OSE concepts with selection of a preferred approach.

Section VI analyzes the space flight operation together with the current and planned capabilities of the deep space network to define probable requirements for mission dependent hardware and software to support the mission.

VOY-D-100
STUDY APPROACH AND GUIDELINES

1. STUDY APPROACH

The last Voyager Spacecraft system study was conducted in November and December of 1965. At that time, the first Voyager mission was scheduled for the 1971 Mars opportunity. As a result of the delay to 1973, this system update was performed to:

a. Reflect changes in the requirements due to the change in mission year.

b. Reflect changes due to other guidelines that have evolved from mission studies conducted by NASA and others.

c. Incorporate changes in technology that have occurred that will be beneficial to Voyager.

d. Incorporate the results of engineering studies that were carried out under Task C.

In this update, as in previous Voyager system designs, the Missile and Space Division of the General Electric Company placed primary emphasis on meeting the major constraints reflected in the mission specification. These restraints are:

1.1. SCHEDULE

The 1973 Mars opportunity places an absolute constraint on the program schedule. To ensure this schedule will be met requires a conservative design that uses a maximum amount of flight-proven hardware and technology to minimize the risk of delays in the development process. The schedule is also enhanced by a design which allows a maximum amount of parallel fabrication and test of the system. This implies a modular construction which allows major portions of the spacecraft to be assembled and tested in parallel with final assembly requiring only the joining of major modules with relatively simple interfaces. Within this approach, defects in flight hardware can be detected and removed much earlier in the process than is the case if system assembly is one long series process.

1.2. PLANETARY QUARANTINE

The probability of contaminating Mars with earth organisms borne by a space vehicle on any given launch must be kept extremely low. During Task C, the ways in which the spacecraft could violate the quarantine constraint were investigated in detail with both analytical and experimental tasks being conducted. This effort and the conclusions resulting therefrom are summarized briefly in Section VOY-D-273 of this volume. The primary conclusion affecting the spacecraft design is that a "clean" spacecraft (not a sterile one) will satisfy the quarantine constraint if moderate restrictions are placed on the mission - (such as minimum periapsis altitude and use of a conservative guidance philosophy). A clean spacecraft is one which is fabricated and tested under reasonable clean room conditions (typically class 100,000) and frequent cleaning operations are performed to remove particulate contamination from the exterior surfaces. This requirement, in turn, requires a design which can be cleaned and does not contain inaccessible regions where particulate can accumulate. Other design areas of concern are cleanliness of the attitude control gas expelled, and attitude verification prior to trajectory corrections or orbit insertion. These are discussed in following sections of this volume.

1.3. MISSION DURATION

A successful 1973 mission requires a spacecraft lifetime in excess of one year. Again, the use of flight-proven hardware and technologies is of benefit to achieving this goal. In addition, the design must be such that thorough testing of all system elements is possible prior to launch to ensure maximum effectiveness in the detection and removal of defects.

Having satisfied these major constraints, the goal of the system design is to maximize the capability of the spacecraft. A prime measure of this capability is the quantity of data returned to earth, and this parameter has received a great deal of attention in the system update. Other important measures are how well the specific science instrument needs are satisfied, and how flexible is the design for accommodating changes in the mission.

The major effort in this system update has been directed at re-examining the basic design approaches selected during Task B within the new guidelines and the present state of technology. Questions such as size of the communication antenna, type of power distribution, and basic selection of the means for generation of control torques were re-examined. To answer these questions, many trade studies were conducted to show the effect on the system of alternate choices. These studies also are discussed in this volume.

Because of time limitations, the implementation of the selected design approach was not pursued beyond the depth necessary to support the higher level trade studies.

2. CONSTRAINTS AND GUIDELINES

The basic requirements for the Voyager systems are contained in the January 1967 issue of General Specification for Performance and Design Requirements for the 1973 Voyager Mission. Basic changes in this document compared to the issue in effect at the time of Task B are:

a. The change in the mission year from 1971 to 1973 affects primarily the communication range to earth at the time of encounter (170 million kilometers or greater for 1973 compared to about 108 million in 1971) and the spacecraft sun distance (maximum of 1.67 AU in 1973).

b. The capability of the Deep Space Network is more conservatively specified than it was in Task B. Engineering Planning Document 283, Revision 2, an applicable document called out in the mission specification, specifies a worst case performance that is 3 db poorer than in the previous study.

c. The power supplied by the spacecraft to the capsule (until capsule separation) is specified at 200 watts continuous. It was previously required only when the spacecraft was sun-oriented and solar power was available.

d. The spacecraft is no longer required to place the capsule in the proper de-orbit attitude before separation. The spacecraft remains oriented to its celestial references, the capsule is separated, and then the capsule performs the necessary rotation to alight the de-orbit propulsion engine. (The spacecraft has the basic capability to perform this maneuver with no added complexity if it is later deemed desirable).

Additional guidelines for this task (Task D) have been issued by Marshall Space Flight Center in several documents listed at the end of this section. Guidelines which had significant impact on the design were:

a. The design should have basic capability to satisfy the 1973 through 1979 Mars missions. In particular, a single propulsion system should be designed for all years.

b. The capability of the Saturn V was specified as shown in Figure 1. Within this total capability, two planetary vehicles must be provided while satisfying the following ground rules;

   1. A 5000 pound project contingency is to be provided.

   2. A capsule weight of 5000 pounds for 1973 through 1979 is required. A capsule weight of 6000 pounds in 1973 and 7000 pounds thereafter is more desirable.

   3. Sufficient usable propellant to impart 1.95 kilometers/second to the planetary vehicle should be provided for all years.

   4. A 5 percent contingency on spacecraft inert weight should be provided.

   5. A 20-day minimum launch period is required.

c. Capability for fueling the spacecraft at the pad while mated to the Saturn V is required. This is in contrast to the Task B approach where fueling was accomplished prior to encapsulation in the shroud.

d. The requirement for magnetic cleanliness of the spacecraft was removed.

e. The basic Spacecraft propulsion system is to use the Lunar Module descent engine. In addition, modular replacement of this engine by the Agena or Titan Transtage engines was to be considered.

f. The preferred method of shroud separation was specified as over-the-nose. While this was not specified in Task B, the configuration design recommended by GE assumed a clamshell separation.

g. It was stated that separation of the forward portion of the Capsule bio-barrier could be accomplished either prior to or after orbit insertion. In Task B this was specified to occur prior to orbit insertion.

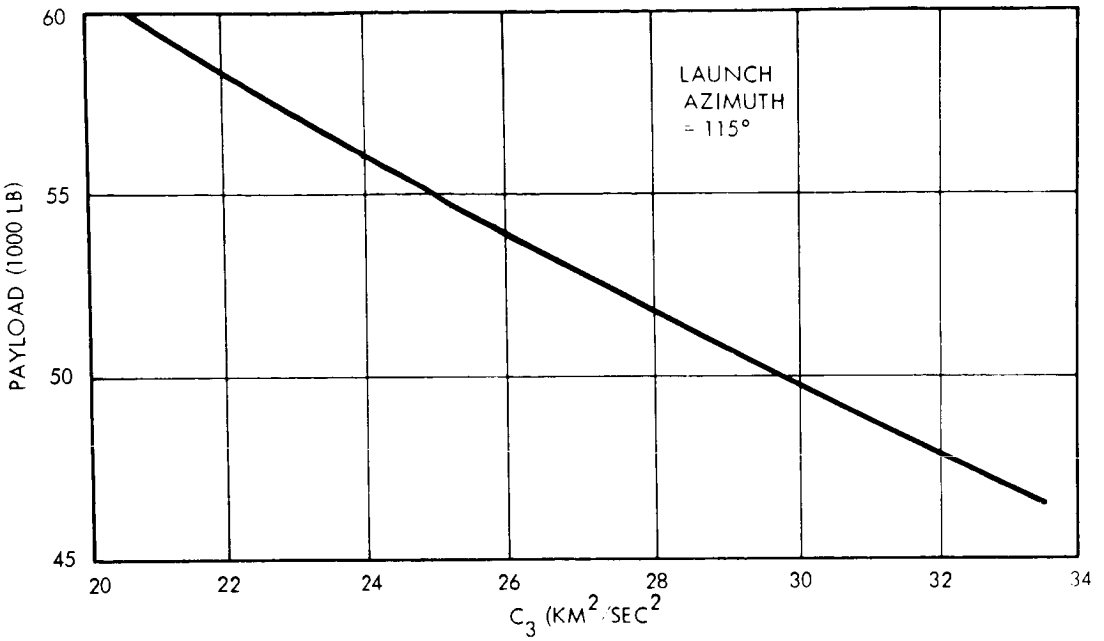

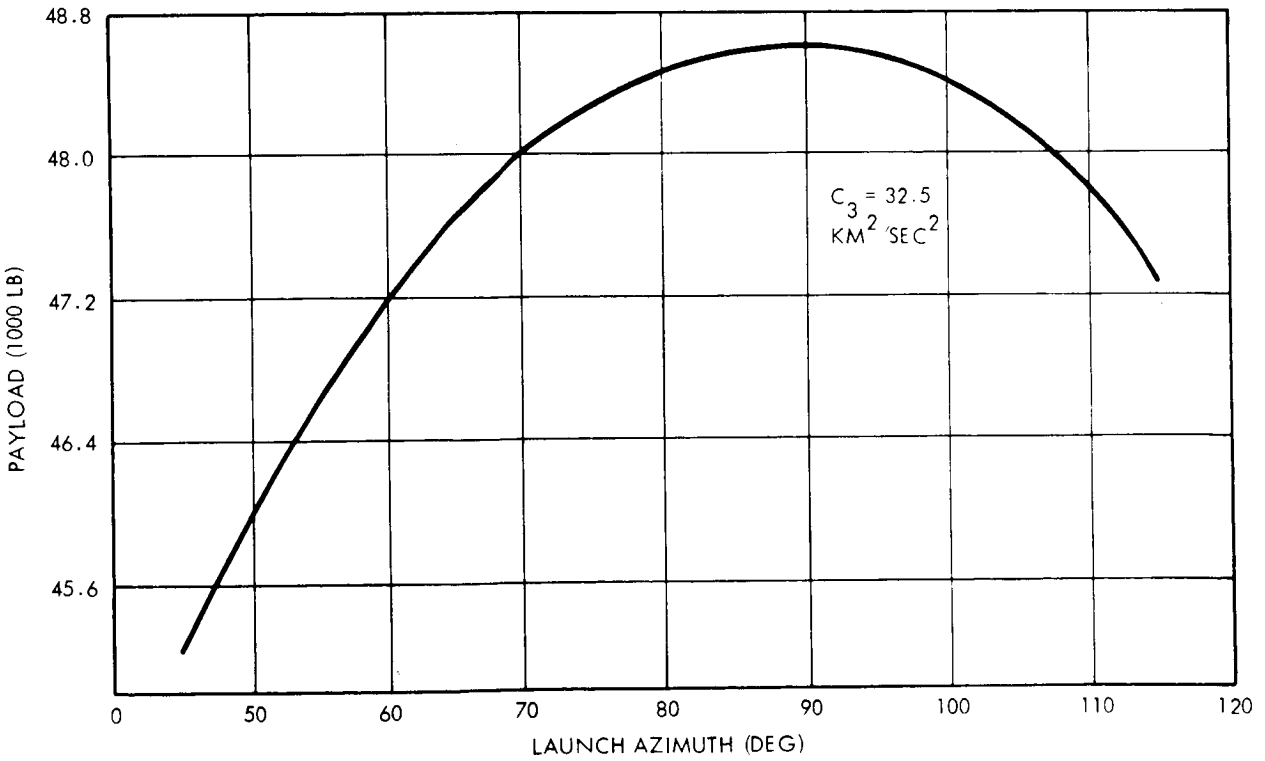

Figure 1. Saturn V Capability

3. MARSHALL SPACE FLIGHT CENTER GUIDELINES

The MSFC issued guidelines for this update are contained in the following documents.

a. Exhibit "A", Contract Guidelines, Phase B, Task D, Voyager Spacecraft System, 16 June 1967.

b. Voyager Spacecraft System Study Guidelines, R-AS-A-67-99, 9 July 1967.

c. Voyager Spacecraft, Phase B, Task D Guidelines, 14 July 1967.

d. R-AS-A-119-67, 12 August 1967.

VOY-D-210
SPACECRAFT DESCRIPTION

1. GENERAL DESCRIPTION

1.1. PLANETARY VEHICLE

A Voyager mission consists of two planetary vehicles launched on a Saturn V launch vehicle. The two planetary vehicles are separated from the last stage, S-IVB, of the Saturn V after injection into an earth to Mars transfer trajectory and operate as independent vehicles thereafter. Each planetary vehicle is composed of a flight spacecraft and a flight capsule with the capsule separating from the flight spacecraft within 30 days after the planetary vehicle is placed into an orbit about Mars. The over-all envelope and configuration of a planetary vehicle is shown in Figure 1.

It is expected that the capsule mission and experiments will be of an evolutionary nature with the capsule for each mission, 1973 through 1979, building on the interpretation of data from previous Voyager and other interplanetary missions. Therefore, the capsule weight is presently defined as a range - 5,000 to 6,000 pounds for the 1973 mission and 5,000 to 7,000 pounds for subsequent missions. For the 1973 mission, the planetary vehicle weight is 20,684 and 22,626 pounds for a 5,000 and 6,000-pound capsule, respectively. With a 5,000-pound capsule, the Saturn V launch vehicle is capable of launching two planetary vehicles with a 30-day launch period and still provide for a 5,000-pound project contingency.

1.2. FLIGHT SPACECRAFT

The primary functions of the flight spacecraft are to support and carry a flight capsule into an orbit about Mars; receive and transmit to Earth data from the capsule during deorbit, descent, entry, and terminal descent; support the scientific instruments; and process and transmit to Earth the data obtained from the spacecraft mounted scientific instruments. To

accomplish these functions, the spacecraft has been designed to be capable of fully accomplishing the mission without ground command provided that the Saturn V launch vehicle injects the planetary vehicle onto a perfect transfer trajectory and a change in pre-programmed instrument sequencing is not required.

The spacecraft, as shown in Figure 2, is fully attitude stabilized throughout the mission using the Sun and Canopus as celestial references during cruise and nominal oribital operations and an onboard inertial system during propulsion maneuvers and occultations of the celestial references. The LEM Descent Engine (LEMDE) and propellant system provides velocity changes at a 1,050-pound thrust level to the spacecraft for correcting the trajectory or trimming the areocentric orbit and at a 9,850-pound thrust level for insertion into an orbit about Mars. While the spacecraft is stabilized to the sun, power is supplied to the spacecraft (and to the capsule before separation) from photovoltaic cells mounted on panels; during maneuver and sun occultation periods, power is obtained from nickel-cadmium batteries. The temperature of the spacecraft is controlled by a combination of super insulation blankets and a variable emissivity louver system for dissipating heat generated by the spacecraft electronic elements.

The scientific data is returned to earth through a 9.5-foot parabolic, mesh antenna radiating 50 watts which is stepped periodically to point the center of the radiated beam to within 17 mrad (0.99 probability) of the spacecraft to earth vector. Two additional low gain wide beam antennas provide for communication between the spacecraft and earth while the spacecraft is not stabilized to the sun and Canopus; a fixed, 90-degree beam width antenna receives data from the capsule from capsule separation through landing. Data from the scientific instruments and capsule are stored on magnetic tape at input rates compatible with the scientific instruments; data from four tape recorders, along with engineering data, are multiplexed for transmission to earth. The communication links also provide ground command to the spacecraft, and angle tracking, two-way doppler measurements and ranging for trajectory and orbit determination.

Figure 1. Planetary Vehicle

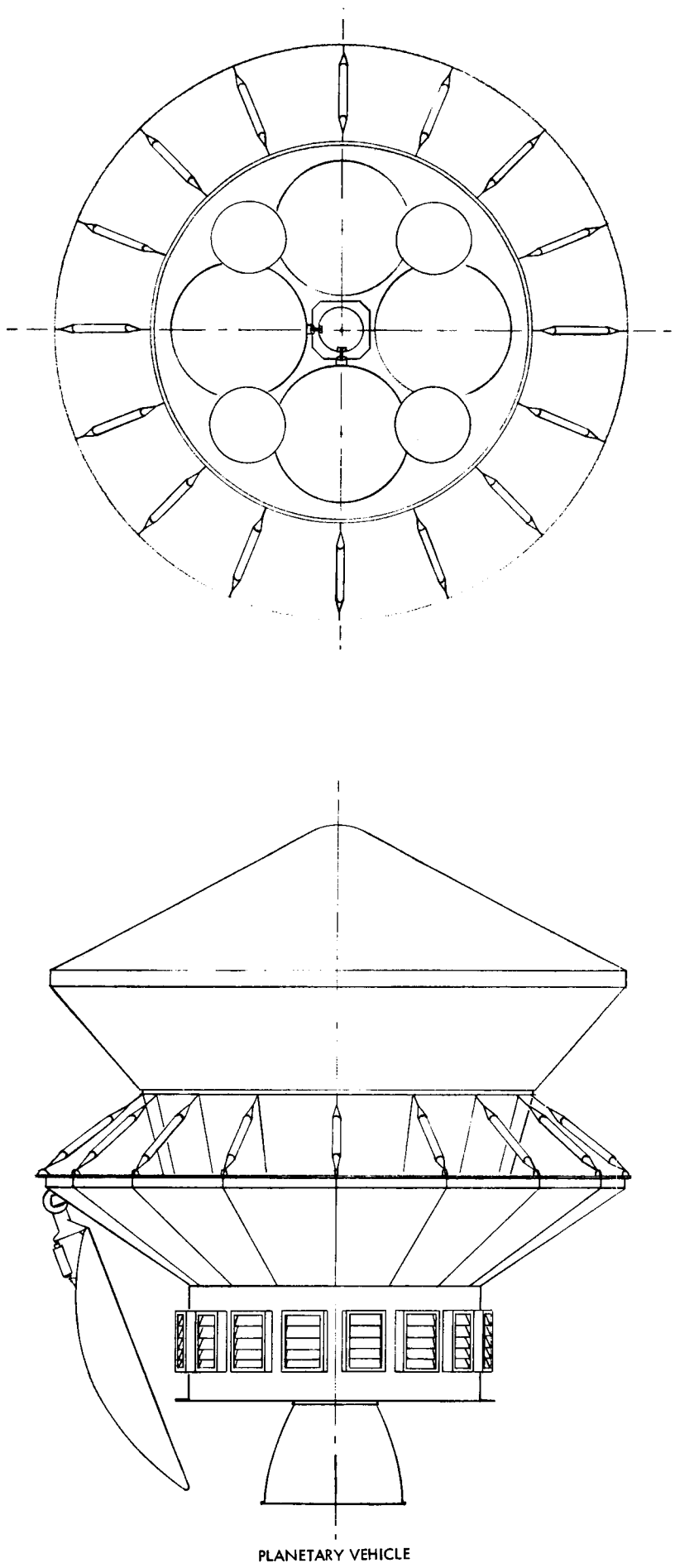

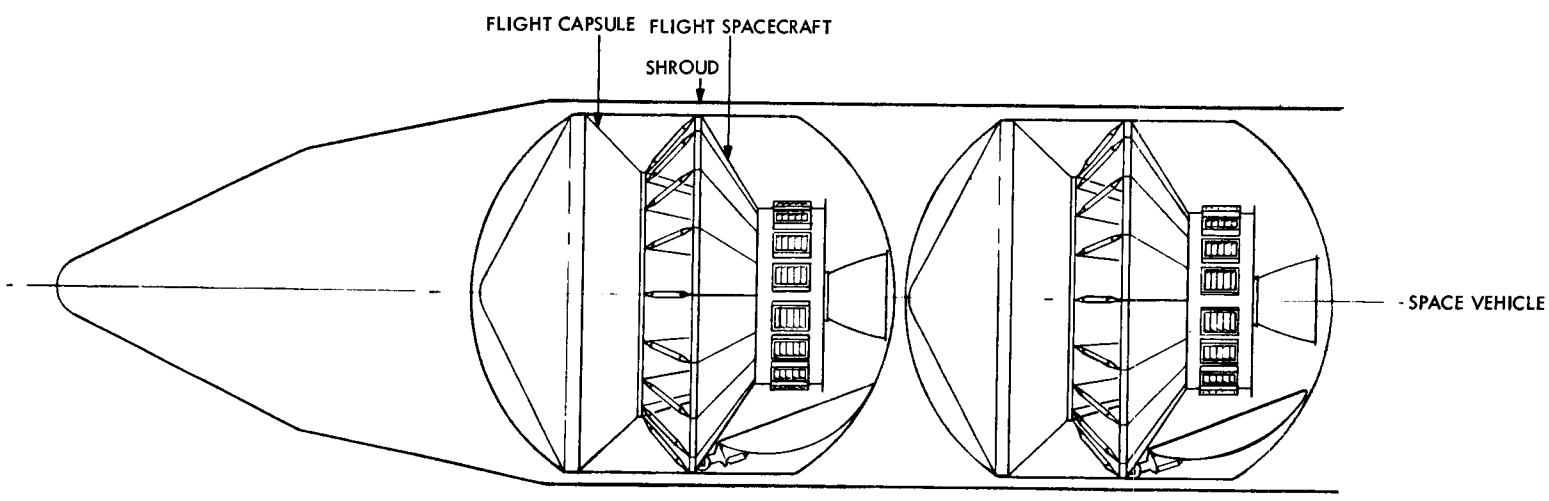

FOLDOUT FRAME 1
3
FOLDOUT FRAME 2
4
VOY-D-210

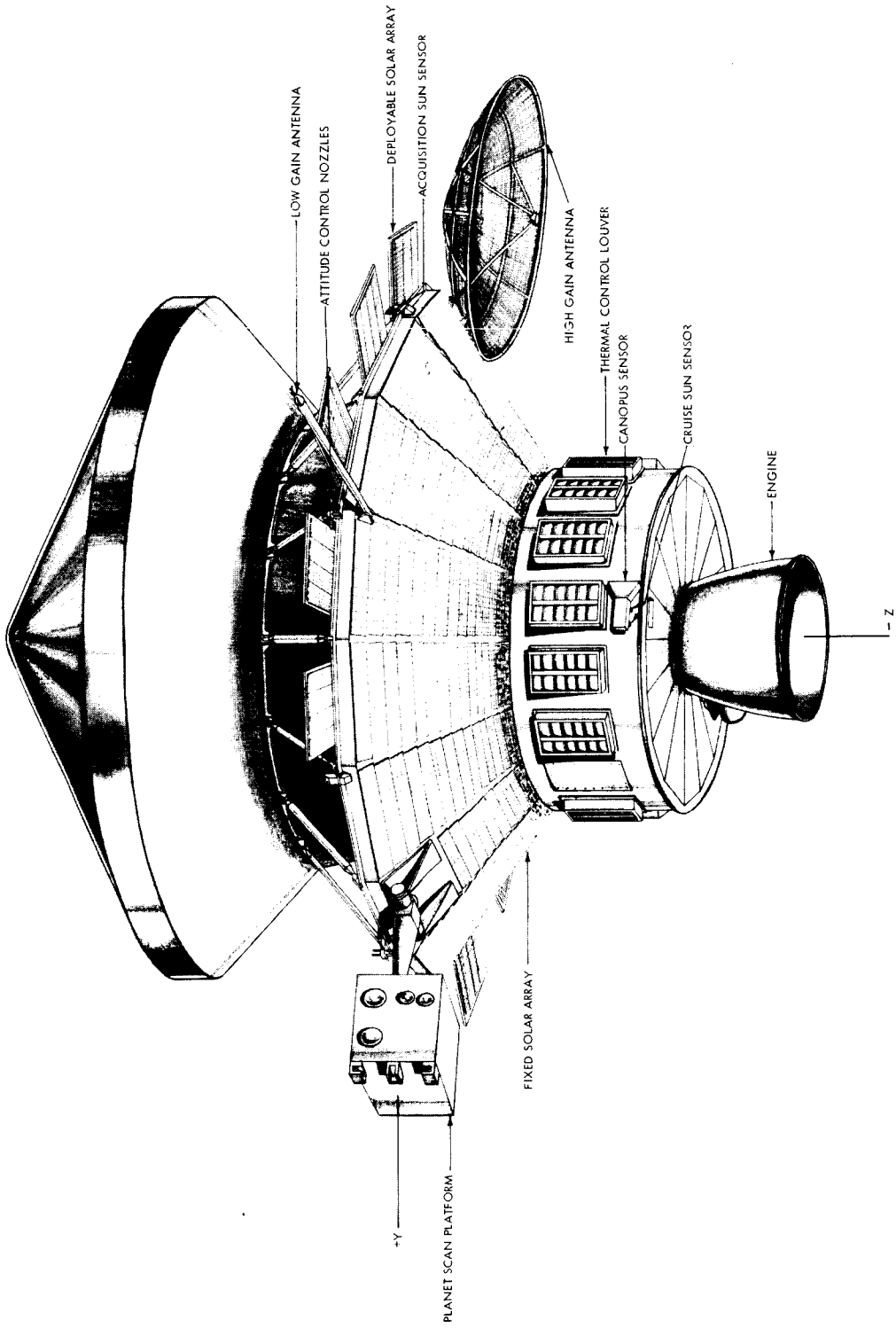

Figure 2. Flight Spacecraft

All the scientific instruments of the baseline science payload are mounted on the Planet Scan Platform (PSP). The instruments are compartmentalized so as to most easily provide the widely different temperature environments required by individual instruments. During orbital operations, a boom perpendicular to the plane of the orbit is erected and continuous motion about this boom points the required instruments to within one degree of the center of the planet. The boom is maintained perpendicular to the orbit plane by stepping each of the two gimbals approximately once per orbit; the motion of the platform about the boom axis is approximately 3 degrees per minute at periapsis passage.

The performance characteristics of the flight spacecraft are noted in Table 1. The major differences as noted from the Task B Design are:

a. A change in the support points, planetary vehicle to shroud, with the electronic module located below the solar array.

b. LEMDE and associated tankage without auxiliary thrusters instead of a solid propellant engine and auxiliary thrusters.

c. Solar array mounted on a conical support structure.

d. Better modularity and accessibility.

e. Increased performance capability as evidenced by a larger antenna, larger PSP, and greater effective solar array area.

1.3. MISSION PROFILE

Launch of the Voyager space vehicle will occur from Cape Kennedy, Florida during the period of August 7 through September 5, 1973 with arrival of the planetary vehicles at Mars occurring between March 1 and March 19, 1974. The flight time between launch and encounter is dependent upon the launch date and will vary between about 220 days for early launches to about 190 days for late launches. The Earth distance (communication distance) at encounter varies between 210 and 240 million kilometers with the shorter distance occuring for the earlier arrival date. The March arrival dates are fixed primarily by the capsule

Table 1. Flight Spacecraft Performance Characteristics

Weights	
Burn Out	5565 lbs
Usable Propellant (Maximum Capability)	12,665 lbs
Usable Propellant (1973 Mission, 5000 lb Capsule)	9994 lbs
Data Rate	
Encounter	40,500 bps
Orbital Operations	40,500; 20,250; 10,121; 1265 bps
Cruise	150 bps
Maneuver	7.5 bps
Data Storage	
390 kps Read-in	2.4×10^9 bits
3.9 kps Read-in	7.2×10^7 bits
Telemetry Channels	
Cruise Sampling Rate of 1.56 sec.	48
Cruise Sampling Rate of 15.6 sec.	145
Cruise Sampling Rate of 312 sec.	300
Command Channels	
Discrete	198
Quantitative	21
Total Capability	246
Instrument Pointing	
Control	1 degree
Accuracy	1/4 degree
Power (at Solar Array)	
Encounter	889 watts
Aphelion	838 watts
Battery (38.5V)	3270 watt-hrs
Maneuvers	
Low Thrust	5
High Thrust	1

landing requirements of between 10 degrees North and 40 degrees South latitude and 10 degrees to 30 degrees from the terminator; for minimum Canopus occultations, the March arrival dates are also preferred. However, earlier arrival dates would result in shorter encounter communication distances; for the 1973 mission, arrival dates as early as February 1 can be supported by the launch vehicle and spacecraft propulsion which would result in an encounter communication distance of 170 million kilometers, or a two-to-one increase in data rate as compared to the March 19 arrival date.

Consideration of propulsion requirements, Canopus and Sun occultations, planet contamination by loose particles from the spacecraft, and surface mapping by the spacecraft mounted cameras resulted in a selection of an orbit of 1,000 x 11,727 kilometers altitude inclined 40 degrees to the Martian equator and with insertion occurring over the Southern hemisphere of Mars. For this orbit, arrival between March 1 and March 19, 1974, and insertion conditions (VOY-D-260) for the desired orbit location, Earth occultations occur for the first 30 days and from about 100 to 180 days after orbit insertion, solar occultations are delayed to about 100 to 120 days after orbit insertion, and 99 percent of the surface of the planet between the extreme latitude excursions of the orbit can be covered in two months; the surface coverage is obtained with a 5.7 degree field-of-view sensor while at altitudes between 1,000 and 3,000 kilometers and lighting angles between 40 and 85 degrees.

The launch and trajectory injection phases of the mission consist of:

a. Burn-out of the first two stages of the Saturn V launch vehicle.

b. First burn of the SIV-B stage to place the space vehicle into a 100 n. mi. parking orbit.

c. Parking orbit coast period during which the nose fairing is separated.

d. Second burn of the SIV-B stage and injection onto the transfer trajectory.

e. Separation of the planetary vehicle from the SIV-B stage in the sequence of forward vehicle, forward shroud section, and aft vehicle. The separation velocities of the two planetary vehicles and forward shroud section are adjusted to prevent interaction between the three elements.

Upon separation from the launch vehicle, the spacecraft attitude control subsystem is enabled and the sun is acquired. A programmed roll of the spacecraft then occurs until Canopus is acquired. Within three to four days, after the initial trajectory has been determined, each planetary vehicle performs a combined trajectory correction and time of flight adjustment maneuver. The first planetary vehicle is given a time of flight adjustment so that its flight time is decreased by four days and the time of flight of the second vehicle is increased by four days. The time of flight adjustment velocity increment for each vehicle varies from about 120 to 60 mps as the launch date is delayed. The separation of arrival dates provides for operational ease in tracking and commanding maneuvers for each planetary vehicle. Two additional trajectory corrections most probably will be made by each vehicle with the first occurring approximately 30 days after transfer trajectory injection and the second ten days before Mars encounter. Provided that the proper attitude is obtained and verified, the relative velocity with respect to Mars is decreased and orbit insertion occurs; the insertion velocity increment necessary to obtain a 1,000 by 11,727 kilometer altitude orbit, properly located, is approximately 1,280 mps; the velocity increment is dependent on the actual trajectory flown with variations in velocity increment due to variations in arrival velocity and rotation of the natural line of apsides.

Within a few days after orbit insertion, the orbit is accurately determined by two way doppler measurements. Depending upon the magnitude of the error in the orbit, a trim of the orbit may be made. The separation of the capsule may occur anywhere between a few days after orbit insertion or orbit trim and 30 days after orbit insertion. From capsule separation to capsule landing, data from the capsule is received by the spacecraft for storage, processing, and transmission to Earth.

If required for mapping of the planet surface or viewing of a specific surface area, an additional orbit trim may occur after capsule separation. Thereafter, nominal orbit operations are continued to the end of mission except during periods of Canopus, Earth, and Sun occultations. During the occultation periods, the spacecraft is commanded by onboard control to vary the mode of operations - switching-on gyros for Sun and Canopus occultations

and inhibiting of data transmission for Earth occultations. Throughout the orbital mission phase, the high gain antenna is stepped so as to point to Earth, the PSP is stepped to provide an axis of rotation normal to the orbital plane, the PSP rotates about the orbit plane normal so as to point to the planet center (except during rewind of the PSP during each orbit period), and data is obtained, stored, processed, multiplexed, and transmitted to Earth.

The spacecraft can be rolled 180 degrees and the second Canopus sensor used for attitude control if scientific instrument viewing is obstructed by spacecraft elements. With the design orbit and the PSP design, it is not anticipated that this will be required for an orbit mission life of 12 months. Completion of the orbital phase is not expected to occur less than six months after orbit insertion and will be terminated by a loss of a critical spacecraft function.

2. SPACECRAFT CONFIGURATIONS

2.1. CONCEPT SELECTION

The spacecraft design characteristics which most affect the selection of a configuration are the capsule and planetary vehicle support, propulsion and electronic storage, and high gain antenna viewing, high gain antenna size, and available solar array area. In selecting a configuration, the more important criteria are planetary quarantine, schedule risk, vehicle weight, expected probability of success, adaptability to future missions (Mars and other planets) and cost. The concepts considered and the details of the selection process are described in VOY-D-220. In summary, after several iterations from Task A through Task C of the Voyager Phase B Studies, several concepts with variations have been developed which can approximately equally fulfill mission performance requirements. The selection of the design concept (Figure 3) which was developed into a preliminary design during this study was made primarily on the basis of modularity and accessibility.

The modularity allows the fabrication and a large portion of the testing to be completed in parallel. In case of design or test difficulties in any one module, the modularity results in a higher confidence in meeting an absolute fixed launch period. The accessibility provides

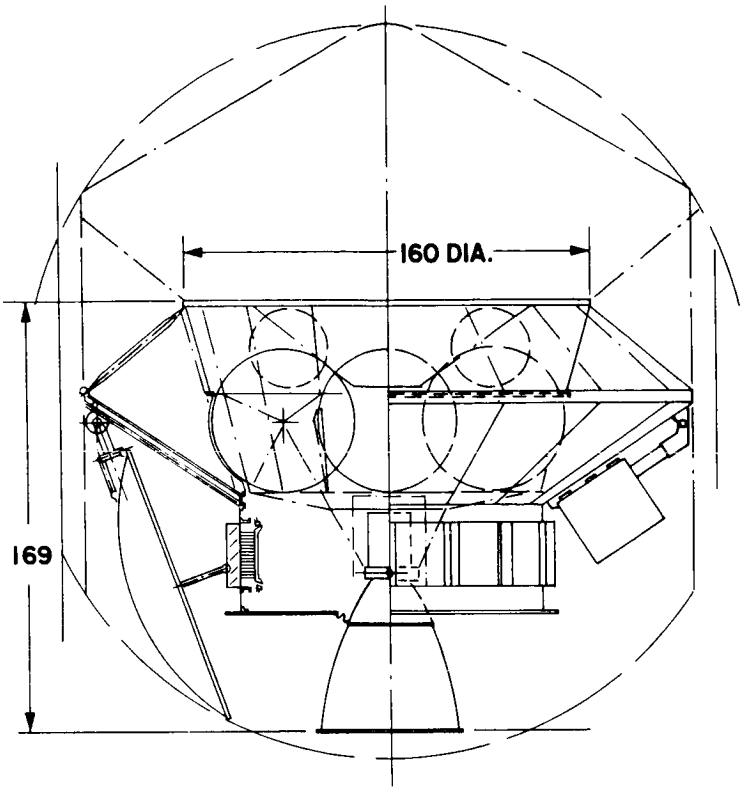

Figure 3. Selected Configuration

for the easy adjustment, testing and replacement of spacecraft components after assembly of the spacecraft, giving additional assurance of being able to meet the required launch period. It should be noted that excellent modularity and assessibility are obtained without a significant penalty to spacecraft performance. The modularity of the selected design concept is shown in Figure 4. It is noted that the three modules - support, propulsion, and electronic - can be fabricated independently and assembled with a minimum of interface connections.

In the process of selecting a configuration concept, several design variations were investigated. These included the number of propellant tanks (4 or 6), propellant tank support (box beam or truss), and the number of electronic bays (12, 16, or 18). For a capsule interface ring of less than 160 inches, four propellant tanks were selected with the truss support system weighing much less than the box beam approach. The optimum number of electronic bays is dependent upon the diameter of the electronic module with the weight per bay, thermal control panel area per bay, number of available electrical connectors per bay, and bay dimensions being design characteristics which must be considered. For the selected concept with an electronic module diameter of 120 inches, 16 bays were selected as optimum.

For the selected configuration, prime design trade-offs included location of appendages (Paragraph 2.5.), location of the support point (Figure 3) and the total effective array area. Moving the support point towards the capsule results in increased heat rejection capability of the electronic bay thermal control louvers, less critical requirements on the planetary vehicle separation mechanism and larger antenna diameters in a given vehicle envelope. Moving the support point away from the capsule results in better high gain antenna viewing, move effective usage of the fixed solar array area, and availability of a greater deployable solar array area. With the support point located towards the center of the two possible extremes, the structural weight is a minimum and the best PSP viewing (day and nighttime for both the experiment and control sensors) is obtained. This trade-off is more fully discussed in VOY-D-220 with a midway support point being chosen. The other primary trade area, effective solar array area, was concerned with the placement of fixed solar array on the bottom of the electronic module or the use of deployable arrays to obtain the required total array area. The fixed array at the bottom of the electronic module has the disadvantage of higher operating temperatures, reduced accessibility to the electronic module, and high temperature gradients between the array and electronic module. Deployable array effects the viewing of the PSP as well as limiting the location of sensors and antennas. However, fixed array including that at the bottom of the electronic module is not sufficient to fulfill the worst case power requirements so some deployed array is required. The choice was, therefore, to use 9 deployed array panels (74.3 sq ft) in combination with the fixed array mounted on the support module (196.0 projected sq ft).

2.2. SUPPORT MODULE

The support module (Figure 5) provides the attachment to the shroud and a support for the fixed and deployed solar array, the PSP, all antennas except the medium gain fixed antenna, and the coarse sun sensors. The lower half of the module consists of sixteen ribs between a lower ring and the main support ring; these ribs carry the load from the electronic module and propulsion engine and tankage with shear loads being taken out by the solar array panels. A series of sixteen struts attached to the main support ring at the rib positions and to the upper ring of the support module carry most of the capsule loads.

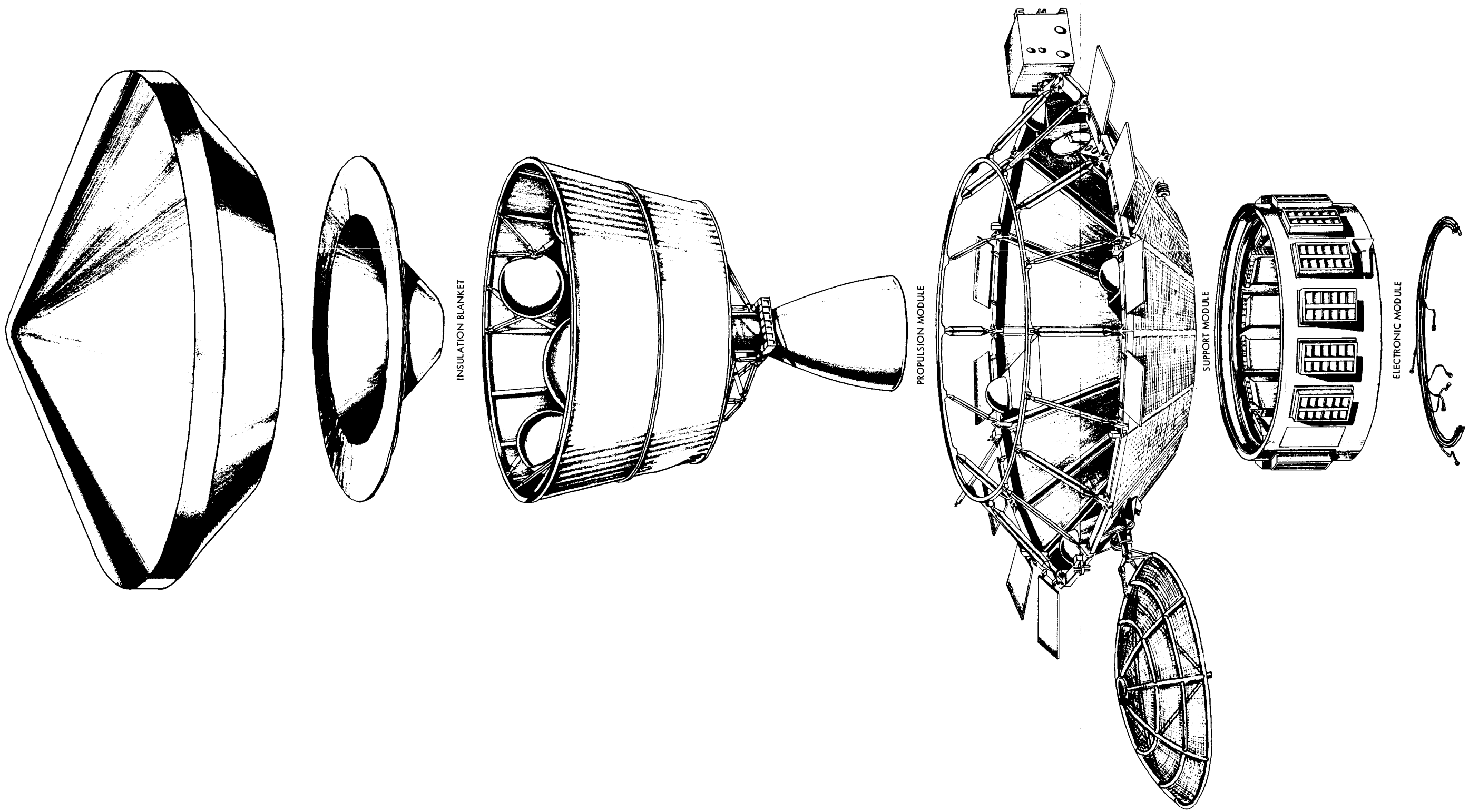

FOLDOUT FRAME 1

Figure 4. Spacecraft Modularity
FOLDOUT FRAME 2

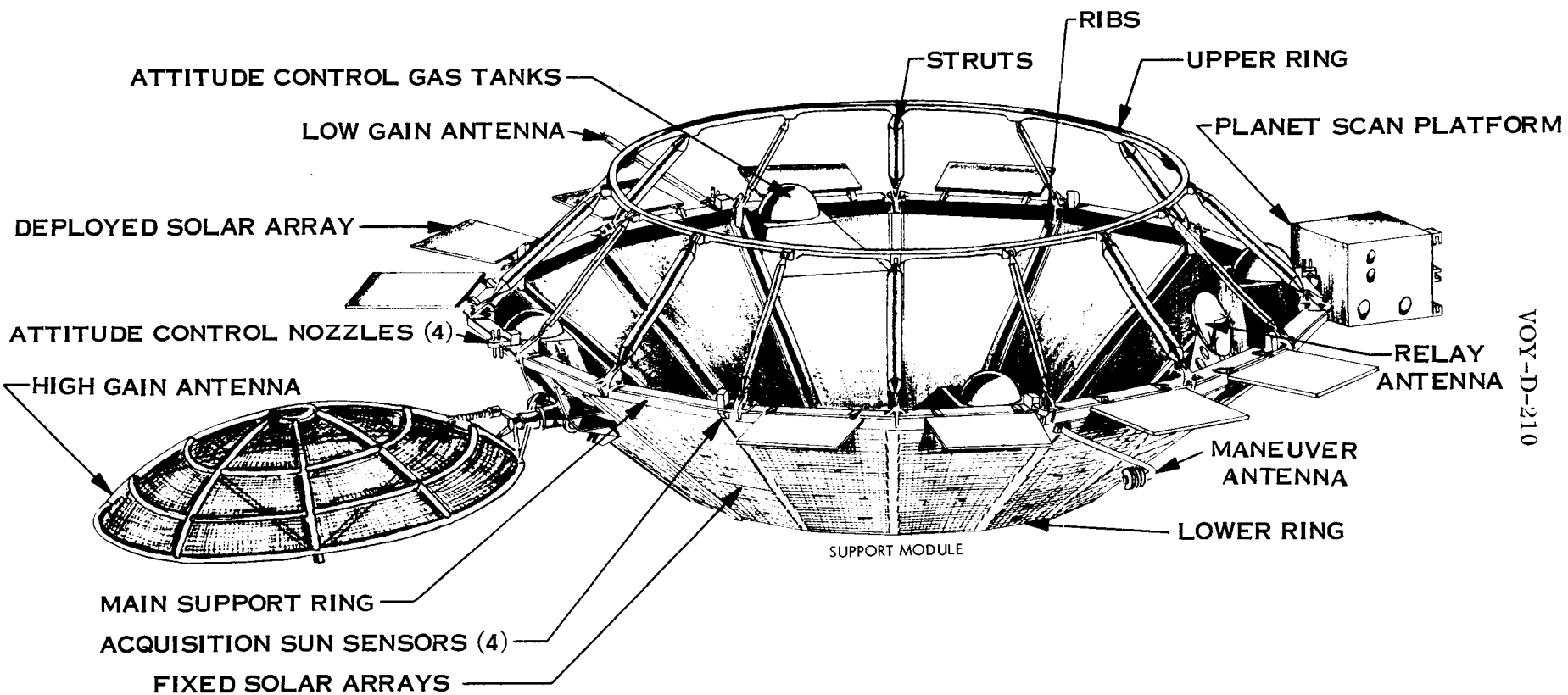

Figure 5. Support Module

In addition to the appendages previously noted, four nitrogen tanks for attitude control gas and the attitude control nozzles are attached to the support module. This allows the attitude control gas system to be completely assembled on the support module and checked out before mating of the three spacecraft modules. The solar array panels can also be mounted to the support module and deployment of the non-fixed panels checked along with the continuity of the complete array before mating of the three modules.

2.3. PROPULSION MODULE

The propulsion module (Figure 6) carries a portion of the lander loads through the ring stiffened shell structure that is the outside envelope of the module as well as the Propulsion Subsystem loads. The propulsion module consists of the ring stiffened shell structure; two trunnion mounted oxidizer and two trunnion mounted fuel tanks; eight tri-pod supports (two per tank) between the propellant tank truss support ring and lower propulsion module ring for supporting the oxidizer and fuel tanks; four trunnion mounted helium pressurization tanks; eight tri-pod supports (two per tank) between the capsule interface ring and propellant tank truss support ring for supporting the helium tanks; a cruciform engine support structure off of the lower propulsion module ring with truss supports from the propellant tank trunnions; a truss engine support structure between the cruciform engine support structure, lower propulsion module ring, and engine gimbal ring; and two actuators mounted between the engine support structure and the head-end of the engine. The upper ring of the propulsion module also serves as the capsule attachment ring. A more detailed description of the engine and tank support structure is given in VOY-D-220.

2.4. ELECTRONIC MODULE

Except for antennas, the scientific instrument sensors, the course sun sensors, and solar cells, all electronic equipment is located in the electronic module (Figure 7). Of the equipment located in the electronic module, only the Canopus sensors and fine sun sensors are located outside of the sixteen electronic bays. The electronic bays are located between two center rings and sixteen longerons which extend between the top and bottom rings of the

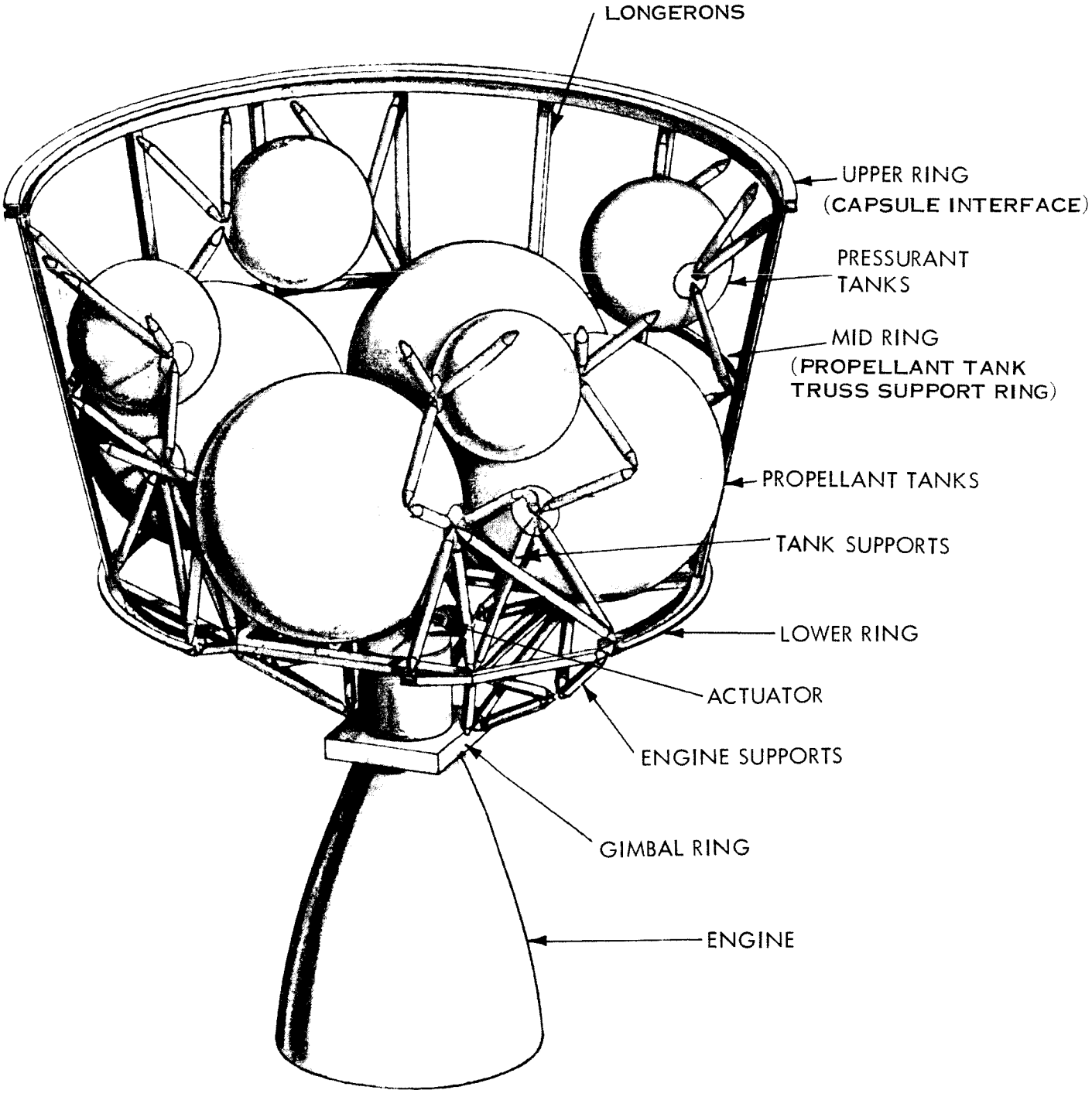

Figure 6. Propulsion Module

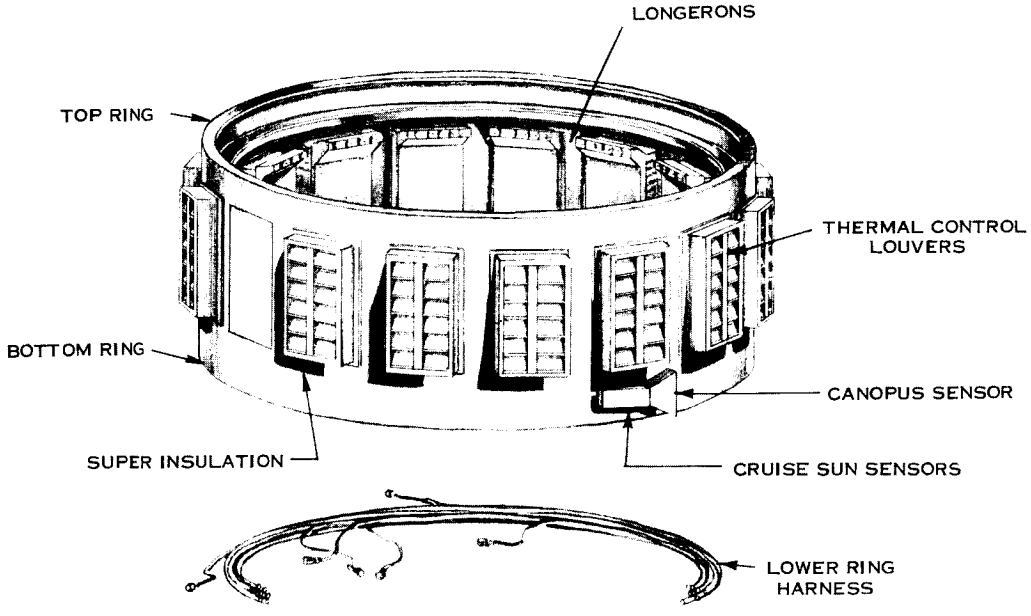

Figure 7. Electronic Module

electronic module forming a cylindrical section of 120 inch diameter and 48-1/4 inches high. Attachment to the support module is made through the top ring. Cover sheets and super insulation form the outer periphery of the cylinder except in areas occupied by the thermal control louver assemblies.

Each of the sixteen electronic bays are 17.8 inches wide by 18 inches high and have a volume of 1,920 cubic inches for the packaging of electronic equipment. A peripheral harness at both the top and bottom of the bays provides interconnection between the bays and external equipment. Access is provided to the electronic bays by either removal of individual thermal control louver assemblies or the bottom of the electronic module.

The arrangement of equipment in the electronic bays and the physical characteristics of the equipment in each bay is noted in Figure 8. Two electronic bays, 3 and 5, are allocated to electronic equipment for the scientific instruments and one bay, 6, to the Data Automation Subsystem which controls sequencing of the scientific instruments and processing of data from the instruments. An additional bay, 13, is allocated to the relay radio receiver and capsule data processing equipment leaving one bay, 4, as a spare.

The thermal control louver system maintains the temperature within each electronic bay between 40 and 70°F if the heat dissipation within the bay is less than 94 watts. The temperature is maintained by a louver system which provides a variable emissivity surface with the effective emissivity being controlled by the bay temperature. The sun shade on each bay prevents heat from the sun from being reflected by the backs of the louver blades into the back plate of the thermal control assemblies.

2.5. APPENDAGES

Because of viewing requirements, the antennas, PSP, and attitude control sensors must be located at specific points about the spacecraft surface. Since both the transfer trajectory and the orbit of Mars about the sun is approximately in the plane of the ecliptic, placement of the

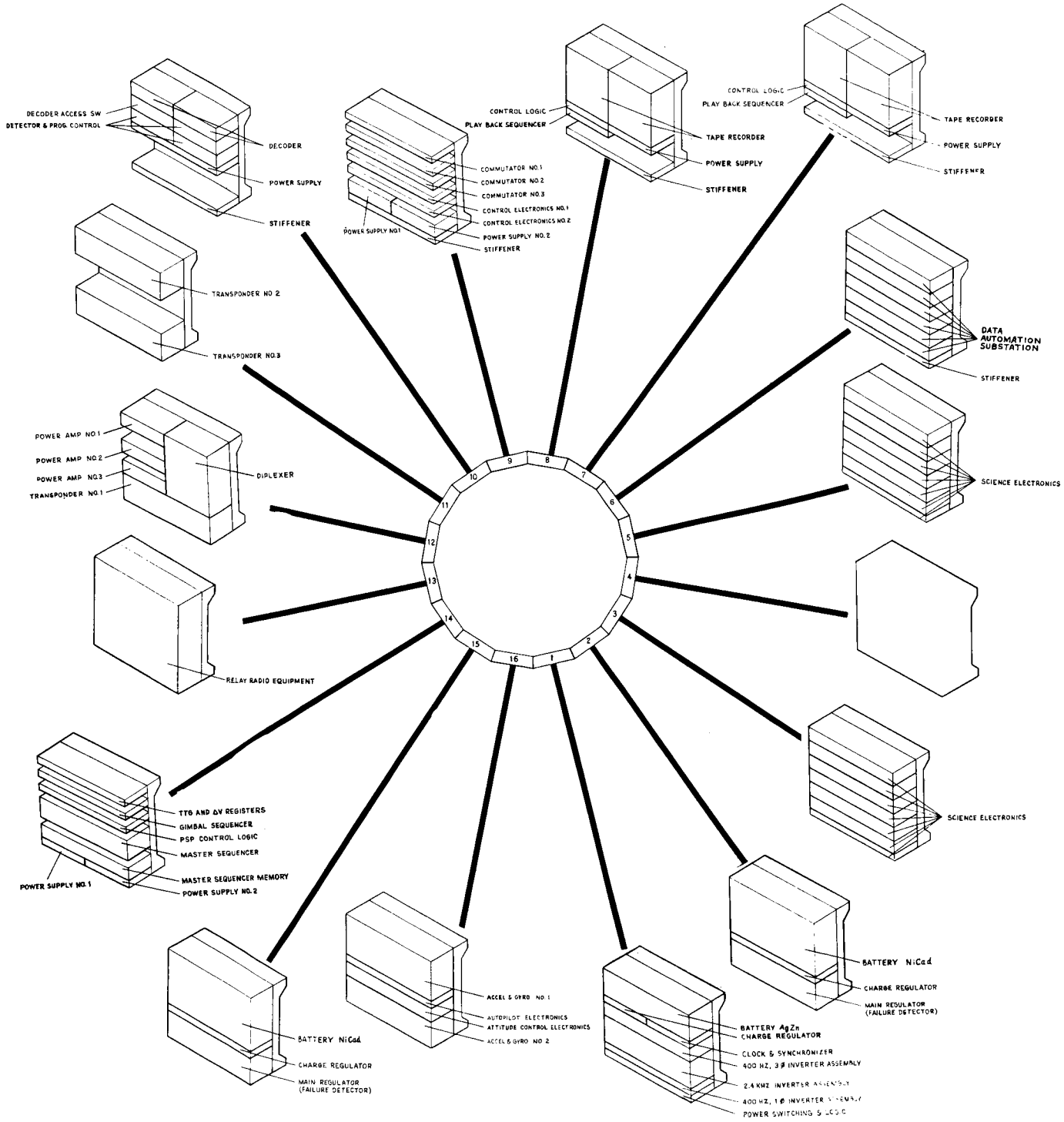

Figure 8. Electronic Equipment Arrangement

Table 2. Equipment Allocations

Bay	Description	Wt. (lb.)	Subassy. Weight	Subassy. Volume (cu. in.)	Packaging Factor (lb./cu. in.)	No. Connectors
1	Power	98.45	96.65	2020	0.048	10
2	Power	111.95	102.75	2020	0.051	10
3	Science E.	65.60	61.00	1750	0.035	Later
4	Spare	4.2	-	-	-	-
5	Science E.	65.60	61.00	1750	0.035	Later
6	Science DAE	54.60	50.00	1750	0.029	10
7	Data Storage	37.30	31.30	1280	0.024	4
8	Data Storage	41.30	35.30	1280	0.028	4
9	Telemetry	37.40	27.20	945	0.029	16
10	Command	39.10	29.90	945	0.032	12
11	Radio	32.60	26.60	1080	0.025	4
12	Radio	54.60	46.70	1550	0.030	4
13	Radio Rel.	56.00	50.00	1750	0.029	4
14	C&S	51.10	42.00	1220	0.034	13
15	Power	111.45	102.00	2020	0.051	10
16	G&C	61.60	43.60	1750	0.025	13
			806.00 lb.	23,110 cu. in.		

Total available Subassembly

Packaging volume - 30,400 cu. in.

Spare volume - 7,290 cu. in.
or 24 %

high gain antenna on the spacecraft y axis (axis approximately normal to the ecliptic) provides the greatest unrestricted viewing of earth by the antenna. Additionally, for most areocentric orbits considered, placement of the PSP on the spacecraft "y" axis provides the best planet viewing; analysis of the design orbit for the 1973 mission indicates less restrictive viewing of the PSP with the PSP located on the +y axis (towards the North celestial pole). Thus, the PSP was located on the +y axis at the maximum distance (support module outer diameter). The high gain antenna then is attached on the -y axis at the support module outer diameter. With attachment at the support module outer diameter, the maximum diameter antenna can be stowed during the launch phase. Attachment of the PSP on both the top and bottom of the support cone, including stowage over the solar array and between the support module and capsule, was also investigated. The selected position, on the solar array side of the support module, results in better viewing for the wide angle planet tracking sensor (as discussed in VOY-D-380.)

During maneuvers, an antenna with a 180-degree beam width in a plane normal to the xy spacecraft plane assures coverage by rolling the spacecraft so that the beam intercepts the earth. By locating this maneuver antenna so that the beam is in the xz spacecraft plane (approximately in the ecliptic) command coverage can also be obtained by the antenna throughout the mission - particularly if the antenna is located on the +x axis as shown in (Figure 5) since the earth is normally located on this side of the sun line. The other low gain antenna is located on the -x axis with the peak of the beam in the sun direction (-z) in order to most adequately fill in the volume not covered by the maneuver antenna. The required coverage of the relay antenna is determined by the spacecraft areocentric orbit size, capsule deorbit trajectory and capsule entry characteristics; the optimum location of the relay antenna is determined by these factors, the relative position of the orbit with respect to the sun line, and spacecraft obstructions. Using the same capsule deorbit trajectory as for the Task B study, the relay antenna was located as shown with the center of the beam at a clock angle of 213 degrees and cone angle of 117.5 degrees. The last antenna, a medium gain fixed antenna, is used for back-up coverage during the early phase of the orbital mission in case of failure of the high gain antenna gimballing mechanism. It is located on the bottom

panel of the electronic module with its beam center at a clock angle of 268 degrees and cone angle of 31 degrees and the major axis of the elliptic dish rotated 25 degrees from the xz plane.

The Canopus sensors should be free from stray light in a fan shaped volume centered on the -y axis. The high gain antenna prohibits placement of the Canopus sensor at the most ideal location, the -y axis at the maximum diameter of the support module. The next best location for the Canopus sensor is, as shown, on the electronic module at the -x axis; the second sensor is located at the +x axis.

In order to provide hemispherical coverage, including viewing in the capsule (+z) direction, the acquisition sun sensors are located at the largest diameter available, hence, on the support module. The cruise sun sensors are located so as to provide the best unobstructed viewing in the sun direction (-z) and, hence, are located on the bottom of the electronic module. The attitude control nozzles are also located at the maximum diameter in order to obtain the greatest moment arm. The nozzles are located on the control axes (x and y) with each nozzle forming a couple with another nozzle.

3. FUNCTIONAL CHARACTERISTICS

3.1. SYSTEM FUNCTIONAL RELATIONSHIPS

The system functional diagram (Figure 9) portrays the functional relationships between the various subsystems of the spacecraft. The signal flow between the subsystems during nominal spacecraft operations is shown as well as a simplified intra-subsystem signal flow for each subsystem. The distribution of power — 2400 Hz, 400 Hz single and three phase, regulated dc, and unregulated dc — is described in VOY-D-340 and is not repeated here. However, the general flow of propellant and pressurant is shown in the system functional diagram.

THIS PAGE INTENTIONALLY LEFT BLANK

PRECEDING PAGE BLANK NOT FILMED.

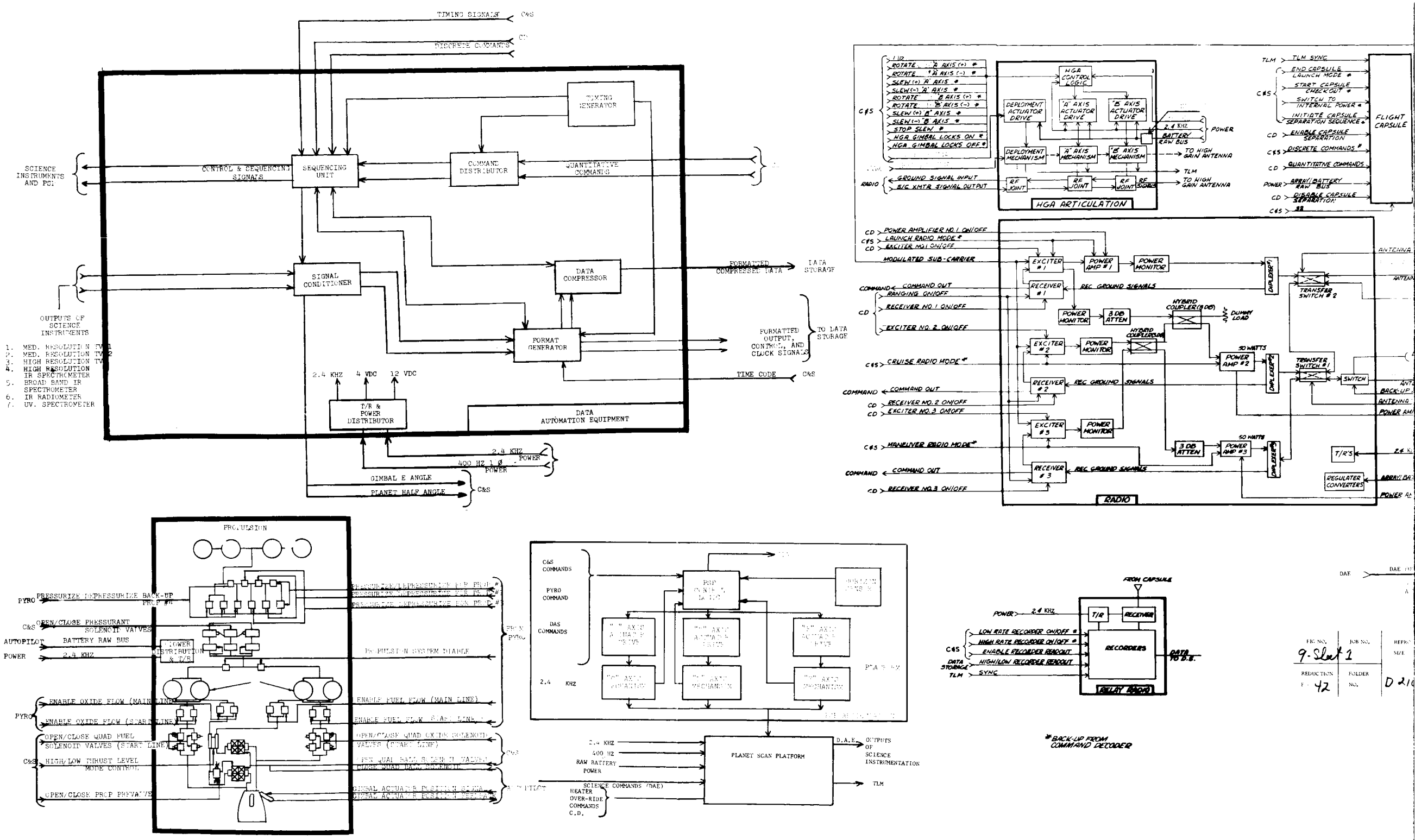

Figure 9. System Functional Diagram
(Sheet 1 of 2)

FOLDOUT FRAME 1

FOLDOUT FRAME 2

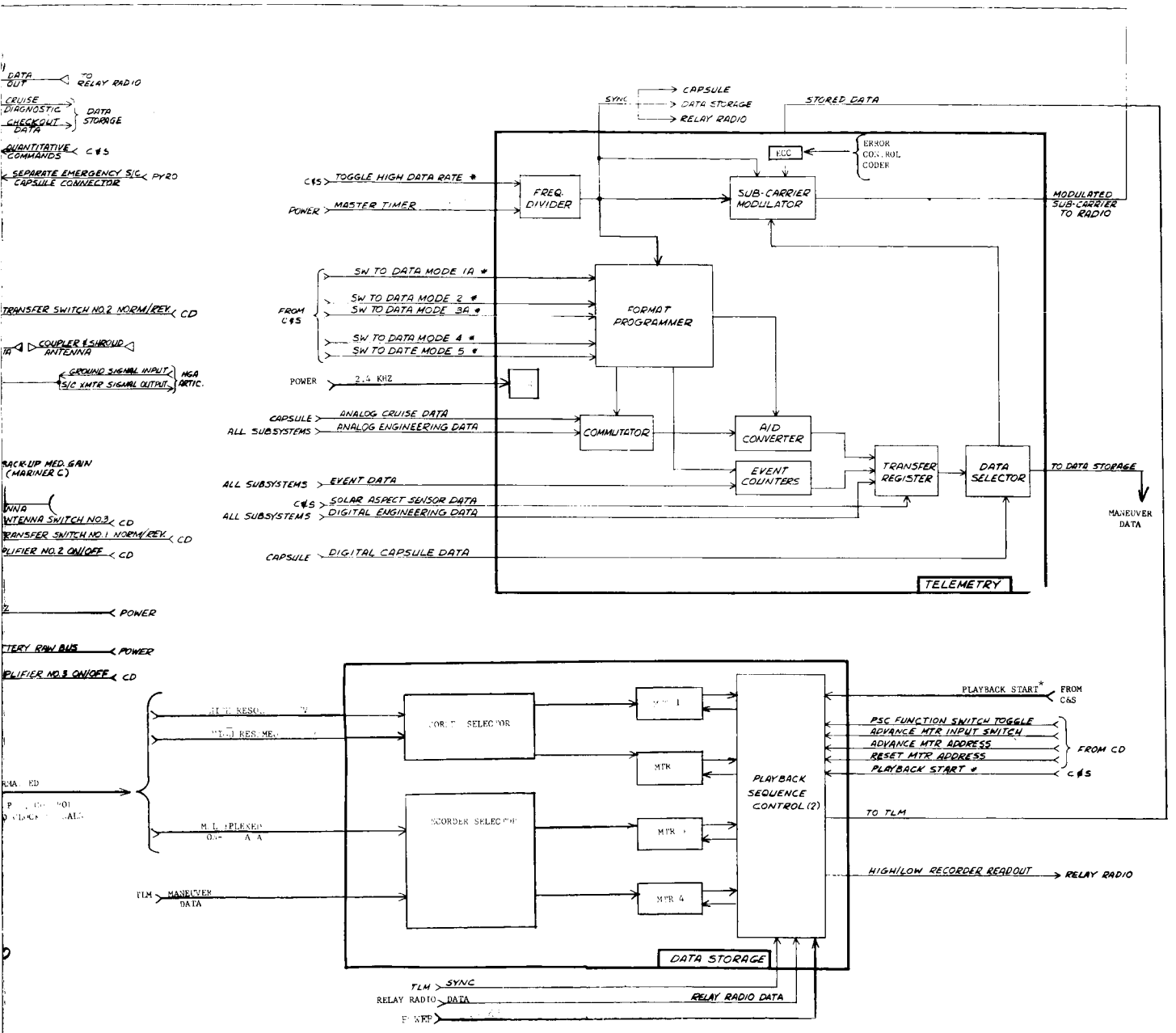

FOLDOUT FRAME 3

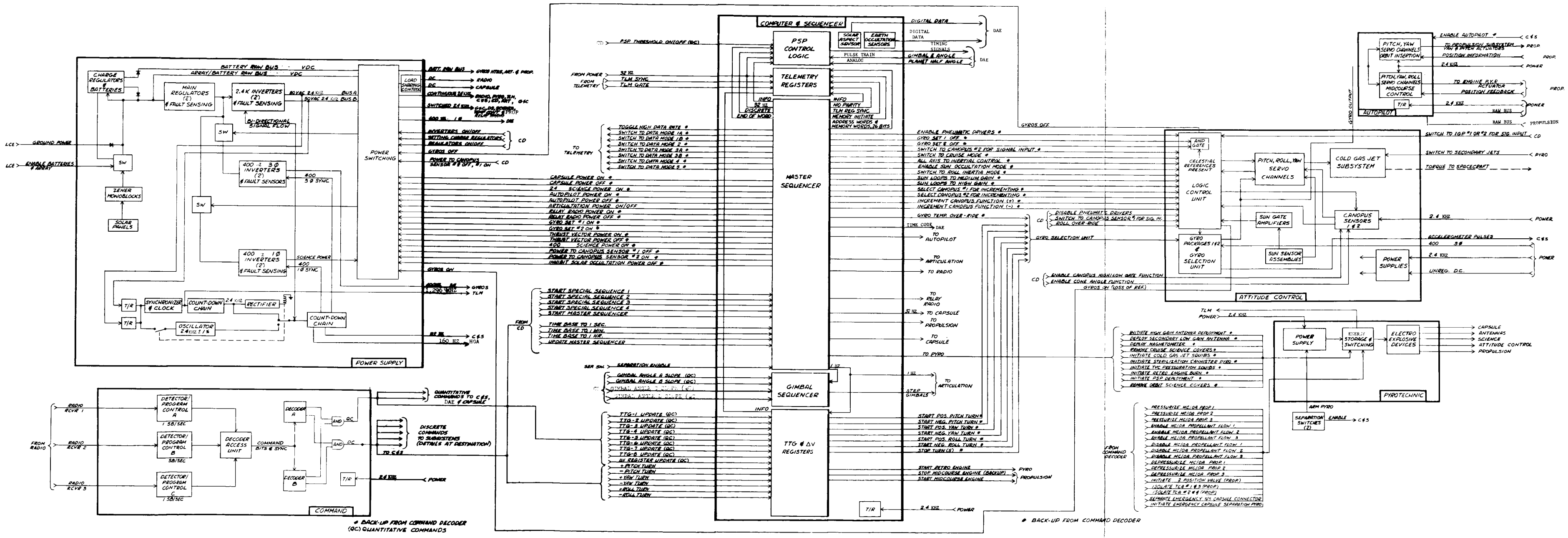

FOLDOUT FRAME 1

FOLDOUT FRAME 2

FOLDOUT FRAME 3

Figure 9. System Functional Diagram (Sheet 2 of 2)

Critical spacecraft functions are provided with a back-up control source. Functions which are controlled by signals originating in the computer and sequencer are generally capable of being commanded by ground through the Command Subsystem. Additionally, intra-subsystem switching of critical functions have a ground command over-ride. By this approach, the complete mission could be completed without ground control, assuming that a perfect trajectory were obtained at separation from the launch vehicle, but ground control based on analysis of diagnostic telemetry is maintained in order to obtain the highest assurance of mission success, or to vary the mission profile based on returned data.

In the diagram of Figure 9, primary command source lines are shown. Commands from the computer and sequencer which are backed-up through the command decoder are indicated by asterisks.

3.2. MASS PROPERTIES

A weight summary for the spacecraft is given in Table 2. A detailed weight statement is given in Appendix A including a pictorial representation of structure weight with allocation to basic vehicle structure, propulsion structure, and equipment and instrumentation structure. The mass properties of the planetary vehicle or flight spacecraft are shown as a function of mission phase in Table 3. The case shown is for a 5,000-pound capsule with a cg at station 247 and for 500 pounds remaining with the spacecraft after capsule separation; station 0 is defined as being at the end of the engine nozzle. The propellant usage is for the velocity profile defined in VOY-D-260.

3.3. POWER PROFILE

Details of the power distribution are presented in VOY-D-340; a summary of the type of power distributed is shown in Table 4. A breakdown of the power requirements as a function of mission phase is given in Table 5. Except for periods of high science and tape recorder loads, (Phases 5 and 9) and sun occulations (Phase 10), the profile is similar to that obtained for the 1971 mission (Task B).

Table 2. Voyager Weight Summary (Sheet 1 of 2)

Item	Weight - Pounds	
Structure		620.1
Propulsion		2015.6
Engine Main	409.00	
Fuel System	376.91	
Oxidizer System	376.91	
Pressuration System	570.13	
Supports	246.00	
Telemetry Sensors	36.70	
Equipment and Instrumentation		2287.7
Structure	65.60	
Guidance, Control & Navigation	202.30	
Instrumentation	357.02	
Electric Power	743.87	
Electric Networks	211.56	
Temperature Control System	149.47	
Attitude Control System	141.90	
Science Equipment	416.00	
Residuals		375.6
Propellants	261.7	
Pressurant	53.9	
Attitude Control System Gas	60.0	
Total Inert Space Craft		5299

Table 2. Voyager Weight Summary (Sheet 2 of 2)

	Total Inert Space Craft		5299
Contingency (5%)			265
	Inert Space Craft with contingency		5564
Usable Propellants			9994
Fuel		3846.92	
Oxidizer		6147.08	
	Total Space Craft at Launch		15,558
Capsule			5000
	Total Planetary Vehicle		20,558
Adapter			126.0
	Total Planetary Vehicle at Launch		20,684

Table 3. Spacecraft Mass Properties

Flight Sequence Description	Case No.	Weight	Center of Mass			Izx	Izy	Ixz	Ioz	Iox	Ioy
			Z(1)	X	Y						
Launch Cond (On Pad)	1	20684	139.0	0.12	0.89	-45.3	-173.4	135.4	12727	17685	17634
Transit Ant Deployed	2	20558	139.3	0.19	0.55	-29.8	-255.5	48.3	12907	17882	17423
After Mid-course Correction	3	19634	140.1	0.20	0.58	-30.5	-257.4	48.3	12566	17674	17142
After Retro Burn (Orbiting)	4	12651	149.9	0.31	0.89	-38.8	-281.5	-48.1	9984	15804	14724
After Capsule Separation	5	8151	113.5	0.48	1.39	-8.1	-192.8	47.6	5670	5099	4020
PSP Deployed	6	8151	114.9	-0.19	4.64	-64.1	75.4	-242.3	7127	6465	4049
After Orbit Adjust	7	6064	112.7	-0.25	6.08	-64.9	93.2	-241.8	6428	6153	3592

(1) Center of Gravity in Inches From Reference 0

(2) Inertias in Slug-ft^2

Table 4. Characteristics of Spacecraft Power

Voltage	Frequency	Regulation	Max. Peak Power, Watts	Max. Avg. Power, Watts	Users	Notes
32-50 volts	dc	---	3000	9	Misc. low duty cycle loads	
32-62 volts	dc	---	750	500	Radio, Capsule, Heaters	Capsule receives 200 W Maximum
50 volts rms	2.4 kc, 1Ø square wave	± 2 percent	600	400	All other Spacecraft loads	
26 volts rms	400 cps, 3Ø stepped square wave	± 5 percent	45	30	Gyros	
26 volts rms	400 cps, 3Ø stepped square wave	± 5 percent	45	30	Gyros	
28 volts rms	400 cps, 1Ø square wave	± 5 percent	30	20	Science, PSP	

Table 5. Power Profile

Mission Phase	(1) Launch to Acquisition	(2) Cruise	(3) Midcourse Maneuver (Typical)	(4) Mars Orbit Insertion (Typical)	Orbit With Capsule: (5) Full Science (41 Min.)	(6) Other Times	(7) Orbit Trim	(8) Capsule Entry & Landing	Orbit Without Capsule: (9) Full Science (41 Min.)	(10) Other Times 5 Hr. 1 Min.	(11) Eclipse (84 min.)	(12) Orbit Trim
RADIO	30.0	30.0	30.0	30.0	30.0	30.0	30.0	30.0	30.0	30.0	30.0	30.0
TELEMETRY	15.0	15.0	15.0	15.0	15.0	15.0	15.0	15.0	15.0	15.0	15.0	15.0
COMMAND	20.2	20.2	20.2	20.2	20.2	20.2	20.2	20.2	20.2	20.2	20.2	20.2
DATA STORAGE			11.0	11.0	37.0	12.0	11.0	11.0	37.0	12.0	11.0	11.0
GUIDANCE + CONTROL	37.3	26.9	39.5	45.7	26.9	26.9	39.5	26.9	32.1	32.1	32.1	39.5
ARTICULATION		5.3	5.3	5.3	5.3	5.3	5.3	5.3	5.3	5.3	5.3	5.3
PYRO CONTROL	1.5	1.5	1.5	1.5	1.5	1.5	1.5	1.5	1.5	1.5	1.5	1.5
COMP. + SEQUENCER	60.0	60.0	60.0	60.0	60.0	60.0	60.0	60.0	60.0	60.0	60.0	60.0
SCIENCE					121.0	4.0			121.0	4.0		
DATA ACQUISITION					50.0	20.0			50.0	20.0	20.0	
PSP HORIZON SENSOR					9.0	9.0			9.0	9.0	9.0	
CLOCK AND SYNCH	8.8	8.8	8.8	8.8	8.8	8.8	8.8	8.8	8.8	8.8	8.8	8.8
ENVIRON. CONTROL											9.0	
RADIO RELAY								50.0				
LOAD SUBTOTAL	172.8	167.7	191.3	197.5	384.7	212.7	191.3	228.7	389.9	217.9	221.9	191.3
HARNESS LOSS	1.7	1.7	1.9	2.0	3.9	2.1	1.9	2.3	3.9	2.2	2.2	1.9
TOTAL INVERTER OUTPUT	174.5	169.4	193.2	199.5	388.6	214.8	193.2	231.0	393.8	220.1	224.1	193.2
THERMAL LOSS	31.6	31.3	32.6	33.0	43.5	33.8	32.6	34.7	43.8	34.1	34.3	32.6
TOTAL 2400 CPS INVERTER INPUT	206.1	200.7	225.8	232.5	432.1	248.7	225.8	265.7	437.6	254.2	258.5	225.8
GYROS	21.0		10.5	21.0			10.5		10.5	10.5	10.5	10.5
LOAD SUBTOTAL	21.0		10.5	21.0			10.5		10.5	10.5	10.5	10.5
HARNESS LOSS	0.2		0.1	0.2			0.1		0.1	0.1	0.1	0.1
TOTAL INVERTER OUTPUT	21.2		10.6	21.2			10.6		10.6	10.6	10.6	10.6
THERMAL LOSS	15.2		7.6	15.2			7.6		7.6	7.6	7.6	7.6
TOTAL 400 CPS 3 PH INVERTER INPUT	36.4		18.2	36.4			18.2		18.2	18.2	18.2	18.2
SCIENCE INSTRU.					10.0				10.0			
PSP GYMBALS					6.0				6.0	6.0	6.0	
LOAD SUBTOTAL					16.0				16.0	6.0	6.0	
HARNESS LOSS					0.2				0.2	0.1	0.1	
TOTAL INVERTER OUTPUT					16.2				16.2	6.1	6.1	
THERMAL LOSS					4.0				4.0	2.8	2.8	
TOTAL 400 CPS 1 PH INVERTER INPUT					20.2				20.2	8.8	8.8	
INVERTER INPUT DIODE LOSS	0.6		0.3	0.6	0.3		0.3		0.6	0.4	0.4	0.3
MAIN REGULATOR OUTPUT	243.0	200.7	244.3	269.4	452.6	248.7	244.3	265.7	476.6	281.6	285.9	244.3
THERMAL LOSS	40.0	37.6	40.0	41.4	51.6	40.3	40.0	41.2	53.0	42.1	42.4	40.0
MAIN REGULATOR INPUT	283.0	238.3	284.4	310.8	504.2	289.0	284.4	307.0	529.5	328.8	328.3	284.4
CAPSULE	200.0	200.0	200.0	200.0	200.0	200.0						
RADIO	75.0	147.0	147.0	147.0	147.0	147.0	147.0	147.0	147.0	147.0	147.0	147.0
GYRO HEATERS	42.0		21.0	42.0			21.0		21.0	21.0	21.0	21.0
PSP HEATERS		5.0	5.0	5.0			5.0	5.0				5.0
UNREGULATED DC LOAD SUBTOTAL	317.0	352.0	373.0	394.0	347.0	347.0	173.0	152.0	168.0	168.0	168.0	173.0
HARNESS LOSS	3.2	3.6	3.8	4.0	3.5	3.5	1.7	1.5	1.7	1.7	1.7	1.7
TOTAL UNREGULATED DC LOAD	320.2	355.6	376.8	398.0	350.5	350.5	174.7	153.5	169.7	169.7	169.7	174.7
UNREGULATED BUS POWER	603.2	593.9	661.1	708.8	854.7	639.5	459.1	460.5	699.2	493.5	498.0	459.1
FAILURE DETECTORS	8.8	8.8	8.8	8.8	8.8	8.8	8.8	8.8	8.8	8.8	8.8	8.8
THRUST VECT CONTR (PEAK)			(701)	(701)			(701)					(701)
SOLENOID VALVES (PEAK)			(448)	(448)			(448)					(448)
ARTICULATION (PEAK)			(112)	(112)			(112)					(112)
DIRECT BATTERY LOAD SUBTOTAL	8.8	8.8	8.8	8.8	8.8	8.8	8.8	8.8	8.8	8.8	8.8	8.8
HARNESS LOSS	0.1	0.1	0.1	0.1	0.1	0.1	0.1	0.1	0.1	0.1	0.1	0.1
TOTAL DIRECT BATTERY LOAD	8.9	8.9	8.9	8.9	8.9	8.9	8.9	8.9	8.9	8.9	8.9	8.9
BATTERY BUS POWER	615.1	8.9	673.0	720.7	8.9	8.9	471.0	8.9	8.9	8.9	509.9	471.0
BATTERY DIODE LOSS	6.2	0.1	6.8	7.3	2.7	0.1	4.8	0.1	0.1	0.1	5.2	4.8
BATTERY POWER OUTPUT	621.3		679.8	728.0	265.2		475.7				515.0	475.7
BATTERY ENERGY OUTPUT (W-HR)				1541.0	181.0						721.0	
BATTERY THERMAL LOSS	127.9	49.6	140.0	149.9	54.6	117.0	97.9		43.7	233.0	106.0	97.9
BATTERY ENERGY INPUT (W-HR)						770.0				1169.0		
BATTERY POWER INPUT		49.6				117.0		49.6	43.7	233.0		
CHARGER OUTPUT		58.6			9.0	126.0		58.6	52.7	242.0		
BATTERY CHARGER THERMAL LOSS	3.0	8.1	3.0	3.0	3.8	14.0	3.0	8.1	7.6	24.0	3.0	3.0
CHARGER INPUT	3.0	66.7	3.0	3.0	12.8	139.9	3.0	66.7	60.3	266.0	3.0	3.0
ARRAY BUS POWER		660.5			612.3	779.4		527.2	759.5	759.5		
HARNESS LOSS		6.7			6.2	7.9		5.3	7.7	7.7		
ARRAY POWER REQUIREMENT		667.2			618.5	787.3		532.5	767.1	767.2		

3.4. MISSION SUCCESS

Figure 10 shows the increasing Mission Expected Worth (see VOY-D-275) that is obtained with the application of redundancy in an optimum manner within the various subsystem areas. Details of the redundancy applied are included in the subsystem sections of this report, and redundancy is applied first in areas where the increase in Mission Expected Worth is greatest. In the proposed updated spacecraft design, in excess of 300 pounds of weight is accounted for by redundant designs.

Table 6 portrays the effect of the application of the recommended redundancy on the probability of successfully completing each mission phase. The improvement, comparing the redundant configuration with that of the single-string, becomes apparent with each succeeding mission phase.

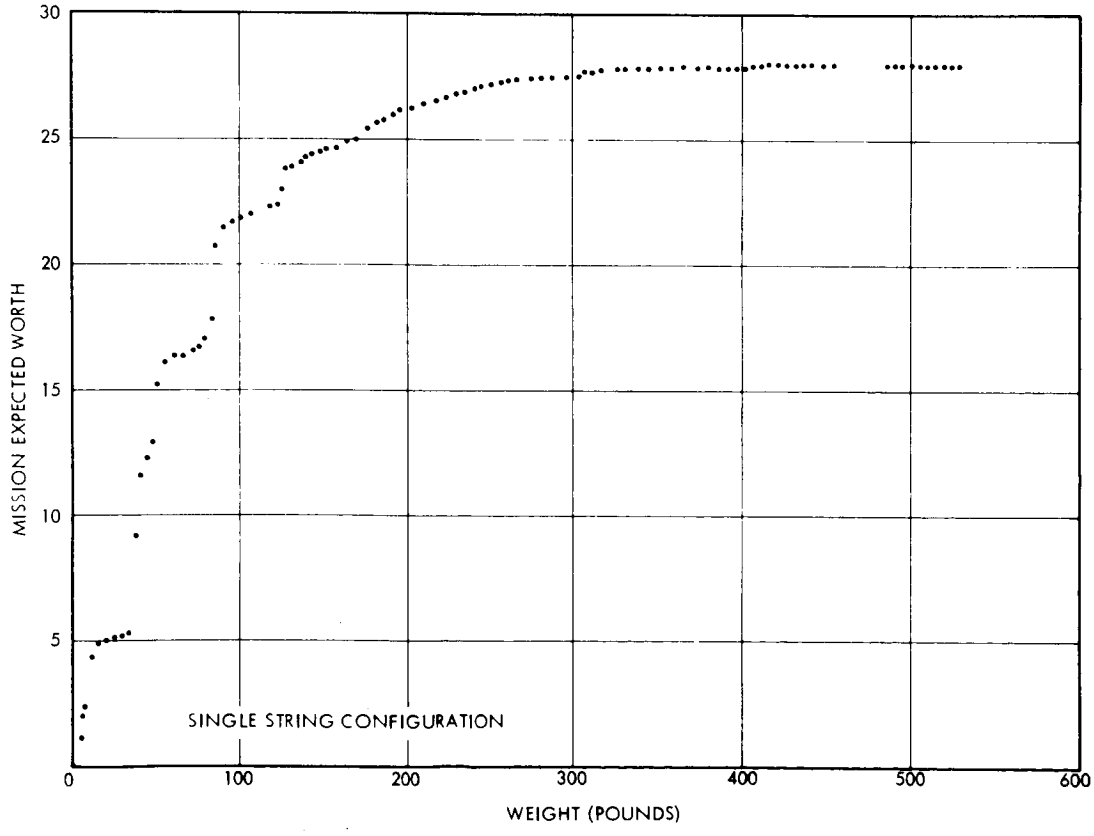

Figure 10. Optimum Redundancy Configurations

Table 6. Mission Phase Probabilities

No.	Mission Phase Name	Probability of Completion: Single-string Configuration	Probability of Completion: Redundant Configuration
1	Launch	0.9190	0.9190
2	Injection	0.8547	0.8547
3	Acquisition	0.8533	0.8547
4	Interplanetary Cruise	0.8525	0.8545
5	Arrival Date Sep. Maneuver	0.8441	0 8507
6	Interplanetary Cruise	0.8352	0.8491
7	Interplanetary Traj. Cor. Mvr.	0.7992	0 8449
8	Interplanetary Cruise	0.7474	0.8340
9	Interplanetary Traj. Cor. Mvr.	0.5861	0.8225
10	Interplanetary Cruise	0.5861	0.8225
11	P/V Mars Orbit Insert	0.5596	0.7987
12	Presep. Orbit Operations	0.5589	0.7984
13	P/V Orbit Trim Mvr.	0.5529	0.7947
14	Presep. Orbit Operations	0.5522	0.7945
15	S/C - Capsule Separation	0.5497	0.7943
16	Capsule Support	0.5495	0.7942
18	Post Landed Orbital Ops.	0.5441	0.7926
19	S/C Orbit Trim Mvr.	0.5338	0.7876
20	Post Landed Orbital Ops.	0.4591	0.7273

4. TELECOMMUNICATION SUBSYSTEM

4.1. SUBSYSTEM DESCRIPTION

The Telecommunication Subsystem (Figure 11) is composed of five subsystems - radio, command, data automation, data storage, and telemetry. The Telemetry Subsystem multiplexes and encodes the engineering data and combines this data with real time capsule data (prior to capsule separation) for transmission at 150 bps; during maneuvers, selected engineering data is processed and transmitted at 7.5 bps. The Data Automation Subsystem controls the operation of the science instruments, and conditions, encodes and formats the data for recording in the Data Storage Subsystem. The recorders, including the one supplied

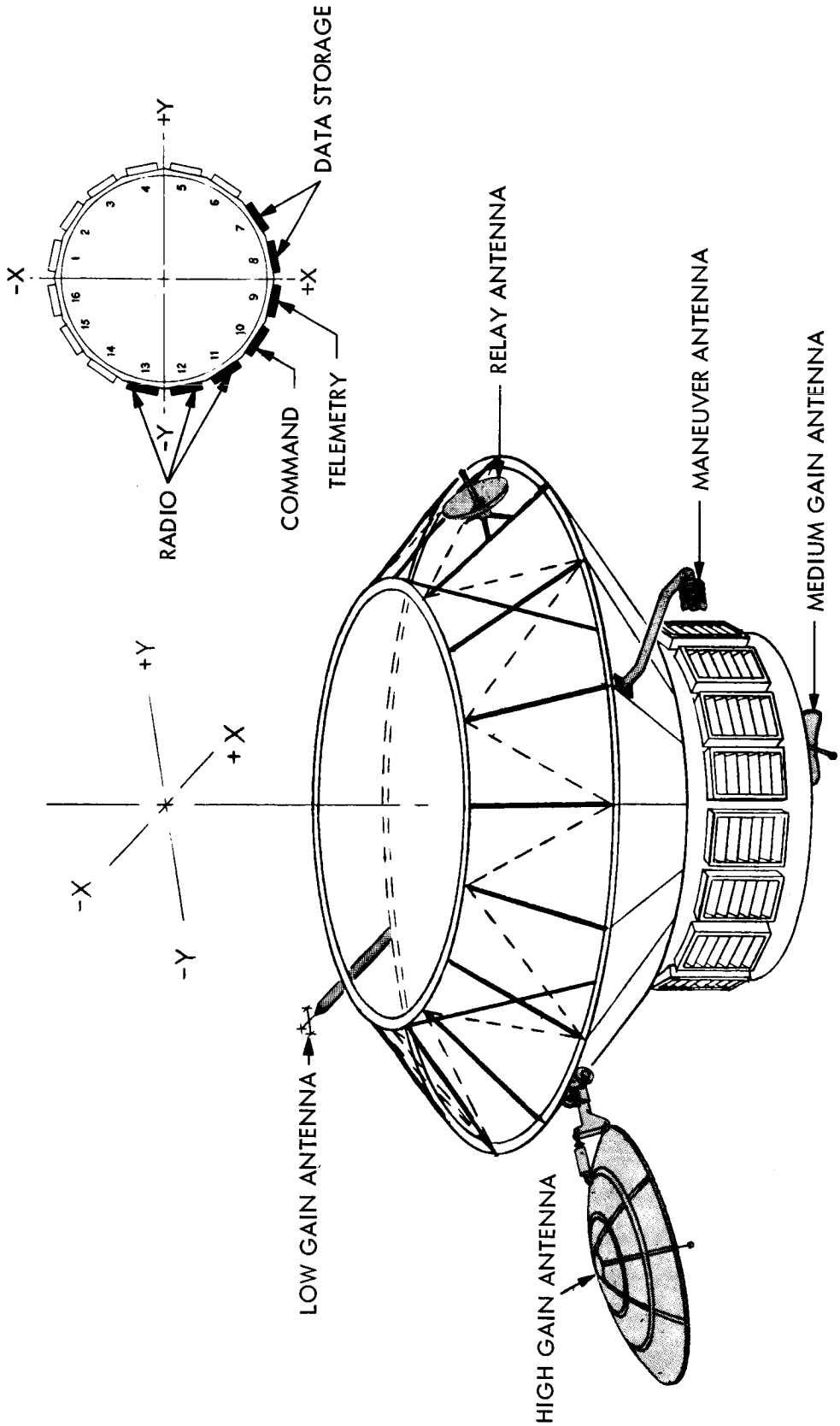

Figure 11. Telecommunication Subsystem

as part of spacecraft mounted capsule equipment, are read out in sequence. This high rate stored data is block coded and is frequency multiplexed with the real time data subcarrier; the composite subcarrier modulates the S-band carrier in the transponder of the Radio Subsystem. A 50-watt power amplifier feeding a steerable 9.5 foot diameter high gain antenna supports data rates of approximately 40, 20, or 10 kilobits per second. A back-up fixed medium gain antenna can support a data rate of 1265 bps for about two months after encounter (March 1, 1974). Low gain antennas are provided for maneuver telemetry and for command reception. The commands are detected, decoded, and distributed to the addressed subsystems by the Command Subsystem. A more detailed description of telecommunications is given in VOY-D-310. The major changes in the subsystem are noted in the remainder of this section.

4.2. DATA TRANSMISSIONS

The data transmission capability of the updated telecommunication system is significantly greater (7 db) than that of the previous design. Major contributors to this improvement are increased antenna size and data coding.

A 9.5-foot diameter dish has replaced the former 7.5-foot dish. Stowage of the larger rigid antenna was made possible by the high-truss spacecraft design, and, although, the larger antenna produces a narrower beam width, pointing errors derived from various sources have been reduced to provide the full advantage of the higher gain. In the period between completion of the Task B Study and the start of the Task D Study, synchronization of bit and words and the obtainment of near theoretical coding gain was adequately demonstrated by test for error control coding. Coding was, therefore, included in the updated system giving nearly double the channel efficiency. An additional gain in channel efficiency is achieved by providing the capability to change the ratios of power in the carrier and data sidebands to match the different requirements for each data transmission mode.

The resulting worst-case data transmission capability of the updated system is shown in Figure 12. Implemented data rates of approximately 40, 20, and 10 kilobits per second can be maintained for 7, 58, and 115 days, respectively, for an encounter date of March 1, 1974.

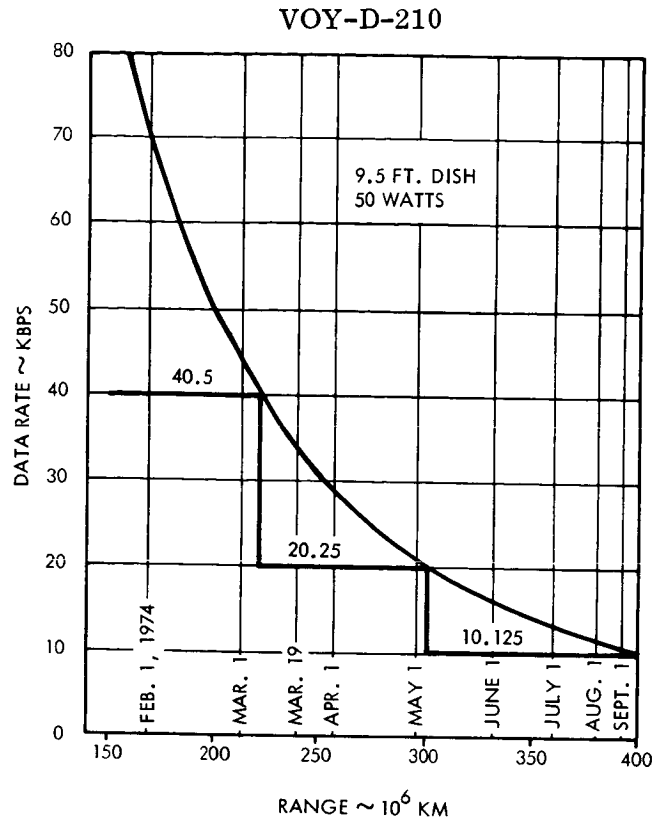

Figure 12. Data Rate - Range Characteristics

For the March 1 arrival date and a 180 day orbital mission, the total data accumulated is over 2×10^{11} bits. The advantage of earlier encounters, from the standpoint of data accumulation, is clearly shown on the graph. For instance, an encounter date of February 1, 1974, would allow transmission at 40 kilobits per second for an extra month, yielding an additional 10^{11} bits of accumulated data or an increase of approximately 50 percent in data accumulation.

Reduced DSIF receiving capability predictions and increased planetary encounter range for the 1973 mission caused the Task B approach to low-rate transmission during orbit insertion and orbit-trim maneuvers to be marginal. The forward-looking low-gain antenna has, therefore, been replaced by a fan-beam antenna (180 degree by 30 degree) with higher gain and capable of transmitting low-rate, 7.5 bps, data to nearly maximum Earth-Mars range.

4.3. DATA STORAGE

Changes in the Data Storage Subsystem have resulted from redefinition of the science payload and the increased data capacity required to maintain the higher data transmission rates throughout an orbit period. Increased storage capacity requirements and higher input data rates have led to the selection of high-density recording. Both digital and analog techniques were considered, and although digital recorders have been selected for the updated design, analog recorders show considerable promise for the high-rate TV data.

Four tape recorders are used to accommodate the new baseline science requirements. Two recorders, each having a storage capacity of 1.2×10^9 bits and an input data rate capability of 390 kilobits per second, are used to store high-rate TV data. Each recorder has the capability of accepting data from either the high-resolution camera or the two medium-resolution cameras. In the nominal mode of operation, data from the high-resolution camera are stored in one recorder while data from the two medium-resolution cameras are interleaved on a frame by frame basis and stored in the other. Two lower-rate recorders, each having a capacity of 3.6×10^7 bits with two read-in rates, 3,900 and 150 bits per second, are included for storage of low-rate multiplexed science data or spacecraft maneuver data.

5. GUIDANCE AND CONTROL SUBSYSTEM

The spatial attitude of the planetary vehicle or spacecraft is maintained throughout the mission by the Guidance and Control Subsystem (Figure 13). To perform this function, three subsystem are required: Attitude Control Subsystem consisting of sensors and gyros, for detecting attitude errors or implementing a commanded spacecraft attitude turn, and the necessary electronics; Reaction Control Subsystem consisting of gas storage, nozzles and solenoids and regulators for controlling the flow of gas; and Autopilot Subsystem which senses a change in attitude during propulsion maneuvers, processes the error, and sends a signal to the propulsion engine actuator to gimbal the engine and remove the attitude error.

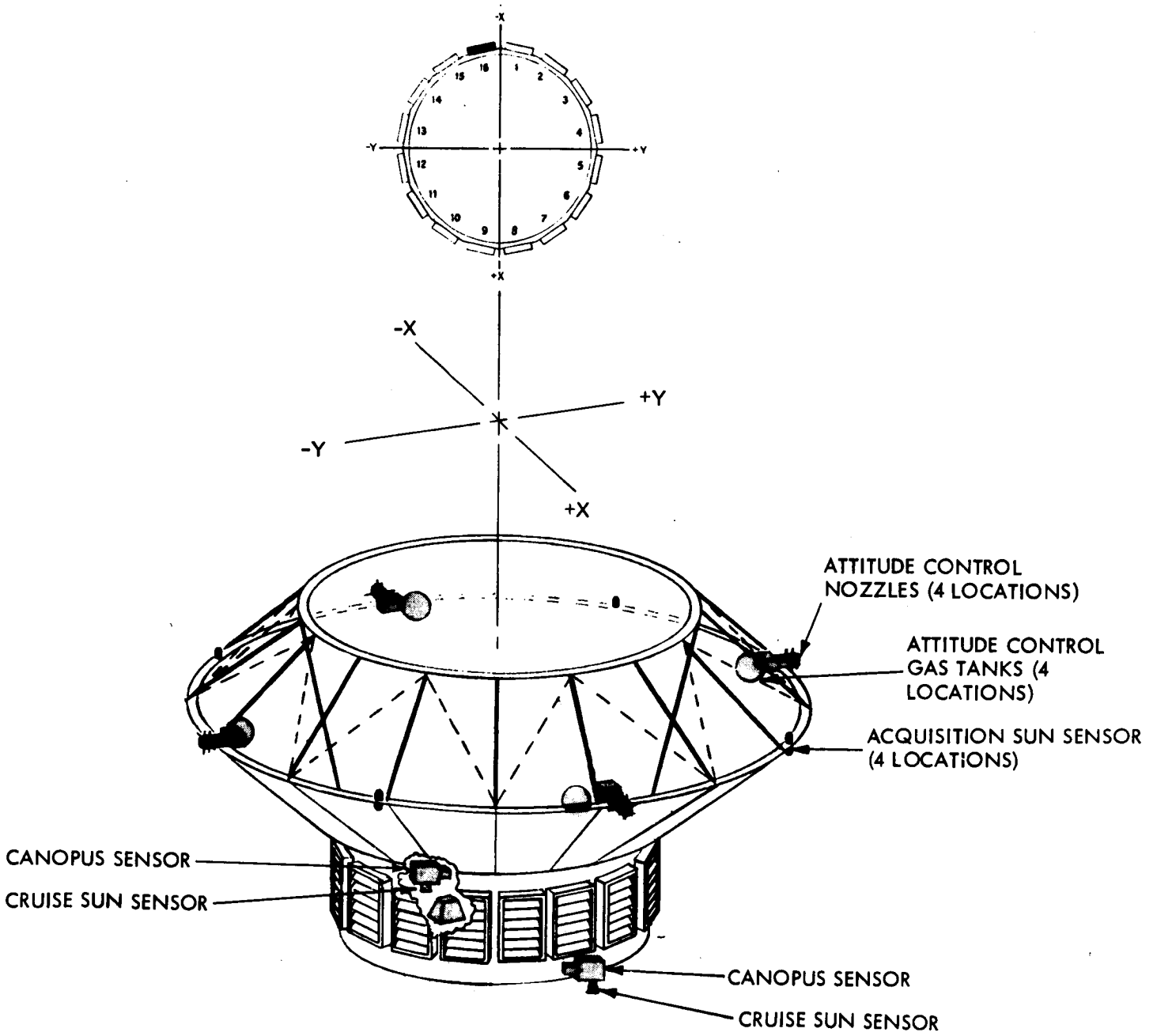

Figure 13. Guidance and Control Subsystems

Except for detailed changes in the electronics of the Attitude Control and Autopilot Subsystems the Guidance and Control Subsystem is the same as that given in the Task B Study Report. However, a large number of analyses were made to either define the design requirements or to investigate alternate ways of implementing the required subsystem functions. The selection of a liquid propellant engine, LEMDE, for the Voyager Spacecraft presented a new group of problems and unknowns. By analysis, it has been shown that control of the engine can be maintained, transient or steady state, by the autopilot even with the uncontrolled movement of the large mass of propellants carried by the spacecraft. Also, an understanding, though incomplete at this time, of the motion of the fluid in a zero gravity field environment was obtained.

A more detailed description of the analyses made and trade-offs investigated is given in VOY-D-320. Performance characteristics of the Guidance and Control Subsystem are as noted in Table 7. In determining the maneuver accuracies, a yaw turn of 165 degrees and a pitch turn of 10 degrees was assumed.

Table 7. Guidance and Control Subsystem Performance Characteristics

Attitude Control Dead-Band	8 mrad
Maneuver Accuracy (3σ)	
Trajectory Corrections	17 mrad
Orbit Insertion	26.5 mrad
Orbit Trims	34.5 mrad
Autopilot Accuracy (3σ)	
Trajectory Corrections	0.076 mps
Orbit Insertion	0.757 mps
Orbit Trims	0.140 mps

6. POWER SUBSYSTEM

The physical location of the Power Subsystem is shown in Figure 14. A complete description of the subsystem is given in VOY-D-340. Power for the spacecraft and capsule are provided by a solar array during periods of full or partial solar illumination and by batteries during periods of solar array disorientation or peak power periods in excess of array capability.

The solar array consists of 16 fixed panels and 9 deployable panels which provide a projected solar array area of 270.3 square feet capable of supplying 838 watts at Mars aphelion. The panels form an annular ring about the spacecraft and contain strings of 2 x 2 centimeter, N/P, silicon solar cells in a series-parallel arrangement. Each string is diode isolated with a zener diode monoblock which limits upper array voltage to 65 volts.

Three batteries provide a total capacity of 3270 watt-hours at 38.5 volts Two of the batteries are of the nickel-cadmium type rated at 20 ampere-hours. This combination has been selected since the mission needs are characterized by a few but deep battery discharges up to the time of capsule separation and thereafter by many but shallow discharges during Martian solar occultations. The high-cycle-life, nickel-cadmium batteries are sized for solar occultations and the silver-zinc battery is sized to make up the energy deficit not available from the nickel-cadium batteries for deep discharges required during maneuvers. Each battery is charged through a separate regulator with charge limit adjustable by command. Power is distributed to the users as unregulated dc or in several forms of regulated ac. The characteristics of the available power are shown in Table 4. All ac busses are supplied from redundant sources with automatic switchover capability in the event of element failure.

The central clock and synchronizer for the spacecraft is contained in the Power Subsystem and provides a 1.296 MHz signal to the telemetry subsystem, 2.4 kHz and 400 Hz signals to the power inverters, 160 Hz for antenna articulation, and a 32 Hz signal to the C&S Subsystem. Frequency accuracy of one part in a million provides the accurate time base required. An

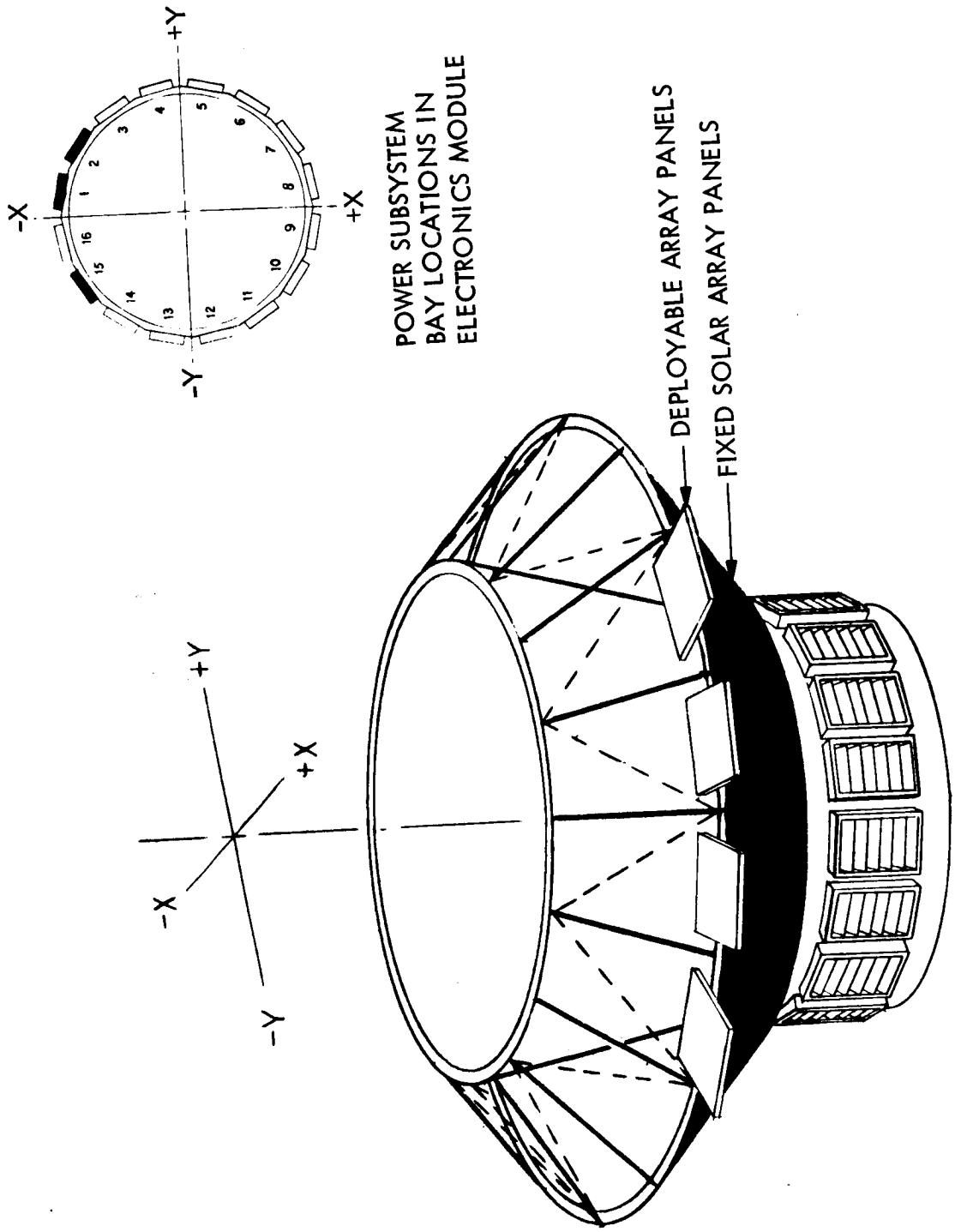

Figure 14. Power Subsystem

oscillator with ± 1 percent frequency accuracy is provided as backup and can supply all signals with the exception of 1.296 MHz. Further backup is available from the free-run capability of the 2.4 kHz inverters.

7. COMPUTER AND SEQUENCER SUBSYSTEM

The Computer and Sequencer is a cycled, special purpose, digital computer, which generates and distributes the onboard commands necessary for the Voyager Spacecraft to perform its mission automatically. In the C&S, critical functions are commanded by special high reliability Time-To-Go Registers. Control of PSP and antenna pointing is provided by a Gimbal Sequencer which provides stepping signals for incremental changes in pointing angle. The Master Sequencer handles all quantitative and all discrete commands except those noted above. The mission sequence of up to 512 command words (18 bits per word) stored in the Master Sequencer and all other stored commands are alterable by ground command. The state of the C&S is preserved during temporary interruption of power with only spacecraft time being interrupted for the duration of the outage. The Computer and Sequence electronics are located in bay 14 (Electronic Module).

The design of the Task B Computer and Sequencer was reviewed in light of updated functional requirements and technological advances. It was determined that the updated functional requirements could be met using the Task B functional design. Consideration was given to incorporating optoelectronic coupling devices and large scale integrated circuits into the design. Although potentially useful, it was determined that the state of development and paucity of reliability data precluded their use with confidence for a 1973 mission.

8. THERMAL CONTROL SUBSYSTEM

The purpose of the Thermal Control Subsystem (Figure 15) is to maintain all components of the spacecraft within required limits for reliable operation throughout the mission life. Active control utilizing thermostatically activated louvers and heaters are incorporated for those portions of the spacecraft such as the electronic bays and external gas lines where

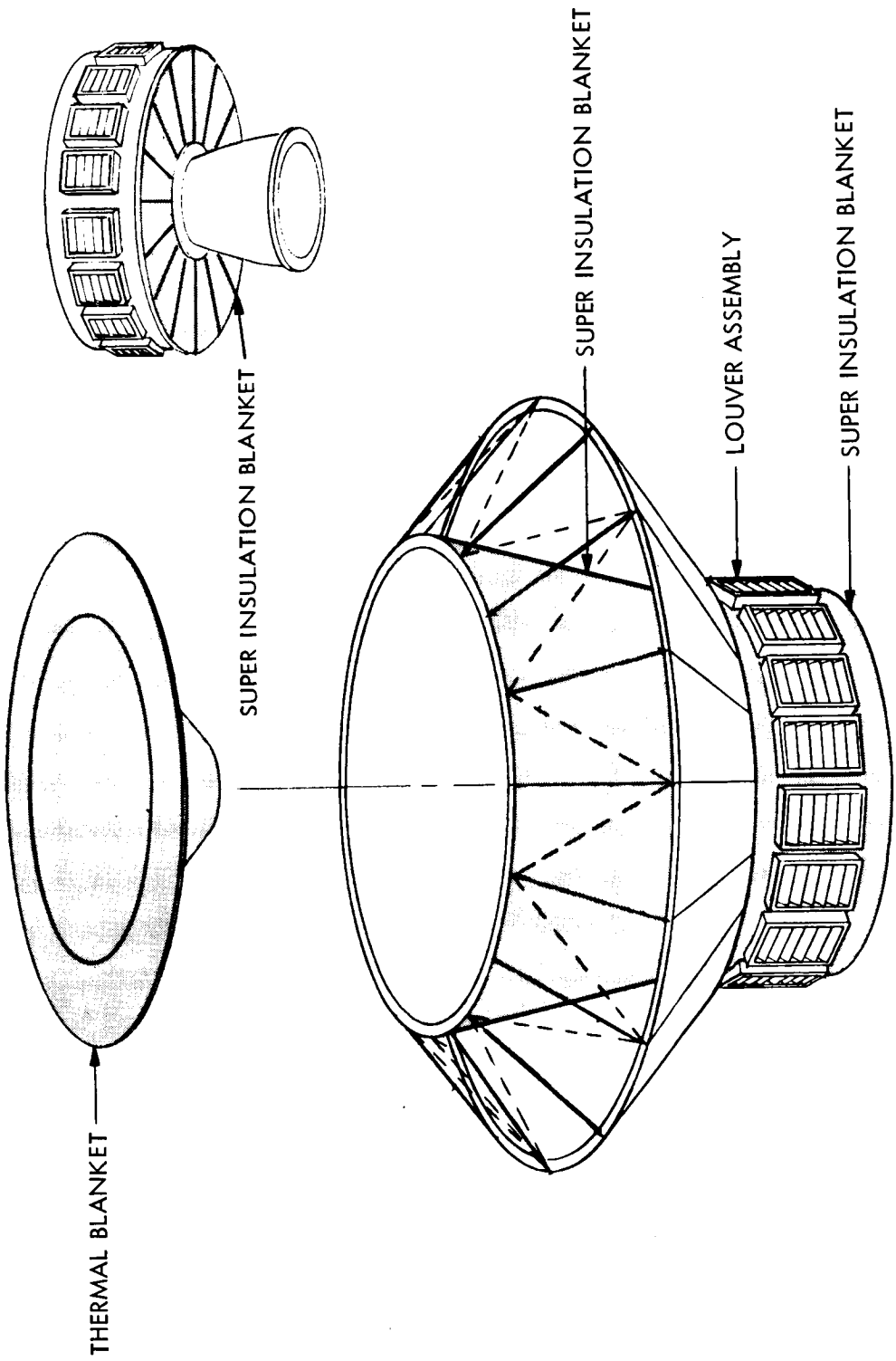

Figure 15. Thermal Control Subsystem

passive control utilizing coatings, multiple layer super insulation blankets, and equipment thermal inertias are not adequate. The equipment in the electronic bays are maintained at 40° to 70°F. by the louver assemblies whose blades open between zero and ninety degrees exposing a 0.825 emissivity backplate and varying the heat radiated by the louver assembly. Except for area covered by the louver assemblies, the spacecraft surface is generally covered by super insulation blankets consisting of layers of aluminized mylar and a 2 mil aluminized mylar cover sheet. Radiative and conductive coupling between the electronic bays and radiative coupling between the bays and propulsion components limit the maximum temperature differential within the controlled spacecraft volume to about 17°F. The temperature rise within electronic bays if the sun-shines directly into a bay during a maneuver or if failure of a shutter assembly occurs is also limited by the integrated design approach.

The PSP presents a different thermal control problem because of the motion of the platform with respect to the sun line. Insulation blankets and heaters provide primary thermal control during cruise and non-operating periods of the science sensors and louvers radiate heat when the sensors are dissipating energy.

9. PROPULSION SUBSYSTEM

9.1. SUBSYSTEM DESCRIPTION

The baseline Propulsion Subsystem (Figure 6) is a bipropellant liquid rocket engine system using the LEMDE thrust chamber assembly. Details of the subsystem are given in VOY-D-370. Helium gas, stored in titanium spheres and regulated by parallel regulators, provides for propellant expulsion. The fuel and the oxidizer, are stored in four equal volume titanium propellant tanks. To provide propellant acquisition for starting, non-rechargeable metal bellows are incorporated within each tank assembly. A separate flow circuit with valving connects the start tanks and thrust chamber assembly. Screens and baffles are incorporated into the tanks to provide propellant motion control during non-operating periods of near zero gravity, and when the system is operating.

The LEMDE is operated at two thrust levels, 1,050 and 9,850 pounds, providing the capability for low minimum impulse bits with acceptable tail-off uncertainties for trajectory and orbit corrections and an acceptable burn period for orbit insertion. A bi-axial gimbal ring and actuator assembly is used to provide ±6 degrees of gimballing for thrust vector control. Provision is also made for isolation of the pressurant storage tanks during launch and periods of long coast. Isolation of the propellant tankage from the downstream components is provided only during launch since quad-redundant valving has been selected for propellant control. Suitable test and fill vent ports for preparing the system for flight are incorporated.

9.2. TRADE-OFFS

In arriving at the baseline configuration, several trade-off studies were conducted. For the pressurization subsystem, the pressurant gas (helium or nitrogen) and type of pressurization (regulated, blowdown, etc.) were investigated. From reliability and weight considerations, a helium gas regulated system was selected.

Tankage studies were conducted to determine the material to be used, and to select a method of mounting into the vehicle structure. Primarily because of a significant weight advantage, 6AL4V titanium was chosen over cryoformed 301 stainless steel. Trunnion mounting for all tanks was selected on the basis of weight and comparative ease of installation. Screens, bellows, and baffles were selected for positive control of fluid motion during all phases of the mission; the investigation of propellant control approaches included diaphragms, bladders, and ullage rockets as well as the selected method.

The need for auxiliary thrusters to meet guidance requirements, simplify autopilot and main engine actuator requirements and reduce leakage, was also investigated. Based on present evaluation, it appears that LEMDE, operating by itself, is a superior system. Therefore, auxiliary thrusters are not included in the baseline design.

In addition to the detailed, in-depth study of the LEMDE system and the associated tradeoff studies, the application of the turbo-pumped Agena system and Transtage thrust chamber assembly was briefly studied. The basic premise in conducting these studies was to consider Agena and Transtage each as a unit replacement for the LEMDE thrust chamber assembly. The main areas of investigation were the weight and performance differences, and configuration advantages. Details of these two systems are presented in VOY-D-370. The LEMDE thrust chamber assembly currently appears to be the only one capable of performing the mission without the use of auxiliary thrusters and without significant design modifications.

10. PLANET SCAN PLATFORM

The function of the PSP (Figure 16) is to protect, environmentally control, and physically support the Mars oriented science sensors.

For the design orbit, the best location for the platform is near the spacecraft y axis with the platform oriented to the spacecraft by a three-axis attitude control servo. Two axes (C&D) are used to erect a perpendicular to the orbit plane with the C axis also providing the deployment function. The perpendicular to the orbit plane changes very slowly with time; accordingly, these axes are controlled open loop by the C&S. The third axis is a closed loop servo using horizon sensors to track the Mars local vertical in the orbit plane. The tracking loop uses a direct drive dc torquer with rate feed back utilizing a dc tachometer rate sensor to smooth the drive. Commanded off-axis pointing is also provided in all three axes. The expected pointing error for either mode is approximately one degree (3σ). Details of the PSP design and operation are given in VOY-D-380.

The instrument packaging concept is illustrated in Figure 17. The packaging approach was developed with the realization that the instruments have not been designed and flexibility rather than extreme detail is important at this time. Provision was made for fixing the orientation of instruments away from the local vertical (as illustrated for the ultraviolet spectrometer) in the event this should be desirable.

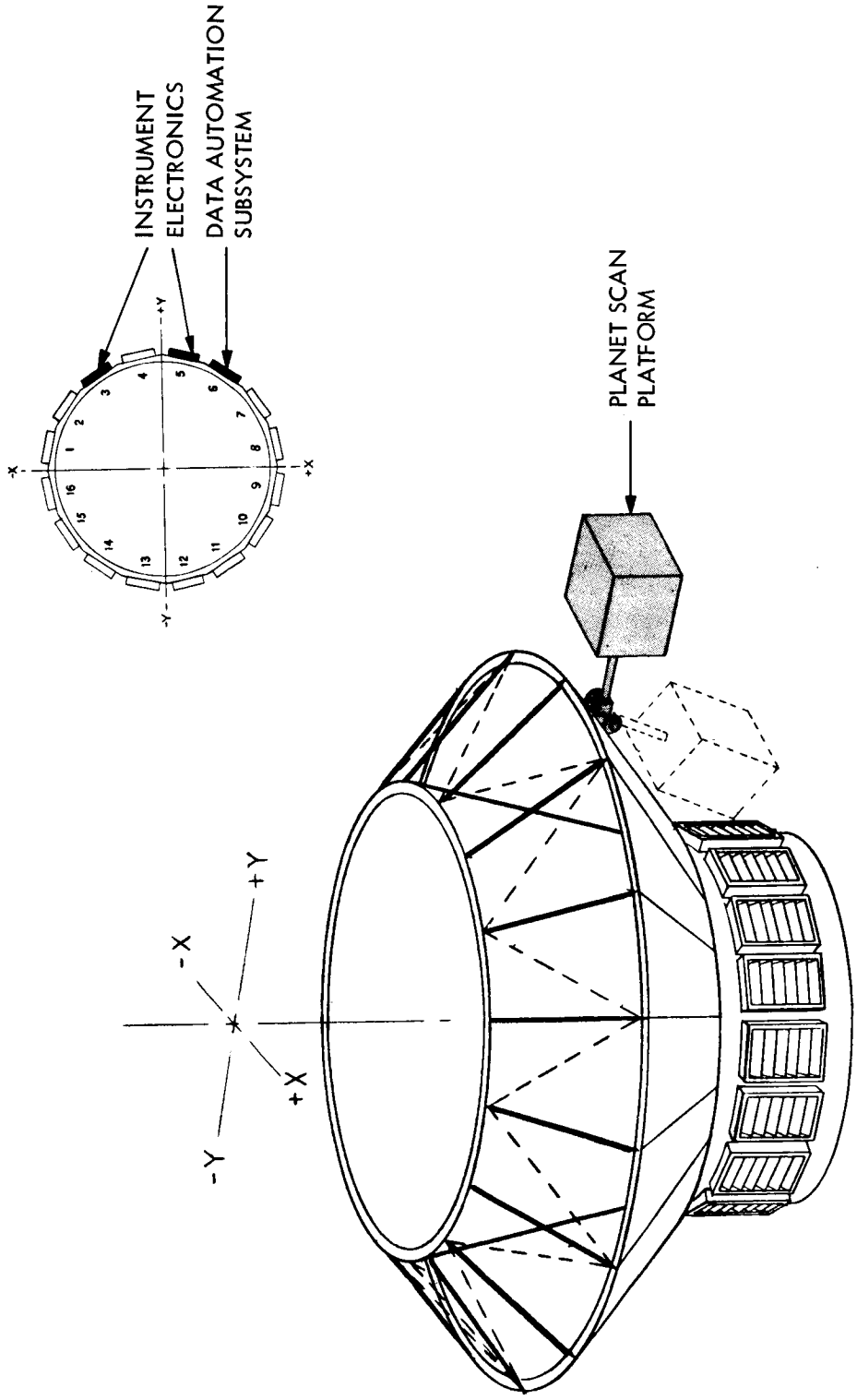

Figure 16. Planet Scan Platform

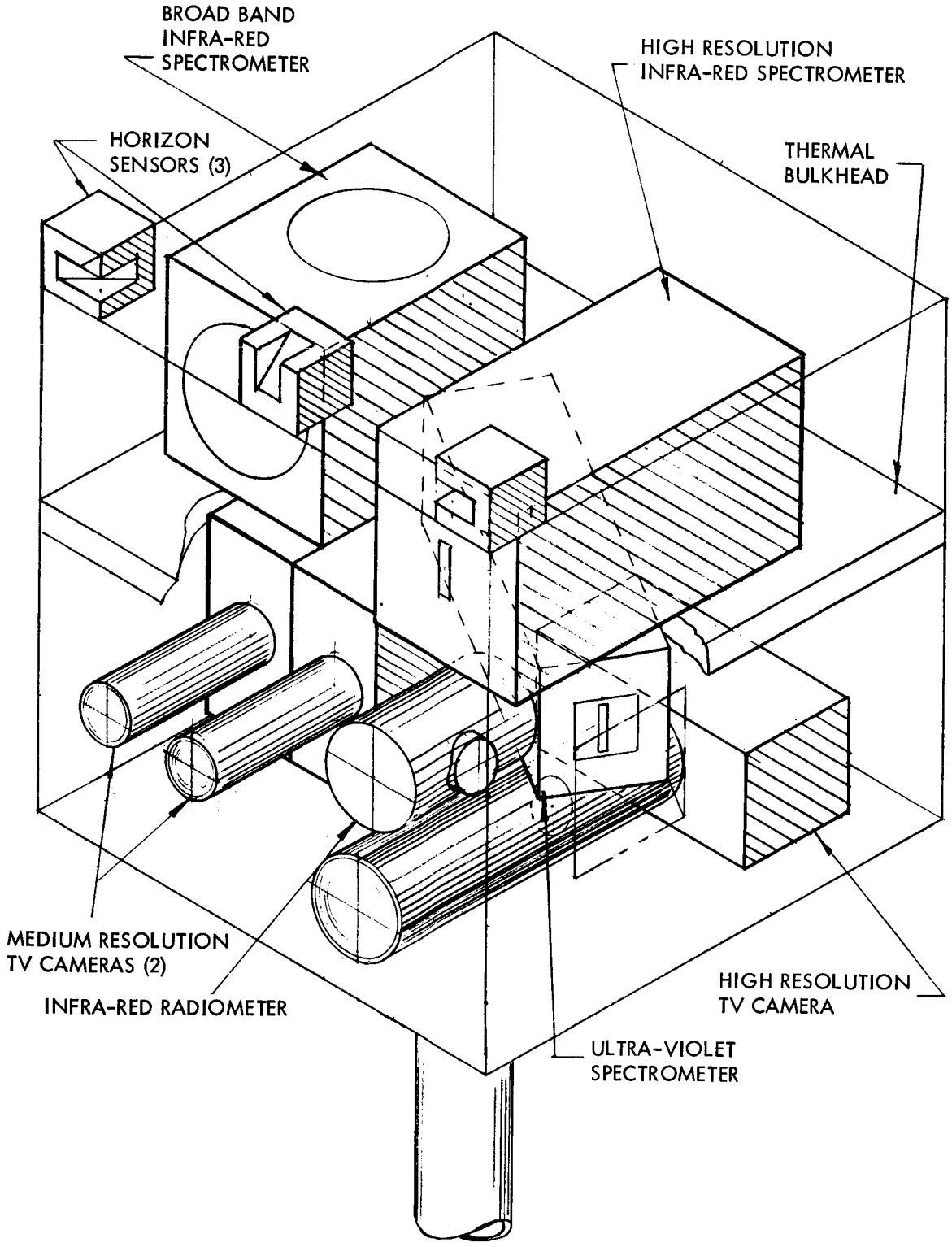

Figure 17. PSP Internal Arrangement

For the purpose of thermal control, an insulating bulkhead is used to separate the PSP into two thermal regions. The first is maintained in the temperature range of 15 to 35°C and houses all instruments except the two infrared spectrometers. The second region is maintained at -43 to -33°C; this second region is located at the top of the package which is a surface of known sun orientation and available for radiative detector cooling. In the preferred design, most of the instrument supporting electronics is located off the PSP in bays 3 and 5 making the power dissipation in the PSP rather low; the long term average dissipation of instruments located on the PSP is approximately 6 watts. The entire platform is insulated to control heat leakage with losses greater than instrument dissipation made up by heaters.

Detector cooling is considered to be a function of the individual science instruments, but the PSP must be configured with appropriate consideration for the cooling requirements of the instruments. Accordingly, the implications of detector cooling were investigated during the study. The conclusion of this study is that realization of detector temperatures below 100°K for extended periods in Mars orbit represents a substantial engineering problem.

11. SPACECRAFT ADAPTABILITY

11.1. GENERAL

For the design trajectories and orbits as defined in VOY-D-260, the maximum planetary vehicle weight which can be launched by the Saturn V launch vehicle within the mission constraints is limited by the 1977 missions to 26,030 pounds; this assumes that the project contingency is allocated to the two planetary vehicles. The propellant tanks have been sized so as to be able to impart a minimum velocity increment of 1.95 km/sec to a 26,030-pound planetary vehicle providing flexibility and growth capability for later Mars missions and other planetary missions.

When the project contingency of 5,000 pounds is subtracted from the launch vehicle capability, the maximum allowable planetary vehicle weight for 1977 is 23,530 pounds. As noted in Table 8 (Column 2), all constraints can not be fulfilled for a 1977 mission if a 7,000-pound

capsule is carried. It is also shown in Table 8 that a 20-day launch period can be provided with the baseline spacecraft weight of 5580 pounds or less if the total minimum velocity increment is decreased from 1.95 km/sec down to 1.835 km/sec or less.

As previously noted, the March arrival dates defined by the design trajectories for the 1973 mission result in long encounter communication distances. With the launch energy required for the 1973 mission, planetary vehicle weights in excess of 23,500 pounds are possible. The curves of Figure 18 indicate how the encounter communication distance can be lowered by utilizing the additional launch capability and propellant tank volume to obtain earlier arrival dates; the earliest arrival date possible is February 1, 1974, for a planetary vehicle with a 6,000-pound capsule. The curves of Figure 18 assumes a 5,500-pound spacecraft burnout weight, the velocities given in VOY-D-260 for the corresponding arrival dates, and a 1,000 x 11,800 kilometer attitude orbit. The two-to-one gain in data rate possible with the February 1 arrival date, as compared to the design trajectory arrival date of March 19, 1974, is not possible unless the capsule landing constraints are relaxed.

Table 8. 1977 Mission Options

Spacecraft Burnout Weight	5564	5594	5580
Capsule Weight	5000	7000	7000
Useable Propellant Weight	9870	11,750	10,824
Total Velocity Increment (km/sec)	1.95	1.95	1.835
Planetary Vehicle Weight	20,560	24,470	23,530
Program Contingency	5000	3120	5000
Launch Period	24	20	20

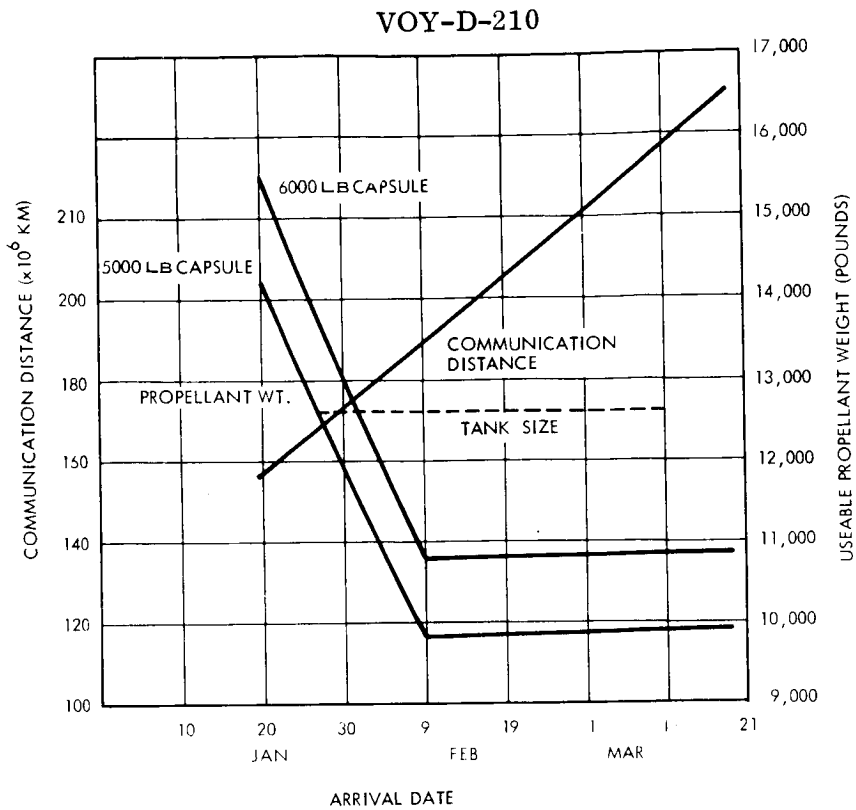

Figure 18. Communication Distance - 1973 Mission

11.2. 1975, 1977, AND 1979 MARS MISSION

In arriving at the spacecraft design for the 1973 Mission, growth and flexibility were also prime considerations. The PSP is positioned to provide good unobstructed viewing. In addition, a second Canopus sensor is included so that by rolling the vehicle 180 degrees, planet viewing which might otherwise be obstructed by the bio-barrier, is possible.

The solar array is presently sized to provide the maximum required power at the maximum sun distance. In later mission years the capsule will carry RTG power generators and the 200 watts will not have to be supplied to the capsule. This power can be used for increased science or other subsystem power loads. If necessary, solar array can also be added to the bottom of the electronic module to obtain an additional 150 to 180 watts. The batteries are sized for an 84 minute sun occultation period compared to a theoretical maximum occulation period of about 94 minutes for the orbit size selected. It is not, therefore, expected that the battery energy requirement will increase beyond the capability provided.

The structure is presently sized to handle a 7,000-pound capsule and 13,000 pounds of propellant. A 7,000-pound capsule is the largest presently being considered for the 1973 thru 1979 missions. The propellant tanks have been sized for a 26,000 pound planetary vehicle (12,665 pounds of useable propellant) which is 1600 pounds greater than a planetary vehicle weight required for carrying a 7000-pound capsule (Table 8). One spare bay is provided for additional spacecraft equipment and space is available in the two bays allocated for science equipment for growth of the science electronics. The thermal control system can handle reasonable increases in power dissipated in the electronic bays.

On the basis of the flexibility in PSP design, growth capability in propellant and capsule weight, worst-case power and array sizing, room for additional electronic equipment and the data storage capacity and transmission rates provided, it is concluded that the spacecraft design described in this report should be adaptable for the 1975, 1977, and 1979 Mars missions.

11.3 EFFECT OF CAPSULE WEIGHT

The "Voyager Spacecraft System Study Guidelines" issued by MSFC and dated July 9, 1967 directed that two different cases of capsule weight be considered for the various mission years:

	1973	1975-1979
Case A	5000 lb	5000 lb
Case B	6000 lb	7000 lb

It was determined that capsule weights from 5000 to 7000 pounds had very little effect on the spacecraft weight. This result is due to the independent design decision of sizing the propulsion system for the maximum Planetary Vehicle weight (26,030 pound) within the performance capability of the Saturn V for all mission years. Table 9 shows the spacecraft weight, propellant weights, program contingency, and available launch period for the two cases.

Table 9. Comparison of Case A and Case B

	Case A		Case B	
	1973	1977	1973	1977
Spacecraft Dry Weight	5013	5013	5038	5038
Unusable Propellant	261	261	276	290
Spacecraft Burnout Weight	5274	5274	5314	5328
Spacecraft Contingency	264	264	266	266
Flight Capsule Weight	5000	5000	6000	7000
Usable Propellant	9970	9832	10956	11750
Separated Planetary Vehicle Weight	20508	20370	22536	24344
Planetary Vehicle Adapter	126	126	126	126
Planetary Vehicle Launch Weight	20634	20496	22662	24470
Total Launch Weight	41268	40992	45324	48940
Project Contingency	5000	5000	5000	3120
Available Launch Period	30	24	26	20

The only differences in the Planetary Vehicle weights, due to a change in capsule weight from 5000 to 7000 pounds, are: (1) a 25 pound difference in spacecraft structure weight; (2) up to 29 pounds difference in unusable propellants due to the change in required propellant; (3) two pounds difference in spacecraft contingency; and (4) a change in propellant weight proportional to the change in capsule weight. In Table 9 it is noted that the dry spacecraft weight remains constant for Case B; since the spacecraft is to carry a 7000 pound capsule, the structure is sized for the heavier capsule even though a 6000 pound capsule is to be carried in 1973. Also shown in Table 9 is a difference in propellant weight for 1973 and 1977 (Case A); a different velocity profile is required for the two years with a higher velocity at the lower thrust level required for the 1973 mission.

For Case B, only data for the 1973 and 1977 missions are shown. The minimum allowable Planetary Vehicle occurs for the 1977 mission; hence, this mission is most limiting on a vehicle carrying a 7000 pound capsule. Other mission effects of Case B are discussed in Section 11.1.

APPENDIX A
COMPONENT DESIGN PARAMETERS

This appendix gives the component design parameters including weight, power input, and allowable temperatures limits. The reference designation given each component allows the continual updating of the component parameter listing by the use of a computer as well as supplying the required function of unambiguous identification of the component. The first two digits note the subsystem requiring the components; the second two digits give the physical location of the component; and the last two digits give a specific component number. The location and subsystem designations are given in Table A-1. A complete listing of the components is given in Table A-2. Figure A-1 defines the structural components in the spacecraft structure, propulsion structure, and equipment and instrumentation structure categories of Table A-2.

Table A-1. Subsystem Reference Designation

010100	Bay No. 1	Power Subsystem	111700	Primary Structure
010200	Bay No. 2	Power Subsystem	122400	Scan Platform
020300	Bay No. 3	Science Electronics	132600	Solar Array
100400	Bay No. 4	Spare Bay	142500	A. C. Gas System
020500	Bay No. 5	Science Electronics	153500	A. C. Independently Mounted Sensors
030600	Bay No. 6	Science DAE	162300	Science Sensors
040700	Bay No. 7	Data Storage	172100	Ant Assemblies
040800	Bay No. 8	Data Storage	181800	Thermal Control
050900	Bay No. 9	Telemetry SSY	191900	Pyrotechnic
061000	Bay No. 10	Command SSY	202000	Harness
071100	Bay No. 11	Radio Subsystem	212200	Propulsion Hardware
071200	Bay No. 12	Radio Subsystem	222700	Total Propellants
071300	Bay No. 13	Radio Subsystem	232800	Meteoroid Protection
081400	Bay No. 14	Computer and Sequencer	242900	Capsule
011500	Bay No. 15	G&C Subsystem	253000	Adapter
091600	Bay No. 16	Power Subsystem		

Table A-2. Component Design Parameters (Sheet of 21)

Description	Weight (lb)	Reference Number	Power Input (Watts) Avg.	Power Input (Watts) Peak	Power Dissipated (Watts) Avg.	Power Dissipated (Watts) Peak	Power Source	Allowable Temp (F) Min.	Allowable Temp (F) Max.
STRUCTURE	620.15								
BASIC SHELL	591.65								
Propulsion Module Skin	112.86	111701							
Upper Ring	73.95	111702							
Reinforcement/ Shear Stiffness	18.80	111703							
Propulsion Module Longeron (16)	29.04	111704							
Lower Ring	49.15	111705							
Support Struts (16)	35.94	111706							
Solar Array Ribs (16)	43.90	111707							
Septer Figs.	62.38	111708							
Upr. Trs Figs.		111709							
Lwr. Trs Ftgs		111710							
Shroud Inter Ring	18.61	111712							

Table A-2. Component Design Parameters (Sheet 2 of 21)

Description	Weight (lb)	Reference Number	Power Input (Watts) Avg.	Power Input (Watts) Peak	Power Dissipated (Watts) Avg.	Power Dissipated (Watts) Peak	Power Source	Allowable Temp (F) Min.	Allowable Temp (F) Max.
STRUCTURE (cont)									
Up. Equip. Instl.	17.31	111714							
Beaded Shear PNL LR (16)	5.76	111715							
Beaded Shear Pnl Up. (16)	5.76	111716							
Bulkhead Lwr.	31.59	111718							
Long. Equip.	29.05	111719							
Equip. Upr Bay Rng. Segmt. (16)	10.27	111720							
Equip. Lwr. Bay Rng. Segmt. (16)	10.27	111721							
Lwr. Segm. Ring (16)	2.97	111722							
Misg. Clips, G.S. & Hardware	34.14	111723							
Meteroid Protection	28.50	232801							

Table A-2. Component Design Parameters (Sheet 3 of 21)

Description	Weight (lb)	Reference Number	Power Input (Watts) Avg.	Power Input (Watts) Peak	Power Dissipated (Watts) Avg.	Power Dissipated (Watts) Peak	Power Source	Allowable Temp (F) Min.	Allowable Temp (F) Max.
PROPULSION	2015.65								
MAIN ENGINE	409.00	012216							
Quad Redund. Ball Valve		212238	265	265.0	265	265.0			
Solenoid Pre-Valves		212239	265	100	100	1000			
Throttle Actuator		212240	90	336.0	90.0	336.0			
FUEL SYSTEM	376.91								
Tank Assembly									
Tanks (2)	226.56								
Baffles & Screens (2)	48.00	212208 212210							
Positive Explosion Bellow Assembly (2)	40.00								
Control Assembly									
Ordnance Valve (2)	16.00	212201							

Table A-2. Component Design Parameters (Sheet 4 of 21)

Description	Weight (lb)	Reference Number	Power Input (Watts) Avg.	Power Input (Watts) Peak	Power Dissipated (Watts) Avg.	Power Dissipated (Watts) Peak	Power Source	Allowable Temp (F) Min.	Allowable Temp (F) Max.
PROPULSION (cont)									
Filter (1)	3.00	212204							
Ordnance Valve (2)	3.50	212201							
Filter (1)	1.50	212204	224	224	224	224			
Solenoid Valve (4)	5.00	212237							
Fill, Vent & Test Assembly									
Fill Valve (1)	1.00	212202							
Fill Valve (1)	4.00								
Test Valve (2)	2.00								
Misc. Hardware									
Tubing & Fitting	16.05	212205							
Bracketry	10.30								
OXIDIZER SYSTEM	376.91								
Tank Assembly									
Tanks (2)	226.56	212212							
Baffles & Screens (2)	48.00								
Positive Explosion Bellows Assembly (2)	40.00								

Table A-2. Component Design Parameters (Sheet 5 of 21)

Description	Weight (lb)	Reference Number	Power Input (Watts) Avg.	Power Input (Watts) Peak	Power Dissipated (Watts) Avg.	Power Dissipated (Watts) Peak	Power Source	Allowable Temp (F) Min.	Allowable Temp (F) Max.
PROPULSION (cont)									
Control Assembly									
Ordnance Valve (2)	16.00	212201							
Filter (1)	3.00	212204							
Ordance Valve (2)	3.50	212201							
Filter (1)	1.50	212204							
Solenoid Valve (4)	5.00	212237	224	224	224	224			
Fill, Vent & Test Assembly									
Fill Valve (1)	1.00								
Fill Valve (1)	4.0	212202							
Test Valve (2)	2.0								
Misc. Hardware									
Tubing & Fittings	16.05	212205							
Bracketry	10.30								
PRESSURIZATION SYSTEM	570.13								
Tanks (4)	500.48	212229 212231							

Table A-2. Component Design Parameters (Sheet 6 of 21)

Description	Weight (lb)	Reference Number	Power Input (Watts) Avg.	Power Input (Watts) Peak	Power Dissipated (Watts) Avg.	Power Dissipated (Watts) Peak	Power Source	Allowable Temp (F) Min.	Allowable Temp (F) Max.
PROPULSION (cont)									
Control Assembly									
Ordnance Valve (6)	10.50	212221							
Ordnance Valve (4)	7.00	212226							
Filter (1)	2.50	212224							
Solenoid Valve (2)	2.50	212225	112	112	112	112			
Regulator (2)	10.00	212220							
Switch Selector (1)	.25	212219							
Pressure Switch (1)	.70	212219							
Check Valve (2)	2.00	21222							
Fill, Vent & Test Assembly									
Fill Valve (3)	3.00								
Test Valve (1)	1.00	212223							
Misc. Hardware									
Relief Valve/ Burst Disc	4.00	212228							
Dist. Manifold	3.00	212227							
Tubing & Fittings	13.70	212219							
Misc. Bracketry	9.50	212219							

Table A-2. Component Design Parameters (Sheet 7 of 21)

Description	Weight (lb)	Reference Number	Power Input (Watts) Avg.	Power Input (Watts) Peak	Power Dissipated (Watts) Avg.	Power Dissipated (Watts) Peak	Power Source	Allowable Temp (F) Min.	Allowable Temp (F) Max.
PROPULSION (cont)									
TELEMETRY SENSORS	36.7	212218							
Pressure Transducer (10)	2.5								
Temperature Sensor	9.2								
Cable & Misc. Bracketry	25.0								
SUPPORTS	246.0								
Propulsion Tanks	44.10	212233							
Helium Tank Supt.	6.40	212234							
Actuator Reactor	6.50	212235							
Engine Support	27.00	212236							
Strut, Trunnion & Ring Fittings	61.00	212217							
Mid. Ring	101.00	212238							
EQUIPMENT & INSTRUMENTATION	2287.72								
STRUCTURE	65.6								

Table A-2. Component Design Parameters (Sheet 8 of 21)

Description	Weight (lb)	Reference Number	Power Input (Watts) Avg.	Power Input (Watts) Peak	Power Dissipated (Watts) Avg.	Power Dissipated (Watts) Peak	Power Source	Allowable Temp (F) Min.	Allowable Temp (F) Max.
EQUIPMENT & INS. (cont)									
GUIDANCE, CONTROL & NAVIGATION	202.30								
A/C Independently Mounted Sensors									
Sun Gage Sensor	0.2	153501						30.0	130.0
Cruise Sun Sensor	1.2	153502						30.0	130.0
Secondary Acquisition Sensor	1.2	153503						30.0	140.0
Canopus Tracker	6.3	153504		1.8	1.8	1.8	2400	-30.0	100.0
Canopus Tracker	6.3	153505		1.8	1.8	1.8	2400	-30.0	100.00
Support Structure and Hardware	1.2	153506							
Earth Null Sensor	1.00	153508						30	130
Computer/Sequencer	35	081401	60	60	60	60	2400 Hz	0.0	120
Control Computer									
Solar Aspect Electronics	5.0	081402						0.0	220
Earth Null Elec.	2.0	081403						0.0	150
A.C. Electronics	8.6	091601	30	30	30.0	30.0	2400	0.0	160
Autopilot	6.0	091602	8.4	8.4	8.4	8.4	2400 Hz	0.0	160

Table A-2. Component Design Parameters (Sheet 9 of 21)

Description	Weight (lb)	Reference Number	Power Input (Watts) Avg.	Power Input (Watts) Peak	Power Dissipated (Watts) Avg.	Power Dissipated (Watts) Peak	Power Source	Allowable Temp (F) Min.	Allowable Temp (F) Max.
EQUIPMENT & INS. (cont)									
Accelmo Gyro	14.50	091603	37.5	125.5	37.5	125.5	(3)	0.0	160
Accelmo Gryo	14.50	091604	0	125.5	0	125.5	(3)	0.0	160
Articulation Eqp.									
PSP Stowage Release, Deploy, & Support	17.00	122411							
High Gain Antenna Actuator & Mechanisms	28.80	172103	17.3	58.00	17.3	58.0	(DC Buss & 2.4 KHZ)	-100	200.0
Mnvr Ant. Mast	1.75								
Broad Coverage Ant. Mast	2.75								
Main Engine Gimbal Actuators	49.00	212240							
INSTRUMENTATION	357.02								
Radio									
Transponder (Rec. & Exc.)	13.3	071101	7.14 8.32	7.14 8.32	7.14 8.32	7.14 8.32	2400 Hz	-10.0	180
Transponder (Rec. & Exc.)	13.3	071102	7.14 0.0	7.14 0.0	7.14 0.0	7.14 0.0	2400 Hz	-10.0	180

Table A-2. Component Design Parameters (Sheet 10 of 21)

Description	Weight (lb)	Reference Number	Power Input (Watts) Avg.	Power Input (Watts) Peak	Power Dissipated (Watts) Avg.	Power Dissipated (Watts) Peak	Power Source	Allowable Temp (F) Min.	Allowable Temp (F) Max.
EQUIPMENT & INST. (cont)									
INSTRUMENTATION (cont)									
Power Amp TWT	8.00	071201	147.0	147.0	97.0	97.0	DC	-35	245
Power Amp TWT	8.00	071202	0	147.0	0	97.0	DC	-35	245
Power Amp (Launch Assy & Backup)	4.00	071203	0.0	75.00	0.0	69.0	DC	-10	180
Transponder (Rec. & Exc.)	13.3	071204	7.14 0.0	7.14 7.14	7.14 0.0	7.14 7.14	2400 Hz	-10.0	180
Diplexer Switch Assembly	13.4	071205	0.0	15.0	0.0	15.5	DC	-10.0	180
Relay Radio (Capsule Descent)	50.00	071301	0	50	0	50.0	2400 Hz	-10.0	180
Command									
Command DET PC	4.2	061001	2.0	2.0	2.0	2.0	(2)	0.0	185
Command DET PC	4.2	061002	2.0	2.0	2.0	2.0	(2)	0.0	185
Command DET PC	4.2	061003	2.0	2.0	2.0	2.0	(2)	0.0	185
Comm. Decoder	5.6	061004	4.5	4.5	4.5	4.5	(2)	0.0	185

Table A-2. Component Design Parameters (Sheet 11 of 21)

Description	Weight (lb)	Reference Number	Power Input (Watts) Avg.	Power Input (Watts) Peak	Power Dissipated (Watts) Avg.	Power Dissipated (Watts) Peak	Power Source	Allowable Temp (F) Min.	Allowable Temp (F) Max.
EQUIPMENT & INST. (cont)									
INSTRUMENTATION (cont)									
Comm. Decoder	5.6	061005	4.5	4.5	4.5	4.5	(2)	0.0	185
DEC ACES SWIT	3.0	061006	0.2	0.2	0.2	0.2	(2)	0.0	185
Power Supply	3.1	061007	20.2	20.2	5.0	5.0	2400 HZ	0.0	185
Telemetry									
Telemetry Electronics	27.2	050900	15.0	15.0	15.0	15.0	2400	0	176
Data System									
Data Auto Eq Include Harness Wt	50.00	030601	50.0	100.0	50.0	100.0	2400 H_z	14.0	167.0
Tape Recorder	15.00	040701					2400 H_z	0.0	158
Tape Recorder	15.00	040702	15	36	15	36	2400 H_z	0.0	158
Tape Recorder	15.00	040801					2400 H_z	0.0	158
Tape Recorder	15.00	040802					2400 H_z	0.0	158
Control Logic	0.65	040703	0.4	0.4	0.4	0.4	2400 H_z	0.0	176
Control Logic	0.65	040803	0.4	0.4	0.4	0.4	2400 H_z	0.0	176
Playback Sequencer	0.65	040704						0.0	176
Playback Sequencer	0.65	040804						0.0	176
Power Supply	4.00	040808	1.0	1.0	0.25	0.25	2400 H_z	0.0	176

Table A-2. Component Design Parameters (Sheet 12 of 21)

Description	Weight (lb)	Reference Number	Power Input (Watts) Avg.	Power Input (Watts) Peak	Power Dissipated (Watts) Avg.	Power Dissipated (Watts) Peak	Power Source	Allowable Temp (F) Min.	Allowable Temp (F) Max.
EQUIPMENT & INST. (cont)									
INSTRUMENTATION (cont)									
Antenna									
Relay Antenna	2.0	172101						-300.0	200.0
Associated Structure	2.0	172102						-300.0	200.0
Hi Gain Antenna	47.60	172103						-100.0	200.0
Maneuver Ant.	1.90	172104						-300.0	200.0
Broad Coverage Antenna	0.12							-300.0	200.0
Medium Gain Antenna	4.4	172105						-300.0	200.0
Supt. Structure	2.0	172106						-300.0	300.0
ELECTRIC POWER	743.87								
Solar Panels									
Solar Panel 1	18.14	132601						-250	250
Solar Panel 2	18.14	132602						-250	250
Solar Panel 3	18.14	132603						-250	250
Solar Panel 4	15.18	132604						-250	250
Solar Panel 5	18.14	132605						-250	250
Solar Panel 6	18.14	132606						-250	250
Solar Panel 7	18.14	132607						-250	250
Solar Panel 8	18.14	132608						-250	250

Table A-2. Component Design Parameters (Sheet 13 of 21)

Description	Weight (lb)	Reference Number	Power Input (Watts) Avg.	Power Input (Watts) Peak	Power Dissipated (Watts) Avg.	Power Dissipated (Watts) Peak	Power Source	Allowable Temp (F) Min.	Allowable Temp (F) Max.
EQUIPMENT & INST. (cont)									
ELECTRIC POWER (cont)									
Solar Panel 9	18.14	132609						-250	250
Solar Panel 10	18.14	132610						-250	250
Solar Panel 11	18.14	132611						-250	250
Solar Panel 12	15.18	132612						-250	250
Solar Panel 13	18.14	132613						-250	250
Solar Panel 14	18.14	132614						-250	250
Solar Panel 15	18.14	132615						-250	250
Solar Panel 16	18.14	132616						-250	250
Deployable Array	156.8	132620						-250	250
Batteries									
Battery AG-Zn	45.00	010101	0.0	25.	0.0	275.0	Charge Reg.	30	80
Battery Ni-Cd	80.00	010201	117	117	35	117	Charge Reg.	30	80
Battery Ni-Cd	80.00	011501	117	117	35	117	Charge Reg.	30	80
Power Control									
Power Switching Logic	7.0	010102	768	1989	4.0	10.0	Reg DC	14.0	167.0
Main Regulator & Failure Detector (FD)	20.75	010202 010212	349	530.7	44.7	54.2	DC	14.0	167.0

Table A-2. Component Design Parameters (Sheet 14 of 21)

Description	Weight (lb)	Reference Number	Power Input (Watts) Avg.	Power Input (Watts) Peak	Power Dissipated (Watts) Avg.	Power Dissipated (Watts) Peak	Power Source	Allowable Temp (F) Min.	Allowable Temp (F) Max.
EQUIPMENT & INST. (cont)									
ELECTRIC POWER (cont)									
Main Regulator & Failure Detector	20.75	011503 011504	0	530.7	0	54.2	DC	14.0	167.0
Charge Regulator	1.50	010103	3.0	35.5	3.0	10.	Array	14.0	167.0
Charge Regulator	2.00	010203	237.5	237.5	12.4	12.4	Array	14.0	167.0
Charge Regulator	2.00	011502	237.5	237.5	12.4	12.4	Array	14.0	167.0
3ϕ Inverters & F.D. (2)	9.50	010104	19.4	38.8	8.8	17.6	Reg DC	14.0	167.0
2.4 KM Inverters & F.D. (2)	17.50	010105	278	440.1	36.5	45.0	Reg DC	14.0	167.0
1ϕ Inverters & F.D. (1)	3.75	010106	10.0	20.2	2.9	5.2	Reg DC	14.0	167.0
Clock & Synchronizer	5.00	010114	9.0	9.0	9.0	9.0	Reg DC	14.0	167.0
Zener, Regulators	8.00	132617					Solar Cells	-250.0	230
Electric Networks	211.56								

Description	Weight (lb)	Reference Number	Power Input (Watts) Avg.	Power Input (Watts) Peak	Power Dissipated (Watts) Avg.	Power Dissipated (Watts) Peak	Power Source	Allowable Temp (F) Min.	Allowable Temp (F) Max.
EQUIPMENT & INST. (cont)									
PYROTECHNICS									
Pyrotechnics Controller	7.50	011612	1.5	6	1.5	6	240Hz Pyro	15.0	185
Pin Pullers	2.20	191901						- 70.0	167.0
Squibs	2.20	191902						- 65.0	167.0
NETWORKS									
Main Harness	93.50	202001						-200.0	250.
Relay Cable	0.55	202002						- 76.0	752.
High-Gain Cable	3.04	202003						- 76.0	752.
Low-Gain Cable	9.05	202004						- 76.0	752.
Medium Gain Cable	2.52	202005						- 10	167
Umbilical	4.50	202006						-250.0	250
SA Harness	26.50	132619						-200	250
Harness Wire Bay 1	4.60	010107						-200	250
Harness Wire Bay 2	4.60	010207						-200	250
Harness Wire Bay 7	1.40	040708						-200	250
Harness Wire Bay 8	1.40	040809						-200	250
Harness Wire Bay 9	5.60	050924						-200	250
Harness Wire Bay 10	4.60	061008						-200	250
Harness Wire Bay 11	1.40	071103						-200	250
Wire Bay 12	3.70	071206						-200	250
Wire Bay 13	1.4	071302						-200	250
Wire Bay 14	4.5	081404						-200	250
Wire Bay 15	4.1	011506						-200	250
Wire Bay 16	5.7	091605						-200	250
PSP Cabling	17.0	124012							

Table A-2. Component Design Parameters (Sheet 16 of 21)

Description	Weight (lb)	Reference Number	Power Input (Watts) Avg.	Power Input (Watts) Peak	Power Dissipated (Watts) Avg.	Power Dissipated (Watts) Peak	Power Source	Allowable Temp (F) Min.	Allowable Temp (F) Max.
EQUIPMENT & INST. (cont)									
TEMPERATURE CONTROL SYSTEM	149.47								
Insulation									
Insulation Orbiter	15.2	181819						-200.0	200.0
Insulation A/C	2.5	181818						-200.0	200.0
Paint	17.5	181817						-300	300.0
Louver & Mechanics									
Shutter Assembly & Face Sheet 1	6.69	181801						-200	200
Shutter Assembly & Face Sheet 2	6.69	181802						-200	200
Shutter Assembly & Face Sheet 3	6.69	181803						-200	200
Insulation & Face Sheet 3	4.14	181804						-300	300
Shutter Assembly & Face Sheet 5	6.69	181805						-200	200
Shutter Assembly & Face Sheet 6	6.69	181806						-200	200
Shutter Assembly & Face Sheet 7	5.59	181807						-200	200

Table A-2. Component Design Parameters (Sheet 17 of 21)

Description	Weight (lb)	Reference Number	Power Input (Watts) Avg.	Power Input (Watts) Peak	Power Dissipated (Watts) Avg.	Power Dissipated (Watts) Peak	Power Source	Allowable Temp (F) Min.	Allowable Temp (F) Max.
EQUIPMENT & INST. (cont)									
TEMPERATURE CONTROL SYSTEM (cont)									
Louver & Mechanisms (cont)									
Shutter Assembly & Face Sheet 8	5.59	181808						-200	200
Shutter Assembly & Face Sheet 9	5.59	181809						-200	00
Shutter Assembly & Face Sheet 10	5.79	181810						-200	200
Shutter Assembly & Face Sheet 11	6.69	181811						-200	200
Insulation & Face Sheet 12	11.57	181812						-300	300
Shutter Assembly & Face Sheet 13	5.79	181813						-200	200
Shutter Assembly & Face Sheet 14	6.69	181814						-200	200
Shutter Assembly & Face Sheet 15	5.79	181815						-200	200
Shutter Assembly & Face Sheet 16	6.69	181816						-200	200
Other Devices									
Solar Array Temp. Sensors	0.2	132618						-250	+250

Table A-2. Component Design Parameters (Sheet 18 of 21)

Description	Weight (lb)	Reference Number	Power Input (Watts) Avg.	Power Input (Watts) Peak	Power Dissipated (Watts) Avg.	Power Dissipated (Watts) Peak	Power Source	Allowable Temp (F) Min.	Allowable Temp (F) Max.
EQUIPMENT & INST. (cont)									
TEMPERATURE CONTROL SYSTEM (cont)									
Other Devices (cont)									
(16) Bay Temp. Sensors	1.6							-300	+300
(14) Shutter Ang. Det.	5.6							-300	+300
Gyro Temp Sensor	0.1	091608						0.0	200
Accel. Temp. Sensor	0.1	091609						0.0	200
Attitude Control Ind. Mounted Sensors	0.2	153507						-300	300
Antenna Temp. Sensor	0.1	172107							
Strip Heats	3.0								
ATTITUDE CONTROL GAS SYSTEM	141.9								
Tank	16.8	142501							
Tank	16.8	142502							
Tank	25.2	142503							

Table A-2. Component Design Parameters (Sheet 19 of 21)

Description	Weight (lb)	Reference Number	Power Input (Watts) Avg.	Power Input (Watts) Peak	Power Dissipated (Watts) Avg.	Power Dissipated (Watts) Peak	Power Source	Allowable Temp (F) Min.	Allowable Temp (F) Max.
EQUIPMENT & INST. (cont)									
ATTITUDE CONTROL GAS SYSTEM (cont)									
Tank	25.2	142504							
Hardware	43.90	142505							
Gas Sys Mtg S	14.00	142514							
SCIENCE EQUIP.	416.00								
Scan Platform									
IR Radiometer	13.00	122401	6	6	6	6	2400		
HRIR Spectrometery	18.00	122402	14	14	14	14	2400		
BBIR Spectrametery	9.00	122403	5	5	5	5	400		
MRTV #1	26.00	122404	35	35	35	35			
MRTV #2	26.00	122405	35	35	35	35			
HRTV	47.00	122406	20	20	20	20			
U.V. Spectrometer	23.00	122409	21	21	21	21	2400 & 400		
PSP Structure & Thermal Control	35.00	122410	5.0	5.0	5.0	5.0	PC		
PSP Gimbal & Control Drive (3)	52.00	122408	15.0	6.5	15.0	16.5			

Table A-2. Component Design Parameters (Sheet 20 of 21)

Description	Weight (lb)	Reference Number	Power Input (Watts) Avg.	Power Input (Watts) Peak	Power Dissipated (Watts) Avg.	Power Dissipated (Watts) Peak	Peak Source	Allowable Temp (F) Min.	Allowable Temp (F) Max.
EQUIPMENT & INST. (cont)									
SCIENCE EQUIP. (Cont)									
Science Body Mounted	45.00	162301							
Science Electronics include Harness Weight	61.00	020501	110.5	110.5	110.5	110.5	(3)	14.0	167.0
Science Electronics include Harness Weight	61.00	020301	110.5	110.5	110.5	110.5	(3)		

Table A-2. Component Design Parameters (Sheet 21 of 21)

Description	Weight (lb)		
RESIDUALS	375.6	TOTAL INERT SPACECRAFT	5299
PROPELLANTS	261.7		
Tanks	105.3		
Random Outage	124.6		
Fuel Bias	31.8		
PRESSURANT	53.9		
Bottles	10.2		
Tanks	43.7		
Attitude Control System Fluids	60.0		
CONTINGENCY	265.0	TOTAL INERT SPACECRAFT WITH CONTINGENCY	5564.0
USEABLE PROPELLANT	9994.00	TOTAL SPACECRAFT AT LAUNCH	15,558
Fuel	3846.92		
Oxidizer	6147.08		
Losses			
CAPSULE	5000.0	TOTAL PLANETARY VEHICLE	20,558
ADAPTER	126.0	TOTAL PLANETARY VEHICLE AT LAUNCH	20,684

(1) See Table 5 for power input for various mission phases.
(2) Power input from subsystem T/R.
(3) Heaters 12 watts, unregulated battery; gyros ϕ watts, 400 Hz, 3ϕ; electronics ϕ watts, 2400 cps.

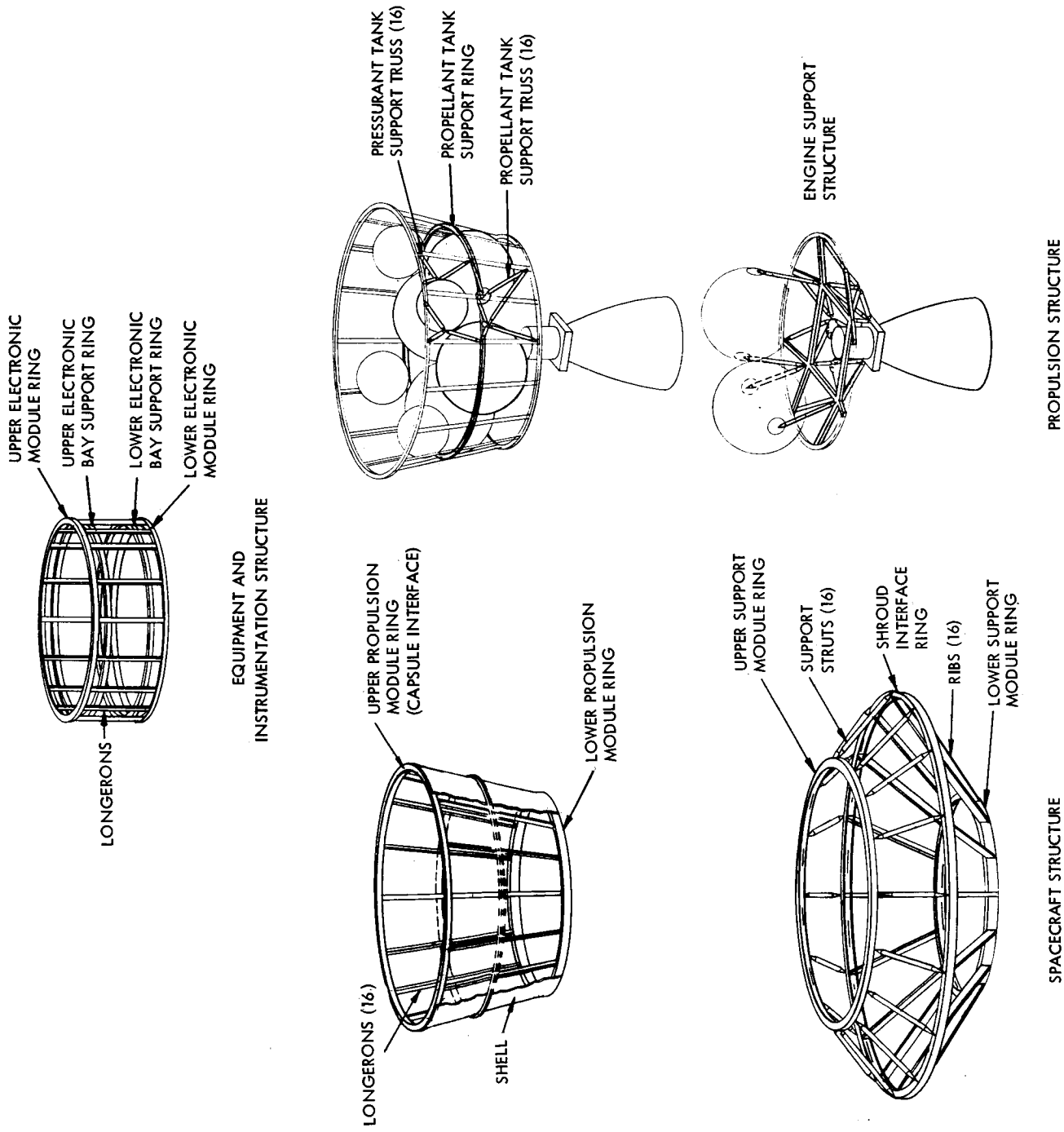

Figure A-1. Structure Breakout

VOY-D-220

SPACECRAFT CONFIGURATION

1. INTRODUCTION

The selected spacecraft is described in VOY-D-210. This section describes the alternatives considered and the rationale used to develop and select the preferred configuration design.

General Electric's experience includes Voyager configuration design for Task A, Task B, Task C and an in-house study of configurations for the LEMDE Propulsion System. This experience was used to the fullest; at the same time, care was taken not to overlook some other possible ways of configuring the design. Previous decisions were reevaluated to insure their continued applicability in light of the new guidelines. The new guidelines most influential in configuration change were the increased interest in higher communication rates and the attendant growth of the antenna, satisfaction of mission objectives for 1973 through 1979, and the use of the LEMDE liquid propulsion system. To implement this approach the effort began with a broad review of possible configuration concepts. These were screened to the most promising concepts for more detailed configuration development and baseline selection. Optimization studies conducted on the baseline design resulted in the preferred configuration. This section describes this spacecraft configuration development effort.

2. CONCEPT DEVELOPMENT AND SCREENING

2.1 BASIC CONCEPTS

The functional subsystems and requirements were reviewed and categorized in order of their effect on the physical definition of a configuration. The four elements considered to have first order effects and the corresponding configuration selection constraints adopted were:

a. Capsule - Must be located at one end of the planetary vehicle for ease of capsule separation.

b. Propulsion - LEMDE Engine.

1. Thrust Chamber - Located at one end of the planetary vehicle with the nominal thrust axis through the center of gravity of spacecraft and center of gravity of the capsule.

2. Tankage - No constraint.

c. Equipment Storage - Bay concept adopted. The bays must view black space during normal flight attitude.

d. Planetary Vehicle Support Adapter - Constrained by shroud geometry.

At this stage no specific geometries were adopted for the propulsion tankage or the support adapter except as restrained by the dynamic envelope as given in Reference 1 and modified by Reference 2.

Six basic configuration concepts were developed by permutation in the relative axial positions of the three elements not constrained from change in location. A seventh basic concept includes the possibility of locating the tankage and equipment bays at the same axial location. Configurations in which the support adapter is located at the same axial position as other elements, were covered by the more detailed description of the adapter which was considered in a latter phase of the study. The seven basic concepts are illustrated in Figure 1.

2.2 CONFIGURATION DEVELOPMENT

In order to have a meaningful basis for evaluating the relative merits of the basic concepts, it was necessary to first develop representative configurations derived from the concepts. At this stage of the effort, some subsystem definitions, influential in configuration design, were under study and not available. Therefore, the tentative guidelines shown in Table 1 were adopted for temporary use. In addition, certain decisions reached in the Task B Study and explained in Reference 3 were reviewed and retained as still appropriate. These were:

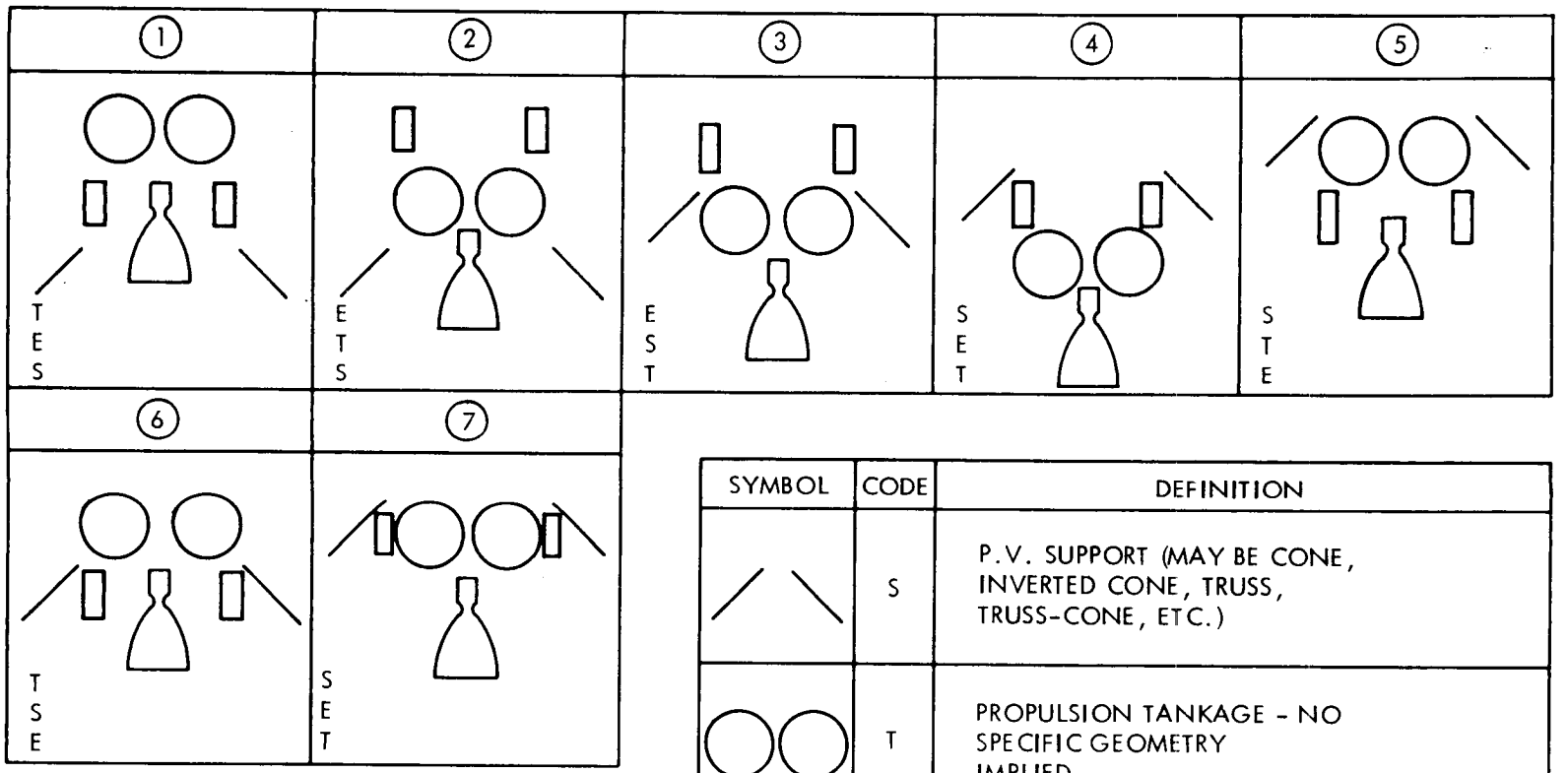

NOTE:

CAPSULE NOT SHOWN-
LOCATED AT TOP OF S/C
IN ALL CASES

SYMBOL	CODE	DEFINITION
	S	P.V. SUPPORT (MAY BE CONE, INVERTED CONE, TRUSS, TRUSS-CONE, ETC.)
	T	PROPULSION TANKAGE - NO SPECIFIC GEOMETRY IMPLIED
	E	ELECTRONIC EQUIPMENT BAYS
		LEMDE TCA MODIFIED FOR VOYAGER

Figure 1. Basic Concepts

Table 1. Tentative Configuration Guidelines I

I. PROPULSION

A. Thrust Chamber Assembly

LEMDE thrust chamber modified for Voyager

B. Propellant Weight and Volume

	Minimum Acceptable	Design Objective
Total propellant weight (pounds)	11,200	12,400
Total fuel weight (pounds)	4,300	4,750
Total oxidizer weight (pounds)	6,900	7,640
Propellant tankage volume (cubic feet)	166	184
Fuel tankage volume (cubic feet)	83	92
Oxidizer tankage volume (cubic feet)	83	92

II. DYNAMIC ENVELOPE

The Dynamic Envelope described in MSFC Guidelines of July 14.

III. HIGH GAIN ANTENNA SIZE

A minimum diameter of 7.5 feet will be accommodated with the ability to accommodate larger antenna diameters (up to 12 feet) desirable.

IV. SOLAR ARRAY

A minimum of 250 square feet of projected solar array area is to be considered. Designs are not to be restricted to fixed arrays only. Ability to accommodate larger array areas up to 350 square feet is desirable.

V. C.G. TO GIMBAL PLANE DISTANCE

A minimum of 20 inches between TCA Gimbal plane and vehicle C.G. A separation of up to 40 inches and beyond is desirable.

VI. EQUIPMENT BAY

An electronics packaging volume of 15 cubic feet. Configurations will have the ability to accommodate thermal radiation panel areas of 4.5 square feet for 16 bay and 6 square feet for 12 bay configurations.

VII. SEPARATION ENVELOPE

The clearance required for over the nose separation as per Dir. V-6230-SMK-097.

VIII. PLANET SCAN PLATFORM

Planet scan platform volume of 10 cubic feet.

- Sun-oriented vehicle with capsule located on the shade side.
- Single PSP
- Toroidally arranged electronic equipment compartments
- Deployable and steerable high gain antenna.

2.2.1 Design Studies

In order to further aid in the configuration development, preliminary studies were conducted in three areas. These areas were electronic equipment packaging, propulsion tankage geometry and equipment bay heat rejection capability as a function of view blockage by spacecraft appendages.

2.2.1.1 Equipment Packaging Study

In the equipment packaging study, the electronic package geometry was taken similar to that used in the Task B study. A fixed dimension of 5 inches in height and 4 inches in width was added to the electronic assembly dimensions to determine the overall area of the thermal plate. The depth of the electronic subassembly was 6 inches, with an additional 4 inches allowed for connectors and wiring. The total volume requirement for electronic equipment (subassemblies) was taken to be 14.5 cubic feet. The equipment was allocated among the various bays by functional breakdown, so as to avoid having more than one subsystem occupying a single bay with a 15 percent spare volume provided in each bay for growth. Only one row of system connectors was permitted at the top and bottom of the bay to allow easy access for mating and demating.

The study was conducted for 12, 16 and 18 bays at diameters of 100 through 160 inches; the resulting packaging parameters are shown on Table 2. Surface areas in the 3.5 square feet range required for heat dissipation and 16 connectors for telemetry bay reduces the number of useful combinations of number of bays and module diameter. In general, the smaller

Table 2. Electronic Packaging Parameters

Sides	Diameter Parameters	100 Inch	120 Inch	144 Inch	160 Inch
12	Area sq. ft.	4.46	4.52	4.46	4.78
	Ht., in.	21.5	18.2	18.2	18.2
	Max. Wt., lb.	101	101	101	101
	No. Conn.	14	18	22	26
	Subassy. Width, in.	20.3	24	24	24
16	Area sq. ft.	3.48	3.44	3.54	3.59
	Ht. in.	23.0	18.0	14.2	13.4
	Max. Wt., lb.	74	74	74	74
	No. Conn.	8	12	16	18
	Subassy. Width	13.9	17.8	22.5	24
18	Area sq. ft.	3.18	3.14	3.18	3.22
	Ht. in.	24.1	18.6	14.6	12.8
	Max. Wt. lb.	63	63	63	63
	No. Conn.	6	10	14	16
	Subassy. Width	11.8	15.2	19.4	22.2

vehicle diameters, combined with a large number of sides were most unsatisfactory, since they resulted in insufficient area for heat dissipation and connector mounting.

2.2.1.2 Propellant Tank Geometry Study

In the preliminary propellant tank geometry study, various shapes, number of tanks and their compatibility with configuration requirements were considered. Pancake and toroidal shapes were discarded primarily due to complexities in development (impact on schedule risk)and increased residual propellant required over other designs. Spherical tanks,

numbering 2, 4, 6 and 8 were examined. Two tank arrangements lead to poor spacecraft packaging efficiency and mass properties characteristics, in particular large C.M. shifts during burn. Use of eight tanks leads to either large spacecraft diameters (greater than 160 inch) or very complex tank nesting arrangements; in either case increased spacecraft weight results. In general, 4 or 6 tank arrangements, depending upon the particular spacecraft configuration, is desirable.

2.2.1.3 Shutter Dissipation Study

Reduction of equipment bay heat dissipation capability caused by solar array view blockage was also studied. The effect of bay heat dissipation capability as a function of axial distance between the electronic equipment bays and the solar array was computed for equipment ring diameters ranging from 120 inches through 160 inches and solar array diameters up to 260 inches. Figure 2 is a typical example of the curves developed.

2.2.1.4 Configurations

Based on the tentative guidelines and the results of the special studies, approximately twenty-five representative configurations were developed, illustrating the seven basic concepts. Fourteen of these were selected for evaluation in the concept screening exercise. These are shown on Figures 3 through 16. The first digit of the configuration number corresponds to the concept it illustrates (see Figure 3). Unlike the basic concepts, the configurations include some consideration of the support and tank geometry. Also those subsystems having second order effects, such as the PSP, high gain antenna and solar array are considered.

2.2.2 Evaluation Criteria

In order to narrow the list of possible concepts down to the few most promising ones, the fourteen configurations were compared on the basis of an evaluation criteria. An evaluation

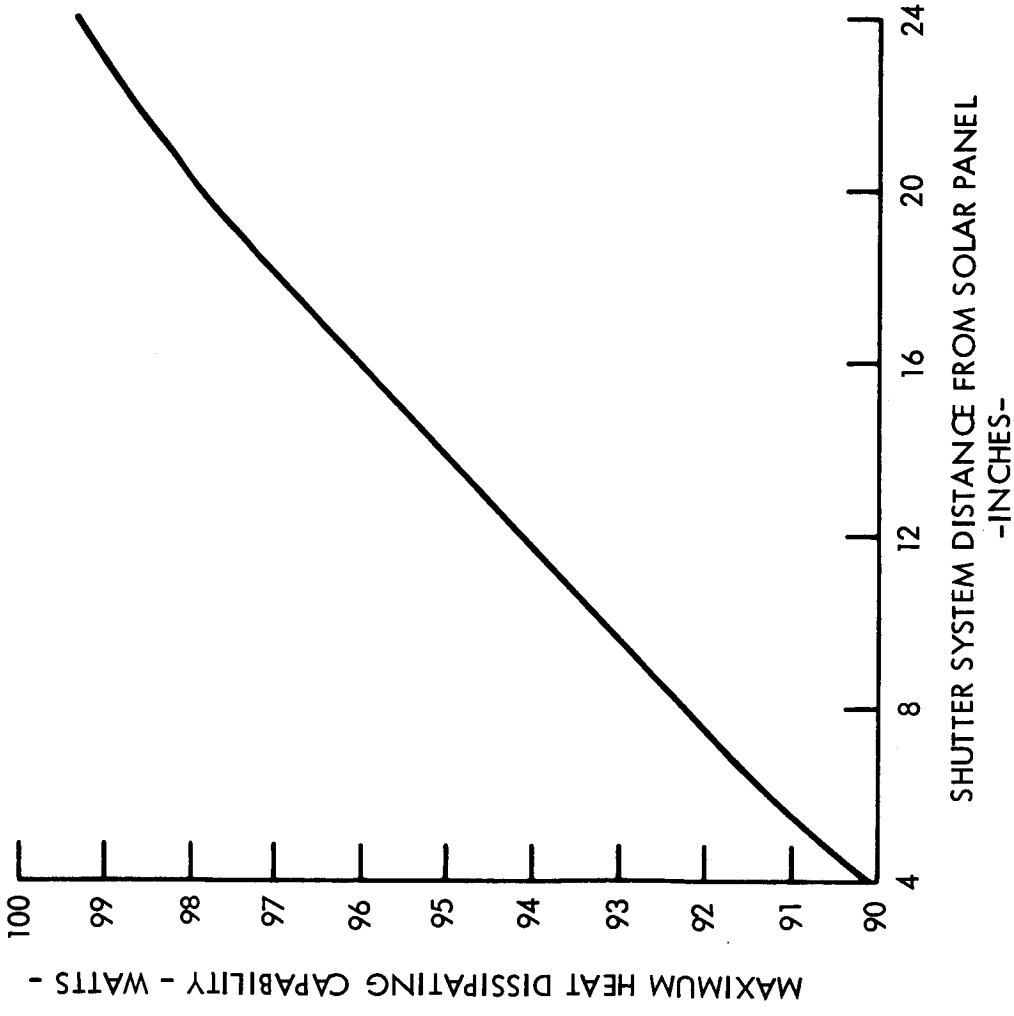

Figure 2. Shutter Heat Dissipating Capability

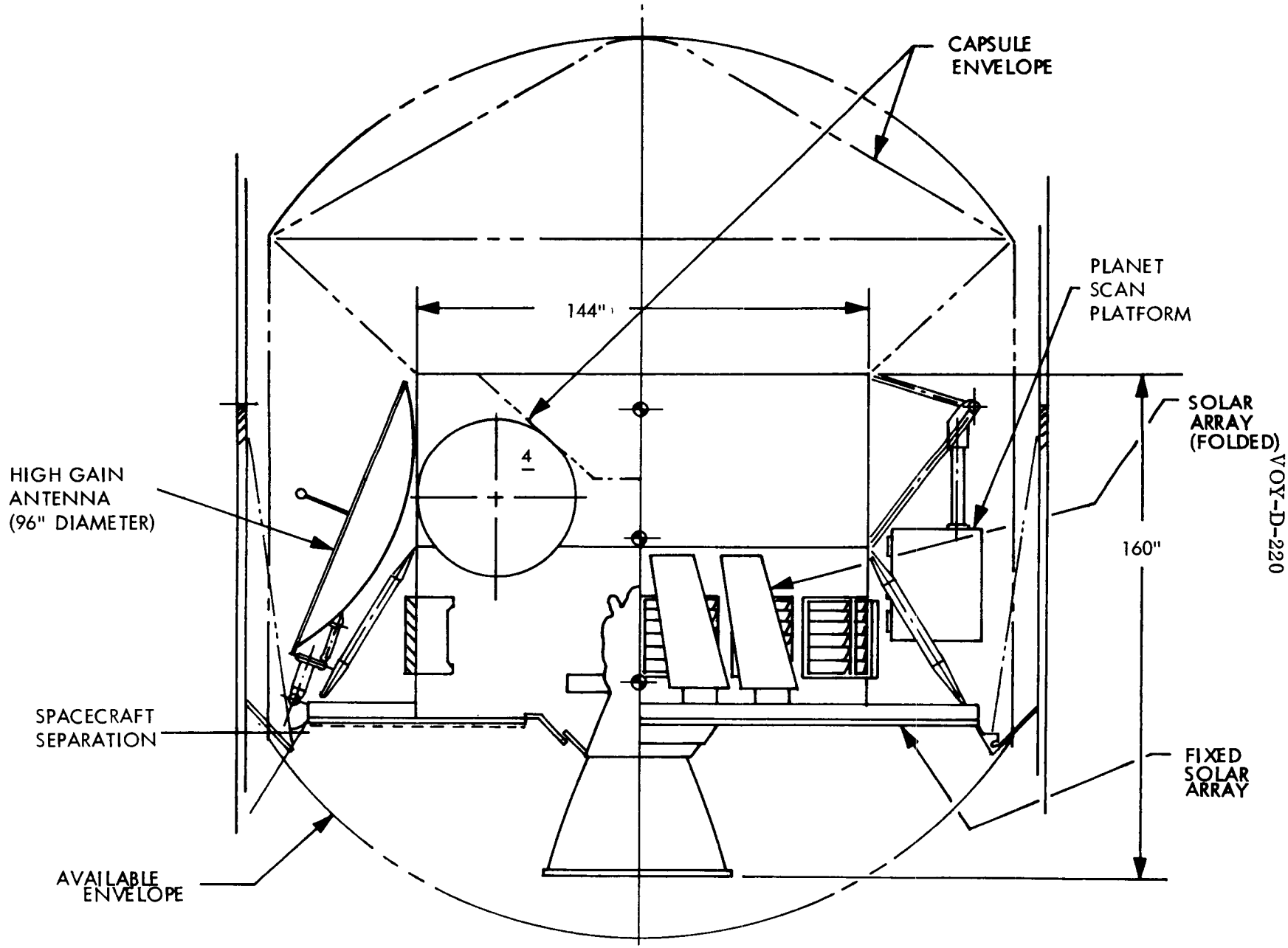

Figure 3. Concept 1 Type 1

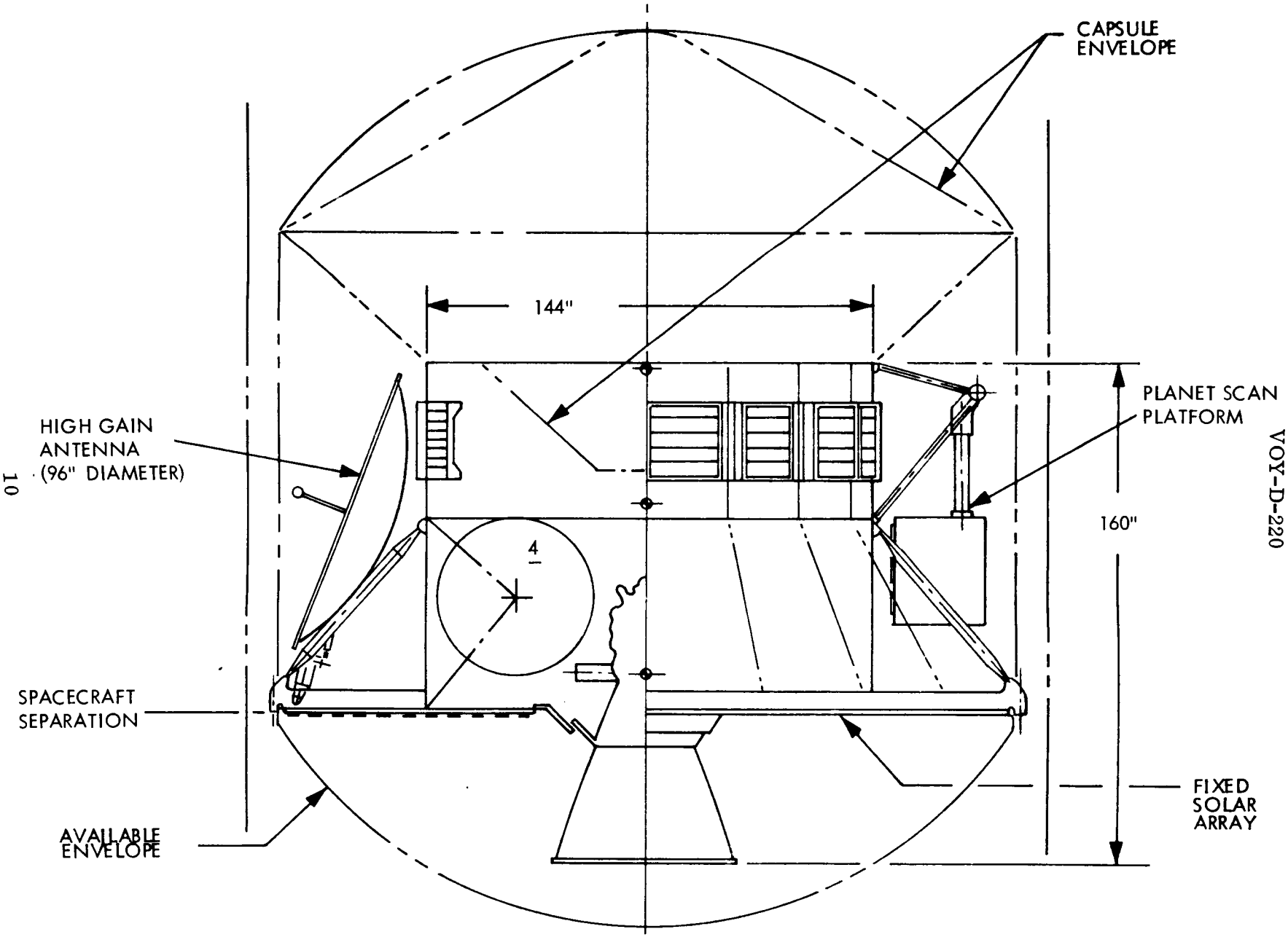

Figure 4. Concept 2 Type 1

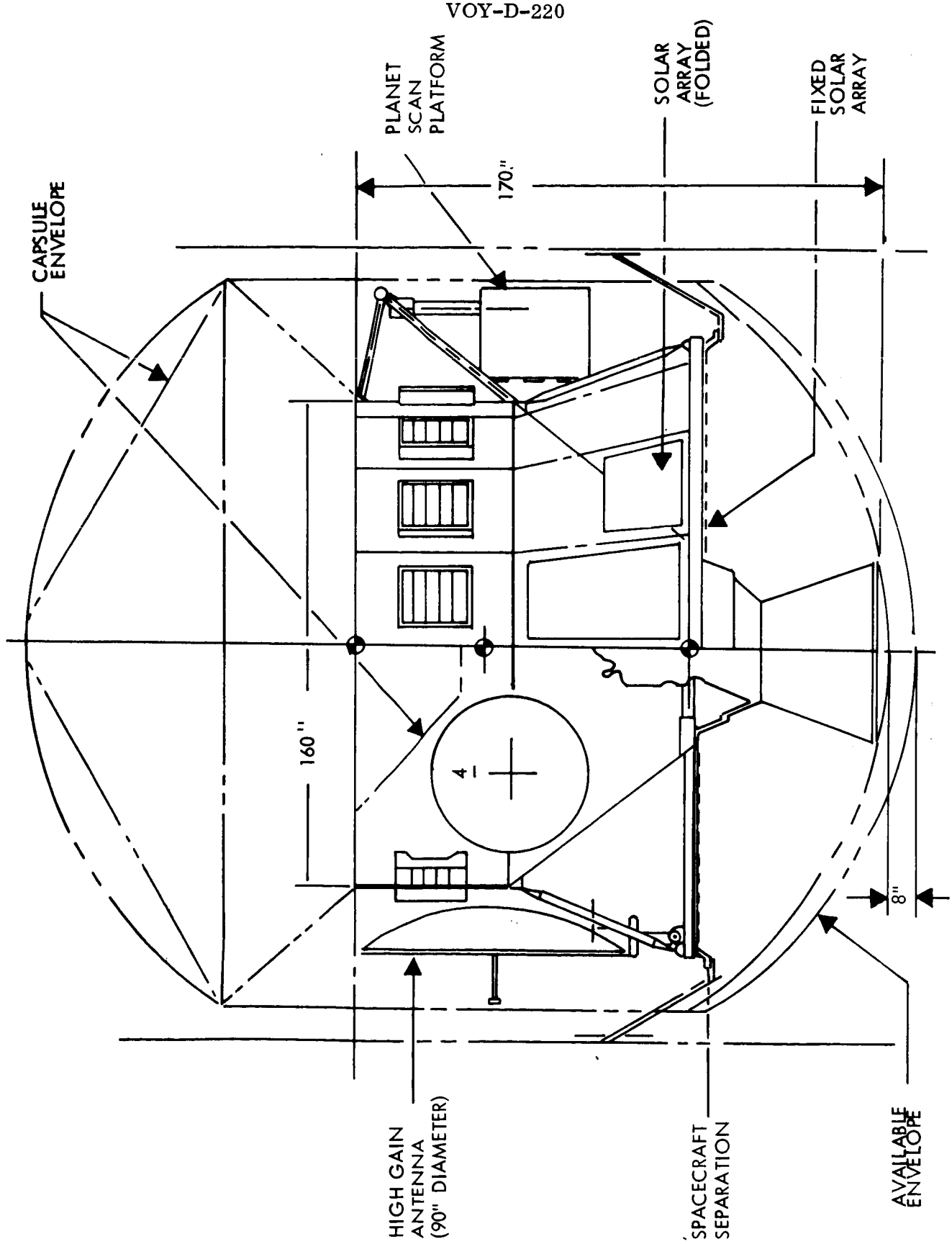

Figure 5. Concept 2 Type 2

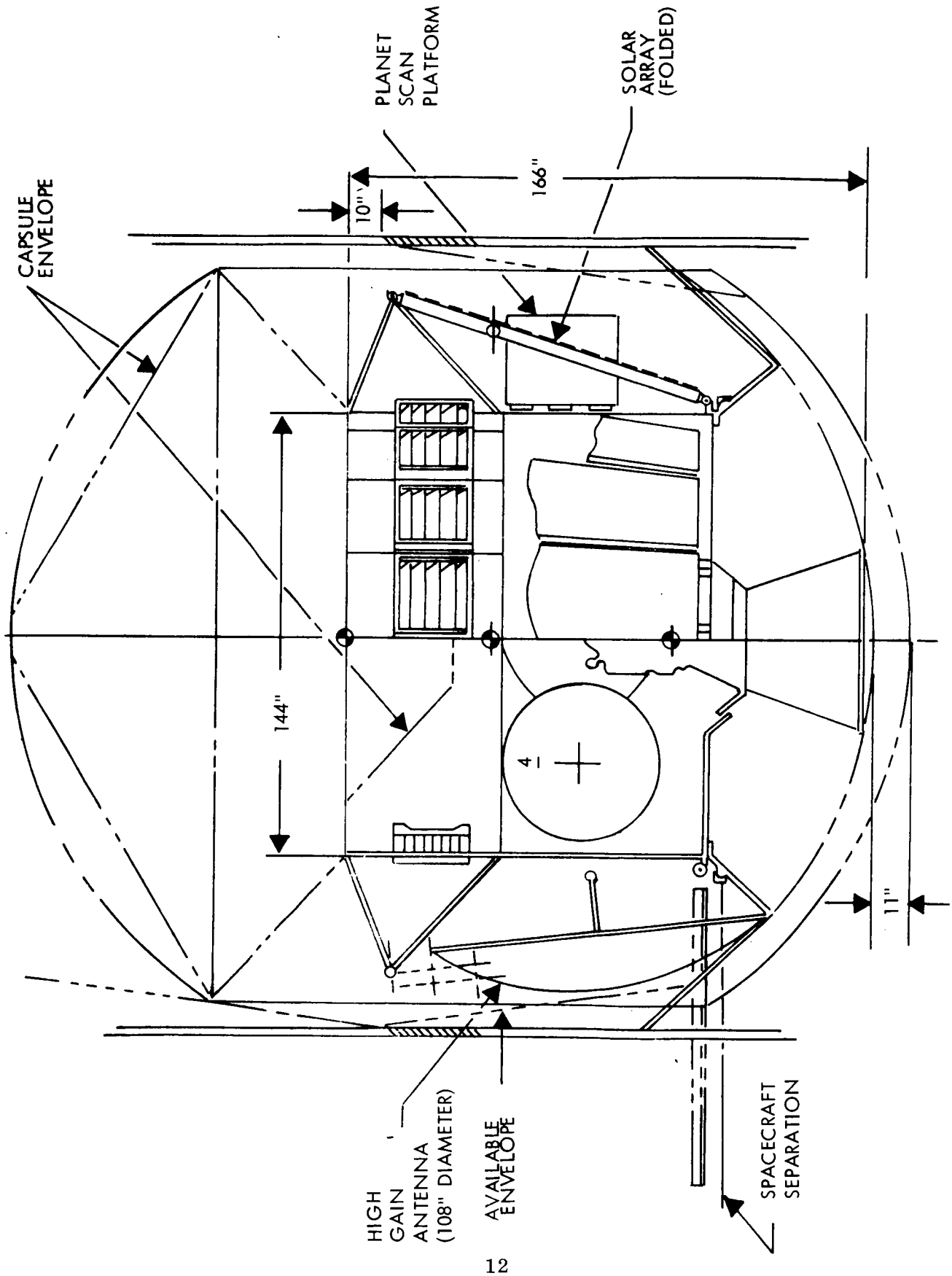

Figure 6. Concept 2 Type 3

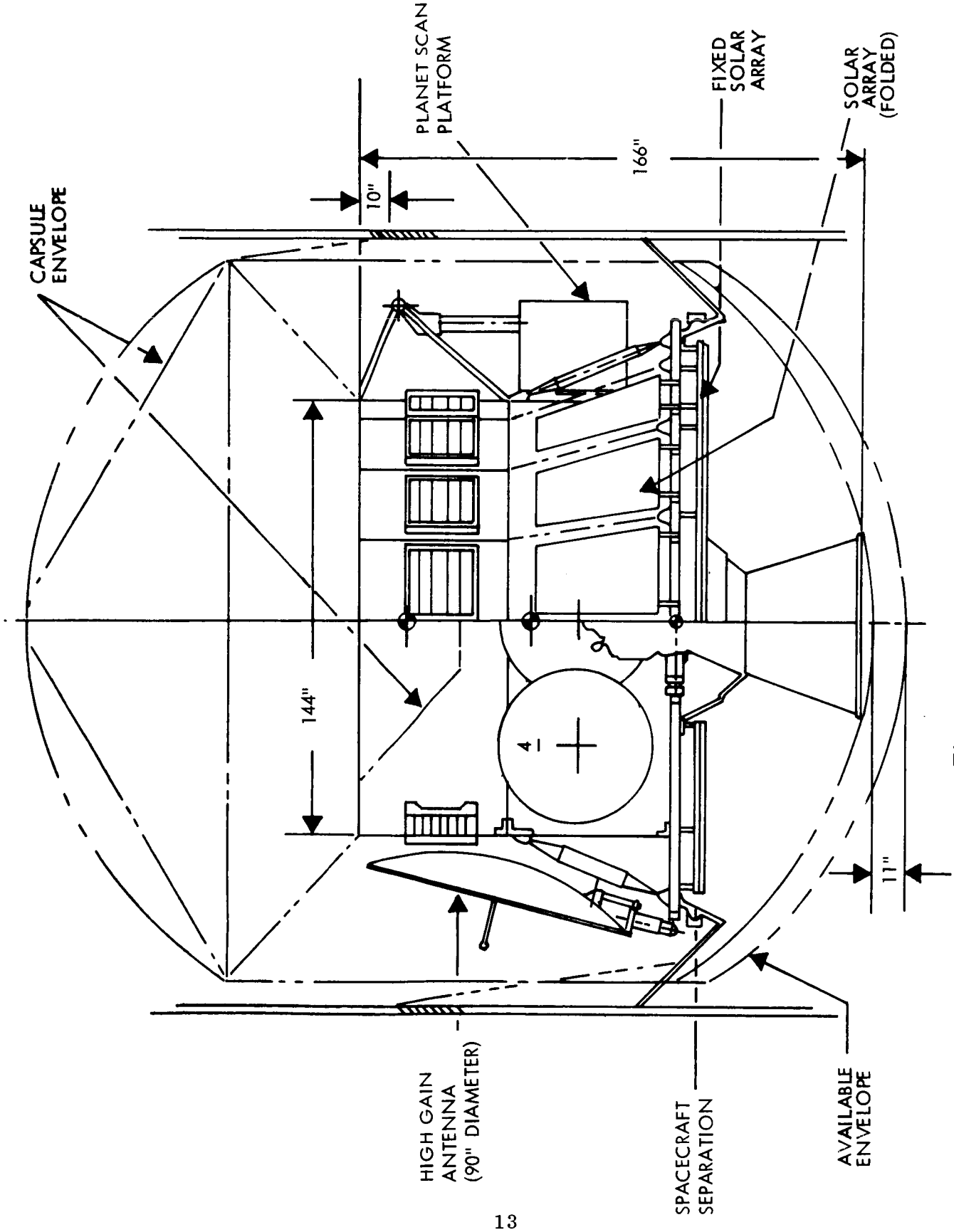

Figure 7. Concept 2 Type 4

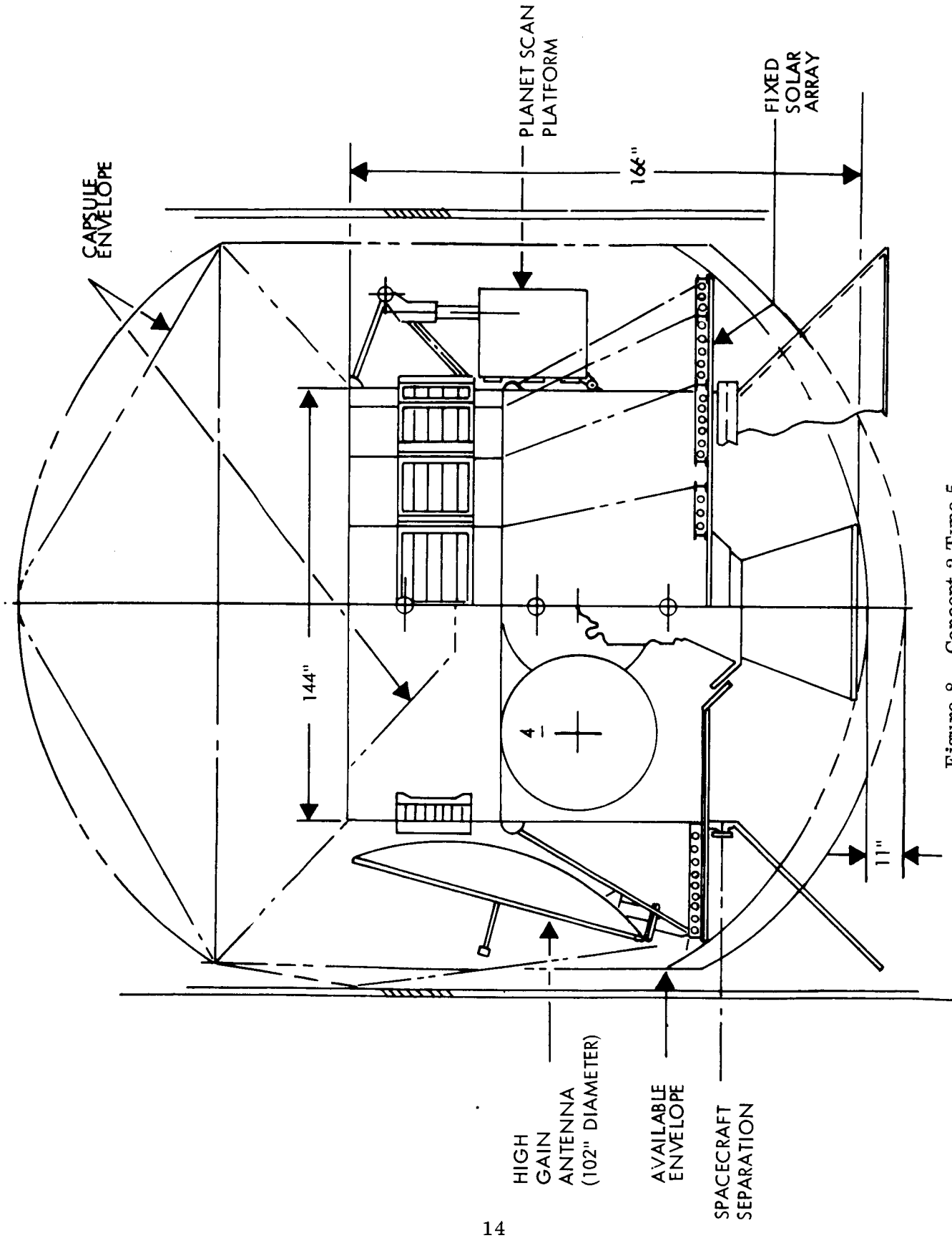

Figure 8. Concept 2 Type 5

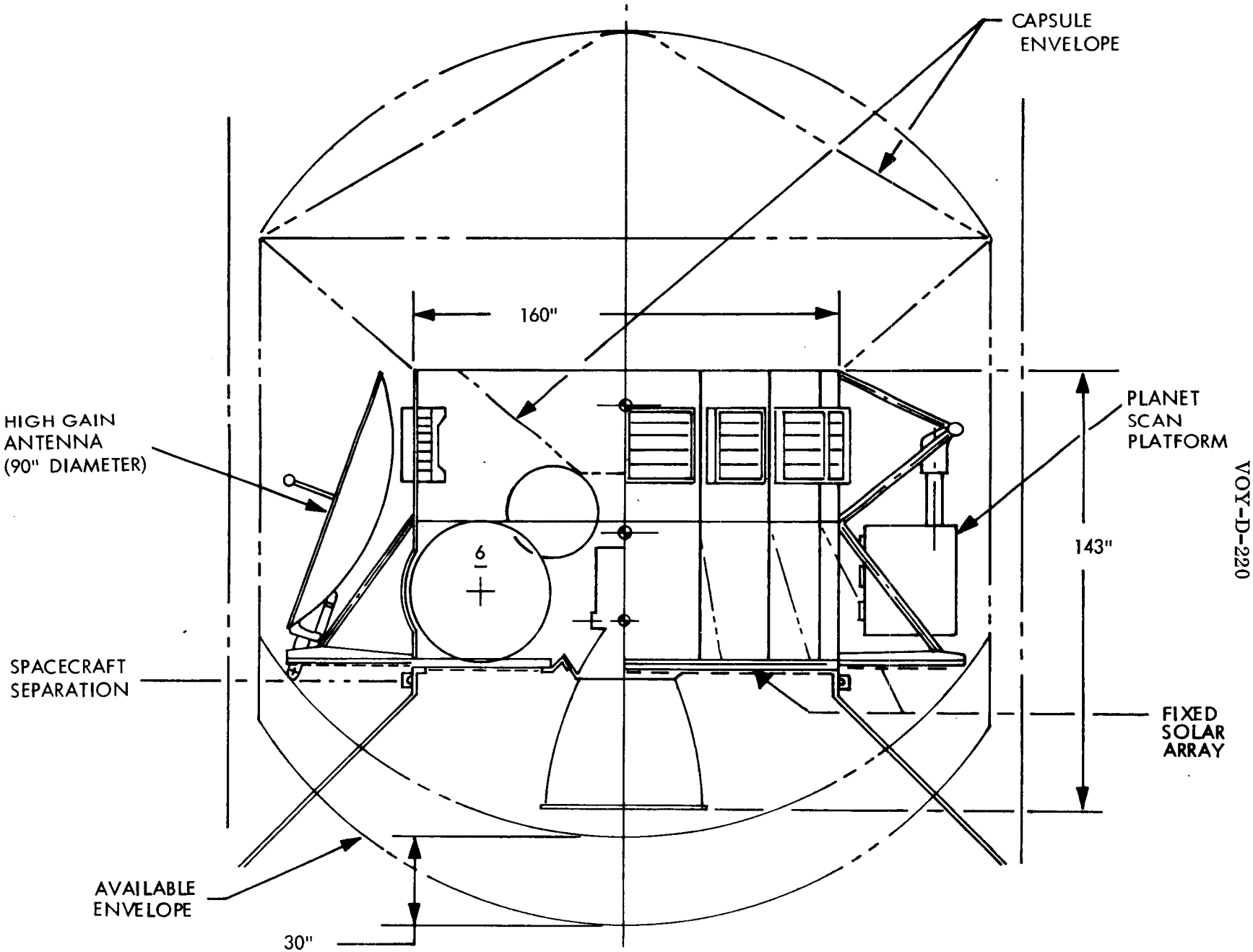

Figure 9. Concept 2 Type 6

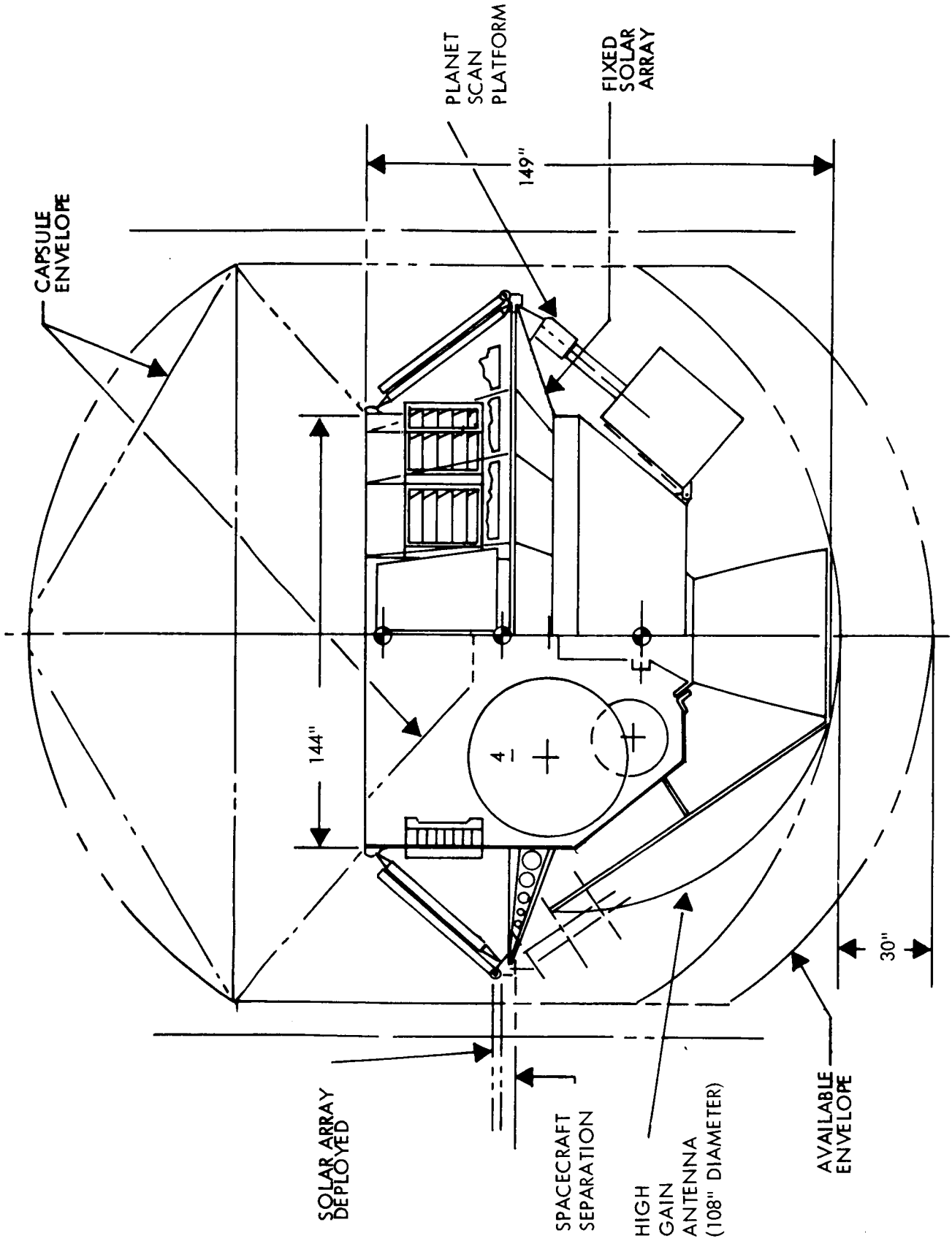

Figure 10. Concept 3 Type 1

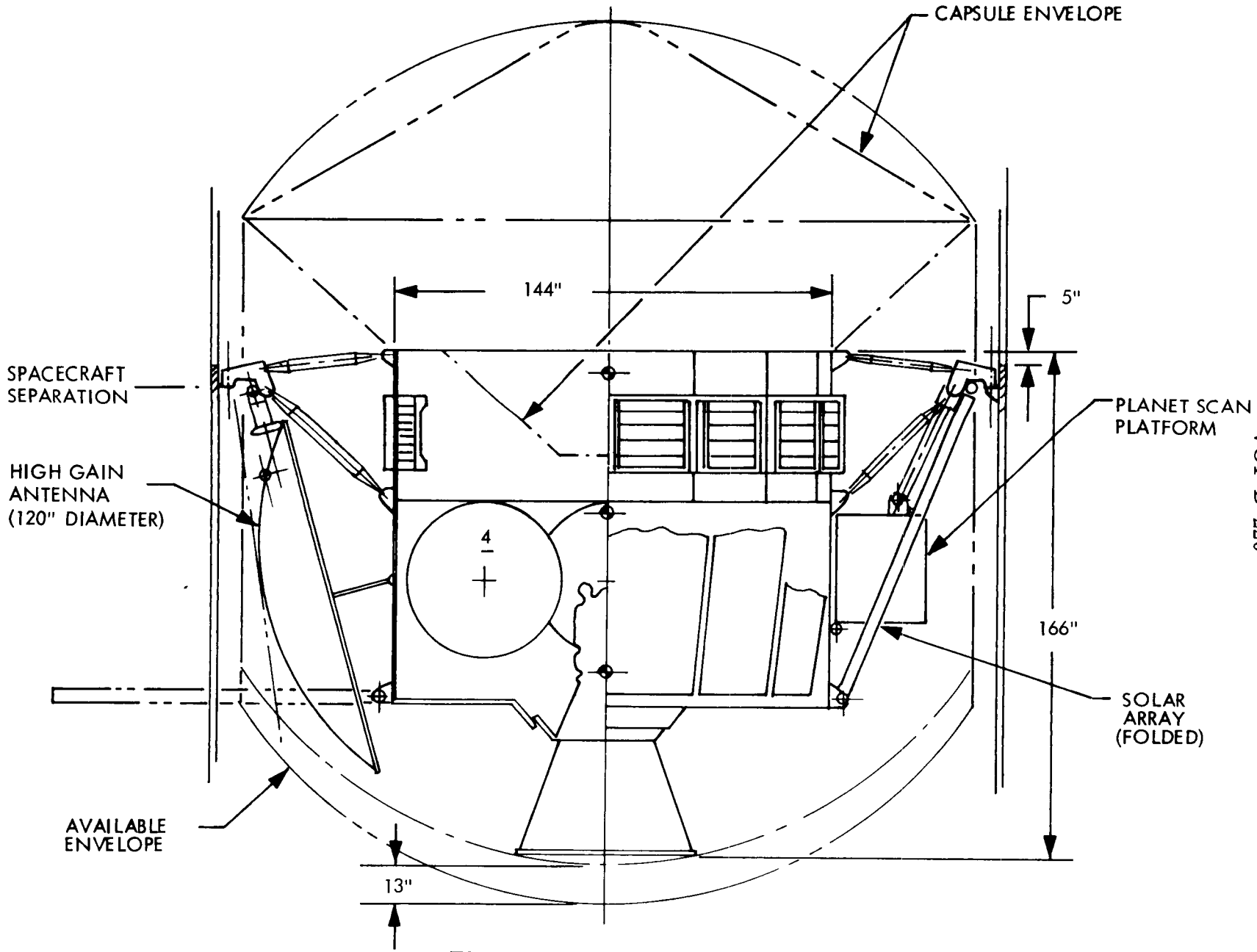

Figure 11. Concept 4 Type 1

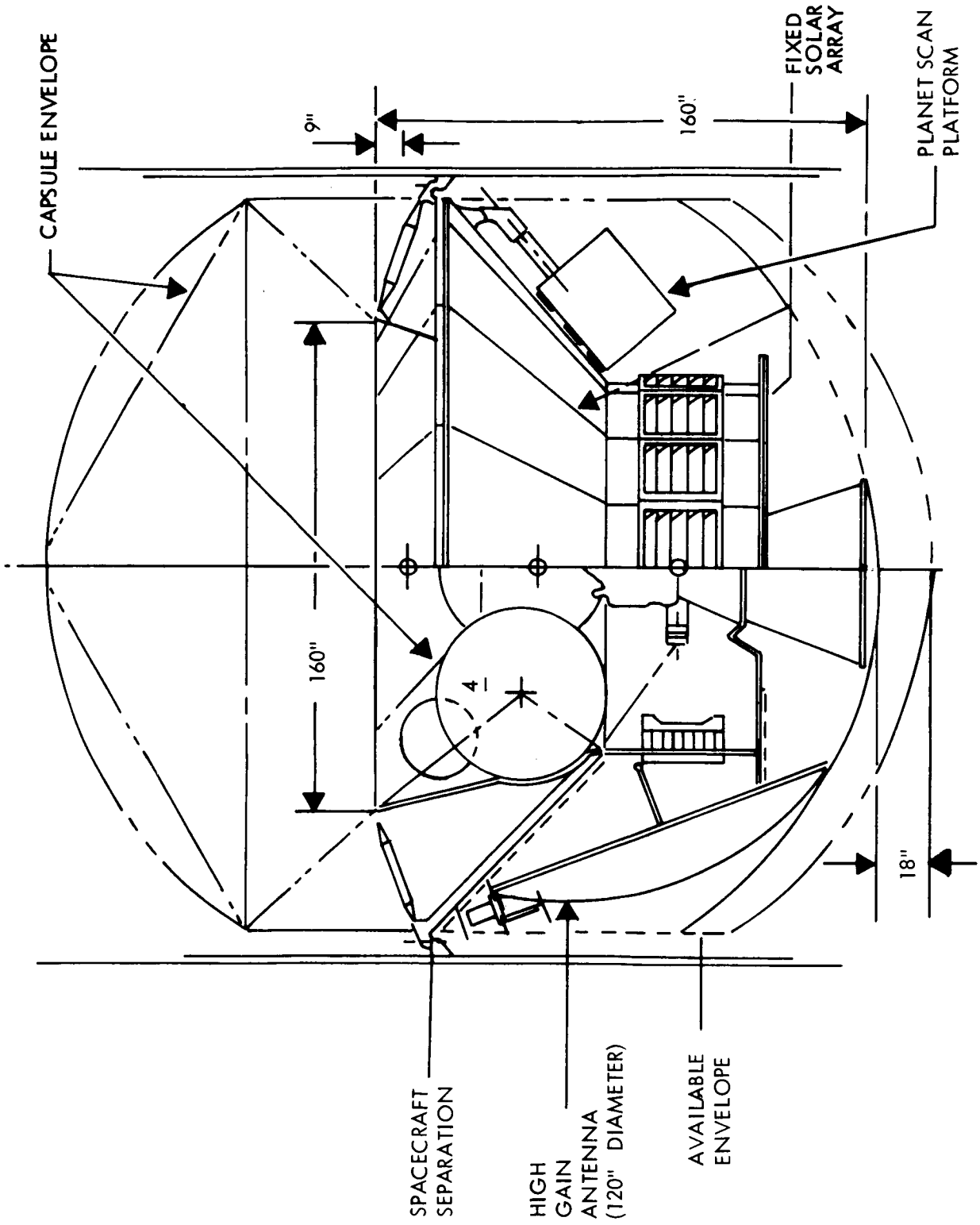

Figure 12. Concept 5 Type 1

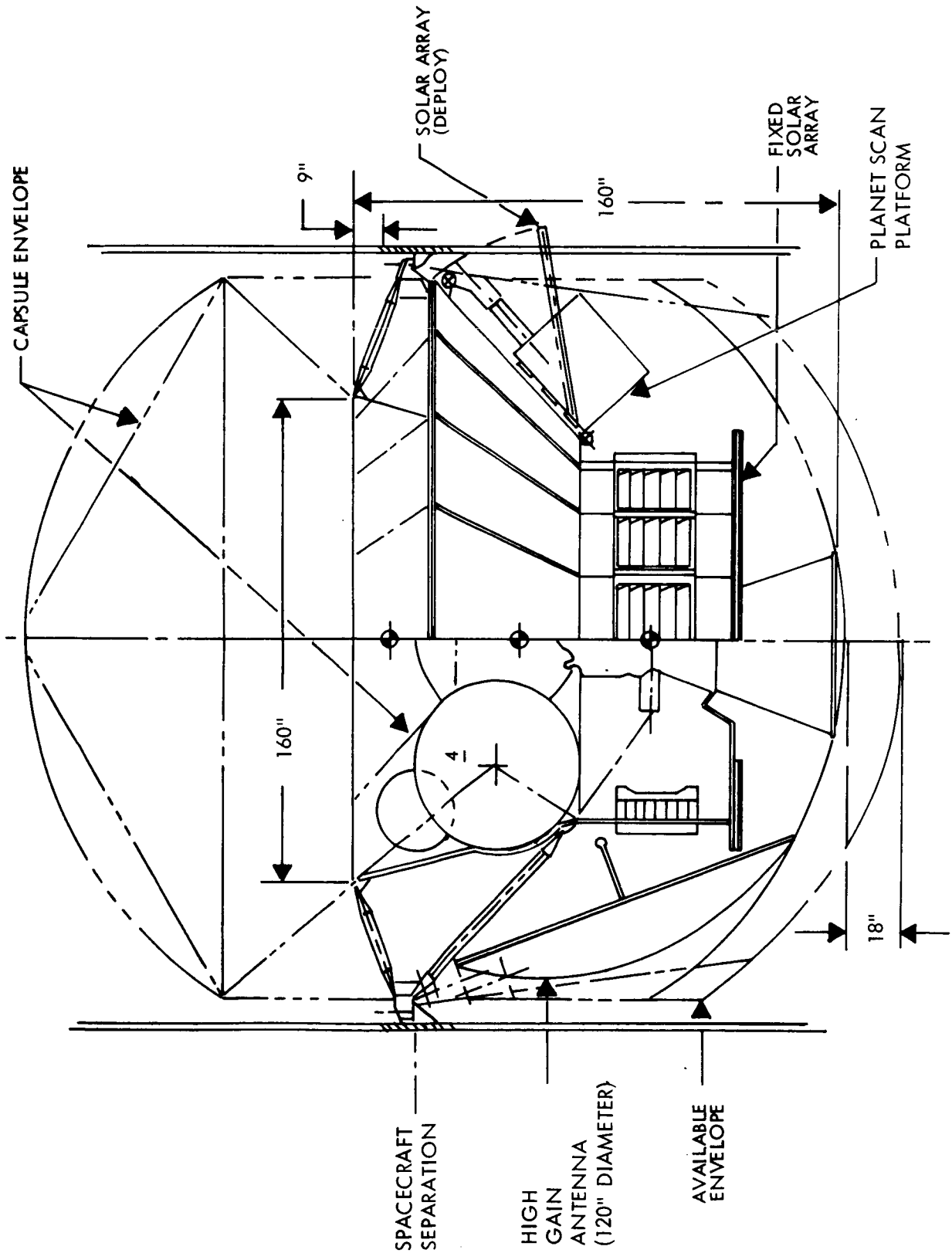

Figure 13. Concept 5 Type 2

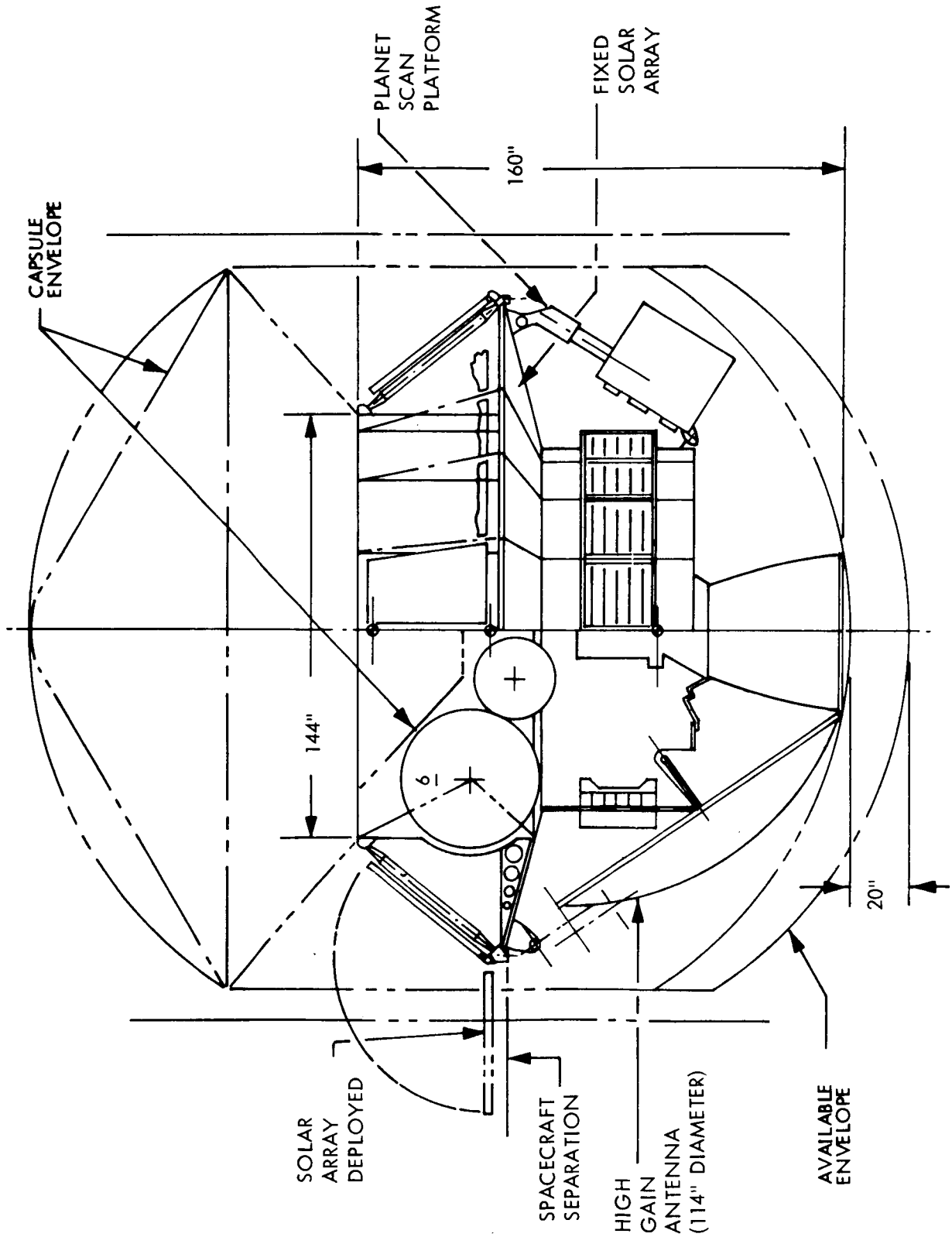

Figure 14. Concept 6 Type 1

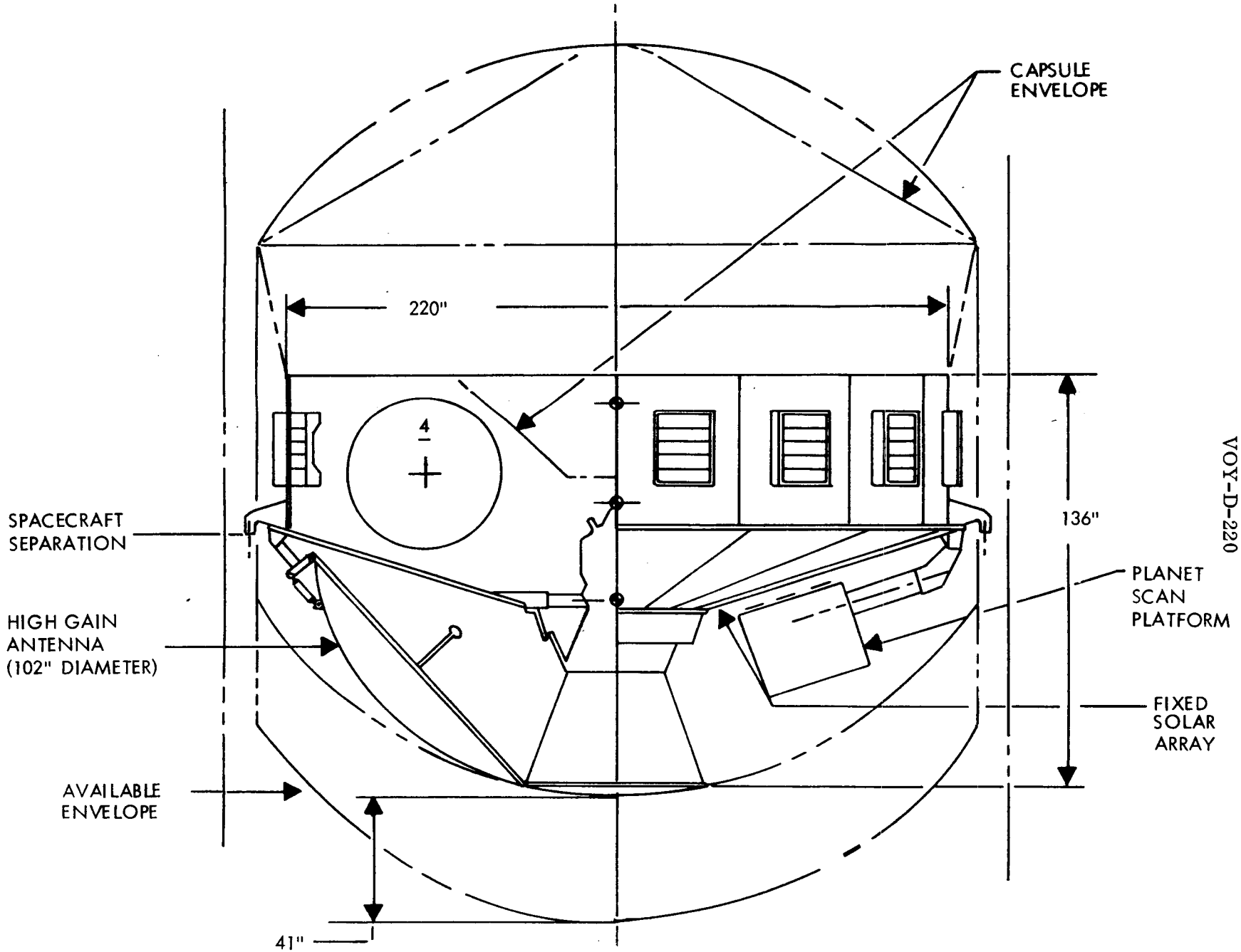

Figure 15. Concept 7 Type 1

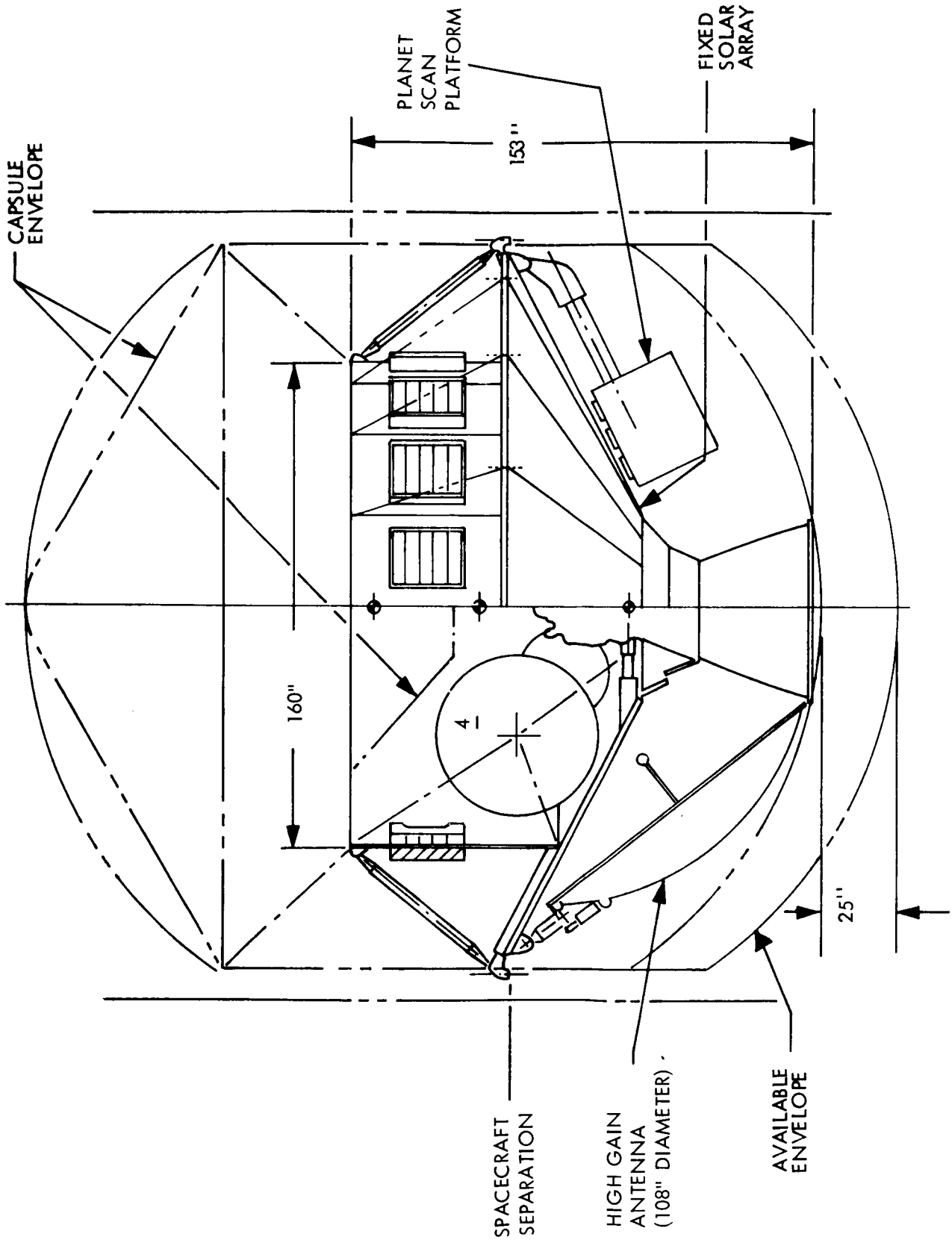

Figure 16. Concept 7 Type 2

criteria similar to that shown on Table 3 was used. The criteria are organized into mission constraints and competing characteristics in accordance with Reference 1. In Table 3, the criteria appear in order of decreasing importance.

2.2.3 Concept Screening

Where possible, numerical estimates of design parameters were computed for each of the fourteen configurations to aid in their evaluation. Some of the design parameter estimates are shown on Tables 4 and 5. It should be noted that due to the preliminary nature of the estimates, particularly in the area of weights, the absolute values may be in error. The differences in estimates between configurations are adequate for screening purposes. The screening was accomplished with contributions from representatives responsible for all major subsystems, systems, manufacturing, test, quality assurance, reliability assurance and program management.

The results of evaluating each candidate configuration, on the basis of these criteria, were tabulated and compared; concepts 2, 5, and 7 scored the highest. Table 6 indicates the advantages and disadvantages, that had the most impact on the screening results, for each concept. The merits of each concept, as exemplified by the best configuration in a particular concept family, are shown. As a result of the screening exercise, concepts 2, 5 and 7 were chosen for further development.

2.3 BASELINE CONFIGURATION SELECTION

Utilizing the then current results of mission and subsystem studies, the tentative configuration guidelines were updated to those shown on Table 7. Based on these guidelines, 1/20th scale drawings of the three candidate configurations were developed. During this effort, further consideration was given to the design and sizing of the primary structure including the propulsion support structure. Figures 17 through 19 illustrate these configurations. It became apparent during the screening process that modularity and its effect on schedule

Table 3. Configuration Evaluation Criteria

A. CONSTRAINTS

1. Quarantine
   - Ability to clean
   - Cold gas impact on separating bio-barriers
   - Capsule line-of-sight to spacecraft
   - Debris caused by moving parts in vicinity of capsule (louvers pinpullers, etc.)
2. Minimum Schedule Risk
   - Modularity
   - Manufacturing and test schedule contingency
   - Assemblability
   - Analyzability (to avoid surprises late in the development cycle)
   - Logistics
   - Development difficulties
   - Accessibility to electronics
   - Accessibility to propulsion
   - Minimum interface interactions
3. L/V and Launch Period
   - Weight

B. COMPETING CHARACTERISTICS

1. Probability of Success
   - Testability
   - Thermal performance
   - Number of deployments
   - Shroud and spacecraft separation
   - Autopilot control
   - Equipment locations (sensors, attitude control jets, antennas)

Table 3. Configuration Evaluation Criteria (Continued)

B. COMPETING CHARACTERISTICS (Continued)

2. Perform Mission Objectives
   - Antenna size
   - PSP viewing
   - Solar array power
3. Future Mars Missions
   - Interface with capsule RTG
   - Adaptable to spacecraft RTG
   - Mission flexibility
   - Growth in propulsion, antenna, power, PSP
4. Cost
   - Design
   - Manufacture
   - Test
   - Compatibility with available facilities
   - Logistics
5. Added 1973 Capability
   - PSP growth
   - Antenna growth
6. Other Planets
   - Meteoroid protection for Jupiter mission
   - Solar array temperature for Venus mission

risk would play a major role in configuration selection. To obtain a better understanding of the capabilities of the configurations in this respect, assembly breakdown studies were conducted for the three configurations. Figures 20 through 22 illustrate assembly breakdowns of the candidate configurations.

Table 4. Design Parameters

Design Parameters		Configurations													
		1-1	2-1	2-2	2-3	2-4	2-5	2-6	3-1	4-1	5-1	5-2	6-1	7-1	7-2
PV Weight (lb)		21311	21310	21251	21253	21352	21215	21326	21337	21341	21318	21354	21260	21237	21164
Adapter Weight (lb)		684	113	841	911	875	857	775	212	113	113	113	198	113	113
S/C Length (in.)		160	160	170	166	166	167	143	149	166	165	165	160	136	153
Δ Payld Mars Orbit (lb)		162	457	151	83	0	146	163	399	389	434	398	445	596	610
Shroud Sep Travel (in.)		87	85	85	89	85	90	80	54	55	59	59	54	57	57
Solar Array Area	Fixed	190	254	185	0	150	216	190	157	0	260	67	148	260	260
	Depld	64	64	65	338	90	64	64	103	350	0	283	60	0	0
Solar Array Temp Earth	R_i	160	160	163	163	160	160	160	168	163	140	168	168	240	140
	R_o	135	135	152	152	135	135	135	154	152	120	154	154		120
Solar Array Temp Mars	R_i	65	65	31	31	65	65	65	69	31	47	69	69	100	47
	R_o	45	45	23	23	45	45	45	56	23	29	56	56		29
No. of Elec Equip Bays		16	16	16	16	16	16	16	16	16	16	16	16	18/24	16
Wt Heaviest Bay (lbs)		75	75	75	75	75	75	75	75	75	75	75	75	63	75
Bay Dimensions (wdth x ht)		22.5 x 14.2	22.5 x 14.2	24 x 13.3	22.5 x 24.2	22.5 x 14.2	22.5 x 14.2	22.5 x 14.2	22.5 x 14.2	22.5 x 14.2	18 x 18	18 x 18	18 x 18	22.2 x 12.8	25.6 x 12.5
No. of PV Support Pts		Cone	16	Cone	Cone	Cone	Cone	Cone	16	16	16	16	16	24	16
No. Avail Cap Suppt Pts		16	16	16	16	16	16	16	16	16	16	16	16	24	16
No. of Propellant Tanks		4	4	4	4	4	4	4	6	4	4	4	4	6	4
HGA Diameter (in.)		96	96	90	96	90	102	90	126	132	132	132	114	102	108
CM Excursion Angle		$2^{\circ}10'$	$1^{\circ}50'$	$1^{\circ}25'$	$1^{\circ}40'$	$2^{\circ}4'$	$2^{\circ}20'$	$3^{\circ}25'$	$2^{\circ}10'$	$1^{\circ}50'$	$2^{\circ}10'$	$2^{\circ}13'$	$1^{\circ}10'$	3°	$1^{\circ}55'$

Table 5. Preliminary Estimates of Array Power

Config. No.	Proj. Area ft^2	Avg. Temp.	Power Density Watts/ft^2 (Mars at aphelion)	Est. Power Watts
1-1	254	52	2.97	754
2-1	318	52	2.97	944
2-2	250	25	3.16	790
2-3	338	25	3.16	1068
2-4	240	52	2.97	713
2-5	280	52	2.97	831
2-6	254	52	2.97	754
3-1	260	60	2.91	757
4-1	350	25	3.16	1106
5-1	260	35	3.08	801
5-2	350	60	2.91	1020
6-1	208	60	2.91	606
7-1	260	100	2.67	694
7-2	117 (insulated)	100	2.65	310
7-2	143 (non insulated)	35	3.08	443
7-2	259 (Total)			753

Table 6. Concept Merit

Concept	Major Advantages	Major Disadvantages	Order of Merit
1-1	• Simplicity • Fair modularity	• Heavier than most • Poor PSP viewing • Inferior accessibility • Poor separation	7
2-2	• Good thermal balance • Simplicity • Fair modularity	• Tended to produce heaviest designs • Poor PSP viewing • Less desirable sensor mounting locations • Poorer S/C separation • Small HGA	3
3-1	• Good PSP viewing • Good thermal performance	• Poor access to equipment bays • Tends to be heavy • Solar array blocks equipment bay on deployment failure	6
4-1	• Abundant solar array • Good thermal performance • Good modularity • Good access to propulsion • Good separation	• Poor PSP viewing • Difficult access to equipment bays • Poor antenna viewing • Possible line of sight between HGA and Capsule	4
5-1	• Very good modularity • Good HGA and PSP viewing • Good access to equipment bays • Good access to propulsion • Good assemblability	• Fair Solar array area • Fair thermal performance • Possible line of sight between HGA and Capsule	1

Table 6. Concept Merit (Continued)

Concept	Major Advantages	Major Disadvantages	Order of Merit
6-1	• Good access to equipment bays and propulsion • Good modularity	• Poor thermal balance • Difficulty mounting sensors	4
7-1	• Light weight • Good HGA and PSP viewing • Good thermal performance • No line of sight to capsule	• Limited access to equipment bays and propulsion • Questionable modularity • Fair electric power	1

Comparisons of the three configurations are based on the evaluation criteria of Table 7. Configuration 2-2 is inferior to the other two due to its higher weight, smaller high gain antenna, and more restrictive PSP viewing capability. The higher weight is a result of the cantilevered support and the large diameter, long length cylindrical section. The high gain antenna is restricted in size by the available length between array and capsule. From Figure 17 it is apparent that PSP viewing is limited by the large axial distance between the capsule and array. A serious logistics problem with this design is that the propulsion module is trapped between the equipment and support modules (see Figure 20). From a schedule contingency point of view, should the support and equipment modules be available, they cannot be mated and checked out until after the propulsion module is available.

It is interesting to note that the 2-2 configuration is very similar to the design recommended by General Electric at the conclusion of Task B. The bus wall diameter has been increased to 160 inches over the 120 diameter of Task B to accommodate the change to Liquid Propulsion System. The increase in spacecraft weight is primarily due to this diameter increase and the capsule weight increase to 7000 pounds. The axial distance between the capsule and solar array accommodates the 7.5 foot diameter HGA on Task B but is not adequate for the

Table 7. Final Configuration Selection Guidelines II

I. PROPULSION

A. LEMDE thrust chamber modified for Voyager

B. Propellant and pressurant weight and volumes
Propellant weight, 13,000 pounds
Propellant tankage volume, 196 cubic feet
Pressurant weight, 75 pounds
Pressurant volume, 29 cubic feet

II. DYNAMIC ENVELOPE

As described by MSFC Guidelines dated July 14, 1967.

III. SOLAR ARRAY POWER

The power available at Mars encounter plus 30 days with the maximum amount of fixed array will be determined. The additional array required to attain 700 watts, 800 watts, and 900 watts will be determined, along with its effect on weight and PSP viewing.

IV. HGA SIZE

The maximum antenna size attainable without cost (other than antenna and its support weight) will be mounted on each design. The maximum antenna size attainable without violating the dynamic envelope will be determined.

V. CM TO GIMBAL PLANE DISTANCE

A minimum of 40 inches between TCA gimbal plane and vehicle CM will be considered. Separations greater than 40 inches are desirable.

VI. EQUIPMENT BAY

Electronic packaging volume of 5 cubic feet will be used. A thermal radiation area of 3.2 square feet will be used for 16 bays.

VII. SEPARATION ENVELOPE

The clearance required for over-the-nose separation will be taken as per V-6230-SMK-097.

VIII. PLANET SCAN PLATFORM (PSP)

A PSP volume of 15 cubic feet and weight of 300 pounds will be used.

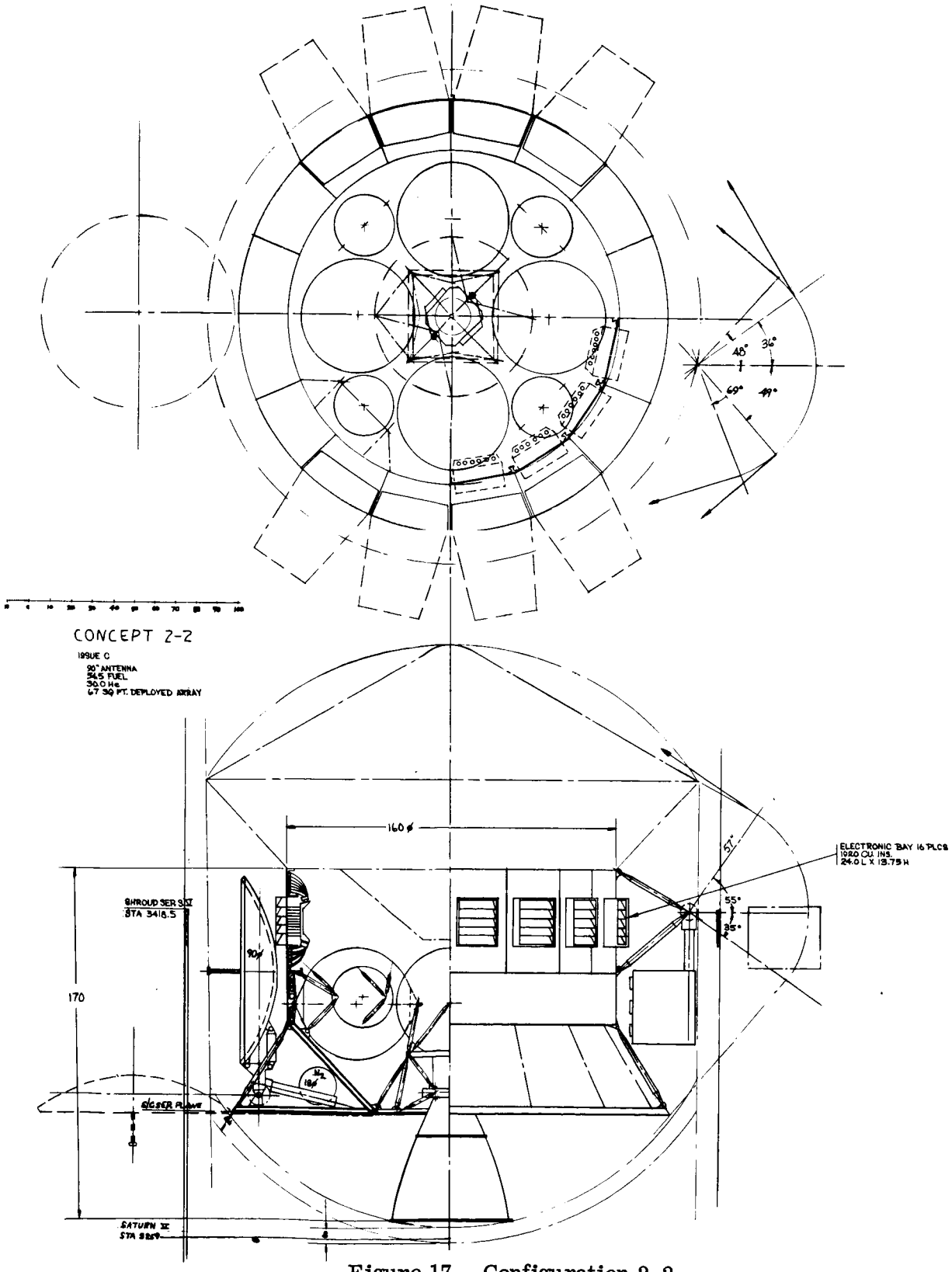

Figure 17. Configuration 2-2

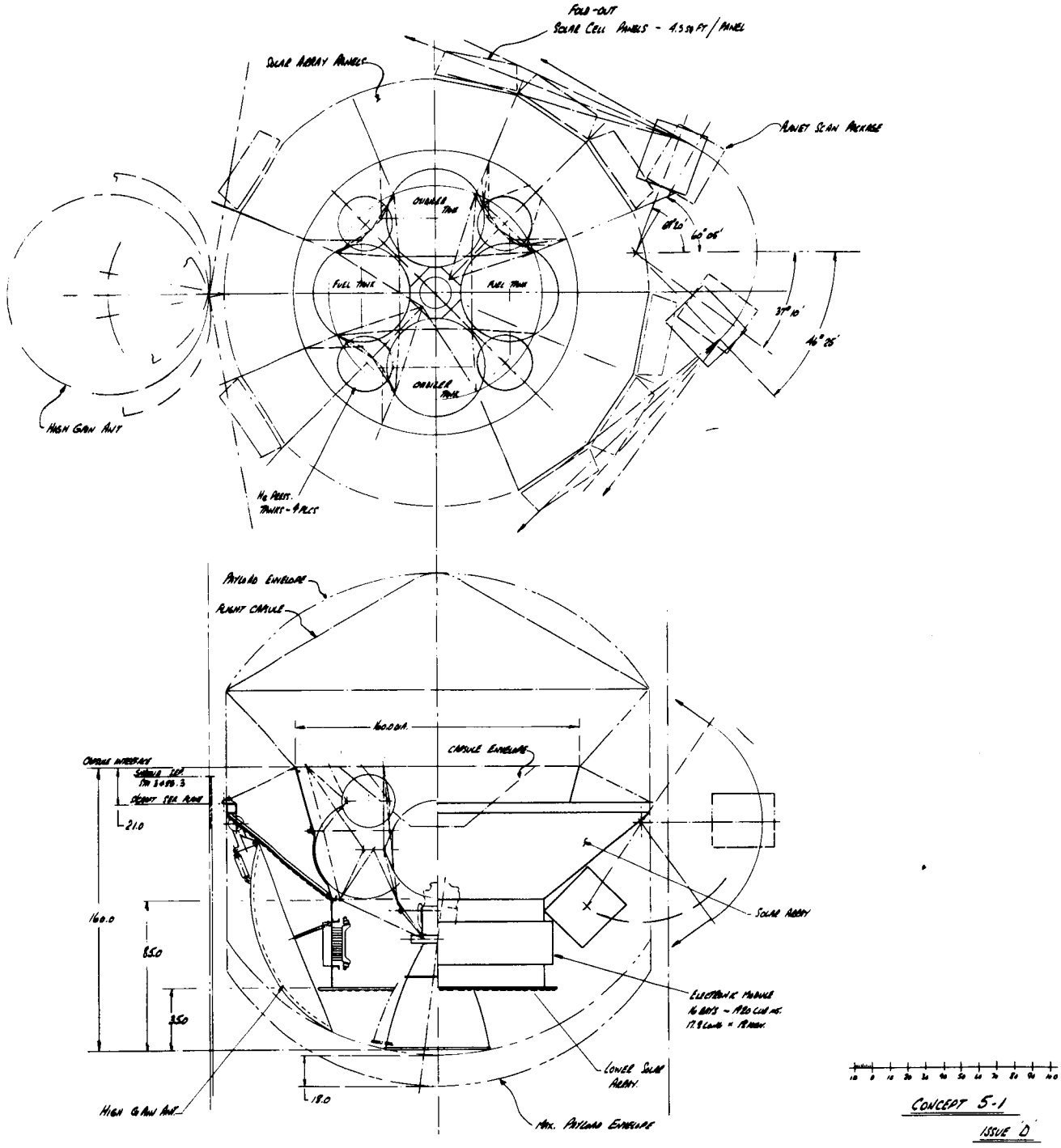

Figure 18. Configuration 5-1

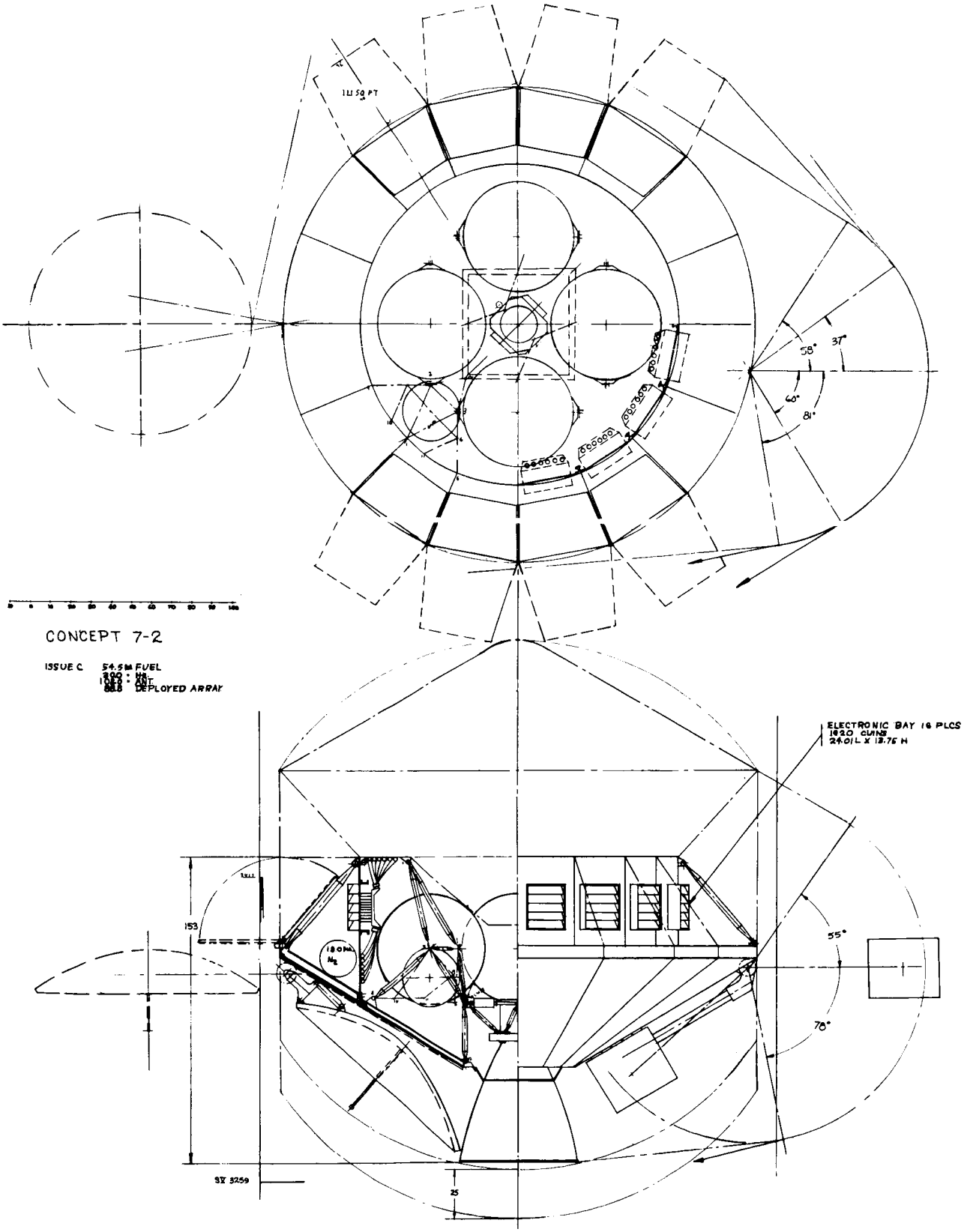

Figure 19. Configuration 7-2

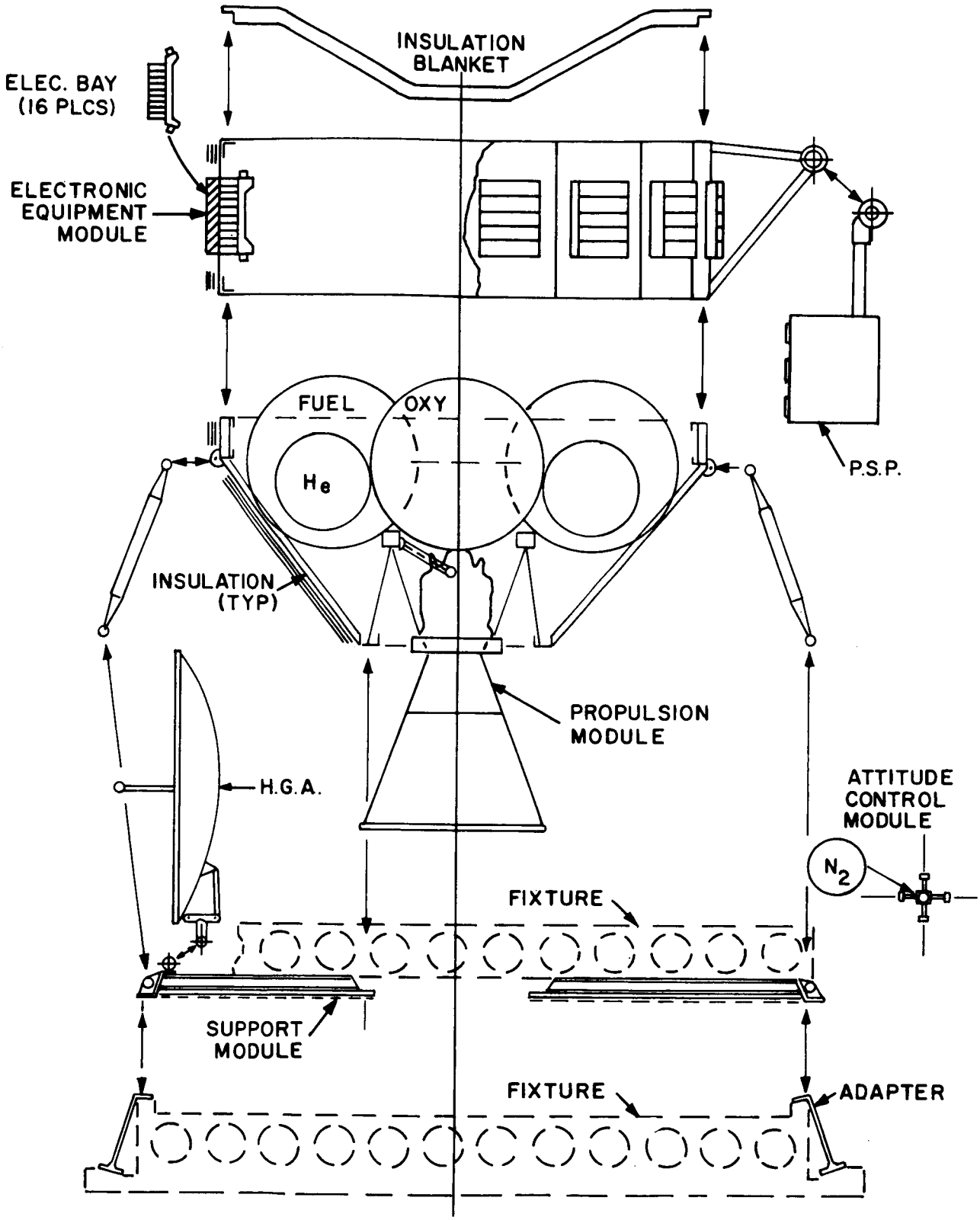

Figure 20. Configuration 2-2, Assembly Breakdown

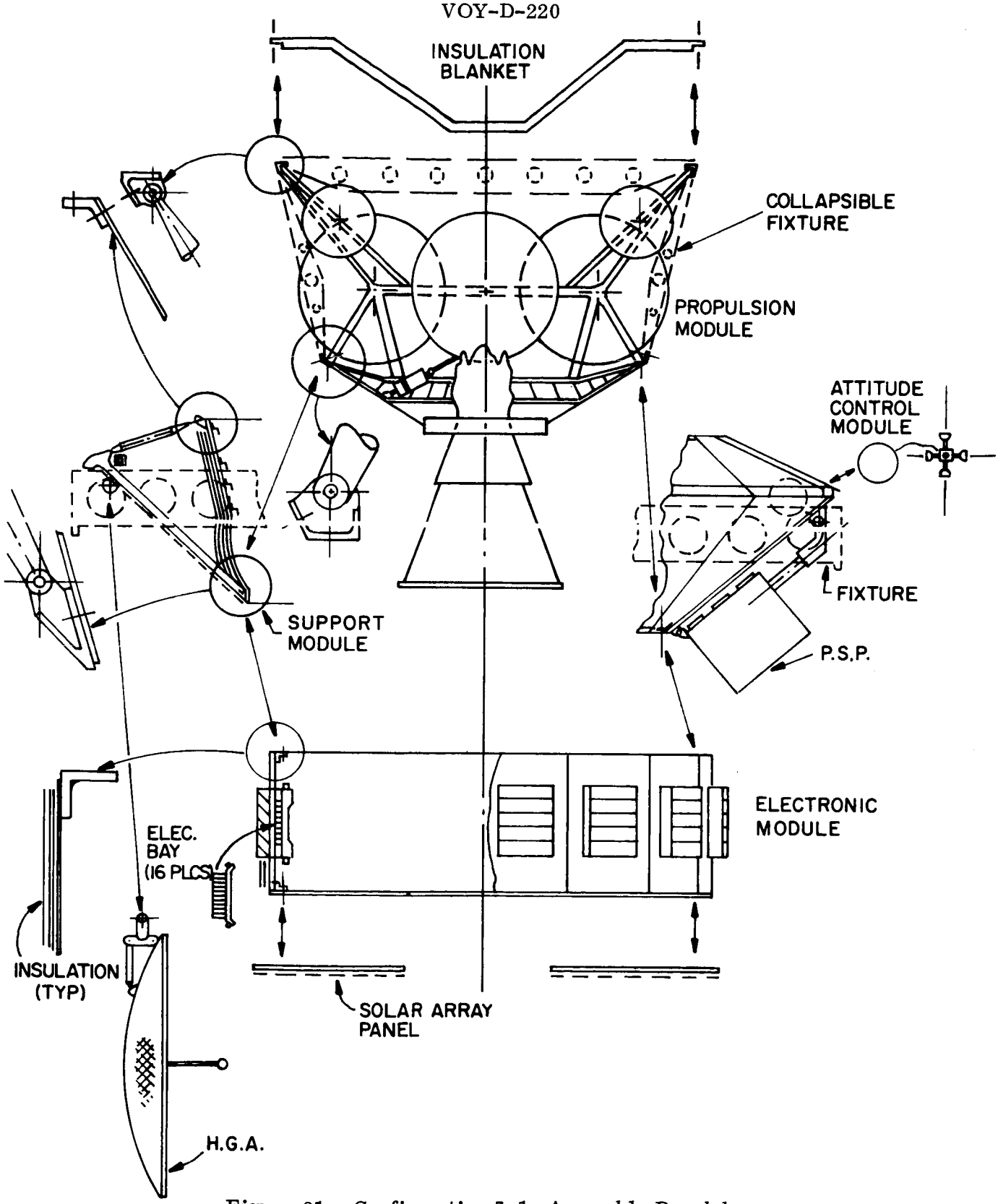

Figure 21. Configuration 5-1, Assembly Breakdown

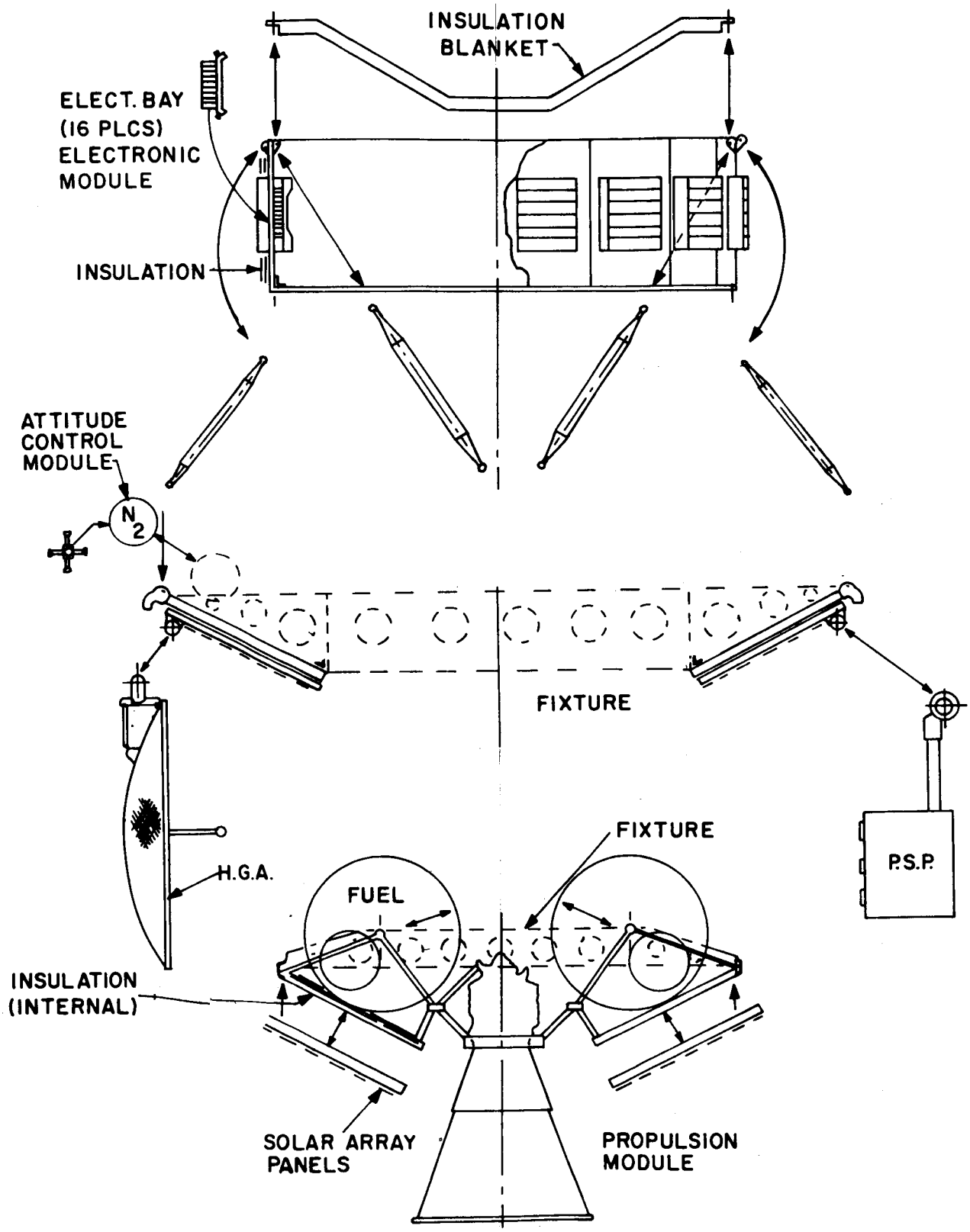

Figure 22. Configuration 7-2, Assembly Breakdown

larger HGA now desired. Over the nose shroud separation in lieu of a clam shell arrangement also makes the large axial distance between capsule and solar array less desirable.

With respect to the competing characteristics category of the evaluation criteria (Table 3), only small differences remain between configurations 5-1 and 7-2. The principal difference between the two configurations is in the minimum schedule risk and launch period categories. The 7-2 configuration is slightly lighter than the 5-1 design. However, in the 5-1 design, the major modules are more self-sustaining (Figure 21). This feature leads to less complex handling and assembly procedures. In addition, the 5-1 configuration has excellent access to the equipment bays and propulsion system in the assembled stage. In view of the large period of time (approximately 4 years) devoted to manufacture and test of the spacecraft, these features are considered most seriously. It is primarily for these advantages that the 5-1 configuration was selected as the baseline design.

3. BASELINE DESIGN DEVELOPMENT STUDIES

Post configuration selection trade studies were performed to:

- Locate the optimum planetary vehicle support point relative to the spacecraft.
- Improve modularity.
- Evaluate the merits of aft biobarrier removal after capsule separation.

3.1 CONFIGURATION MODIFICATION

One difficulty remaining with the 5-1 configuration is that there is a line-of-sight between the large deployed antenna and the top of the capsule while the bio-barrier is off. This results in a potential quarantine problem as discussed in VOY-D-273. The problem could be removed by lowering the PV support point. The items considered in this trade study are:

- Reduction in structural and solar array weight as a function of lowering the support location.

- Equipment bay heat rejection capability, spacecraft thermal gradient as a function of support location.
- Fixed solar array electrical power as a function of support location.
- Maximum antenna size as bounded by capsule line-of-sight and envelope restrictions as a function of support point location.
- HGA viewing capability as a function of support point location.
- PSP viewing and stowage considerations as a function of support point location.
- Additional deployed solar array capability as a function of support point location.

Raising or lowering the planetary vehicle - shroud interface location, over the range considered, has little effect on the spacecraft thermal performance, fixed solar array electric power, HGA viewing, or PSP viewing and stowage. Figure 23 illustrates the capsule line-of-sight bound and envelope restriction on the antenna size as a function of support point location. Figure 24 shows the reduction of weight and increase in deployable solar array capability as the support point is lowered. The decreased weight is primarily due to the decreased total solar array area for the same projected area. The increased solar array deployment capability depends on the increased distance between the capsule interface envelope and support points. Figure 25 is a combination of these two figures. The design point chosen, indicated by a star, results in a 15-inch drop in support point location while maintaining a 114-inch diameter antenna. At this design point, the line of sight difficulty is removed, and sufficient deployable solar array is available to allow removal of the fixed array under the equipment module. This permits increased accessibility to the electronic bays and propulsion unit and some reduction in propulsion nozzle weight due to decreased insulation requirements.

The assembly breakdown, Figure 21, shows the propulsion module supported by collapsible fixtures. Removal of these fixtures from inside the spacecraft complicates assembly procedures. This problem is overcome by making the conical shell a permanent part of the

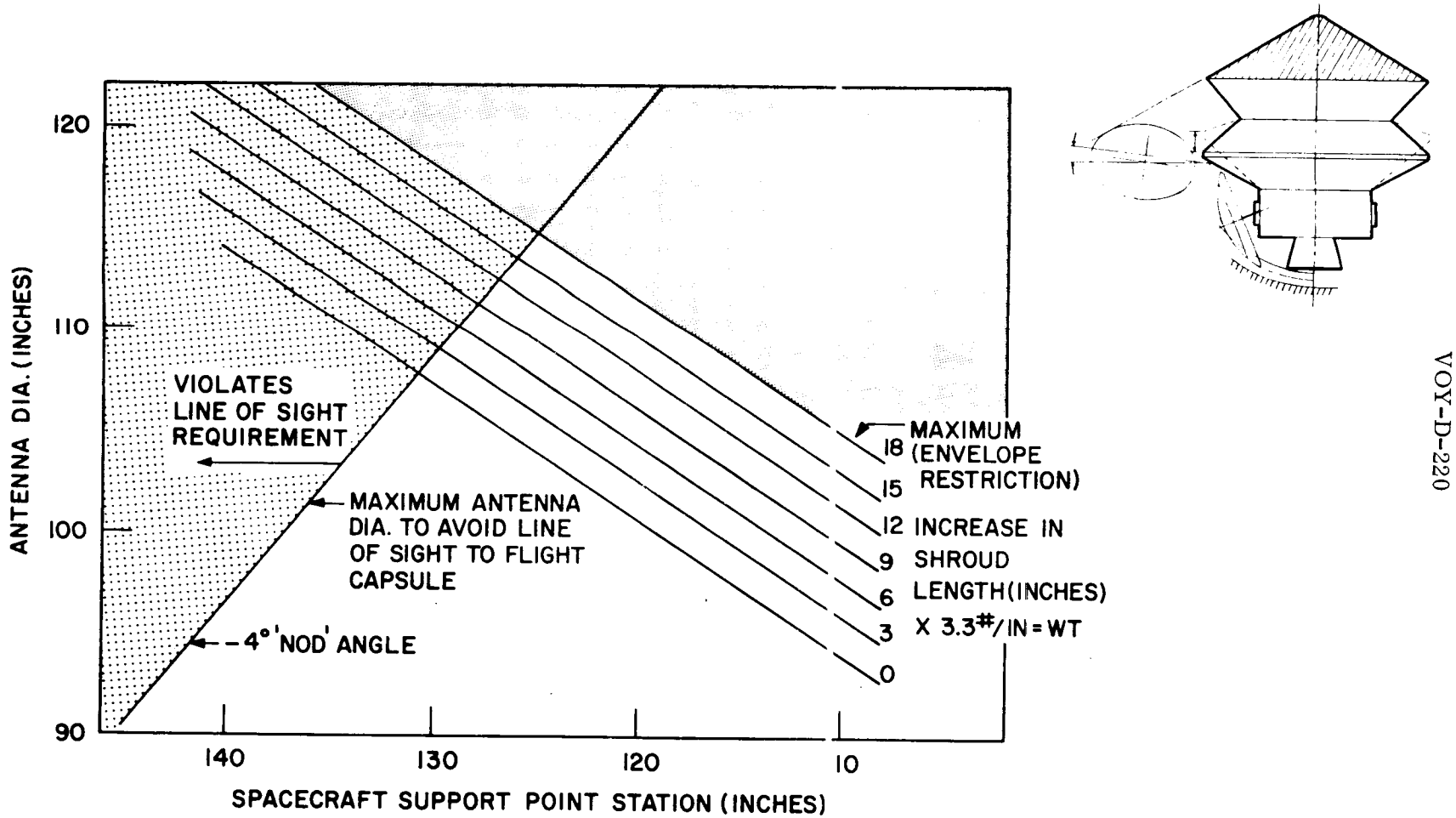

Figure 23. Antenna Diameter Versus Support Point Location

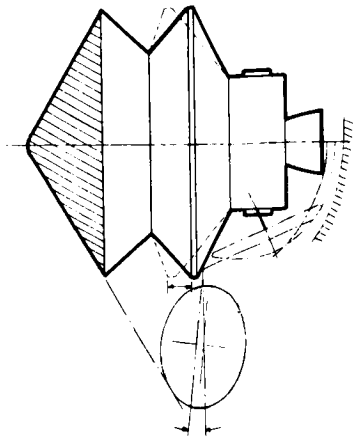

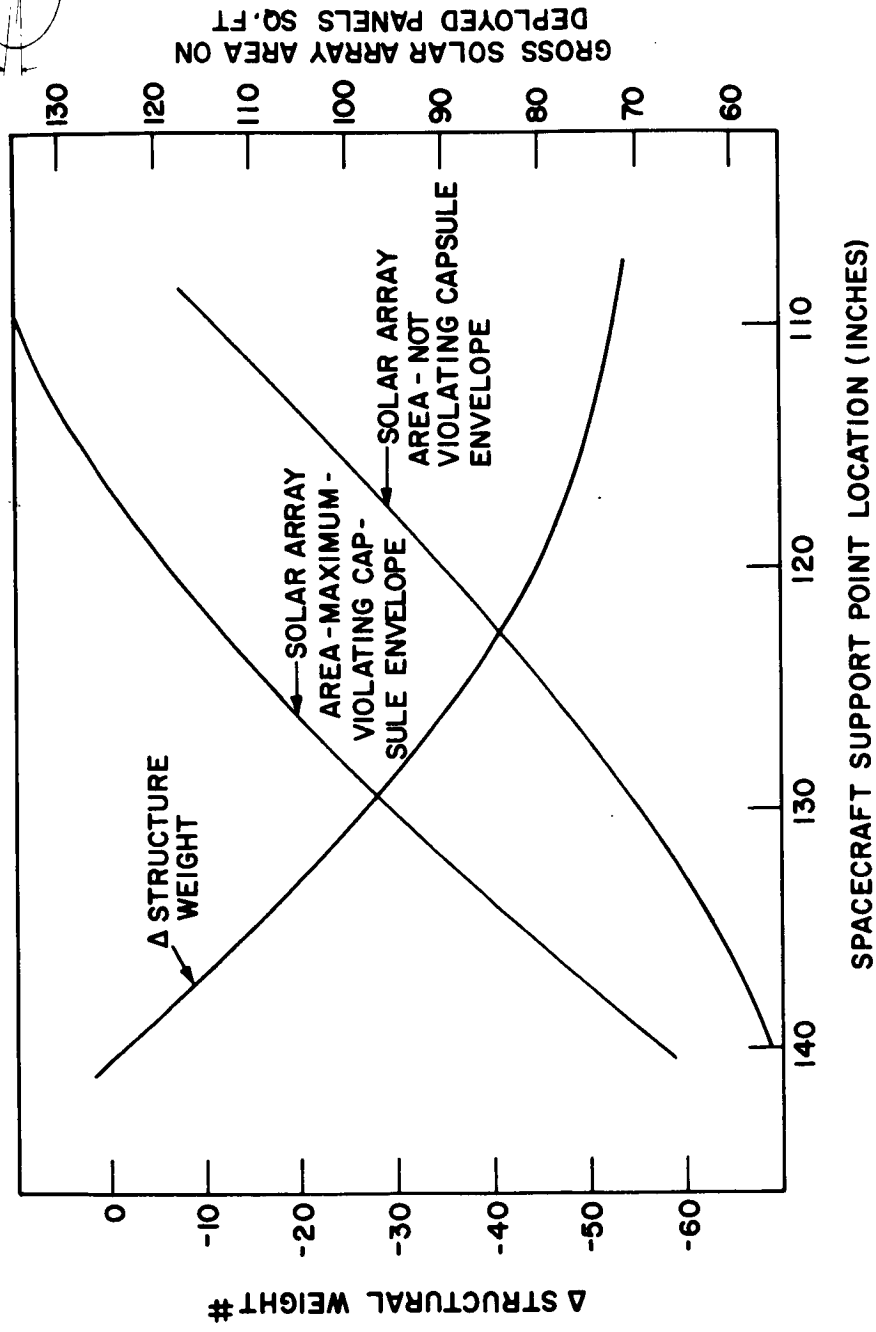

Figure 24. Weight and Array Area versus Support Point Location

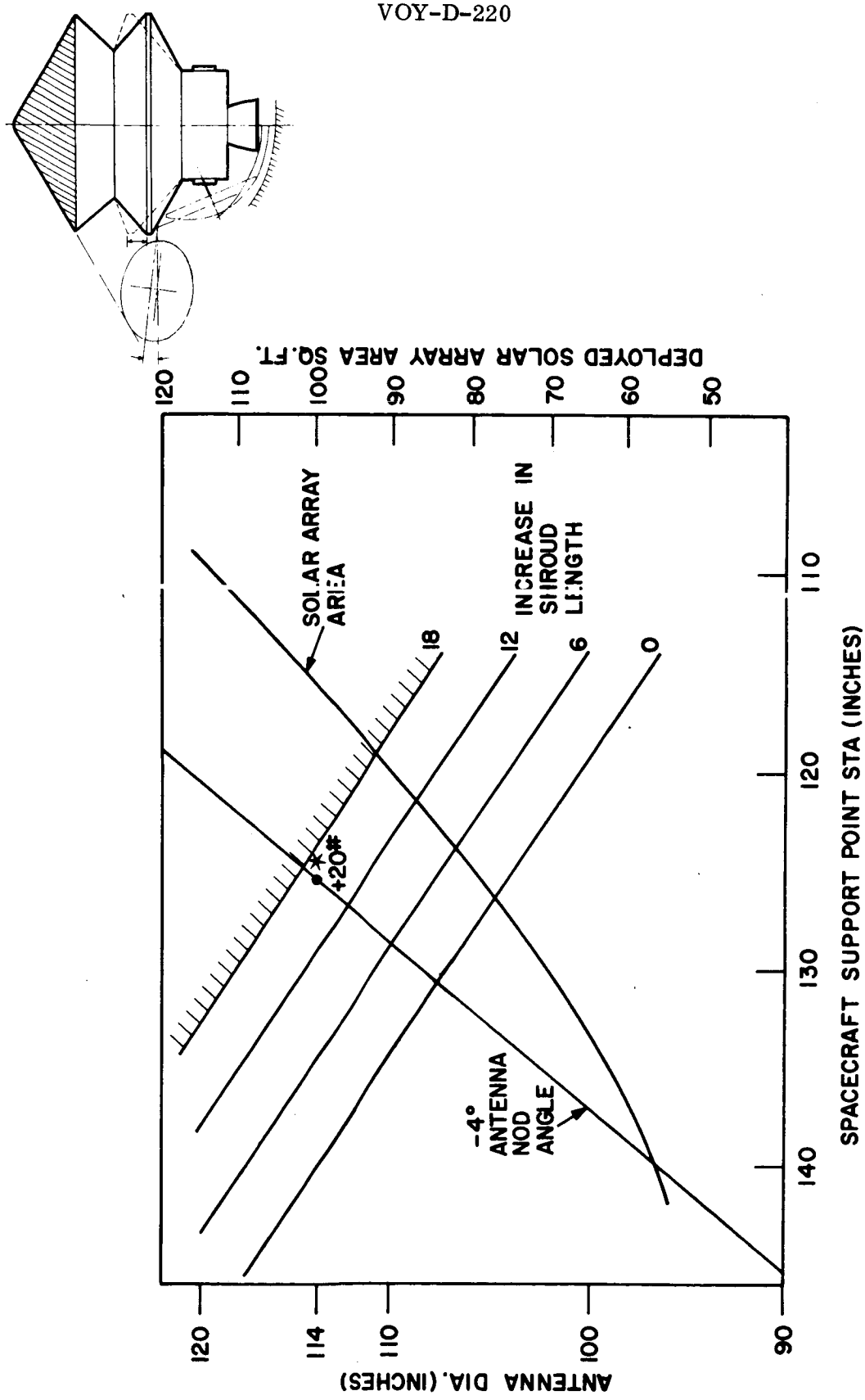

Figure 25. Truss Point Location Trade-off

propulsion module. The support module is stiffened by jury struts connecting the three rings as shown in Figure 26.

With the elimination of the solar array from beneath the electronic module, as described earlier, all solar panels are consolidated on the support module. Also since access to the inside of the equipment module is facilitated, the equipment bay electrical connectors were turned inward. The more difficult access to the connectors through hand holes from the outside is avoided. Figure 27 illustrates access to the connectors.

3.2 AFT BIO-BARRIER SEPARATION

The question of whether the aft bio-barrier should be left on the spacecraft or separated after the capsule has been ejected was the subject of a trade-off study. The basic areas of consideration taken into account were: (a) Planetary Quarantine, (b) Thermal, (c) Micro-meteoroid protection, (d) Mass property changes, (e) Reliability, (f) Planet Scan Platform (PSP) viewing. Figure 28 is a schematic diagram of the spacecraft with the aft bio-barrier broken into two main sections, with the "A" section being that portion of the barrier which is adjacent to the thermal blankets, and section "B", that area of the barrier which is essentially a fin when the capsule is ejected, leading to large heat leaks from the spacecraft.

To show each investigated area in its proper perspective, the total trade-off considerations may be written as a function of each area's preference with a weighting factor applied to the particular area in question.

3.2.1 Quarantine Consideration

Preferred Operation: Aft bio-barrier left attached to the spacecraft. The barrier has a periapsis altitude of 1000 KM, weighs 500 pounds with a frontal area of 314 square feet, and an associated drag coefficient of approximately 2. The M/C_DA is 0.025 slugs/ft^2. From Figure 29 it can be shown that the orbit lifetime of the barrier before decay into the atmosphere would be in the vicinity of 10^7 years. Therefore, contamination of the planet by the

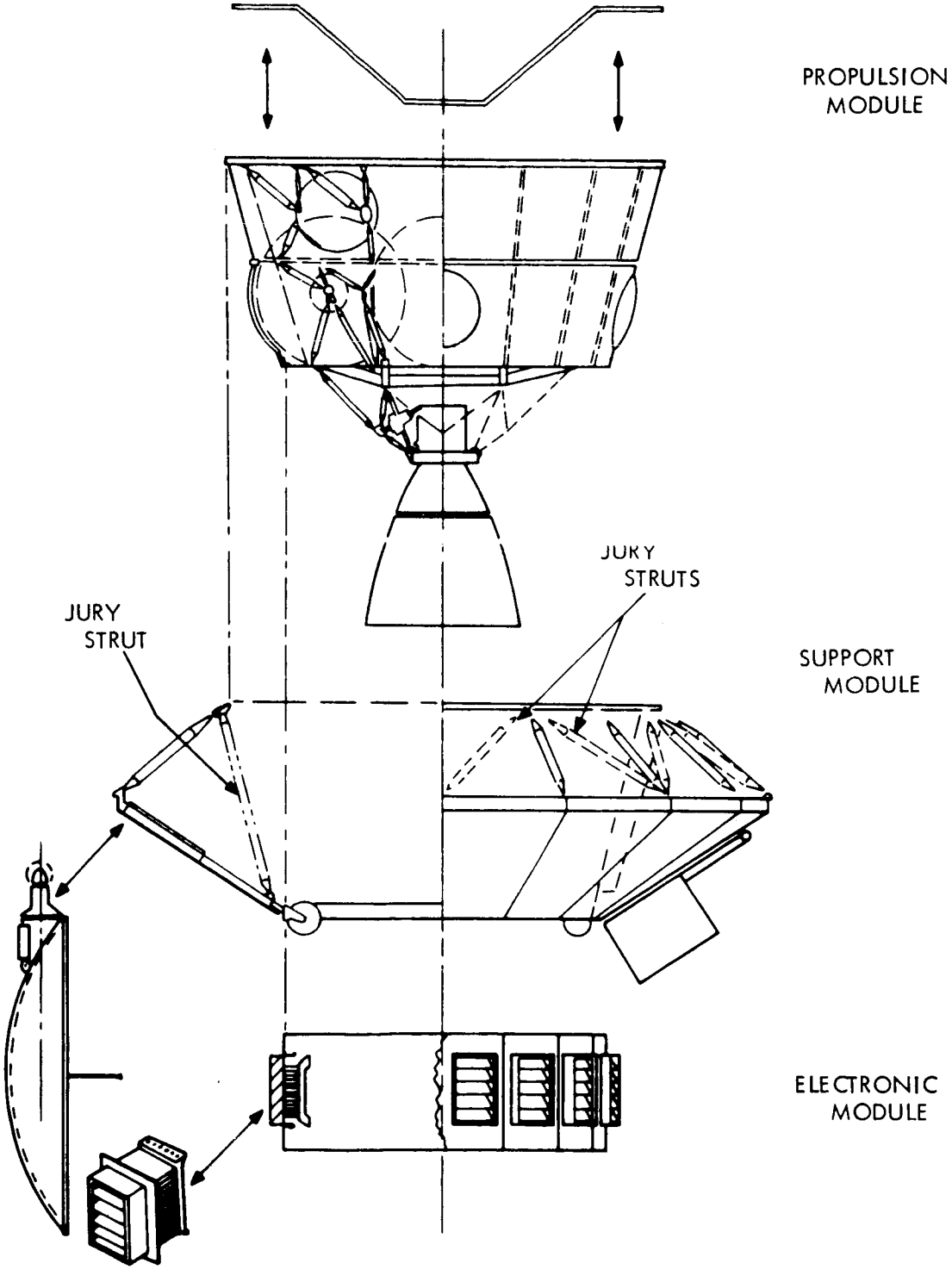

Figure 26. Support Module Jury Struts

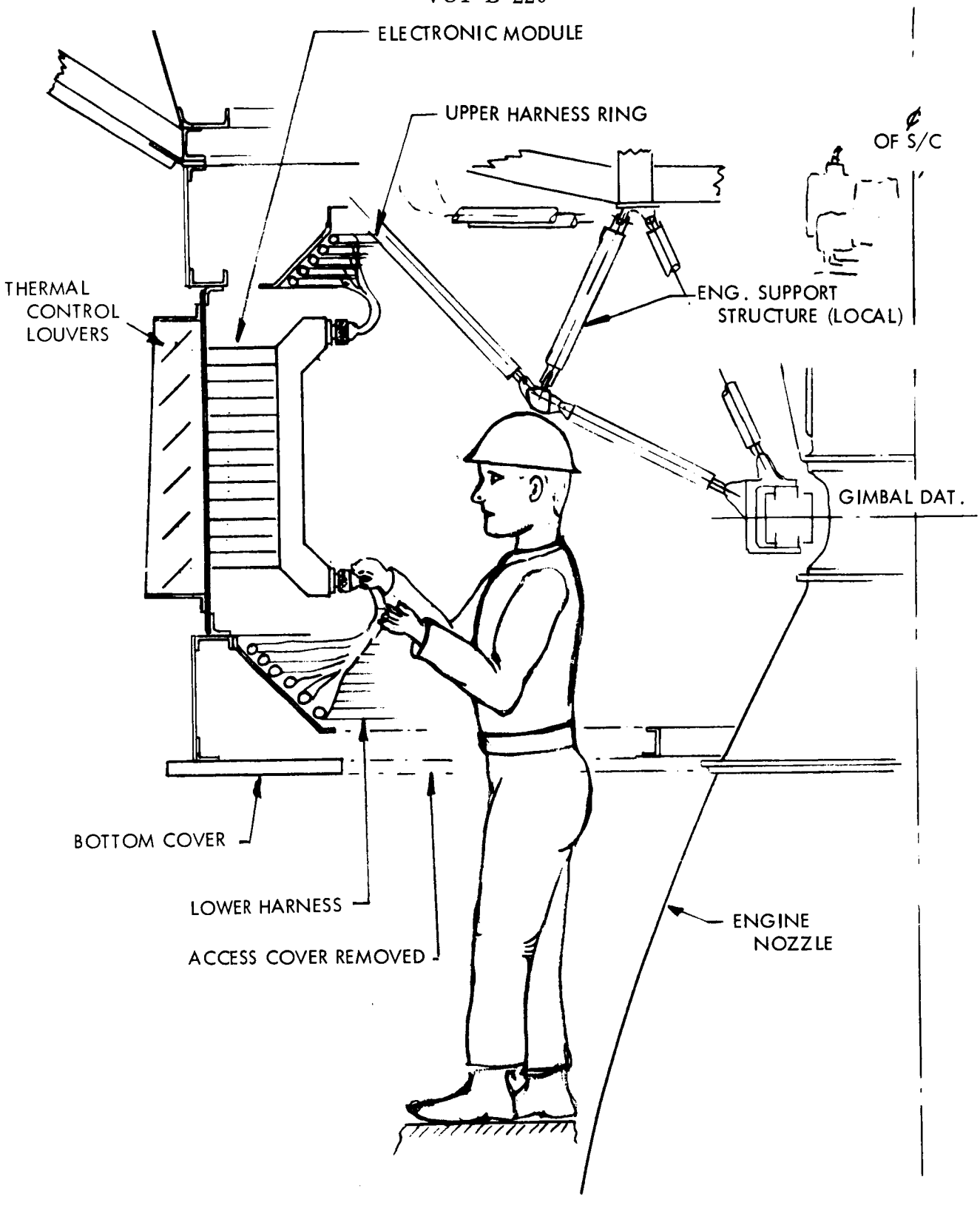

Figure 27. Electronic Module Access

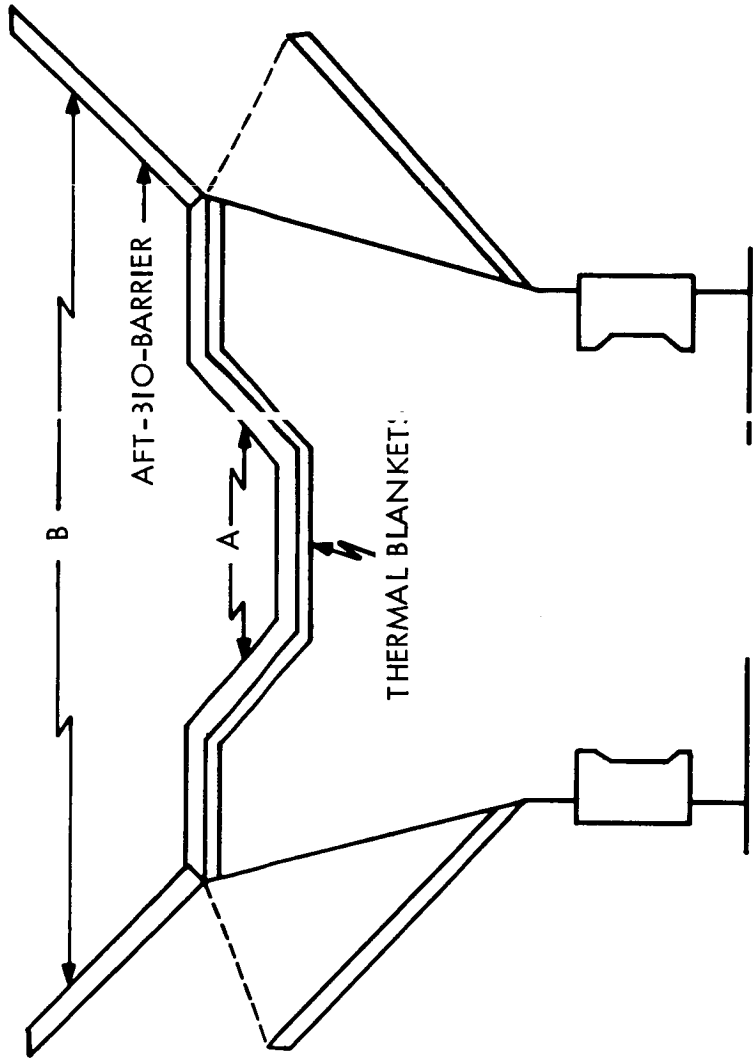

Figure 28. Schematic Showing Bio-Barrier in Two Sections

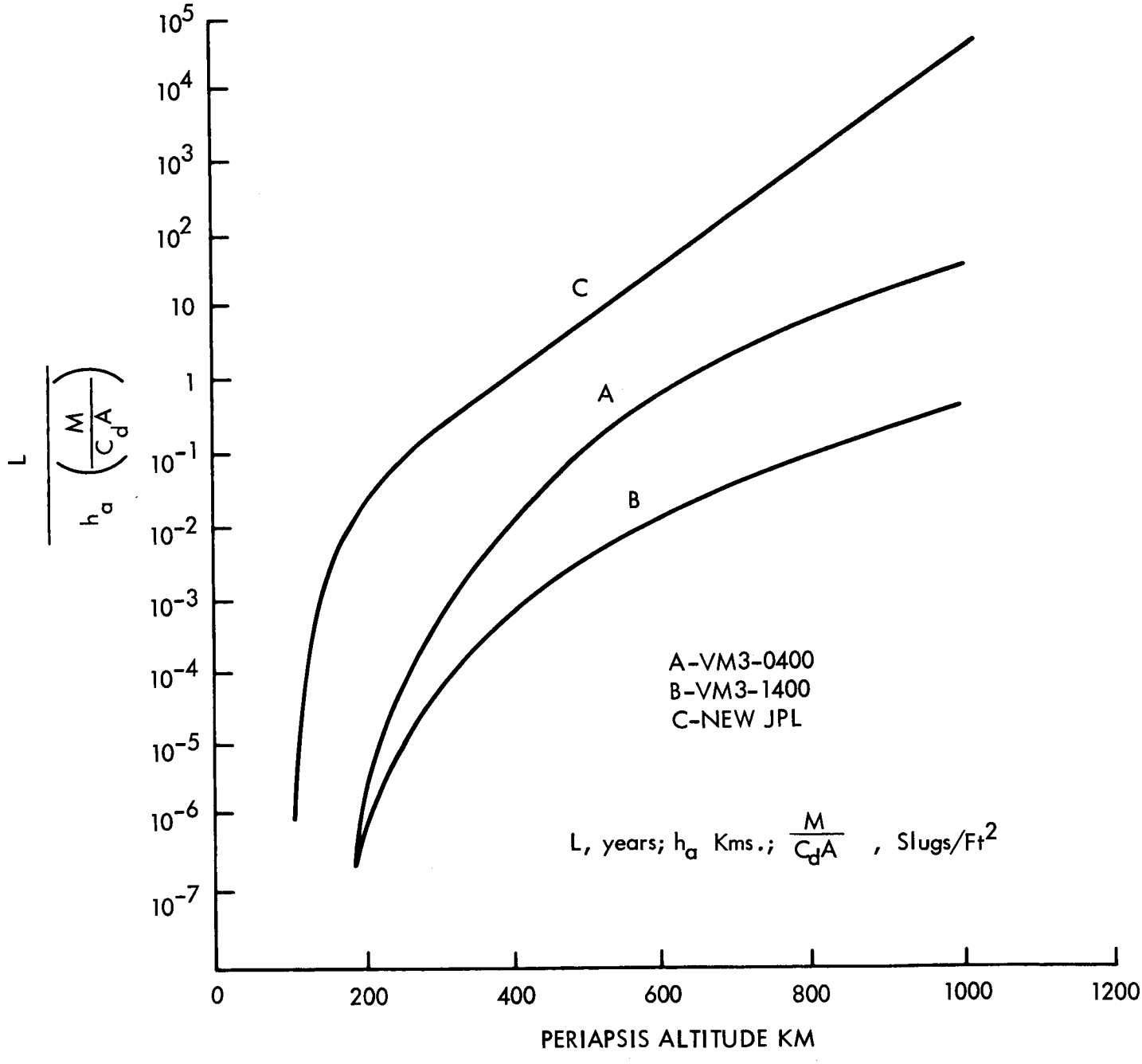

Figure 29. Linearized Orbit Life

ejected barrier cannot be weighted heavily in the determination of the operating mode. The other major consideration under the trajectory investigation is the possible collision between the spacecraft and the barrier. However, when the separation devices provide a separation velocity of 1 to 1.5 mps, the probability of any collision between the two objects would be infinitesimal. This conclusion is the same as found for the forward bio-barrier even though the aft bio-barrier weight (and therefore the M/C_DA) is different.

3.2.2 Thermal Consideration

Preferred Operation: Aft bio-barrier removed from the spacecraft. The heat loss from the spacecraft to the barrier would be excessive without well insulated structural attachments. Reduction of the thermal leak to an acceptable level may be accomplished by use of an interface connection with high thermal resistance (Figure 1 VOY-D-250). Studies show that were this thermally resistant interface not used, an added insulation weight of 20 pounds applied to all exposed barrier surfaces would be necessary to hold the heat leak to approximately 20 watts. Figure 30 shows the plot of heat leak from the spacecraft as a function of the added insulation weight.

3.2.3 Micrometeoroid Protection

Preferred Operation: Aft bio-barrier left attached to the spacecraft. Although the zero penetration probability is greater when the barrier is left attached, the degradation in the non-penetration probability between the barrier-on and barrier-off condition is only 0.000882.

3.2.4 Mass Property Changes

Preferred Operation: Aft bio-barrier left attached to the spacecraft. The mass property changes between the two modes of operation have their principal effect in the required gimbal angle of the LEMDE nozzle. In the worst firing condition (during orbit adjust after

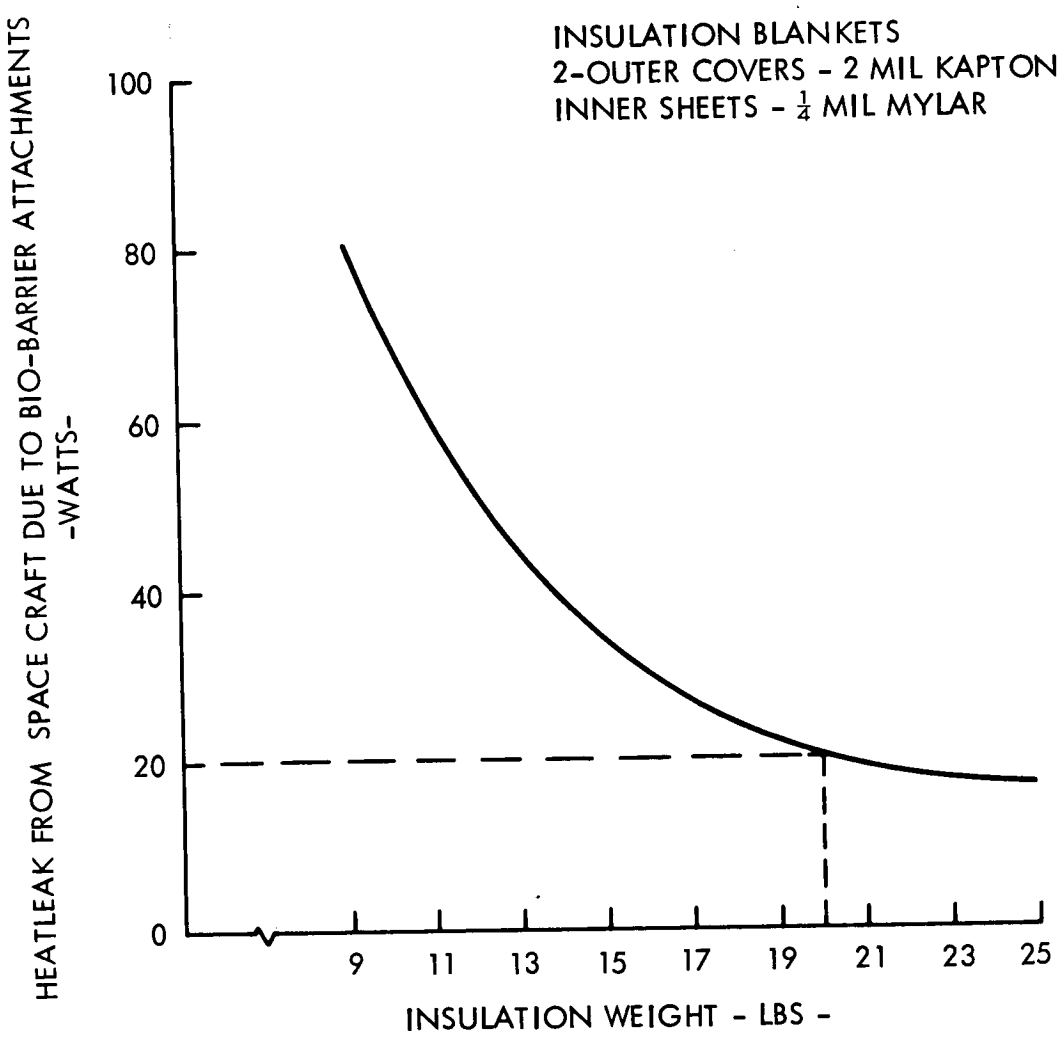

Figure 30. Heat Leak from Spacecraft versus Bio-Barrier Fin Insulation Weight

capsule separation), the analysis has shown that the engine must gimbal $1^{\circ}15'$ more if the engines are fired with the bio-barrier off instead of with it left attached.

3.2.5 Reliability

Preferred Operation: Aft bio-barrier left attached to the spacecraft. The probability of a successful ejection would be of the order of 0.999995.

3.2.6 PSP Viewing

Preferred Operation: Aft bio-barrier removed from the spacecraft. The scan platform boom is deployed normal to the orbit plane. The cone and clock angles bounded by curve A of Figure 31, define the boom cone and clock angle region for which no view blockage exists, with the aft-barrier removed. Curve B of Figure 31 defines the corresponding region with the aft-barrier retained. The boom cone and clock angles required for the first six months of the design orbit are shown by curve C of Figure 31. It can be concluded that for the present design conditions no significant viewing advantage is obtained by barrier removal.

3.2.7 Conclusion

At present there is no significant advantage to be gained by removal of the aft bio-barrier in orbit. In fact, the added complexity of providing for separation is sufficient reason to warrant bio-barrier retention.

3.3 LOCATION OF EXTERNALLY MOUNTED EQUIPMENT

This section discusses the rationale for placement of the Sun and Canopus sensors, the attitude control jets and tanks, and the various communication antennas. Figure 32 shows the location of these components with their respective fields of view. In order to present the rationale for the location of this equipment it is necessary to briefly discuss the Spacecraft orientation criteria.

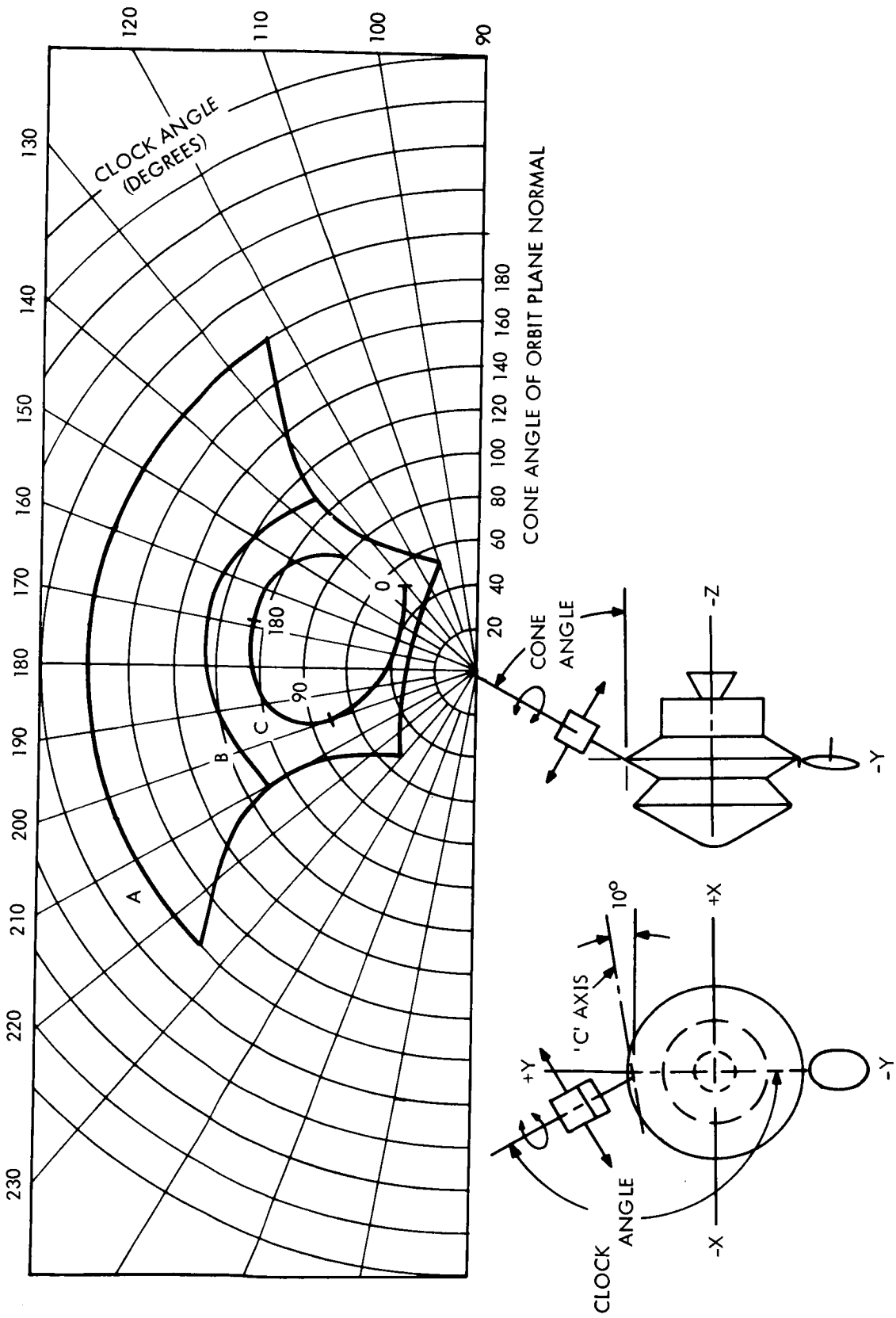

Figure 31. PSP Attitude Control Sensor Coverage

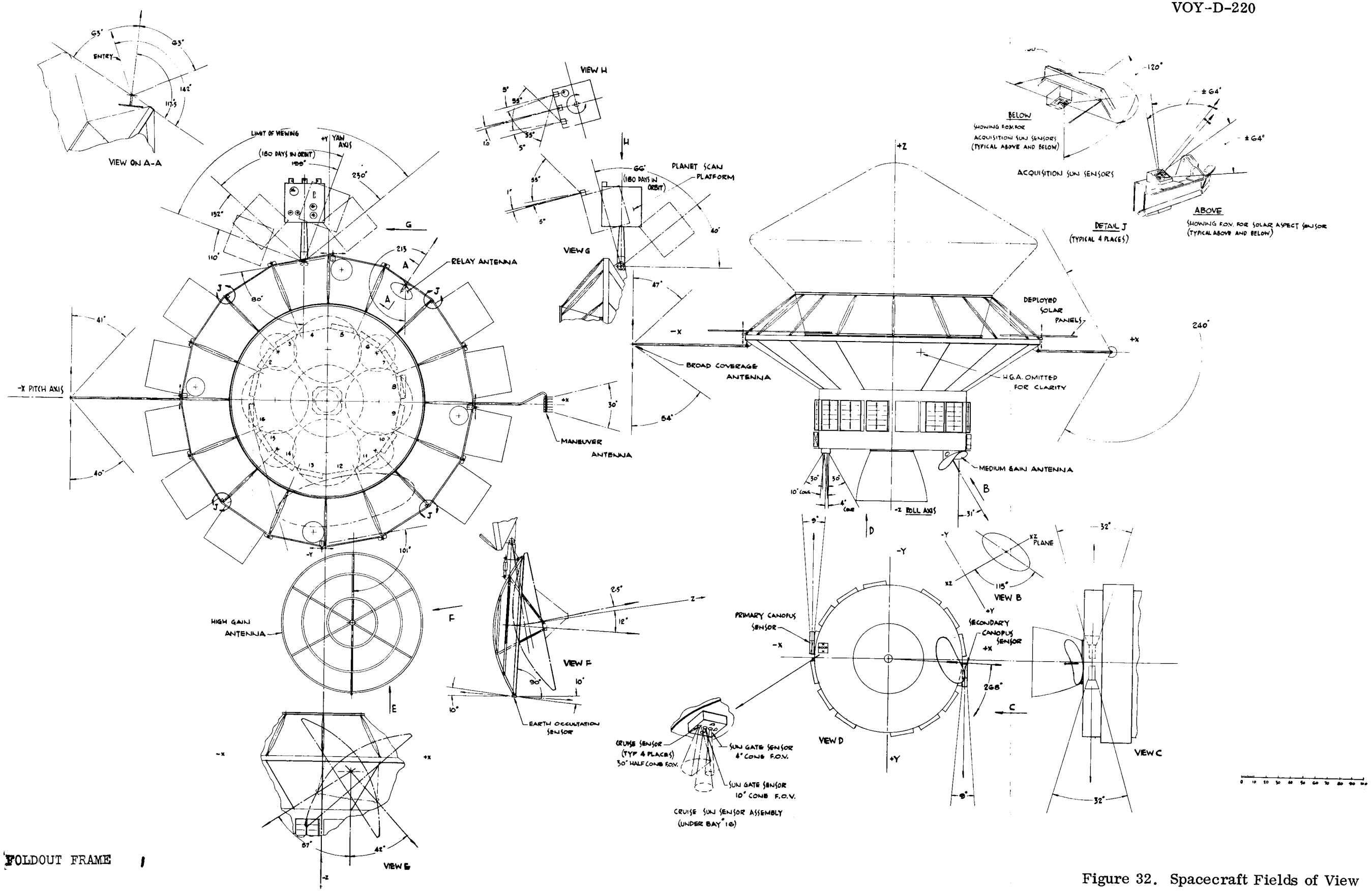

FOLDOUT FRAME 1

Figure 32. Spacecraft Fields of View

FOLDOUT FRAME 2

The Voyager mission requires a spacecraft which examines Mars by means of scientific instruments and transmits the resulting data to Earth via antennas. The long communication distances and large data rates demand high pointing accuracies for the HGA, thus, a stable platform for mounting the antenna. The spacecraft provides such a platform by means of an active attitude control system which is Sun and Canopus referenced.

The location on the spacecraft to provide adequate viewing for these sensors and antennas therefore must be considered a serious constraint during the development of a spacecraft configuration.

3.3.1 Sun Sensors

The spacecraft will align itself with its -Z axis pointing to the Sun. Pointing within ± 5 degrees is achieved by mounting an array of eight coarse Sun sensors; four of these sensors are attached symmetrically to each side of the fixed portion of the solar array at maximum radial distance from the Z axis, to provide a 4π steradian field of view. Accurate pointing of the spacecraft Z axis with respect to the Sun, within $\pm .25$ degrees, is controlled by the fine sun sensor assembly which is located on the portion of the electronic module environmental shield facing the Sun. The -X axis is convenient to associated guidance and control electronic equipment located in Bay number 16.

3.3.2 High Gain Antenna and Canopus Sensor

Before the location of the Canopus sensors is discussed, it is necessary to consider the location of the 114-inch diameter high gain antenna and the planet scan package (PSP). Due to its size this antenna must be deployed after separation of the planetary vehicle from the launch vehicle. Also, the antenna has a two axes gimbal mount with the gimbal axis located approximately in the plane and normal to the ecliptic plane. Because the spacecraft transit trajectory is approximately in the ecliptic plane, uninterrupted Earth pointing by the antenna

is only possible by locating it near either the North or South Pole (±Y axis) of the spacecraft. A curve of the antenna pointing angles for various missions is given in VOY-D-260.

The planet scan package viewing and the rationale for its location near the North Pole (+Y axis) of the spacecraft is described in VOY-D-380. This places the high gain antenna near the South pole (-Y axis) of the spacecraft. The rationale for employing two Canopus sensors is discussed in VOY-D-320. A Canopus sensor must be mounted with its axes normal to the sun direction (-Z axis). In order to minimize the possibility of stray light interference from the PSP and HGA, it is necessary to locate the Canopus sensors close to the X axis at the maximum radial distance from the spacecraft center line. Two alternate mounting locations may be provided on the spacecraft; one above the solar array in the shade, the other on the side of the electronic module. The latter position was selected because the viewing angles between the sensors and other spacecraft elements was the highest providing for the best protection against the sensor receiving false signals due to stray light reflected from the spacecraft. In addition, the primary Canopus sensor, which looks south, may be mounted on a machined bracket along with the fine Sun sensor, close to the guidance and control bay; thus the two critical sensors may be aligned to each other on a common base reducing alignment errors.

3.3.3 Other Antennas

The medium gain antenna serves as a back up in the event of articulation failure of the high gain antenna. It is fixed on the spacecraft at a viewing angle to provide communication coverage for a period from Mars encounter until approximately 2 months after encounter. It is located on the portion of the electronic module environmental shield facing the Sun on the +X axis at a maximum radial distance from the spacecraft center line. Radiative heat from the propulsion engine skirt during firing results in a maximum temperature on the antenna surface at 250^{0}F. An alternate location on the solar array surface would result in a loss of 10 square feet of solar cell area.

The broad coverage antenna is deployed beyond the deployed solar panels on the -X axis to provide communications coverage early in the mission and provides back up for the high gain antenna. When stowed it is parasitically coupled to the shroud and serves as a launch antenna. An additional low gain antenna, the maneuver antenna, has a higher gain and a fan shaped beam for use at long communication distances. This antenna is deployed to a position of the +X axis beyond the deployed solar panels providing an uninterrupted field of view in the XZ plane.

A fixed relay antenna is mounted behind the solar array pointing in the 117.5 degrees and 213 degrees cone clock angle direction. This pointing was determined by the cone and clock angles of the capsule from separation to impact.

3.3.4 Attitude Control

The 4 nozzle assemblies consisting of roll, pitch and yaw jets with solenoids for the attitude control system are positioned at either end of the principal axes of the spacecraft. They are located at the extremity of the fixed solar array - between the deployable panels on the X axis and adjacent to the high gain antenna on the -Y axis and the PSP on the +Y axis. A small saving of gas weight could be effected by placing the jets at the tip of the deployable panels but a significant loss in reliability would result due to the requirement for flexible lines over the hinges and dependency on the panel deployment. The spherical attitude control gas tanks are mounted on the support module immediately adjacent to the nozzle assemblies. An alternate mounting for these tanks inside the body of the spacecraft would necessitate cylindrical tanks due to space limitations resulting in a 45 pound weight penalty; the weight penalty for micrometeoroid shielding of the spherical tanks at the selected location is 2 to 3 pounds.

3.4 PROPELLANT LOADING

In the Task B design, loading of propellants at the Explosive Safe Facility only was considered because of design constraints imposed by the then current mission specification.

Further considerations of the handling and safety problems associated with off-pad fueling has resulted in provision for on-pad fueling in the system update design. Major considerations in providing for the on-pad fueling are maintenance of the design modulatiry; extra weight of lines, valves, and fuel; and the shroud access requirements. In the latter, both the location of the access with respect to field or separation joints and the size of the access panel must be considered.

3.4.1 Selected Approach

The selected approach for on-pad fueling is shown in Figure 33. A panel is mounted off the cruciform engine support structure for the mounting of valves and fittings. Even though this panel extends into the electronic module, the design modularity is not broken. A drip tray is included to catch and dump propellant spilled during loading. The panel and access opening, shroud and spacecraft, are located at approximately the X axis of the spacecraft away from appendages such as the high gain antenna and planet scan platform.

With the selected approach, the length of fueling lines which must be carried with the spacecraft are a minimum eliminating concern about propellant trapped in the fueling lines. The shroud access panel is located away from shroud joints and, hence, in a low stress region. The large unobstructed volume between the shroud access panel and the spacecraft mounted panel provides for ease of the loading operation.

3.4.2 Alternate Approaches

Before deciding on the approach described above, two additional locations for on-board fueling were studied; these locations are shown in Figure 34. Both of these locations suffer from the shroud access location being in the vicinity of the shroud in-flight separation plane. In addition, with the fueling panel located near the top of the propulsion module, the access panel in the shroud will be larger; this location, however, does maintain the spacecraft

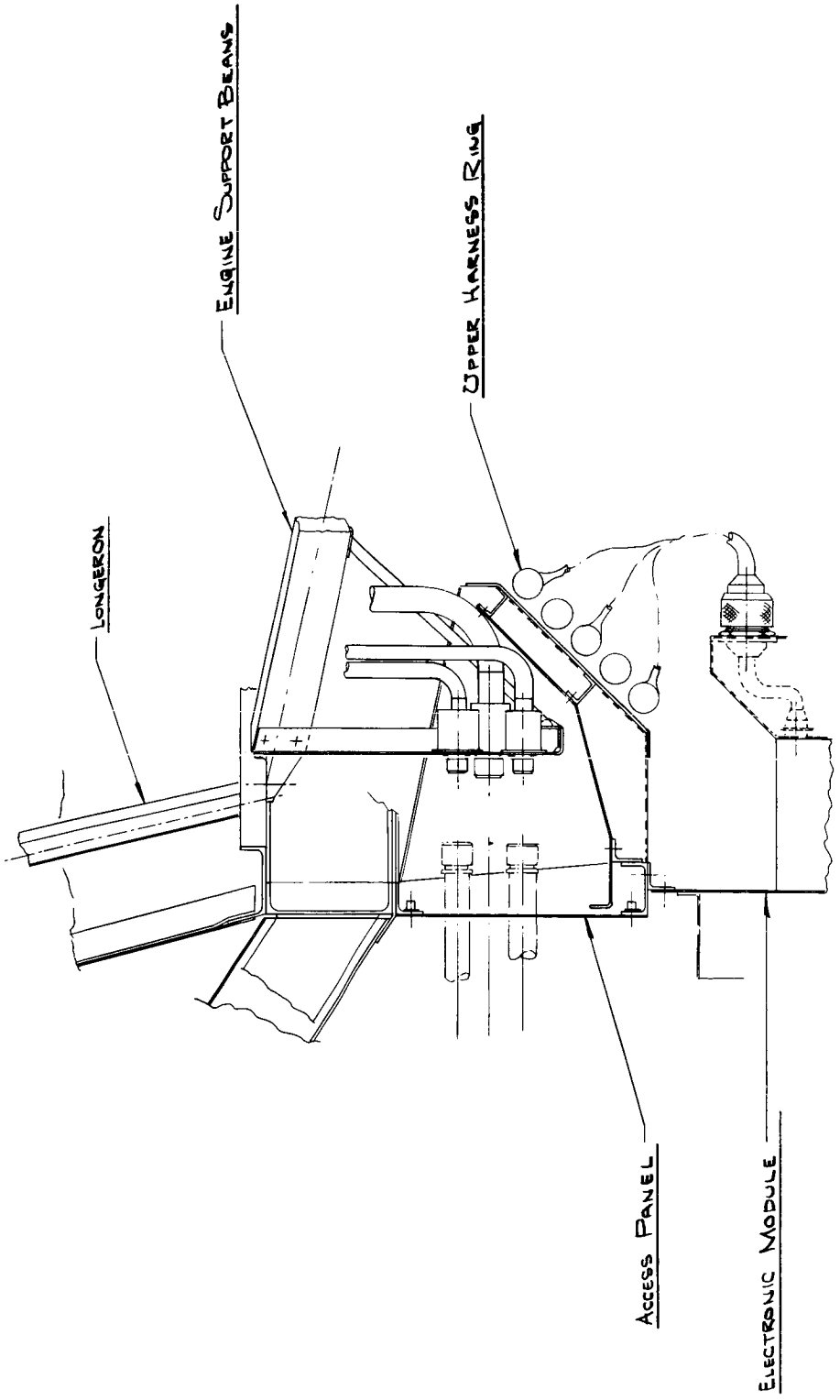

Figure 33. Propulsion Servicing Panel

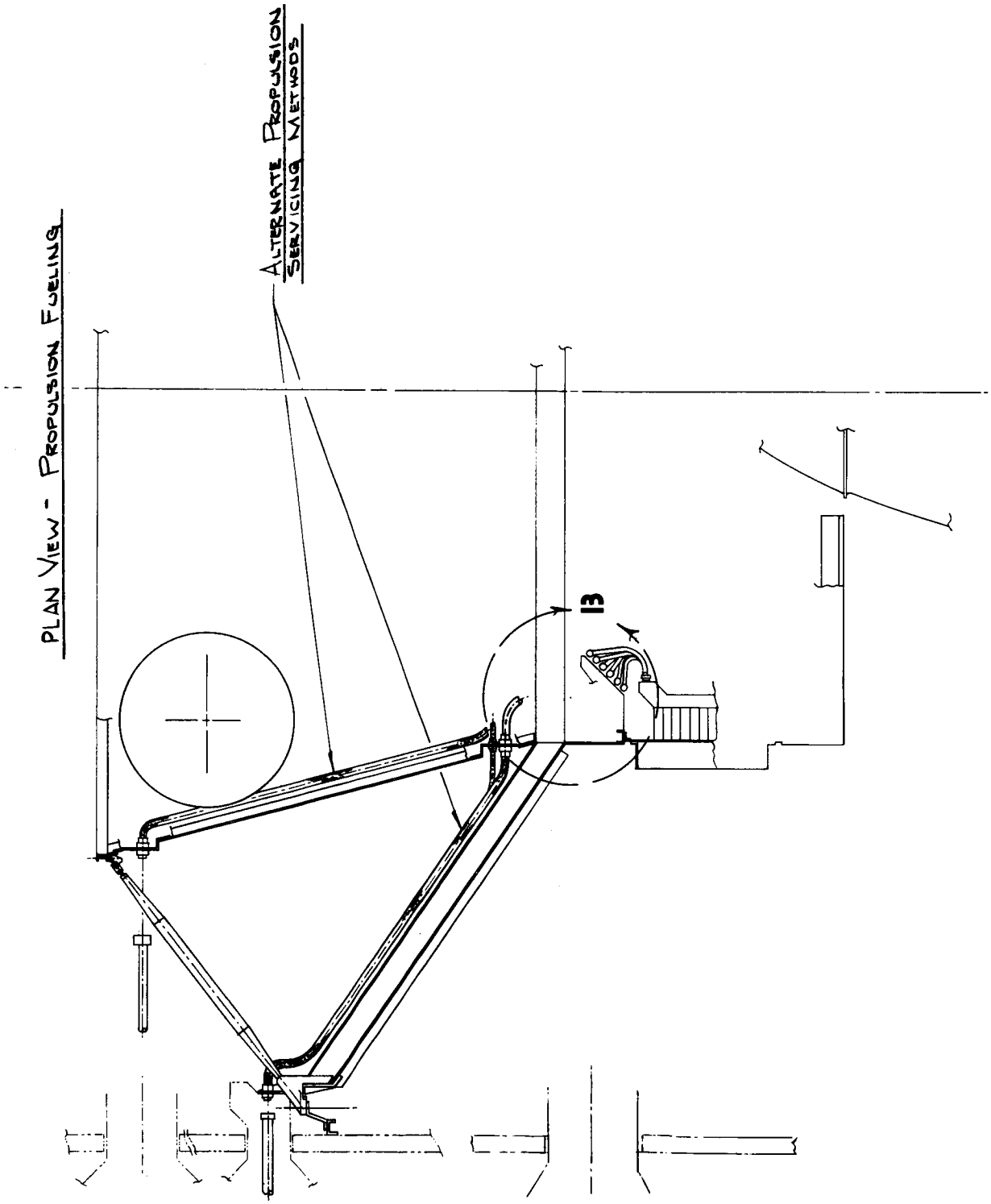

Figure 34. Propulsion Servicing Alternates

design modularity. Also, gravity draining of the loading lines cannot be accommodated with either of those approaches.

The other location for the propellant loading, near the spacecraft shroud attachment plane, has many disadvantages the most serious of which is loss of modularity. The loading lines are attached to the support module requiring a checkout of these lines after mating of the support and propulsion modules. Other disadvantages for this location are as follows:

a. Long spacecraft loading lines requiring draining of the line or designing for the problems associated with fuel in the loading lines.

b. Valves at both the shroud end and spacecraft end of the lines are required.

c. Spillage could run down the lines and drip on the back of the array making clean-up difficult.

As noted from the above discussion, the selected approach of propellant loading is superior to any other approach which was developed in the study.

3.5 ALTERNATE SPACECRAFT TO SHROUD ATTACHMENT

The baseline spacecraft to shroud attachment is shown in Figure 35. In this design the support module extends out to the dynamic envelope where it attaches to the planetary vehicle adapter. A more detailed description of this arrangement is presented in VOY-D-260. Use of an adapter permits the separation interface and the planetary vehicle - shroud field joint to be separate interfaces.

An alternate spacecraft to shroud attachment is shown in Figure 36. In this design the planetary vehicle support module extends to the shroud. This eliminates the adapter ring and results in an additional 14 square feet of fixed solar array. The difficulties with this concept are associated with possible planetary vehicle separation clearance problems and

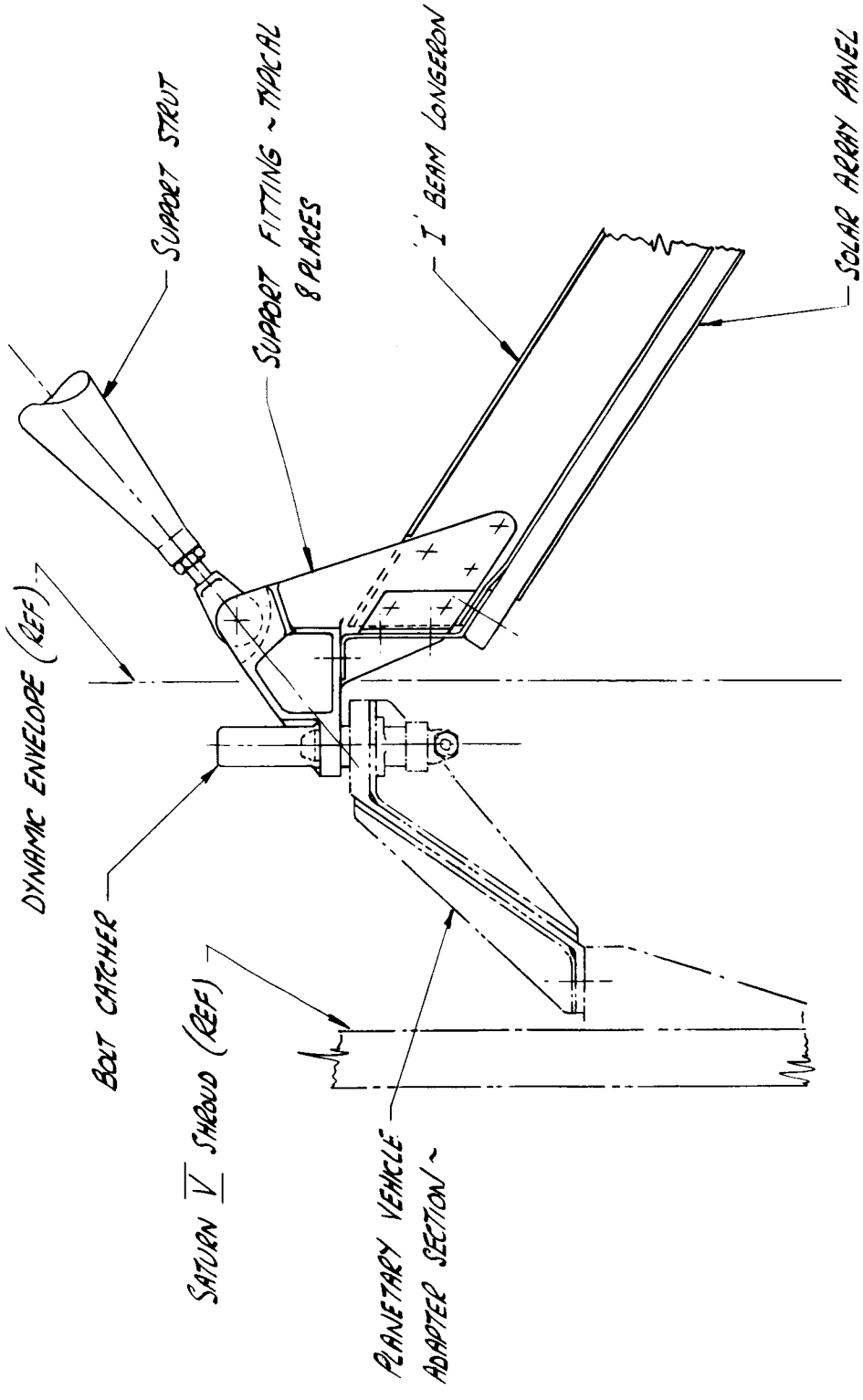

Figure 35. Spacecraft to Shroud Attachment

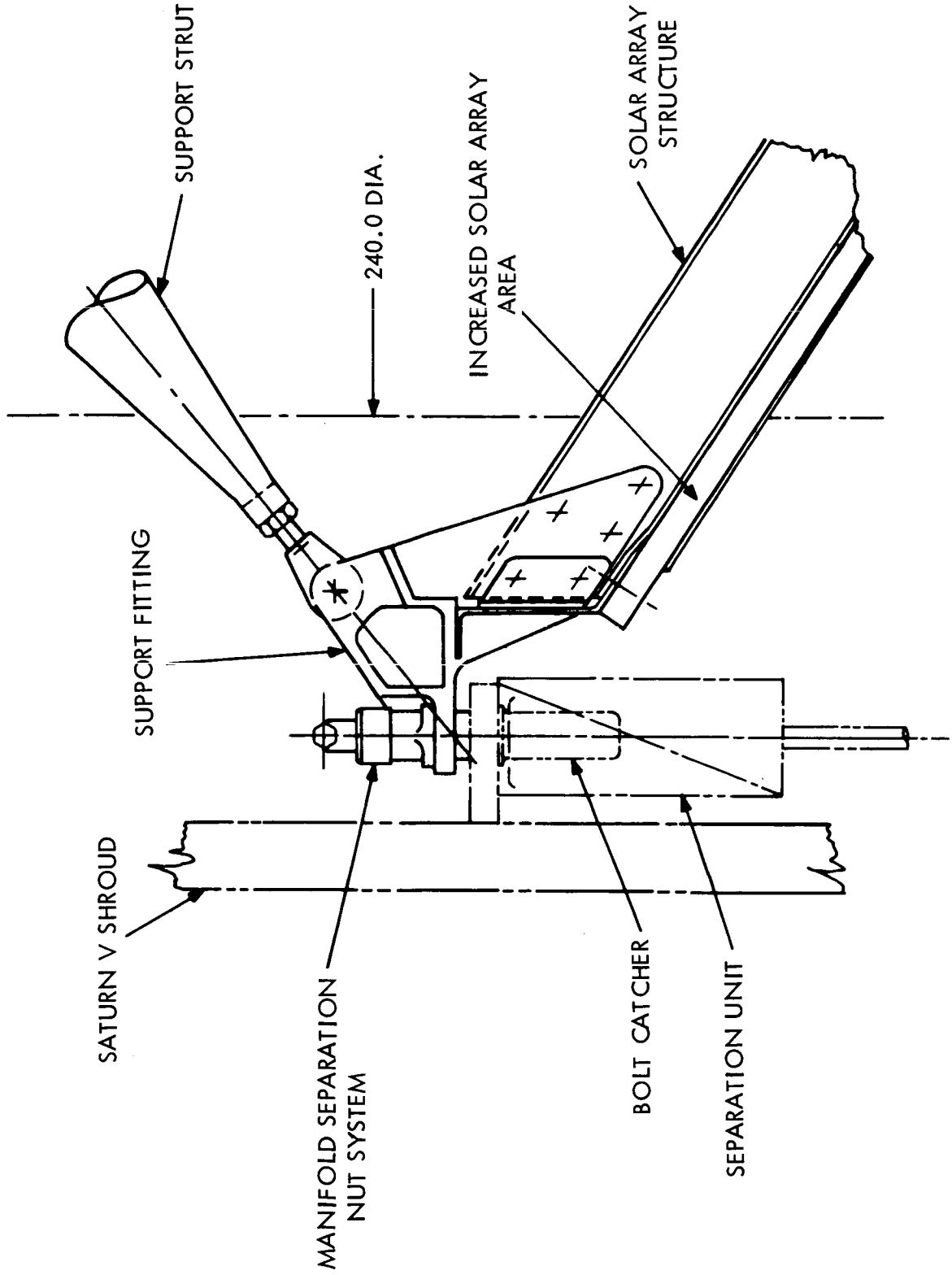

Figure 36. Alternate Spacecraft to Shroud Attachment

interface complexities. The interface complexities arise from combining the separation and field joints. Such considerations as interface tolerances and final settings on the separation springs are potential problem areas.

Final determination of the optimum interface arrangement will require detailed design studies in conjunction with the shroud designers.

3.6 RESULTS OF DEVELOPMENT STUDIES

As a result of the baseline development studies, the preferred design became the configuration shown on Figure 37 and Figure 38.

4. ALTERNATE THRUST CHAMBER ADAPTATION

This section discusses the spacecraft configuration changes necessary to accommodate (1) The Bell Agena Thrust Chamber, and (2) The Aerojet Transtage Thrust Chamber in place of the LEMDE. Changes in the Propulsion System itself are discussed in VOY-D-370.

Both of these engines have smaller profiles, weigh less and have radiatively cooled skirts which must be insulated in a manner similar to that for the LEMDE. Therefore, the substitution of either of these engines does not basically affect the spacecraft configuration, except that the addition of auxiliary thrusters may be necessary to provide the minimum impulse bit required for midcourse maneuvers. A thruster installation is shown in Figures 39 and 40.which may be applied to either the Agena or the Transtage adaptation.

Figure 39 shows the Agena thrust chamber mounting. The existing spacecraft structure is shown in phantom with the revised structure for the engine mounting shown in solid line. This thrust chamber uses a head end gimbal mount, located at Sta. 79.0. attached to a cruciform beam assembly which ties into the existing spacecraft propulsion unit structure. Auxiliary thrusters are shown mounted at Sta. 26 on the principal X and Y spacecraft axes

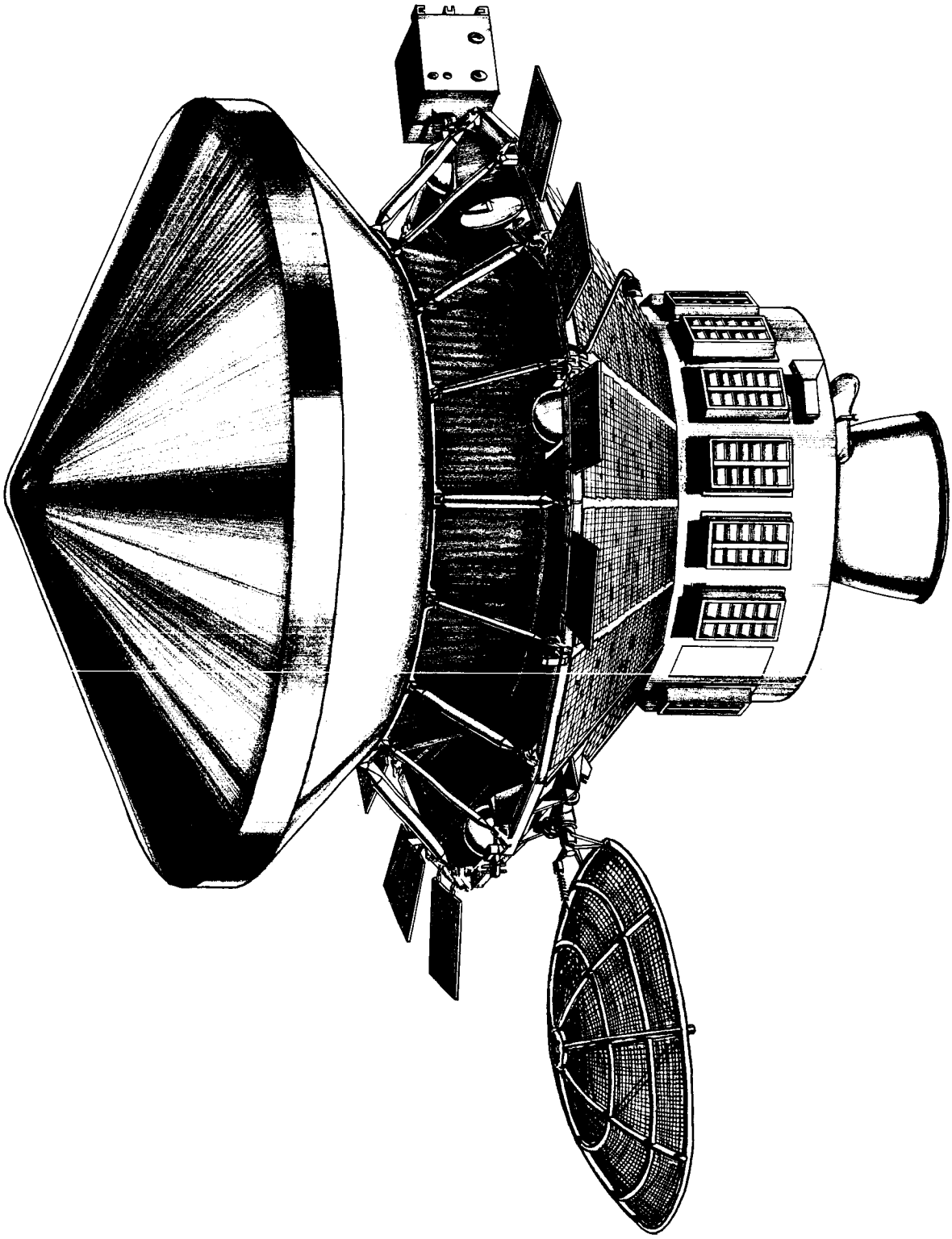

Figure 37. Spacecraft Design (Artists' Concept)

at a radius of 38.0 inches from the center line. This location for the thrusters avoids interference with other components such as the stowed high gain antenna, the medium gain antenna and the cruise sun sensor. The turbo pump exhaust duct for the Agena engine is modified to clear the skirt at the maximum gimbal angle and the auxiliary thruster located on the +Y axis.

Figure 40 shows the Transtage thrust chamber. The existing structure is shown in phantom as for the Agena adaptation, with the modification for the engine mounting shown in solid. The Transtage engine has a throat gimbal similar to the LEMDE so the adaptation is very simple with minimum changes to the LEMDE spacecraft structure. The engine actuator attachment points have been altered to place their centerlines on the spacecraft principal axes.

The change in structural support weight associated with the mounting of each of these alternate thrust chambers from the LEMDE design is insignificant.

5. REFERENCES

1. Performance and Design Requirements for the 1973 Voyager Mission General Specification for January 1, 1967 by JPL, SE002BB 001-1B21 File SEIDC, Task 544-1DC11-1-2810.

2. Voyager Spacecraft Phase B Task D Guidelines, July 14, 1967 MSFC.

3. Voyager Spacecraft System, Phase 1A Task B Preliminary Design, Spacecraft Functional Description, Vol. A by GE for JPL, DIN 65 SD 4514, January 31, 1967.

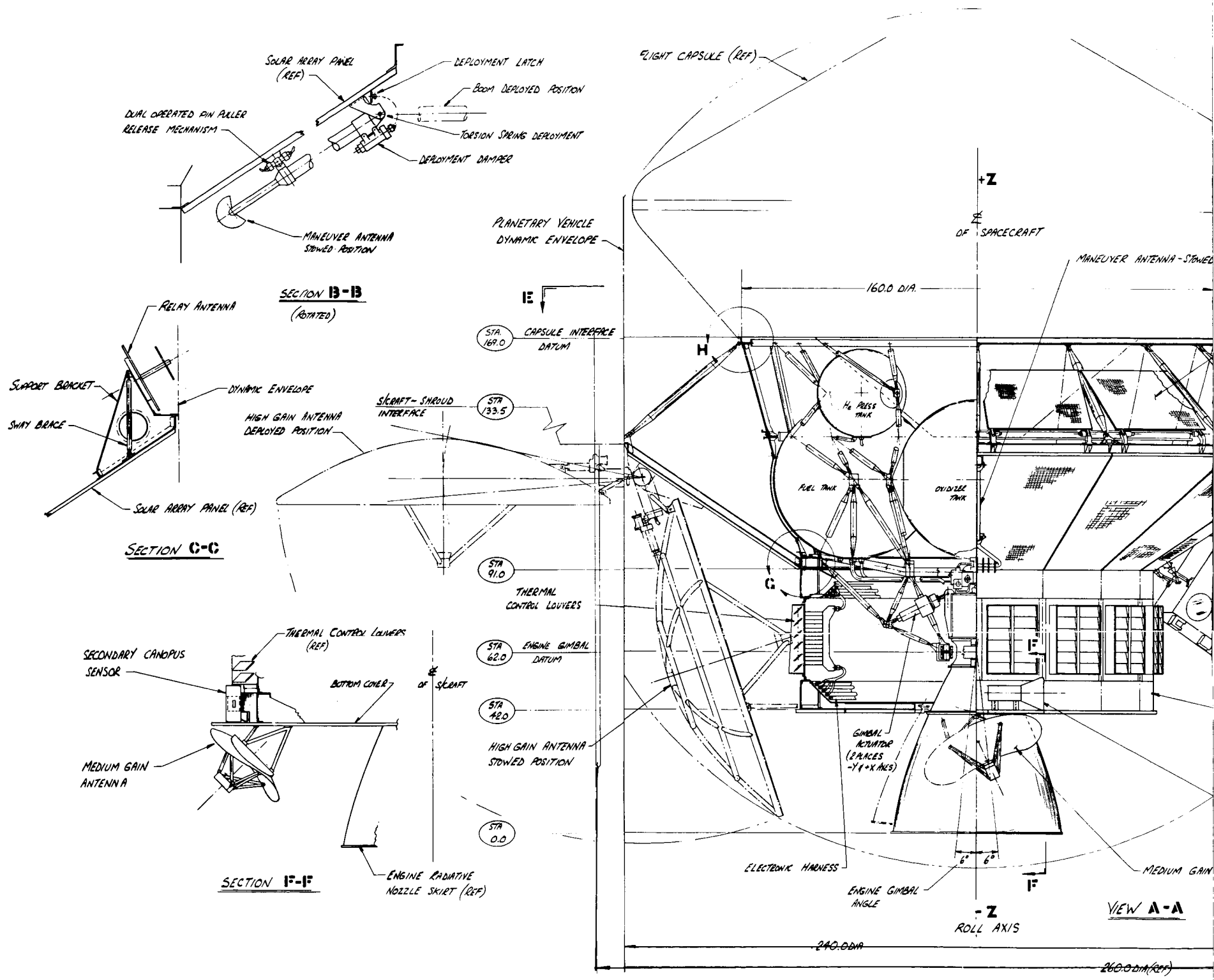

FOLDOUT FRAME 1

FOLDOUT FRAME

TABLE SHOWING BAY ALLOCATIONS OF ELECTRONIC EQUIPMENT

BAY NO.	SUBSYSTEM	BAY NO.	SUBSYSTEM
1	POWER	9.	TELEMETRY
2.	POWER	10.	COMMAND
3.	SCIENCE ELECTRONICS	11	RADIO
4.	SPARE BAY	12.	RADIO
5.	SCIENCE ELECTRONICS	13.	RELAY RADIO
6.	SCIENCE DAE	14.	GUIDANCE & CONTROL
7.	DATA STORAGE	15.	POWER
8.	DATA STORAGE	16.	GUIDANCE & CONTROL

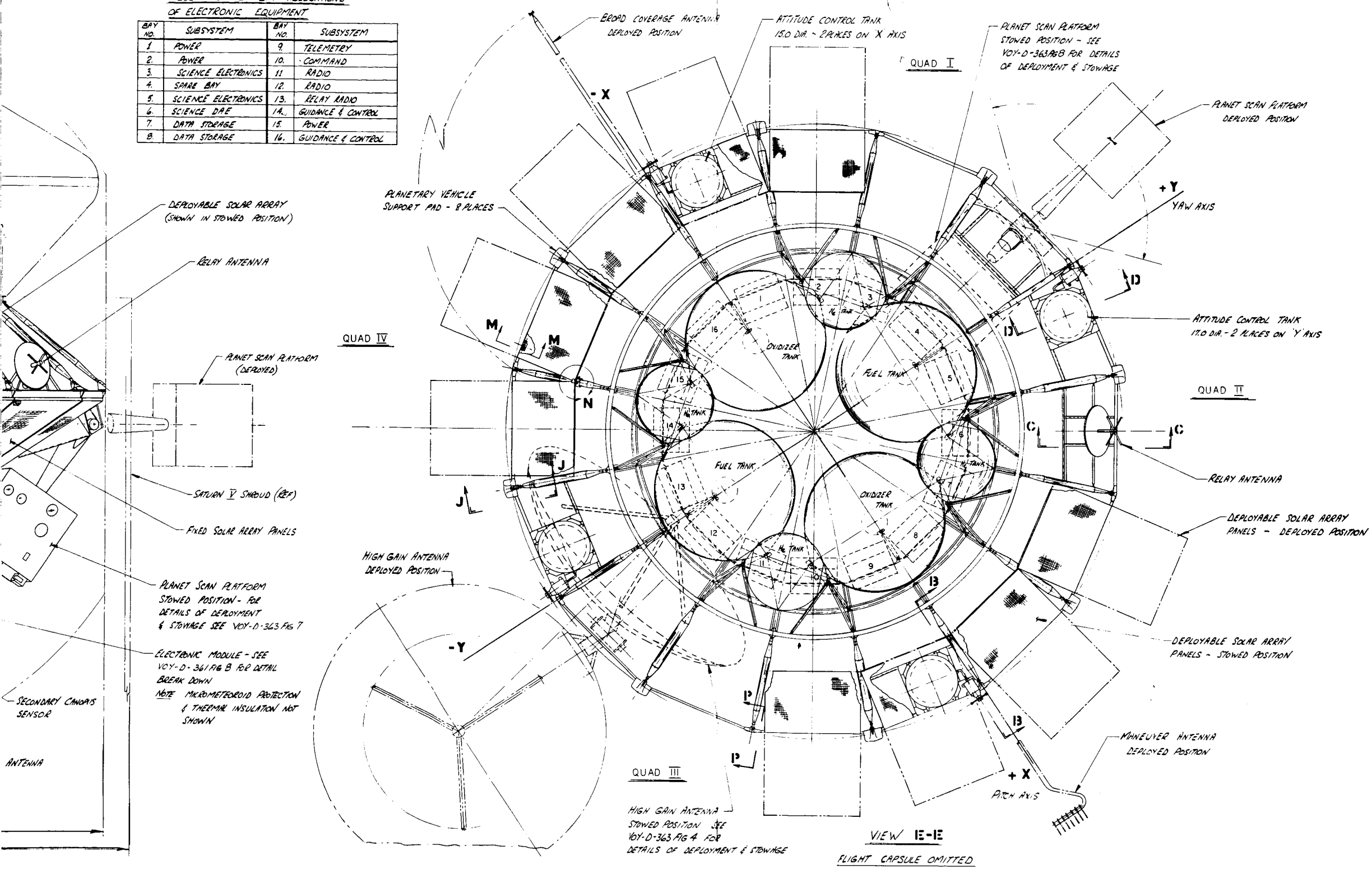

Figure 38. Spacecraft General Arrangement (Sheet 1 of 2)

FOLDOUT FRAME 2

FOLDOUT FRAME 3

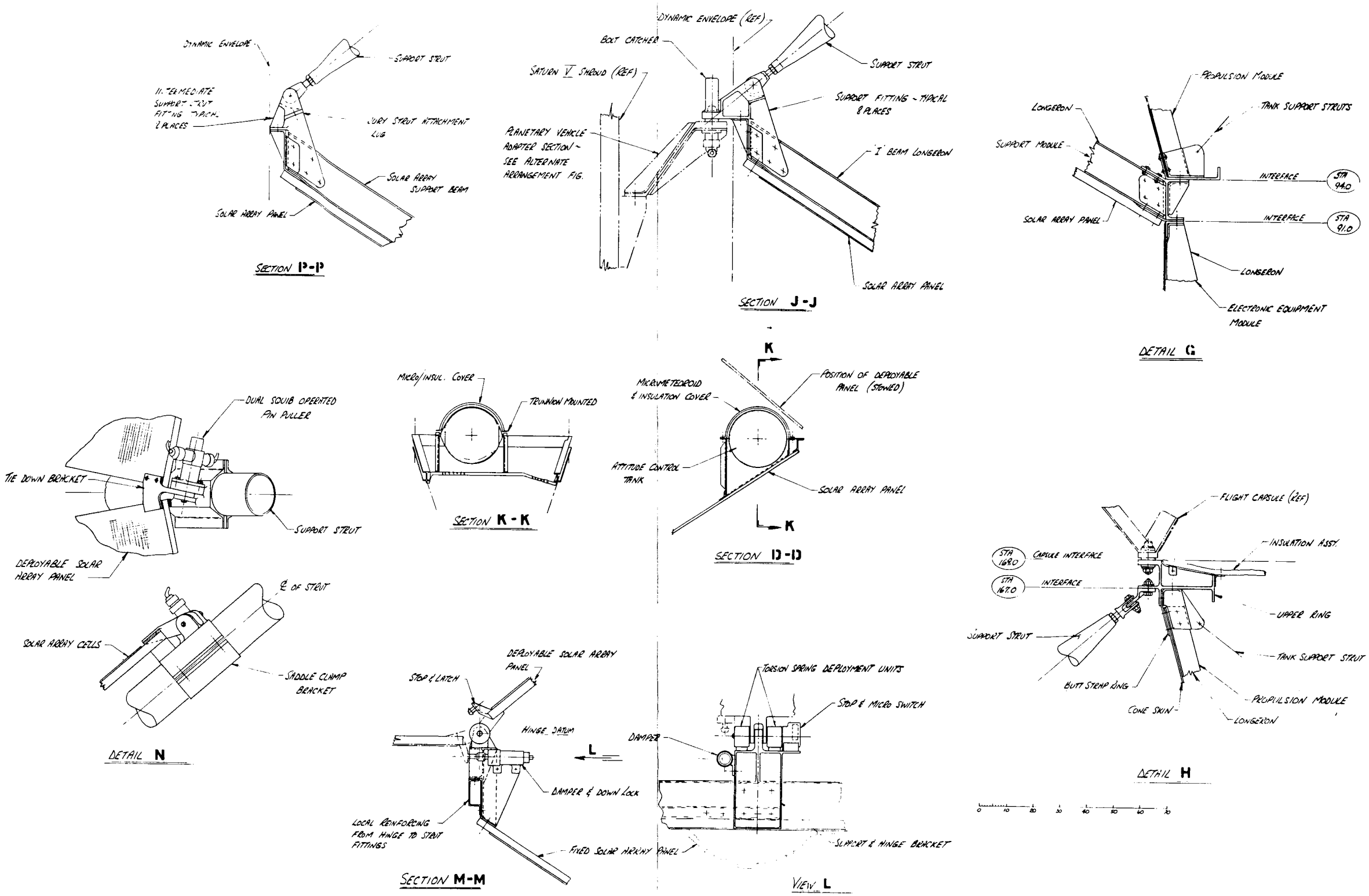

Figure 38. Spacecraft General Arrangement (Sheet 2 of 2)

FOLDOUT FRAME 1

FOLDOUT FRAME 2

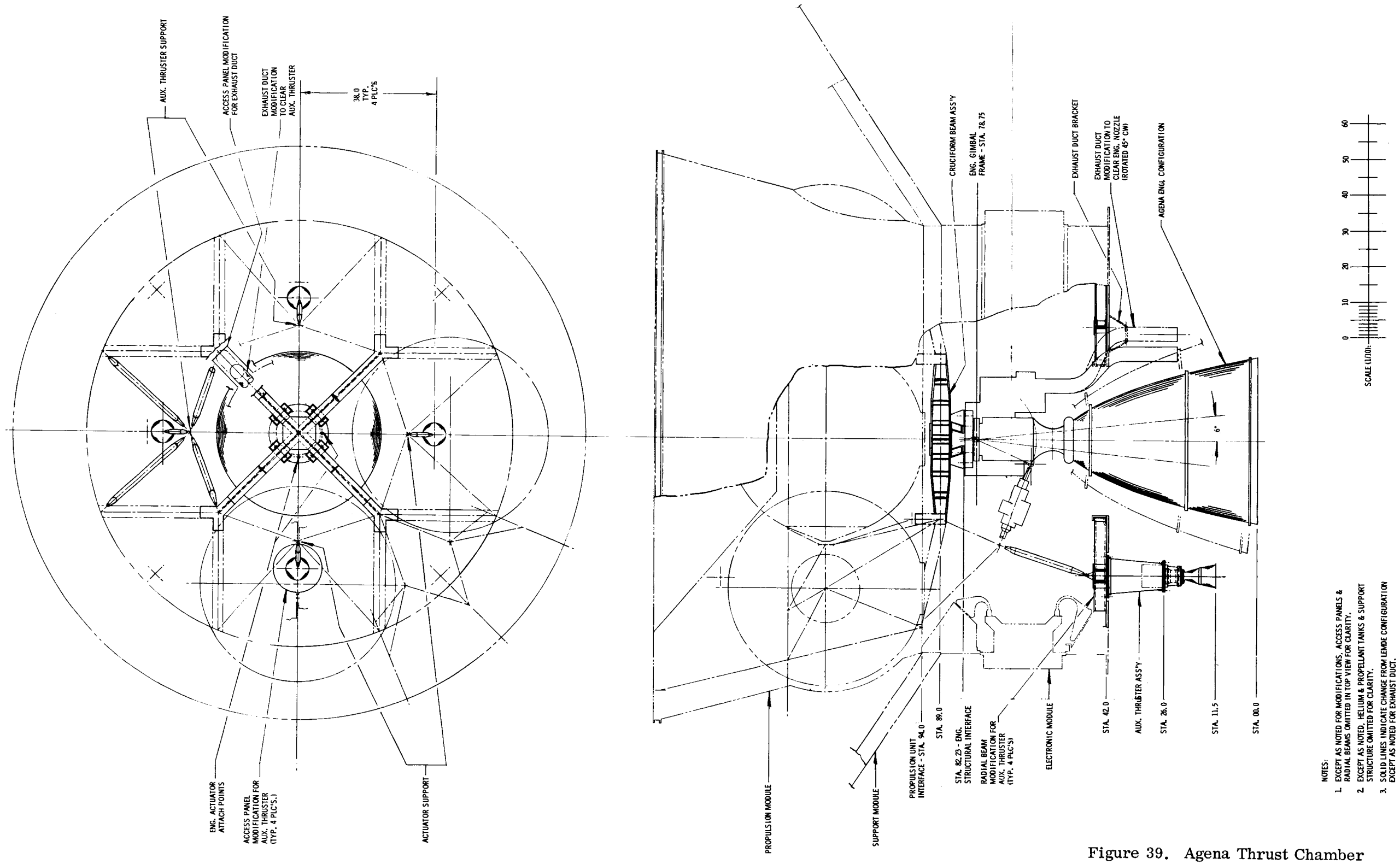

NOTES:
1. EXCEPT AS NOTED FOR MODIFICATIONS, ACCESS PANELS & RADIAL BEAMS OMITTED IN TOP VIEW FOR CLARITY.
2. EXCEPT AS NOTED, HELIUM & PROPELLANT TANKS & SUPPORT STRUCTURE OMITTED FOR CLARITY.
3. SOLID LINES INDICATE CHANGE FROM LEMDE CONFIGURATION EXCEPT AS NOTED FOR EXHAUST DUCT.

Figure 39. Agena Thrust Chamber Adaptation

FOLDOUT FRAME 2

FOLDOUT FRAME 1

67

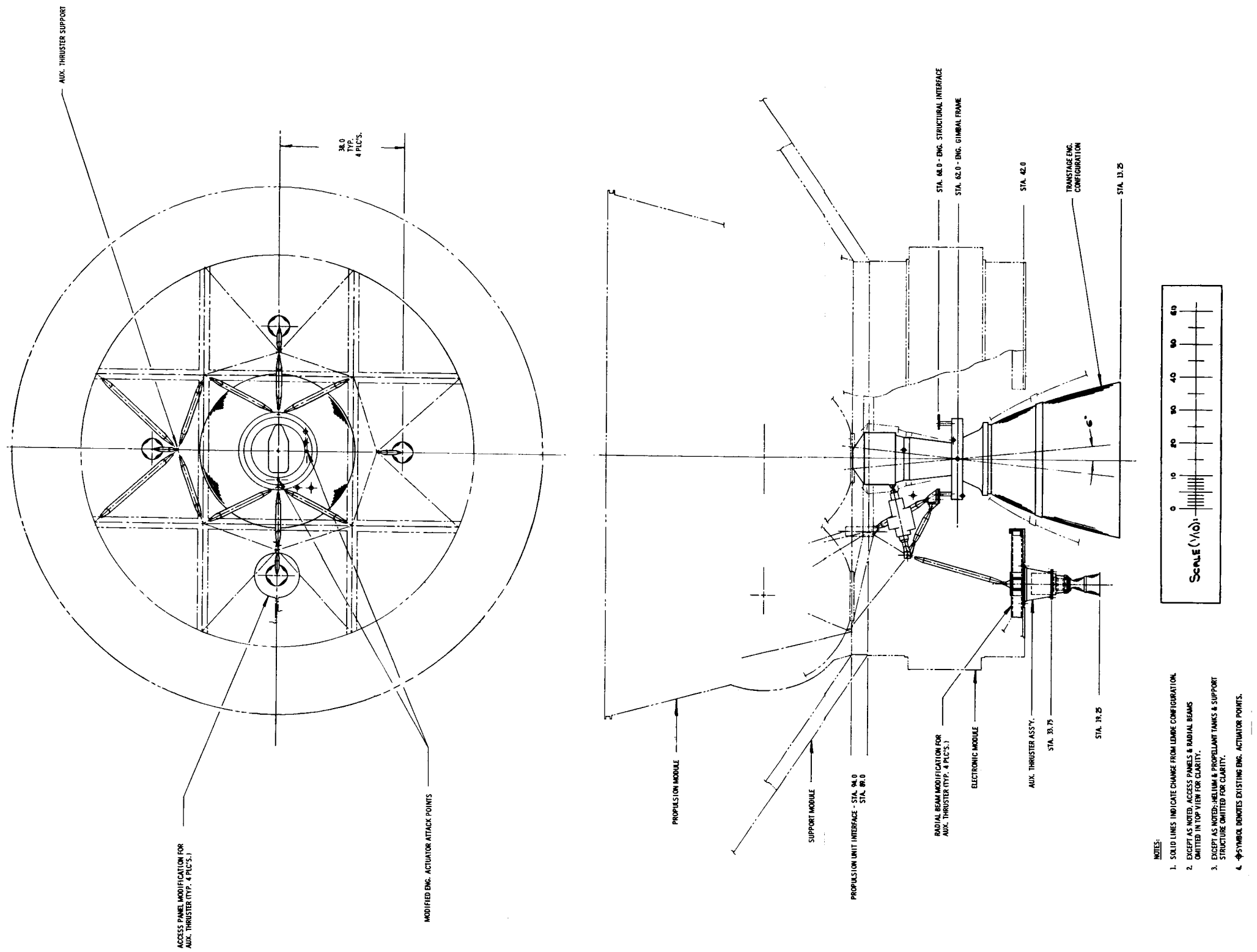

Figure 40. Transtage Thrust Chamber Adaptation

FOLDOUT FRAME 1

FOLDOUT FRAME 2

VOY-D-230
FUNCTIONAL SYSTEM INTEGRATION

1. INTRODUCTION

This section provides the functional integration of the Voyager system update. The functional system integration consists of the preparation of a consistent sequence of events, the commands necessary to perform the events, and the telemetry required to ascertain that the events have been properly executed or for diagnosis of trouble if anomalies occur during flight.

The sequence of events defines the nominal occurrences required to initiate each event, the change in power required to accomplish the event, and the component affected by the event.

The spacecraft command list has been developed from the sequence of events, the requirements of the spacecraft subsystems and the analysis of critical failure modes. Both onboard and ground commands necessary to satisfy the mission requirements and to circumvent the critical failure modes are included.

The diagnostic engineering telemetry required has been compiled from three principal sources: measurements necessary to monitor spacecraft events; measurements necessary to detect critical failure modes; and a continuing program of hypothesizing performance anomalies and methods of ascertaining the cause of the anomalies.

2. SEQUENCE OF EVENTS

2.1. MISSION SUMMARY

The mission phases which comprise the 1973 Voyager mission sequence are principally derived from those defined in the referenced mission profile summary*.

*Performance and Design Requirements for the 1973 Voyager Mission, General Specification for, (JPL), January 1, 1967, SE-002-BB-001-1B21.

A highlight summary of the 1973 Voyager mission sequence follows.

The planetary vehicles (PV 1 and PV 2) are checked out, conditioned, and initialized for launch during the prelaunch phase just prior to lift-off. At the completion of the launch phase, the S-IVB stage and the attached planetary vehicles are in an earth parking orbit from which they are placed on a heliocentric transfer trajectory toward Mars. At the end of the injection phase, the planetary vehicles and shroud section are separated from the S-IVB with a relative velocity between them in order to provide adequate spatial separation for subsequent orientations, maneuvers, and thrusting. Immediately after separation from the S-IVB stage, the planetary vehicles initiate their own acquisition phase during which they achieve a 3-axis stabilization using the sun and Canopus as references, deploy solar arrays and antennas, terminate the launch mode for certain components, and commence to use solar energy as a source of electrical power. The completion of the acquisition phase of each planetary vehicle leads to the interplanetary cruise phase during which the planetary vehicle maintains its 3-axis stabilized voyage to Mars; the cruise phase is interrupted three times at appropriate positions in its trajectory to make trajectory corrections. After each of these corrections, the planetary vehicle is returned to the mode appropriate for the cruise phase.

The first trajectory correction, the arrival date separation maneuver, is performed by PV 1 approximately 3 days after launch. The planetary vehicle is controlled to perform a maneuver consisting of an orientation, under gyro references, away from the sun and Canopus references, and a thrusting action designed to partially remove the trajectory bias, to correct for injection errors and to provide a separation in the time of arrival at Mars between the planetary vehicles. At an apporpriate later time, nominally 1 day, PV 2 performs its arrival date separation maneuver.

The two remaining trajectory corrections are referred to as interplanetary trajectory corrections. The first correction occurs for PV 1 at approximately 30 days after launch and the second correction at approximately 10 days before arrival. The correction maneuvers are similar to the arrival date separation maneuver, differing only in the thrusting direction and

the velocity imparted to the planetary vehicle during the thrust action. After each of the two trajectory corrections, the planetary vehicle returns to the cruise mode. Capsule power is momentarily interrupted after maneuvers to inhibit array/battery load sharing. The corrections to PV 2 follow those of PV 1 nominally by 8 days.

The conclusion of the cruise phase occurs at the commencement of the Mars orbit insertion phase. The orbit insertion maneuver, like the trajectory correction maneuvers, is very nearly identical to the arrival date separation maneuver differing in the thrusting direction and the velocity magnitude imparted to the planetary vehicle. The insertion maneuver also differs somewhat in procedure due to the extremely small opportunity window available for the maneuver. The spacecraft attitude must be verified on the ground prior to ignition. Due to the arrival date separation maneuver, PV 2 accomplishes the insertion maneuver nominally 8 days after PV 1.

After insertion into a Mars orbit, the planetary vehicle enters into a phase of orbital operations during which the orbit geometry is determined, surveillance data is obtained in support of the selection of the capsule landing site, and selective science data is acquired. One of the more pertinent activities of this phase is the deployment of the planetary scan platform, which is subsequently controlled to point to Mars along the local vertical in order to orient the science sensors mounted on the platform. An antenna-mounted earth sensor signals earth occultations and switch telecommunications to the occultation mode.

Once in orbit, a PV orbit trim maneuver may be performed, as required, to optimize the orbit. The orbit trim maneuver is very nearly identical to the arrival date separation maneuver and differs from it in the same manner as does the trajectory correction maneuvers. The planet scan platform is retracted during orbit trim maneuvers. At the conclusion of the maneuver, the planetary vehicle returns to the orbital operations mode.

The capsule separation phase terminates the planetary vehicle orbital operations mode. During this phase, the forward biobarrier and capsule are separated while the spacecraft

remains 3-axis stabilized to the sun and Canopus. Biobarrier separation occurs five minutes prior to capsule separation. The capsule and the capsule-spacecraft radio relay link are checked out and then capsule power is shifted to capsule internal batteries. The capsule separates from the spacecraft only if enabled by a ground signal and then orients itself for a retro-propulsion thrusting designed to cause the capsule to enter the Martian atmosphere and land at the selected landing site. The spacecraft remains oriented to the sun and Canopus during separation. Low and high rate data from the capsule is relayed to the spacecraft during capsule descent. The spacecraft stores the data for later transmission to earth. A nominal time for capsule separation indicated in the sequence of events is 7 days after orbit insertion.

After the landing of the capsule the spacecraft enters the spacecraft orbital operations phase, during which the scientific instruments are programmed for long term capabilities of surveillance and spectrometric measurement of Mars. Science data is stored on tape recorders while being acquired near periapsis passage and read out of the recorders for transmission to earth during the remainder of the orbit. The spacecraft orbit operations phase may be interrupted for an orbit trim maneuver as described previously. The orbiting spacecraft will not encounter sun occultations during the first 105 days of Mars orbit for the nominal orbital parameters. When sun or Canopus occultations do occur, inertial references will be employed.

2.2. FLIGHT SEQUENCE OF EVENTS

The Flight Sequence of Events is a detailed listing of the primary occurrences and events which comprise the mission. The sequence is developed from a basic top level mission plan and encompasses the integrated requirements of all subsystems and design restraints.

Inherently, the sequence cannot be finalized until all subsystem design and mission parameters are completely defined. Consequently, the sequence is continuously under revision as these parameters are selected. The sequence of events presented in this section represents the integration of all currently available information.

As part of this system update study, a Voyager mission sequence computer program (VMSC) was developed. Basically, computer input card data is provided for each event within the sequence, and for each component affected by the event, provided that the component requires electrical power to operate.

The principal computer output formats are as follows:

Format 1.	Sequence of Events by Time and Time Related Power Usage Profile.
Format 2.	Sequence of Events by Command Source.
Format 3.	Sequence of Events by Affected Subsystem.
Format 4.	Sequence of Events by Affected Component.
Format 5.	Sequence of Events by Component Location.
Format 6.	Subsystems by Location and by Component.

The VMSC program facilitated the continuous revision to the flight sequence previously discussed. Event, component, command source and power requirement data were readily revised via changes to selected key punch input cards. The program provides, among other things, an upper-bound power profile useful in the design of the Power Subsystem and related equipment.

The sequence of mission events, shown in Table 1. is presented with the following column heading format:

Hours -	Refers to time from launch. The launch period is from
Seconds -	August 7 to September 5, 1973, with planetary arrival of the first vehicle falling between March 1 and March 11, 1974. PV 2 will arrive 8 days after PV 1.

Event Description - Occurrences within the mission.

Command Source - Source of command to initiate event.

Power Supply - The seven electrical power buses, described in Section 3., are combined under the headings:

DC=raw battery power
(37 - 52 VDC) and (37 - 65 VDC)
2.4=2.4 kHz power, single phase
400=400 Hz power (single & 3-phase)

The power requirement profile is shown for all events under these headings. Initial power is indicated at lift-off.

Component - Component affected by event (reference number from Appendix A, VOY-D-210).

Significant mission phases are indicated by double-space breaks in the computer printout. Only the printout "Events by Time", format 1, is displayed in Table 2. Except where specifically noted, all events are for PV 1. In the orbital modes, operations are repetitive and, for brevity, only one orbit is shown in the table. The computer is capable of printing out any number of repetitive orbits.

The radio modes, data modes, science categories and abbreviations used in the sequence of events are defined in Table 1.

3. COMMAND LIST

The Command Subsystem provides for 246 distinct commands. Most of these commands are outputed by the Command Subsystem in the form of a single pulse, which is utilized to accomplish the desired command action. However, a few of the commands contain binary data for subsequent use by the affected subsystem. Those command words which contain information regarding only a need for a momentary pulse are designated discrete commands, while those command words which contain additional binary data to be transferred to a subsystem are designated quantitative commands. The major user of quantitative commands

Table 1. Flight Sequence - Symbols and Abbreviations

Launch Radio Mode	6-watt amplifier, low gain and parasitic antenna.
Maneuver Radio Mode	50-watt amplifier, maneuver antenna.
Cruise Radio Mode	50-watt amplifier, high gain antenna.
Data Mode 1	Maneuver mode-data transmission at 7.5 bps, data storage at 150 bps.
Data Mode 2	Cruise mode-data transmission at 150 bps.
Data Mode 3	Orbit mode-data transmission of stored science data at 40,500/20,250/10,125 bps depending on range, and at 150 bps for engineering data.
Data Mode 4	Cruise recorder readout mode-transmission of stored maneuver data at 10,125 bps and cruise engineering data at 150 bps.
Data Mode 5	Capsule checkout mode-capsule checkout data transmitted at 100 bps and orbital engineering data at 50 bps.
Orbit Science	Science used in orbit but not PSP-mounted.
PSP Science	Science mounted on PSP.
ACS	Attitude Control System
ANT	Antenna
CAPSLE, CAPS	Flight Capsule
C/O	Checkout
CD	Command Decoder
CS, C & S	Computer and Sequencer
C & S2	Computer and Sequencer - PV 2
DAE	Data Automation Equipment
DS	Data Storage Subsystem
G & C	Guidance and Control Subsystem
HGA	High Gain Antennae
INH	Inhibit
LCE	Launch Complex Equipment
LV	Launch Vehicle
PSP	Planet Scan Platform
PV1	Forward Planetary Vehicle
PV2	Aft Planetary Vehicle
POWER	Power Subsystem
PYRO	Pyrotechnic Subsystem - PV 1
PYRO 2	Pyrotechnic Subsystem - PV 2
RADIO	Radio Subsystem
R. RAD	Relay Radio Subsystem
S 1	Separation Switch No. 1
SCI	Science Subsystem
SW	Switch
TVC	Thrust Vector Control

Table 2. Voyager Mission Sequence (Sheet 1 of 9)

HOUR	SECS	EVENT DESCRIPTION	COMMAND SOURCE	POWER SETTING DC	2.4	400	COMPONENT
- 24	0	*PRELAUNCH					
- 24	0	UPDATE/INSERT STORED COMMANDS	LCE				
- 24	0	CHARGE PV BATTERIES	LCE				
- 0	600	INITIALIZE PV TO LAUNCH MODE	LCE				
- 0	600	INITIALIZE ACS(GYROS + ELECT)	LCE				
- 0	600	RADIO TO LAUNCH MODE	LCE				
- 0	600	CAPSULE TO LAUNCH MODE	LCE				
- 0	600	SW TO INTERNAL PV POWER	LCE				
- 0	180	INITIALIZE C+S	LCE				
- 0	60	*LAUNCH/INJECTION/EARTH ORBIT					
- 0	60	UMBILICAL RELEASE	LCE				
0	0	LIFT OFF		313.0	196.0	21.0	
0	150	S-IC CUTOFF + JETTISON	LV				
0	155	S-II IGNITION	LV				
0	520	S-II CUTOFF + JETTISON	LV				
0	520	S-IVB IGNITION NO.1	LV				
0	660	S-IVB CUTOFF	LV				
0	660	EARTH ORBIT INSERTION					
0	1260	JETTISON FWD NOSE FAIRING	LV				
0	2460	ASSUME 30 MIN IN PARKING ORBIT					
0	2460	S-IVB IGNITION NO.2	LV				
0	2490	PV TRANSIT TRAJECT INJECTION					
0	2670	PV1 INFLT DISCONNECT SEPARAT	LV				
0	2670	PV1 SEPARATION (3FT/SEC)	LV				
0	2670	ARM PV1 PYROTECHNICS	S1	313.0	197.5	21.0	191900
0	2670	ENABLE C+S(PV1)	S1	313.0	197.5	21.0	081401
0	2730	*PV1 ACQUISITION					
0	2730	ENABLE HI THRUST COLD GAS JETS	CS001	337.0	197.5	21.0	142505
0	2820	END CAPSULE LAUNCH MODE	CS149				
0	2880	INITIATE HGA DEPLOYMENT	CS052	387.0	205.5	21.0	172103
0	2940	DEPLOY SOLAR PANELS	CS051				
0	2970	DEPLOY BROAD COVERAGE ANTENNA	CS053				
0	2985	DEPLOY MANEUVER ANTENNA	CS054				
0	3000	*PV 2 SEPARATION					
0	3000	REMOVE SHROUD	LV				
0	3180	PV2 INFLT DISCONNECT SEPARAT	LV				
0	3185	PV2 SEPARATION (1FT/SEC)	LV				
0	3185	ARM PV2 PYROTECHNICS	S1				
0	3185	ENABLE C+S(PV2)	S1				
0	3240	ANTENNA DEPLOYMENT COMPLETE		362.0	202.8	21.0	172103
0	3300	*SUBSEQ. EVENTS FOR PV1 ONLY					
1	330	*TV1 ACQUISITION (CONT)					

Table 2. Voyager Mission Sequence (Sheet 2 of 9)

HOUR	SECS	EVENT DESCRIPTION	COMMAND SOURCE	POWER SETTING DC	2.4	400	COMPONENT
1	330	SUN ACQUIS COMPLETE(20 MIN)		562.0	202.8	21.0	142505
1	340	SWITCH TO CRUISE MODE	CS032				
2	930	CANOPUS ACQ. COMPLETE(70 MIN)					
2	935	HGA CONTROL ON	CS078				
2	935	HGA MOVES TO PREPROG POSITION					
2	1530	SWITCH TO CRUISE RADIO MODE	CS116	434.0	202.8	21.0	071200
2	1530	DATA RECEPT ON EARTH VERIF ACQ					
2	1800	GYRO NO.1 OFF	CS082	422.0	187.8	10.5	091603
2	1800	GYRO NO.2 OFF	CS084	410.0	172.8	0.	091604
3	0	*FIRST CRUISE PERIOD					
3	0	UPDATE ANT POINTING(AS REQD)					
3	0	STEP ANT GIMBAL A (+)	CS096	435.0	175.5	0.	172103
3	0	STEP ANTENNAE GIMBAL B (+)	CS100				
3	40	STEPPING COMPLETE		410.0	172.8	0.	172103
3	40	UPDATE CANOPUS SENSOR POINTING					
3	45	MONITOR PV PERFORMANCE					
72	0	*ARRIVAL DATE SEP, MANEUVER					
72	0	UPDATE C+S MASTER SEQUENCER	CD186				
72	600	LOAD C+S TIME TO GO REGISTERS					
72	600	ROLL MANEUVER TIMES	CD905				
72	600	PITCH MANEUVER TIMES	CD906				
72	600	YAW MANEUVER TIMES	CD907				
72	600	ENGINE START TIME	CD908				
72	600	ENGINE STOP TIME	CD909				
75	0	GYRO NO.1 ON	CS081	510.0	187.8	10.5	091603
75	60	SUPPLY PRESS TO SOLEN VALVES	CS055				
75	60	ENABLE MAIN FUEL FLOW	CS065				
75	60	ENABLE MAIN OXID FLOW	CS066				
75	90	PRESSURIZE PROPELL TANKS	CS121	622.0	187.8	10.5	212229
75	1800	SW TO DATA MODE 1 (MANEUVER)	CS108	622.0	198.8	10.5	040808
75	1860	SW TO MANEUVER RADIO MODE	CS117				
75	3000	GYRO TEMP OVERRIDE	CS031	534.0	198.8	10.5	091603
75	3000	AUTOPILOT ON	CS076	534.0	207.2	10.5	091602
75	3060	SELECT PITCH+YAW INERTIAL MODE	CS022	510.0	207.2	10.5	142505
75	3060	SELECT ROLL INERTIAL MODE	CS026				
75	3120	START ROLL TURN(+)	CS018	534.0	207.2	10.5	142505
76	0	STOP ROLL TURN	CS020	510.0	207.2	10.5	142505
76	60	START PITCH TURN (+)	CS012	534.0	207.2	10.5	142505
76	540	STOP PITCH TURN	CS014	510.0	207.2	10.5	142505
76	600	START YAW TURN (+)	CS015	534.0	207.2	10.5	142505
76	1080	STOP YAW TURN	CS017	510.0	207.2	10.5	142505
76	1080	TURN TIMES BASED ON 180 DEG					
76	1800	ATTITUDE VERIFICATION COMPLETE					
76	1800	IF NO VER=INH BURN BY GRD COMM					
76	1800	HGA GIMBAL LOCKS ON	CS105	535.0	209.9	10.5	172103
76	1800	SELECT THRUST LEVEL(LOW)	CS129	625.0	209.9	10.5	212240
76	1800	TVC POWER ON(MAX. PWR.=1000W)	CS092	625.0	209.9	10.5	212217
76	1830	OPEN PREVALVE	CS133	925.0	209.9	10.5	212239
76	1860	OPEN OXID START VALVE	CS127				
76	1860	OPEN FUEL START VALVES(IGNITE)	CS125	1373.0	209.9	10.5	212237

Table 2. Voyager Mission Sequence (Sheet 3 of 9)

HOUR	SECS	EVENT DESCRIPTION	COMMAND SOURCE	POWER SETTING DC	2.4	400	COMPONENT
76	1872	OPEN MAIN PROPELL VALVES	CS131	1636.0	209.9	10.5	212238
76	1875	CLOSE START TANK VALVES(FUEL)	CS126	1190.0	209.9	10.5	212237
76	1875	CLOSE START TANK VALVE(OXID)	CS128				
76	1875	GIMBALLING BY AUTOPILOT					
76	1875	BURN TIME ASSUMED 260 SECONDS					
76	2120	CLOSE MAIN PROPELL VALVES	CS132	925.0	209.9	10.5	212238
76	2125	CLOSE PREVALVE	CS134	825.0	209.9	10.5	212239
76	2140	HGA GIMBAL LOCKS OFF	CS106	800.0	207.2	10.5	172103
76	2140	TVC POWER OFF	CS095	600.0	207.2	10.5	212217
76	2155	THROTTLE ACTUATOR OFF		510.0	207.2	10.5	212240
76	2155	AUTOPILOT POWER OFF	CS077	510.0	198.8	10.5	091602
76	2160	CLOSE PRESSURIZATION SOL VALVE	CS122	498.0	198.8	10.5	212225
76	2170	SW TO CRUISE MODE	CS032	422.0	198.8	10.5	142505
76	3070	SUN ACQUIS COMPLETE(15 MIN)		422.0	198.8	10.5	142505
78	70	CANOPUS ACQUIRED					
78	70	GYRO NO.1 OFF	CS082	410.0	163.8	0.	091603
78	80	CAPSULE POWER OFF	CS074	210.0	163.8	0.	242900
78	90	CAPSULE POWER ON	CS073	410.0	163.8	0.	242900
78	120	SW TO CRUISE RADIO MODE	CS116				
78	150	SW TO DATA MODE 4(READOUT)	CS111	410.0	188.8	0.	040808
78	510	SW TO DATA MODE 2(CRUISE)	CS109	410.0	172.8	0.	040808
78	1800	*SECOND CRUISE PERIOD					
78	1800	REPEAT FIRST CRUISE PERIOD					
720	0	*FIRST INTERPLNTRY CORRECTION					
720	0	REPEAT ARR DATE SEP MNVR EXCPT					
720	0	DO NOT SUPPLY PRESS TO SOL VLV					
720	0	BURN TIME ASSUMED 30 SECONDS					
720	0	DISABLE PRESS TO SOL VALVES	CS056				
726	0	*THIRD CRUISE PERIOD					
726	0	REPEAT FIRST CRUISE PERIOD					
726	0	SW SUN SENSORS TO MED GAIN	CS027				
4776	0	*SECOND INTERPLNTRY CORRECTION					
4776	0	REPEAT ARR DATE SEP MANEUVER					
4776	0	BURN TIME ASSUMED 10 SECONDS					
4782	0	*FOURTH CRUISE PERIOD					
4782	0	REPEAT FIRST CRUISE PERIOD					
4782	0	SW SUN SENSORS TO HIGH GAIN	CS028				
5015	0	*MARS ORBIT INSERTION					
5015	0	UPDATE C*S MASTER SEQUENCER	CD186				
5015	600	LOAD C*S TIME TO GO REGISTERS					
5015	600	ROLL MANEUVER TIMES	CD905				
5015	600	PITCH MANEUVER TIMES	CD906				

Table 2. Voyager Mission Sequence (Sheet 4 of 9)

HOUR	SECS	EVENT DESCRIPTION	COMMAND SOURCE	POWER SETTING DC	2.4	400	COMPONENT
5015	600	YAW MANEUVER TIMES	CD907				
5015	600	ENGINE START TIME	CD908				
5015	600	ENGINE STOP TIME	CD909				
5015	1080	GYRO NO.1 ON	CS081	510.0	187.8	10.5	091603
5015	1080	GYRO NO.2 ON	CS083	610.0	202.8	21.0	091604
5015	1080	BOTH GYROS ON DURING INSERTION					
5016	900	PRESSURIZE PROPELLANT TANKS	CS121	722.0	202.8	21.0	212225
5016	1080	GYRO TEMP OVERRIDE	CS031	634.0	202.8	21.0	091603
5016	1080	GYRO TEMP OVERRIDE	CS031	546.0	202.8	21.0	091604
5016	1080	SW TO DATA MODE 1 (MANEUVER)	CS108	546.0	213.8	21.0	040808
5016	1140	SW TO MANEUVER RADIO MODE	CS117				
5016	2880	AUTOPILOT ON	CS076	546.0	222.2	21.0	091602
5016	2940	SELECT PITCH+YAW INERTIAL MODE	CS022	522.0	222.2	21.0	142505
5016	2940	SELECT ROLL NERTIAL MODE	CS026				
5017	1080	START ROLL TURN (+)	CS018	546.0	222.2	21.0	142505
5017	1560	STOP ROLL TURN	CS020	522.0	222.2	21.0	142505
5017	1620	START PITCH TURN (+)	CS012	546.0	222.2	21.0	142505
5017	2100	STOP PITCH TURN	CS014	522.0	222.2	21.0	142505
5017	2160	START YAW TURN (+)	CS015	546.0	222.2	21.0	142505
5017	2640	STOP YAW TURN	CS017	522.0	222.2	21.0	142505
5017	2640	TURN TIMES BASED ON 180 DEG					
5019	1680	ATTIT VERIF COMPLETE					
5019	3300	HGA GIMBAL LOCKS ON	CS105	547.0	224.9	21.0	172103
5019	3360	TVC POWER ON(MAX. PWR.=1000W)	CS092	747.0	224.9	21.0	212217
5019	3420	SELECT THRUST LEVEL(HIGH)	CS130	837.0	224.9	21.0	212240
5019	3570	OPEN PREVALVE	CS133	937.0	224.9	21.0	212239
5020	0	OPEN OXID START VALVE	CS127				
5020	0	OPEN FUEL START VLV(IGNITION	CS125	1385.0	224.9	21.0	212237
5020	12	OPEN MAIN PROPELL VALVES	CS131	1650.0	224.9	21.0	212238
5020	15	CLOSE START TANK VALVES(FUEL)	CS126	1202.0	224.9	21.0	212237
5020	15	CLOSE START TANK VALVE(OXID)	CS128				
5020	15	GIMBALLING BY AUTOPILOT					
5020	15	BURN TIME ASSUMED 204 SECONDS					
5020	204	CLOSE PROPELLANT VALVES(MAIN)	CS132	937.0	224.9	21.0	212238
5020	209	CLOSE PREVALVE	CS134	837.0	224.9	21.0	212239
5020	225	HGA GIMBAL LOCKS OFF	CS106	812.0	222.2	21.0	172103
5020	225	TVC POWER OFF	CS093	612.0	222.2	21.0	212217
5020	230	THROTTLE ACTUATOR OFF		522.0	222.2	21.0	212240
5020	230	AUTOPILOT POWER OFF	CS077	522.0	213.8	21.0	091602
5020	235	CLOSE PRESSURIZATION SOL VALVE	CS122	410.0	213.8	21.0	212225
5020	240	SW TO CRUISE MODE	CS032	434.0	213.8	21.0	142505
5020	240	CAPSULE POWER OFF	CS074	234.0	213.8	21.0	242900
5020	250	CAPSULE POWER ON	CS073	434.0	213.8	21.0	242900
5020	890	PERIAPSIS PASSAGE OCCURS					
5020	1190	SUN ACQUIS COMPLETE		434.0	213.8	21.0	142505
5020	1299	EARTH OCCULTATION OCCURS	CS120				
5020	3407	EARTH OCCULTATION COMPLETE	CS119				
5021	1790	CANOPUS ACQUIRED					
5021	1800	SW TO DATA MODE 4 (READOUT)	CS111	434.0	218.8	21.0	040808
5021	1800	ENABLE CANOPUS OCCULTAT. MODE	CS034				
5021	1800	GYRO NO.2 OFF	CS084	422.0	203.8	10.5	091604
5021	2100	SW TO DATA MODE 3 (ORBIT)	CS110	422.0	198.8	10.5	040808
5021	2220	*PV ORBITAL OPERATIONS					

Table 2. Voyager Mission Sequence (Sheet 5 of 9)

HOUR	SECS	EVENT DESCRIPTION	COMMAND SOURCE	POWER SETTING DC	2.4	400	COMPONENT
5021	2220	SW TO CRUISE RADIO MODE	CS110				
5021	2250	DEPLOY PLANET SCAN PLATFORM	CS067				
5021	2580	400 HZ SCIENCE POWER ON	CS085	422.0	218.8	10.5	030601
5021	2580	PSP CONTROL ON	DA042	422.0	218.8	16.5	122408
5021	2580	PSP MOVES TO PREPROGRAM POSIT					
5021	2610	REMOVE SCIENCE COVERS	CS068				
5024	570	MORNING TERMINATOR PASSAGE					
5024	1069	CANOPUS OCCULTATION OCCURS					
5024	1070	APOAPSIS PASSAGE OCCURS					
5025	709	CANOPUS OCCULTATION COMPLETE					
5027	1550	PSP SCIENCE ON	DAE	422.0	248.8	16.5	030601
5027	1850	IRRADIOMETER ON	DA032	422.0	254.8	16.5	122401
5027	2090	HIGH RESOLUTION TV ON	DA019	422.0	274.8	16.5	122406
5027	2690	HIGH RESOL IR SPCTRMTR ON	DA022	422.0	288.8	16.5	122402
5027	2690	BRD BND IR SPCTRMTR ON	DA027	422.0	293.8	21.5	122403
5027	2690	UVSPECTROMETER ON	DA036	422.0	309.8	26.5	122409
5027	2870	MED RESOL TV NO.1 ON	DA006	422.0	344.8	26.5	122404
5027	2900	MED RESOL TV NO.2 ON	DA008	422.0	379.8	26.5	122405
5027	3470	RECORDERS TO PEAK POWER	DAE	422.0	405.8	26.5	040808
5028	740	MED RESOL TV NO.1 OFF	DA007	422.0	370.8	26.5	122404
5028	770	MED RESOL TV NO.2 OFF	DA009	422.0	335.8	26.5	122405
5028	1070	HIGH RESOL TV OFF	DA020	422.0	315.8	26.5	122406
5028	1250	PERIAPSIS PASSAGE OCCURS					
5028	1260	CAPSULE POWER OFF	CS074	222.0	315.8	26.5	242900
5028	1270	CAPSULE POWER ON	CS073	422.0	315.8	26.5	242900
5028	1395	EVENING TERMINATOR PASSAGE					
5028	1448	HIGH RESOL IR SPCTRMTR OFF	DA023	422.0	301.8	26.5	122402
5028	1448	BRD BND SPCTRMTR OFF	DA028	422.0	296.8	21.5	122403
5028	1610	PLAYBACK COMPLETE	DAE	422.0	270.8	21.5	040808
5028	1659	EARTH OCCULTATION OCCURS	CS120				
5028	3410	UV SPECTROMETER OFF	DA037	422.0	254.8	16.5	122409
5029	167	EARTH OCCULTATION COMPLETE	CS119				
5029	650	IR RADIOMETER OFF	DA033	422.0	248.8	16.5	122401
5029	660	PSP SCIENCE OFF	DAE	422.0	218.8	16.5	030601
5118	0	*FIRST PV ORBIT TRIM MANEUVER					
5118	0	PERFORMED ONLY IF NECESSARY					
5118	0	ENG BURN ASSUMED AT PERIAPSIS					
5120	1800	RETRACT PLANET SCAN PLATFORM	CS135	422.0	218.8	18.0	122408
5120	1800	PSP GIMBAL LOCKS ON	CS159				

Table 2. Voyager Mission Sequence (Sheet 6 of 9)

HOUR	SECS	EVENT DESCRIPTION	COMMAND SOURCE	POWER SETTING DC	2.4	400	COMPONENT
5120	1800	PRECEEDING DISABLES PSP SCI					
5120	2270	UPDATE C+S MASTER SEQUENCER	CD186				
5120	2820	LOAD C+S TIME TO GO REGISTERS					
5120	2820	ROLL MANEUVER TIMES	CD905				
5120	2820	PITCH MANEUVERS TIMES	CD906				
5120	2820	YAW MANEUVER TIMES	CD907				
5120	2820	ENGINE START TIME	CD908				
5120	2820	ENGINE STOP TIME	CD909				
5120	3450	MORNING TERMINATOR PASSAGE					
5121	349	CANOPUS OCCULTATION OCCURS					
5121	350	APOAPSIS PASSAGE					
5121	1810	SW TO DATA MODE 1 (MANEUVER)	CS106				
5121	1810	SW TO MANEUVER RADIO MODE	CS117				
5121	3589	CANOPUS OCCULTATION COMPLETE					
5122	2400	PRESSURIZE PROPELL TANKS	CS121	534,0	218,8	18,0	212225
5122	3000	AUTOPILOT ON	CS076	534,0	227,2	18,0	091602
5122	3300	SELECT PITCH+YAW INERTIAL MODE	CS022	510,0	227,2	18,0	142505
5122	3300	SELECT ROLL INERTIAL MODE	CS026				
5123	0	START ROLL TURN (+)	CS018	534,0	227,2	18,0	142505
5123	480	STOP ROLL TURN	CS020	510,0	227,2	18,0	142505
5123	540	START PITCH TURN (+)	CS012	534,0	227,2	18,0	142505
5123	1020	STOP PITCH TURN	CS014	510,0	227,2	18,0	142505
5123	1080	START YAW TURN (+)	CS015	534,0	227,2	18,0	142505
5123	1560	STOP YAW TURN	CS017	510,0	227,2	18,0	142505
5123	1560	TURN TIMES BASED ON 180 DEG					
5125	360	ATT VERIF COMPLETE					
5125	360	IF NO VER-INH BURN BY GRD COMM					
5125	450	HGA GIMBAL LOCKS ON	CS105	535,0	229,9	18,0	172103
5125	450	SELECT THRUST LEVEL(LOW)	CS129	625,0	229,9	18,0	212240
5125	480	TVC POWER ON(MAX. PWR.=1000W)	CS092	825,0	229,9	18,0	212217
5125	510	OPEN PREVALVE	CS133	925,0	229,9	18,0	212239
5125	530	PERIAPSIS PASSAGE OCCURS					
5125	530	OPEN OXID START VALVE	CS127				
5125	530	OPEN FUEL START VLVS(IGNITION)	CS125	1373,0	229,9	18,0	212237
5125	542	OPEN MAIN PROPELL VALVES	CS131	1638,0	229,9	18,0	212238
5125	545	CLOSE START TANK VALVES(FUEL)	CS126	1190,0	229,9	18,0	212237
5125	545	CLOSE START TANK VALVE(OXID)	CS128				
5125	545	GIMBALLING BY AUTOPILOT					
5125	545	BURN TIME ASSUMED 600 SECONDS					
5125	675	EVENING TERMINATOR PASSAGE					
5125	939	EARTH OCCULTATION OCCURS					
5125	1145	CLOSE MAIN PROPELL VALVES	CS132	925,0	229,9	18,0	212238
5125	1150	CLOSE PREVALVE	CS134	825,0	229,9	18,0	212239
5125	1165	HGA GIMBAL LOCKS OFF	CS106	800,0	227,2	18,0	172103
5125	1165	TVC POWER OFF	CS093	600,0	227,2	18,0	212217
5125	1180	THROTTLE ACTUATOR OFF		510,0	227,2	18,0	212240
5125	1180	AUTOPILOT POWER OFF	CS077	510,0	218,8	18,0	091602
5125	1185	CLOSE PRESSURIZATION SOL VALVE	CS122	398,0	218,8	18,0	212225
5125	1185	DISABLE PRESS TO SOL VALVE	CS056				
5125	1185	SW TO CRUISE MODE	CS032	422,0	218,8	18,0	142505
5125	2085	SUN AQUIS COMPLETE		422,0	218,8	18,0	142505
5125	3047	EARTH OCCULT COMPLETE					
5126	2685	CANOPUS ACQUIRED					
5126	2730	PSP GIMBAL LOCKS OFF	CS160				

Table 2. Voyager Mission Sequence (Sheet 7 of 9)

HOUR	SECS	EVENT DESCRIPTION	COMMAND SOURCE	POWER SETTING DC	2.4	400	COMPONENT
5126	2730	DEPLOY PLANET SCAN PLATFORM	CS135				
5126	2755	CAPSULE POWER OFF	CS074	222.0	218.8	18.0	242900
5126	2765	CAPSULE POWER ON	CS073	422.0	218.8	18.0	242900
5126	2790	SW TO CRUISE RADIO MODE	CS110				
5126	2820	SW TO DATA MODE 4 (READOUT)	CS111	422.0	223.8	18.0	040808
5126	3090	DEPLOYMENT COMPLETE		422.0	223.8	16.5	122408
5126	3090	PSP REACQUIRE AND TRACK	DA043				
5126	3090	PRECEDING ENABLES PSP-SCI					
5126	3180	SW TO DATA MODE 3 (ORBIT)	CS110	422.0	218.8	16.5	040808
5126	3240	*SECOND PV ORBITAL PERIOD					
5126	3240	UPDATE HGA POINTING (AS READ)					
5126	3240	UPDATE PSP POINTING (AS REQD)					
5129	210	MORNING TERMINATOR PASSAGE					
5129	709	CANOPUS OCCULTATION OCCURS					
5129	710	APOAPSIS PASSAGE OCCURS					
5130	349	CANOPUS OCCULTATION COMPLETE					
5132	1190	PSP SCIENCE ON	DAE	422.0	248.8	16.5	030601
5132	1490	IR RADIOMETER ON	DA032	422.0	254.8	16.5	122401
5132	1730	HIGH RESOLUTION TV ON	DA019	422.0	274.8	16.5	122406
5132	2330	HIGH RESOL IR SPECTROMETER ON	DA022	422.0	288.8	16.5	122402
5132	2330	BRD BAND IR SPECTROMETER ON	DA027	422.0	293.8	21.5	122403
5132	2330	UV SPECTROMETER ON	DA036	422.0	309.8	26.5	122409
5132	2510	MED RESOL TV NO.1 ON	DA006	422.0	344.8	26.5	122404
5132	2540	MED RESOL TV NO.2 ON	DA008	422.0	379.8	26.5	122403
5132	3060	RECORDERS TO PEAK POWER	DAE	422.0	405.8	26.5	040808
5133	560	MED RESOL TV NO.1 OFF	DA007	422.0	370.8	26.5	122404
5133	590	MED RESOL TV NO.2 OFF	DA009	422.0	335.8	26.5	122405
5133	710	HIGH RESOL TV OFF	DA020	422.0	315.8	26.5	122406
5133	890	PERIAPSIS PASSAGE OCCURS					
5133	900	CAPSULE POWER OFF	CS074	222.0	315.8	26.5	242900
5133	910	CAPSULE POWER ON	CS073	422.0	315.8	26.5	242900
5133	1035	EVENING TERMINATOR PASSAGE					
5133	1088	HIGH RESOL IR SPECTROMETER OFF	DA023	422.0	301.8	26.5	122402
5133	1088	BRD BAND IR SPECTROMETER OFF	DA028	422.0	296.8	21.5	122403
5133	1251	PLAYBACK COMPLETE	DAE	422.0	270.8	21.5	040808
5133	1299	EARTH OCCULTATION OCCURS	CS120				
5133	3050	UVSPECTROMETER OFF	DA037	422.0	254.8	16.5	122409
5133	3407	EARTH OCCULTATION COMPLETE	CS119				
5134	290	IR RADIOMETER OFF	DA033	422.0	248.8	16.5	122401
5134	300	PSP SCIENCE OFF	DAE	422.0	218.8	16.5	030601
5185	2730	MORNING TERMINATOR PASSAGE					
5185	3229	CANOPUS OCCULTATION OCCURS					
5185	3230	APOAPSIS PASSAGE OCCURS					
5186	2869	CANOPUS OCCULTATION COMPLETE					
5188	1100	*FLIGHT CAPSULE SEPARATION					

Table 2. Voyager Mission Sequence (Sheet 8 of 9)

HOUR	SECS	EVENT DESCRIPTION	COMMAND SOURCE	POWER SETTING DC	2.4	400	COMPONENT
5188	1100	SW TO DATA MODE 5(CAPS C/O)	CS112				
5188	1700	START CAPSULE CHECKOUT	CS150				
5189	110	PSP SCIENCE ON	DAE	422,0	248,8	16,5	030601
5189	410	IR RADIOMETER ON	DA032	422,0	254,8	16,5	122401
5189	650	HIGH RESOLUTION TV ON	DA019	422,0	274,8	16,5	122406
5189	1250	HIGH RESOL IR SPECTROMETER ON	DA022	422,0	268,8	16,5	122402
5189	1250	BRD BAND IR SPECTROMETER ON	DA027	422,0	293,8	21,5	122403
5189	1250	UV SPECTROMETER ON	DA036	422,0	309,8	26,5	122409
5189	1430	MED RESOL TV NO,1 ON	DA005	422,0	344,8	26,5	122404
5189	1460	MED RESOL TV NO,2 ON	DA008	422,0	379,8	26,5	122405
5189	1980	RECORDERS TO PEAK POWER	DAE	422,0	405,8	26,5	040808
5189	3080	MED RESOL TV NO,1 OFF	DA007	422,0	370,8	26,5	122404
5189	3110	MED RESOL TV NO,2 OFF	DA009	422,0	335,8	26,5	122405
5189	3230	HIGH RESOL TV OFF	DA020	422,0	315,8	26,5	122405
5189	3410	PERIAPSIS PASSAGE OCCURS					
5189	3420	CAPSULE POWER OFF	CS074	222,0	315,8	26,5	242900
5189	3430	CAPSULE POWER ON	CS073	422,0	315,8	26,5	242900
5189	3555	EVENING TERMINATOR PASSAGE					
5190	8	HIGH RESOL IR SPECTROMETER OFF	DA023	422,0	301,8	26,5	122402
5190	8	BRD BAND IR SPECTROMETER OFF	DA028	422,0	296,8	21,5	122403
5190	171	PLAYBACK COMPLETE	DAE	422,0	270,8	21,5	040808
5190	219	EARTH OCCULTATION OCCURS	CS120				
5190	1970	UVSPECTROMETER OFF	DA037	422,0	254,8	16,5	122409
5190	2327	EARTH OCCULTATION COMPLETE	CS119				
5190	2810	IR RADIOMETER OFF	DA033	422,0	248,8	16,5	122401
5190	2820	PSP SCIENCE OFF	DAE	422,0	218,8	16,5	030601
5194	2900	UPDATE + VER STORED CAPS COMMS					
5195	1640	INHIBIT PSP GIMBAL	DA041	422,0	218,8	10,5	122408
5195	1640	PRECEEDING INHIBS PSP SCI ON					
5195	1670	RELAY RADIO ON	CS079	422,0	268,8	10,5	071301
5195	1700	ENABLE CAPSULE SEPAR SEQUENCE	CD236				
5195	1730	SW TO CAPSULE INTERNAL POWER	CPSLE	222,0	268,8	10,5	242900
5196	800	SEPARATE BIOBARRIER	CS070				
5196	920	LOW RATE RECORDER ON	CS145				
5196	1100	CAPSULE SEPARATION					
5196	1110	ENABLE LO THRUST COLD GAS JETS	CS069				
5196	2300	CAPSULE DEORBIT MOTOR FIRES					
5196	2600	HIGH RATE RECORDER ON	CS146				
5197	3518	CAPSULE IMPACT					
5198	170	PERIAPSIS PASSAGE					
5198	218	LOW RATE RECORDER OFF	CS145				
5198	218	HIGH RATE RECORDER OFF	CS146				
5198	255	EVENING TERMINATOR PASSAGE					
5198	280	RELAY RADIO OFF	CS080	222,0	218,8	10,5	071301
5198	320	SW TO DATA MODE 3 (ORBIT)	CS110				
5198	380	ENABLE PSP GIMBAL	DA043	222,0	218,8	16,5	122408
5198	459	EARTH OCCULTATION OCCURS					
5198	2567	EARTH OCCULTATION COMPLETE					
5198	2580	ENABLE RELAY RECORD READOUT	CS147				
5202	506	COMPL RELAY RECORD REAADOUT					
5202	506	*SPACECRAFT ORBITAL OPERATION					
5202	506	REPEAT SECOND PV ORBITAL PER					

Table 2. Voyager Mission Sequence (Sheet 9 of 9)

HOUR	SECS	EVENT DESCRIPTION	COMMAND SOURCE	POWER SETTING DC	2.4	400	COMPONENT
5284	180	*FIRST S/C ORBIT TRIM MANEUVER					
5284	180	PERFORMED ONLY IF NECESSARY					
5284	180	ENG. BURN ASSUMED AT APOAPSIS					
5284	180	REPEAT PV ORB. TRIM MAN.EXCEPT					
5284	180	ENABLE PRESS TO SOL VALVES					
5284	180	DISABLE PRESS TO SOL VALVES					
5284	180	DELETE CAPSULE COMMANDS					
7536	0	*FIRST SUN OCCULTATION OCCURS					
7536	0	105DAYS AFTER INSERTION					
7540	1500	GYRO NO.1 ON	CS081				
7541	1500	GYRO TEMP OVERRIDE	CS031				
7541	1788	ENABLE SUN OCCULTATION MODE	CS033				
7541	1848	SUN OCCULTATION OCCURS					
7542	2082	SUN OCCULTATION COMPLETE					
7542	3000	GYRO NO. 1 OFF	CS082				

is the computer and sequencer which uses the binary information to control the mode of the computer and sequencer, to update the master sequencer, and to fill several special registers. Other users of quantitative commands from the Command Subsystem are the Guidance and Control Subsystem, the Data Automation Subsystem, and the flight capsule.

In the command list (Table 3) the source of a command action is indicated by a letter prefix to the command numbers. Commands from the Command Subsystem are prefixed by the letter D, commands from the computer and sequencer are prefixed by the letter S, and commands from the Data Automation Subsystem are preceded by the letter A. Quantitative command data outputted by the Command Subsystem is indicated by allocation of the 900 series of numbers prefixed by the letter D. Commands derived from the quantitative command data routed to the flight capsule are not presented in this command list. All of the S commands issued from the computer and sequencer are derived from the quantitative command D904; similarly all of the A commands issued from the Data Automation Subsystem are derived from the quantitative command D917.

Many command functions are controlled by either of two commands; those commands that are normally utilized are designated as primary commands while those commands which represent non-normal command actions are designated "backup" commands. The command list for the Data Storage Subsystem lists only backup commands since this subsystem receives its primary control as a result of commands sent to the Radio Subsystem.

The total spare commands (D commands) from the Command Subsystem is 28, which represents a margin of 11 percent of the 246 total D commands.

Explanation of the abbreviations used in the command list is given in Table 4.

Table 3. Command Listing (Sheet 1 of 5)

GUIDANCE AND CONTROL SUBSYSTEM					
Command		Command Function	Command		Command Function
Primary	Backup		Primary	Backup	
S001	D001	Enable Pneumatic Drivers	S028	D030	Pitch & Yaw Sun Sensor High Gain
S002	D002	Disable Pitch and Yaw Pneumatic Drivers	S029	D031	Enable Autopilot
S003	D003	Enable Pitch and Yaw Pneumatic Drivers	S030	D032	Disable Autopilot
S006	D006	Disable Roll Pneumatic Driver	S031	D033	Gyro Temperature Override
S007	D007	Enable Roll Pneumatic Driver	S032	D034	Enable Cruise Mode
D008		Select Gyro Package No. 1	S033	D035	Enable Sun Occultation Mode
D009		Select Gyro Package No. 2	S034	D036	Enable Canopus Occultation Mode
S008	D010	Gyro Rate Mode	D037		Select Canopus Sensor No. 1
S009	D011	Gyro Position Mode	D038		Select Canopus Sensor No. 2
S012	D014	Start Pitch (+) Turn	S035	D039	Enable Canopus Sensor No. 1 High Gate
S013	D015	Start Pitch (-) Turn	S036	D040	Disable Canopus Sensor No. 1 High Gate
S014	D016	Stop Pitch Turn	S037	D041	Enable Canopus Sensor No. 2 High Gate
S015	D017	Start Yaw (+) Turn	S038	D042	Disable Canopus Sensor No. 2 High Gate
S016	D018	Start Yaw (-) Turn	S039	D043	Canopus Sensor No. 1 Cone Position 1
S017	D019	Stop Yaw Turn	S040	D044	Canopus Sensor No. 1 Cone Position 2
S018	D020	Start Roll (+) Turn	S041	D045	Canopus Sensor No. 1 Cone Position 3
S019	D021	Start Roll (-) Turn	S042	D046	Canopus Sensor No. 1 Cone Position 4
S020	D022	Stop Roll Turn	S043	D047	Canopus Sensor No. 2 Cone Position 1
S021	D023	Select Pitch and Yaw Celestial Mode	S044	D048	Canopus Sensor No. 2 Cone Position 2
S022	D024	Select Pitch and Yaw Inertial Mode	S045	D049	Canopus Sensor No. 2 Cone Position 3
S025	D027	Select Roll Celestial Mode	S046	D050	Canopus Sensor No. 2 Cone Position 4
S026	D028	Select Roll Inertial Mode	D918		Position Engine Gimbal Pitch
S027	D029	Pitch & Yaw Sun Sensor Medium Gain	D919		Position Engine Gimbal Yaw
PYROTECHNIC SUBSYSTEM					
S051	D055	Deploy Solar Panels	S062	D066	Fourth Post-Thrust Depressurization Pyro
S052	D056	Initiate High Gain Antenna Deployment	S063	D067	Enable Start Fuel Flow Pyro
S053	D057	Deploy Broad Coverage Antenna	S064	D068	Enable Start Oxidizer Flow Pyro
S054	D058	Deploy Maneuver Antenna	S065	D069	Enable Main Fuel Flow Pyro
S055	D059	First Pre-Thrust Pressurization Pyro	S066	D070	Enable Main Oxidizer Flow Pyro
S056	D060	First Post-Thrust Depressurization Pyro	S067	D071	Initiate PSP Deployment
S057	D061	Second Pre-Thrust Pressurization Pyro	S068	D072	Remove Science Instrument Covers
S058	D062	Second Post-Thrust Depressurization Pyro	S069	D073	Initiate Cold Gas Jet Pyro
S059	D063	Third Pre-Thrust Pressurization Pyro	S070	D074	Initiate Sterilization Cannister Separation
S060	D064	Third Post-Thrust Depressurization Pyro	D075		Disable Propulsion System Pyro
S061	D065	Fourth Pre-Thrust Pressurization Pyro	D076		Arm Disable Propulsion System Pyro

Table 3. Command Listing (Sheet 2 of 5)

POWER SUBSYSTEM					
Command		Command Function	Command		Command Function
Primary	Backup		Primary	Backup	
D080		Charge Regulator No. 1 OFF	S075	D104	2.4 KHZ Science Power On
D081		Charge Regulator No. 1 Setting "A"	D105		2.4 KHZ Science Power Off
D082		Charge Regulator No. 1 Setting "B"	S076	D106	Autopilot Power On
D083		Charge Regulator No. 2 OFF	S077	D107	Autopilot Power Off
D084		Charge Regulator No. 2 Setting "A"	S078	D108	Articulation Power On/Off
D085		Charge Regulator No. 2 Setting "B"	S079	D109	Relay Radio Power On
D086		Charge Regulator No. 3 OFF	S080	D111	Relay Radio Power Off
D087		Charge Regulator No. 3 Setting "A"	S081	D112	Gyro Set No. 1 On
D088		Charge Regulator No. 3 Setting "B"	S082	D113	Gyro Set No. 1 Off
D089		Main Regulator - Switch to No. 1	S083	D114	Gyro Set No. 2 On
D090		Main Regulator - Switch to No. 2	S084	D115	Gyro Set No. 2 Off
D093		2.4 KHZ Inverter - Switch to No. 1	S085	D116	400 HZ Science Power On
D094		2.4 KHZ Inverter - Switch to No. 2	D117		400 HZ Science Power Off
D097		Select 400 HZ Inverter No. 1	S086	D118	Canopus Sensor No. 1 Power On
D098		Select 400 HZ Inverter No. 2	S089	D119	Canopus Sensor No. 1 Power Off
D099		Select Master Clock OSC. No. 1	S090	D120	Canopus Sensor No. 2 Power On
D100		Select Master Clock OSC. No. 2	S091	D121	Canopus Sensor No. 2 Power Off
S073	D102	Capsule Power On	S092	D122	Thrust Vector Control Power On
S074	D103	Capsule Power Off	S093	D123	Thrust Vector Control Power Off
HIGH GAIN ANTENNA ARTICULATION/ACTUATION SUBSYSTEM					
S096	D128	Rotate 3/16° (+) "A" Axis	S102	D134	Slew (+) "B" Axis
S097	D129	Rotate 3/16° (-) "A" Axis	S103	D135	Slew (-) "B" Axis
S098	D130	Slew (+) "A" Axis	S104	D136	Stop Slew
S099	D131	Slew (-) "A" Axis	S105	D137	HGA Gimbal Locks On
S100	D132	Rotate 3/16° (+) "B" Axis	S106	D138	HGA Gimbal Locks Off
S101	D133	Rotate 3/16° (-) "B" Axis			
TELEMETRY SUBSYSTEM					
S108	D140	Switch to Data Mode 1	S113	D145	Advance High Data Rate
S109	D141	Switch to Data Mode 2	D146		Exchange Programmers
S110	D142	Switch to Data Mode 3	D147		Exchange Channels
S111	D143	Switch to Data Mode 4	D148		Exchange Block Coders
S112	D144	Switch to Data Mode 5			

Table 3. Command Listing (Sheet 3 of 5)

Command		Command Function	Command		Command Function
Primary	Backup		Primary	Backup	
DATA STORAGE SUBSYSTEM					
	D150	Reset PSC Address		D153	Exchange PSC Functions
	D151	Advance PSC Address		D154	Playback Start
	D152	Advance MTR Input Switch Position		D155	Playback Interrupt
RADIO SUBSYSTEM					
S115		Switch to Launch Radio Mode	D162		Power Amplifier No. 3 On/Off
S116		Switch to Cruise Radio Mode	D163		Receiver No. 1 On/Off
S117		Switch to Maneuver Radio Mode	D164		Receiver No. 2 On/Off
D157		Exciter No. 1 On/Off	D165		Receiver No. 3 On/Off
D158		Exciter No. 2 On/Off	D166		Antenna Switch No. 1 Norm/Rev
D159		Exciter No. 3 On/Off	D167		Antenna Switch No. 2 Norm/Rev
D160		Power Amplifier No. 1 On/Off	D168		Antenna Switch No. 3 Norm/Backup
D161		Power Amplifier No. 2 On/Off	D169		Ranging On/Off
COMPUTER AND SEQUENCER SUBSYSTEM					
D900		HGA Gimbal Angle "A" Slope	D915		PSP Turn Off Threshold
D901		HGA Gimbal Angle "B" Slope	S154	D171	Start Special Sequence 1
D902		PSP Gimbal Angle "C" Slope	S155	D172	Start Special Sequence 2
D903		PSP Gimbal Angle "D" Slope	S156	D173	Start Special Sequence 3
D904		Modify/Scan Word in Memory	S157	D174	Start Special Sequence 4
D905		TTGR 1 Update	D181		Set Time Base to 1 Second
D906		TTGR 2 Update	D182		Set Time Base to 1 Minute
D907		TTGR 3 Update	D183		Set Time Base to 1 Hour
D908		TTGR 4 Update	S119	D184	Inhibit Earth Occultation Mode Data Switch
D909		TTGR 5 Update			
D910		TTGR 6 Update	S120	D185	Enable Earth Occultation Mode Data Switch
D911		TTGR 7 Update			
D912		TTGR 8 Update	D186		Update Master Sequence
D913		Δ V Register Update	D187		Start Master Sequence
D914		PSP Turn On Threshold			

Table 3. Command Listing (Sheet 4 of 5)

PROPULSION SUBSYSTEM					
Command		Command Function	Command		Command Function
Primary	Backup		Primary	Backup	
S121	D193	Open Pressurant Solenoid Valve No. 1	S128	D200	Close Quad Oxidizer Solenoid Valves
S122	D194	Close Pressurant Solenoid Valve No. 1	S129	D201	Select Low Thrust Level Mode
S123	D195	Open Pressurant Solenoid Valve No. 2	S130	D202	Select High Thrust Level Mode
S124	D196	Close Pressurant Solenoid Valve No. 2	S131	D203	Open Quad Ball Solenoid Valves
S125	D197	Open Quad Fuel Solenoid Valves	S132	D204	Close Quad Ball Solenoid Valves
S126	D198	Close Quad Fuel Solenoid Valves	S133	D205	Open Propulsion Prevalve Solenoid
S127	D199	Open Quad Oxidizer Solenoid Valves	S134	D206	Close Propulsion Prevalve Solenoid
			S161	D192	Throttle Actuator Power Off
SCIENCE AND DATA AUTOMATION EQUIPMENT SUBSYSTEM					
D917		DAE Sequencer Update	A021		HRTV Camera Expose
A001		Normal MRTV Operation	A022		HRIR Spectrometer Power On
A002		Stereo MRTV Operation	A023		HRIR Spectrometer Power Off
A003		MRTV Sequence Start	A024		HRIR Spectrometer Optical Position
A004		MRTV Sequence Period	A025		BBIR Spectrometer Motor On
A005		MRTV Sequence Frames	A026		BBIR Spectrometer Motor Off
A006		MRTV Camera No. 1 Power On	A027		BBIR Spectrometer Electronics On
A007		MRTV Camera No. 1 Power Off	A028		BBIR Spectrometer Electronics Off
A008		MRTV Camera No. 2 Power On	A029		BBIR Spectrometer Optical Position
A009		MRTV Camera No. 2 Power Off	A030		IR Radiometer Motor On
A010		MRTV Camera No. 1 Filter Color	A031		IR Radiometer Motor Off
A011		MRTV Camera No. 2 Filter Color	A032		IR Radiometer Electronics On
A012		MRTV Camera No. 1 Optical Position	A033		IR Radiometer Electronics Off
A013		MRTV Camera No. 2 Optical Position	A034		UV Spectrometer Motor On
A014		MRTV Camera No. 1 Expose	A035		UV Spectrometer Motor Off
A015		MRTV Camera No. 2 Expose	A036		UV Spectrometer Electronics On
A016		HRTV Sequence Start	A037		UV Spectrometer Electronics Off
A017		HRTV Sequence Period	A038		UV Spectrometer Optical Position
A018		HRTV Sequence Frames	A039		UV Spectrometer Low Data Rate
A019		HRTV Camera Power On	A040		UV Spectrometer High Data Rate
A020		HRTV Camera Power Off	S144	D220	DAS Power On
			S148	D231	DAS Power Off

Table 3. Command Listing (Sheet 5 of 5)

PLANETARY SCIENCE PLATFORM ARTICULATION					
Command		Command Function	Command		Command Function
Primary	Backup		Primary	Backup	
S159	D239	PSP Gimbal Locks On	S143	D215	Stop Slew
S160	D240	PSP Gimbal Locks Off	D216		Heater No. 1 Power On
S135	D207	Rotate 3/16° (+) PSP C Axis	D217		Heater No. 1 Power Off
S136	D208	Rotate 3/16° (-) PSP C Axis	D218		Heater No. 2 Power On
S137	D209	Rotate 3/16° (+) PSP D Axis	D219		Heater No. 2 Power Off
S138	D210	Rotate 3/16° (-) PSP D Axis	A041	D220	PSP "E" Gimbal Hold
S139	D211	Slew (+) PSP C Axis	A042	D221	PSP "E" Gimbal Acquire/Track
S140	D212	Slew (-) PSP C Axis	A043	D222	PSP "E" Gimbal Continue/Track
S141	D213	Slew (+) PSP D Axis	A044	D223	PSP "E" Gimbal (+) Slew
S142	D214	Slew (-) PSP D Axis	A045	D224	PSP "E" Gimbal (-) Slew
RELAY RADIO SUBSYSTEM					
S145	D227	Low Rate Recorder On/Off	S147	D229	Enable Recorder Readout
S146	D228	High Rate Recorder On/Off	D230		Disable Recorder Readout
FLIGHT CAPSULE					
S149	D232	End Capsule Launch Mode	D236		Enable Capsule Separation
S150	D233	Start Capsule Checkout	D237		Disable Capsule Separation
S151	D234	Switch to Internal Power	D290		Capsule Sequencer Update
S152	D235	Initiate Capsule Separation Sequence			

Table 4. Definition of Abbreviations

BBIR	Broadband Infrared
DAE	Data Automation Equipment
HGA	High Gain Antenna
HRTV	High Resolution Television
IR	Infrared
MRTV	Medium Resolution Television
MTR	Magnetic Tape Recorder
PSC	Playback Sequence Control
PSP	Planet Scan Platform
TTGR	Time-to-Go Register
UV	Ultraviolet
Δ V	Delta Velocity

4. TELEMETRY LIST

The telemetry commutator for Voyager provides three sampling rates (in any given mode) to format the various engineering measurements into a single digital bit stream. The organization of the commutator is shown on Figure 1. There are a total of 8 high-speed decks (A through H), 16 medium-speed decks (M100 through M1600), and 15 low-speed decks (L100 through L1500).

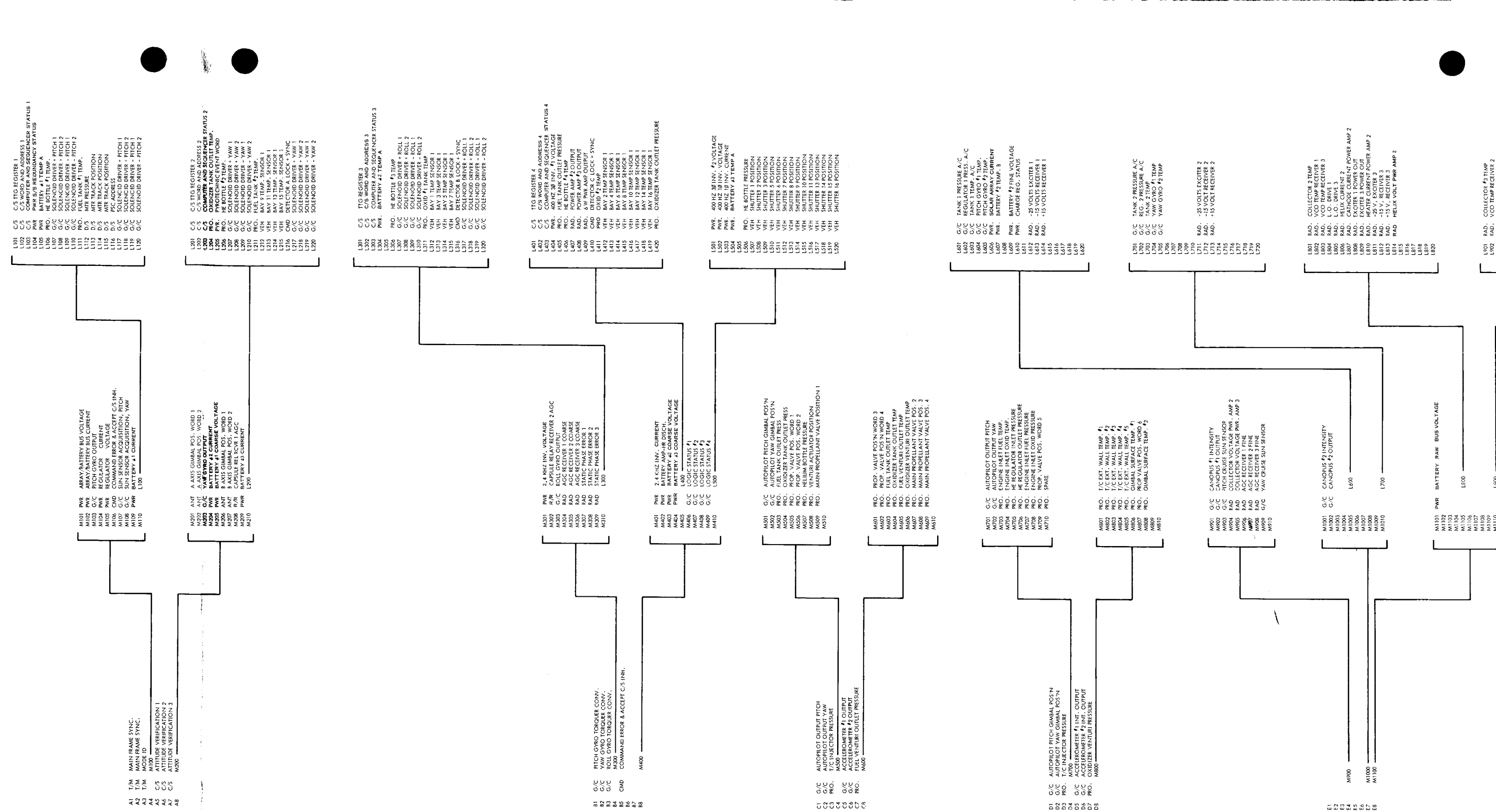

FOLDOUT FRAME

FOLDOUT FRAME 1

FOLDOUT FRAME 2

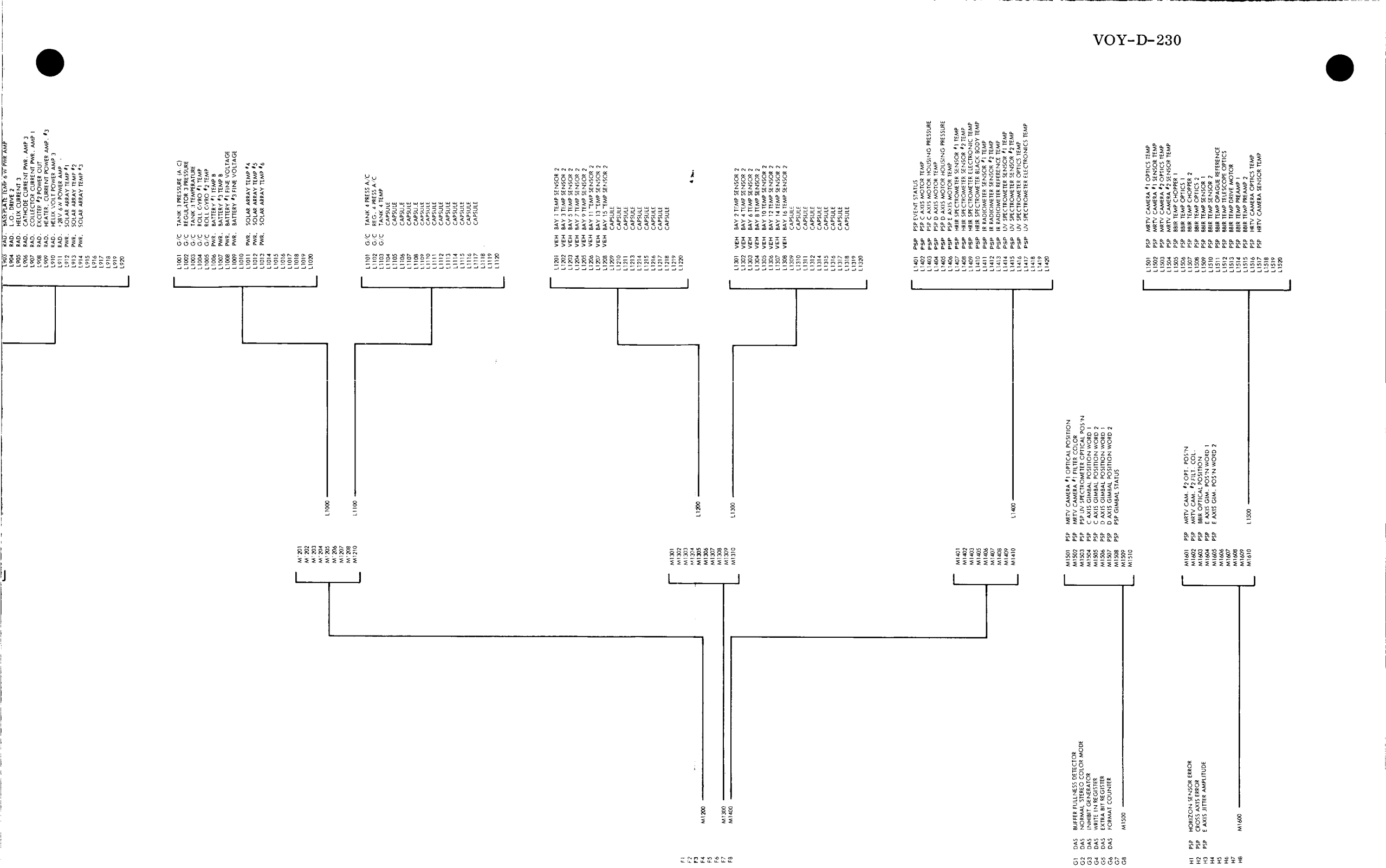

Figure 1. Telemetry Deck Format

FOLDOUT FRAME 3

FOLDOUT FRAME 4

Five telemetry modes have been provided by the Telemetry Subsystem to accommodate the data requirements of the different phases of the Voyager Mission. These data modes include data sampling and real time transmission as well as selected data storage and delayed transmission of engineering data as noted in Table 5. Table 5 reveals several aspects of the data modes. These aspects are:

a. Channels of the medium deck are sampled 1/10th as often as the high deck channels.

b. Channels of the low deck are sampled 1/20th as often as the channels of the medium deck and 1/200th as often as the channels of the high deck.

c. During the maneuver mode, data is collected for storage on a tape recorder at a rate 10 times faster than real time data is being transmitted (7.5 bps).

d. The highest rate of sampling and real time transmission (150 bps) occurs during the cruise and cruise recorder readout modes.

Table 5. Telemetry Data Modes

Mode	High Decks		Medium Decks		Low Decks	
	Decks	Sampling Period	Decks	Sampling Period	Decks	Sampling Period
1. Maneuver						
Realtime Data	A&B	14.92 sec	100-400	149.2 sec	100-500	2984 sec
Stored Data	A&B&C&D	1.49 sec	100-800	14.92 sec	100-500	298.4 sec
2. Cruise	A&B&E&F	1.49 sec	100-1400	14.92 sec	100-1400	298.4 sec
3. Orbit	A&B&E& F&G&H	2.24 sec	100-400 900-1600	22.4 sec	100-1500	448 sec
4. Cruise Recorder Readout	A&B&C&D	1.49 sec	100-1400	14.92 sec	100-1400	298.4 sec
5. Capsule Checkout	A&B& Capsule Data	2.24 sec	100-400	22.4 sec	100-500	448 sec

e. Stored data collected during the maneuver mode is read out during the cruise recorder readout mode without interrupting the cruise real time data.

f. Coded telemetry data from the flight capsule is time multiplexed with the two full time transmission decks (decks A&B) during the capsule checkout mode; the flight capsule data occupies the same sampling time as four decks nominally used for spacecraft telemetry.

Table 6, "Telemetry Channel Assignment", presents by subsystem, the channels assigned to the various subsystem functions. Additional information is included concerning maximum input voltage to the encoder and the engineering units for each measurement. The encoder will accept low-level dc inputs from 0 to +100 MVDC, a bipolar dc input from -1.6 to +1.6 VDC, and high level dc inputs from 0 to +3.2 volts. The type of input to the encoder is indicated under max volts in Table 6. The telemetry matrix will also accept digital coded data; this type of input is signified under max volts as dig. (digital). Digital data, when sampled, bypasses the encoder and enters by means of a buffer into the digital data stream outputted by the encoder. Most of the digital data is used to indicate some type of event count or status of a switch and thus are labeled as events in the engineering units column of Table 6. In those instances where the digital data sampled represents an analog quantity, the descriptive engineering units are defined.

Table 6. Channel Assignments (Sheet 1 of 11)

1. GUIDANCE AND CONTROL

T/M Channel	Function		Maximum Volts	Eng. Units
M901	Canopus #1 Intensity		3.2	Bright
M1001	Canopus #2 Intensity		3.2	Bright
M902	Canopus #1 Output		1.6	Deg.
M1002	Canopus #2 Output		1.6	Deg.
M103	Pitch Gyro Output		1.6	Deg-Deg/sec
M203	Yaw Gyro Output		1.6	Deg-Deg/sec
M303	Roll Gyro Output		1.6	Deg-Deg/sec
B1	Pitch Gyro Torquer Current		3.2	Amps
B2	Yaw Gyro Torquer Current		3.2	Amps
B3	Roll Gyro Torquer Current		3.2	Amps
M107	Sun Sensor Acquisition Pitch		1.6	Deg.
M108	Sun Sensor Acquisition Yaw		1.6	Deg.
M903	Pitch Cruise Sun Sensor		100 MV	Deg.
M909	Yaw Cruise Sun Sensor		100 MV	Deg.
L107	Solenoid Driver + Pitch 1		Dig.	Events
L117	Solenoid Driver + Pitch 1	(R)	Dig.	Events
L108	Solenoid Driver + Pitch 2		Dig.	Events
L118	Solenoid Driver + Pitch 2	(R)	Dig.	Events
L109	Solenoid Driver - Pitch 1		Dig.	Events
L119	Solenoid Driver - Pitch 1	(R)	Dig.	Events
L110	Solenoid Driver - Pitch 2		Dig.	Events
L120	Solenoid Driver - Pitch 2	(R)	Dig.	Events
L207	Solenoid Driver + Yaw 1		Dig.	Events
L217	Solenoid Driver + Yaw 1	(R)	Dig.	Events
L208	Solenoid Driver + Yaw 2		Dig.	Events
L218	Solenoid Driver + Yaw 2	(R)	Dig.	Events
L209	Solenoid Driver - Yaw 1		Dig.	Events
L219	Solenoid Driver - Yaw 1	(R)	Dig.	Events
L210	Solenoid Driver - Yaw 2		Dig.	Events
L220	Solenoid Driver - Yaw 2	(R)	Dig.	Events
L307	Solenoid Driver + Roll 1		Dig.	Events
L317	Solenoid Driver + Roll 1	(R)	Dig.	Events
L308	Solenoid Driver + Roll 2		Dig.	Events
L318	Solenoid Driver + Roll 2	(R)	Dig.	Events
L309	Solenoid Driver - Roll 1		Dig.	Events
L319	Solenoid Driver - Roll 1	(R)	Dig.	Events
L310	Solenoid Driver - Roll 2		Dig.	Events

Table 6. Channel Assignments (Sheet 2 of 11)

T/M Channel	Function	Maximum Volts	Eng. Units
L320	Solenoid Driver - Roll 2	Dig.	Events
M406	Logic Status #1	Dig.	Events
M407	Logic Status #2	Dig.	Events
M408	Logic Status #3	Dig.	Events
M409	Logic Status #4	Dig.	Events
D1	Autopilot Pitch Gimbal Position	3.2	Deg.
M501	Autopilot Pitch Gimbal Position	3.2	Deg.
D2	Autopilot Yaw Gimbal Position	3.2	Deg.
M502	Autopilot Yaw Gimbal Position	3.2	Deg.
C1	Autopilot Amplifier Output Pitch	3.2	VDC
M701	Autopilot Amplifier Output Pitch	3.2	VDC
C2	Autopilot Amplifier Output Yaw	3.2	VDC
M702	Autopilot Amplifier Output Yaw	3.2	VDC
C5	Accelerometer #1 Output	3.2	F/S^2
D6	Accelerometer #2 Output	3.2	F/S^2
D5	Accelerometer #1 Integrator Output	3.2	F/S
C6	Accelerometer #2 Integrator Output	3.2	F/S
L601	Tank 1 Pressure	3.2	PSI
L701	Tank 2 Pressure	3.2	PSI
L1001	Tank 3 Pressure	3.2	PSI
L1101	Tank 4 Pressure	3.2	PSI
L602	Regulator 1 Pressure	3.2	PSI
L702	Regulator 2 Pressure	3.2	PSI
L1002	Regulator 3 Pressure	3.2	PSI
L1102	Regulator 4 Pressure	3.2	PSI
L603	Tank 1 Temperature	100 MV	Deg. F.
L703	Tank 2 Temperature	100 MV	Deg. F.
L1003	Tank 3 Temperature	100 MV	Deg. F.
L1103	Tank 4 Temperature	100 MV	Deg. F.
L604	Pitch Gyro #1 Temperature	100 MV	Deg. F.
L704	Yaw Gyro #1 Temperature	100 MV	Deg. F.
L1004	Roll Gyro #1 Temperature	100 MV	Deg. F.
L605	Pitch Gyro #2 Temperature	100 MV	Deg. F.
L705	Yaw Gyro #2 Temperature	100 MV	Deg. F.
L1005	Roll Gyro #2 Temperature	100 MV	Deg. F.

Table 6. Channel Assignments (Sheet 3 of 11)

2. PROPULSION

T/M Channel	Function	Maximum Volts	Eng. Units
C3	T/C Injector Pressure	3.2	PSI
D3	T/C Injector Pressure (R)	3.2	PSI
M801	T/C External Wall Temp. #1	100 MV	Deg. F.
M802	T/C External Wall Temp. #2	100 MV	Deg. F.
M803	T/C External Wall Temp. #3	100 MV	Deg. F.
M804	T/C External Wall Temp. #4	100 MV	Deg. F.
M805	T/C External Wall Temp. #5	100 MV	Deg. F.
M505	Propulsion Valve Position Word 1	Dig.	Events
M506	Propulsion Valve Position Word 2	Dig.	Events
M507	Propulsion Valve Position Word 3	Dig.	Events
M508	Propulsion Valve Position Word 4	Dig.	Events
M709	Propulsion Valve Position Word 5	Dig.	Events
M807	Propulsion Valve Position Word 6	Dig.	Events
L106	Helium Bottle #1 Temp.	100 MV	Deg. F.
L206	Helium Bottle #2 Temp.	100 MV	Deg. F.
L306	Helium Bottle #3 Temp.	100 MV	Deg. F.
L406	Helium Bottle #4 Temp.	100 MV	Deg. F.
L111	Fuel Tank #1 Temp.	100 MV	Deg. F.
L211	Fuel Tank #2 Temp.	100 MV	Deg. F.
L311	Oxidizer Tank #1 Temp.	100 MV	Deg. F.
L411	Oxidizer Tank #2 Temp.	100 MV	Deg. F.
M603	Fuel Tank Outlet Temp.	100 MV	Deg. F.
M604	Oxidizer Tank Outlet Temp.	100 MV	Deg. F.
M507	Helium Bottle Pressure	3.2	PSI
L506	Helium Bottle Pressure	3.2	PSI
M503	Fuel Tank Outlet Pressure	3.2	PSI
L405	Fuel Tank Outlet Pressure	3.2	PSI
M504	Oxidizer Tank Outlet Pressure	3.2	PSI
L420	Oxidizer Tank Outlet Pressure	3.2	PSI
M605	Fuel Venturi Outlet Temp.	100 MV	Deg. F.
M606	Oxidizer Venturi Outlet Temp.	100 MV	Deg. F.
M703	Engine Inlet Fuel Temp.	100 MV	Deg. F.
M704	Engine Inlet Oxidizer Temp.	100 MV	Deg. F.
M705	Helium Regulator Inlet Press.	3.2	PSI
M706	Helium Regulator Outlet Press.	3.2	PSI
M707	Engine Inlet Fuel Press.	3.2	PSI

Table 6. Channel Assignments (Sheet 4 of 11)

T/M Channel	Function	Maximum Volts	Eng. Units
M708	Engine Inlet Oxidizer Press.	3.2	PSI
M806	Gimbal Surface Temp. #1	100 MV	Deg. F.
M807	Gimbal Surface Temp. #2	100 MV	Deg. F.
C7	Fuel Venturi Outlet Press.	3.2	PSI
D7	Oxidizer Venturi Outlet Press.	3.2	PSI
M508	Venturi Actuator Position	3.2	%
M509	Main Propellant Valve Pos. 1	3.2	%
M607	Main Propellant Valve Pos. 2	3.2	%
M608	Main Propellant Valve Pos. 3	3.2	%
M609	Main Propellant Valve Pos. 4	3.2	%

3. RADIO

T/M Channel	Function	Maximum Volts	Eng. Units
M304	AGC Receiver 1 Coarse	3.2	DBM
M305	AGC Receiver 2 Coarse	3.2	DBM
M306	AGC Receiver 3 Coarse	3.2	DBM
M307	Static Phase Error 1	1.6	CPS
M308	Static Phase Error 2	1.6	CPS
M309	Static Phase Error 3	1.6	CPS
M904	Collector Voltage Pwr. Amp. 2	1.6	VDC
M905	Collector Voltage Pwr. Amp. 3	1.6	VDC
M906	AGC Receiver 1 Fine	100 MV	DBM
M907	AGC Receiver 2 Fine	100 MV	DBM
M908	AGC Receiver 3 Fine	100 MV	DBM
L407	Power Amplifier #2 Output	3.2	WAT
L408	Power Amplifier #3 Output	3.2	WAT
L409	6W Power Amplifier Output	3.2	WAT
L612	-25 Volts Exciter 1	1.6	VDC
L613	-15 Volts Receiver 1	1.6	VDC
L614	+15 Volts Receiver 1	1.6	VDC
L711	-25 Volts Exciter 2	1.6	VDC
L712	-15 Volts Receiver 2	1.6	VDC
L713	+15 Volts Receiver 2	1.6	VDC
L802	VCO Temp. Receiver 1	100 MV	Deg. F.
L902	VCO Temp. Receiver 2	100 MV	Deg. F.

Table 6. Channel Assignments (Sheet 5 of 11)

T/M Channel	Function	Maximum Volts	Eng. Units
L803	VCO Temp. Receiver 3	100 MV	Deg. F.
L804	L.O. Drive 1	100 MV	MW
L904	L.O. Drive 2	100 MV	MW
L805	L.O. Drive 3	100 MV	MW
L806	Helix Current 2	3.2	MA
L905	Helix Current 3	3.2	MA
L808	Exciter 1 Power Out	3.2	WAT
L908	Exciter 2 Power Out	3.2	WAT
L809	Exciter 3 Power Out	3.2	WAT
L810	Heater Cur. Pwr. Amp. 2	3.2	MA
L909	Heater Cur. Pwr. Amp. 3	3.2	MA
L811	-25V Exciter 3	1.6	VDC
L812	-15V Receiver 3	1.6	VDC
L813	+15V Receiver 3	1.6	VDC
L801	Collector #2 Temp.	100 MV	Deg. F.
L901	Collector #3 Temp.	100 MV	Deg. F.
L903	Baseplate Temp. 6W Pwr. Amp.	100 MV	Deg. F.
L907	Cathode Current Pwr. Amp. 1	3.2	MA
L807	Cathode Current Pwr. Amp. 2	3.2	MA
L906	Cathode Current Pwr. Amp. 3	3.2	MA
L814	Helix Volt Pwr. Amp. 2	1.6	VDC
L910	Helix Volt Pwr. Amp. 3	1.6	VDC
L911	+28V 6W Pwr. Amp.	3.2	VDC
M208	Capsule Relay Receiver 1 AGC	1.6	DBM
M302	Capsule Relay Receiver 2 AGC	1.6	DBM

4. SCIENCE DATA AUTOMATION EQUIPMENT

T/M Channel	Function	Maximum Volts	Eng. Units
G1	Buffer Fullness Detector	Dig.	Events
G2	Normal/Stereo Color Mode	Dig.	Events
G3	Inhibit Generator	Dig.	Events
G4	Write In Register	Dig.	Events
G5	Extra Bit Register	Dig.	Events
G6	Format Counter	Dig.	Events

Table 6. Channel Assignments (Sheet 6 of 11)

5. COMMAND

T/M Channel	Function	Maximum Volts	Eng. Units
B5	Cmd. Error & Accept C/S Inhibit	Dig.	Events
M106	Cmd. Error & Accept C/S Inhibit	Dig.	Events
L216	Detector A Lock + Sync	Dig.	Events
L316	Detector B Lock + Sync	Dig.	Events
L410	Detector C Lock + Sync	Dig.	Events

6. POWER

T/M Channel	Function	Maximum Volts	Eng. Units
M101	Array/Battery Bus Voltage	3.2V	VDC
M102	Array/Battery Bus Current	3.2V	Amp.
M104	Regulator #1 Current	3.2V	Amp.
M105	Regulator #1 Voltage	3.2V	VDC
M301	2.4 KHZ Inverter #1 Voltage	3.2V	VAC
M401	2.4 KHZ Inverter #2 Voltage	3.2V	VAC
M402	Battery Amp-Hr Discharge	3.2V	AHR
L606	Solar Array Current	3.2V	Amp.
L104	Power S/S Redundancy Status	Dig.	Events
M1101	Battery Raw Bus Voltage	3.2V	VDC
L404	400 HZ 3Ø Inv. #1 Voltage	3.2V	VAC
L501	400 HZ 3Ø Inv. #2 Voltage	3.2V	VAC
L502	400 HZ 1Ø Inv. Voltage	3.2V	VAC
L503	400 HZ 1Ø Inv. Current	3.2V	Amp.
L105	Battery #1 Temp. A	100 MV	Deg. F.
L607	Battery #2 Temp. B	100 MV	Deg. F.
M205	Battery #1 Coarse Voltage	3.2V	VDC
L609	Battery #2 Fine Voltage	3.2V	VDC
L610	Charge Reg. States	Dig.	Events
M109	Battery #1 Current	Dig.	Amp.

Table 6. Channel Assignments (Sheet 7 of 11)

T/M Channel	Function	Maximum Volts	Eng. Units
L504	Battery #3 Temp. A	100 MV	Deg. F.
L304	Battery #2 Temp. A	100 MV	Deg. F.
M404	Battery #3 Coarse Voltage	3.2V	VDC
M403	Battery #2 Coarse Voltage	3.2V	VDC
M204	Battery #2 Current	3.2V	Amp.
L912	Solar Array Temp. #1	100 MV	Deg. F.
L913	Solar Array Temp. #2	100 MV	Deg. F.
L914	Solar Array Temp. #3	100 MV	Deg. F.
L1006	Battery #1 Temp. B	100 MV	Deg. F.
L1007	Battery #3 Temp. B	100 MV	Deg. F.
L1008	Battery #1 Fine Voltage	3.2V	VDC
L1009	Battery #3 Fine Voltage	3.2V	VDC
M209	Battery #3 Current	3.2V	Amp.
L1011	Solar Array Temp. #4	100 MV	Deg.
L1012	Solar Array Temp. #5	100 MV	Deg.
L1013	Solar Array Temp. #6	100 MV	Deg.

7. VEHICLE

T/M Channel	Function	Maximum Volts	Eng. Units
M201	A Axis Gimbal Pos. Word 1	Dig.	Events
M202	A Axis Gimbal Pos. Word 2	Dig.	Events
M206	B Axis Gimbal Pos. Word 1	Dig.	Events
M207	B Axis Gimbal Pos. Word 2	Dig.	Events
L205	Pyrotechnic Event Word	Dig.	Events
L312	Bay 1 Temp. Sensor 1	100 MV	Deg. F.
L412	Bay 2 Temp. Sensor 1	100 MV	Deg. F.
L313	Bay 3 Temp. Sensor 1	100 MV	Deg. F.
L413	Bay 4 Temp. Sensor 1	100 MV	Deg. F.
L314	Bay 5 Temp. Sensor 1	100 MV	Deg. F.
L414	Bay 6 Temp. Sensor 1	100 MV	Deg. F.
L315	Bay 7 Temp. Sensor 1	100 MV	Deg. F.
L415	Bay 8 Temp. Sensor 1	100 MV	Deg. F.
L212	Bay 9 Temp. Sensor 1	100 MV	Deg. F.
L416	Bay 10 Temp. Sensor 1	100 MV	Deg. F.

Table 6. Channel Assignments (Sheet 8 of 11)

T/M Channel	Function	Maximum Volts	Eng. Units
L213	Bay 11 Temp. Sensor 1	100 MV	Deg. F.
L417	Bay 12 Temp. Sensor 1	100 MV	Deg. F.
L214	Bay 13 Temp. Sensor 1	100 MV	Deg. F.
L418	Bay 14 Temp. Sensor 1	100 MV	Deg. F.
L215	Bay 15 Temp. Sensor 1	100 MV	Deg. F.
L419	Bay 16 Temp. Sensor 1	100 MV	Deg. F.
L1201	Bay 1 Temp. Sensor 2	100 MV	Deg. F.
L1301	Bay 2 Temp. Sensor 2	100 MV	Deg. F.
L1202	Bay 3 Temp. Sensor 2	100 MV	Deg. F.
L1302	Bay 4 Temp. Sensor 2	100 MV	Deg. F.
L1203	Bay 5 Temp. Sensor 2	100 MV	Deg. F.
L1303	Bay 6 Temp. Sensor 2	100 MV	Deg. F.
L1204	Bay 7 Temp. Sensor 2	100 MV	Deg. F.
L1304	Bay 8 Temp. Sensor 2	100 MV	Deg. F.
L1205	Bay 9 Temp. Sensor 2	100 MV	Deg. F.
L1305	Bay 10 Temp. Sensor 2	100 MV	Deg. F.
L1206	Bay 11 Temp. Sensor 2	100 MV	Deg. F.
L1306	Bay 12 Temp. Sensor 2	100 MV	Deg. F.
L1207	Bay 13 Temp. Sensor 2	100 MV	Deg. F.
L1307	Bay 14 Temp. Sensor 2	100 MV	Deg. F.
L1208	Bay 15 Temp. Sensor 2	100 MV	Deg. F.
L1308	Bay 16 Temp. Sensor 2	100 MV	Deg. F.
L507	Shutter 1 Position	3.2	Deg.
L508	Shutter 2 Position	3.2	Deg.
L509	Shutter 3 Position	3.2	Deg.
L510	Shutter 5 Position	3.2	Deg.
L511	Shutter 6 Position	3.2	Deg.
L512	Shutter 7 Position	3.2	Deg.
L513	Shutter 8 Position	3.2	Deg.
L514	Shutter 9 Position	3.2	Deg.
L515	Shutter 10 Position	3.2	Deg.
L516	Shutter 11 Position	3.2	Deg.
L517	Shutter 13 Position	3.2	Deg.
L518	Shutter 14 Position	3.2	Deg.
L519	Shutter 15 Position	3.2	Deg.
L520	Shutter 16 Position	3.2	Deg.

Table 6. Channel Assignments (Sheet 9 of 11)

8. DATA STORAGE

T/M Channel	Function	Maximum Volts	Eng. Units
L112	MTR Pressure	Dig.	High/Low
L113	MTR Track Position	Dig.	Position
L114	MTR Track Position	Dig.	Position
L115	MTR Track Position	Dig.	Position
L116	PSC Address	Dig.	Position

9. COMPUTER AND SEQUENCER

T/M Channel	Function	Maximum Volts	Eng. Units
A5	Attitude Verification 1	Dig.	Deg.
A6	Attitude Verification 2	Dig.	Deg.
A7	Attitude Verification 3	Dig.	Deg.
L101	TTG Register 1	Dig.	Events
L201	TTG Register 2	Dig.	Events
L301	TTG Register 3	Dig.	Events
L401	TTG Register 4	Dig.	Events
L102	Word and Address 1	Dig.	Events
L202	Word and Address 2	Dig.	Events
L302	Word and Address 3	Dig.	Events
L402	Word and Address 4	Dig.	Events
L103	Computer and Sequencer Status 1	Dig.	Events
L203	Computer and Sequencer Status 2	Dig.	Events
L303	Computer and Sequencer Status 3	Dig.	Events
L403	Computer and Sequencer Status 4	Dig.	Events

10. SCIENCE

T/M Channel	Function	Maximum Volts	Eng. Units
H1	PSP Horizon Sensor Error	1.6	Deg.
H2	PSP Cross Axis Error	1.6	Deg.
H3	PSP E Axis Jitter Amplitude	3.2	Deg.

Table 6. Channel Assignments (Sheet 10 of 11)

T/M Channel	Function	Maximum Volts	Eng. Units
M1501	MRTV Camera #1 Optical Position	Dig.	Events
M1502	MRTV Camera #1 Filter Color	Dig.	Events
M1503	UV Spectrometer Optical Position	Dig.	Events
M1504	C Axis Gimbal Position Word #1	Dig.	Events
M1505	C Axis Gimbal Position Word #2	Dig.	Events
M1506	D Axis Gimbal Position Word 1	Dig.	Events
M1507	D Axis Gimbal Position Word 2	Dig.	Events
M1508	PSP Gimbal Status	Dig.	Events
L1401	PSP Event Status	Dig.	Events
L1402	PSP C Axis Motor Temp.	100 MV	Deg. F.
L1403	PSP C Axis Motor Housing Press.	3.2	PSI
L1404	PSP D Axis Motor Temp.	100 MV	Deg. F.
L1405	PSP D Axis Motor Housing Press.	3.2	PSI
L1406	PSP E Axis Motor Temp.	100 MV	Deg. F.
L1407	HRIR Spectrometer Sensor #1 Temp.	100 MV	Deg. F.
L1408	HRIR Spectrometer Sensor #2 Temp.	100 MV	Deg. F.
L1409	HRIR Spectrometer Sensor Elect. Temp.	100 MV	Deg. F.
L1410	HRIR Spectrometer Sensor Blackbody Temp.	100 MV	Deg. F.
L1411	IR Radiometer Sensor #1 Temp.	100 MV	Deg. F.
L1412	IR Radiometer Sensor #2 Temp.	100 MV	Deg. F.
L1413	IR Radiometer Sensor Reference Temp.	100 MV	Deg. F.
L1414	UV Spectrometer Sensor #1 Temp.	100 MV	Deg. F.
L1415	UV Spectrometer Sensor #2 Temp.	100 MV	Deg. F.
L1416	UV Spectrometer Sensor Optics Temp.	100 MV	Deg. F.
L1417	UV Spectrometer Sensor Electronics Temp.	100 MV	Deg. F.
L1501	MRTV Camera #1 Optics Temp.	100 MV	Deg. F.
L1502	MRTV Camera Sensor Temp.	100 MV	Deg. F.
L1503	MRTV Camera #2 Optics Temp.	100 MV	Deg. F.
L1504	MRTV Camera #2 Sensor Temp.	100 MV	Deg. F.
L1505	BBIR Temp. Chopper 1	100 MV	Deg. F.
L1506	BBIR Temp. Optics 1	100 MV	Deg. F.
L1507	BBIR Temp. Chopper 2	100 MV	Deg. F.
L1508	BBIR Temp. Optics 2	100 MV	Deg. F.
L1509	BBIR Temp. Sensor 1	100 MV	Deg. F.
L1510	BBIR Temp. Sensor 2	100 MV	Deg. F.
L1511	BBIR Temp. Opaque Reference	100 MV	Deg. F.
L1512	BBIR Temp. Telescope Optics	100 MV	Deg. F.

Table 6. Channel Assignments (Sheet 11 of 11)

T/M Channel	Function	Maximum Volts	Eng. Units
L1513	BBIR Temp. Drive Motor	100 MV	Deg. F.
L1514	BBIR Temp. Preamp 1	100 MV	Deg. F.
L1515	BBIR Temp. Preamp #2	100 MV	Deg. F.
L1516	HRTV Camera Optics Temp.	100 MV	Deg. F.
L1517	HRTV Camera Sensor Temp.	100 MV	Deg. F.

11. CAPSULE

T/M Channel	Function	Maximum Volts	Eng. Units
L1104	These channels have been reserved for		
L1105	unassigned capsule functions such as		
L1106	voltages, currents, temperatures,		
L1107	events, status, etc.		
L1108			
L1109			
L1111			
L1112			
L1113			
L1114			
L1115			
L1116			
L1117			
L1209			
L1210			
L1211			
L1212			
L1213			
L1214			
L1215			
L1216			
L1217			
L1218			
L1309			
L1310			
L1311			
L1312			
L1313			
L1314			
L1315			
L1316			
L1317			
L1318			

VOY-D-240
BASELINE SCIENCE DEFINITION

1. INTRODUCTION AND SUMMARY

The spacecraft design update for the 1973 Mars Mission is complicated to some degree by the fact that the scientific experiments for the mission will not be selected before 1968. The requirements imposed on the spacecraft by the experiments can influence the design requirements for every spacecraft subsystem and the overall spacecraft configuration. The approach taken during this study was to anticipate the selection of the experiments and their requirements, using the best available information, and to provide a high degree of flexibility where possible in the spacecraft design. The flexibility and growth provisions provided by the design are discussed throughout this study report; this section is concerned with the selection of a hypothetical baseline payload and the requirements imposed on the spacecraft design by this baseline payload.

The hypothetical baseline payload was established using the following criteria:

a. The hypothetical baseline payload will constitute the best estimate that can presently be made of the final science payload.

b. Only high priority experiments will be included; i.e., those which are the most important in the exploration of Mars.

c. The hypothetical baseline payload may press, but must not exceed, realistic mission support capabilities.

A summary of the science experiments selected for the baseline payload is shown in Table 1. If additional experiments can be supported by the spacecraft, the following experiments are recommended on a first priority basis:

a. Photopolarimeter

b. Micrometeorite Detector

c. Cosmic Ray Telescope

Table 1. Baseline Science Experiments

Experiment	Weight (lb)	Power (watts)	Data (bits/orbit)
1. Photoimaging			
Medium Resolution TV Camera #1	38	35	8.65×10^8
Medium Resolution TV Camera #2	38	35	8.65×10^8
High Resolution TV Camera	59	20	2.88×10^8
2. High Resolution IR Spectrometry	30	14	5.85×10^5
3. Broadband IR Spectrometry	16	5	4.68×10^6
4. IR Radiometry	20	6	1.44×10^7
5. UV Spectrometry	32	16	1.24×10^7
6. Radio Occultation	-	-	-
7. Celestial Mechanics	-	-	-

2. BASELINE SCIENCE PAYLOAD DESCRIPTION

2.1 EXPERIMENT SELECTION RATIONALE

The selection of the baseline experiments for Voyager '73 is made on the basis of two separate considerations:

a. Scientific Merit - the ability of the experiment to obtain specific scientific data about the Martian environment. Priorities are assigned on the basis of providing general broad based information which has relevance to a number of scientific areas and which is required in the planning of later highly specialized scientific investigations.

b. Specific Information - the ability of the experiment to obtain information that will be most useful in an engineering sense for the design of subsequent Voyager missions.

As an example of the application of this rationale, consider a photoimaging mission. One objective is to locate areas on the surface of the planet that look promising for future biological exploration, e.g., say a dark homogeneous area showing strong seasonal response to the wave of darkening and with a strong rejuvenative character when inundated by a severe dust storm. An estimate of the surface relief on a scale compatible with the size of the lander is desirable before considering such an area as a soft landing site. Thus, the capability is contained in a single experiment for obtaining both scientific and engineering data and a high priority for such an experiment is established.

Similar arguments can be advanced for the other baseline experiments; some of the arguments are presented below. Additional instruments, discussed in Paragraph 3, fulfill the rationale and could amend the baseline scientific instrument payload in the future.

The selected high resolution IR spectrometer experiment provides detailed information about the abundance of H_2O vapor, the surface reflectivity in selected wavelength regions, and the temperature structure within the Martian atmosphere as a function of altitude. Although not included in this instrument, effort should be made to extend the experiment to cover the fundamental CO_2 band at 4.3 microns. In addition to the scientific value, the determination of the temperature structure of the atmosphere will resolve the ambiguities existing in model atmospheres of the planet. The establishment of reliable model atmospheres is perhaps the single most important engineering objective for an early Martian experiment, as it greatly enhances the confidence level that can be assigned to a soft lander system. This experiment, along with the other IR experiments included in the baseline payload, provides an integrated capability for determining the prevailing microclimatic and selected aerological conditions as well as providing engineering data needed for soft lander system designs.

The broadband infrared (IR) spectrometer, when looking at the atmosphere, provides needed information about the chemical composition, particularly carbon dioxide, of the Martian atmosphere. This radiatively active gas is an important constituent in estimating the infrared heat loss of the planet. Furthermore, this experiment will scan the surface to supply data on

the compositional analysis of the surface rocks of Mars. The biological importance in discovering rocks containing water of crystalization is of course obvious.

The infrared radiometer, a light weight, highly reliable experiment, is designed to provide a thermal map of the Martian surface and cloud top temperatures with a spatial resolution previously unobtainable from terrestrial observations. From a scientific point of view, such data is invaluable if the thermal budget of the planet is to be understood. Such data also has direct bearing on determining the driving mechanism in the meteorologically active lower atmosphere of the planet. The latter results in winds which in turn are of engineering interest.

The ultraviolet (UV) spectrometer provides molecular, atomic, and ionic compositional analysis of the Martian atmosphere and the ultraviolet reflectivity of the Martian surface/atmosphere. The construction of model atmospheres at the higher altitudes depends strongly on the atmospheric constituents present at the near surface levels. While the IR spectrometer is capable of providing data on the CO_2 molecule, the UV experiment provides additional data with regard to atomic constituents such as argon, nitrogen, and hydrogen as well as O_3 and O_2. Molecules undergoing fluorescence in such atmospheres and detectable in the ultraviolet include nitric oxide, CO, and nitrogen. This experiment, therefore, not only provides fundamental scientific data but also data needed in the construction of model atmospheres.

In the following paragraphs, discussion of the individual experiments will include a definition of the experiment objectives as related to the 1973 mission, functional and physical descriptions, operational sequences, and performance and data characteristics.

2.2. PHOTOIMAGING EXPERIMENT

2.2.1. Experiment Description

The specific objectives for the photoimaging experiment are twofold:

a. Mapping of most of the planet at a resolution on the order of 100 meters. A fraction of this mapping will be performed in stereo and color.

b. Reconnaissance of selected areas of the planet at a resolution of approximately 10 meters.

As shown in Figure 1, three TV cameras are used in this experiment. Two Return Beam Vidicons perform the medium resolution mapping, while a Secondary Electron Conduction Vidicon takes the high resolution pictures. These tubes were selected for their high sensitivity, good spatial resolution, long storage capability, and rugged construction. The physical characteristics of each camera are also given in Figure 1.

In the mapping mode of operation, all three cameras are boresighted and nominally pointed at the planet along the local vertical. The two medium resolution cameras take alternate frames of a mapping sequence. This technique permits an increase in ground resolution for a limiting data record speed and allows the two medium resolution cameras to back-up each other in a degraded mapping mode. A sequence of overlapping frames taken when the spacecraft is between 1000 and 3000 km of altitude and between solar illumination angles of 40 and 80 degrees consists of 72 frames. Since a zoom lens is not provided, although quite desirable, the ground coverage of each frame will increase with altitude. To maintain the overlap between frames fairly constant as spacecraft altitude and velocity changes, the time between subsequent frames can be varied.

The design orbit has a period of approximately one-third the period of the planet's axial rotation. The offset between adjacent ground traces must be less than 100 km if some overlap is to be obtained between frames in adjacent ground traces. This condition will be approximately satisfied if the orbit period differs by about 5 minutes from exactly one-third of the

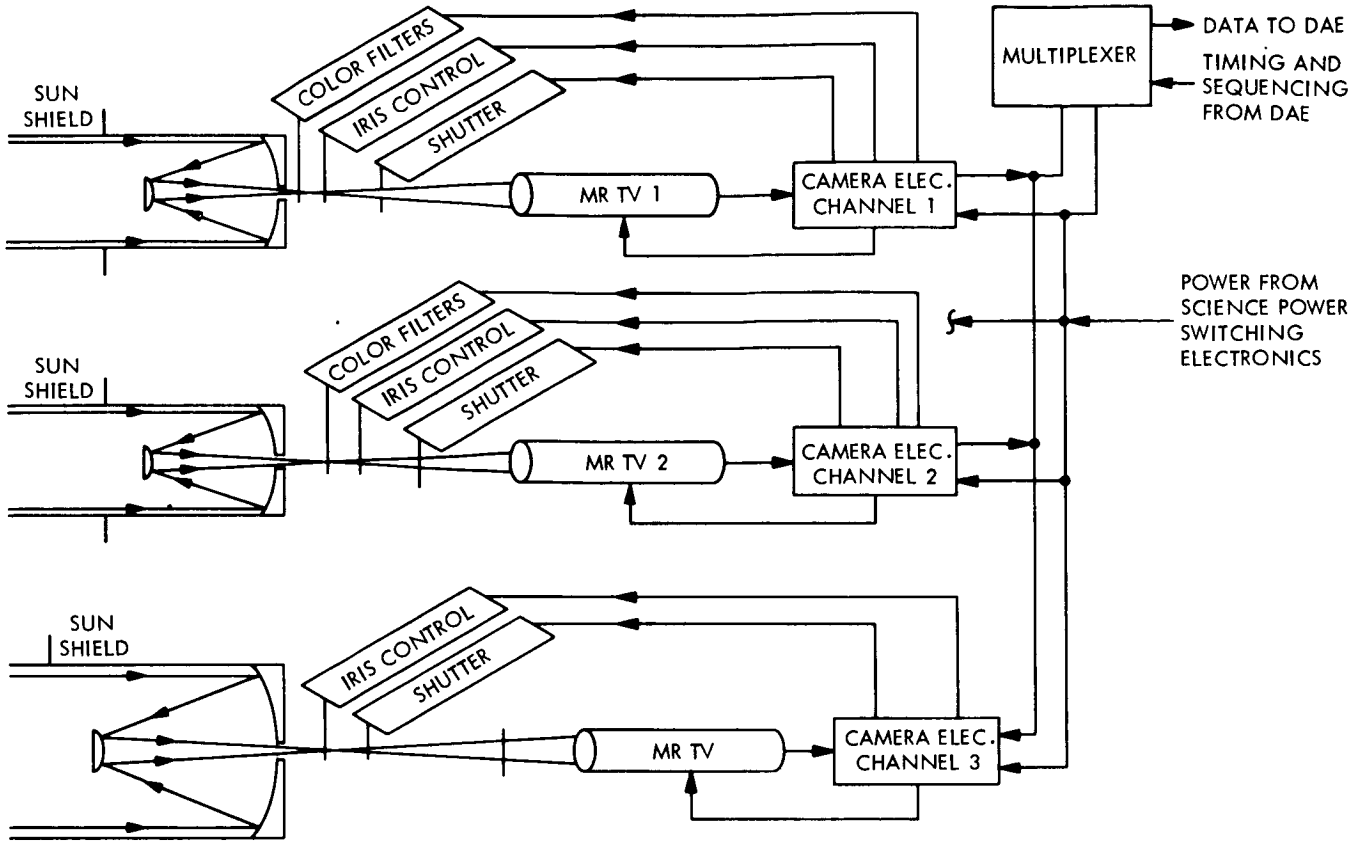

CHARACTERISTICS	MEDIUM RES. CAMERA 1	MEDIUM RES. CAMERA 2	HIGH RES. CAMERA
WEIGHT:			
OPTICS	10 LB	10 LB	25 LB
CAMERA HEAD	16	16	22
ELECTRONICS	12	12	12
	38	38	59
DIMENSIONS:			
OPTICS	4D x 10 IN.	4D x 10 IN.	7D x 20 IN.
CAMERA HEAD	6 x 6 x 12	6 x 6 x 12	7 x 7 x 15
ELECTRONICS	6 x 6 10	6 x 6 x 10	6 x 6 x 10
POWER:	35 WATTS	35 WATTS	20 WATTS
FIELD OF VIEW:	5.7°	5.7°	0.57°
TEMPERATURE LIMITS:		OPERATING	NONOPERATING
OPTICS AND AND CAMERA HEAD		-20°C TO 35°C	-40°C TO 60°C
ELECTRONICS		-10°C TO 50°C	-40°C TO 70°C

Figure 1. Medium and High Resolution Television Systems

planet's axial rotation period. Depending on the amount of overlap between adjacent traces, a tolerance on the orbit period can be established. Assuming a ± 10-percent overlap tolerance, the orbit period error should be less 0.5 minute.

As shown in Figure 2, when in the nominal operational mode, the high resolution camera will take a 0.57 x 0.57-degree frame nested inside every third 5.7 x 5.7-degree medium resolution frame. For the stereo mode of operation, as shown in Figure 3, viewing directions to the proper angles fore and aft of the suborbital point along the ground trace have been assumed to be accomplished by optical deflection. Since each medium resolution camera can be optically pointed either in the "stereo" direction or "nominal" (local vertical) direction, a total of four pictures of the same area, each through a different color filter, can be obtained. This scheme permits stereo and multicolored pictures to be taken without the need for additional cameras.

2.2.2. Data Flow and Performance

The photoimaging experiment provides about 98 percent of the total orbital data which is telemetered back to earth. The data flow is constrained by both the maximum transmission data rate of 40 kbps and the digital recorder maximum read-in rate of 390 kbps. The performance and data flow for the proposed 10-meter and 100-meter resolution photoimaging systems are given in Table 2. Data from the high resolution camera is stored on a digital recorder. A second digital recorder stores data from the first medium resolution camera for 30 seconds and then switches for 30 seconds to the second medium resolution camera. The remaining 30 seconds of the 60 seconds between frames is required for image erase in each vidicon. By accepting data alternately from the two cameras, the recorder need not be started and stopped for each frame, but can run continuously, resulting in more reliable operation and a capability for higher resolution mapping. The total telemetry requirement is near 40×10^3 kbps for a 72-frame sequence and transmission of data for the full spacecraft orbital period.

Stringent intensity resolution requirements and development status seem to favor digital recording techniques. If, however, analog recording is used, a higher storage rate can be obtained, thus allowing more rapid mapping with a wider field of view.

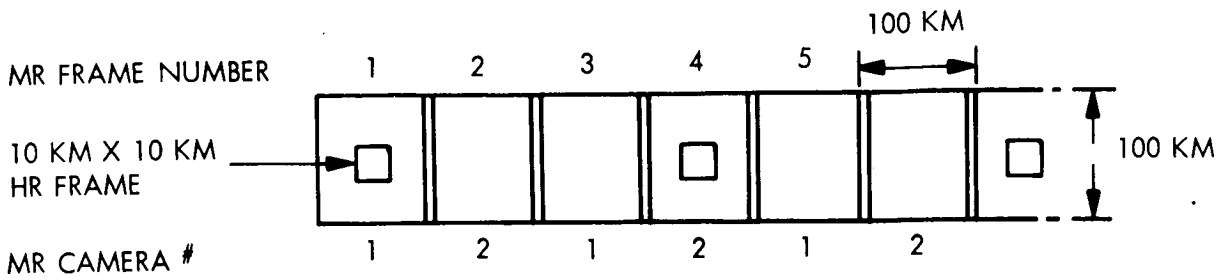

Figure 2. Nominal Mapping Sequence with 100-Km Swathwidth

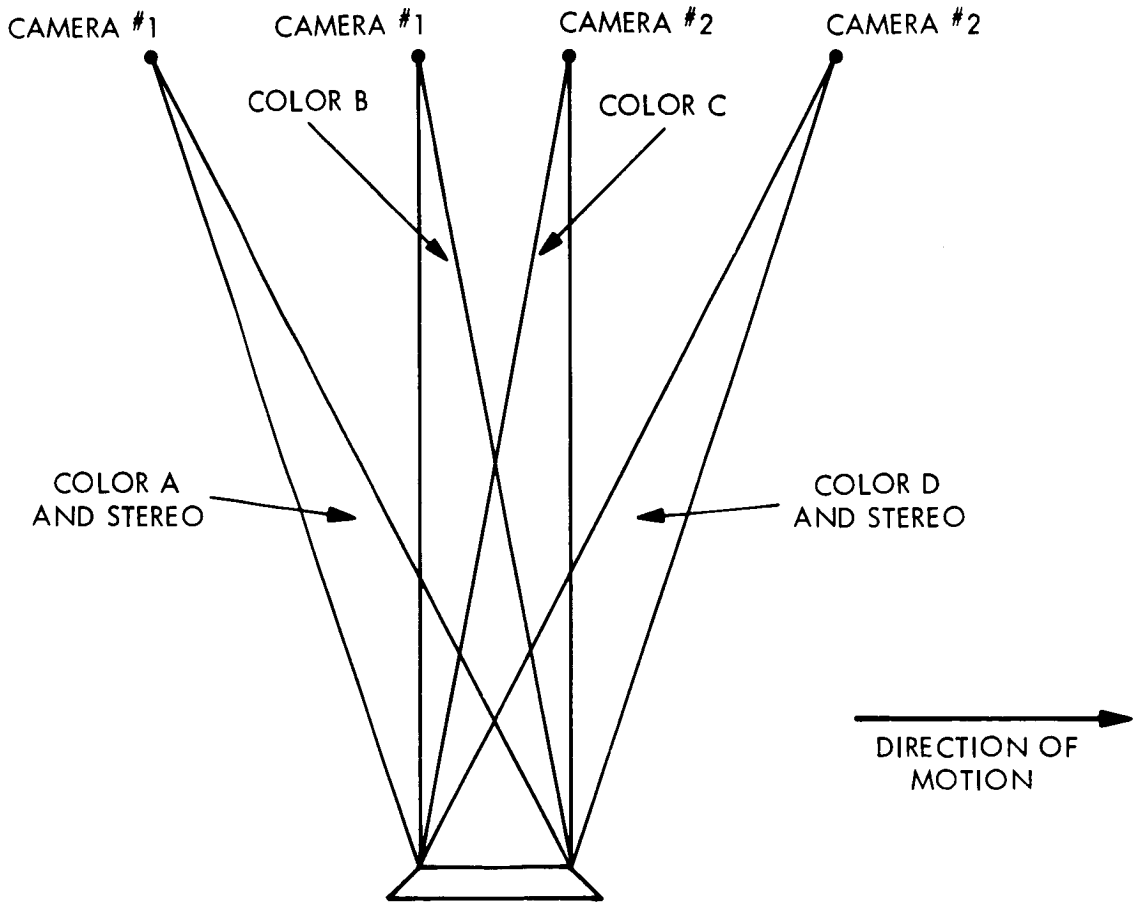

Figure 3. Geometry for Stereo and Color Modes

Table 2. Data Flow and Performance of Photoimaging Experiment

Performance Characteristic	High Resolution	Medium Resolution (Nominal: Digital Storage)	Medium Resolution (Analog Storage)
Ground Resolution (m)	10	100	100
Scan Lines/Frame	1400	1400	1400
Density (Line Pairs/mm)	27.5	27.5	27.5
Time Between Frames (sec)	90	30	15
Time Between Single Camera Frames (sec)		60	30
Readout Time (sec)	30	30*	15*
Erase Time (sec)	30	30	15
Analog Readin Rate (Hz)	32×10^3	32×10^3	64×10^3
Bits/Frame	15.6×10^6	15.6×10^6	15.6×10^6
Bits/Frame Stored**	11.7×10^6	11.7×10^6	11.7×10^6
Storage Readin Rate (bps)	3.9×10^5***	3.9×10^5***	7.6×10^5
Frames/Orbit	24	72	72
Bits/Orbit	2.88×10^8	8.65×10^8	8.65×10^8
Format (mm)	25.4	25.4	25.4
Field of View (degrees)	0.57 x 0.57	5.7 x 5.7	11.4 wide
Ground Coverage (km)	10 x 10	100 x 100	2 x 100 x 100
Telemetry Rate (bps)	10×10^3	30×10^3	30×10^3

*Two cameras taking alternate frames, i.e., twice the readout time for single camera.

**Of the eight bits per sample defining grey levels, only six will be stored continually. Only about every tenth sample will contain all eight bits for calibration.

***Near estimated current state-of-art limitation on series digital recorder input rate.

As shown in Table 2, with analog recording the two medium resolution cameras take alternate frames but in adjacent ground strips (see Figure 4). This technique allows most of the area between ± 40 degrees latitude to be mapped within about 2 months. This data is for the design orbit of 1000 x 11,727-km altitude and 40 degrees inclination. Since the number of pictures taken in series (odd number or even number frames of Figure 4) is 36 instead of 72 as for digital recording, the altitude range can be limited to 1000 to 2000 km.

In all cases spatial resolution can be traded for intensity resolution or coverage. For instance, the Return Beam Vidicon has the capability for twice the 1400 scan lines specified, but the number of grey levels would decrease by orders of magnitude below the 64 to 256 requirement. Similarly, if 300-meter ground resolution were acceptable, the field of view could be increased to about 18 degrees and the area of interest mapped about three times faster within the same data-rate constraints. Further tradeoff possibilities are discussed in the Engineering Task on Photoimaging in Volume IV.

2.3. HIGH RESOLUTION INFRARED SPECTROMETRY

High resolution IR spectra of the planetary surface and intervening atmosphere will be recorded continuously for a portion of the area included in medium resolution TV coverage and to a distance of 10 degrees beyond the terminators. The instrument will be aligned with the

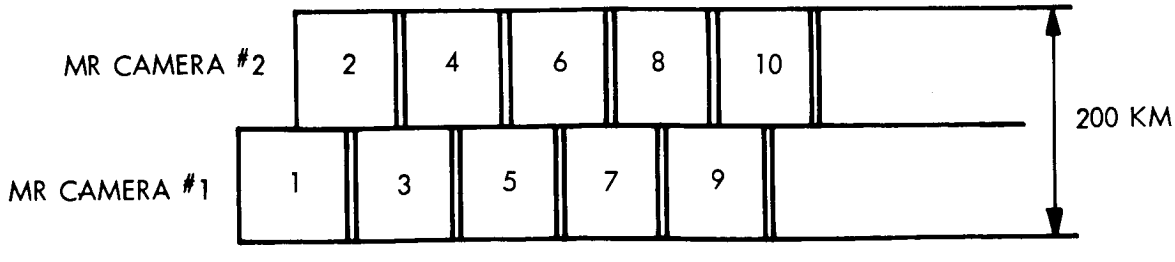

Figure 4. Mapping Sequence with 200-Km Swathwidth

medium resolution cameras. Prior to and following the TV mapping mode, a mirror will be positioned so that the instrument can view the atmosphere above the limb or other areas; the image of the slit will be tangential to the limb. The specific objectives of this experiment are:

a. Determination of atmospheric constituents and temperature variation.

b. Measurement of surface reflectivities and temperatures.

c. Study of clouds and cloud-top temperatures.

d. Biological studies.

The infrared detectors (PbSe) can be used in an uncooled mode providing a $D^* \cong 10^8$, a time constant approximately equal to 4μ sec and a long wave cutoff $\lambda_c = 4.0\mu$. An InSb detector operated in a PEM mode will extend cutoff to $\lambda_c = 7.0\mu$ with a $D^* \cong 10^8$ and a time constant of about 0.2μ sec. While the entire spectral range between 1.5 and 7.0 microns cannot be covered with the system shown (Figure 5) to the same spectral resolution, it may be worth while to consider a slight extension to cover the fundamental CO_2 pressure broadened band centered at 4.3 microns. High resolution spectra of the spatial distribution of this band as a function of altitude and areographic coordinates would be of great value in the evaluation of model atmospheres for the planet.

2.4. BROAD BAND INFRARED SPECTROMETER

2.4.1. Experiment Description

The objectives of this experiment are as follows:

a. Atmosphere - Detection of factors indicative of life (polyatomic molecules associated with biological processes, and atmospheric constituents which limit the UV flux at the surface); study of physical characteristics (identification of constituents and their geographical and altitudinal variation, oxidation and reduction processes, atmospheric photochemistry, and gas temperatures).

b. Surface - Detection of molecules indicative of life, surface temperatures, albedo, and composition.

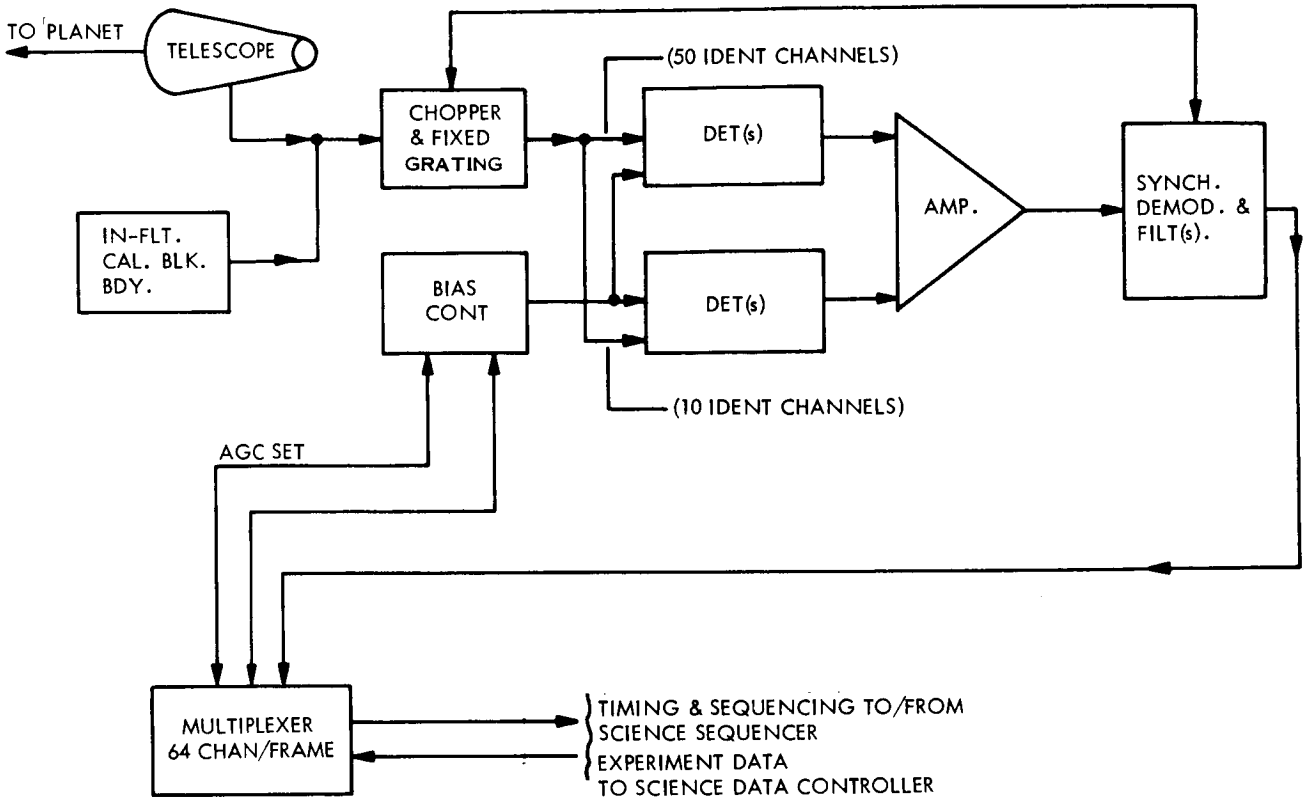

WEIGHT:
SPECTROMETER 16 LB
ELECTRONICS 14 LB

FIELD OF VIEW: 1° BY 4°

SPECTRAL RANGES: 1.5 TO 2 MICRONS AND 3.0 TO 4 MICRONS

DIMENSIONS: 10 x 12 x 20 IN.

POWER: 14 WATTS

DATA RATE: 150 BITS · SEC^{-1}

TEMPERATURE:

	OPERATING	STORAGE
SPECTROMETER	-60° TO 10°C	
DETECTORS (PbSe)	-60°C TO 20°C	
ELECTRONICS	-30° TO 50°C	-30° TO 50°C

Figure 5. High Resolution Infrared Spectrometer

The spectrometer, Figure 6, is optically aligned with the medium resolution photoimaging cameras and will record spectra continually of the central portions of the areas viewed by TV and also extended viewing to a distance of 10 degrees beyond the terminator. Data will be acquired at all times the spacecraft is at an altitude of 4000 km or less. On command, a mirror will reflect other selected regions such as the atmosphere above the limb, into the telescope. This mode will normally be utilized prior to or following a TV sequence with the image of the spectrometer slit oriented tangential to the limb.

2.4.2. Special Requirements

All known sensitive infrared detectors capable of measuring radiation to 15 microns require cooling. Mercury-doped germanium (HgGe), which has been selected for use on the Mariner 1969 flyby mission, exhibits very good detectivity at about 27°K. A two stage N_2Ne cryostat with two pressure vessels weighing a total of 13 lb will enable the Mariner detector to operate satisfactorily. In VOY-D-380 (Thermal Control of the Planetary Scan Platform), the use of Joule-Thomson cooling on a six month orbiting mission is shown to be unfeasible.

Two relatively new detectors (mercury-cadmium-telluride and lead-tin-telluride) have detectivities (D*) in the higher temperature range which approximate that of HgGe at a temperature of 27°K. PbSnTe, now a laboratory item, appears to be the more desirable detector and may be commercially available in small quantities within a year. It is probable that one of these new detectors will operate satisfactorily in the 80° to 100°K range, eliminating the requirement for passive cooling to 27°K. It is indicated in VOY-D-380 that passive cooling to 80° to 100°K may be feasible; additional studies are required to ascertain this. Depending upon the wavelength and detectivity characteristics of the new detector, it may be necessary to substitute another detector for PbSe in channel 2 in order to overlap the spectral coverage of the detectors.

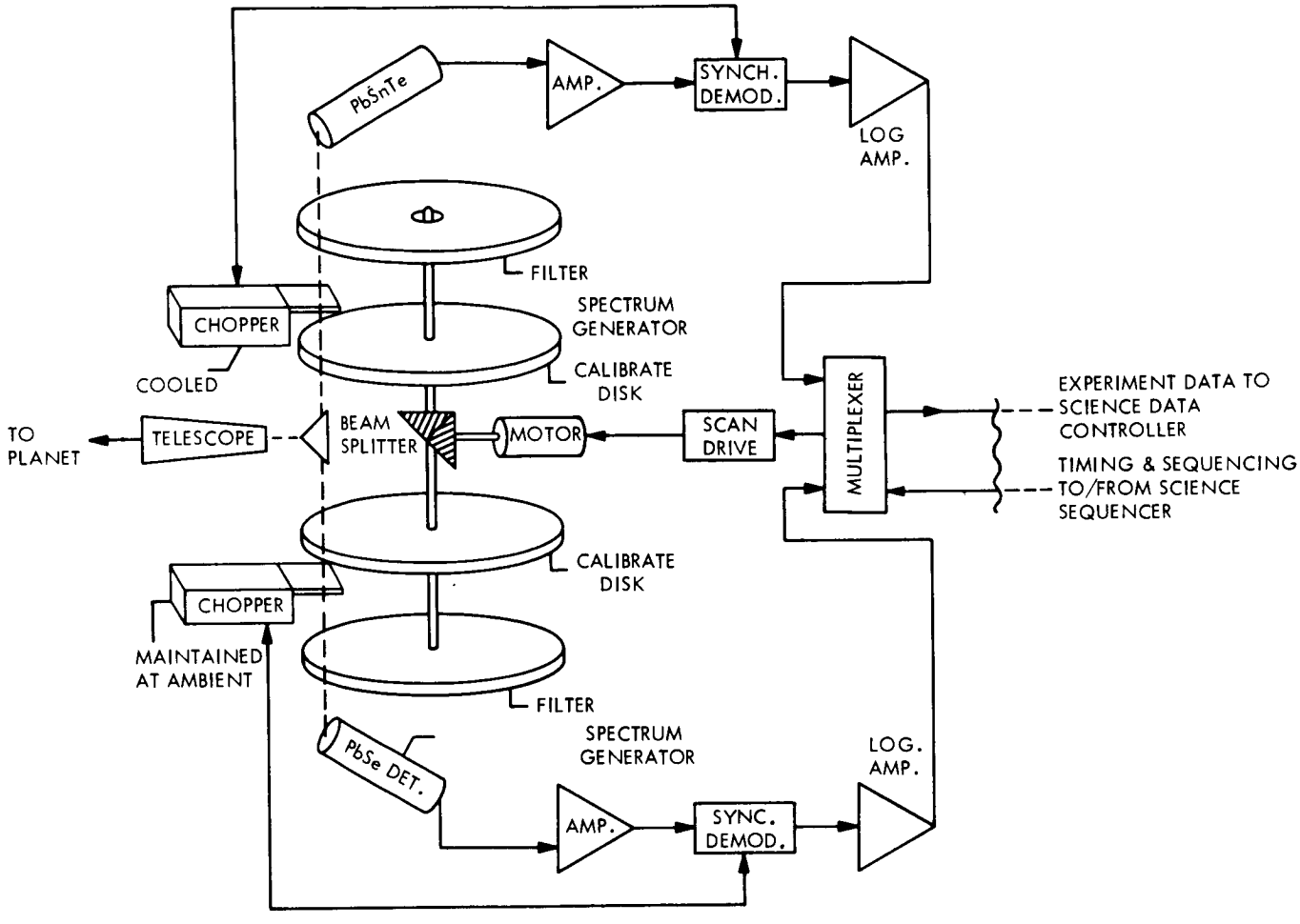

WEIGHT: 16 LB

DIMENSIONS: 12 x 11 x 14 IN.

POWER: 5 WATTS

DATA RATE: 1.2×10^3 BITS · SEC^{-1}

FIELD OF VIEW: 0.17° x 2.87°

SPECTRAL RANGE:
CHANNEL 1 - 4 TO 15 MICRONS
CHANNEL 2 - 1.5 TO 6 MICRONS

SPECTRAL RESOLUTION: 1% INSTANTANEOUS CENTRAL WAVELENGTH FROM 1.5 TO 15 MICRONS

TEMPERATURE:

	OPERATING	STORAGE
CHANNEL 1 DETECTOR	80° TO 100°K	
CHANNEL 2 DETECTOR (PbSe)	130°K	
CHANNEL 1 CHOPPER	130° ± 5°K	
CHANNEL 2 CHOPPER	235° ± 5°K	
TELESCOPE AND MONOCHROMATOR	-38° ± 5°C	-38° ± 5°C
ELECTRONICS	-40° TO +40°C	-50° TO +55°C

Figure 6. Broadband Infrared Spectrometer

2.5. INFRARED RADIOMETER

Objectives of the infrared radiometer experiment are:

a. Mapping of surface temperatures, including thermal abnormalities (volcanos, fault lines, etc.)

b. Identification of cloud features.

A scan mirror, driven by a stepping motor, directs radiation from space, the planet, and a thermal reference source into two optical detectors. The detectors, which are composed of five bismuth antimony junction thermopiles, measure radiation intensities in selected regions (e.g., 0.5-0.75 and 8-13 microns). The rotating mirror scans a 120-degree field of view (± 60 degrees from the photoimaging field of view.)

The primary purpose of the experiment is the accurate measurement of day and night temperatures. Daylight views include the integrated effects of thermal and reflected radiation from the surface and atmospheric absorption. Observations of the darkened side identify thermal effects. Data derived from this instrument will supplement infrared spectrometer data in the complex analysis of lines and bands. The instrument is schematically shown in Figure 7, with physical characteristics noted at the bottom of the figure.

2.6. ULTRAVIOLET SPECTROMETER

2.6.1. Experiment Description

The ultraviolet spectrometer (Figure 8) will observe various levels of the day and night atmospheres above the limb and will also view the planetary surface. A rotating mirror will render it capable of viewing the nadir and observing areas recorded by the visual imaging devices. The scientific objectives for the equipment are as follows:

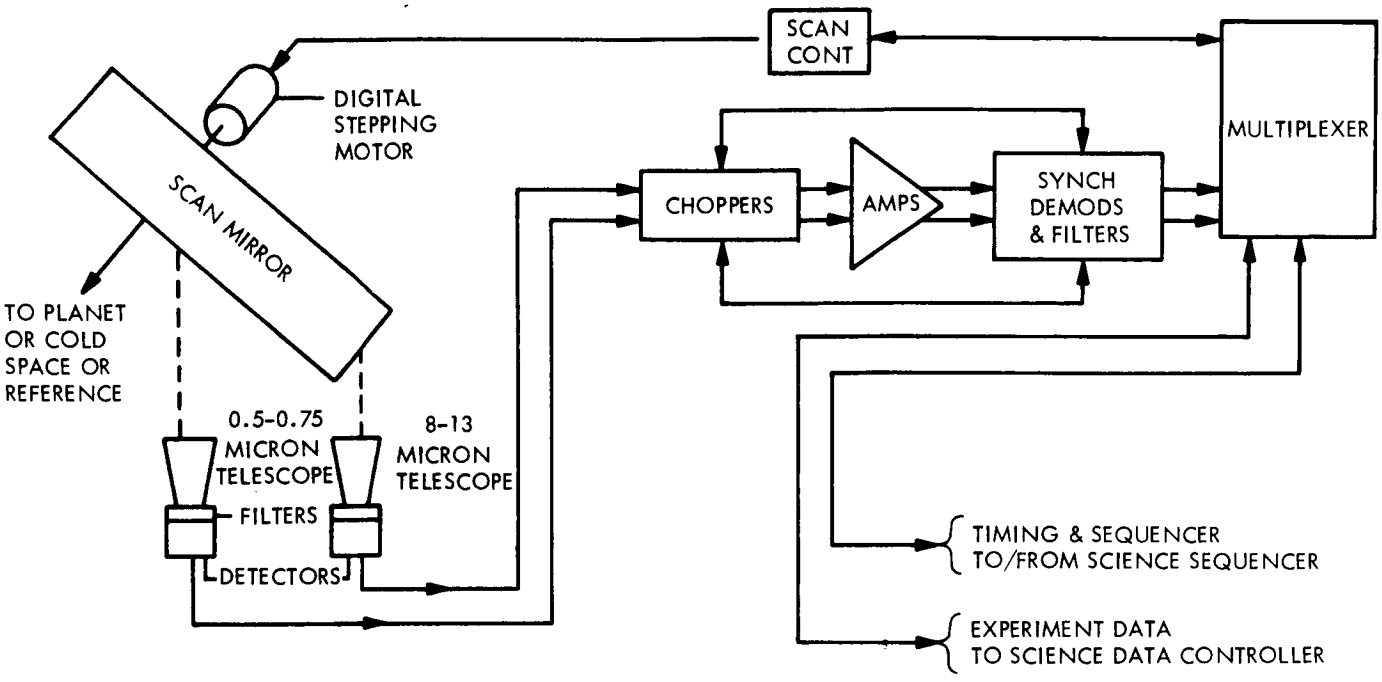

WEIGHT: 20 LBS.

DIMENSIONS:
RADIOMETER 7 IN. DIAM. x 10 IN.
ELECTRONICS 7 x 7 x 10 IN.

POWER: 6 WATTS

DATA RATE: 2.4×10^3 BITS · SEC^{-1}

TEMPERATURE:

	OPERATING	STORAGE
RADIOMETER	-20° TO + 50°C	-50° TO +55°C
ELECTRONICS	-20° TO + 50°C	-50° TO +55°C

FIELD OF VIEW: 0.57° x 0.57°

SPECTRAL RANGE:
CHANNEL 1 - 0.5 TO 0.75 MICRON
CHANNEL 2 - 8 TO 13 MICRONS

SENSITIVITY: ±0.1°K AT 300°K
±0.4°K AT 140°K

Figure 7. Infrared Radiometer

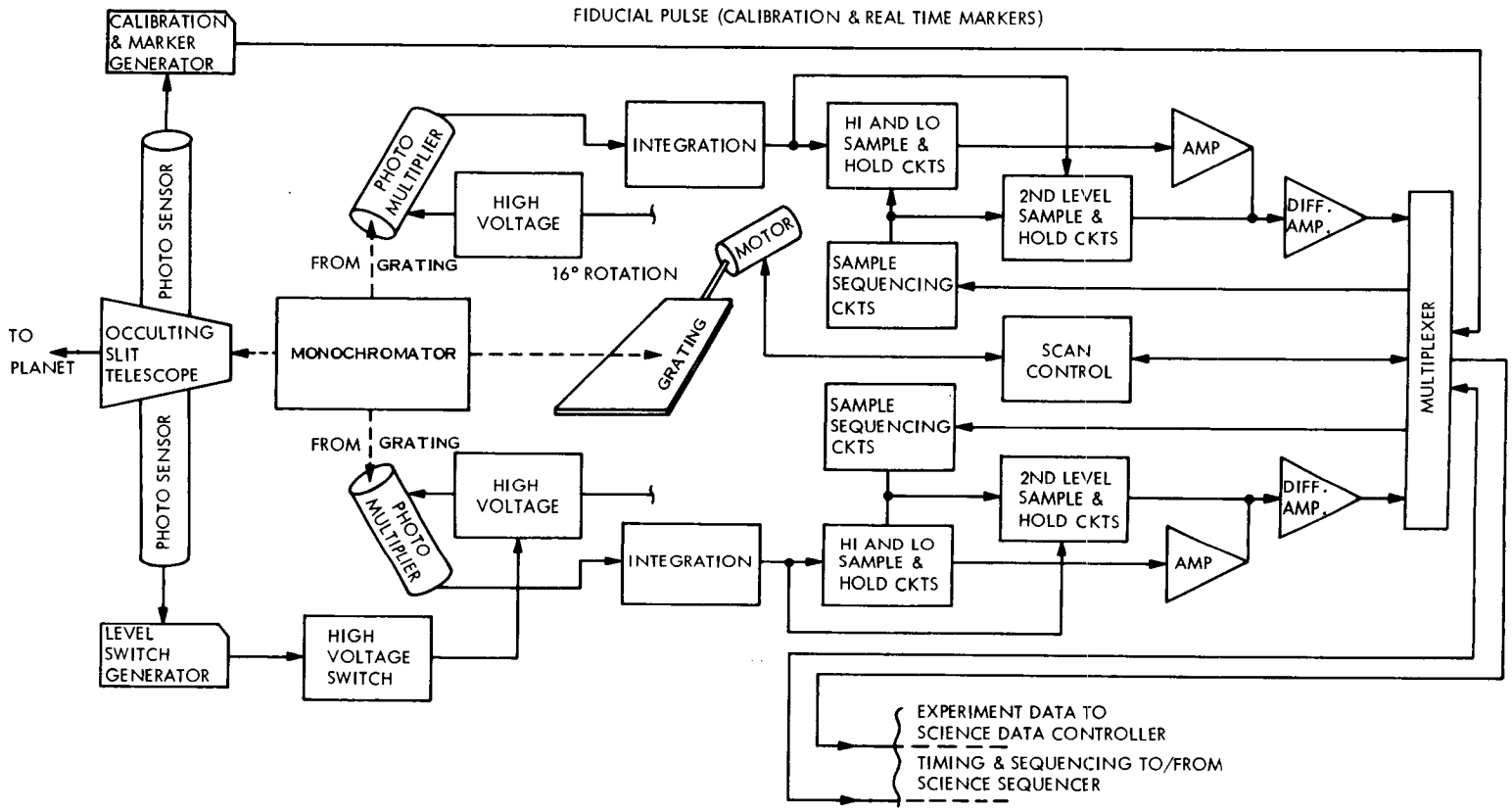

WEIGHT: 32 LBS

DIMENSIONS:
SPECTROMETER 24 x 8 x 8 IN.
ELECTRONICS (3) 6 x 6 x 1.5 IN.

POWER: 16 WATTS

FIELD OF VIEW: 2° BY 6 MIN. OF ARC

SPECTRAL RANGE:
CHANNEL 1 - 1100 TO 2200 Å
CHANNEL 2 - 1500 TO 4300 Å

SPECTRAL RESOLUTION: 20 Å (IN FIRST ORDER SPECTRA)

HIGH DATA RATE: 2400 BITS · SEC^{-1} (INTERMITTENTLY)
LOW DATA RATE: 150 BITS · SEC^{-1} (CONTINUALLY)

MEASUREMENT ACCURACY: 5%

DYNAMIC RANGE, CHANNELS 1 AND 2: 50 RAYLEIGHS PER 20 Å INTERVAL TO 50 KILORAYLEIGHS

TEMPERATURE:
OPERATING 0° TO 40°C
STORAGE -55° TO +55°C

Figure 8. Ultraviolet Spectrometer

a. Identification of atmospheric constituents by measuring resonance re-radiation and molecular absorption.

b. Determination of scale heights of constituents.

c. Measurement of Rayleigh scattering in the lower atmosphere.

d. UV reflectivity of surface.

Prior to the time a landing site is identified for the lander, the UV spectrometer will continuously record spectra of the views seen by the medium resolution photoimaging devices. In the surface mode, it will normally operate at spacecraft altitudes less than 4000 km. When operating in the atmospheric mode, the spectrometer will be commanded to observe the atmosphere at specified angular distances above the limb prior to and following a surface mapping sequence and at varying spacecraft distances from the planet. It will analyze photochemical reactions in both the day and night environments. Operating within constraints imposed by the PSP maneuverability, the ultraviolet spectrometer will occasionally view the planet and its atmosphere from relatively large distances (i.e., approaching apoapsis).

2.6.2. Special Requirements

Most surfaces are poor reflectors of ultraviolet radiation. Mirrors with acceptable reflectivities from 1100 Å to the visible are usually composed of vacuum-deposited fresh aluminum overcoated in the same vacuum with 250 Å of magnesium fluoride, yielding a reflectivity of 80 percent at 1200 Å.

The instrument electronics will become saturated if the optics point as near as 10 degrees to the sunline. Power must be turned off if the sun is in the field of view.

The photomultiplier sensors are readily affected by nuclear radiation. If RTG electrical power supplies are utilized on the lander, the instrument must be shielded or re-designed to operate in a moderate-level radiation field.

2.7. RADIO EXPERIMENTS

Using two RF frequencies, it is possible to unambiguously separate the ionospheric layer in an atmosphere as a function of height. For Mars, this ionospheric layer, if it exists, is at a low altitude and not amenable to direct orbiter or flyby experiments. It is assumed that the normal radio tracking data for the orbiter will be processed in such a way as to recover this information.

From the tracking data, it is possible to record the time rate of change of the node of the aerocentric orbit which in turn may be used to infer higher order terms in the gravitational potential of the planet. This in turn can be used to infer bounds on the internal density distribution of the planet. When considered in conjunction with certain theoretical models for the planet, an estimation of whether or not the planet is differentiated can be made. It is assumed that such an attempt will be made on the part of the NASA radio tracking facility.

3. ADDITIONAL EXPERIMENTS WITH BASELINE PAYLOAD INSTRUMENTS

3.1. EXPERIMENTS USING BASELINE PAYLOAD INSTRUMENTS

3.1.1. A Study of Phobos

The larger of the Martian moons, Phobos, as shown in Table 3, cross the orbit of the spacecraft if the apoapsis altitude is between 10,000 and 20,000 km.

Table 3. Parameters of Martian Moons

Parameter	Phobos	Deimos
Mean distance from primary	9,400 km	23,500 km
Diameter	16 km	8 km
Orbital Period	7^h38^m	$1^d6^h21^m$
Orbit Inclination	1.8°	1.4°
Orbital Eccentricity	0.019	0.003

It is apparent, therefore, that at times Phobos and the orbiter could be in close proximity and available for study by the baseline instruments.

Phobos, which is an unresolved object in a terrestrial telescope, has for a number of years been used to estimate the dynamical flattening of its primary. The dynamical flattening disagrees with the geometrical value (optically derived) by a factor of two, and this discrepancy has resulted in an ambiguous determination about the physical composition of Mars. Part of this discrepancy may rest in the inferred size of Phobos, based on assumed albedos. The diameter of 16 km listed in Table 3 is derived from such indirect measurements.

It is proposed, therefore, that the photoimaging system aboard the orbiter be directed to obtain whole disc pictures of Phobos from which direct diameter measurements can be obtained. Surface irregularities showing up in these pictures (craters, large basin formations, etc.) would be extremely interesting from a planet evolutionary sense.

Using the other base line instruments, in particular the IR spectrometer and IR radiometer, additional information about the surface mineralology and thermal temperature of Phobos could be obtained. In particular, the former could be used to detect the iron oxides, e.g., hematite, limonite, and geothite, which are common to the primary. Detection of the iron oxides would be strong argument for the origin of Phobos from part of the Martian crust. If not detected, a captive process may be more attractive in attempting to fix its origin.

3.1.2. Surface Dynamics

There are certain dynamical changes taking place on the planet that are generally not considered under the baseline measurement objectives. Among these are circulation dynamics and the effects of wind erosion on the planet. It is proposed, therefore, that at the time of strong dust storms, surface mapping of the planet be terminated and TV tracking of the mass motions of such storms be undertaken in an effort to obtain wind velocities and the effects on surface features before and after such an event.

3.2. EXPERIMENTS REQUIRING ADDITIONAL INSTRUMENTS

3.2.1. A Photopolarimeter Experiment

There currently exists discrepancies in the determination of the Martian surface pressure. Occultation experiments yield a surface pressure of 4 to 6 mb, terrestrial spectroscopic observations yield 12 to 15 mb, and terrestrial polarimetric observations 25 to 30 mb. A possible explanation for the discrepancy between the spectroscopic and polarimetric measurements is the existence of an aerosol component in the Martian atmosphere which increases the diffuse power of the air by a factor and detected by the polarimeter and not by the spectrometer. This possibility could be resolved by adding a photopolarimeter to the science payload and recording the output of both the photopolarimeter and spectrometers when looking in essentially the same direction. Add to this a TV picture of any clouds present and the possibility of resolving the problem is greatly enhanced.

Since the occultation experiment will be performed at least once per orbit, a statistically meaningful set of occultation data will be obtained, raising the confidence level of the occultation surface pressure measurements and certainly averaging out any link irregularities that may have biased the flyby data. The possibility exists, therefore, in correlating all three types of data used in remote surface pressure determinations and the dependence of such data on aerosol/gas components. To aid in estimating engineering parameters involved in soft lander designs, the ambiguity in pressure as determined by remote sensing should, of course, be reduced to as small a value as possible.

Surface polarimetry of Mars has long been used to classify the material of the bright areas as belonging to a class of iron oxides, e.g., hematite, limonite, and geothite, which give Mars its predominately red color. These terrestrial observations refer to extensive Martian areas (several hundred kilometers in extent). An averaging over this extent has little relevance to laboratory prepared samples used as a standard of comparison, which is an objection to the terrestrial observation that needs to be resolved. Thus polarimetry at a spatial scale of 1-km ground resolution is proposed in an effort to remove such an objection.

The dark areas, such as Syrtis Major, should be studied as well. In particular, a record of such an area before, while covered by a dust storm, and when clear again, would be of biological significance, since these areas appear to have some rejuvenative character; a study of them throughout such an event (dust storm) may indicate whether or not this rejuvenation is only a meteorological phenomenon or must be ascribed to another process, such as biological.

3.2.2. Micrometeoroid Detectors

While the average micrometeoroid flux at Mars is expected to be the same as that determined by the Mariner probes (essentially the interplanetary value), it is possible that a sporadic component exists similar to that on earth (meteor showers). The existence of such a shower component can only be determined by measurements over long periods of time; the long life time of the orbiter is ideally suited for making such measurements. Both a cometary and asteroidal component is possible; the latter being associated with Mar's proximity to the asteroid belt.

The existence of an asteroidal component will, if significant, alter the observed crater count age determinations for the Martian surface. In the data obtained from the Mariner pictures (Mariner IV), a transition in the slope of the number of craters versus size plots is noted as the crater size decreases. This is not currently understood. This may be due to the fact that only one percent of the planet has been covered by Mariner IV photographs, or it may be that the obliteration rate of small craters is higher on Mars than presently estimated, due to a higher sporodic component in the meteoritic influx rate incident on the planet. Micrometeoroid detectors on board the spacecraft could answer this problem involving long term surface erosion.

3.2.3. Cosmic Ray Telescope

At the time of a solar flare, it would be valuable to directly monitor the flux and energy of the arriving ionizing radiation from the sun and to correlate this component with the observed atmospheric effects recorded by the UV spectrometer. Under these conditions, additional data

can be derived about the constituents of the Martian atmosphere and an estimate made as to its transparency to such irradiation. The latter has, of course, biological significance. The size and weight of such an instrument is small and, if included, would be body mounted.

4. SEQUENCING AND PROFILES

The performance of most experiments at or near periapsis will produce the best surface and atmospheric spatial resolution. For this reason, most data will be recorded within a distance of 3000 kilometers from the surface. The orbit has a nominal periapsis altitude of 1000 km and apoapsis altitude of 11,727 km resulting in a period of 8.15 hours. Data will also be recorded at distances greater than 3000 kilometers; several interesting missions at the larger distances are identified in Paragraph 3.

During the initial weeks in orbit, a prime scientific objective is the identification of significant sites onto which a lander may later descend. Spectrometric and radiometric data will also be obtained for each area covered by the medium resolution photoimaging system. Attempts will be made to detect the presence of methane, chlorophyll, and other biologically-related materials. Analyses of atmospheric and surface properties as a function of "geographical" position will provide important scientific and environmental details.

The operating sequence for the baseline instruments is described in Table 4. The additional instruments (photopolarimeter, cosmic ray telescopes, and micrometeoroid detectors) recommended on a first priority basis for inclusion in the science package would not appreciably affect the cumulative data rate if added, but would require an increase in power of about 7 percent. The cosmic ray telescope and micrometeoroid detectors would operate continually in orbit. The photopolarimeter would operate when the spacecraft is 50 minutes before to 50 minutes after periapsis passage.

All of the baseline instruments use power continually from the time noted as "power-on" to "power-off." In Table 4 the spectrometers and radiometer are assumed to collect data continually while power is on with no warm up being required.

Table 4. Scientific Instrument Sequence, Data Rate, and Power Requirements

	Bits Per Second	Bits Per Orbit	Turn On (Minutes from Periapsis)*	Turn Off (Minutes from Periapsis)	Power (Watts)
1. Medium Resolution TV Camera No. 1	3.9×10^5	8.65×10^8	-44	-2.5	35
2. Medium Resolution TV Camera No. 2	3.9×10^5	8.65×10^8	-44	-2.5	35
3. High Resolution TV Camera	3.9×10^5	2.88×10^8	-44	-2.5	20
4. High Resolution IR Spectrometer	150	5.85×10^5	-50	+15	14
5. Broad Band IR Spectrometer	1200	4.68×10^6	-50	+15	5
6. IR Radiometer	2400	1.44×10^7	-50	+50	6
7. UV Spectrometer					
High Data Rate	2400	1.24×10^7	-50	+36	16
Low Data Rate	150	7.74×10^5			
Totals (Maximum Rates):					
Utilizing UV High Data Rate Mode	1.18×10^6	2.05×10^9			131 (Maximum)
Utilizing UV Low Data Rate Mode	1.17×10^6	2.04×10^9			

*The timing sequence applies to a typical orbit.

Each of the two medium-resolution TV cameras takes a picture once each minute. Following each exposure (a fraction of a second), the time to read the data into the tape recorder is 30 seconds. The time to erase the picture is also 30 seconds. The cameras are consecutively sequenced, resulting in a continuous recorder read-in for a sequence of 72 frames per orbit. One high resolution picture is taken for every three medium resolution pictures (once every 90 seconds). All cameras require a 5-minute warm up time.

The times at which sequencing events occur as shown in Figure 9 are approximate. The conditions shown are for the first orbit after insertion, with the periapsis assumed to be located directly over the evening terminator. The sequencing times noted in Figure 9 are typical and dependent upon the characteristic of the actual orbit obtained. The cumulative data rate for the science and the power required for the instruments is also noted in Figure 9; the case shown is for the UV spectrometer in the high data rate mode during a solar flare.

On some occasions, it will be desirable for science instruments and the PSP to depart from the programmed normal mode to study special subjects. The following are representative situations where the PSP or specific instruments, or both, will operate on ground command.

1. Operation of medium resolution TV in stereo or color modes.
2. Determination of the location of the lander with high resolution following its landing.
3. Observation of advancing dust storms, frost lines, dark wave, etc.
4. Studies of other events important in scientific research: nearby passage of Phobos and more distant observations of Deimos, observations of atmospheric and surface photo-chemical changes following Class III solar flares, etc.

During the first several weeks in orbit, priority will be given to the mapping mission. Much of the planet between $\pm 40^\circ$ latitude will have been mapped within 2 months, and increasing attention can then be devoted to the observation of other interesting scientific phenomena.

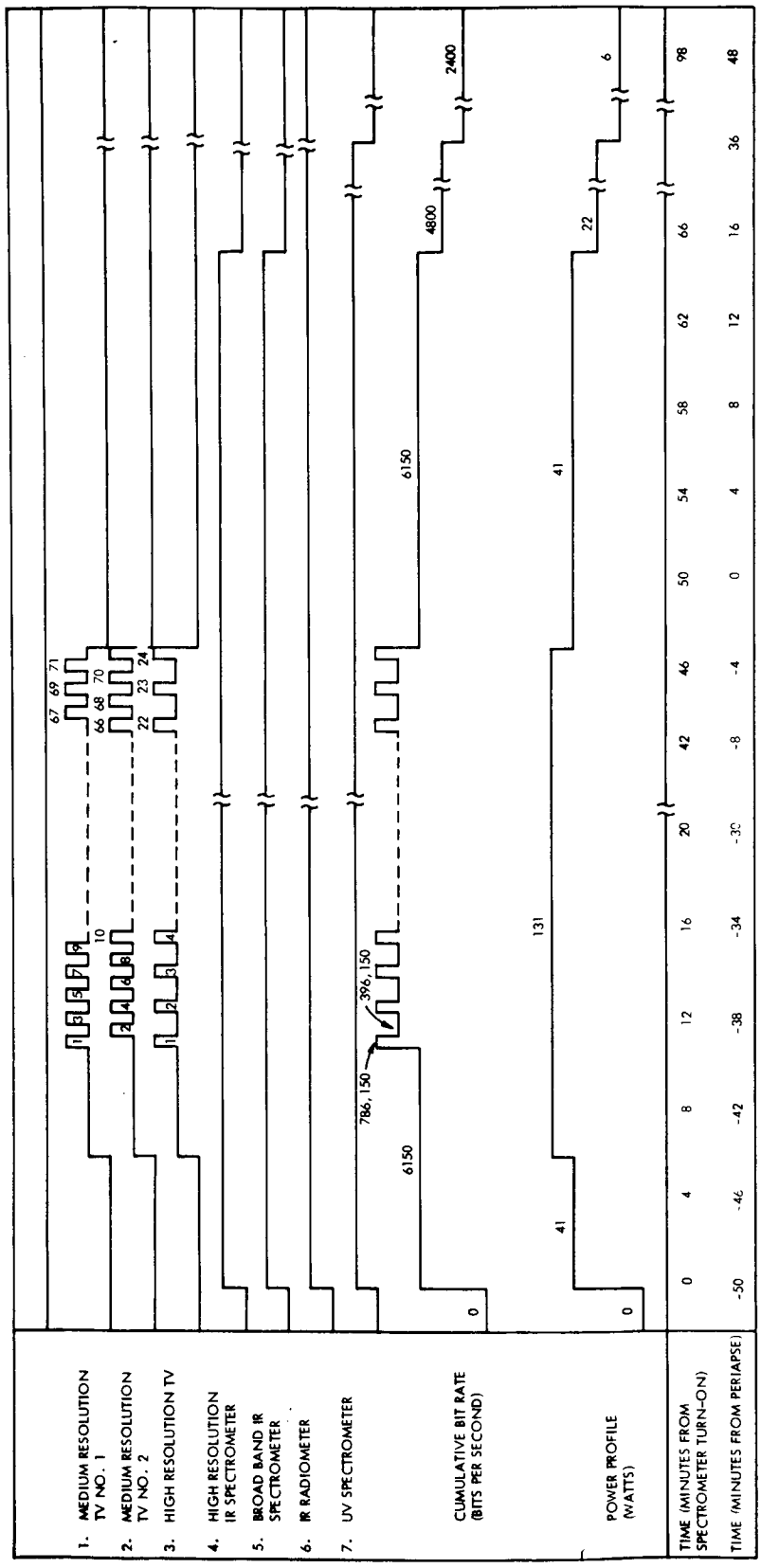

Figure 9. Nominal Instrument Data Acquisition and Power Profiles for First Few Orbits

It will also be noted that a considerable degree of flexibility is available with the optical pointing mechanisms which are attached to each of the spectrometers. One or more of the spectrometers may be oriented to view the atmosphere above the limb during active solar periods, while TV cameras continue the mapping mission. Typically, the ultraviolet spectrometer and high resolution infrared spectrometer will view the horizon while the broadband infrared spectrometer continues to record data in the TV mapping mode. The infrared radiometer, although boresighted with the TV camera, scans the planet from limb to limb continually while the PSP operates in the normal mode.

The scientific instruments utilize single phase, 400 and 2400 Hz power. The cumulative power requirements are graphically illustrated in Figure 9. Table 5 specifies the allocation of power as a function of time between the two power sources. Transients caused by instruments being turned on or off will last less than one second. An evaluation of the effect of transients on operating instruments cannot be performed until detailed information about the instruments is available.

Table 5. Cumulative Scientific Instrument Power Requirements

Time Period (Minutes from Periapsis)	2400 H_z Power (watts)	400 H_z Power (watts)	Total Power (watts)
Prior to -50 Min	0	0	0
-44 to -50	31	10	41
-3 to -44	121	10	131
-3 to +15	31	10	41
+15 to +36	17	5	22
+36 to +50	6	0	6
Following +50 to next cycle	0	0	0

VOY-D-250
INTERFACE REQUIREMENTS

1. GENERAL

The Voyager Flight Spacecraft is involved in four interfaces with other Voyager systems. One interface exists between the flight spacecraft and the flight capsule. These two systems comprise a planetary vehicle, of which two are launched by a single Launch Vehicle System. Another interface exists between the planetary vehicles and the launch vehicle. The space vehicle, which consists of the two planetary vehicles and the launch vehicle, in turn has a mutual interface, prior to launch with the Launch Operations System, and after launch with the Mission Operations System.

The period of operational interface between the flight capsule and flight spacecraft is initiated when they are mated together to become a planetary vehicle, continues through separation of the Flight Capsule from the flight spacecraft, and is concluded when radio contact is terminated after the flight capsule lands on the Martian surface. The physical interface between a planetary vehicle and the launch vehicle, with the major interfaces existing between the flight spacecraft portion, extends from the time that the planetary vehicle(s) are joined to the launch vehicle shroud by an adapter, continuing through launch and is concluded after both planetary vehicles have been separated from the launch vehicle. Concurrent in time with the interface between the planetary vehicle(s) and the launch vehicle is a second interface concerning those operations at the launch area when either the individual portions of the space vehicle or any combination of them, up to and including the total vehicle, are present. This interface requirement is concluded only after the planetary vehicles have been launched and separated from the launch vehicle. The final interface requirement is that between the Mission Operations System and both planetary vehicles. This interface starts with the separation of the planetary vehicles from the launch vehicle and continues through the interplanetary cruise and maneuvering, the Mars orbit insertion, the Flight Capsule separation, and throughout the orbiting life of the flight spacecraft. The remainder of this section describes briefly each of these major interfaces.

2. CAPSULE INTERFACE

2.1 INTRODUCTION

The flight capsule is mated to the flight spacecraft for approximately half of their mission life. For most of this period, the capsule is in a somewhat dormant state and is dependent on the flight spacecraft for contact with the earth, power for heating and in-flight operation, and protection from the environment by maintaining it at a fixed attitude with respect to the sun. Additionally, the spacecraft must take the capsule into orbit about Mars, possibly help determine the capsule landing area by aerial mapping of the surface, initiate the capsule mission, and then receive and transmit to earth the capsule entry data.

Because of this strong dependence of the capsule on the spacecraft and the high scientific importance of the capsule mission, the capsule-spacecraft interface is a critical interface. Fortunately, this interface can be maintained relatively simple. Operational, power thermal, radio, mechanical, and OSE interfaces exists. The major interface considerations will be discussed in this section. In discussing these interfaces, certain assumptions have been made with respect to definition of the capsule design; where applicable, data obtained from the McDonnell-GE capsule study team is used.

2.2 CAPSULE FLIGHT PROFILE

Approximately eight hours prior to the capsule separation, a capsule checkout period is initiated. Test sequencers for the Capsule Bus and Surface Laboratory, which may be mounted on the spacecraft (Bay 13) as part of the capsule support equipment, sequence the capsule equipment to verify the capsule readiness. The capsule data may be multiplexed onboard the capsule or sent to spacecraft mounted commutators via hardwire and the electrical interface. Commutators included as part of the spacecraft mounted equipment would have the advantage of reduced operating life for these commutators. This capsule data is multiplexed with spacecraft data and transmitted to earth. If the readiness of the capsule is verified by ground, and capsule separation authorization received by the spacecraft Command Subsystem, the separation sequencer is initiated.

Approximately five minutes before capsule separation, the forward half of the bio-barrier is separated. This separation must be designed to cause a negligible torque and minimum force on the spacecraft. The capsule inertial system takes its references from the spacecraft attitude, placing requirements on the accuracy of the spacecraft attitude control and alignment between the capsule and spacecraft. Based on analyses conducted in Task B, the spacecraft attitude accuracy is sufficient for this purpose. The bio-barrier separation and capsule separation are initiated by the Capsule Bus System.

Approximately 20 minutes after capsule separation, which occurs at a relative velocity of a quarter to a half a meter per second, the capsule reorients itself and fires a deorbit engine. Throughout the deorbit and until entry, data is received from the capsule at a rate which may be between a few hundred and a few thousand bits per second. This data is multiplexed with spacecraft data by the spacecraft Telemetry Subsystem for transmission to earth. Starting at entry through landing, capsule data is received at rates in excess of 50,000 bps and stored in spacecraft mounted capsule recorders for eventual transmission to earth. The location of the relay receiving antenna is noted in Section VOY-D-311. It is assumed that capsule support, except for aerial surveillance, ceases within minutes after capsule landing.

2.3 MECHANICAL INTERFACE

Each Flight Capsule is mounted forward of its corresponding flight spacecraft and is wholly contained within the envelope defined in "Performance and Design Requirements for the 1973 Voyager Mission, General Specification For" dated January 1, 1967. The only attachment is at the interface plane; the electrical inflight disconnect and the spacecraft-to-capsule field joint is located at planetary vehicle station 169.0.

The flight capsule/flight spacecraft physical interface is a field joint as shown in Figure 1. This interface consists of two circular mating rings, one terminating the capsule adapter, and the other terminating the spacecraft upper structure. The mechanical interface is structurally joined by 8 bolt/nut combinations symmetrically located around the interface

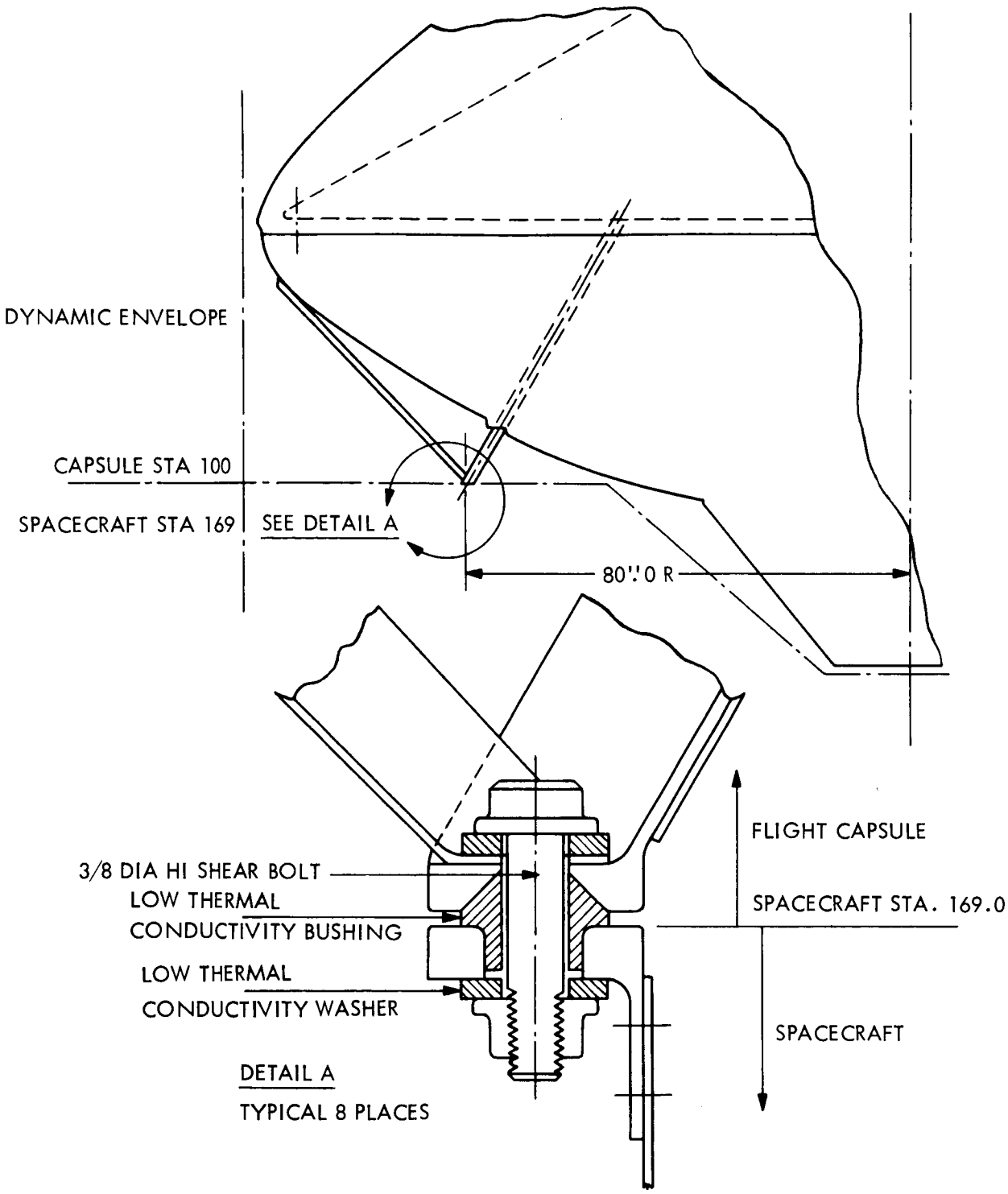

Figure 1. Capsule Mechanical Interface

rings on a nominal 160-inch diameter bolt circle. One bolt hole is offset circumferentially to key the rotational position of the flight capsule to the proper position on the flight spacecraft. Ample bolt hole clearance is provided to ease attachment/detachment procedures and yet maintain reasonable tolerance.

The primary load conditions for the flight spacecraft/flight capsule interface occur during ground handling, launch, Mars orbit insertion, and capsule separation. The maximum design loads occur during launch, and these loads are the result of various combinations of capsule inertial reactions to the Saturn V rigid body and vibratory accelerations. The interface structure is designed with a 1.25 factor of safety. The load factors and resulting interface ultimate loads for a 7,000 lb. Flight Capsule (designed such that the interface is compatible for later missions) are shown in Table 1. The vibratory load factors have been converted to those of an equivalent rigid body to obtain the maximum flight capsule load factors.

Table 1. Flight Capsule Load Factors

	Load Factor	Max. Ultimate Loads
Longitudinal	+1.50g's -4.75g's	+13,120 lb -41,600 lb
Lateral	0.40g's	3,500 lb
Total Bending	-	269,000 in. -lb
Torsion	Small	Small

The capsule mass properties for the 1973 mission are assumed to be as shown in Table 2.

Table 2. 1973 Flight Capsule Mass Properties

Total Weight	CG Location	I_x	I_y	I_z
5,000 lbs	(Worse Case) 77 in. From Interface (Station 247)	(Slug - Ft.^{2}) 4,700	4,700	4,700

2.4 THERMAL INTERFACE

Thermal design considerations dictate that this spacecraft-capsule interface area be designed in such a way as to hold heat transfer between the two vehicles to a minimum. In order to meet this criteria, the forward section of the spacecraft is covered with super insulation material which insulates the bio-barrier from the interior spacecraft structure.

Another major source of heat leakage from the spacecraft is at the interface mechanical attachments. The heat leak at these points may be minimized by utilizing a gap between the two interface rings using tapered insulation shear carrying bushings and completing the isolation of the attachment bolts with a low conductivity material (See Figure 1.)

The lower half of the bio-barrier acts as a radiating fin after capsule separation and becomes a major heat leak source for the spacecraft. After considering the reliability, PSP viewing, micrometeroid protection and other considerations (as well as the thermal problem), it was concluded that the lower bio-barrier half should not be separated from the spacecraft (VOY-D-220). However, the several hundred degree Farenheit differential between the open side of the canister and attachments will require careful design of the attachments in order to relieve the thermal stresses.

The thermal interaction between the spacecraft and capsule, due to RTG's mounted on the capsule, was also considered. With the proposed location of the RTG radiators pointing almost normal to the roll axis, the heat intercepted by the spacecraft has a negligible effect.

2.5 TELEMETRY INTERFACE

As previously noted, equipment for checking out the capsule and commutating capsule in flight data (before separation) may be mounted on the spacecraft. A schematic of such an arrangement is given in Figure 2. However, it is assumed that all processing of capsule data will be done by capsule equipment with a single input to the spacecraft telemetry. The spacecraft mounted equipment can be located in Bay 13 along with the capsule tape recorder(s) used for storing capsule entry data. An additional telemetry interface is the relay antenna

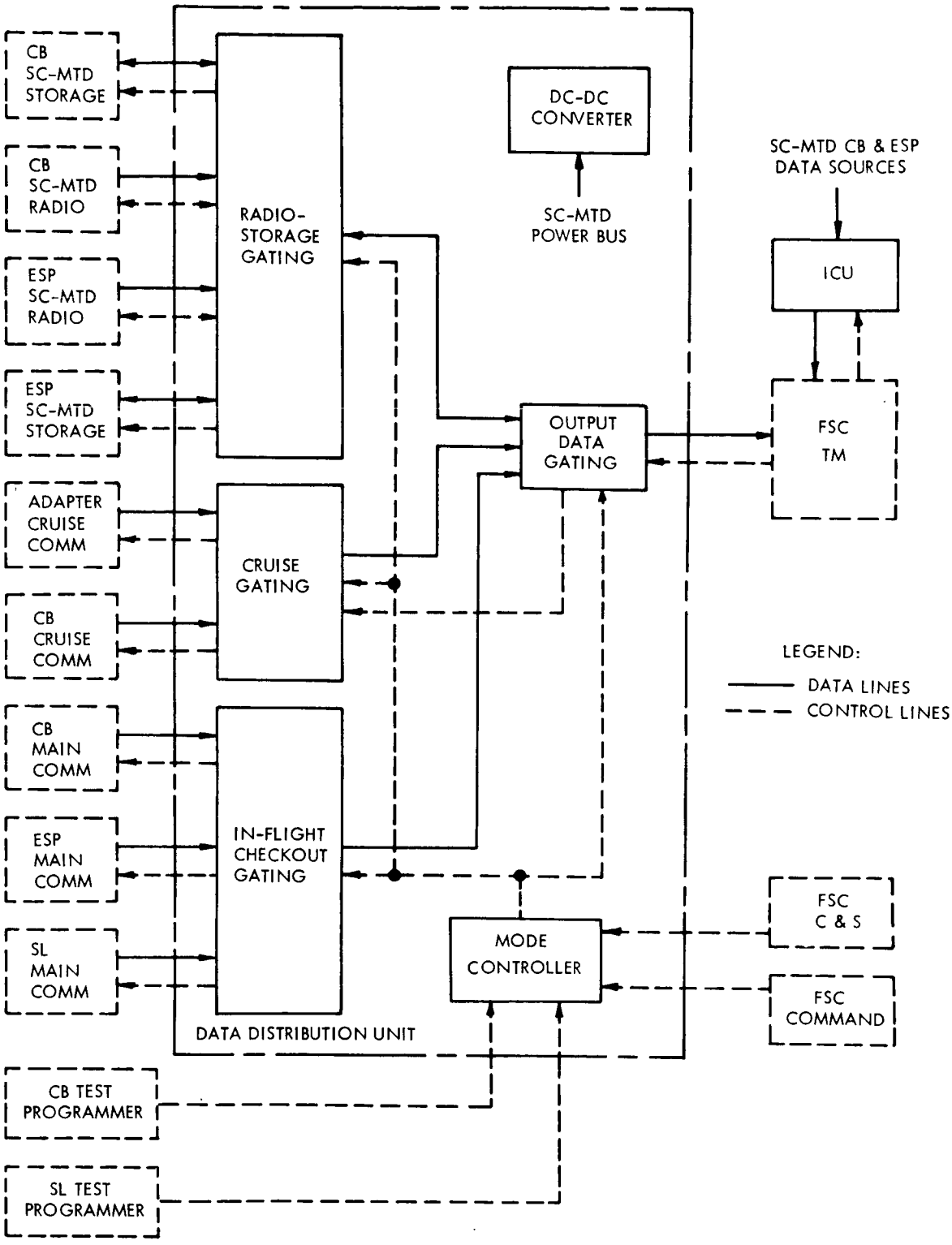

Figure 2. Spacecraft Mounted Flight Capsule Telemetry Support Equipment

and receiver. The receiver is assumed to be capsule system furnished equipment. Provisions have been made for mounting the antenna for unobstructed capsule viewing from separation to a few minutes after landing. The receiver equipment will be located in Bay 13.

2.6 ELECTRICAL INTERFACE

The flight spacecraft provides 200 watts of unregulated (37 - 65 volt) raw array/battery DC power to the flight capsule from liftoff through transfer to internal power prior to spacecraft/capsule separation. The transfer of power is interrupted only for ten second periods after maneuvers in order to relieve a spacecraft adverse load sharing problem. In addition, 50 watts of 2.4 kHz, 1ϕ, square wave power is supplied to the relay radio and other spacecraft mounted capsule bus support equipment from shortly before spacecraft/capsule separation until after capsule landing and termination of relay radio operation.

Approximately 170 watts of the 200 watts supplied to the capsule is used for maintaining the capsule temperature within allowable limits. However, the rate of temperature change in the interior of the capsule is estimated to be a few degrees Farenheit per hour if this power is interrupted. The necessity for supplying this power during maneuvers results in additional spacecraft batteries weighing 21.5 pounds. Further consideration of the requirement to supply 200 watts to the capsule during spacecraft maneuvers is recommended.

The electrical physical interface is assumed to occur at the spacecraft-capsule interface plane. The requirements for fault protection, grounding, and EMI, as noted in the Task B Study report, are considered to be still valid.

2.7 OPERATIONAL INTERFACES

The spacecraft trajectory and orbit location about Mars was, to a large degree, determined by the capsule landing (lighting and latitude) requirements. With respect to the capsule mission, the following conclusions may be reached as a result of the trajectory and orbit studies:

a. Illumination requirements can be fulfilled for landings near both the evening and morning terminators.

b. Direct earth communication links can be readily established by the capsule with landings near the morning terminator.

c. Up to two hours of communication after landing can be realized with only a moderate degradation of the illumination angle for evening terminator landings.

d. Velocity requirements for evening terminator landings with immediate communication requirements are feasible.

e. Approaches from the north are eliminated because the landing latitude constraint is violated.

Selection of the design orbit with periapsis and capsule landing point near the evening terminator imposes thermal control hardships on the capsule and limits the initial direct communication time. However, the detrimental aspects to the flight spacecraft, if a periapsis and capsule landing point near the morning terminator were chosen, outweigh the hardships imposed on the capsule.

In Section VOY-D-273, several potentially important capsule recontamination mechanisms are discussed. In order to minimize the possibility of recontaminating the capsule utilizing one of these mechanisms, the bio-barrier is removed five minutes before spacecraft/capsule separation. Consideration was given to possibly turning the attitude control gas jets off during separation to prevent recontamination from this source, but further investigation must take place concerning the orientation accuracy requirement compatibility before accepting this separation procedure. The requirement for line-of-sight restrictions between the exposed capsule and any spacecraft appendages has been complied with, and this consideration had an important role in defining the spacecraft/launch vehicle support point location, as well as the high gain antenna size.

An interface will also exist between OSE for the flight capsule and flight spacecraft during planetary vehicle checkout, launch operations, and mission operations. These interfaces will be defined at a later date when a better definition of the flight capsule becomes available.

3. LAUNCH VEHICLE INTERFACE

3.1 INTRODUCTION

This section discusses the requirements placed on the planetary vehicles by the launch vehicle system and the requirements placed on the launch vehicle system by the planetary vehicles. These requirements are based upon NASA data and, where necessary, assumption s which are explained in the appropriate sections. It was assumed in this study that the launch vehicle system includes the launch vehicle, the nose fairing and structural shroud, encapsulation diaphragms, and umbilical lines. The structural shroud is defined as that portion of the enclosure which encapsulates the two planetary vehicles. The nose fairing is that portion of the enclosure located above the structural shroud.

Before mating with the launch vehicle, each planetary vehicle is encapsulated in a section of the structural shroud. Each end of the shroud section is sealed by a diaphragm. These two assemblies are each supported and handled by the AHSE (assembly, handling and shipping equipment) designed to lift and transport the encapsulated planetary vehicle. From the time the planetary vehicles leave the explosive-safe assembly facility, they will remain encapsulated for launch pad operations.

The spacecraft system and the launch vehicle system have functional, physical, electrical signal and power, RF, and environmental control interfaces. Each of the interfaces is shown in Figure 3 and described below.

3.2 FUNCTIONAL INTERFACES

Two identical planetary vehicles are launched together on the specified trajectory. The spacecraft system is able to maintain launch readiness in fueled and mated condition for the full duration of the launch period. The launch vehicle system is capable of maintaining readiness for a daily firing window of two hours or more for a 30-day period, and have a probability of 0.99 for accomplishing the launch. The Launch Vehicle will have parking-orbit capability and a guaranteed gross injection weight capability of 52,000 lbs. on Mars

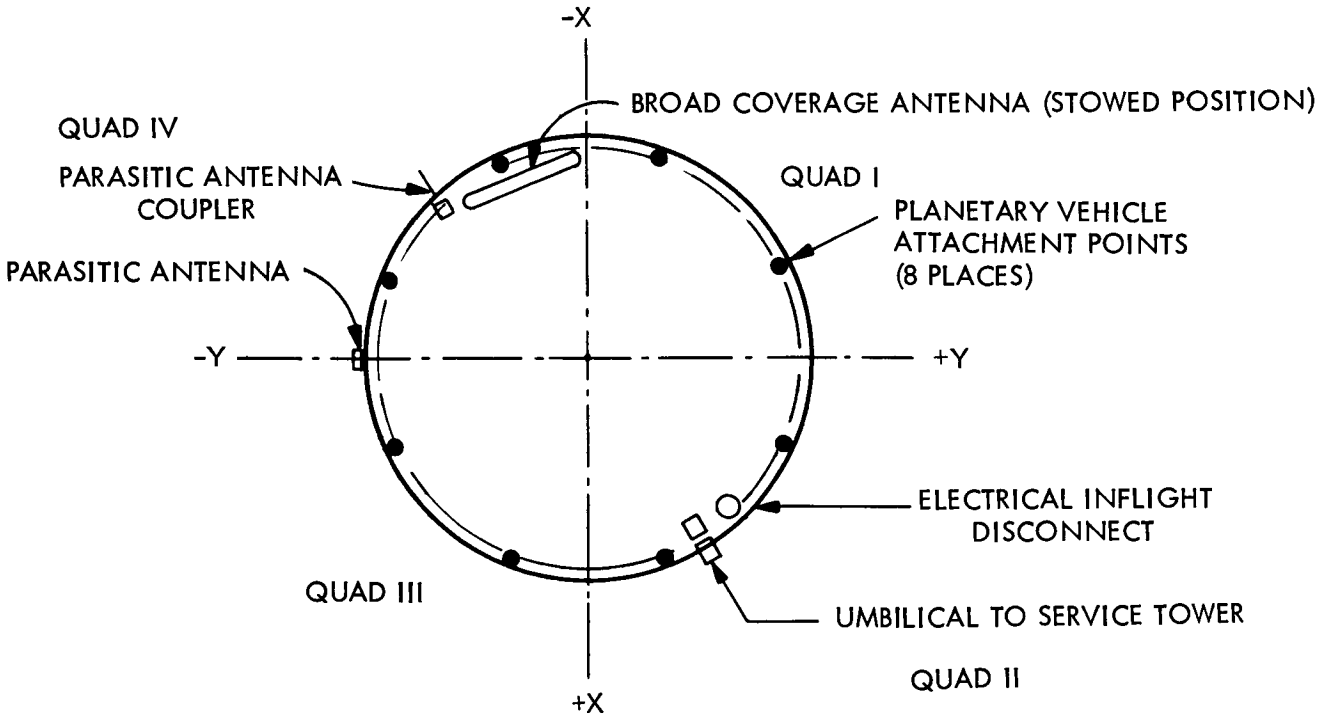

SECTION A-A

FOLDOUT FRAME 1

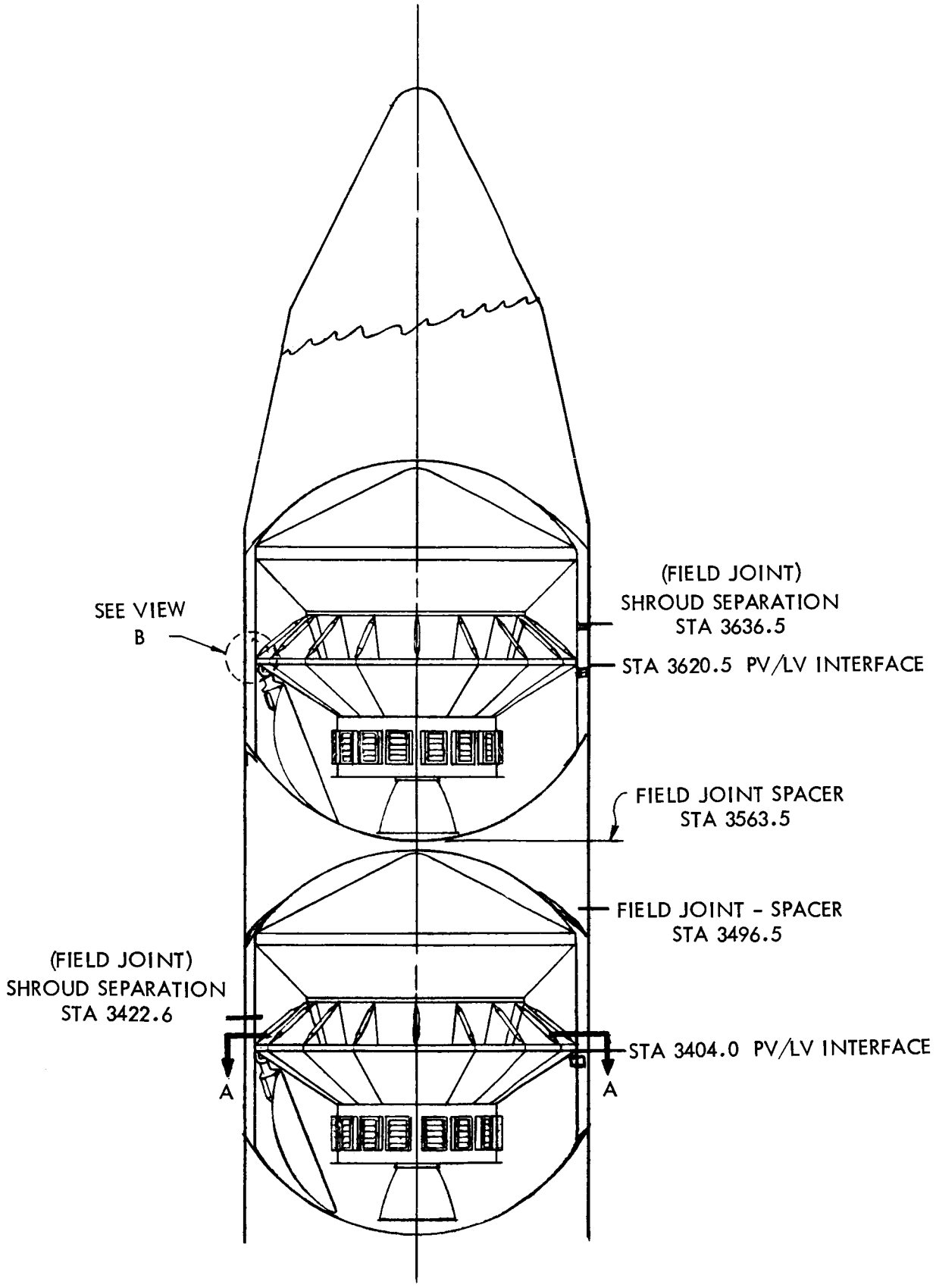

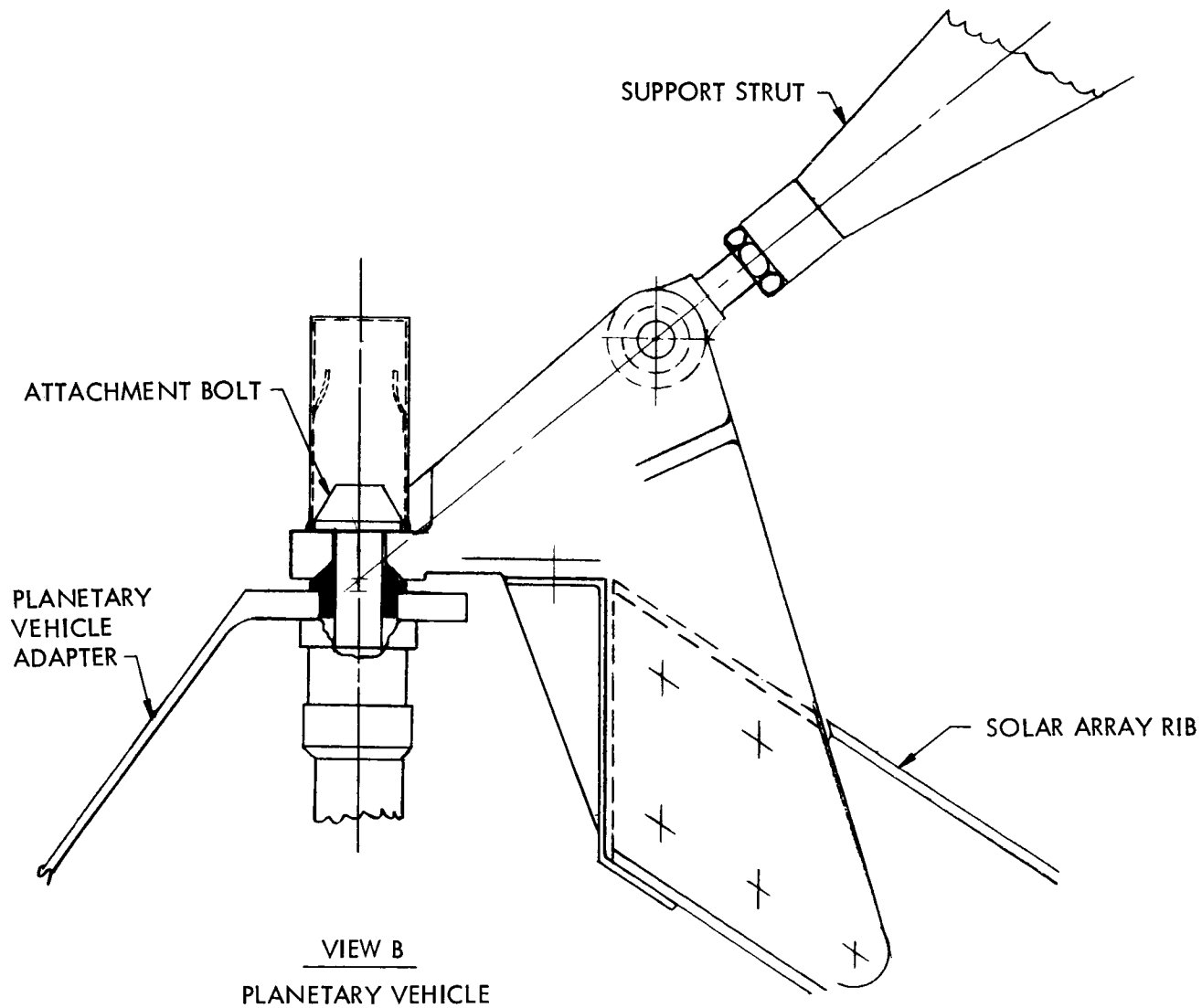

VIEW B

PLANETARY VEHICLE
SEPARATION ATTACHMENTS
(8 PLACES)

Figure 3. Launch Vehicle Interfaces

trajectory with a C_3 of 28 km^2/sec^2 based upon a lauch azimuth of 115 degrees. The Saturn IVB stage is capable of providing the final burn after an interval of 2 to 90 minutes in nominal parking orbit. The launch vehicle trajectory is biased from an optimum Mars trajectory in order to satisfy the planetary quarantine constraint.

During ascent through the Earth's atmosphere, the planetary vehicles are enclosed in the launch vehicle nose fairing and structural shroud; the aerodynamic nose fairing is jettisoned during the parking orbit. Each planetary vehicle is separated from launch vehicle by firing eight squib-actuated separation nuts, thus allowing for actuation of sixteen separation springs (two springs at each attachment point).

At the time of separation of the forward planetary vehicle, it is given a relative velocity by the separation system with respect to the aft planetary vehicle and S-IVB stage. The maximum angular rate at separation must be less than 3 deg/sec. The launch vehicle will contribute less than 1 deg/sec and the maximum angular tipoff rate attributable to the separation system must be less than 2 deg/sec. Subsequent to separation of the forward planetary vehicle, the shroud covering the aft planetary vehicle is separated. The aft planetary vehicle is then separated with from the S-IVB stage. A relative velocity between the forward and aft planetary vehicles insures the required dispersion at the time of the first mid-course maneuver 2 to 5 days after injection. The aft shroud section must also be given a relative velocity with respect to the two planetary vehicles. Suitable separation velocities between all elements can be achieved with identical separation springs on each PV due to the changing mass of the vehicle being left behind. An analysis of the PV separation and selection of suitable velocities is contained in VOY-D-364.

3.3 PHYSICAL INTERFACE

The identical mechanical interfaces between the planetary vehicle and the structural shroud are at launch vehicle stations 3404.0 and 3620.5. These mechanical interfaces are the only structural supports for the planetary vehicle. Each planetary vehicle is attached to the adapter structure with eight 1/2-inch diameter bolts (one at each of the eight attachment points). The adapter, in turn, is attached to a shroud ring.

The launch vehicle inflight electrical disconnects (IFD) are positioned approximately at the mechanical interface between the planetary vehicle and the structural shroud. The launch vehicle system must provide a means of access for mating of the IFD's.

3.4 ELECTRICAL SIGNAL AND POWER INTERFACE

The electrical interface between the planetary vehicles and the launch vehicle system is illustrated in Figure 4 and includes ground power, launch monitor control and spacecraft and capsule environmental telemetry. Prior to liftoff, the planetary vehicles are switched from launch complex to internal power. All electrical exchanges are accomplished by means of launch complex umbilicals to each planetary vehicle and wires from the planetary vehicles to the launch vehicles. The umbilical connections are located in the structural shroud adjacent to each planetary vehicle adapter.

Planetary vehicle environmental measurements such as vibration, acoustic, pressure, and temperature are made and transmitted over the launch vehicle telemetry system. Limited spacecraft status data is also transmitted over the launch vehicle telemeter.

The disconnect leads from each planetary vehicle are routed to the launch vehicle as shown in Figure 4.

Since squib firing circuits can not be routed through inflight separation connectors, certain direct wiring is required from the launch vehicle. The squib-actuated pin-pullers which release the inflight disconnects and the explosive nuts of the planetary vehicle separation systems are activated by the launch vehicle in the proper timing sequence. It is also assumed that the launch vehicle will supply the power since the planetary vehicle pyrotechnics subsystem is not armed until separation protecting against inadvertant or spurious commands prior to separation causing a premature squib firing.

Each separation nut for each planetary vehicle has two electro-explosive devices. In addition, each planetary vehicle has two pin-pullers for the inflight disconnect. The inflight disconnect

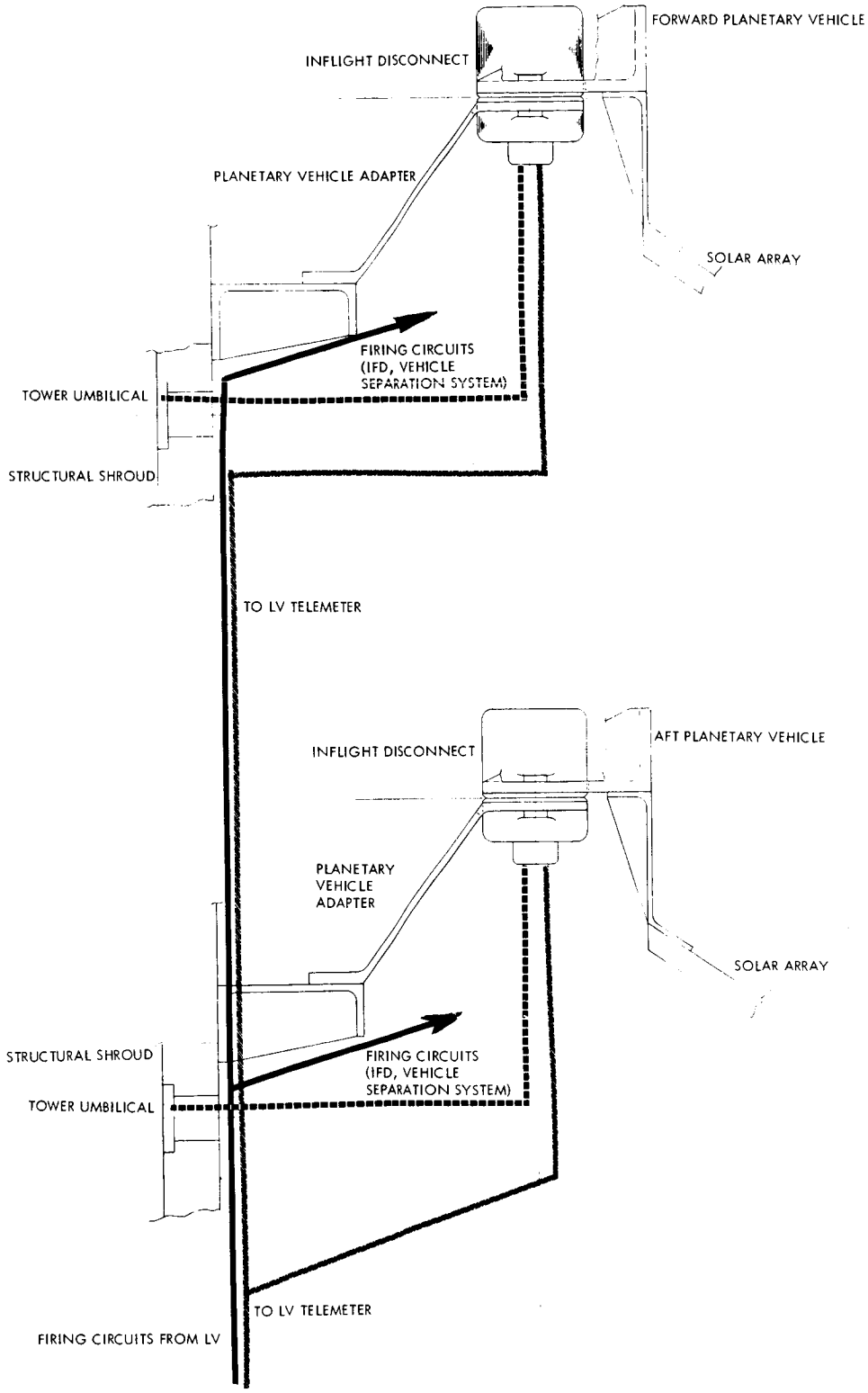

Figure 4. LV/PV Electrical Interfaces

is operated before planetary vehicle separation with each pin-puller actuated by a single Apollo standard initiator (ASI). The firing current for the ASI is 5 amps minimum, so 10 amps will be required for the IFD. Each ASI of the separation system also requires a minimum firing current of 5 amps, so that a total of 80 amperes is required for separation.

3.5 RF INTERFACE

The output RF signals from each planetary vehicle are picked up by means of a parasitic antenna coupler located on the shroud. One coupler is mounted on the shroud adjacent to the aft planetary vehicle-shroud interface, and one is mounted on the shroud adjacent to the forward planetary vehicle-shroud interface. Each signal is carried to an antenna on the exterior surface of the structural shroud. The antennas are located so that both flight spacecraft are in communication with the Cape 71 DSIF station during the launch phase.

3.6 ENVIRONMENTAL CONTROL INTERFACE

Thermal and humidity environments are provided by the launch vehicle system to the encapsulated planetary vehicles from time of explosive safe assembly through nose fairing separation. It is assumed that the encapsulating diaphragms are supplied with the nose fairing and structural shroud. The diaphragms remain with the shroud at the time of nose fairing or shroud separation.

The thermal analysis section, VOY-D-362, defines the effect of aerodynamic heating of the shroud on the spacecraft. The current estimates of maximum shroud temperature are well within acceptable limits.

4. LAUNCH OPERATION SYSTEM INTERFACE

The Launch Operations System, LOS, with which the Voyager Planetary Vehicle must interface, includes both facilities and services. These supporting facilities and services exist at both Kennedy Space Center and Cape Kennedy. The planetary vehicle support by the LOS will be required in three general areas: (1) the hangar or Spacecraft Checkout Facility (SCF),

(2) the Explosives Safe Area or Hazardous Materials Handling Area, and (3) the Launch Complex. For each of these locations, a supporting facility will be delineated by appropriate facility interface documents. Service support will also be required and documented by procedure/documents. In general, Voyager will make use of the available services at KSC and ETR but will require nothing unusual in the way of services. Facilities requirements are not completely determined, but no changes are envisioned from those defined in the Task B Study Report other than provisions for on-pad propellant loading.

A general description of the interface is given in this section. It is not the intent to specify the interface, but to identify the area and nature of the interface so that problems will be exposed. The interface, both functional and physical, is as follows:

a. Launch Complex 39

1. Propellant Loading - Propellant servicing equipment and operators are required for on-pad loading of propellants. It is assumed that KSC will provide this capability. Loading rates, quantities and accuracies must be determined by the spacecraft contractor. As discussed in Volume IV, existing Apollo Lunar Module fluid service equipment may be used.

2. Pressurization - On-pad pressurization capability may be required. This would consist of pressurized nitrogen provided by KSC.

3. Umbilical Requirements - Electrical and mechanical umbilical capability will be required. This could take the form of an interface with the shroud manufacturer. The requirement includes transfer of electrical signals to the LCE and provision of dry, filtered air or nitrogen for the cooling the planetary vehicle under the shroud.

4. Mobile Service Tower - Power, communications and equipment space will be required at the appropriate levels of the MST. Present ground rules on planetary vehicle accessibility preclude the need for a tent. The Voyager program must provide requirements for power, communications, and floor space to KSC. Any test equipment or special equipment required would be provided by the Voyager program.

5. Propellant Sensing Alarms - Sensing alarms for fuel and oxidizer fumes must be provided. Since the sensors must sense fumes inside the shroud, there will be an alarm interface between the LOS and Planetary Vehicle.

6. Hoisting Requirements - The hammerhead crane on the umbilical tower must be capable of hoisting a planetary vehicle and its encapsulating shroud to the top of the booster. With on-pad fueling of the spacecraft, the capability of the crane should be sufficient.

7. Launch Control Center - Power, communication and space is required in the LCC firing room for the OSE used to control the prelaunch and launch of the Voyager spacecraft. The OSE must have an interface with the LC39 hardline running between the Vertical Assembly Building and the launch pad. The number and type of hardlines must be specified by the Voyager Spacecraft contractor. In addition, a data/control link tie-in to the Spacecraft Checkout Facility will be required, as well as a communication interface with DSIF 71.

b. Explosives Safe Area or Hazardous Materials Handling Area. The requirements for this area are essentially the same as those noted in the Task B Study Report, except for the deletion of the propellant loading requirement. It is expected that a new facility or expansion of existing facilities will be required with mating of the spacecraft and capsule occurring in this facility. KSC will provide service and storage for pyrotechnics, pressurized gases and clean working areas.

c. Spacecraft Checkout Facility - A high bay, clean area is required for spacecraft inspection and test. This area must accommodate the spacecraft test equipment, per Voyager specified dimensions, loads, and environmental control. The exact facility location is not critical, as long as the required communication between system test equipment and other OSE elements can be implemented.

d. Communications

1. Voice Communications - Extensive voice communication capability will be required between the SCF, ESA, DSIF 71 and LC39. The normal facility communications systems should be more than adequate. Exact requirements in terms of operator stations, locations and nets must be specified by the Voyager program.

2. Data Links - Existing data links at KSC and AFETR more than meet Voyager requirements.

3. RF Antennas - A system of several RF antennas in the 2,100-2,200 mc range is required to link the Voyager planetary vehicle with the DSIF and the system test equipment. It is assumed that KSC will provide these to Voyager specifications. Antennas required at these places are:

   a. Hangar Roof

   b. Mobile Service Tower

   c. Umbilical Tower

5. MISSION OPERATIONS SYSTEM AND DEEP SPACE NETWORK INTERFACE

5.1 GENERAL

Following inflight separation from the launch vehicle, all communications between the Voyager Spacecraft System and ground operations on earth will be accomplished through the Deep Space Network (DSN). The DSN as configured for Voyager will consist of: (1) tracking and data acquisition equipment, facilities, and software which are independent of the Voyager mission, (2) Mission Operations System (MOS) which includes hardware and software which are mission dependent. The Voyager Spacecraft System communication interface with ground operations includes:

a. On the Spacecraft - Compatibility between Spacecraft Telecommunication Subsystem design and the DSN.

b. On the Ground - Configuring mission dependent hardware (MDHW) and Mission Dependent software (MDSW) associated with the MOS.

A definition of the overall DSN is given in VOY-D-600 including Mission Dependent Equipment requirements (hardware and software).

While the Voyager Spacecraft interfaces with the DSN only at the Deep Space Station (DSS) antennas, data paths are required from the Space Flight Operations Facility (SFOF) to the DSS antennas and back. Appropriate data analysis and displays for spacecraft control must be coordinated by mission operations personnel following a mission operations plan. All of

these functions make maximum use of existing equipment, facilities and software (Mission Independent Equipment). Only where this is not adequate will the Voyager program supply mission dependent equipment.

The requirements for the MOS/DSN interface were given in the Task B study report. The following is a summary of these requirements with changes as noted.

5.2. RF REQUIREMENTS

The Spacecraft-mounted transmitter and receiver is compatible with the existing and planned DSS for the Voyager time period. This interface consists of an up-link made up of simultaneous ranging and command data transmitted by the DSS and a down-link containing engineering data, scientific data, and the ranging code. The data is contained on three subcarriers of the spacecraft transmitted signal which is coherent with the received DSS transmitted signal. The frequencies selected shall allow for simultaneous operation with two spacecrafts with adequate signal separation to prevent cross talk.

5.3. DATA PROCESSING

5.3.1. Engineering Data

The Spacecraft engineering data will be in one of several selected formats transmitted at rates of 150, 37.5 or 7.5 bps; this data will be contained on a separate subcarrier. The DSS must remove the subcarrier and establish bit sync using the detected frame sync. The data format can then be established and the data decommutated. Data will be displayed within the DSS only to the extent required to support DSS operations and transmitted to the SFOF in near realtime.

The SFOF will receive the data and will perform automatic spacecraft status analyses continuously, drive display devices with raw data, and provide recommendations for switching to spacecraft alternate modes or elements using pre-programmed analyses. The data will

also establish that automatic sequences are being carried out properly, obtain thermal balance characteristics and power consumption, monitor significant parameters for trends, and obtain a record of the performance of all subsystems for anomaly analysis.

5.3.2. Scientific Data

The scientific data will be transmitted at one of four commanded data rates (1.265, 10.125, 20.25, 40.5 Kbps) on a separate subcarrier. An added requirement results from the spacecraft use of error control coding which requires that the data be decoded at the DSS; this will require MDE. The recorded data will be identified by correlating the engineering data word indicating source of data. The data will be transmitted to the SFOF where it will be processed in near realtime using the wide band data link. Each scientific instrument will require separate display and processing MDE.

5.4. COMMAND REQUIREMENT

The MOS operating personnel will initiate commands to update the spacecraft automatic sequences, for controlling spacecraft housekeeping functions, and the science equipment operation, to initiate functional redundancy provisions, and to overcome operational anomalies. The commands will be initiated in the SFOF with complete verification of proper reception by the spacecraft being required. The commands will be one of four types.

a. Realtime discrete

b. Stored sequences released in sequence based on time lag

c. Discrete commands-executed after a specified time lag following receipt by the spacecraft

d. Command data for the capsule (via the Spacecraft Command Subsystem).

The specific spacecraft to be commanded is selected by the DSS transmitter frequency as well as by using a preamble sequence peculiar to that spacecraft. Command data will be sent after establishing PN lock as indicated by the engineering data. The commands will be verified as sent by the DSS as well as at the SFOF. If the data is improper, the DSS will alter the

command, causing rejection of the command by the spacecraft. The DSS will use the engineering data to establish the sequence of accepted and rejected commands and retransmit commands as required. The DSN command transmission structure will include points at which spacecraft verification of acceptance must be obtained before proceeding.

5.5 TRAJECTORY ESTABLISHMENT

The DSN must provide data for establishing the trajectory. This will require ranging and the determination of range rate, position, and time. This data will be transmitted to the SFOF from the DSS for trajectory establishment.

5.6 COMPUTER PROGRAMS

An extensive computer program library will be required to support the Voyager mission. The majority of these will be MDE. The type of computer programs required are as follows:

a. TLM Processing (SFOF and DSS)

b. Command Processing (SFOF and DSS)

c. Spacecraft Status

d. Trajectory Determination

e. Maneuver Parameter

f. Planetary Orbit Determination

g. Orbit Trim Parameter

h. Data Display

i. Spacecraft Simulation

j. Pad/Launch Operations

k. DSN Acquisition

l. DSS-SFOF Data Interchange

m. Personnel Training

VOY-D-260
TRAJECTORY AND GUIDANCE ANALYSIS

1. INTRODUCTION

This section discusses the various trajectory and guidance aspects of the voyager mission and determines flight profiles, velocity requirements and launch vehicle payload capability. System design parameters such as communication distance, vehicle-sun distance, antenna gimbal/orientation angles, and occultation durations are included herein. Special emphasis is placed on guidance accuracy and its significance in the execution of the assigned mission maneuvers.

A brief summary of the trajectory and guidance analysis results is given below. It is recognized that these conclusions may change in the face of further analyses or with the consideration of additional or modified mission constraints.

a. Type I trajectories are recommended presently for all launch years.

b. A total propulsion requirement (ΔV) of 1.95 km/sec appears adequate.

c. Launch periods are approximately 20 to 30 days for the selected arrival dates of the four launch opportunities.

d. Direct areocentric orbits with landing and periapsis locations near the evening terminator are recommended.

e. Direct capsule-earth link, established immediately after landing, results in a moderate degradation of landing illumination for landings near the evening terminator.

f. The preliminary orbit size is:

   1. Periapsis altitude, 1,000 km
   2. Apoapsis altitude, 11,727 km
      Orbital Period 8.15 hrs.

g. Trip times vary from 190 days to 240 days

h. An areocentric orbit inclination of 30 to 40 degrees appears satisfactory.

i. The guidance accuracy during all thrusting maneuvers is 2.24 degrees (3σ). The velocity accuracy is dependent on the vehicle weight and thrust level.

j. Orbital period control:

   1. Pre-trim, 18 minutes (3σ)
   2. Post-trim, 22 seconds (3σ)

2. MISSION BACKGROUND

The objective of the Voyager mission is to advance the planetary scientific exploration of the solar system. Mars is the first planet under consideration and present plans call for launch in 1973 with subsequent arrivals in early 1974. Planetary vehicles will be capable of

a. Placing science instruments in orbit about Mars.

b. Placing science instruments on the surface of Mars.

c. Conducting observation of Martian phenomena for specified periods of time.

d. Transmitting the data to Earth.

The vehicles will be designed to permit launches during the 1975, 1977 and 1979 launch opportunities as well. The mission concept specifies presently that two planetary vehicles will be launched by one Saturn V launch vehicle. Aim points for the Saturn V injection and mid-course maneuvers are selected to satisfy quarantine constraints. Furthermore, a major mid-course maneuver that results in eight days difference in the arrival dates of the two planetary vehicles in 1973 and four days for the remaining years is to be conducted.

2.1 MISSION CONSTRAINTS

The mission constraints are as defined in the following two documents:

a. "Performance and Design Requirements for the 1973 Voyager Mission, General Specification for." January 1, 1967, SE 002 BB 001-1B21 Jet Propulsion Laboratory.

b. "Voyager Spacecraft System Study Guidelines" Letter R-AS-A67-99 July 9, 1967 NASA, George C. Marshall Space Flight Center.

The above applicable documents contain tentative gross mission plans and requirements for the Voyager mission. Document 1 quotes a preferred order of competing mission characteristics which in turn infers a similar priority on various mission constraints. These priorities are summarized below in decreasing order of importance for the first four competing characteristics.

2.1.1 Competing Characteristic:

a. Achievement of a planetary vehicle (P/V) Mars orbit insertion

Mission Constraint:

1. Planetary vehicle orbit insertion shall occur in view of Goldstone.

2. Adequate velocity allowance for orbit insertion for 1973, 75, 77 and 79 launch opportunities.

3. Periapsis altitude: 500 to 1,500 km
   Apoapsis altitude: 10,000 to 20,000 km

b. Achievement of a flight capsule landing

1. Nominal capsule deorbit: Three to 12 days after orbit insertion (capability for capsule support and separation shall be provided for up to 30 days after insertion).

2. Landing site shall lie between 10 degrees north and 40 degrees south latitude.

c. Performance of entry science experiments

1. The capsule landing point shall lie between 15 degrees and 30 degrees from the terminator.

2. The selected landing site shall allow the orbiter to obtain high resolution pictures of the region within 600 km of the specified site.

d. Performance of orbital science experiments

1. First three months: sub-periapsis point shall be between 0 degrees and plus 45 degrees from a terminator.

   Second three months: sub-periapsis point shall lie between minus 30 degrees and plus 90 degrees from a terminator.

2. First six months: the Mars latitude of the sub-periapsis point shall lie between 60 degrees south and 40 degrees north latitude.

3. Minimum areocentric orbit inclination shall be 30 degrees.

4. First thirty days: no sun occultation by Mars. From 30 days to 6 months after encounter, sun occultation shall not exceed the smaller of 8 percent of each orbit period or 60 minutes.

5. First 30 days: loss-of-Canopus lock not permitted.

6. Early earth occultations are desired with the occultation line covering a wide range of latitude and solar zenith angles.

7. For UV experiments, it is required that the angle between the orbit plane and the ecliptic plane not exceed 45 degrees.

8. First three months: The angle between the orbit plane and terminator plane shall not be less than 30 degrees.

   Second three months: This angle shall not be less than 30 degrees for more than a total period of one month.

9. The angle between the normal to the satellite orbit plane and the Earth-Mars line shall be at least ( ) degrees until 30 days after the last orbit trim maneuver.

e. Other general mission specifications include the following (not in priority):

1.

Year	Trajectory Type	Launch Azimuth
1973 and 1979	I	90 degrees to 115 degrees
1975 and 1977	I	45 degrees to 115 degrees
1975 and 1977	II	90 degrees to 115 degrees

2. Launch period: 30 days minimum

3. Arrival date separation: 8 days (1973), 4 days (1975, 1977, 1979)

4. Declination of outbound asympote: $|DLA| > 5$ degrees

5. Minimum launch window: 1 hour

6. The probability of contaminating Mars by Voyager space vehicle borne terrestial organisms shall not exceed 10^{-3} for all potential Voyager sources of contamination while biological studies are being conducted.

Recently, MSFC issued revised requirements (second referenced document) that take precedence over the first applicable document. These include, in part, the following:

a. A minimum of 1.95 km/sec Δ V capability shall be provided for the following maneuvers: arrival date separation of 8 days for the 1973 opportunity and 4 days for succeeding years, mid-course correction, orbit insertion and orbit trim.

b. A reasonable launch period is considered to be a minimum of 20 days for all launch years - if possible.

One obvious omission from the above summary is a communication time requirement, either directly with earth or with the orbiter, for the capsule immediately after landing. With the communication modes unresolved, various operational modes were examined to determine the influence on trajectory and orbit selection.

Although the above lists include approximately 20 constraints, only 5 of the constraints have a real significant impact on trajectory selection, spacecraft design, or spacecraft capability. These are listed briefly below in descending order of importance:

a. No loss-of-Canopus lock

b. Capsule landing between 15 degrees and 30 from terminator

c. Landing site between 10 degrees N to 40 degrees S latitude

d. Minimum launch window of 20 days

e. Solar occultation (max 8 percent of orbit period)

In order to avoid loss-of-Canopus lock, late arrivals (April 74) must be planned for the 1973 launch opportunity. This action results in long communication distances (260×10^6 km) and longer flight times (230 days) at encounter.

With the specification that the landing be between 15 degrees and 30 degrees from the terminator, and the landing site be between 10 degrees North and 40 degrees South latitude, the allowable range of areocentric orbit inclinations and direction of periapsis approaches are restricted to 30 to 55 degrees with approaches from the south. Apsidal rotation requirements are also affected.

The minimum launch window of 20 days during the 1975 and 1977 launch opportunities for Type I flights, limits the allowable payload weight to 52,000 lbs. (no program contingency); thereby specifying allowable spacecraft weight for the 1973 and 1979 opportunities as well.

These constraints are considered in detail in the subsequent sections.

2.2 MISSION CONSIDERATIONS

2.2.1 Geometry

It is apparent from the above summary of mission specifications that mission capability depends to a high degree on the geometry between the spacecraft and celestial bodies at the planet. This geometry consists of the areocentric orbit inclination, direction of planetary approach and the approach hyperbola periapsis location relative to the sun, earth, Canopus and equatorial plane of Mars. Figure 1 depicts the geometrical arrival conditions at the planet in a simplified manner. The figure also shows the evening terminator, desired landing zone and approximate on-the-surface earth communication zone. The positions of the natural periapsis represent the line-of-apsides of the resulting areocentric orbit providing

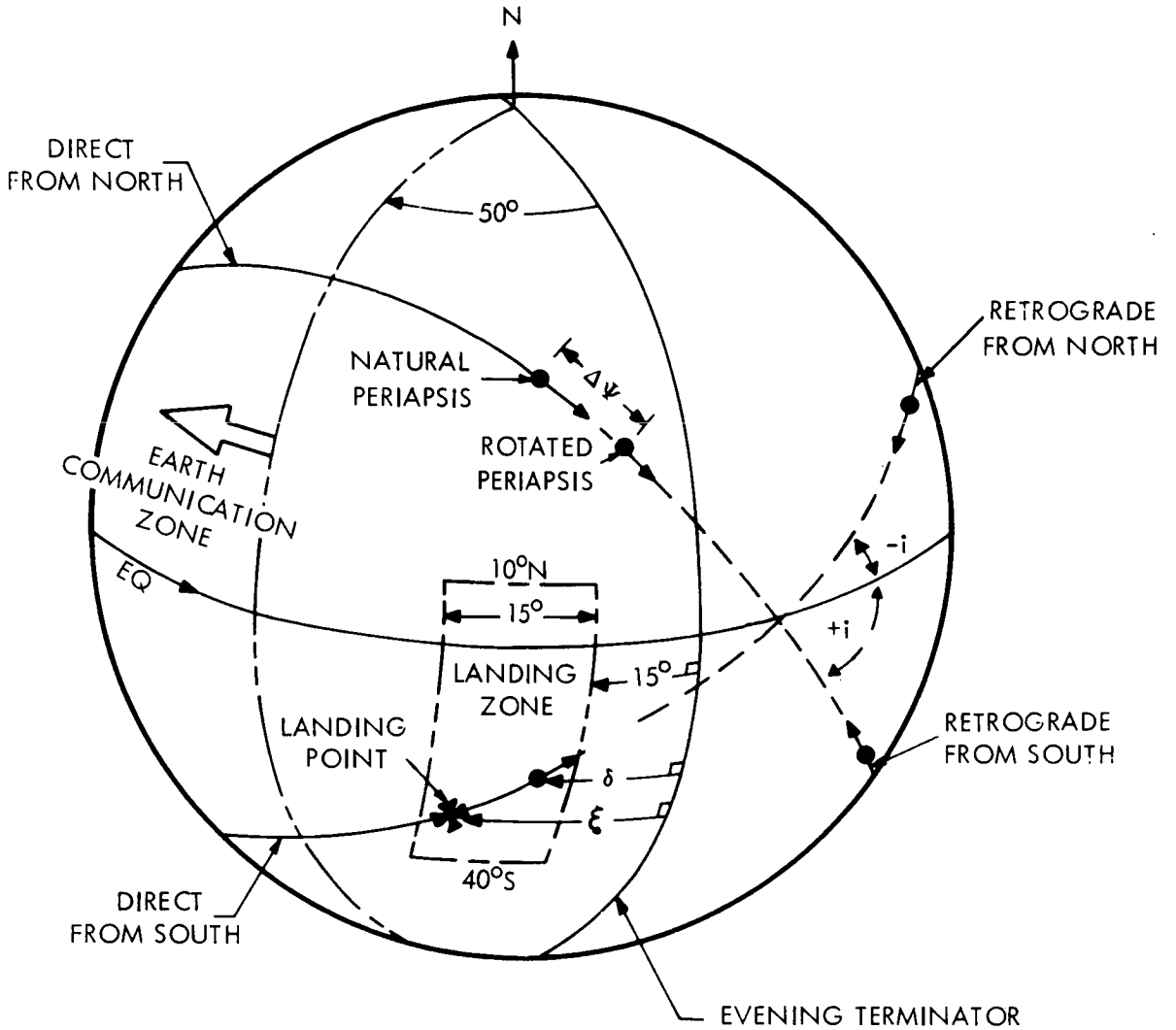

$\delta \sim$ ILLUMINATION ANGLE OF THE SUB-PERIAPSIS POINT MEASURED IN A GREAT CIRCLE PLANE NORMAL TO THE TERMINATOR

$\xi \sim$ ILLUMINATION ANGLE OF THE CAPSULE LANDING POINT MEASURED IN A GREAT CIRCLE PLANE NORMAL TO THE TERMINATOR

$i \sim$ AREOCENTRIC ORBIT INCLINATION

$|i| < 90° \sim$ DIRECT OR POSIGRADE ORBITS

$|i| > 90° \sim$ RETROGRADE ORBITS

$\Delta\psi \sim$ APSIDAL ROTATION OBTAINED AT THE TIME OF ORBIT INSERTION

$(+)\Delta\psi \sim$ ROTATION IN DIRECTION OF VEHICLE MOTION

$(-)\Delta\psi \sim$ ROTATION OPPOSITE TO VEHICLE MOTION

Figure 1. Arrival Geometry

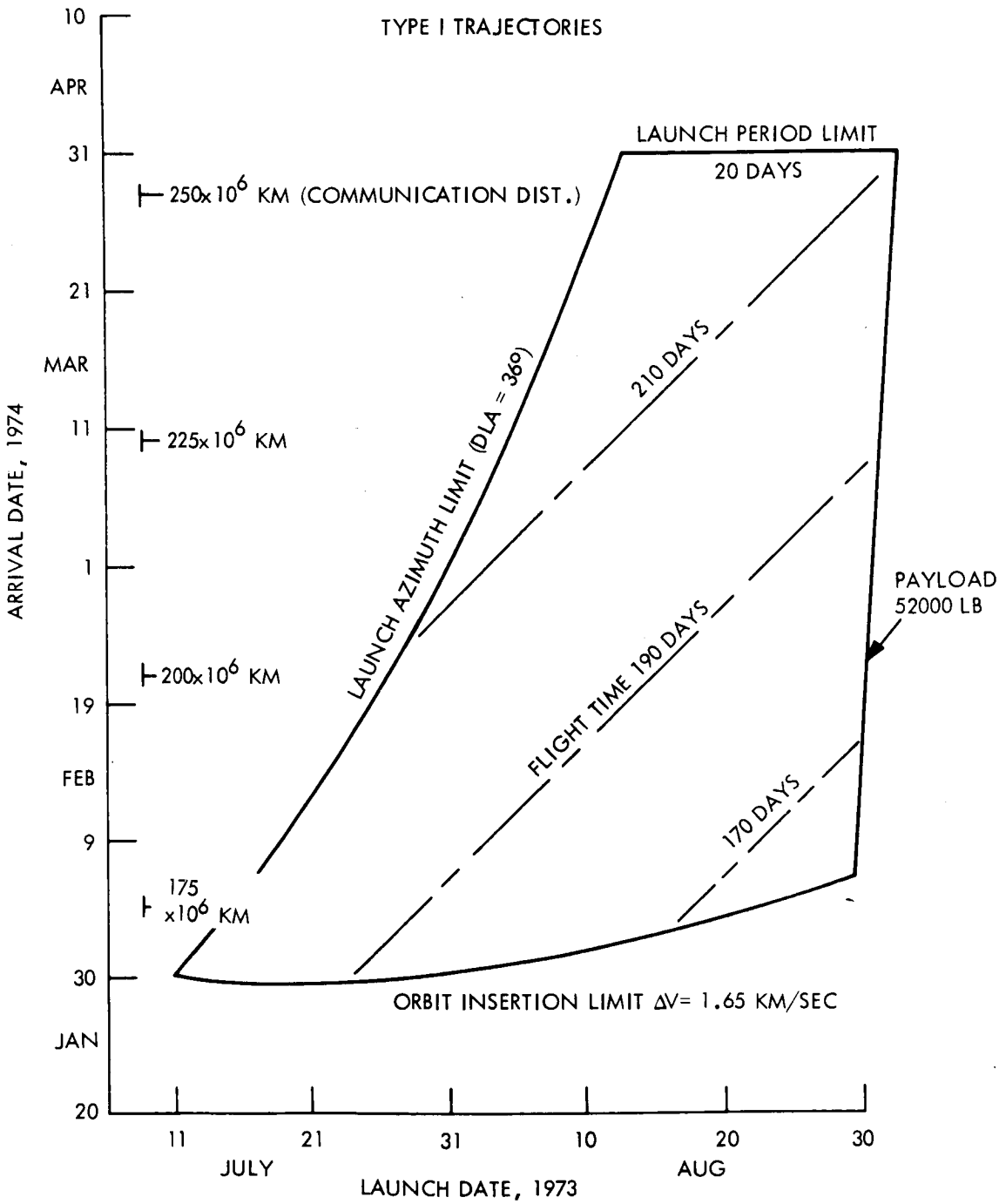

Figure 2. 1973 Mission Envelope - Type I Trajectories

that the orbit insertion maneuver is executed at the periapsis of the approach hyperbola with the insertion velocity colinear with the approach velocity. The apsidal rotation, $\Delta \psi$, is achieved by performing the orbit insertion maneuver at a preselected point on the approach hyperbola. Positive rotations imply an apsidal shift in the direction of vehicle motion while negative rotations are opposite to the direction of motion. Positive inclinations in this report connote northerly approaches. Orbit inclinations less than 90 degrees represent direct (posigrade) approaches and retrograde orbits are given by inclinations greater than 90 degrees. The orbit location is controlled by both the orbit inclination and arrival date.

In the discussion that follows and based on Task B study results, the landing point is assumed to be located 17 degrees of central angle prior to periapsis passage. The effect of changing this relative landing position can be determined by simply interpreting the change as an apsidal rotation.

2.2.2 Mission Options

Figure 1, although drawn pictorially, does represent approximately the actual arrival situation at Mars. The planetary vehicle, for any trans-Mars trajectory, can be made to approach Mars with almost any inclination. This choice of areocentric orbit inclination combined with available choices of launch and arrival dates, plus the capability to perform apsidal rotations results in a number of mission alternatives. These alternatives include:

a. Evening or morning terminator periapsis locations (capsule landings)

b. Early versus late arrivals

c. Type I or Type II heliocentric trajectories

d. Southerly or northerly approaches

e. Direct or retrograde areocentric orbits

Establishing periapsis or landing points near the evening terminator requires smaller apsidal rotations than establishing landing and periapsis points near the morning terminator for both Type I and Type II trajectories. The morning terminator landing zone, however, affords an immediate capsule - earth communication link after touchdown.

Early arrivals exhibit longer launch periods, shorter communication ranges, shorter flight times, larger insertion velocity impulse, and lower trajectory sensitivity. Later arrivals for a given launch envelope generally have the opposite characteristics but do result in lower planetary approach speeds and consequently smaller velocity (ΔV) requirements. As will be demonstrated, the desired choice of early arrival date can be preempted by the imposed mission constraints.

Type II trajectories have inherent characteristics of longer flight times and longer communication distances. Although these characteristics are not desirable, Type II trajectories do ease the launch azimuth requirements and because of their approach geometry, morning terminator landings are made more accessible for the 1975 and 1977 opportunities.

Solar occultations are less prevalent with direct orbits than with retrograde orbits, and loss of Canopus lock is generally experienced with inclinations from 10 degrees to 150 degrees and minus 30 degrees to minus 130 degrees for a 40 degree by 60 degree light sensitive sensor field of view. For the 1973 mission solar occultations during the early orbital phase occurs for a smaller range of arrival parameters if the periapsis is located near the evening terminator. Retrograde orbits exhibit large earth occultation zones at the time of orbit insertion and in general require larger apsidal rotations than direct orbits. Occultations are also significantly affected by arrival date, apsidal rotations and orbit size.

Another important mission consideration is the planetary quarantine constraint. This constraints necessitates the use of a somewhat complex injection and midcourse maneuver policy, and also may influence the final aerocentric orbit size selection.

3. MISSION ANALYSIS

The necessity of performing mission analysis tasks is evident especially in the light of the many mission constraints and alternatives. This becomes even more apparent when reference is made to Figure 2. This figure shows the allowable launch envelope for 1973 as bounded by the allowable declination of the departure asymptote (DLA<36 degrees), a payload requirement of 52,000 LB (C_3 = 28 km^2/sec^2), an orbit insertion ΔV limit of 1.65 km/sec and a 20-day launch window. Although a large region of acceptable launch and arrival dates is available, only a portion may actually be available when the remaining constraints are considered. Thus, the intent is to examine the alternatives, assess the governing constraints, determine the velocity requirements, suggest operational modes and recommend design flight profiles. This is accomplished by making a mission comparison of the launch opportunities from 1973 to 1979 with five major considerations in mind, namely:

a. Type I (1973 and 1979), Type I and II (1975, 1977).

b. Evening versus morning terminator periapsis locations and capsule landing zones.

c. Direct or retrograde orbits.

d. Communication distances.

e. Flight times.

3.1 APSIDAL ROTATION REQUIREMENTS

Figure 3 is a summary chart showing apsidal rotation requirements for both morning and evening terminator landings (periapsis location near morning or evening terminator) and for direct and retrograde orbits. The planetary approach velocity (VHP) is used as the independent parameter since it best represents nearly constant arrival conditions. The figure includes Type I and Type II flights for the years 1975 and 1977 but does not include retrograde orbits for Type I trajectories. This latter consideration is eliminated for landings near the morning terminator because of the exceedingly high apsidal rotation requirements

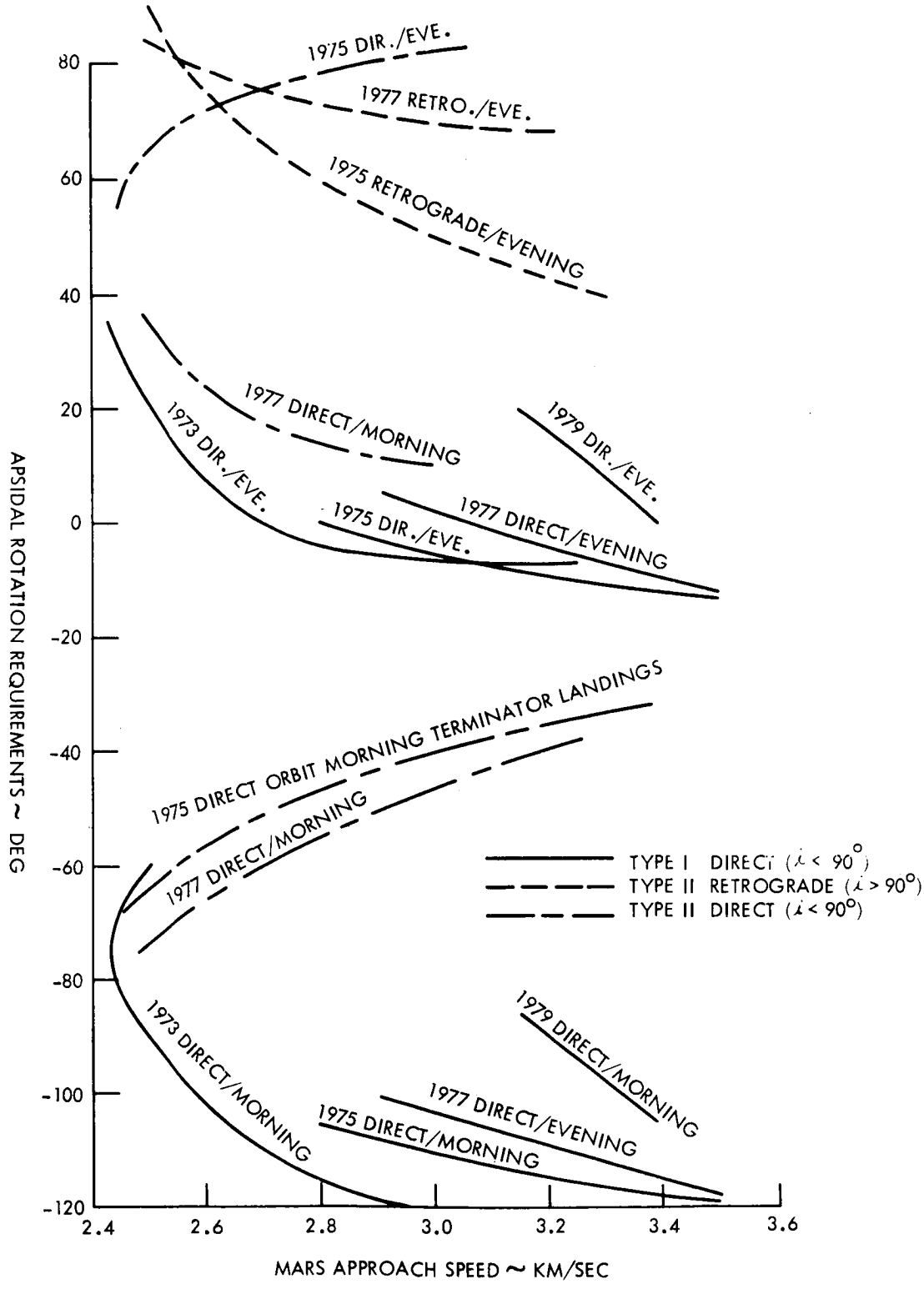

Figure 3. Mission Comparison - Apsidal Rotation Requirements

($\Delta\psi > 110$ degrees). Use of retrograde orbits for landings near the evening terminator have been similarly excluded because of poor earth occultation characteristics and high apsidal rotation requirements ($\Delta\psi > 60$ degrees). Note that apsidal rotation requirements are less than 30 degrees for all Type I trajectories with landings in the vicinity of the evening terminator.

Direct orbits with capsule landings near the morning terminator require apsidal rotation magnitudes greater than 90 degrees for Type I trajectories and greater than 40 degrees for Type II trajectories except for the 1977 direct orbit - evening terminator landing case. Retrograde orbits from Type II trajectories with subsequent landings near the evening terminator require rotations between 40 degrees and 90 degrees.

Figure 3 is based on satisfying the landing illumination and landing latitude requirements and does not include a direct capsule-earth link requirement after landing. However, preliminary analyses indicate that approximately the same apsidal rotation would be required (but in the opposite direction) to establish a capsule-earth direct link. This requirement concerns only landings near the evening terminator since morning terminator landings are automatically in view of the earth. These apsidal rotation requirements can be directly converted to velocity requirements as demonstrated in Section 5.3.

3.2 VELOCITY REQUIREMENTS

Figure 4 presents estimates of the velocity requirements (ΔV) for the various mission cases. As expected, use of Type I trajectories with direct orbits and periapsis locations near the morning terminator results in extremely large ΔV requirements for all launch opportunities except 1973. For this year, ΔV requirements are on the order of 2.1 km/sec for approach speeds of 2.45 km/sec. Type I trajectories with landings near the evening terminator require a velocity allowance of less than 2.0 km/sec. Velocity requirements for Type II trajectories are generally greater than 1.9 km/sec except for the direct orbit/evening terminator case (1977) which is comparable to similar cases for Type I trajectories.

The velocity requirements shown in Figure 4 include allowances for the arrival-time separation maneuvers, mid-course corrections, and gravity losses. The total allowance for 1973

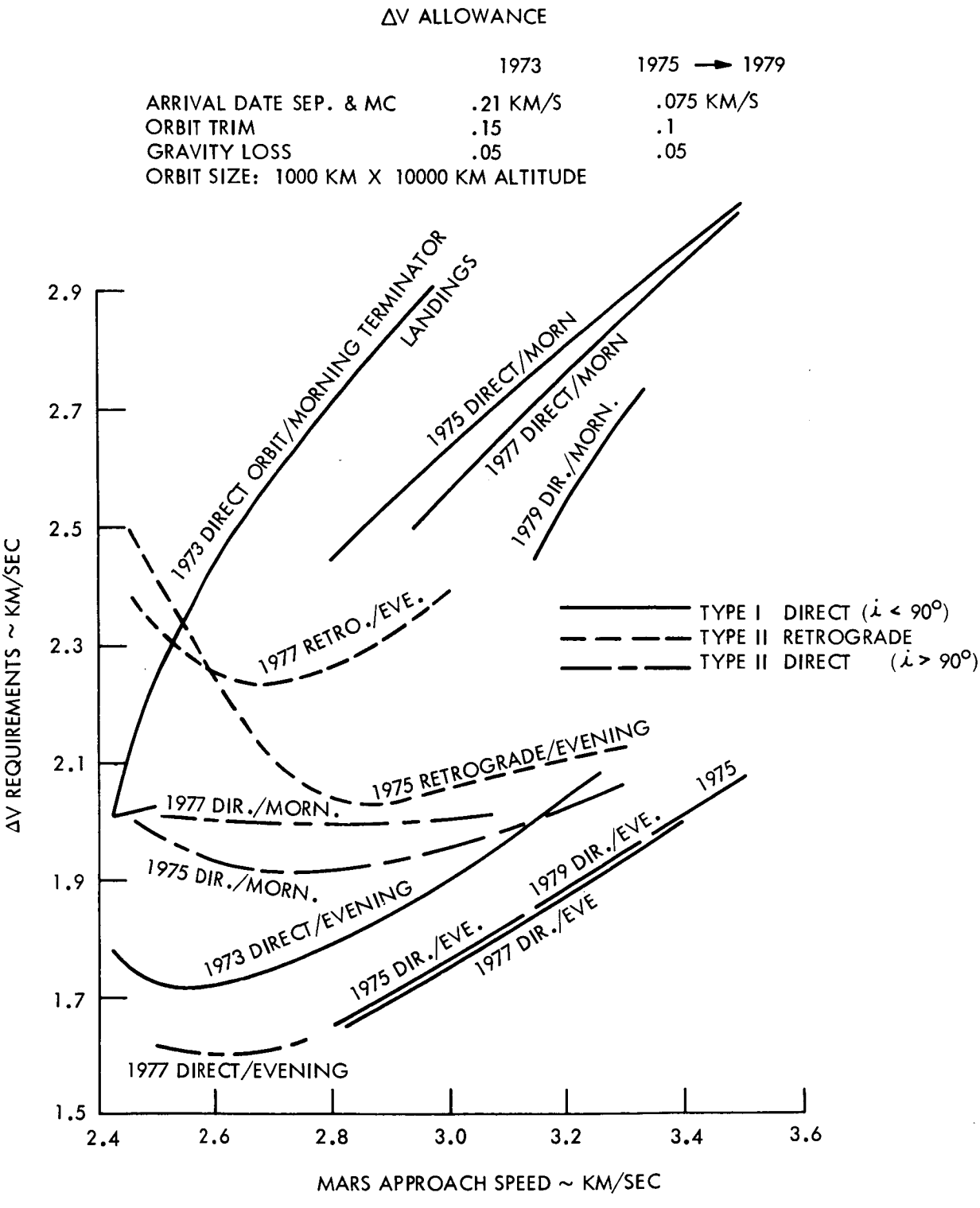

Figure 4. Mission Comparison - Velocity Requirements

is 0.41 km/sec and 0.225 km/sec for the remaining launch opportunities. Preliminary data indicate that the gravity losses for orbit insertion are approximately 0.005 km/sec which would result in a decrease of 0.045 km/sec in the above velocity allowance. The time of flight allowance is actually a variable and is dependent upon the launch and arrival dates.

3.3. LAUNCH PERIODS AND FLIGHT CHARACTERISTICS

Figure 5 presents the launch periods for the 1973 and 1979 mission opportunities. Again, constant approach velocities are utilized as the independent variable and can be interpreted as near constant arrival dates. Note that a period of 20 days can be obtained with an approach speed of 2.45 km/sec or greater for 1973 and 3.2 km/sec or greater for 1979. Figure 5 also includes scales for corresponding trip times and earth communication distances at encounter. Flight times are on the order of 200 days and 240 days respectively for 1973 and 1979 launch opportunities. Communication distances for the 1973 opportunity will range from 175×10^6 km for early February 74 arrivals (VHP=3.25 km/sec) to 270×10^6 km for early April 74 arrivals (VHP=2.45 km/sec). For the 1979 launch opportunity, the communication distance is approximately 265×10^6 km for an August 1980 encounter (VHP=3.2 km/sec).

Figure 6 presents information for Type I and II trajectories for the 1975 mission opportunity. The figure indicates that flight times for Type II trajectories are generally 100 days longer than for Type I flights.

It is expected that Type I flights for this opportunity will have an encounter date of late April, 1976 (VHP = 3.25 km/sec) thereby resulting in a communication distance of 240×10^6km. Type II flights however, even for the quickest transits, result in a communication distance of 325×10^6km for an encounter date of early July, 1976 (VHP = 2.45 km/sec).

Furthermore, communication distances for Type II trajectories are usually longer for any arrival date by 100×10^6km. Only a small gain can be seen, in terms of launch period size, between Types I and II trajectories for approach speeds greater than 2.6 km/sec. If the total pre-orbit insertion ΔV allowance is increased from 0.072 km/sec to 0.1 km/sec to allow for larger time-of-flight adjustment velocity, then the launch period for Type II trajectories can be increased by 10 to 15 days.

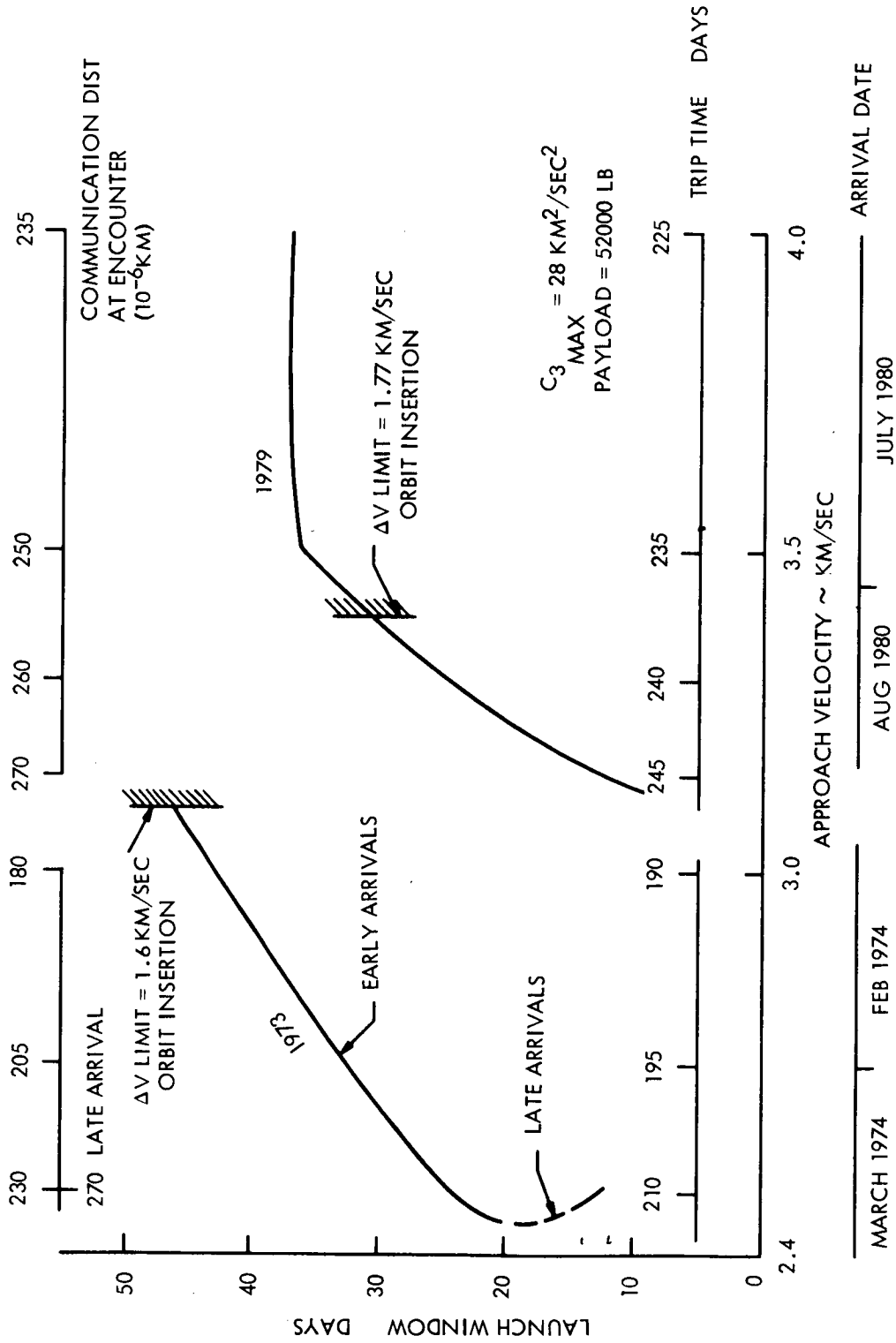

Figure 5. Launch Period Comparison - Type I Trajectories

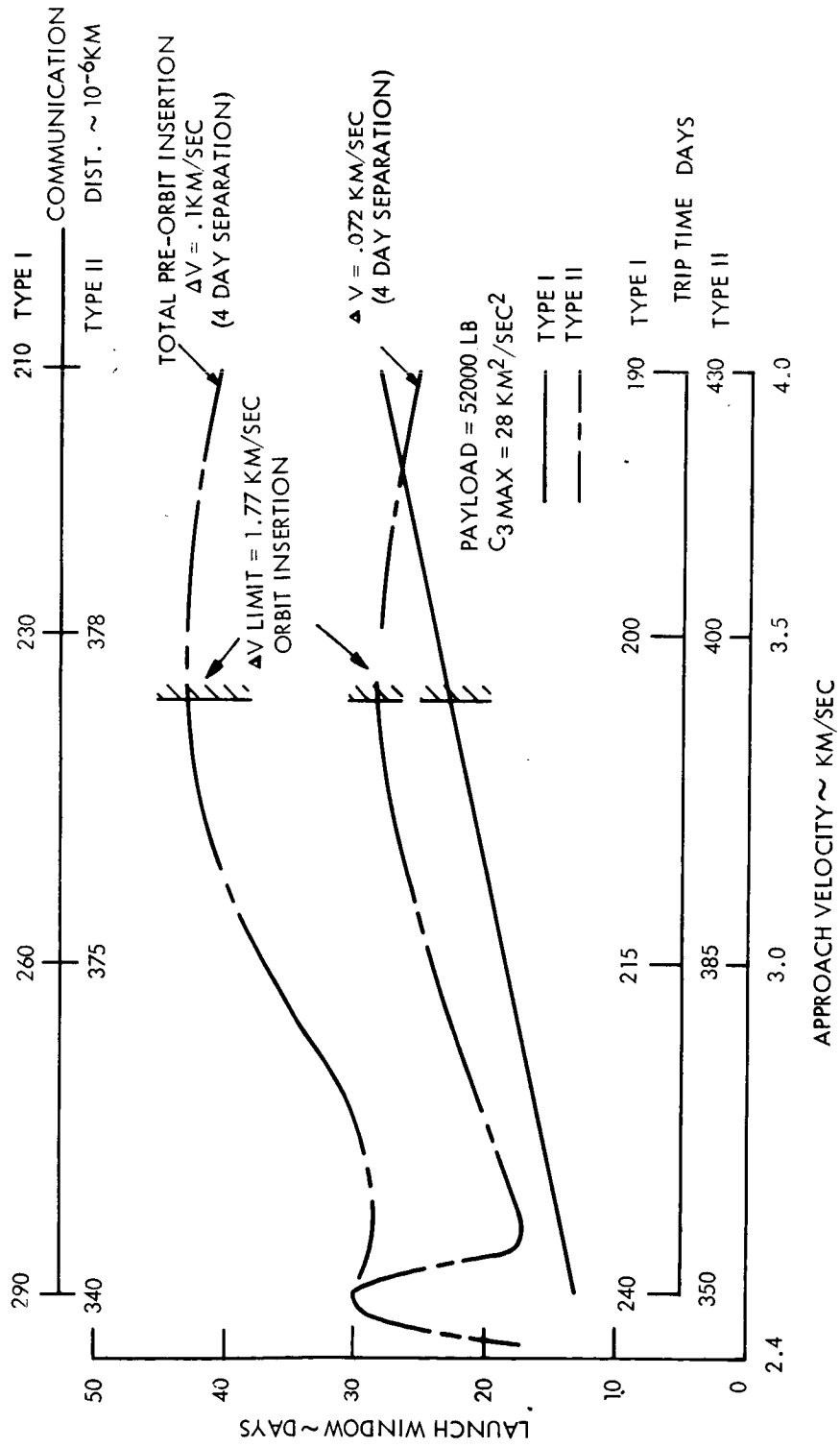

Figure 6. Launch Period Comparison of Trajectory Types - 1975 Launch Opportunity

Figure 7 similarly shows mission characteristics for the 1977 launch opportunity. It is again noted that flight times for Type II trajectories are generally over 60 days longer than for Type I flights. Communication distances for Type II trajectories are correspondingly longer by 15×10^6 to 100×10^6 km.

For Type I flights, the design trajectory arrival date is in mid June 1978 (VHP = 3.25 km/sec) with a corresponding communication distance of 270×10^6km. Type II flights with early arrival dates in mid July 1978 (VHP = 2.75 km/sec) result in a communication distance of 285×10^6km. Although communication distances are comparable, the Type II flight time is 80 days longer. These differences in flight time and communication distances become even more pronounced when Type II arrivals in mid September 1978 (VHP = 2.75km/sec) are used. For this situation, the flight time increases to 250 days and communication distance increases to 330×10^6km.

The two available launch periods for the Type II flights stem from the fact that for a given approach speed, two different arrival dates and two different ZAP* angles can be obtained. It is desirable to approach with small ZAP* Angles for the direct orbit/morning terminator and retrograde orbit/evening terminator landing conditions and with large ZAP angles for the direct orbit/evening terminator case. This latter case corresponds to "Early Arrivals" as noted in Figure 7. The choice of ZAP angle is not available for the 1975 mission because of the characteristic of the earth departure asymptote constraint ($|DLA| > 5$ degrees) which eliminates the "Earlier Arrival" case.

The data given in this section (3.3) reflect a payload limit of 52,000 lb and the orbit insertion ΔV limit of 1.6 km/sec (1973) and 1.77 km/sec (1975-1979). These values correspond closely to the updated Voyager system and are derived in Section 3.6 and Section 3.7.

3.4. CAPSULE LANDING PHASE

The capsule landing phase extends from deorbit to landing. Achievement of a capsule landing and performance of entry science experiments rank number two and three as competing mission characteristics. The prime mission requirements for this phase are noted in Section 2.1.

*ZAP Angle: The included angle between planetary approach asymptote and the Mars-Sun line.

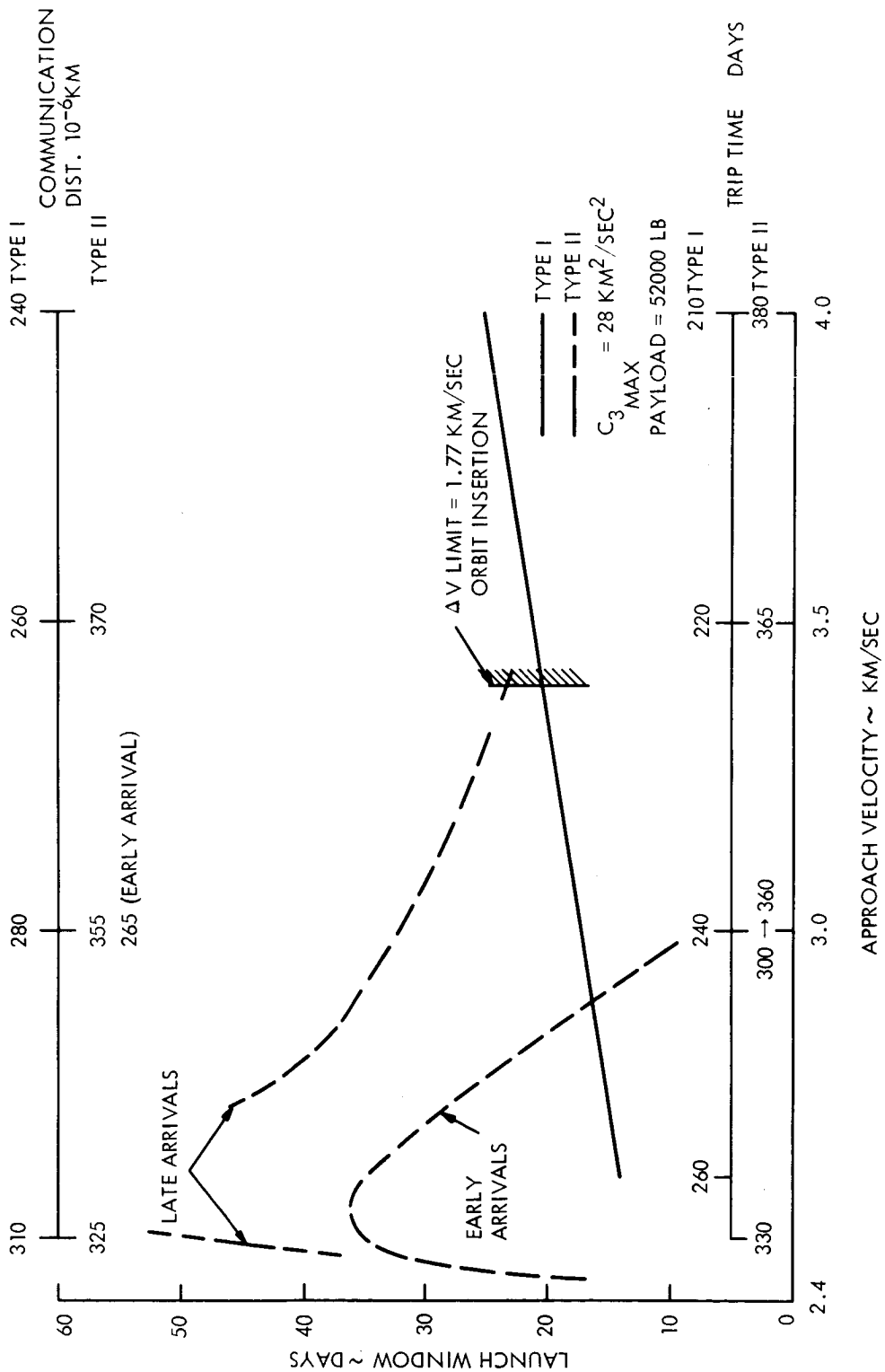

Figure 7. Launch Period Comparison of Trajectory Types - 1977 Launch Opportunity

3.4.1. Deorbit and Landing Illumination

Figure 8 presents the landing illumination angle as defined in Figure 1 for direct orbit inclinations and a March 11, 1974 arrival. The figure represents typical landings near the evening terminator and also shows the effects of delaying deorbit for 12 days and 30 days. The apsidal rotation (in this case $\Delta \psi$ of + 17 degrees) has been selected to maximize the landing potential for inclinations greater than $|30|$ degrees. For the desired range of illumination and for deorbit delays up to 12 days, two arrival windows avail themselves and extend from approximately an inclination of -18 degrees to minus 47 degrees for southerly approaches and 46 degrees to 62 degrees for northerly approaches. Note that both of these arrival inclination ranges allow 30-day deorbit delays with only moderate lighting degradation. An auxiliary scale of landing point latitude (for zero days delay) has been included in this figure and is based on a landing point located at a 17-degree range angle (343 degrees true anomaly) prior to sub-periapsis passage.

In order to meet the specified landing zone latitude band (10 degrees North to 40 degrees South) and entry lighting constraint, only arrivals from the south can be utilized for the March 1, arrival date and 17 degrees apsidal rotation. The windows presented can be slightly improved by a lesser apsidal rotation, a capsule impact point farther from periapsis, or by a combination of these two actions.

Figure 9 presents similar data for typical landings near the morning terminator; an apsidal rotation of minus 75 degrees. This condition is presented here because it remains as a possible mission condition for the 1973 opportunity and because it is very instructive for aspects of mission planning. Two important observations can be made in this figure. First, landing point latitudes are not as sensitive to orbit inclination for morning terminator landings, and secondly, the illumination angle decreases with time in the arrival lighting window. The acceptable inclination range for the case shown and for a southern injection is 30 degrees to 42 degrees and can be improved with a minor decrease in apsidal rotation to a range of 30 degrees to 47 degrees.

Although solar occultations of the orbiter are effectively reduced by landings near the morning terminator, Canopus occultation probability and duration are increased. The converse is true for evening terminator landings.

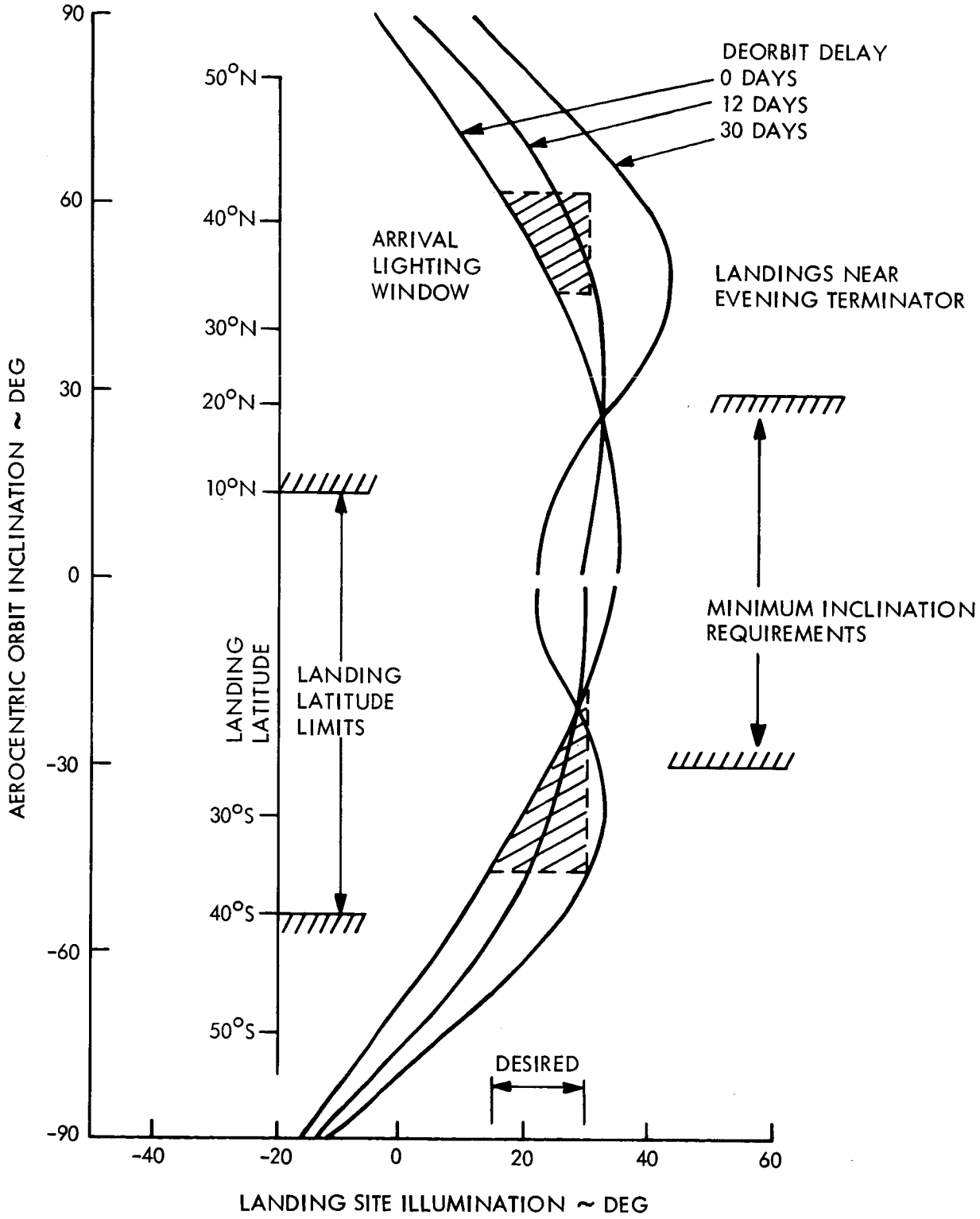

Figure 8. Landing Site Illumination - Evening Terminator Landings

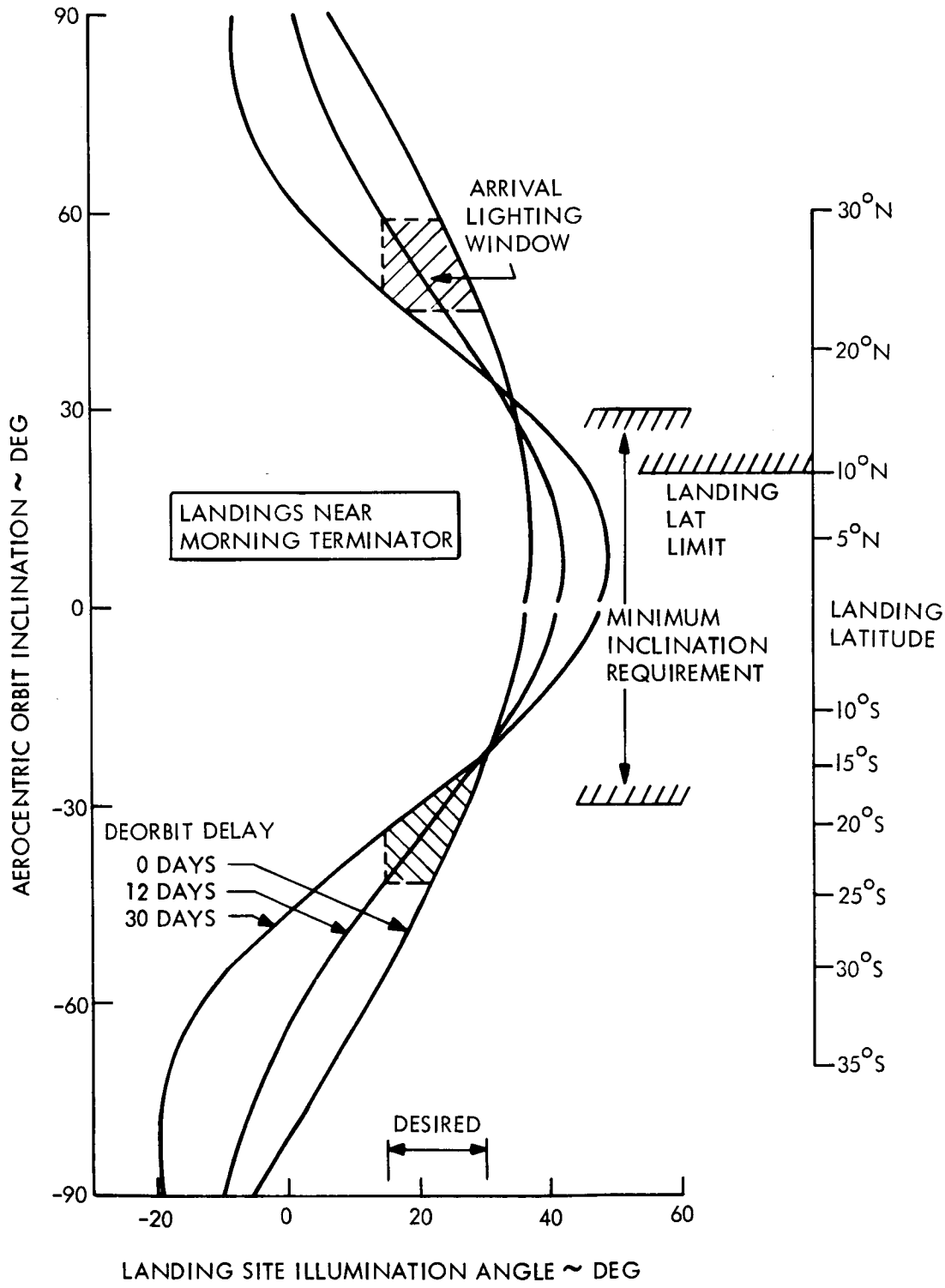

Figure 9. Landing Site Illumination - Morning Terminator Landings

3.4.2. Earth Communication Considerations

The above discussion does not consider requirements for earth communications immediately after landing. Two operational modes are implied in the previous discussion: (a) use of the orbiter as a relay link and (b) delayed capsule-earth direct link. This latter mode requires that the capsule remain dormant after landing until a direct-earth line-of-sight is established. This situation occurs frequently for evening terminator landings as the earth is usually below the horizon at the time of landing; approximately a 10-hour wait is necessary before earth comes into view again. Capsule landings near the morning terminator have long periods (6 to 8 hours) of possible direct earth communications immediately after landing.

If a direct capsule-earth link is required for a specified duration immediately after landing, then the landing latitude and illumination constraints must be mitigated for evening terminator landings. Figures 10 and 11 have been prepared to show the magnitude of apsidal rotations required to establish direct capsule-earth communication periods after landing for early and late arrivals in 1974. One hour of communication time is deducted from the data of Figures 10 and 11 to allow for a minimum earth elevation of 15 degrees. Apsidal rotations of minus 45 degrees (early arrival, Feb 1 1974) and a minus 20 degrees (late arrival, Mar 11, 1974) are required to obtain a 2-hour useful communication period. These rotation requirements are based on ensuring a 2-hour communication period for inclinations (southerly approaches) of 30 degrees and greater for the assumed capsule landing point location. Table 1 shows the corresponding velocity requirements to obtain a 1-hour and 2-hour useful direct capsule-earth communication link after landing for various arrival dates.

Table 1. Velocity Propulsion Requirements (ΔV)

Arrival Date (1974)	Earth Communication Period	
	1 hr.	2 hr.
February 1	2.205 km/sec	2.33 km/sec
February 22	1.79 km/sec	1.87 km/sec
March 11	1.69 km/sec	1.72 km/sec
April 1	1.63 km/sec	1.65 km/sec

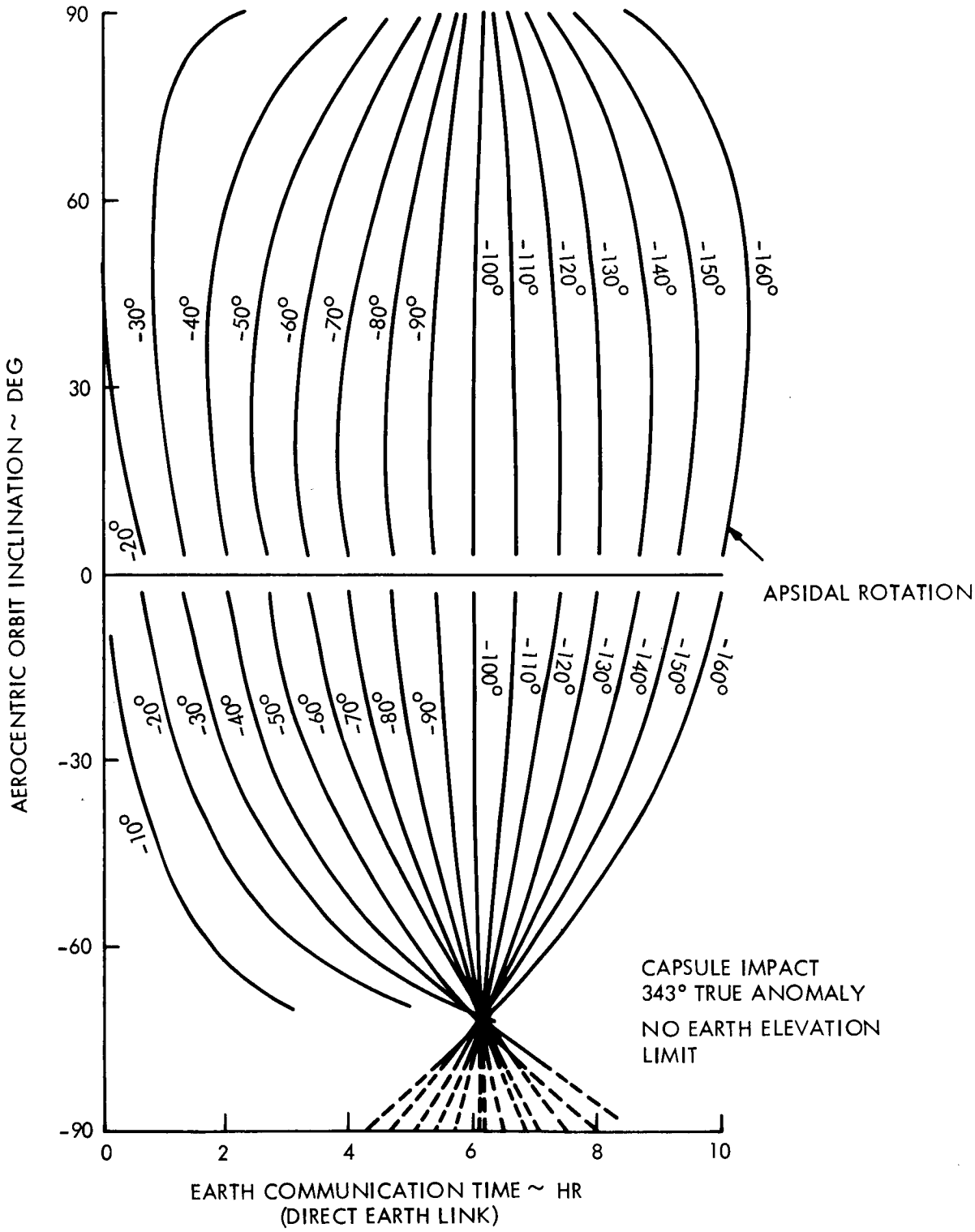

Figure 10. Capsule Post-Landing Earth Communication Time - February 1, 1974 Arrival

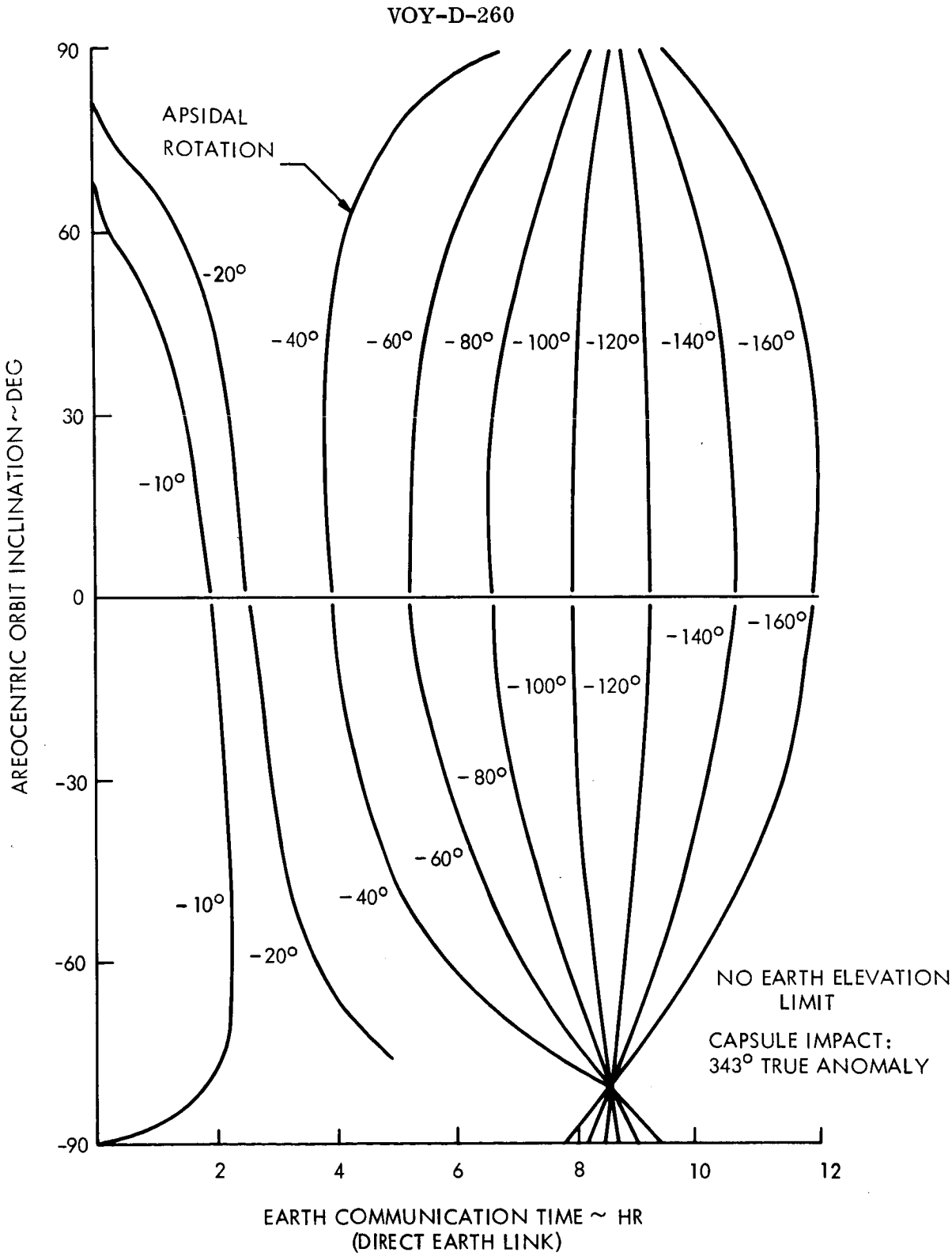

Figure 11. Capsule Post-Landing Earth Communication Time - March 11, 1974 Arrival

3.4.3. Degradation of Landing Illumination

In the event that a direct capsule-earth communication link is specified immediately after landing, the question arises as to what will be the degradation in evening terminator landing illumination. Figure 12 displays the extent of degradation for both 1-hour and 2-hour useful communication requirements. If the present landing latitude specification is observed, it can be seen that the minimum landing illumination angle (ξ) increases to approximately 40 degrees or 45 degrees for the 1-hour communication requirement. For the 2-hour communication requirement, the resulting illumination angle will be between 45 degrees and 50 degrees. These increases represent an increment of 10 degrees to 20 degrees over the maximum desired value of 30 degrees. Also noted in Figure 12 is the allowable inclination range for a relieved landing latitude constraint of 50 degrees south. It is doubtful that the increased inclination range (-30 degrees to -50 degrees) can be gainfully used since avoidance of Canopus occultations requires the use of low inclinations. The figure reveals also that illumination differences are minimized if later arrivals (March 74) are planned requiring relatively low planetary approach speeds.

3.5. ORBITAL PHASE

The orbital phase begins at the time of orbit insertion and extends for the duration of the mission. During this time, the orbiter is performing scientific data collection and mapping tasks. The major mission constraints for this phase concern maintaining the sub-periapsis point in daylight and within a designated latitude band of 60 degrees south to 40 degrees north. In addition, the minimum orbit inclination should be $|30|$ degrees, and solar occultations and loss of Canopus lock should be avoided for the first 30 days. Recently, there has been some indication from MSFC that up to 1.5 hours loss-of-Canopus lock will be acceptable for the first 30 days.

3.5.1. Sub-periapsis Illumination

Figure 13 presents the variation of the sub-periapsis illumination angle δ (defined in Figure 1) with elapsed time after orbit insertion for a 1,000 x 10,000 km altitude orbit. The data in this figure correspond to capsule landing points (initial periapsis locations) near the evening terminator and the morning terminator for an arrival date of March 11, 1974. It appears that lighting conditions are suitable in either case for determining a landing site selection although evening terminator landings initially exhibit higher contrast conditions. If color TV experiments are to be conducted, landings near the evening terminator appear more attractive since

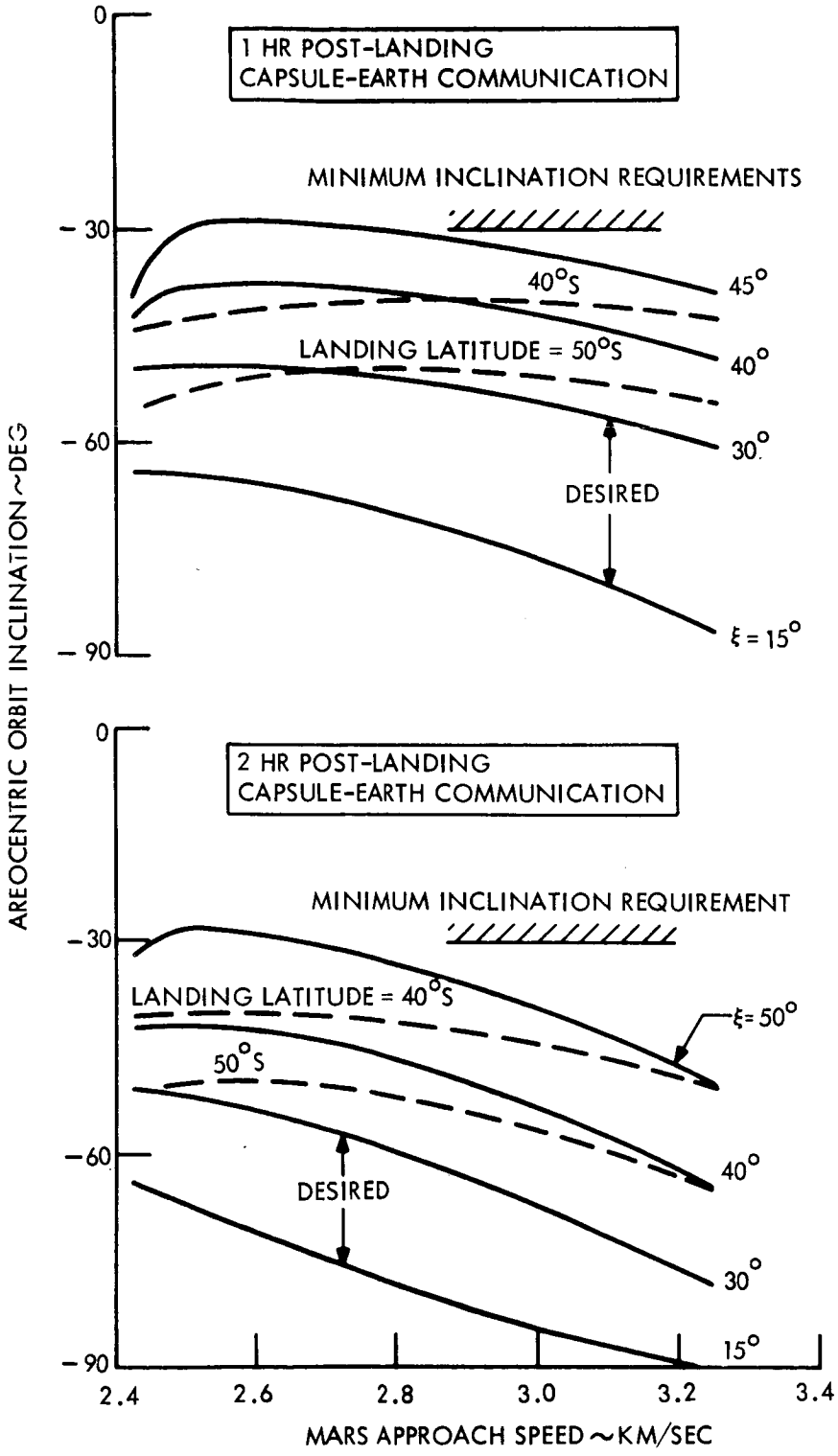

Figure 12. Degradation of Landing Illumination - Evening Terminator Landings

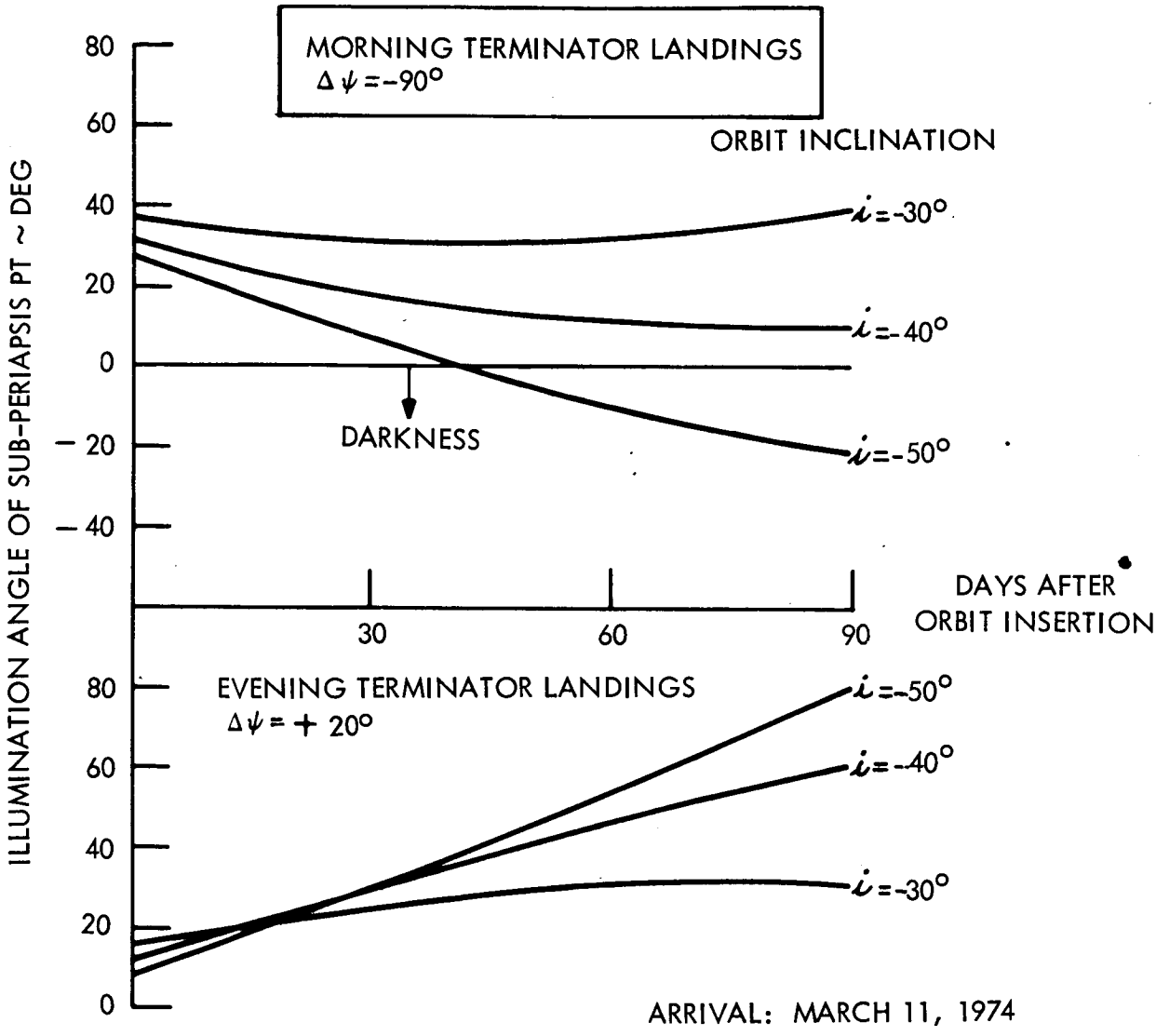

Figure 13. Sup-Periapsis Point Illumination - 1 x 10 Orbit

illumination angles increase with time. It is also noted that inclinations must be restricted for landings near the morning terminator because of the sub-periapsis point drifting into darkness.

The effect on the lighting conditions by changing the orbit size to a 1,000 x 20,000 km altitude orbit is shown in Figure 14. It can be seen that the sub-periapsis point encounters darkness sooner for morning terminator landings and that the maximum inclination restriction is decreased further.

3.5.2. Periapsis Movement

The highest resolution mapping pictures are obtained in the vicinity of periapsis passage. Thus, it is desirable to have the sub-periapsis point cover a wide latitude band (preferably between 60 degrees south and 40 degrees north) during the course of the mission. Figure 15 demonstrates the extent of the periapsis movement for the first three months after orbit insertion (March 11, 1974) and for capsule landings in the region of the evening and morning terminators. The evening terminator case results in a latitude movement of approximately twice that of the morning terminator landing case for a 1,000 x 10,000 km altitude orbit. Increasing the apoapsis latitude to 20,000 km reduces the over-all movement of periapsis as shown in Figure 16 but does not reduce the relative merit of evening terminator landings. Variation in arrival date do not appreciably change the trends noted in the above figures.

3.6. PAYLOAD CAPABILITY

The second referenced applicable document provided the payload capability of the Saturn V launch vehicle. This payload data has been correlated with launch periods during the various mission opportunities and the results are given in Figure 17 for Type 1 trajectories. The payload shown in this figure represents the net injected weight capability. The injected weight values include two planetary vehicles plus adapters for structural attachment between planetary vehicles and shroud. No program weight contingency has been assumed in the payload shown. From Figure 17 it can be seen that the 1975 and 1977 launch opportunities are the most limiting in terms of payload, and that significant increases in payload can be obtained by slightly decreasing the launch period. It is seen that the maximum allowable injection weight of two planetary vehicles is 52,000 pounds. Using Type I trajectories, a program contingency weight of 2,500 pounds per planetary vehicle results in a maximum planetary vehicle weight of 23,500 pounds.

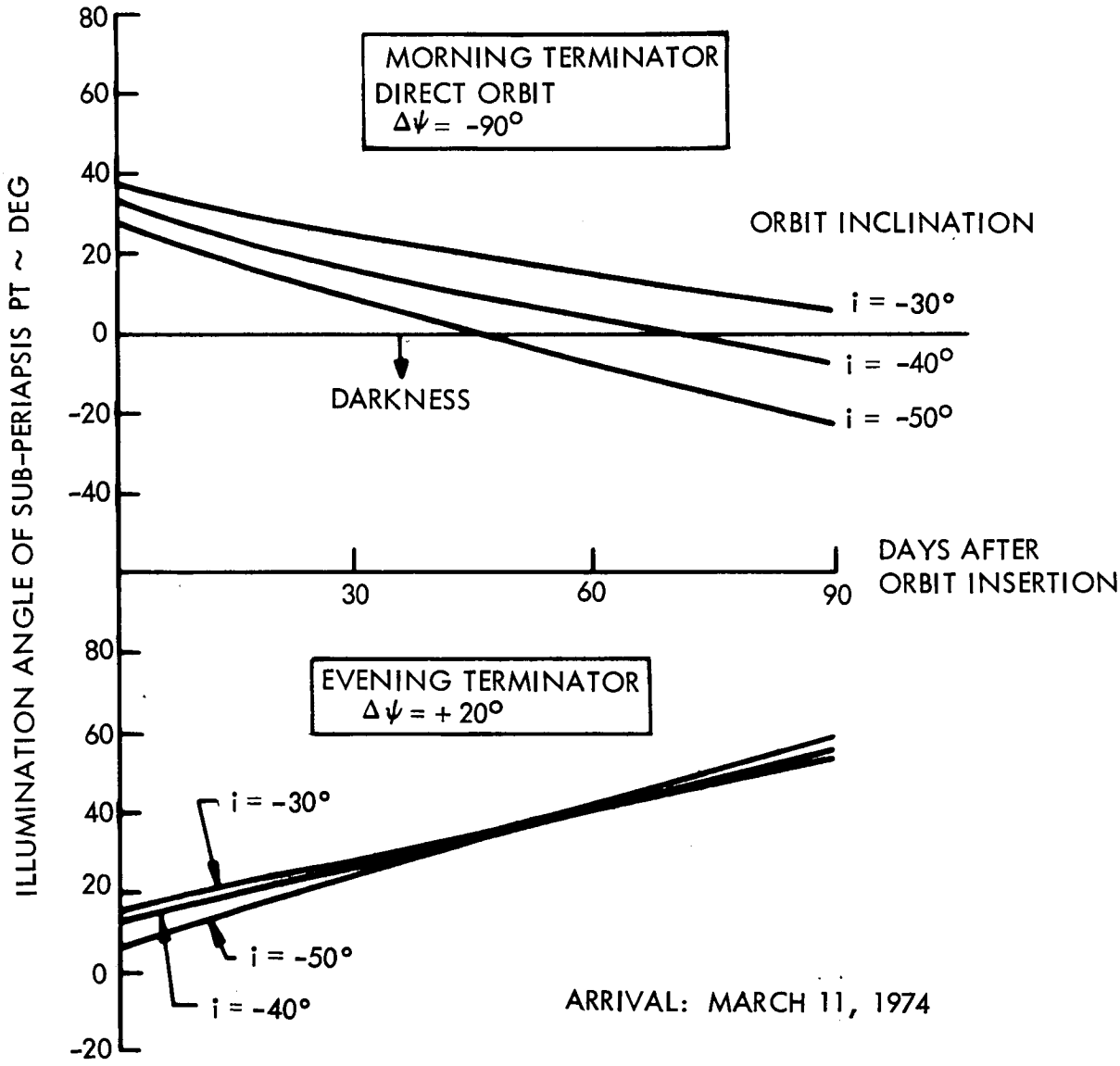

Figure 14. Sub-Periapsis Point Illumination - 1 x 20 Orbit

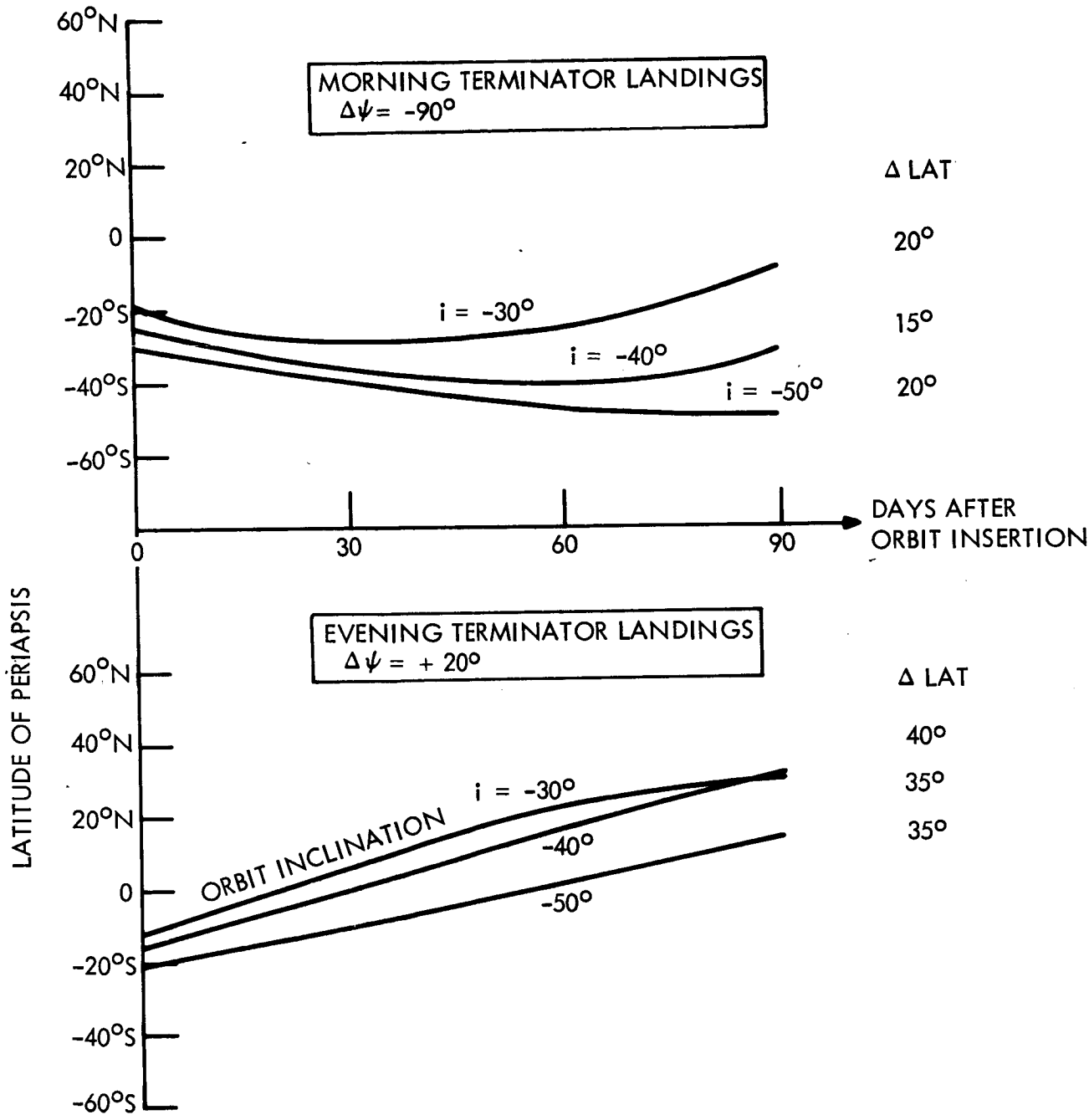

Figure 15. Latitude Movement of Periapsis - 1 x 10 Orbit

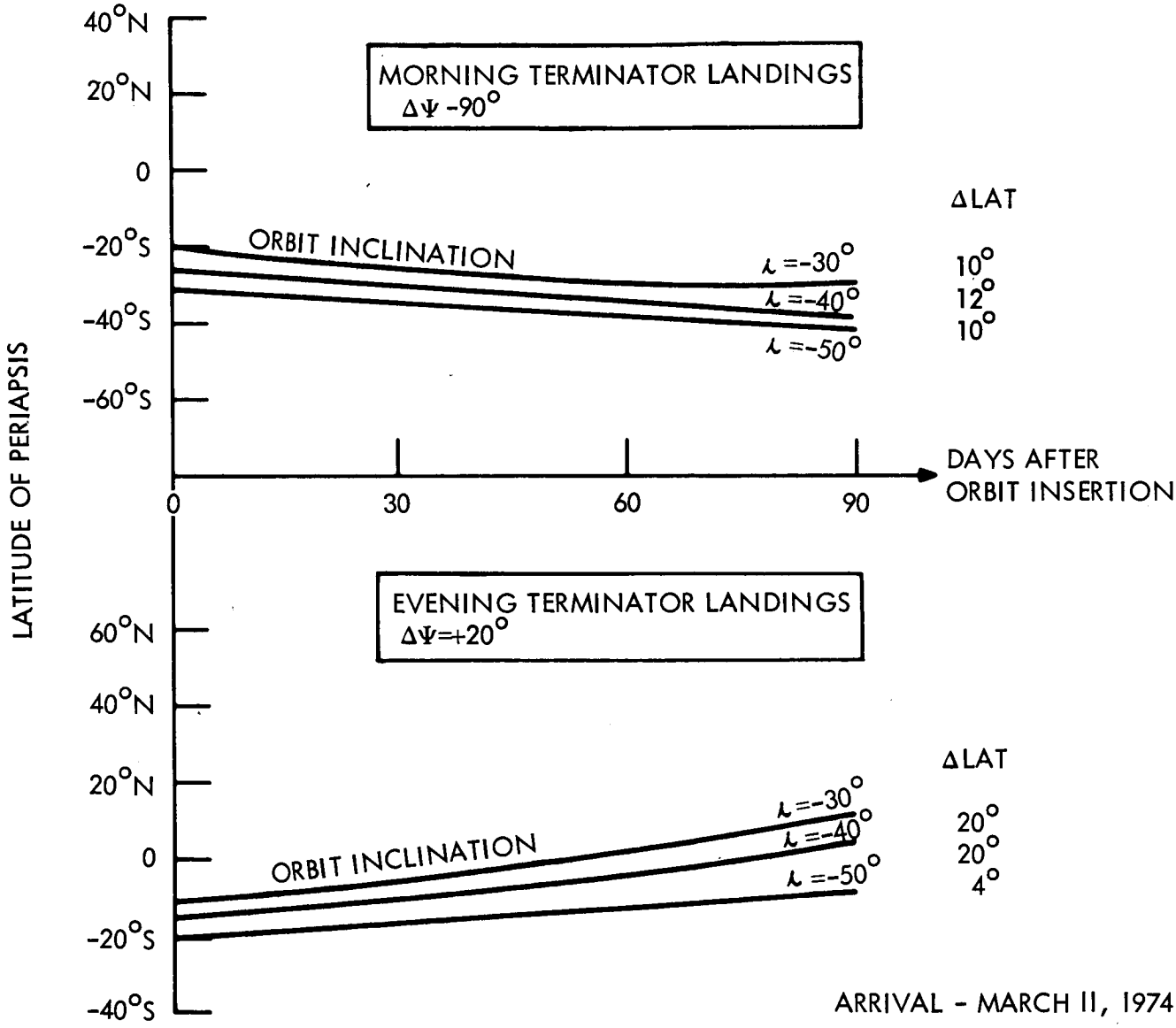

Figure 16. Latitude Movement of Periapsis - 1 x 10 Orbit

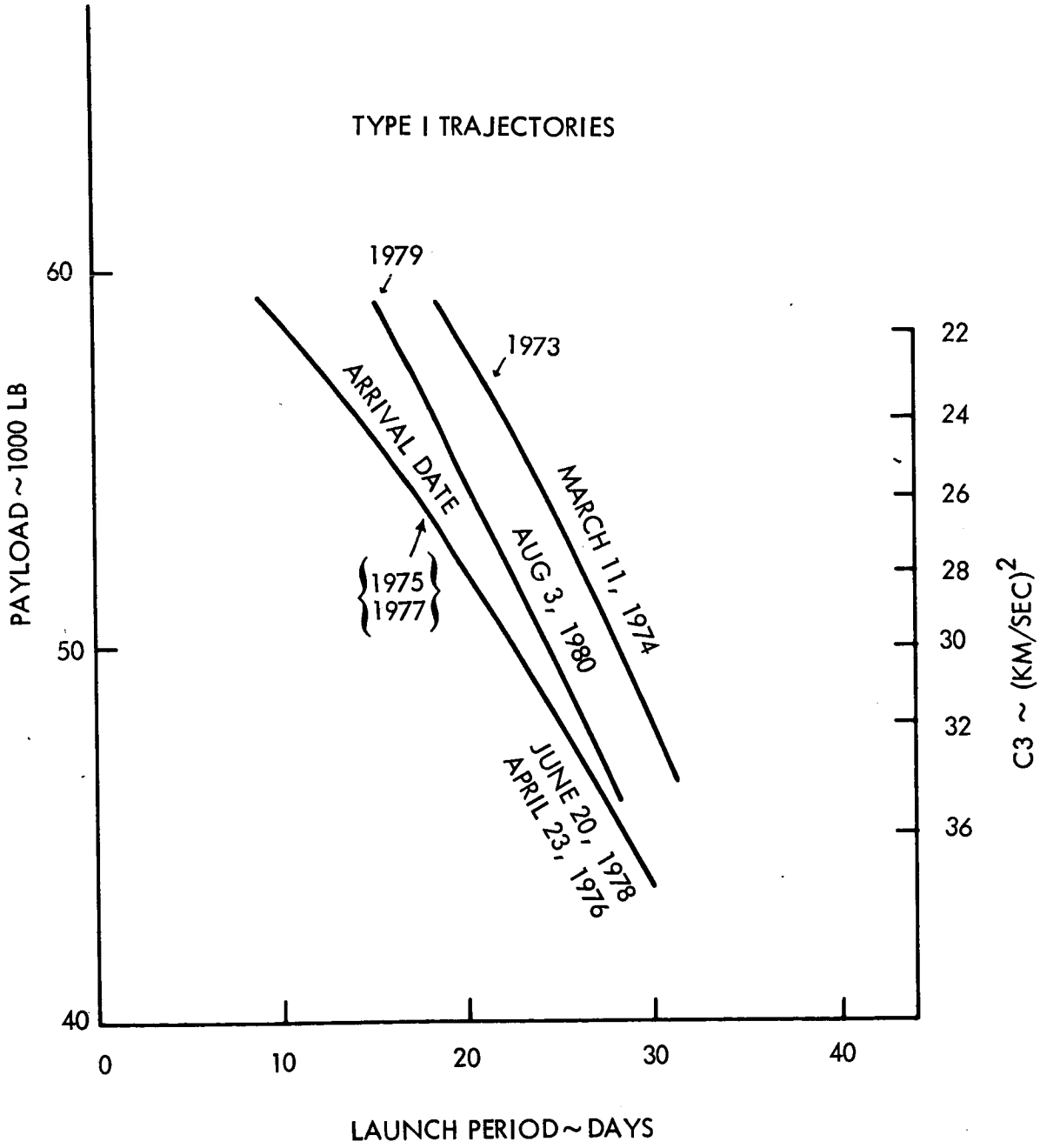

Figure 17. Mission Performance - Net Allowable Injected Weight

The sensitivity of useful weight (burn-out weight) to velocity requirements is also important. For example, with a 2.0 km/sec velocity capability and an I_{sp} of 300 seconds, 50 percent of the injected planetary vehicle weight is propellant. If the propulsion capability is increased by 0.1 km/sec, a loss in useful payload of over 350 pounds can be expected for an assumed injected weight of 25,000 pounds.

3.7. SUMMARY

Having reviewed some of the mission considerations and having performed over-all mission comparisons, some observations can be made at this time.

a. With the widening of the launch azimuth corridor ($45 < \text{azimuth} < 115°$), Type I trajectories (1975 and 1977) become acceptable in terms of both payload capability and launch period. These trajectories are even more desirable from the standpoint of communication distance, flight time and trajectory sensitivity. Therefore, Type I trajectories for all mission opportunities (1973 to 1979) can be employed.

b. Retrograde orbits are eliminated from consideration because of their greater velocity requirements and poorer solar and earth occultation characteristics. Thus, only direct orbits need be considered in meeting mission goals.

c. Selection of landing zones and, hence, location of the orbit periapsis near the evening terminator is the most promising from the standpoint of propulsion requirements. In fact, periapsis locations near the morning terminator are extremely expensive for all considered Type I launch opportunities except for the 1973 opportunity; it is possible to land near the morning terminator for this opportunity with practical ΔV requirements.

d. Illumination requirements can be fulfilled for landings near both the evening or morning terminators.

e. Direct earth-communication links can most readily be established by the capsule with landings near the morning terminator.

f. Up to two hours of communication after landing can be realized with only a moderate degradation of illumination angle for evening terminator landings.

g. Velocity requirements for evening terminator landings with immediate capsule-earth direct communication requirements are practical.

h. Approaches from the north are eliminated because the landing latitude constraint is violated.

i. In light of useful vehicle weight sensitivity to ΔV, minimum propulsion requirements are highly desirable. It appears that a ΔV requirement of 1.95 km/sec is adequate for achievement of Mars mission goals.

Table 2 has been prepared to allow a quick qualitative assessment of the various mission considerations and is based on the observations noted above. The following Voyager flight specifications have been selected:

a. Type I trajectories for all launch opportunities

b. Landings and periapsis locations near the evening terminator for all operational modes.

c. Direct planetary orbits - southerly approach.

The velocity requirement (ΔV) associated with this selection is 1.95 km/sec and allowing for the arrival date separation and orbit trim maneuvers, results in an orbit insertion ΔV allowance of approximately 1.6 km/sec (1973) and 1.77 km/sec (1975 to 1979).

Some important trade-off areas that remain include more detail analyses of 1975, 1977 and 1979 flights for both Type I and II trajectories. These areas include comparisons of arrival windows, communications distances, flight times, implication of establishing direct capsule-earth communication links and behavior of illumination and landing conditions with orbit inclination. It is also desirable to ascertain the effect of relieving various mission constraints for the 73 to 79 opportunities for improvement of mission and spacecraft capability.

4. DESIGN TRAJECTORY AND ORBIT SELECTION

In the selection of design trajectories and orbits for this study, it is realized that priorities of mission specifications and operational modes may change. With this in mind, certain selections are made based on the available information and data that have been assembled to date.

4.1. TRAJECTORY SELECTION

The selection of design trajectories is graphically shown in Figure 18. This figure presents the allowable orbit inclination as determined by solar occultation, and capsule landing illumination and landing latitude constraints. Although not shown in the figure, loss-of-Canopus lock cannot be avoided for inclinations greater than 30 degrees. Table 3 gives the duration of loss-of-lock for different arrival dates and inclination, and is based on the lighted limb of the planet falling within a rectangular sensor field of view of 40 degrees by 60 degrees. Figure 18 shows a design selection point in mid-March having an orbit inclination of minus 40 degrees. Although it is very possible to select a design point for an orbit inclination of minus 30 degrees in early April and thereby reduce or eliminate loss-of-Canopus lock, the selection is a

Table 2. Trajectory Selection

Mission Requirement	Operational Modes: 1. Orbiter Relay 2. Capsule direct direct delayed transmission		3. Capsule direct link immediate transmission		Trajectory Type: I		II	
	Morn. Term.	Eve. Term.	Morn. Term.	Eve. Term.	Dir	Retro	Dir	Retro
1. No solar occultations (first 30 days)	✓	✓	✓	✓				
2. Satisfactory periapsis illumination for landing site selection	X	✓	X	✓				
3. Periapsis movement for photographic coverage	X	✓	X	✓				
4. Minimal canopus occultations	X	✓	X	✓				
5. Landing site illumination (30° > and > 15°	✓	✓	✓	X				
6. Early earth occultation	X	✓	X	✓				
7. Minimal propulsion requirement	X	✓	X	✓	✓	X	✓	X
8. Minimal flight time					✓	✓	X	X
9. Short communication distance					✓	✓	X	X
10. Earth communication at insertion and deorbit					✓	X	✓	X

Selection:
(1) Type I trajectories
(2) Evening terminator
(3) Direct planetary orbits

✓ satisfied
X not satisfied (less than desirable)

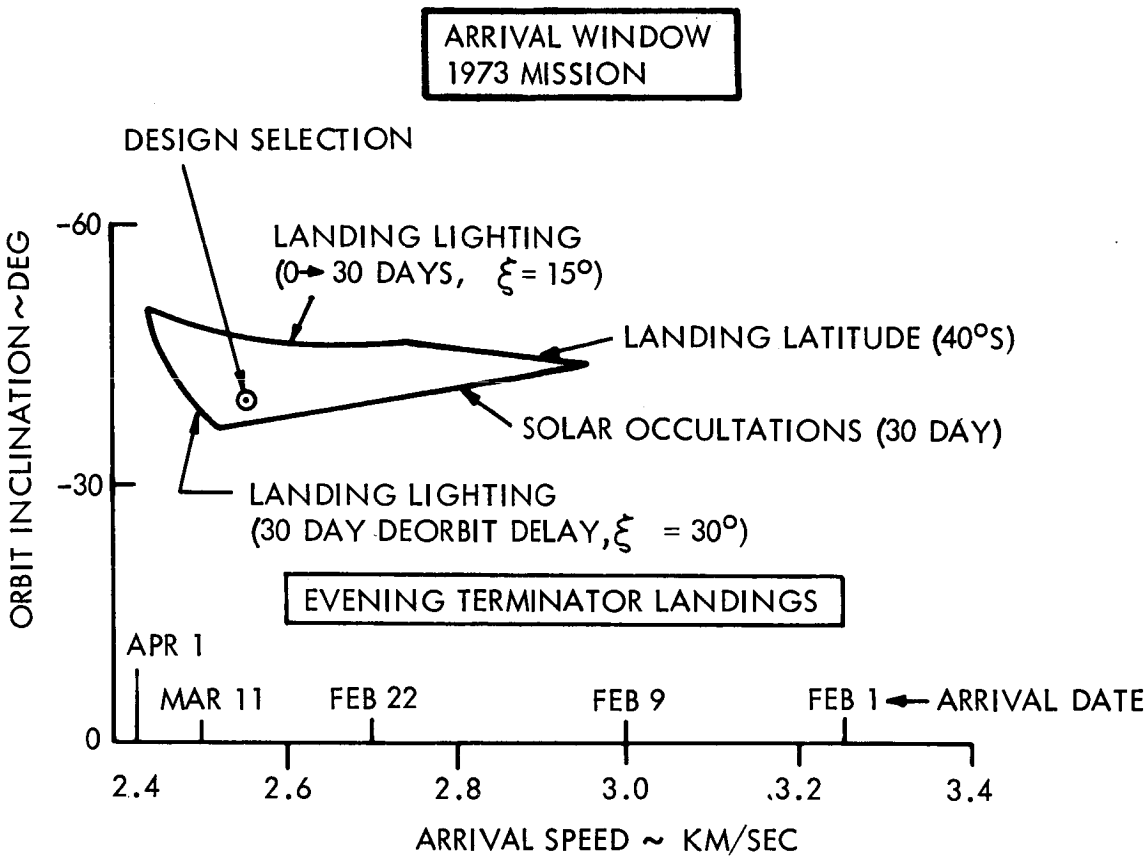

DESIGN TRAJECTORIES

YEAR	LAUNCH	ARRIVAL	FLT. TIME	VHP	ORBIT INCLINATION
1973	AUG. 10	MAR. 15	217 DAYS	2.52 KM/SEC	40°
	AUG. 10	MAR. 7	209	2.55	40°
	AUG. 19	MAR. 9	202	2.49	40°
	AUG. 19	MAR. 1	194	2.59	40°
	SEPT. 4	MAR. 9	196	2.50	40°
	SEPT. 4	MAR. 11	188	2.56	40°
1975	SEPT. 30	APR. 23	206	3.30	45°
1977	NOV. 5	JUN. 30	227	3.35	45°
1979	DEC. 9	AUG. 3	240	3.30	45°

Figure 18. Design Trajectory Selection

compromise between increased communication distance, photographic coverage and loss-of-Canopus lock. For this reason, and because a certain duration of loss-of-lock might be tolerated, the six design trajectories were selected in the March arrival date area. It is important to note that if direct capsule-earth links are required after landing, the favored arrival time span is again located in the mid-March to early April region.

The table in Figure 18 lists the six selected design trajectories together with three provisionally selected design trajectories for the launch years of 1975, 1977 and 1979.

Table 3. Loss-of-Canopus Lock Duration

Arrival Date	Apsidal Rotation	Inclination	Duration
Feb. 1, 1974	-7°	30° 40°	7 min. 73 min.
Feb. 23, 1974	0°	30° 40°	17.5 min. 65 min.
March 11, 1974	+20°	30° 40°	14 min. 54 min.
April 1, 1974	+35°	30° 40°	1.5 min. 31 min.

4.2. PLANETARY ORBIT SIZE SELECTION

The effects of quarantine constraints and science and engineering requirements must be considered in the selection process that determines the aerocentric orbit size, i.e. periapsis and apoapsis altitudes. The following discussion highlights the major factors and arguments involved in the selection process and although based on limited data, a preliminary recommendation of an orbit size is advanced at this time.

The probability of contaminating the planet is a function of many variables; one of the more sensitive parameters being the periapsis altitude of the spacecraft orbit. The spacecraft orbit determines the decay time for particles ejected from the spacecraft which is more limiting on orbit selection than spacecraft orbit decay.

During the quarantine study performed under Task C, the probability of ejecta contamination was determined for two orbit sizes; a 500 km x 10,000 km altitude orbit and a 1,000 km x 10,000 km altitude orbit. The study assumed "clean" manufacturing, the best estimate of the Martian atmosphere, an 11 year quarantine time period, and some decontamination or filtering of the ejected attitude control gas.

Figure 19 presents the probability of ejecta contamination. The solid line is the projected probability, P (c/h), of ejecta contaminating the planet given the orbit periapsis altitude.

Present estimated guidance errors result in a maximum periapsis error (3σ) of 300 kilometers. If this error is assumed to be normally distributed about the desired periapsis altitude and using the above assumptions, the expected probability of ejecta contamination is given by the following equation:

$$\overline{P\ (c)} = \int_0^\infty P\ (c/h)\ p\ (h)\ dh$$

where h is the periapsis altitude of the orbit,
p (h) is the normal distributed altitude due to guidance errors, and
P (c/h) is the probability of contamination given the orbit altitude

The dashed line in Figure 10 represents $\overline{P\ (c)}$, the expected probability of contamination.

The horizontal line noted (at the top of the figure) in Figure 19 is the allocation of probability of contamination assigned to all ejecta sources. However, a margin of safety should be adopted that provides for uncertainties in the quarantine analysis including the ability to determine all ejecta sources. It is felt strongly that a minimum safety margin be at least one order of magnitude less than the allocation for all ejecta. This margin is noted in Figure 19 and it can be seen that the minimum periapsis altitude that can be established from the quarantine and guidance viewpoint alone is approximately 800 km.

The orbital parameters that affect science returns are: a) periapsis altitude, b) orbital period, c) argument of periapsis (or latitude of periapsis), d) inclination and e) ascending node relative to the terminator. The argument of periapsis, inclination and position of the ascending node are preselected to satisfy the landing latitude and lighting constraints, and the orbital illumination constraints (including occultations) as noted in Section 3. Periapsis altitude and orbital period, or equivalent orbit size, are the remaining orbit parameters that affect scientific returns. An assessment of the on-board science experiments, with regard to resolution and coverage, revealed that the one most important criterion for best return in value of scientific data is expressed in terms of linear resolution-minimum separation between two objects before they become completely distinguishable. The improvement in resolution increases inversely with decrease in altitude.

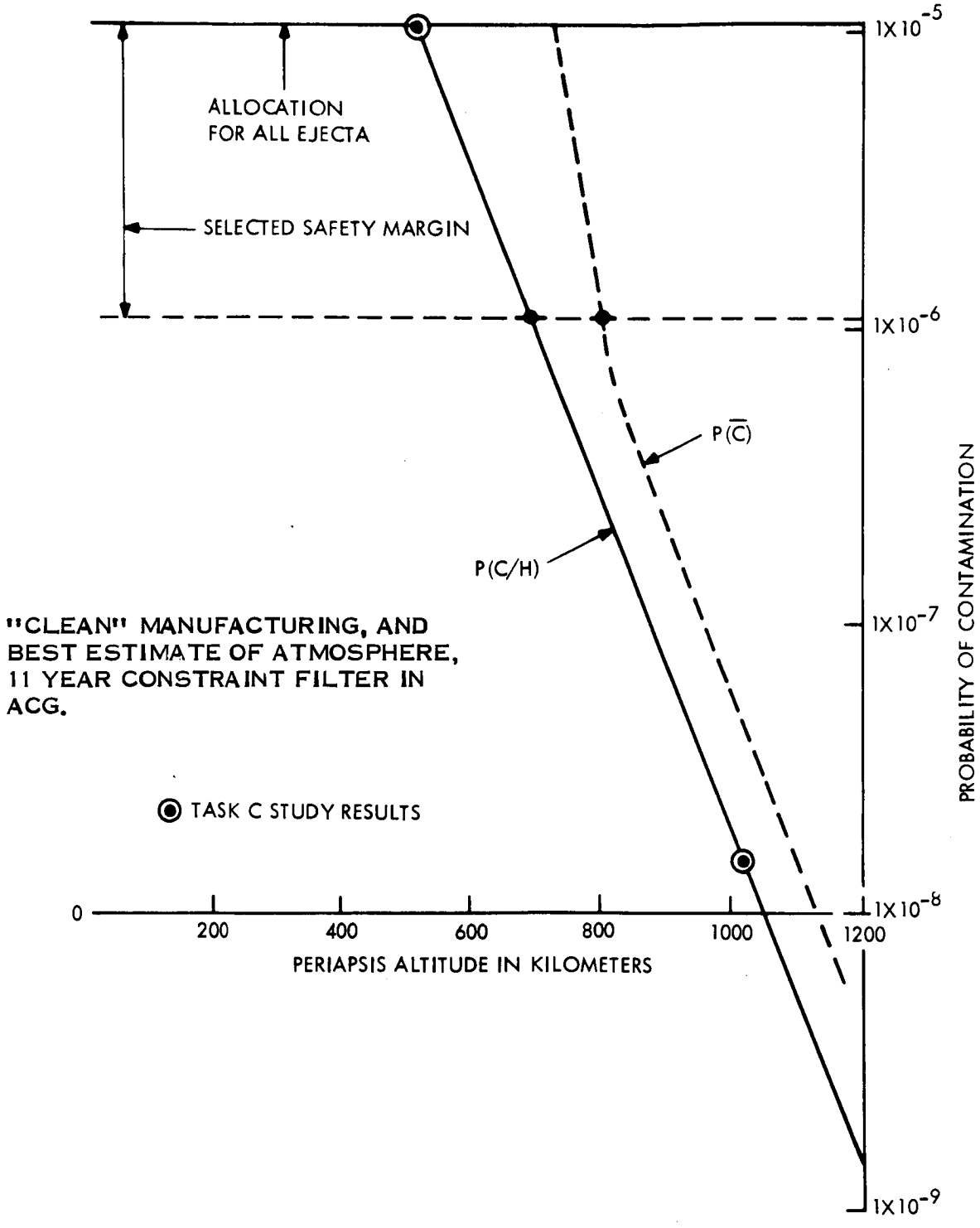

Figure 19. Probability of Contamination Vs Orbit Altitude

Operational considerations that affect orbit size selection include sun, earth, and Canopus occultations. Solar occultations influence battery weight and solar array size and their effects early in the orbital mission can be minimized by establishing highly inclined orbits having high periapsis altitudes. Canopus occulations influence attitude control system design. Canopus occultation effects can be minimized by selecting low inclined orbits that also have high periapsis altitudes. Both sun and Canopus occultations can have an adverse effect on mission success with sun occultations also affecting the weight available for science data return. Earth occultations together with orbit size influence data storage requirements. Studies have shown that for the 1973 mission design trajectories, the periapsis altitude must be greater than 980 km in order to avoid solar occultations early in the mission with a 99.9 percent certainty.

Mapping requirements for landing site selection and surface coverage presently favor sub-synchronous orbits with nearly repeating ground tracks. However, the apoapsis altitude must be selected between 10,000 km and 20,000 km as specified in the previous list of mission constraints. Thus, there are many sub-synchronous orbital periods that are compatible with mission specifications and that result in nearly repeating ground tracks; orbits having periods between 8 hrs and 12 hrs cover the useful range of selection. Although orbits with higher apoapsis altitudes may more readily avoid solar and Canopus occultations, they initially result in a lesser surface coverage and surveillance of fewer landing zones.

In arriving at an orbit period selection, the rate of coverage accumulation, number of landing zones that can be reconnoitered, time interval before coverage overlap occurs, and velocity impulse required to establish the orbit must also be considered. For example, coverage overlap can be realized after one day for 8.15 hour and 12.224 hour orbital periods, but the 8.15 hour orbital period allows reconnoitering of three potential landing zones as compared to two landing zones for an orbit with a period of 12.224 hours. If orbital periods of 9.82 hours and 9.22 hours are selected, the former allows the reconnoitering of five landing zones and the latter nine landing zones. However, a time lapse of two days and three days respectively is needed before overlapping coverage can be obtained. Thus, emphasis has been placed at this time on orbits having periods of 8.15 and 12.224 hours.

The percent of increased coverage between the 8.15 -hour orbit 12.224-hour orbit can be determined from Figure 20. The figure represents the accumulation of continuous daylight coverage (illumination region of 40 degrees to 85 degrees from the sub-solar point) whenever the orbiter is below 2,000 km and with 25 percent overlapping ground coverage. A sensor field-of-view cone angle of 10 degrees is also assumed. For up to two months of flight, the 8.15 hour orbit coverage is 50 percent more than that of the 12.224 hour orbit. It is not expected that orbit period uncertainties will significantly change this coverage since the uncertainty in orbital period as shown in section 5.4 can be controlled to 21 seconds (3 σ) by an orbit trim maneuver.

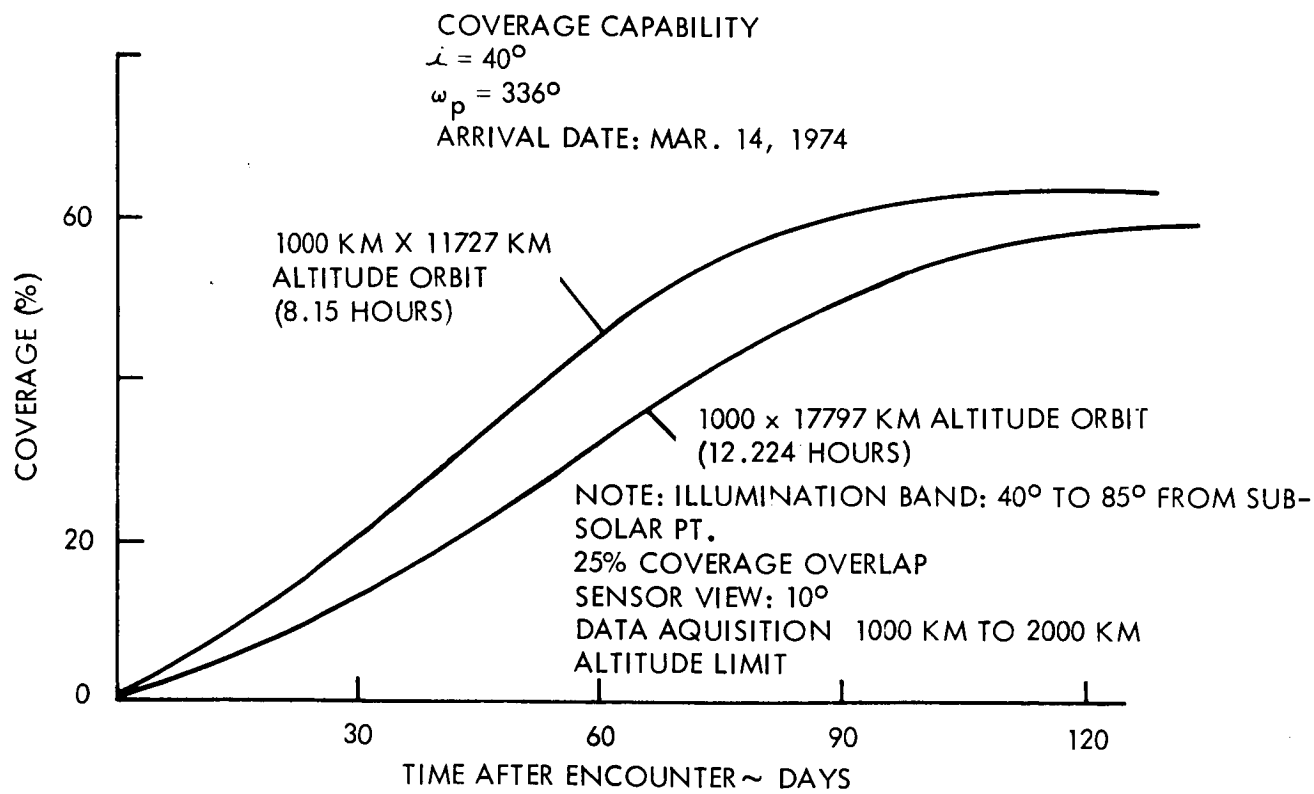

Figure 20. Surface Coverage

A summary of orbit selection consideration is given in Table 4. An orbit with a 8.15 hour orbital period is tentatively selected because it provides a higher rate of coverage and allows an appraisal of three landing zones as well as fulfilling all other requirements. The resulting orbit size has a periapsis altitude of 1,000 km and an apoapsis altitude of 11,727 km. If future analyses prove the desirability of larger orbit periods, they can be accommodated easily without increasing velocity requirements or modifying the vehicle design.

Table 4. Orbit Selection Consideration

	Periapsis Alt.	Apoapsis Alt.
1. Quarantine Constraint with insertion inaccuracies	>830 km	High
2. Science: Surfacing Mapping & Landing site selection	Subsynchronous with low Periapsis	
3. Engineering:		
a) Solar & Earth occultations with insertion inaccuracies	>980 km	High
b) Capsule Deorbit to impact communication	<1000 km	<20,000 km

It is mentioned here that the inclination constraint between the orbit and terminator planes (constraint 8, section 2.1) is satisfied at all times and in fact the inclination between the orbit plane and terminator plane is always greater than 30 degrees (mission spec.) for over 180 days of mission time. However one constraint that is completely incompatible with the arrival date for all years is the inclination requirement ($<30^\circ$) between the orbital plane and ecliptic plane (Constraint 7). After orbit insertion the angle between the two planes is approximately 60 degrees and does not decrease to less than 45 degrees (mission spec.) until 80 days after orbit insertion.

Table 5 catalogs the solar and earth occultation durations for the six afore mentioned design trajectories. Note that solar occultations are avoided for the first 30 days in compliance with mission specifications and also that early earth occultations are experienced. However, maximum solar occultations on the order of 85 minutes are experienced late in the mission. This duration is greater than the specification of 60 minutes, and results in an increased system weight of 50 lb. The maximum occultation can be decreased by increasing the orbit inclination resulting in lack of compliance with other restraints. The longer solar occultations is accepted

Table 5. Sun and Earth Occultation Durations (minutes) per Orbit

Trajectory		Days after Encounter												
		0	15	30	45	60	75	90	105	120	135	150	165	180
1	Sun	0	0	0	0	0	0	0	0	68.04	83.3	78.3	59.2	0.6
	Earth	39.2	31.8	12.9	0	0	0	0	0	15.2	65.7	77.6	71.2	48.5
2	Sun	0	0	0	0	0	0	0	0	60.9	82.2	80.6	65.1	32.4
	Earth	40.8	35.1	21.6	0	0	0	0	0	0	59.2	76.4	74.0	57.0
3	Sun	0	0	0	0	0	0	0	0	70.8	81.5	74.9	56.3	0
	Earth	38.8	32.3	17.8	0	0	0	0	0	34.8	65.4	73.8	68.1	50.6
4	Sun	0	0	0	0	0	0	0	0	63.7	81.9	79.2	63.4	33.8
	Earth	40.6	35.7	24.6	0	0	0	0	0	0	59.1	73.9	72.5	57.9
5	Sun	0	0	0	0	0	0	0	39.0	76.4	70.1	55.4	34.3	21.4
	Earth	32.0	22.6	0	0	0	0	0	0	62.3	68.2	64.1	51.9	37.4
6	Sun	0	0	0	0	0	0	0	0	77.4	74.7	61.9	39.3	3.9
	Earth	35.1	27.1	5.4	0	0	0	0	29.3	58.1	69.1	68.0	57.2	40.0

as a compromise. The design trajectories selected for the 1975 to 1979 opportunities exhibit occulation characteristics similar to those presented in Table 5.

4.3. DESIGN TRAJECTORY DATA

The trajectory parameters that directly influence design concepts include earth communication distance, spacecraft - sun distance, earth cone and clock angles, and occultation durations. Communication distance affects power, antenna size and quantity of data return. Vehicle-sun distance and corresponding power requirements determine solar array size. Antenna gimbal angles are derived from earth cone and clock angles while occultations directly affect onboard power, data return, and attitude control requirements.

Figure 21 presents the communication distances for three design trajectories. Two of the trajectories were taken from the six previously selected design trajectories for 1973. The third trajectory represents an early arrival (January 24, 1974) and is included to show specifically the range in variation in design parameters that are possible for the 1973 launch opportunity. It can be seen that communication distances are comparable over the mission duration. However, at the time of encounter and shortly thereafter when small communication distances are desired, a difference of 80×10^6 km between early and late arrivals can be experienced. This can be a serious problem since the quantity of data return is affected.

Figure 22 shows the vehicle-sun distance for the same design trajectories. The difference in sun distance for the the trajectories is approximately 20×10^6 km at the time of encounter and again with the early arrival having the shorter distance. Sun distance affects solar array power output at the time of encounter but does not alter array performance over the duration of the mission.

The corresponding earth cone and clock angles are given in Figure 23. These angles essentially determine the high gain antenna gimbal angles. At first glance, it appears that a wide variation will be required in the antenna gimbal angles. However, transforming to a vehicle body axis system that uses a rotation and nod gimbal angle (in that order) for antenna pointing, the variations are small as illustrated in Figure 24. It is seen that the antenna rotation angle (clockwise + about the -y body axis) varies between ± 50 degrees and the nod angle (about the x body axis, - below the xz plane) varies between -12 degrees to +3 degrees.

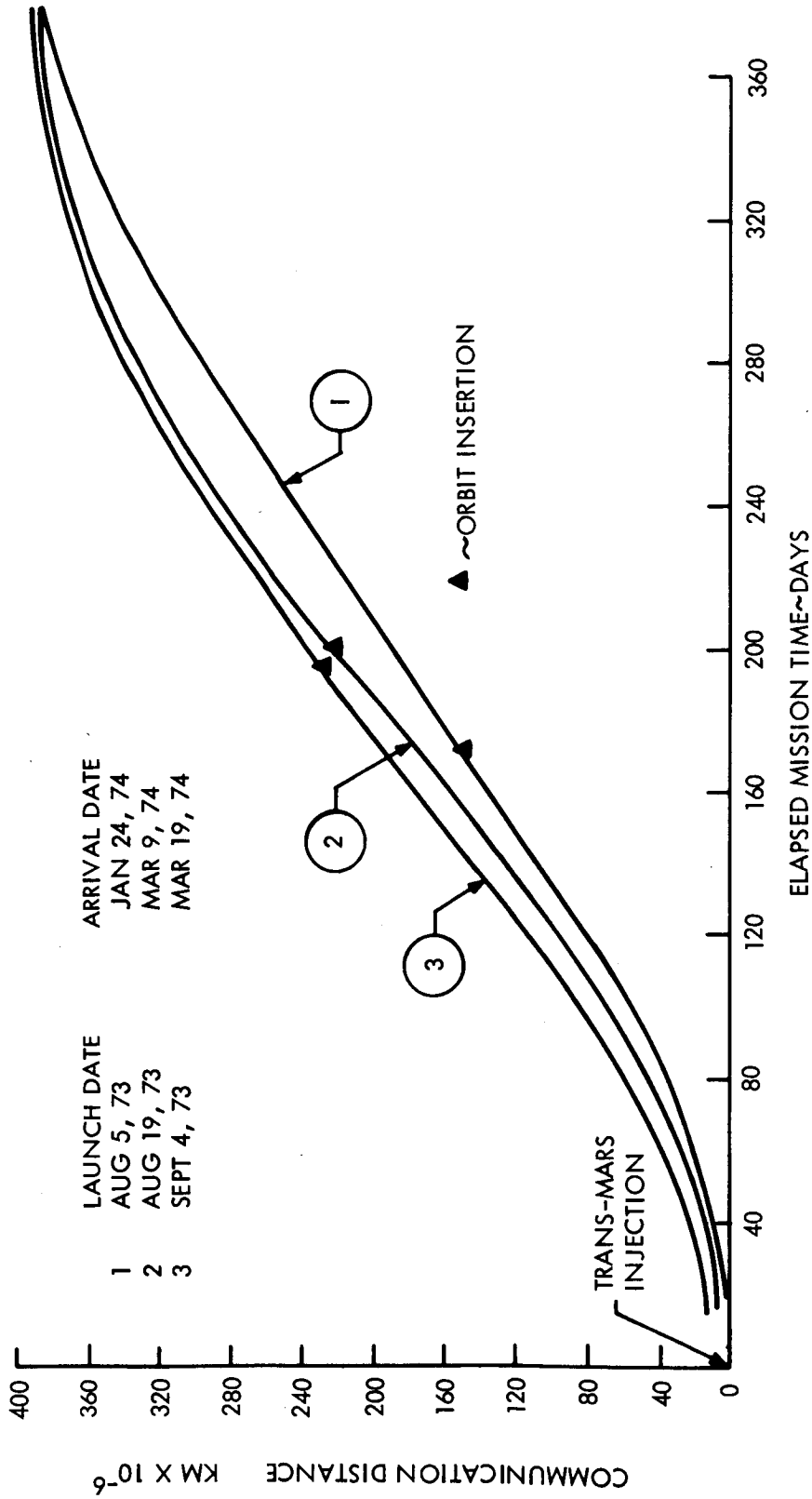

Figure 21. Communication Distance - Mars 1973 Trajectories

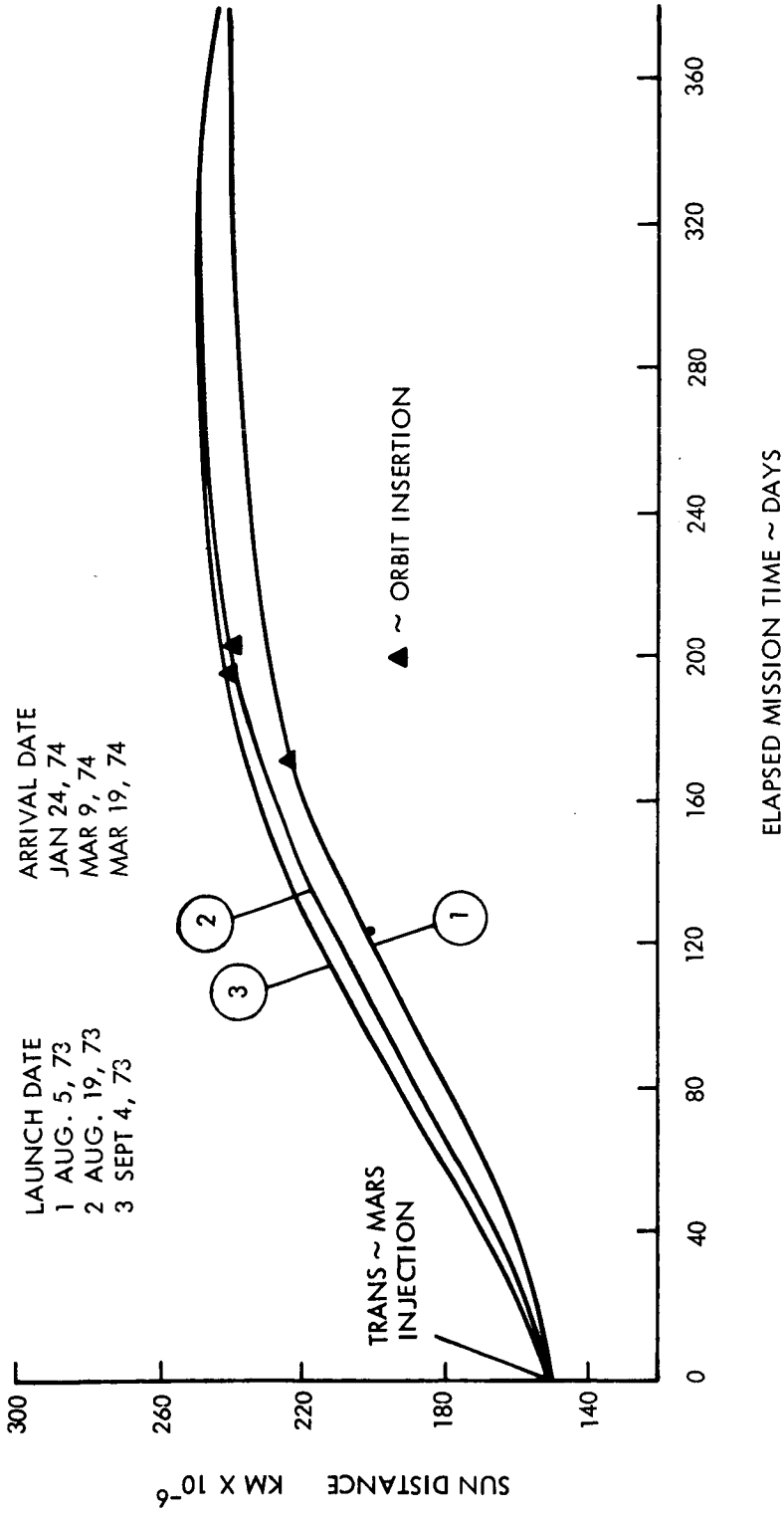

Figure 22. Vehicle - Sun Distance

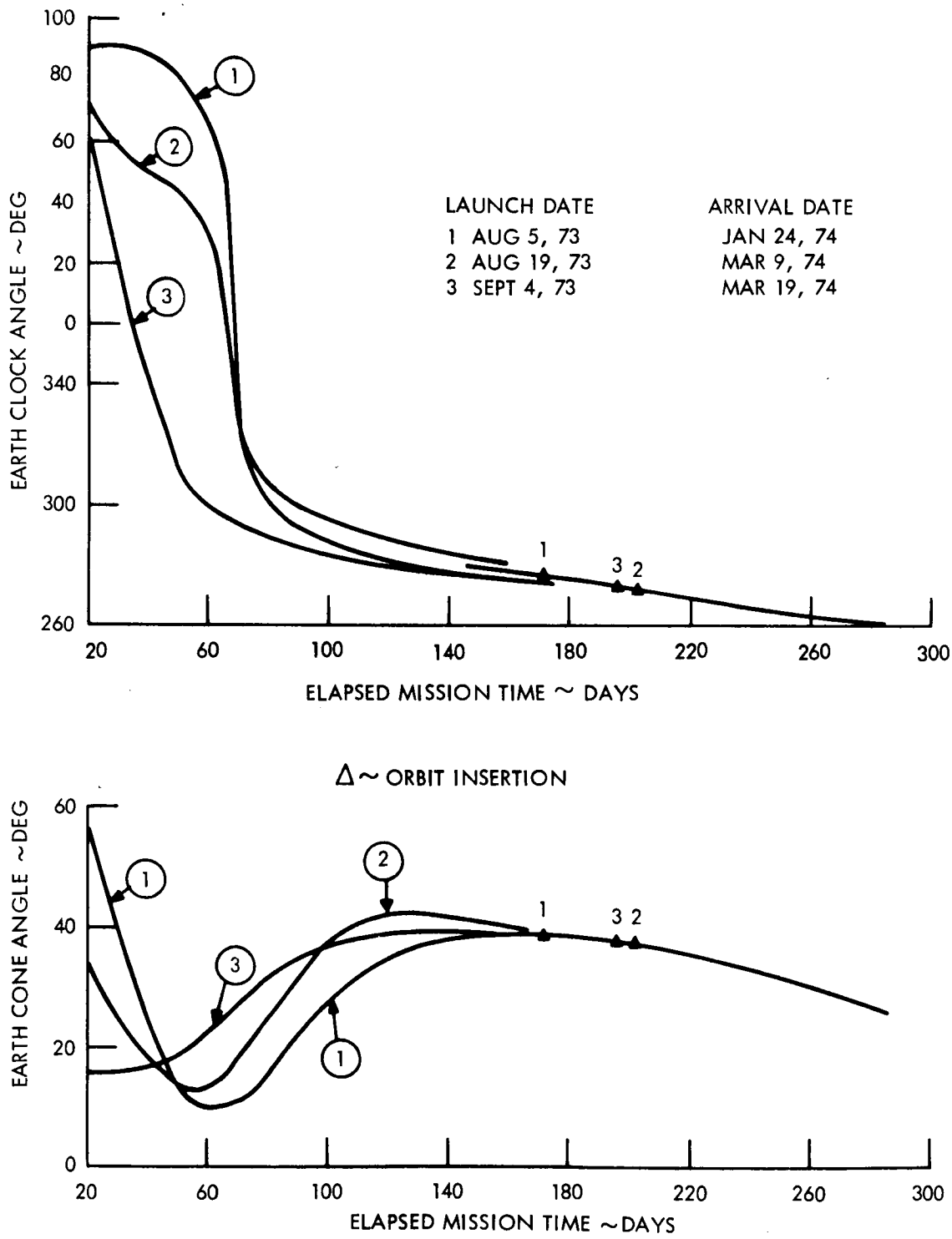

Figure 23. Earth Clock and Cone Angles

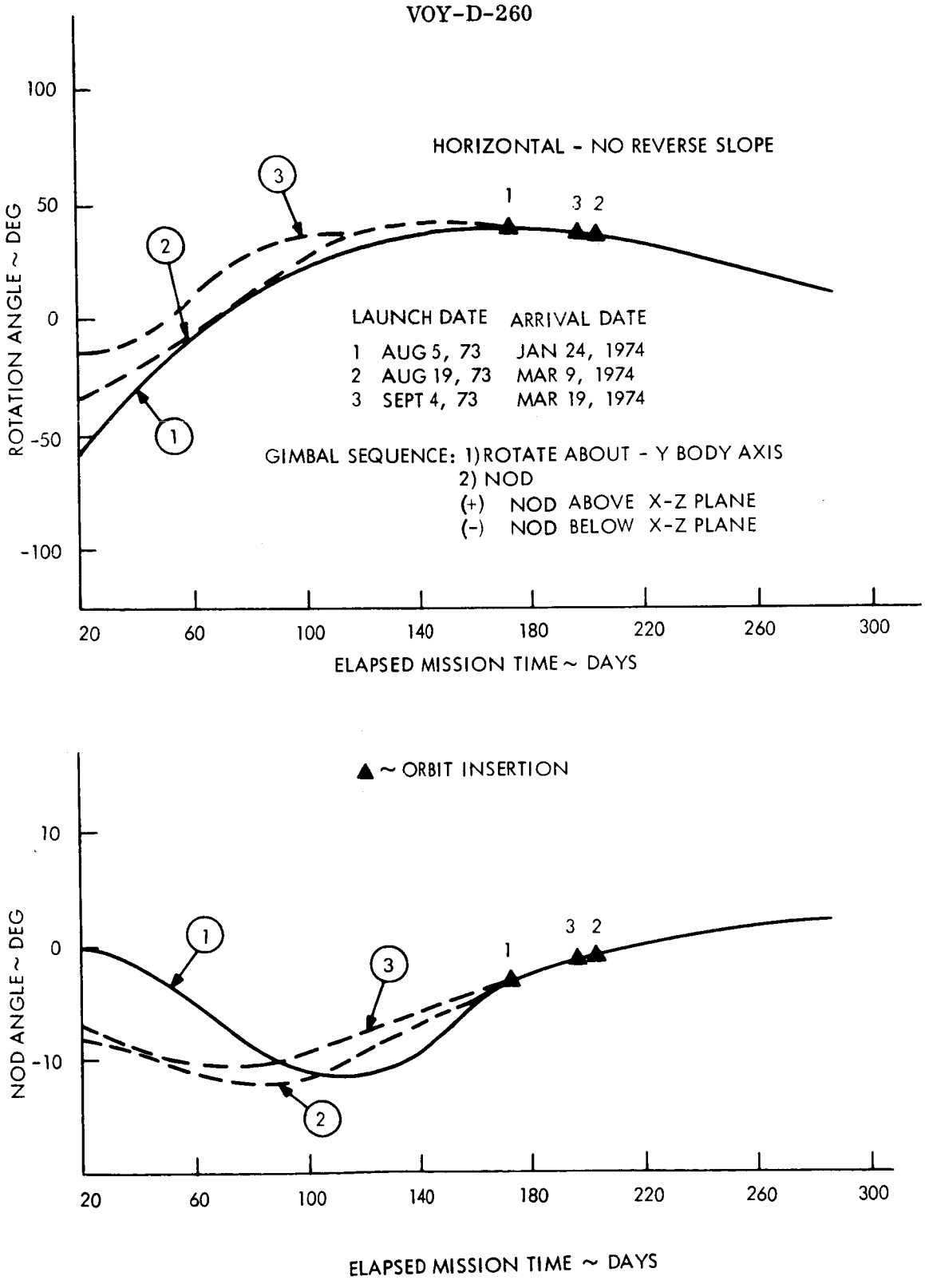

Figure 24. Antenna Gimbal Angles

5. OPERATIONAL CONSIDERATIONS

After the two planetary vehicles are injected into the trans-Mars trajectory, there remains the task of guiding the vehicles to the final orbital conditions at Mars. This task includes tracking the vehicles and conducting midcourse corrections, and orbit insertion and orbit trim maneuvers. However, in executing these maneuvers, certain error sources which affect final accuracies are present that must be considered in meeting the quarantine constraint. The error sources include;

a. Injection inaccuracies
b. Tracking or orbit determination uncertainties
c. Maneuver execution inaccuracies

In the discussion below, a guidance philosophy is outlined which accounts for the various errors and determines allowable execution errors to satisfy quarantine constraints. In addition, execution error sources such as gyro drift, autopilot capability to cope with C.G. uncertainties and thrust tailoff uncertainties are statistically analysed to derive pointing and thrusting errors. Finally, a typical 1973 flight is investigated to determine insertion accuracy and final orbit trim accuracy.

5.1. GUDIANCE PHILOSOPHY

In determining à mid-course guidance philosophy for an interplanetary mission such as Voyager, the overriding constraint is the requirement that the probability of spacecraft impact on the planet be very small - on the order of 10^{-5}. This necessitates that the initial aim point (at injection) be biased from the final desired aim-point for the first and sometimes second correction. It is assumed that the final desired aim-point is very close to the planet, say 1,000 to 5,000 km. The distance the actual point is biased from the desired aim-point is dependent on the size of the position uncertainty at encounter due to both guidance and orbit determination errors and the location of the desired aim-point about the planet.

For the Voyager mission, two spacecraft are launched with the same launch vehicle. The first midcourse velocity correction is required to remove random errors due to booster injection inaccuracies and to provide a time-of-flight adjustment. This latter velocity impulse is applied in order to separate the time of arrival between the two spacecraft. Since the time-of-flight adjustment is pre-determined, the velocity magnitude is known and therefore is referred to as

a deterministic quantity. This first correction may also be used to remove the launch vehicle bias. However both this correction (about 20 m/sec to remove a bias of 400,000 km) and the velocity required to correct for injection errors (about 5 m/sec) are small compared to the time-of-flight velocity correction (100-200 m/sec for an eight day separation during the 1973 Mars mission). In addition, the bias correction impulse and flight time impulse are very nearly normal to each other.

Ideally, this first correction would place the spacecraft on a trajectory that would produce exactly the proper planet encounter conditions. However, there will be uncertainties in the required velocity impulse. The resultant velocity errors together with orbit determination uncertainties will produce uncertainties in the encounter conditions. Thus a procedure must be investigated for removing the encounter errors using one or two additional velocity corrections. The parameters which can be varied in obtaining this procedure are:

a. The points along the trajectory at which the velocity corrections are made.
b. The accuracy to which corrections can be made.
c. The probability of impact.

The velocity correction required at any point along the trajectory to remove encounter errors is easily computed by the use of sensitivity coefficients. With a velocity correction computed and an execution accuracy assumed, the velocity errors after the second correction are computed and together with the orbit determination uncertainty, new uncertainties in encounter conditions are determined. If the final aim-point is not obtained within the required accuracy and within the imposed probability of impact, an additional correction is required and the above process is repeated.

After the first mid-course correction, the resultant velocity errors can be propagated to the impact parameter plane in terms of a position dispersion ellipse. A locus of aim-points that satisfies the probability of impact can also be determined. If the final desired aim-point lies outside the locus of aim-points that satisfy the probability of impact, no biasing is required at the first correction. If biasing is required, the type of biasing must then be specified. Three types of biasing have been investigated: minimum, radial, and tangential. For the minimum bias case, a point on the locus is chosen which minimizes the distance to the desired aim-point. For the radial bias case, a point on the locus is chosen which is on a radial line

through the desired aim-point. For the tangential case, a point on the locus is chosen which is on a line perpendicular to the radial line through the desired aim-point; the desired aim-point referred to is the aim-point for the second mid-course correction. Thus, the first and second aim-points may be interdependent; the type of biasing chosen is dependent on the dominant system errors. For large velocity shut-off errors, the tangential bias technique minimizes the possibility of an impact, while a radial bias would be used if the pointing errors were dominant. For nearly equal errors (magnitude and pointing) the minimum bias technique yields minimum velocity correction requirements. For the second correction, if a bias is required, the radial technique is used since the position error dispersions are very nearly circular.

It is the purpose here to determine the guidance accuracy requirements and velocity correction requirements for a typical 1973 Earth-Mars trajectory. An analytic formulation, similar to that given in reference 1, which statistically treats the various error sources and biasing techniques, has been used to derive the guidance accuracies presented below. The sequence of impact probability after each mid-course correction is based on the requirement that the total probability of impact of the launch vehicle or either spacecraft be less than 3×10^{-5} and that each spacecraft is identical in operation.

The assumptions and ground rules employed for this typical case are:

a. Three mid-course corrections are used.

b. Corrections occur at 2 days after injection, at the mid-point of the trajectory, and at 10 days before encounter.

c. The probability of impact without additional maneuvers after each correction is 10^{-4}, 10^{-5}, 10^{-5}, respectively.

d. Minimum aim-point biasing.

e. The resolution and autopilot errors are negligible.

f. The 1 σ impact parameter errors due to orbit determination are:

	Position (km.)	Time (min.)
1st correction	665	5
2nd correction	250	2.33
3rd correction	140	1

g. Mars atmospheric height is 400 km.

h. Periapsis altitude of the approach hyperbola is 1,000 km.

i. Inclination of the approach hyperbola relative to the Mars equator is 40 degrees direct.

j. First mid-course velocity correction for injection guidance errors is 5 m/sec (1σ).

k. The trajectory parameters and approach conditions are:

1.	Launch Date:	August 10, 1973
2.	Arrival Date:	March 15, 1974
3.	Trip Time:	217 days
4.	C3:	16.571 km^2/sec^2
5.	Declination	32.20 deg.
6.	Approach Speed:	2.520 km/sec
7.	Capture Radius:	8125 km.
8.	Aim Point	
	Impact Parameter:	8891 km.
	Orientation angle:	54.37 deg.
9.	Time of arrival separation velocity (± 4 days)	124.35 m/sec.

Figure 25 presents the limits on the guidance accuracies required to satisfy the constraints for the typical trajectory analyzed. It is assumed here that the guidance (or execution) accuracies are constant for each mid-course correction. Any combination of pointing and shut off errors below the solid curve in the figure will satisfy the contamination constraint for this trajectory and aim-point.

The RSS velocity requirement for the first mid-course correction is 124.5 m/sec. This includes the flight time separation and the injection guidance correction requirements. The sum of the RSS velocity corrections for the 2nd and 3rd corrections is shown in the figure as dashed lines. As will be shown subsequently for midcourse maneuvers the anticipated standard deviation pointing error and thrust error deviations are .0067 radians and less than .2% respectively. These values fall well within the limit required to meet the quarantine constraint and indicate that the total velocity correction for the second and third midcourse maneuvers is 7 mps (1σ).

5.2. MANEUVER ACCURACY

The maneuver accuracy was investigated in terms of the various contributing error sources. These error sources are:

Table 6. Center of Gravity Offset-Errors

COMPONENT	DISTRIBUTION	MEAN	STANDARD DEVIATION (DEGREES)
GYRO DRIFTS			
.001285 (Y + P) + .0884	Gaussian	0.0	.3116
TURN UNCERTAINTIES			
1) Turn rates			
σ_{TRY} = .00133Y	Gaussian	0.0	.2195
σ_{TRP} = .00133P	Gaussian	0.0	.0133
2) Timer resolution ±.5 second	Uniform ± .089°	0.0	.0515
SPACECRAFT DEVIATIONS			
1) Control system deadband	Uniform ± .458	0.0	.253
2) Sensor repeatability	Gaussian	0.0	.047
3) Control electronics drift	Gaussian	0.0	.0155
4) Sensor mounting alignment	Gaussian	0.0	.0167 to .167
ATTITUDE CONTROL ERRORS DURING THE MANEUVER	Uniform ± .458	0.0	.263
AUTOPILOT ERROR			
1) Center of gravity offset	Gaussian	0.0	.001 to .4
2) Thrust misalignment	Gaussian	0.0	.06916
3) Transient error	Gaussian	0.0	.001 to .1
4) Autopilot feedback gain	Gaussian	2 to 8	Negligible

a. Gyro drifts
b. Turn uncertainties
c. Spacecraft deviations from the celestial references
d. Altitude control errors during the turn maneuver
e. Autopilot errors
f. Magnitude uncertainty of the velocity vector

Appendix A.1 gives an analysis of the maneuver pointing errors and the uncertainty of the velocity vector.

Table 6 gives the statistical properties of all the error sources, for a yaw-pitch turn sequence of 165 degrees and 10 degrees respectively. Four error sources were parameterized in the study:

a. The sensor mounting alignment
b. The autopilot feedback gain
c. The autopilot transient errors
d. The center of gravity offset errors

Using a sensor mounting alignment error of .0835 (1σ) degrees, an autopilot feedback gain of 4.0, a transient error of .1 (1σ) degrees, and the three sigma values for the center of gravity offset errors given in Table 6, the values of the three sigma maneuver pointing error for a yaw-pitch turn sequence of 165 degrees-10 degrees were obtained as given in Table 7. Impulse variability data was obtained from the engine manufacturer and converted to the three sigma thrusting magnitude errors given in Table 7.

5.3. ORBIT INSERTION ACCURACY

After the last mid-course correction in an inter-planetary transfer trajectory, a position dispersion ellipse about the desired final aim-point in the impact parameter plane exists due to the propagation of velocity execution errors and orbit determination errors at the time of the last correction. An investigation of the effects of additional tracking after the last mid-course correction has been made. It was found from this investigation that the probability of being in a region about the desired aim-point (and consequently in some region about the desired

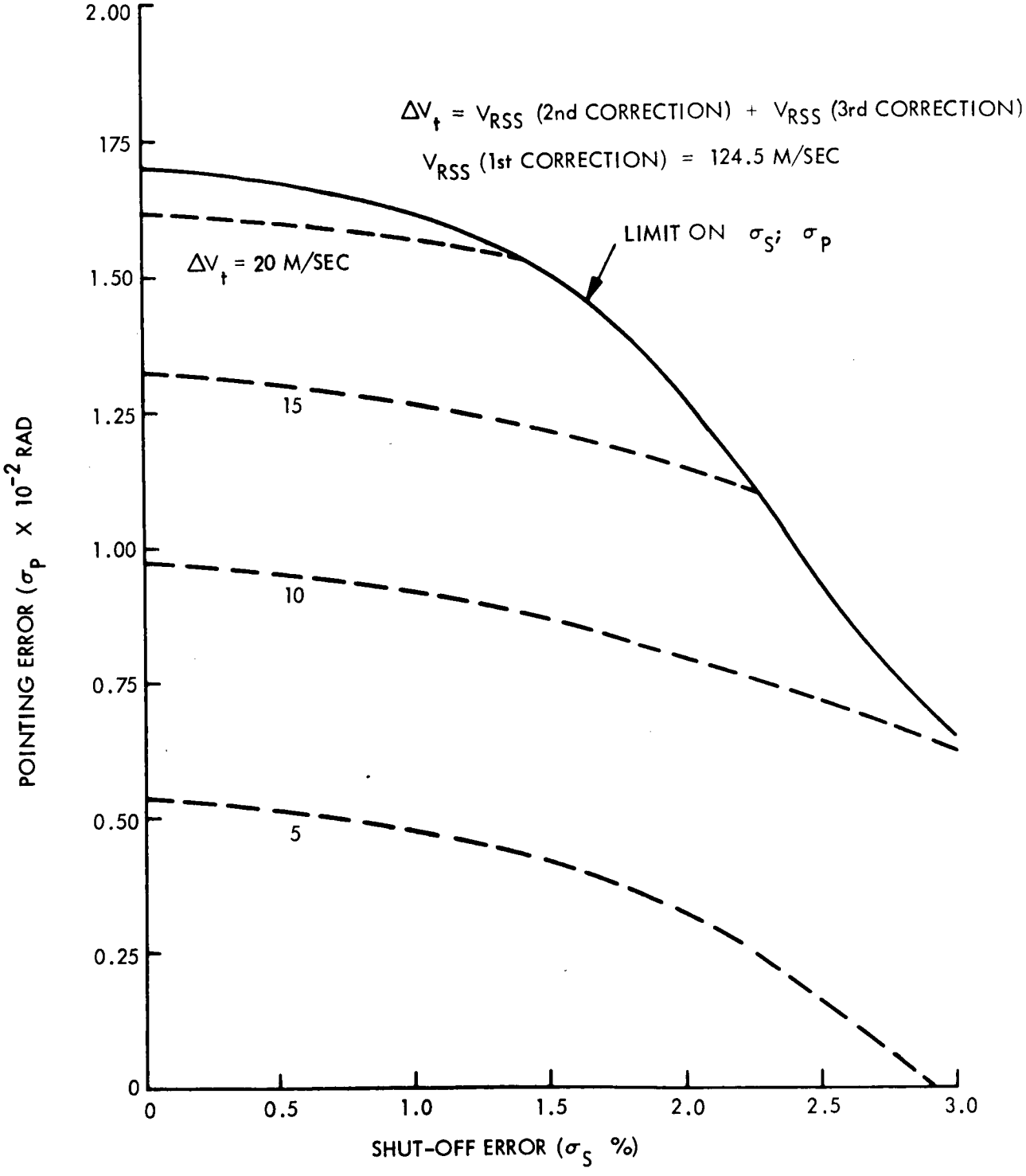

Figure 25. Guidance Accuracy Requirements 1973 Earth-Mars Trajectory

Table 7. Summary of Maneuver Errors

Maneuver	Center of Gravity Offset Errors (degrees) (3σ)	Pointing Errors of each component (degrees) (3σ)	ΔVelocity** Errors (m/sec) (3σ)
Midcourse Corrections	.01716	.975 ± .1765*	.0756
Orbit Insertion	.566	1.52 ± .1924	.757
Orbit Trims with capsule on	.72	1.674 ± .20	.140
Orbit Trims with capsule off	1.03	1.98 ± .2627	.280

*The plus/minus errors are based on a 99.7 percent confidence

**The Δ velocity errors should include an error which is proportional to the total delta velocity due to accelerometer error. However, at a 1,000 pound thrust level this error is negligible.

periapsis altitude) is only dependent on the guidance errors and orbit determination errors up to the time of the last mid-course correction. The advantage of additional tracking is that the actual aim-point (and actual periapsis altitude) may be determined to some higher degree of accuracy, thus allowing a change in the orbit insertion maneuver (if this flexibility has been provided) to obtain an orbit size and location closer to the desired orbit.

It is the purpose here to determine the errors in the final areocentric orbit due to errors in the orbit insertion. The orbital errors of interest are deviations from the nominal periapsis altitude, apoapsis altitude, period, and apsidal rotation. The error sources are navigation-impact parameter error, time of ignition error, system-velocity shut-off error, and pointing error.

Two modes of nominal orbit insertion were studied.

a. Minimum ΔV insertion
b. Tangential insertion.

In order to define the nominal orbit insertion conditions, several parameters must be specified:

a. Approach Speed: 2.5 km/sec
b. Orbit Size: 1,000 x 10,000 km altitude
c. Apsidal Rotation: + 20 deg.

The insertion velocity impulse that must be applied to transfer the spacecraft from the approach hyperbola to an areocentric ellipse is a minimum for a periapsis to periapsis transfer. This establishes the location of the periapsis of the ellipse for zero apsidal rotation. By injecting into the elliptical orbit from some point on the hyperbola other than the periapsis, the line of apsides of the ellipse may be rotated. The amount the line of apsides is rotated is the difference between the true anomaly on the approach hyperbola at which the transfer takes place and the true anomaly on the ellipse at which insertion occurs. The velocity impulse that must be applied is the vector difference between the velocities on the hyperbola and ellipse at the transfer point. Figure 26 illustrates the minimum insertion velocity required to rotate the line of apsides of a 1,000 x 10,000 km altitude elliptical orbit for approach velocities at Mars of 2.5, 3.0 and 3.5 km/sec.

Since Figure 26 depicts the minimum insertion velocity impulse for varying apsidal rotation, it is important to note that the altitude of the approach hyperbola is a variable. For a 1,000 x 10,000 km elliptical orbit and an approach velocity of 3.5 km/sec, apsidal rotations of 10 degrees and 30 degrees are attained by transferring from an approach trajectory with periapsis altitudes of 1,027 km and 1,369 km respectively. The minimum velocity impulse required for these rotations are 1.87 and 1.97 km/sec. Had the periapsis altitude of the approach hyperbola been 1,000 km, velocity impulses of 1.89 and 2.60 km/sec would have been required.

Tables 8 and 9 show dispersion in orbital size, period and argument of periapsis. These tables represent the case where post-midcourse maneuver tracking data are not used to update the orbit insertion maneuver. The 1 σ error sources in performing the insertion maneuver are also noted in the tables. The magnitude of the impact error (140 km, 1 σ) at the time of orbit insertion is given by Figure 27.

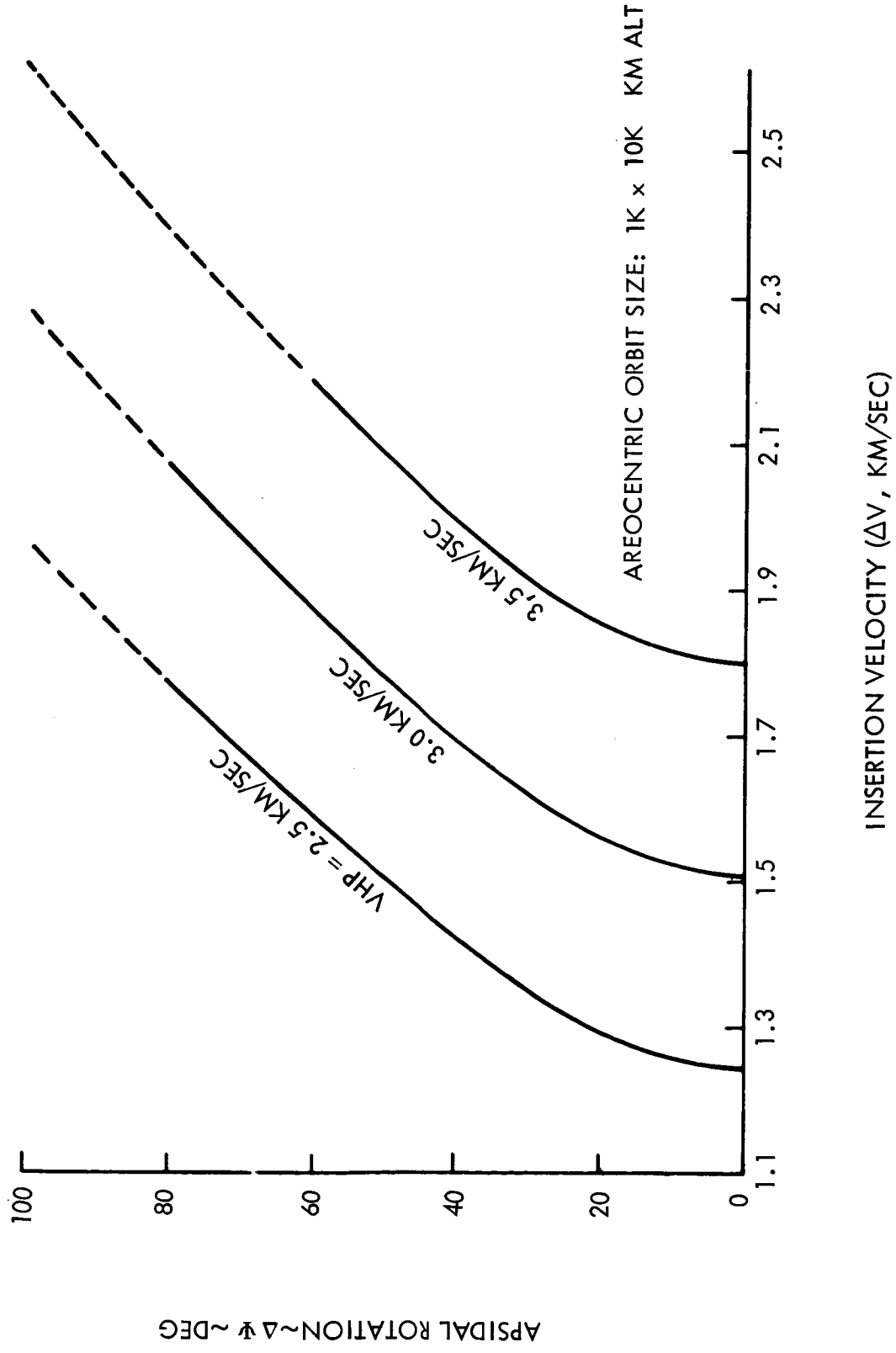

Figure 26. Insertion Maneuver Requirements

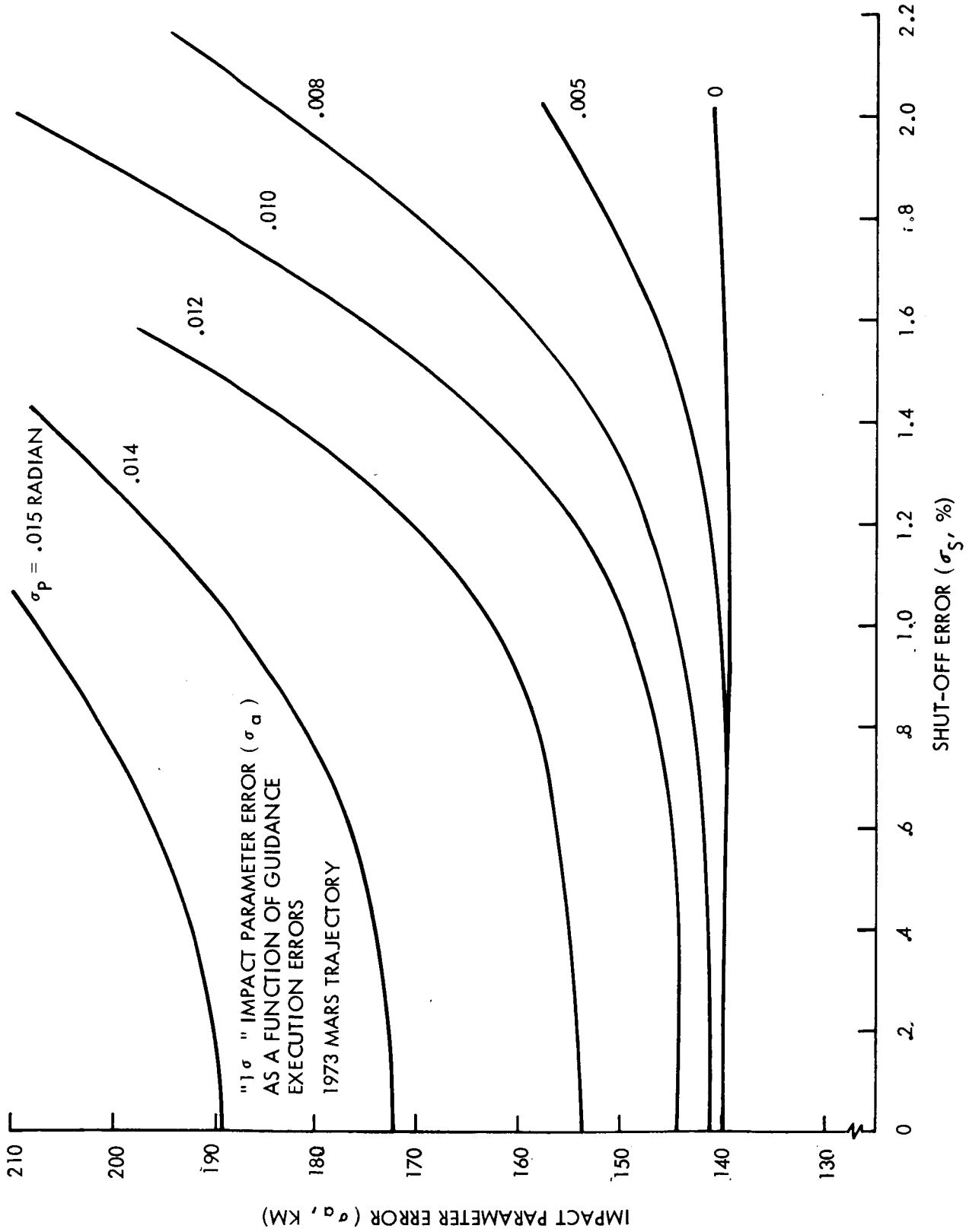

Figure 27. System Update Design

Table 8. Orbit Insertion Accuracy

Minimum ΔV Insertion
(w/o Post-Midcourse Maneuver Tracking)

Orbit Error	Periapsis Altitude (km)	Apoapsis Altitude (km)	Period (min.)	Apsidal Rotation (deg.) or Argument of Periapsis
1σ Error Source				
Impact Parameter(B) 140 km	71.27	238.42	11.14	- .08
Ignition Time(t) 40 sec	-26.55	106.00	2.85	-1.12
Velocity Shutoff(V) .02 percent	- 0.12	7.0	0.26	.01
Pointing(θ) .57 deg	- 9.6	58.1	1.74	- .52
	RSS $\cong$ 77.	RSS $\cong$ 267.	RSS $\cong$ 11.6	RSS $\cong$ 1.22

Table 9. Orbit Insertion Accuracy

Tangential Insertion
(w/o Post-Midcourse Maneuver Tracking)

Orbit Error	Periapsis Altitude (km)	Apoapsis Altitude (km)	Period (min.)	Apsidal Rotation (deg.) or Argument of Periapsis
1σ Error Source				
Impact Parameter(B) 140 km	75.53	276.56	12.68	- .24
Ignition time(t) 40 sec	21.29	207.13	6.70	- .90
Velocity Shutoff(V) .02 percent	- .12	7.0	.26	.01
Pointing(θ_T) .57 deg	-12.2	16.2	.15	.59
	RSS $\cong$ 80.	RSS $\cong$ 347.0	RSS $\cong$ 14.5	RSS $\cong$ 1.1

In comparing these two modes of insertion it is seen that the major error sources are the time of ignition and the uncertainty in the impact parameter. Orbital errors resulting from pointing inaccuracy and velocity shut-off errors are approximately the same for each mode of insertion.

From the data of Tables 8 and 9, it is noted that the resultant 1 σ orbit period dispersion is on the order of 11 to 15 minutes. It is also pointed out again that the above analysis did not consider the use of tracking data after the final midcource maneuver. In order to gain an insight to the degree of orbit insertion improvement, it is presumed that post-maneuver tracking can reduce the 1 σ impact parameter uncertainty (B) to 70 km and the 1 σ firing time error to 20 seconds.

The 1 σ period uncertainty with post-maneuver tracking is then 6.0 minutes as shown in Table 10. However, from a photographic mapping viewpoint, where a specific coverage overlap may be desirable, orbital period control is most important. Although the above tables are based on attaining a 1,000 x 10,000 km altitude orbit, the results are nevertheless typical for the selected orbit size of 1,000 x 11,727 km.

Table 10. Orbit Insertion Accuracy

Minimum ΔV Insertion
(with Post-Midcourse Maneuver Tracking)

Orbit Error	Periapsis Altitude (km)	Apoapsis Altitude (km)	Period (min.)	Apsidal Rotation (deg.)
1σ Error Source				
Impact Parameter (B) 70 km	35.63	119.21	5.57	-.04
Ignition Time (t) 20 sec	-13.27	53.0	1.42	-.56
Velocity Cutoff (V) .02 percent	- .12	7.0	.26	.01
Pointing (θ_1) .57 deg	- 9.6	58.1	1.74	0.52
	RSS $\cong$ 39.3	RSS $\cong$ 143.0	RSS $\cong$ 6.0	RSS $\cong$ .77

5.4. ORBIT TRIM ACCURACY

Orbit trim maneuvers are designed to correct orbit dispersions caused by the orbit insertion maneuver and to adjust the orbital elements to more desirable values. Presently, the nominal orbit insertion maneuver is designed to achieve a planetary orbit that satisfies all important mission constraints, such as illumination conditions, periapsis location, and occultation restrictions. Velocity requirements to adjust periapsis altitude, apoapsis altitude, argument of periapsis and orbit inclination were given in the Task B study report and therefore are not included again. To date, requirements to significantly alter the nominal orbit size and orientation after orbit insertion have not been uncovered and, therefore orbit trim maneuves are considered to be primarily conducted for establishing or maintaining the nominal conditions. Since small dispersions in apsidal rotation and inclination have negligible effect on illumination, periapsis location, occultation constraints, and more important, mapping coverage capability, orbit trim maneuvers are relagated to orbit period and orbit size (periapsis-apoapsis) control.

Orbit period control is very important especially when a specific overlap in coverage is desired. For example, if it is desired to have mapping coverage within overlap bounds of 15 percent and 35 percent, the probability of achieving the proper orbital period, without orbit trim and without using post-midcourse maneuver tracking data, is approximately .025. If post-midcourse maneuver tracking data is used to update the orbit insertion maneuver, then the probability of achieving an acceptable orbital period only increases to .05. In either case, the need for an orbit trim maneuver is apparent. Using the orbit trim accuracy data presented in section 5.2, preliminary calculations indicate that the orbital period for a nominal 1,000 x 11,727 km altitude orbit can be controlled to within 0.36 minutes (3σ) and the probability of establishing an acceptable orbital period that obtains the desired coverage overlap is .997. The corresponding (3σ) velocity requirement is 28.0 m ps for the case where post-midcourse maneuver tracking data is not utilized and 14 mps when the additional tracking data is used.

The above discussion refers to the case where the orbit trim maneuver is performed after capsule separation. If the orbit trim maneuver is performed prior to capsule separation, orbital period can be controlled to within .18 min (3σ).

APPENDIX A
MANEUVER ACCURACY

A.1. INTRODUCTION

The maneuvers considered in this system analysis study include the midcourse corrections, orbit insertion, and orbit trim. In performance of these mission maneuvers, a pair of turns about two of the spacecraft axes are required. In all cases, it is desired to direct the roll axis through the required thrust vector. The redirection of the roll axis is accomplished by a combination of pitch and yaw turns. Flexibility of choosing the order of the turns (i.e., yaw-pitch vs pitch-yaw) allows the minimization of the maneuver errors. The sequence which requires the lowest sum of angles will result in shorter maneuver times and, therefore, smaller maneuver pointing errors.

A.1.1. TURN APPROACHES

Figure A-1 illustrates the turns required to redirect the roll axis near the initial yaw-axis and initial x-y plane. In this example, the pitch-yaw sequence will have minimum pointing error. Figure A-2 illustrates redirecting the roll axis close to the initial pitch axis and x-y plane. In this example, the yaw-pitch sequence will yield the lowest maneuver pointing error.

In the analysis which follows, only a yaw-pitch sequence will be considered since these are the most likely sequences to be encountered during the mission. The analysis of the maneuver errors involves successive coordinate transformations which include the effects of system errors. A math model of the maneuver was developed which considers the problem geometrically by successive multiplications of coordinate transformations.

A.1.2. MATH MODEL

The error analysis for the maneuvers is considered in the following discussion. The geometry of the problem is modeled by matrix coordinate transformations of the effects of each system error and the normal rotation characteristics of the vehicle. The basic equation is:

$$\left[Y\right]\cdot\left[P\right]\cdot\left[\xi x\right]\cdot\left[\xi x\right]\cdot\left[-G_{x,y,z}\right] = \left[\delta_{x,y,z}\right]\cdot\left[\Delta_{x,y}\right]\cdot\left[Y\right]\cdot\left[\Delta Y\right]\cdot\left[\Delta_{y}\right]\cdot\left[-\Delta X\right]\cdot\left[P\right]\cdot\left[\Delta P\right]\cdot\left[-\Delta_{y,z}\right] \qquad \text{(A-1)}$$

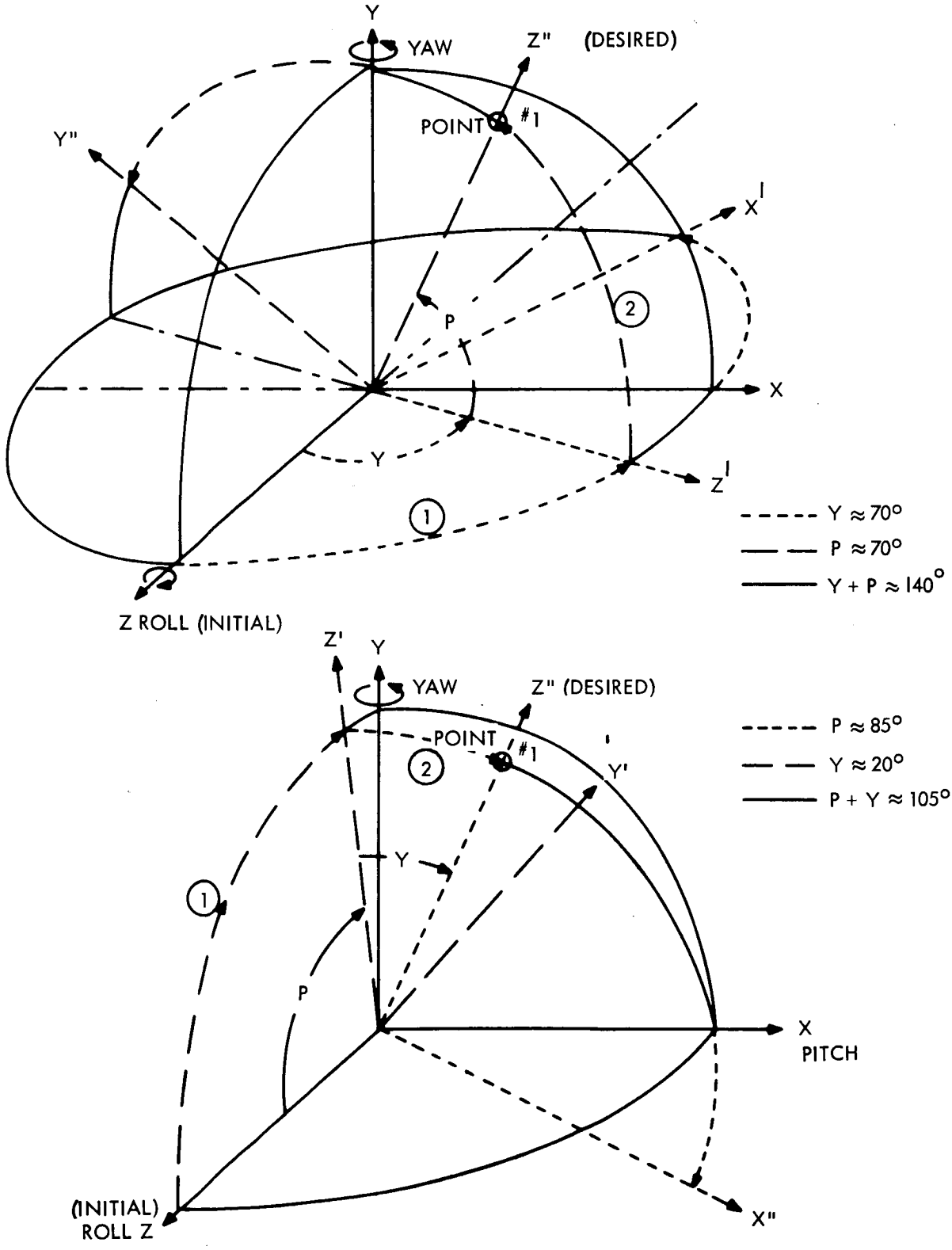

Figure A-1. Y-P and P-Y Turns to Reach Point No. 1

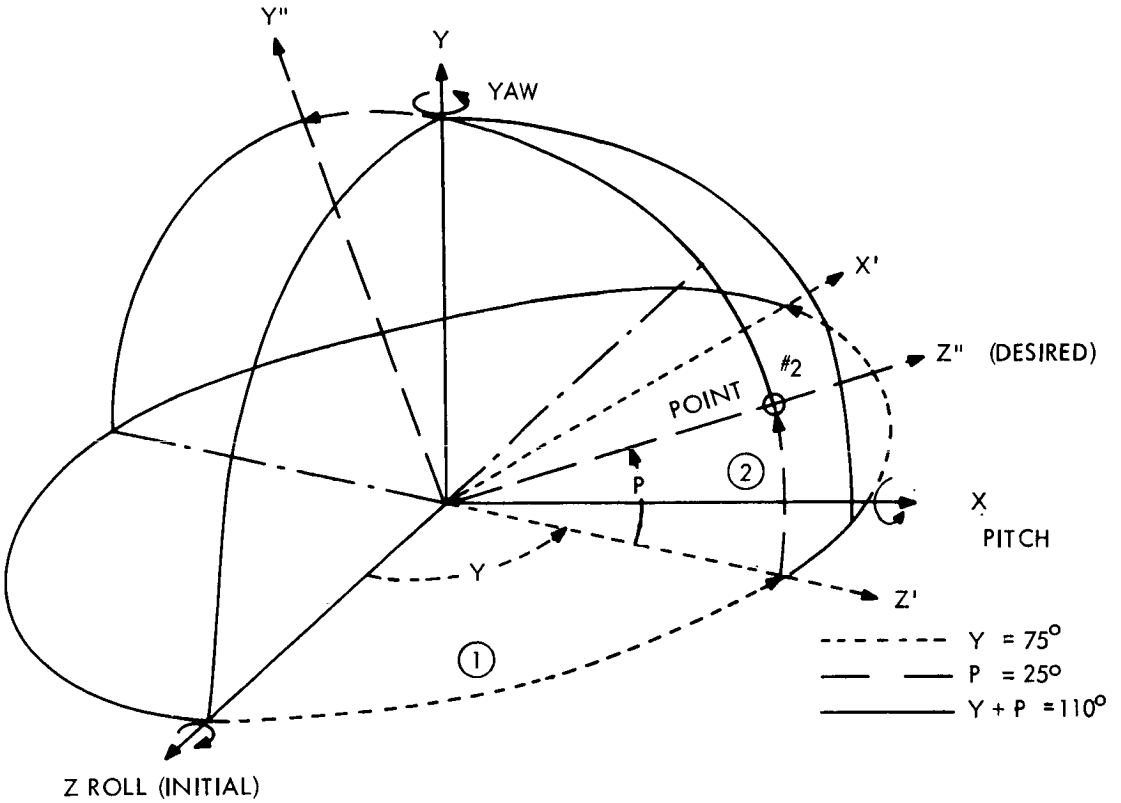

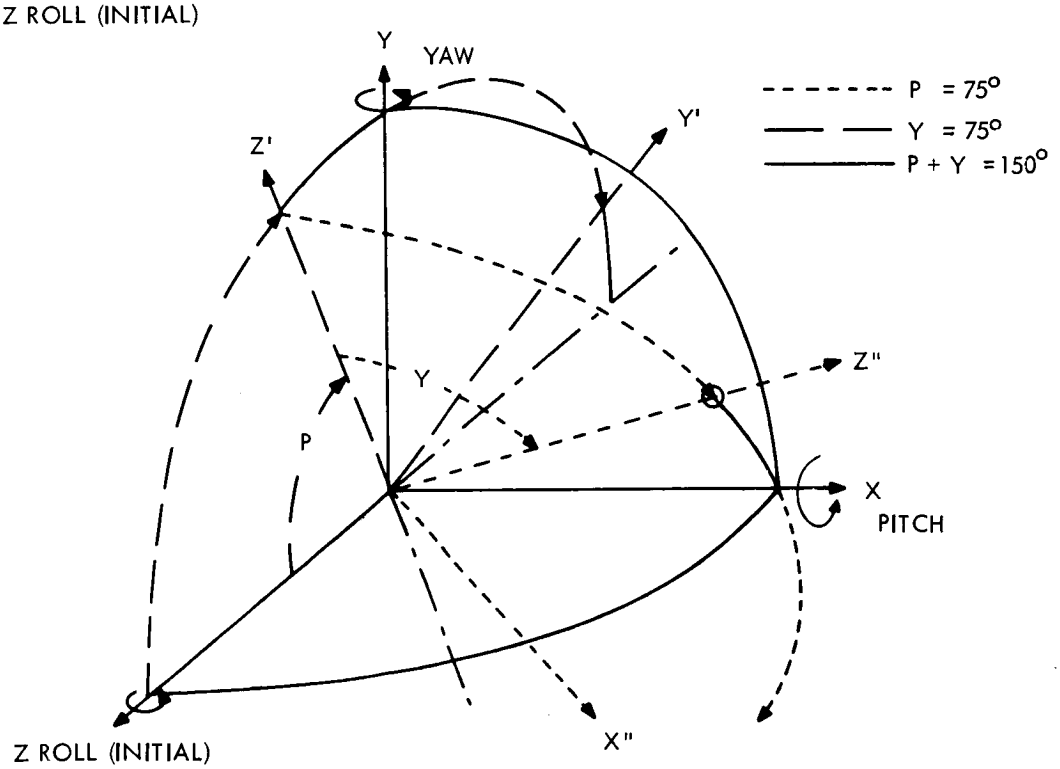

Figure A-2. Y-P and P-Y Turns to Reach Point No. 2

where

Y	is the yaw turn
P	is the pitch turn
ξ_x	is the final pitch error
ξ_y	is the final yaw error
$G_{x,y,z}$	are the gyro drifts during the turn
ΔP	is the pitch turn uncertainty
ΔY	is the yaw turn uncertainty
$\delta_{x,y,z}$	are the initial spacecraft deviations from the celestial references
$\Delta_{x,y,z}$	are the errors in the attitude control gas system during the gyro sensing mode

Equation (A-1) can be solved for ϵ_x and ϵ_y, the final pitch and yaw errors. Performing the reduction and assuming that second order and higher error terms can be neglected and adding autopilot errors (A_x, A_y), the following equations are obtained for the two orthognal components of error:

$$\xi_x = G_x - (\delta_z + \Delta_z) \operatorname{Sin} Y + (\Delta P - \Delta_x) + (\delta_x + \Delta_x) \operatorname{Cos} Y + A_x \tag{A-2}$$

$$\xi_y = G_y + (\delta_x + \Delta_x) \operatorname{Sin} Y \operatorname{Sin} P + (\delta_z + \Delta_z) \operatorname{Cos} Y \operatorname{Sin} P + (\Delta Y \operatorname{Cos} P - \Delta_y) + (\delta_y + \Delta_y) \operatorname{Cos} P + A_y \tag{A-3}$$

Thus the contributing errors are:

a. The deviations of the spacecraft from celestial references (δ), at time of switching to gyro references and includes the attitude control gas dead bands.

b. The uncertainties in the actual magnitude of executed turns (ΔY and ΔP).

c. The control system dead band errors during the turn ($\Delta_{x,y,z}$).

d. Autopilot errors during the thrusting.

The following sequence illustrates how each error contributes to the maneuver pointing error:

a. First the gyros are allowed to warm up. The time required will be on the order of one hour.

b. After warmup and at some arbitrary time, the gyro nulls are aligned with the celestial references. Attitude control deadband, alignment errors, control electronics drift and normal sensing error contribute to the location of the gyro nulls.

c. At a fixed time later, the yaw turn begins and during this turn only attitude control errors with respect to the gyro nulls on the roll and pitch axes contribute to shifts in the yaw null. Turn rate uncertainty determines the uncertainty in the magnitude of the turn.

d. At the completion of the yaw turn, the spacecraft is allowed to attitude stabilize using an inertial reference.

e. At a fixed time later, the pitch turn begins and during this turn only the roll and yaw errors in the attitude control deadbands contribute to pitch null location through vehicle coupling. The uncertainty in the turn is related to the turn rate uncertainty.

f. At the completion of the pitch turn, the spacecraft is attitude stabilized.

g. When the thrust is supplied, the autopilot directs the thrust vector through the center of gravity, using the gyro nulls as an error reference. The location of the center of gravity, the steady-state error in the autopilot and the transient errors in the autopilot contribute to the autopilot errors. Gyro drift errors are proportional to the time interval beginning with the alignment of the gyro nulls to the completion of the thrusting.

A.3. ERROR ANALYSIS

The error sources are discussed in the following subparagraphs and each is described by a probability distribution and appropriate statistics.

A.3.1. BODY DEVIATIONS

The deviations of the spacecraft from celestial references is a function of four dominant sources. These are the Attitude Control Subsystem (ACS) deadband during the optical sensing mode, the sensor mounting alignments, the sensor repeatability, and the control electronics drift and noise. Table A-1 lists the distribution of each of these sources and the associated statistics.

A.3.2. GYRO DEADBANDS

The gyro deadbands in the inertial sensing mode contribute to the maneuver pointing error modified by the turn magnitude as indicated in Equations A-2 and A-3. The Attitude Control Subsystem does not change the magnitude of the deadbands when switching from the optical mode to the inertial mode; therefore, a variation of ±0.458 degree is expected with a uniform probability distribution. The distribution is modified by the values of cos (P), sin (P), or cos (Y) as determined by Equations A-2 and A-3.

Table A-1. Body Deviation Error Sources

Error Source	Symbol	Distribution Uniform	Mean	Variance $(\text{Degrees})^2$
Control System Dead Band (1) (Optical Sensing Mode)	$\delta_x, \delta_y, \delta_z$	$-0.458°$ to $+0.458°$	0.0	0.06992
Sensor Repeatability (3)	$\delta_x, \delta_y, \delta_z$	Gaussian	0.0	0.00222
Control Electronics Drift	$\delta_x, \delta_y, \delta_z$	Gaussian	0.0	0.00028
Sensor Mounting Alignment	$\delta_x, \delta_y, \delta_z$	Gaussian	0.0	0.00028

ASSUMPTIONS

(1) All error sources are independent.

(2) Each component $(\delta_x, \delta_y, \delta_z)$ is assumed to be independent and described by a distribution with a mean and variance equal to the distribution of the other two components.

(3) Sensor Repeatability is due to variations in linearity and in null position with time and temperature.

A.3.3. GYRO DRIFTS

The gyro drift is determined by the length of time involved in the turn. The drifts in the nulls in pitch and yaw are considered to be independent and estimated to be described by a Gaussian distribution with three times the standard deviation to be 0.25 degree per hour.

The turn rate is designed to be 3.14 milliradians per second. Thus, the standard deviation for the gyro drift is given by the following equation:

$$\sigma_g = 0.001285\ (Y + P) + 0.0833\ (T) \qquad \text{(A-4)}$$

where:

Y is the yaw turn in degrees

P is the pitch turn in degrees

σ_g is the standard deviation in degrees

T is the sum of the following time intervals in hours.

a. The time from alignment with the celestial references to the start of the yaw turn (assumed to be 1/2 hour)

b. The time from the end of the yaw turn to the start of the pitch turn (assumed to be 1/60 hour)

c. The time from the end of the pitch turn to the end of the application of the thrust (assumed to be 1/2 hour)

Thus

$$\sigma_g = 0.001285\ (Y + P) + 0.0884 \tag{A-5}$$

$$\sigma_g^2 = (0.001285\ (Y + P) + 0.0884)^2 \tag{A-6}$$

A.3.4. TURN UNCERTAINTIES

The pitch and yaw turns are subject to errors due to variations in the turn rate, and the accuracy of resolution of the Computer and Sequencer (C&S) timer.

The turn rate of the gyros is 3.14 milliradians per second. The turn rate uncertainty was assumed to be ±0.4 percent (3σ) of the mean turn rate. Therefore, the standard deviation of the turn due to turn Gaussian rate variations is

$$\sigma_{try} = 0.00133\ Y \tag{A-7}$$

$$\sigma_{trp} = 0.00133\ P \tag{A-8}$$

where

Y is the yaw turn in degrees

P is the pitch turn in degrees

$\sigma_{try}\ \sigma_{trp}$ is the standard deviation of the yaw or pitch turn rate variation in degrees

The resolution of the C&S timer is ±0.5 seconds. The distribution is uniform, and, therefore, the distribution of the turn uncertainty due to the C&S timer is also uniform (±0.089 degrees). The total turn uncertainty is described by the sum of the two error sources.

A.3.5. AUTOPILOT ERRORS

The autopilot controls the thrust vector so that this vector is directed through the center of gravity of either the spacecraft or spacecraft and capsule. There are basically two error categories in which all of the autopilot error sources may be classified. These two error categories are steady-state errors and transient errors. The steady-state errors are those which remain after the autopilot has achieved steady-state conditions. Transient errors are the remaining errors in the autopilot because of insufficient time to obtain steady-state operation. Each of these categories of errors are analyzed separately.

A.3.5.1. Steady-State Errors

The steady-state error is a function of alignment errors, center of gravity errors and feedback gain in the autopilot. Alignment errors are those associated with the misalignment of the thrust vector to the vehicle axes. This includes:

a. Thrust misalignment relative to the engine, which is 0.2 degree (3σ Gaussian)

b. Engine misalignment relative to the vehicle which is considered as being 0.05 degrees (3σ Gaussian).

Thus the autopilot alignment error (δ_t) is 0.2085 degrees (3σ Gaussian).

The center of gravity errors are associated with the lateral displacement of the thrust axis from the vehicle center of mass, expressed as an angle (δ_{cg}). Uncertainties in the lateral displacement of the center of mass are listed below. These uncertainties were based upon the Task B design. However, they are considered to be representative of the present design. The uncertainties are mainly due to antenna and scan package movements.

a. Maximum uncertainty during midcourse maneuvers is 0.09 inches (3σ Gaussian)

b. Maximum uncertainty during the retromaneuver is 0.573 inches (3σ Gaussian)

c. Maximum uncertainty during orbit trim maneuvers is 1.0 inches (3σ Gaussian)

Table A-2 gives the distances between the thrust hinge point and the center of mass. Using these distances, the above displacement uncertainties can be converted to angular uncertainties as follows:

a. Midcourse 0.0716 degrees (3σ Gaussian)

b. Orbit insertion 0.566 degrees (3σ Gaussian)

c. Orbit adjust 1.03 degrees (3σ Gaussian)

Thus, the center of gravity errors are expressed in terms of the angle (δ_{CG}), and this angle is described as having a Gaussian distribution with a mean equal to zero and a standard deviation depending upon the maneuver to be performed.

Table A-2. Summary of Distance Between the Thrust Hinge Point and CG

Mission description	ℓ inches
Transit Separated spacecraft- antenna deployed before midcourse correction.	71.9
After midcourse correction antenna deployed	72.9
After retro burn capsule on	85.2
After orbit adjust psp deployed capsule off	46.9

The analysis of the autopilot performance of steady-state error depends upon the spacecraft response to the disturbance torques resulting from the relative center of mass offset and the thrust misalignment. Figure A-3 illustrates the geometry and sign convention used in the definition of the spacecraft.

Using small angle approximations, the thrust direction is given by

$$\beta = \delta - \theta + \delta_t \tag{A-9}$$

where β is the thrust vector angle

θ is the response angle

δ_t is the misalignment angle

δ is the error angle.

The steady-state pointing error is given by the following equation:

$$\beta_{ss} = \delta_{ss} - \theta_{ss} + \delta_t \qquad \text{(A-11)}$$

However, in the steady-state, the net torque on the spacecraft will be reduced to zero, so that

$$\delta_{ss} = -\delta_{CG} - \delta_t \qquad \text{(A-11)}$$

Thus, the steady-state thrust pointing error β_{ss} is

$$\beta_{ss} = -\delta_{CG} - \theta_{ss} \qquad \text{(A-12)}$$

The spacecraft response (θ) to the disturbance torques resulting from the relative center of mass offset and the thrust misalignment is given by

$$\frac{\theta(S)}{\delta_T + \delta_{CG}(S)} = \frac{G(S)}{1 - K_\theta \; G(S)\, H(S)} \qquad \text{(A-13)}$$

where $G(S)\ H(S)$ is the open loop transfer function

K_θ is the feed back gain

$G(S)$ is the forward transfer function

The steady-state spacecraft attitude resulting from the step input of disturbances is given by:

$$\theta_{SS} = \lim_{s \to o} S\ \theta(S) = \frac{\delta_T + \delta_{CG}}{K_\theta} \qquad \text{(A-14)}$$

Using the above results in equation (A-12) yields the following equation for the steady-state thrust pointing error.

$$\delta_{SS} = -\delta_{CG}\left(1 + \frac{1}{K_\theta}\right) - \delta T/K_\theta \qquad \text{(A-15)}$$

If the feedback gain is chosen large, then the steady-state thrust pointing error is approximately equal to the angular offset of the center of mass.

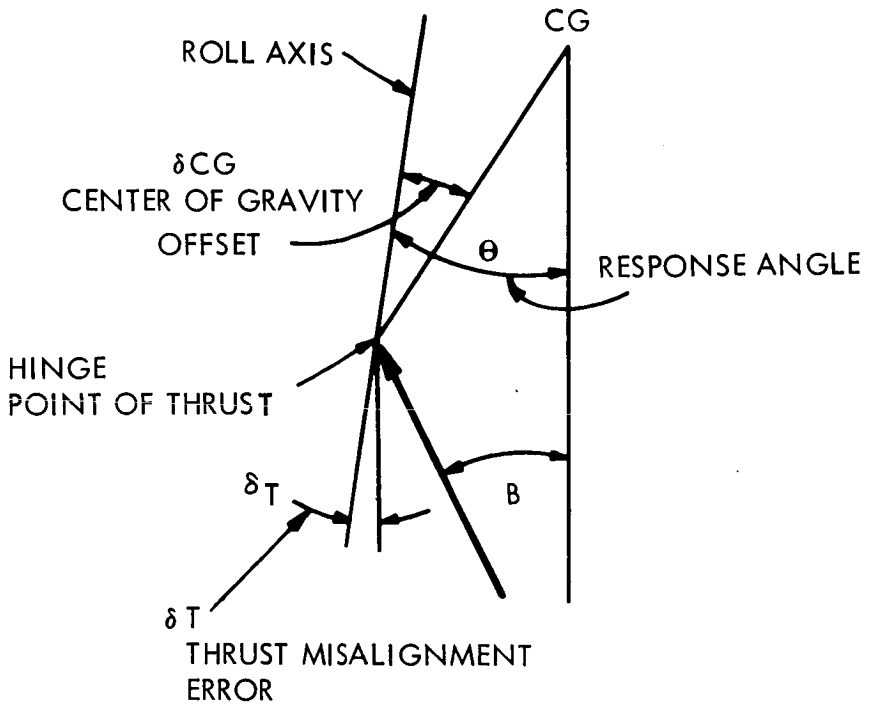

Figure A-3. Geometry and Sign Convention

The probability distribution β_{SS} is Gaussian since it is the result of the summation of two Gaussian random variables. The variance of β_{SS} is

$$\sigma^2_{\beta_{SS}} = (1 + \frac{1}{K_\theta})^2 \sigma^2_{\delta_{CG}} = (\frac{1}{K_\theta} \sigma_{\delta_T})^2 \qquad \text{(A-16)}$$

The mean or expected value of the steady-state thrust pointing error is zero since the two contributors have zero means.

Since the variance of the offset in mass varies with the maneuver to be performed, so will the steady-state thrust pointing error.

Figure A-4 illustrates the relationship between the magnitude of steady-state pointing errors and the feedback gain. This plot was developed for the following conditions:

a. The thrust misalignment variance $\sigma_T^2 = 0.0049$ (degrees^2)

b. The center of mass offset variance has been parameterized and allowed to vary from 0.001 to 0.4 (degrees^2).

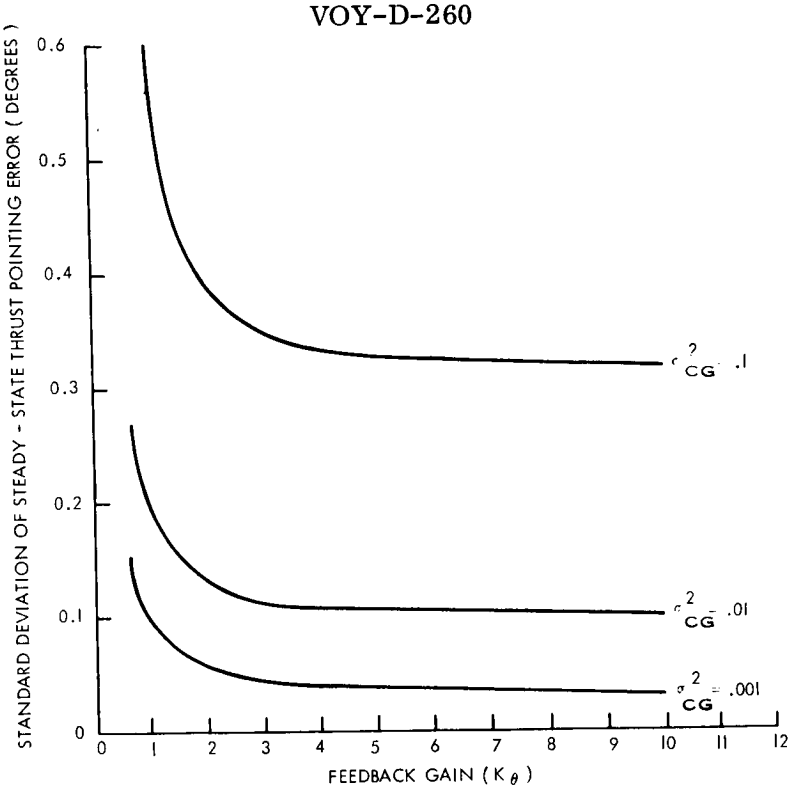

Figure A-4. Pointing Error vs Feedback Gain

The center of mass will shift during the thrusting of the maneuver, however such changes in the center of gravity present a ramp driving function for the autopilot. The response is due to such a disturbance is given by

$$\theta_{ss} = \lim_{s \to o} s \; \theta(s) = \infty \tag{A-17}$$

Thus, such center of mass shifts will not be completely compensated for by the autopilot. However, these shifts will be in the direction of reducing the initial error due to the shift of the center of mass. This compensation is obtained because the center of mass moves further from the pivot point of the propulsion nozzle as the fuel is consumed. Since, these effects will tend to reduce the steady-state error it is conservative to neglect such shifts during the application of thrust. This effect should be checked by simulation.

Because the center of mass uncertainty was felt to be a prime variable in the analysis and the center of mass is dependent upon the final design of the spacecraft, this variable was parameterized in the results presented in Paragraph A.2.3.

A.3.5.2. Transient Errors

The transient errors resulting from the termination of thrust before the autopilot can remove all errors and maintain the steady-state error are being investigated by a 3-axes simulation of the vehicle and the autopilot.

One of the main causes of long transient errors is the fluid motion within the fuel tanks. These fluid motions are to be included in the simulation so their effects can be observed.

Because the results of the three axes simulation was not available at the time of this writing, the transient errors were parameterized in the next section. The analysis was conducted for the transient standard deviations (σ_{tr}) of 0.001, 0.01, and 0.1 degrees.

A.4. RESULTS

Equations A-2 and A-3 were programmed on a digital computer and all of the components of uncertainty were sampled by the Monte Carlo method. Two hundred samples were taken by each error source, and the two components of error ξ_x and ξY were determined. The resultant cone angle error ξ_z of the two components,

$$\xi_z = \sqrt{\xi_x^2 + \xi_y^2} \tag{A-18}$$

was calculated and its distribution analyzed for various values of σ_{CG}, σ_{tr}, Y, P, and K_θ.

In general, it was found that the distribution of ξ_z could be represented by the Rayleigh distribution. This implies that the two components of ξ_x and ξy can be considered to be independent with a normal distribution described by a zero mean and a standard deviation given by the following equation.

$$\sigma_{\xi y} = \sigma_{\xi x} = \xi_z \cdot \sqrt{2/\pi} \tag{A-19}$$

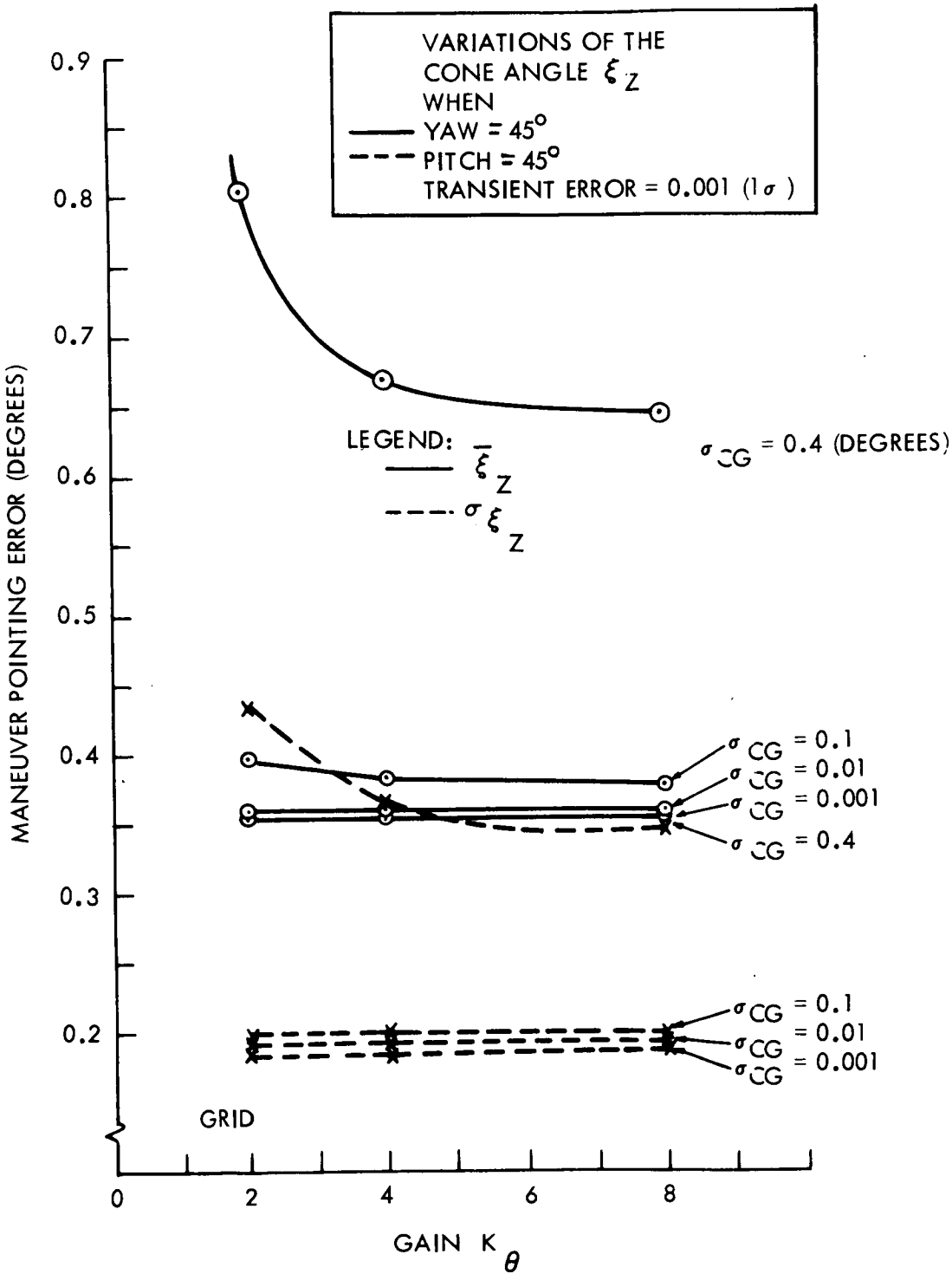

Figure A-5. Maneuver Error Parameters (Transient Error = 0.001)

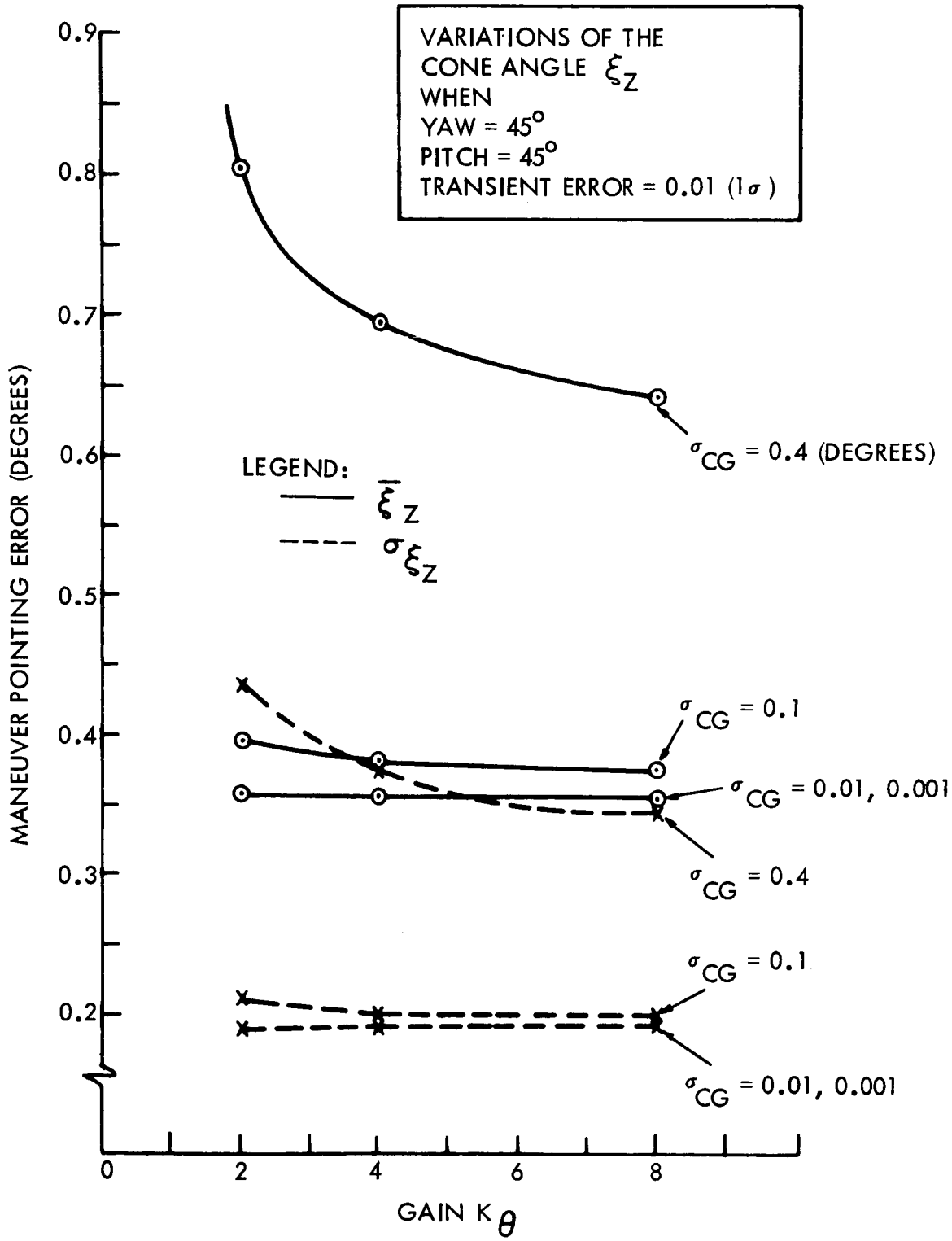

Figure A-6. Maneuver Error Parameters (Transient Error = 0.01)

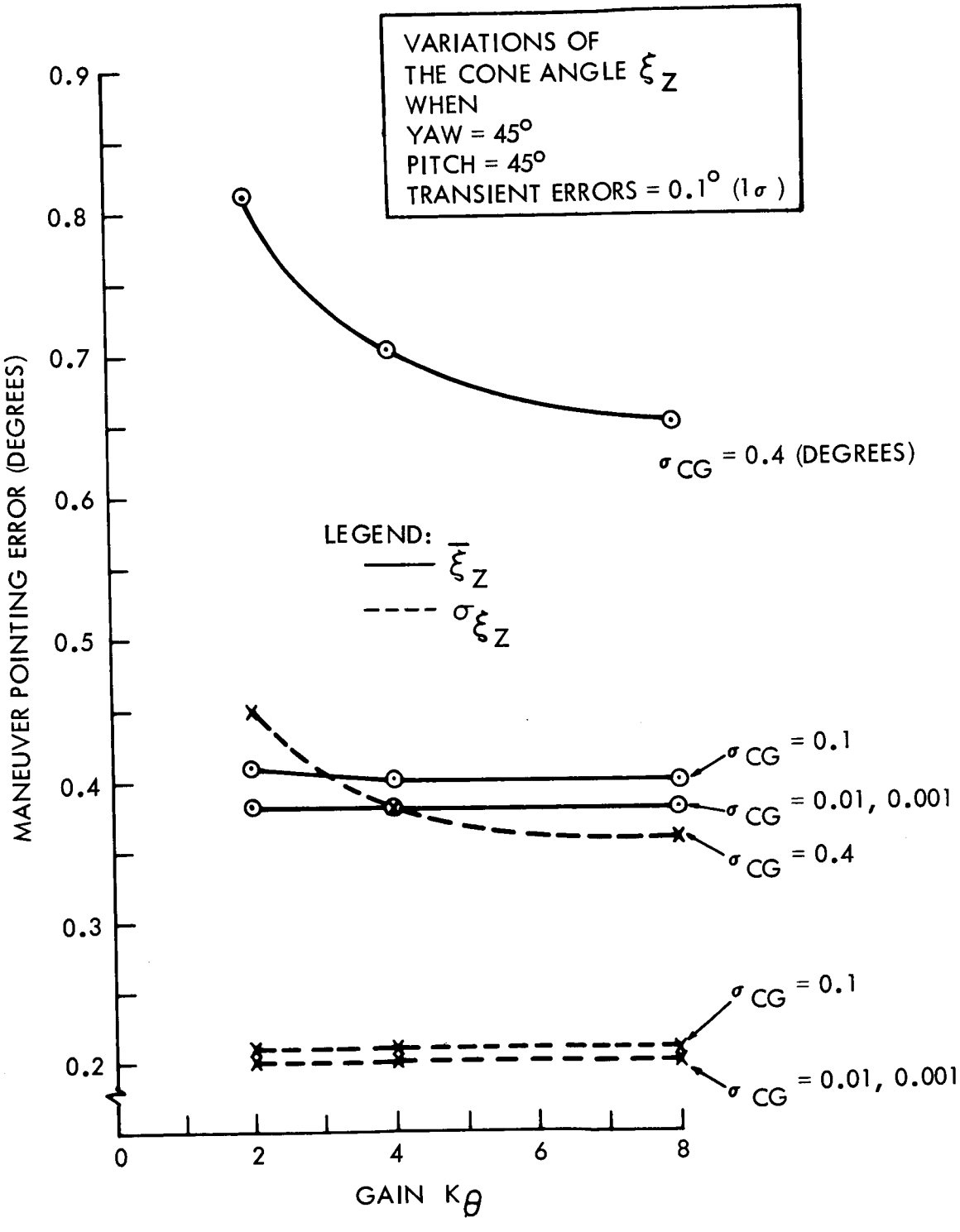

Figure A-7. Maneuver Error Parameters (Transient Error = 0.1)

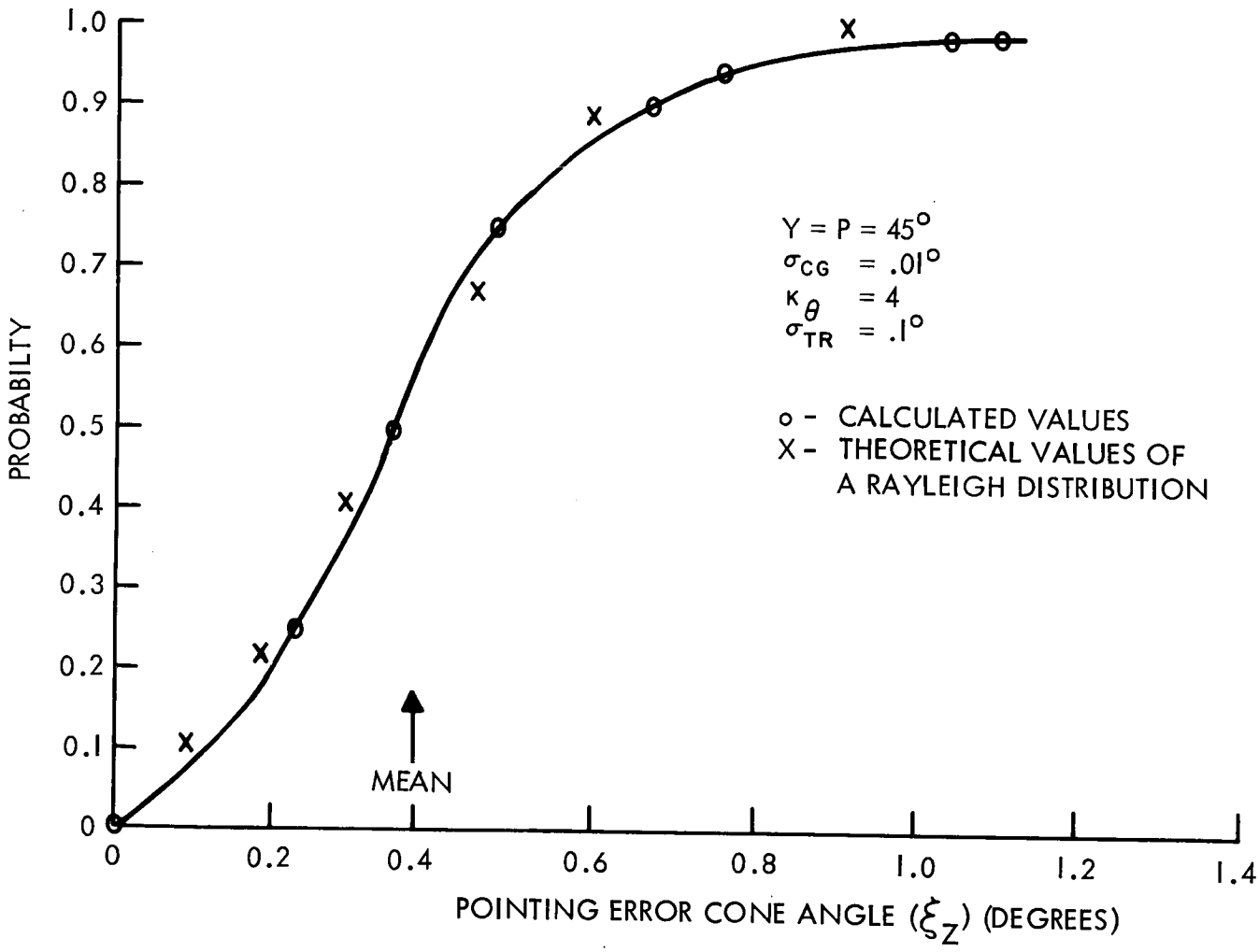

Figure A-8. Typical Cumulative Probability Function of the Cone Angle

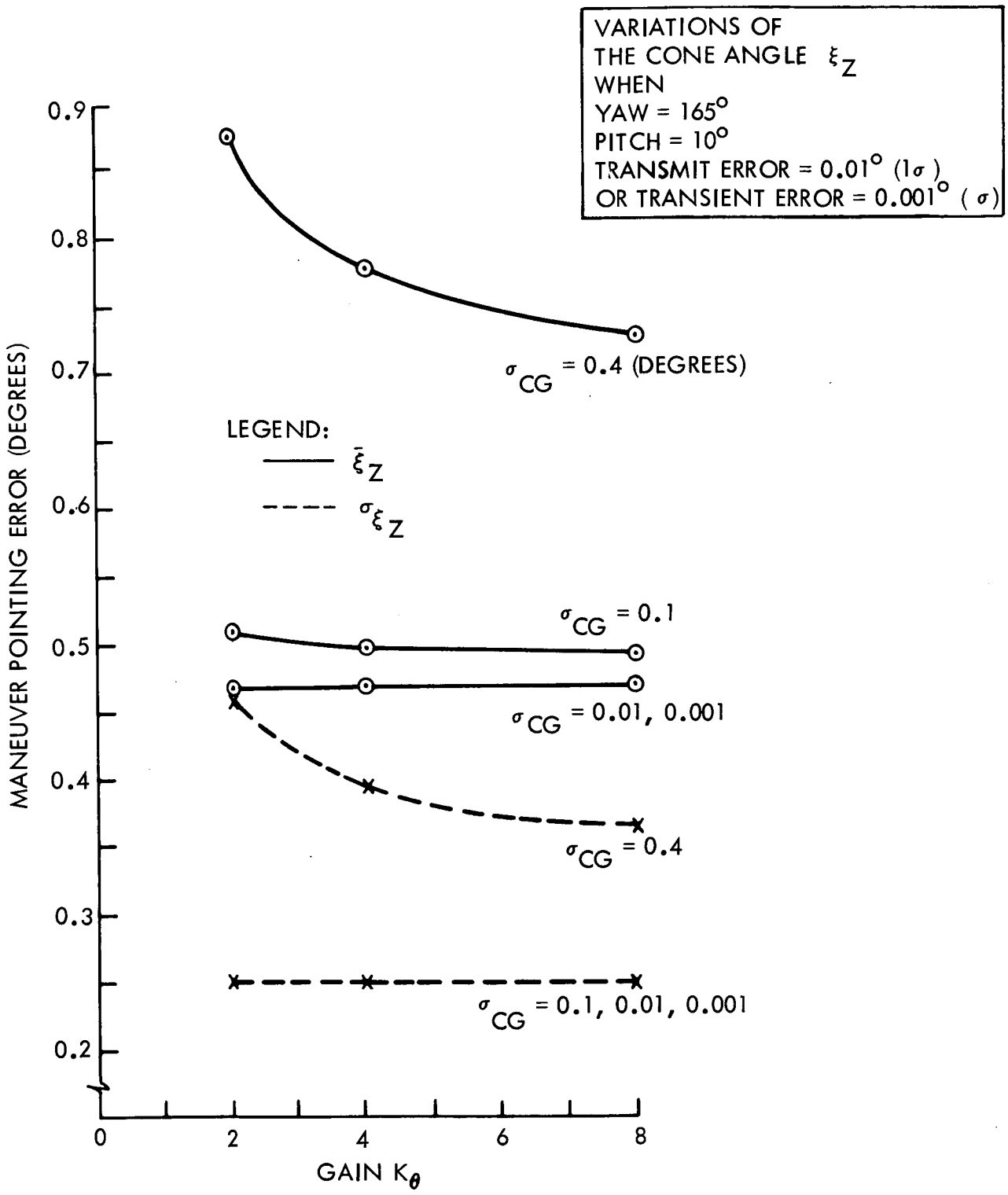

Figure A-9. Maneuver Error Parameterizations (Transient Error = 0.001)

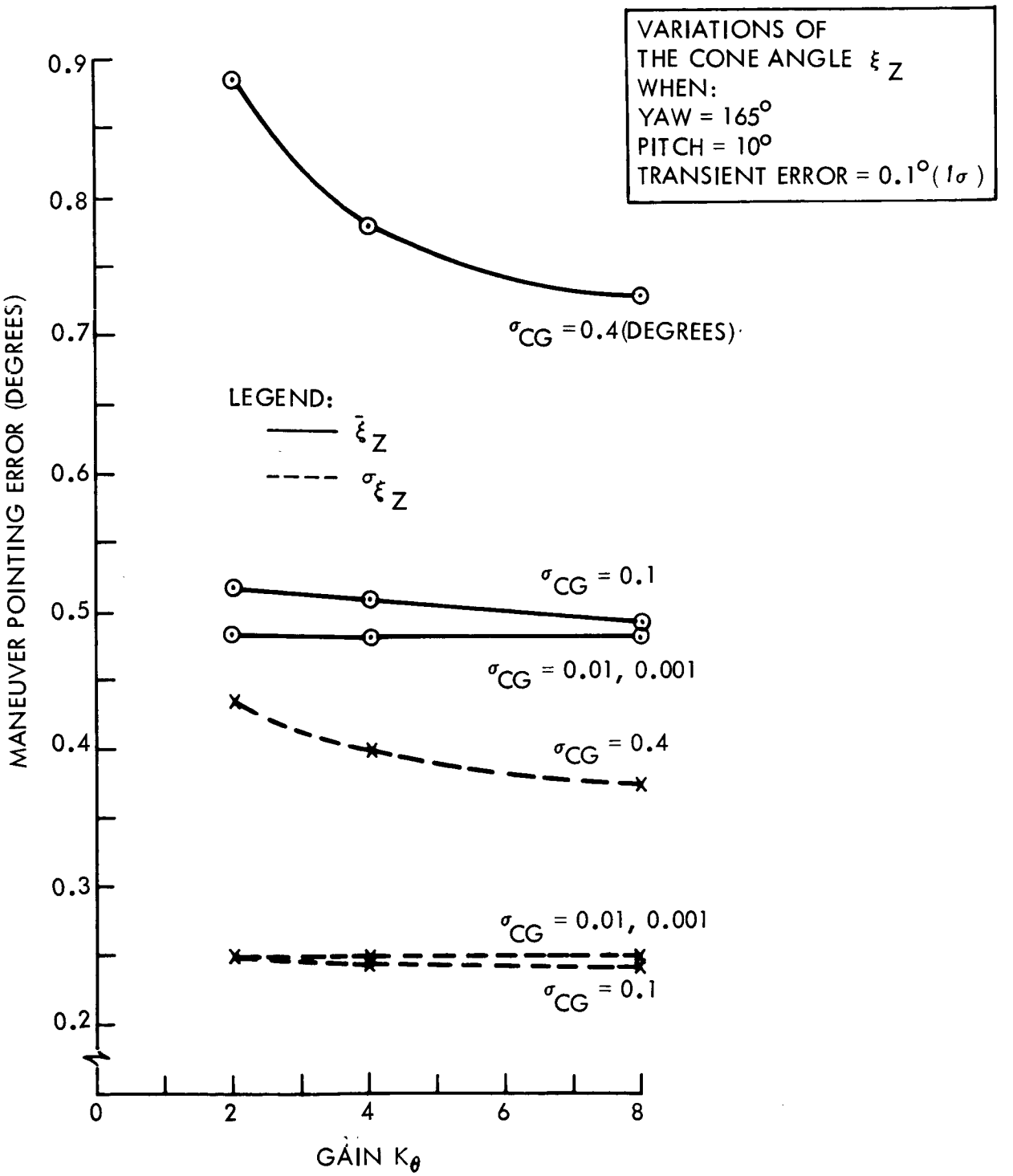

Figure A-10. Maneuver Error Parameterizations (Transient Error = 0.1)

In all cases there was a variation of $\bar{\xi}_z$ with the parameter investigated; thus, the distribution of the components ξ_y and ξ_x were not stationary and depended upon the yaw-pitch turn.

Two turns were investigated in detail. These were a yaw-pitch turn of 45 - 45 degrees and a yaw-pitch turn of 165 - 10 degrees. The feedback gain K_θ was varied from 2 to 8 and the standard deviations of the transient error (σ_{tr}) and center of mass offset (σ_{CG}) were varied over a range from 0.001 to 0.1 degrees, and 0.001 to 0.4 degrees, respectively.

Figures A-5, A-6 and A-7 give the mean, ξ_z, and the standard deviation, σ_{ξ_z} as a function of the transient error, center of gravity offset and the feedback gain for a yaw-pitch turn of 45 - 45 degrees. Figure A-8 illustrates a typical cumulative probability function of ξ_z. The shape of this function suggests the Rayleigh distribution. Figures A-9 and A-10 give the mean ξ_z and the standard deviation σ_{ξ_z} as a function of the transient error, center of gravity offset and feedback gain for a yaw-pitch turn of 165 - 10 degrees. For this turn sequence, the distribution of the cone angle ξ_z was investigated and also found to be nearly Rayleigh.

Figure A-11 is a plot of a Rayleigh distribution parameterized in terms of the mean, ξ_z. Various texts describe the Rayleigh distribution and give tables of the distribution, in addition the cumulative probability is given by the following equation.

$$P(\xi_z \leq E_z) = 1 - \mathrm{Exp}\left(-\pi E_z^2 / 4\bar{\xi}_z^2\right) \tag{A-20}$$

Confidence in the estimates can be established by noting that the standard deviation of the mean is the ratio of the measured estimate of the standard deviation and the square root of the number of Monte Carlo samples; i.e.,

$$\sigma_{\bar{\xi}_z} = \sigma_{\xi_z} / (200)^{1/2} \tag{A-21}$$

Typical values of the standard deviation estimate $\sigma_{\bar{\xi}_z}$ is 0.30 (degrees). Thus, the standard deviation of the estimate of the mean is typically

$$\sigma_{\bar{\xi}_z} = 0.30/(200)^{1/2} = 0.02125 \text{ (degrees)} \tag{A-22}$$

The mean values noted in the previous figures lie within ± 0.0625 degrees (3σ) with 99.7 percent confidence. The respective confidence limits of the standard deviation of the components ξ_x, ξ_y are ± 0.05 degrees (3σ).

One additional variable was investigated. This variable was the alignment errors of the sensor mountings. The standard deviation of this variable was varied over one order of magnitude from 0.0167 to 0.167 degrees while the feedback gain was held constant at 4.0 and the center of gravity shift and transient errors were varied from 0.001 to 0.1 (1σ) degrees. Figures A-12 and A-13 present the results of this investigation. Notice that an alignment of sensor mountings of 0.0835 degrees (1σ) does not significantly effect the mean ξ_z.

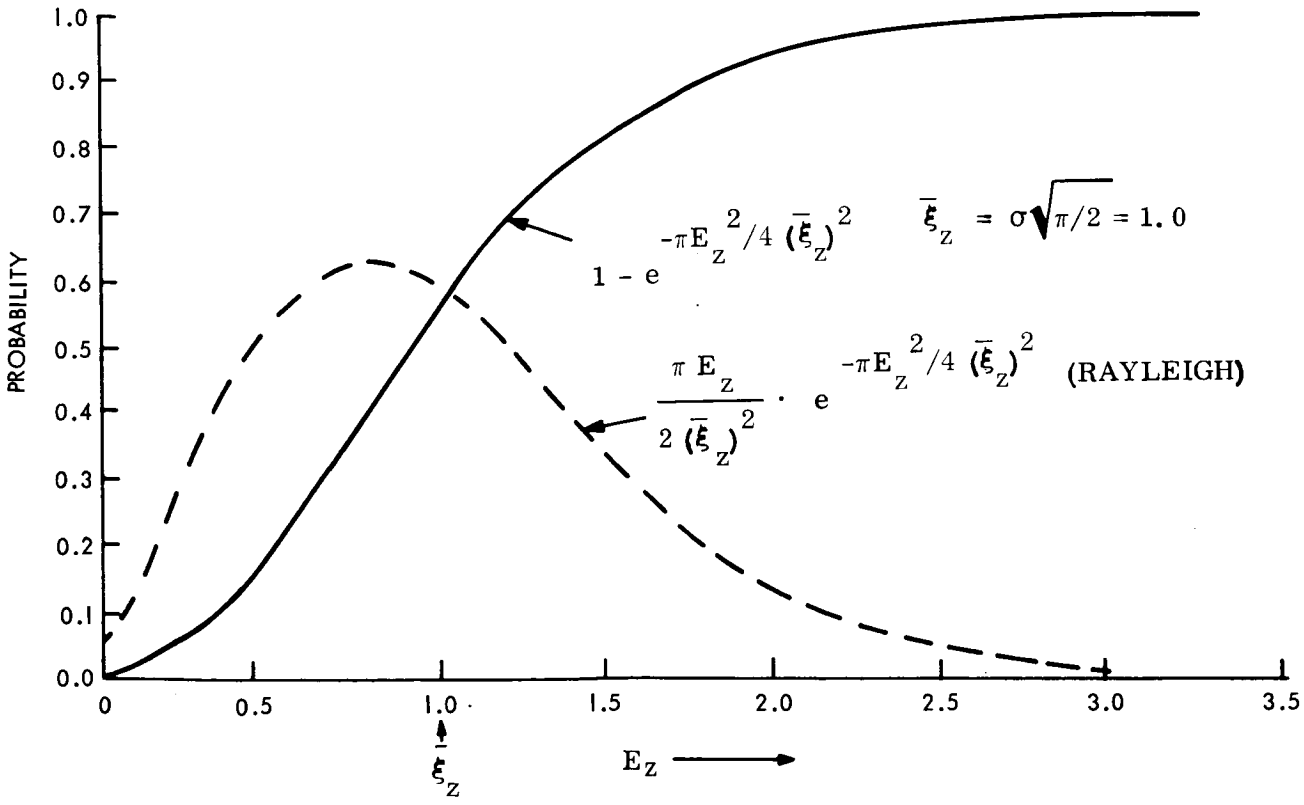

Figure A-11. Probability Distribution of Pointing Error as a Function of Pointing Error and the Mean Error

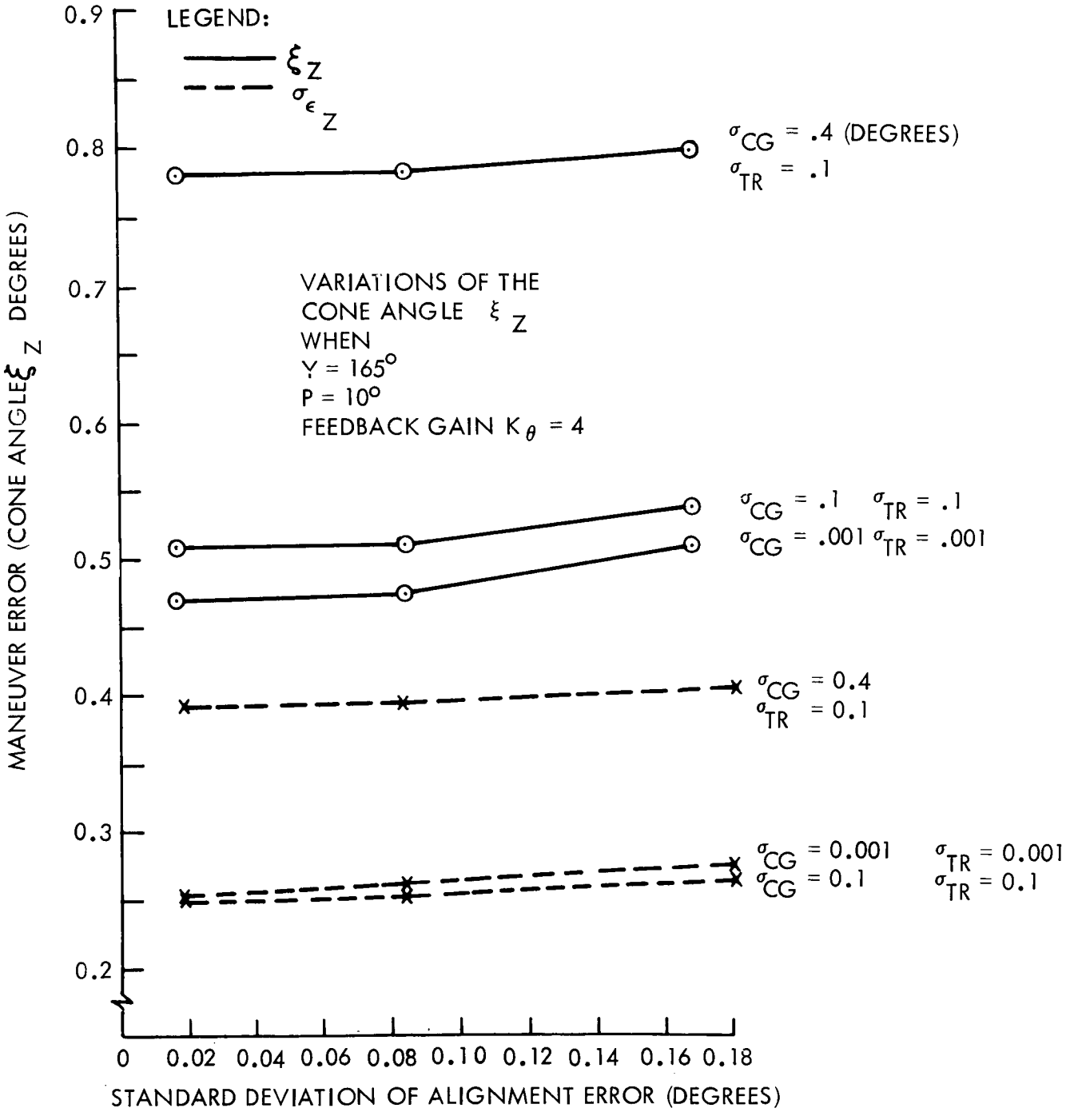

Figure A-12. Investigation of Alignment for a 165 - 10 Degree Turn

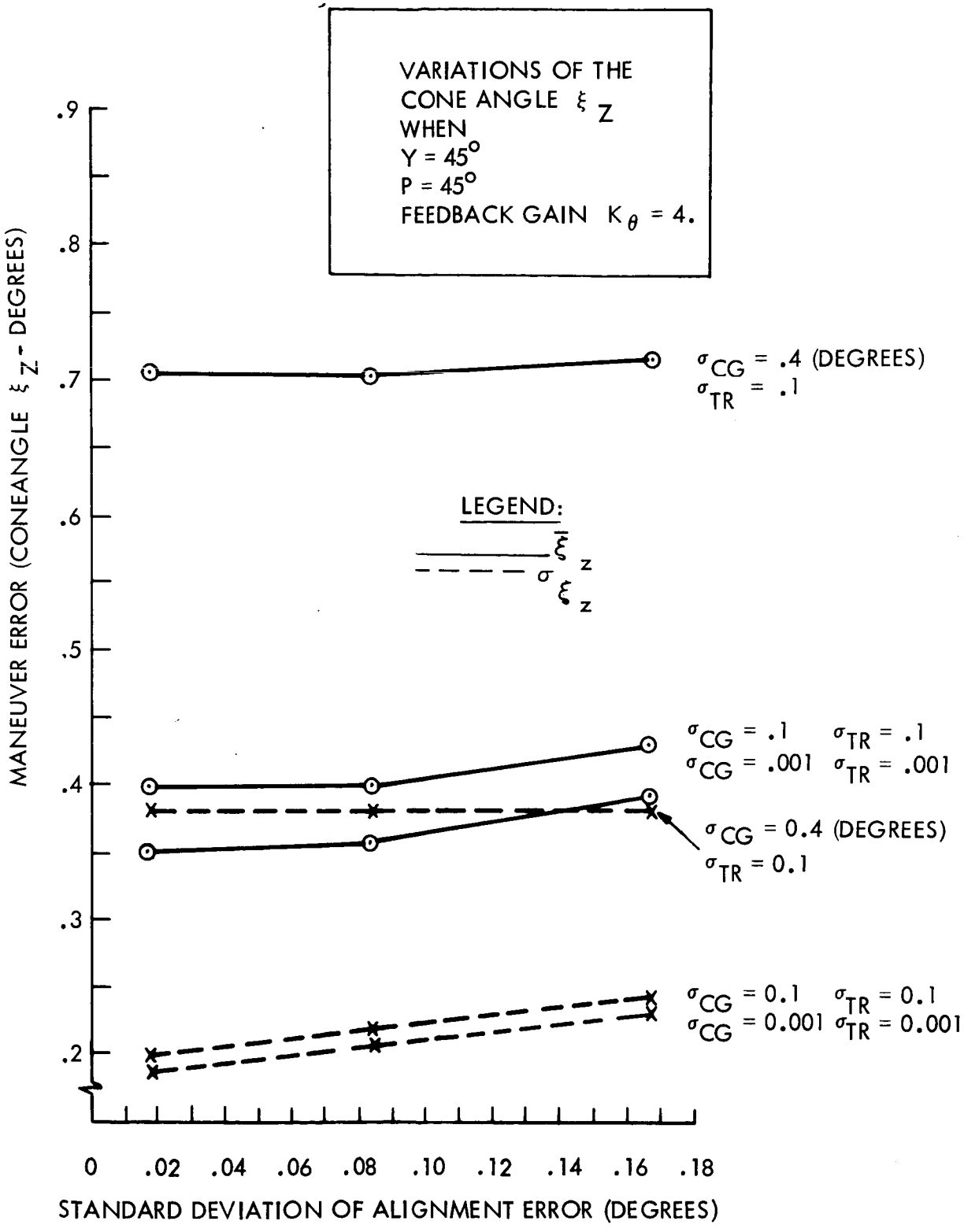

Figure A-13. Investigation of Alignment Error for a 45 - 45 Degree Turn

A.5. CONCLUSIONS

The largest 3 σ maneuver pointing error for the component errors of ξ_x and ξ_y established in this study is 2.13 $\pm$ 0.291 degrees. This occurs for a center of gravity offset standard deviation of 0.4 degrees, a yaw-pitch turn sequence of 165 to 10 degrees, a feedback gain of the autopilot of two, and an alignment standard deviation of 0.0165 degrees. Increasing the alignment to 0.0835 degrees will increase this 3 σ value to 2.13 $\pm$ 0.30 degrees. Using the center of gravity offset errors for the Task B design as typical of the offset errors for the new configuration, the pointing errors for each component error of ξ_x and ξ_y are estimated as:

a.	During midcourse maneuvers	0.975 ± .1756 (3 σ) degrees
b.	During orbit insertion	1.52 ± .1924 (3 σ) degrees
c.	During orbit trims capsule off	1.98 ± .2627 (3 σ) degrees.

The impulse accuracy of the thrust vector was obtained from the engine manufacturer. The estimates of 3 σ velocity errors are:

a.	During midcourse maneuvers	0.0756 (3σ) m/sec
b.	During orbit insertion	0.757 (3σ) m/sec
c.	During orbit trims capsule off	0.280 (3σ) m/sec ·

VOY-D-271
TRANSMITTER POWER-ANTENNA GAIN SELECTION

1. INTRODUCTION AND SUMMARY

The product of the antenna gain and the transmitted power is of major importance because of the desire for high data rates in the Voyager Mars missions. Communication distances in the 1973 mission are larger than those considered in the Task B design. This increase in communication distance results in a larger gain-power product required to maintain the same data rate. In addition the specified worse case capability of the DSN has decreased 3 db compared to that in Task B. Improvement of the power-gain product involves many subsystems; therefore, a trade study was conducted to establish the optimum gain-power product for a given Spacecraft. This trade study involves the following subsystems:

a. Radio Subsystem
b. Power Subsystem
c. Computer and Sequencer Subsystem
d. Attitude Control Subsystem

In these subsystems, the antenna size, solar array size, solar pressure balance, attitude control dead band, antenna stepping control, traveling wave tube wattage, and thermal control are varied to optimize the power-gain product as a function of system weight.

The design base for this trade study was the General Electric Task B design. Design approaches which depart from the Task B design were not considered; i.e., erectable antennas, closed loop antenna control, substantial increased computer capabilities, etc. The major design trade-offs are associated with the antenna pointing error, the antenna gain, the transmitter power and the resulting power gain product. These major design trade-offs are as follows:

a. The antenna pointing error as a function of weight can be optimally assigned to Attitude Control Subsystem dead band or the Computer and Sequencer Subsystem antenna stepping control. In paractice, there is an optimum assignment which minimizes the antenna pointing error for a given weight.

b. For an optimum antenna gain-weight characteristic, weight can optimally be allocated to the antenna and its solar pressure balancing method and to the Attitude Control and Computer and Sequencer Subsystems to reduce the pointing variations.

c. The transmitter power obtainable is also a function of weight; the weight increases due to solar array area, temperature controls of the power amplifier tube, and the weight of the power tube.

d. The power-gain product versus weight of all affected components is optimized by the proper assignment of weight to obtain the transmitter power and the antenna gain. The optimum product for a given weight defines the antenna size, solar array size, solar pressure balance method, attitude control dead band, antenna stepping control requirement, traveling wave tube wattage, and thermal control requirements.

This system study was reported in depth in milestone report, VOY-P-TM-12, "Antenna and Solar Array Sizing Trade Study." The following sections have been summarized from the trade study.

2. ANTENNA GAIN

2.1 POINTING ERROR ANALYSIS

Error analysis for the High-Gain Antenna (HGA) is modeled by matrix coordinate transformations of the effects of each system error and the normal rotation characteristics of the vehicle. The coordinate transformation matrixes may be approximated by the following equations:

$$\theta_x = \sum_i K_{xi} E_i \tag{1}$$

$$\theta_y = \sum_i K_{yi} E_i \tag{2}$$

Where θ_x and θ_y are the orthogonal components at the resultant pointing error, θ_z.

K_{xi} is the first order derivative of error in the x direction with respect to the error from the ith source, and

E_i is the magnitude of the error from the ith source.

This approximation is valid when the errors are small enough to employ the small angle approximations and the products of small rotations are negligible. It has been shown that a conservative estimate of the resultant error can be made by assuming independence of the two components.

The antenna pointing error results primarily from three error sources: the dead band of the Attitude Control Gas Subsystem, and the curve fit accuracy and quantization error of the high gain antenna pointing control. For antenna pointing control, the required pointing direction is linearized as a function of time and the antenna pointing direction with respect to the spacecraft is changed in steps. The error due to linearizing the pointing direction as a function of time is defined as the curve fit accuracy, and the deviation from the linearized antenna pointing direction due to stepped control is the quantization error. The magnitude of each error is controllable by the expenditure of weight, computer and sequencer excess memory capacity and a negligible change in reliability.

Figure 1 gives the weight of the Attitude Control Subsystem as a function of the expected pointing error. Both the curve fit accuracy and gimbal quantization error can be varied over the range necessary without penalty to the system weight or reliability.

2.2 ANTENNA GAIN VERSUS WEIGHT

The antenna gain is a function of the antenna size, the pointing error, the frequency of the transmitted signal, and the aperture efficiency. In addition, as the antenna increases in size,

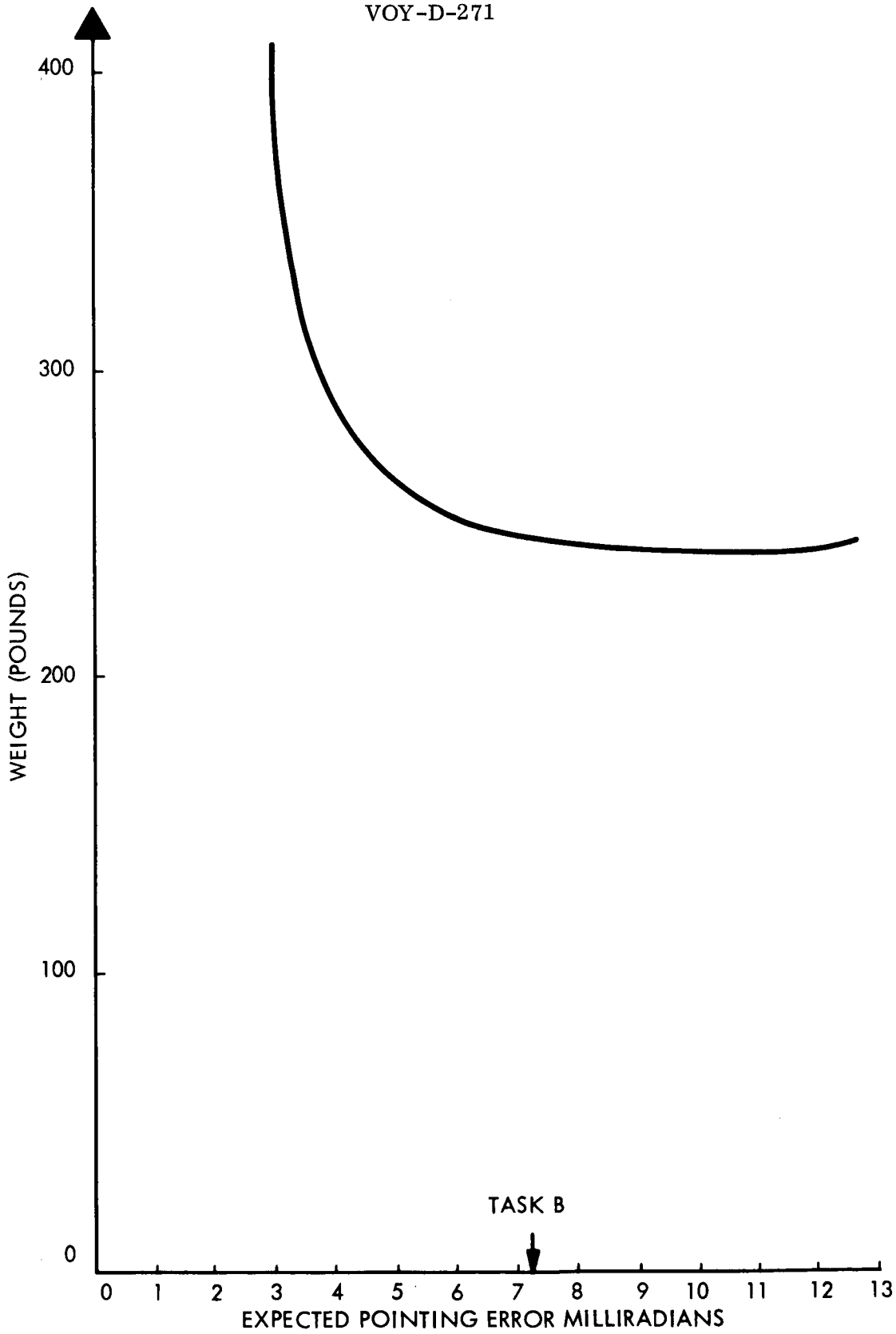

Figure 1. Weight of the Attitude Control Subsystem As A Function of Expected Pointing Error

solar radiation pressure produces a mechanical couple which must be counteracted by either increased attitude control gas or by the implementation of a solar vane.

Figure 2 shows the antenna gain as a function of the reflector size and pointing error. Aperture efficiency and frequency are fixed and defined in VOY-D-311.

The antenna weight is a function of the reflector size, deployment mechanism and actuator weight. The weight shown in Figure 3 includes these mechanisms and is sized in all cases for the resonant frequency needed to satisfy autopilot requirements.

As the antenna becomes larger, solar pressure exerts a mechanical couple about the spacecraft center of gravity. This couple must be balanced either by additional firings of the attitude control gas jets or by a solar vane. Either method requires additional weight, and there is an optimum allocation of weight to the solar vane and attitude control gas as a function of the high gain antenna size.

Figure 4 gives the optimum weight of the antenna and the balance method as a function of antenna size. Below eight feet, pressure balance is not required. Between 8 feet and 12.2 feet, additional control gas is the optimum method to balance the solar torque. Above 12.2 feet, the optimum method is a solar vane. No optimum combination of a solar vane and use of attitude control gas for solar pressure balancing was found because of the initial weight required for deployment of a solar vane.

2.3 OPTIMIZATION OF ANTENNA SIZE AND POINTING ERROR

The antenna gain is optimized as a function of the expected pointing error and the antenna size. From this optimization for a given weight, the optimum allocations of weight to the antenna and its balancing method and to the reduction of pointing error by increasing the weight of the attitude control gas and by increasing the number of gimbal commands in the Computer and Sequencer Subsystem have been determined.

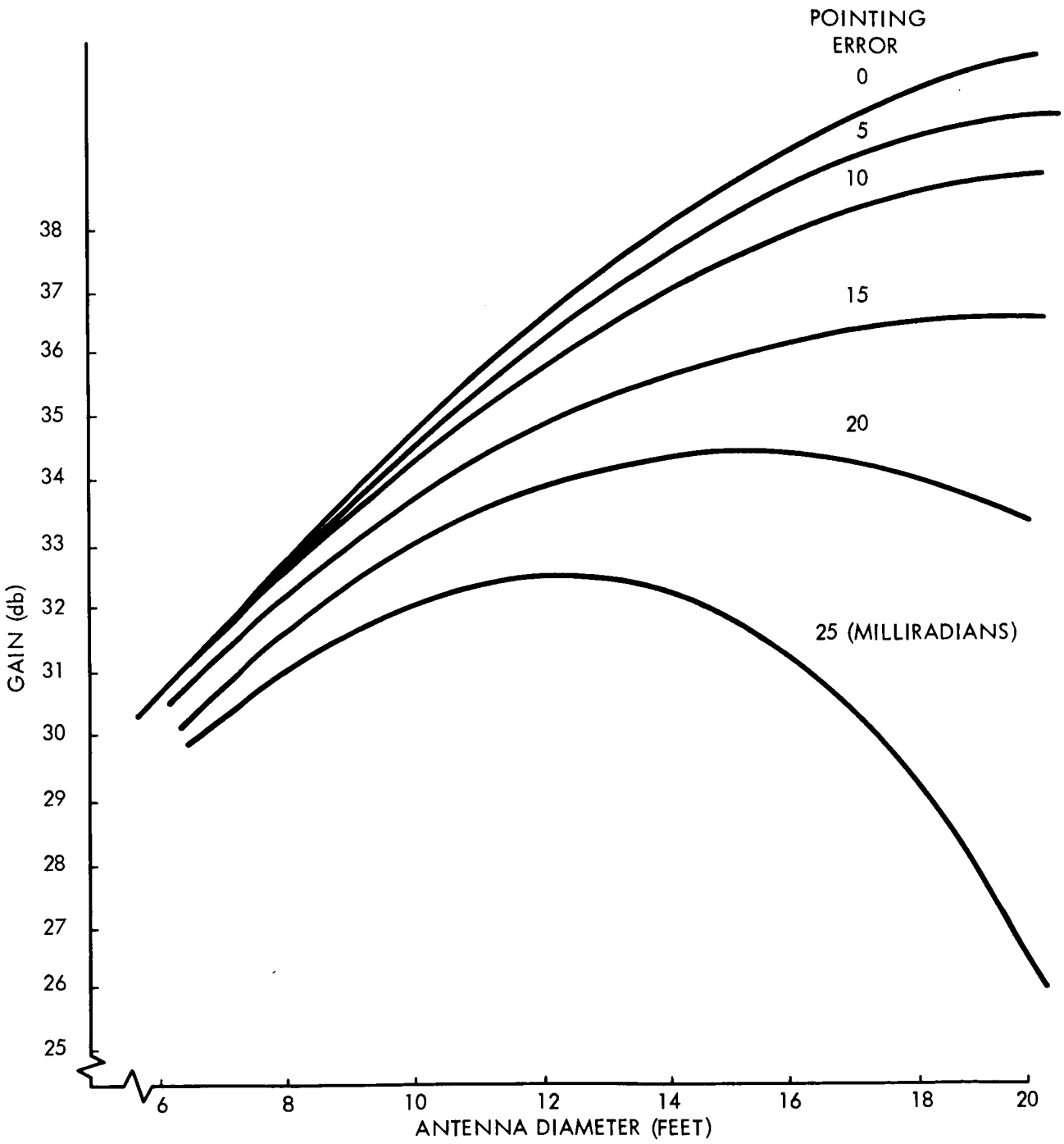

Figure 2. Gain-Pointing Error Relationships

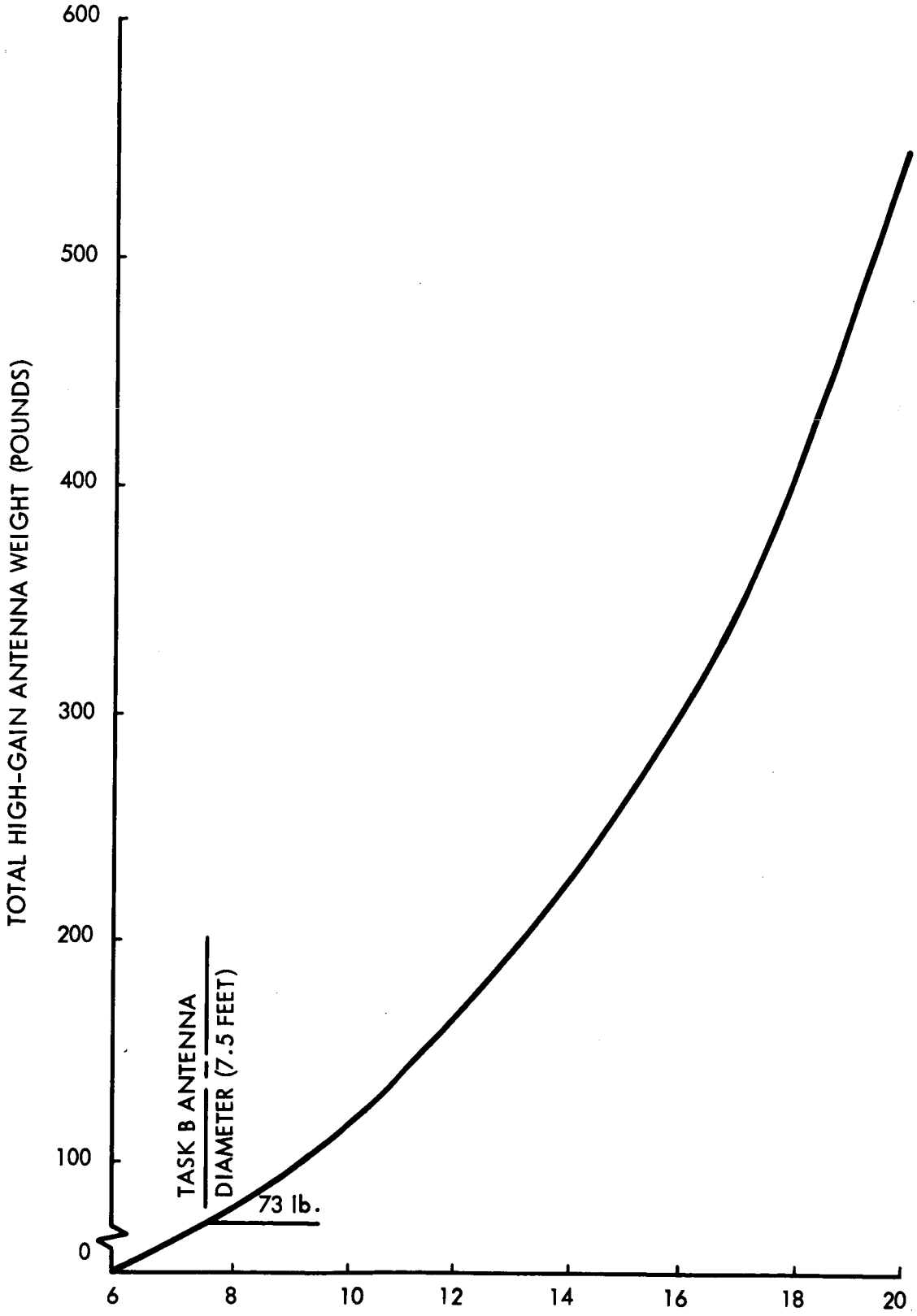

Figure 3. High-Gain Antenna Weight As A Function of Antenna Diameter

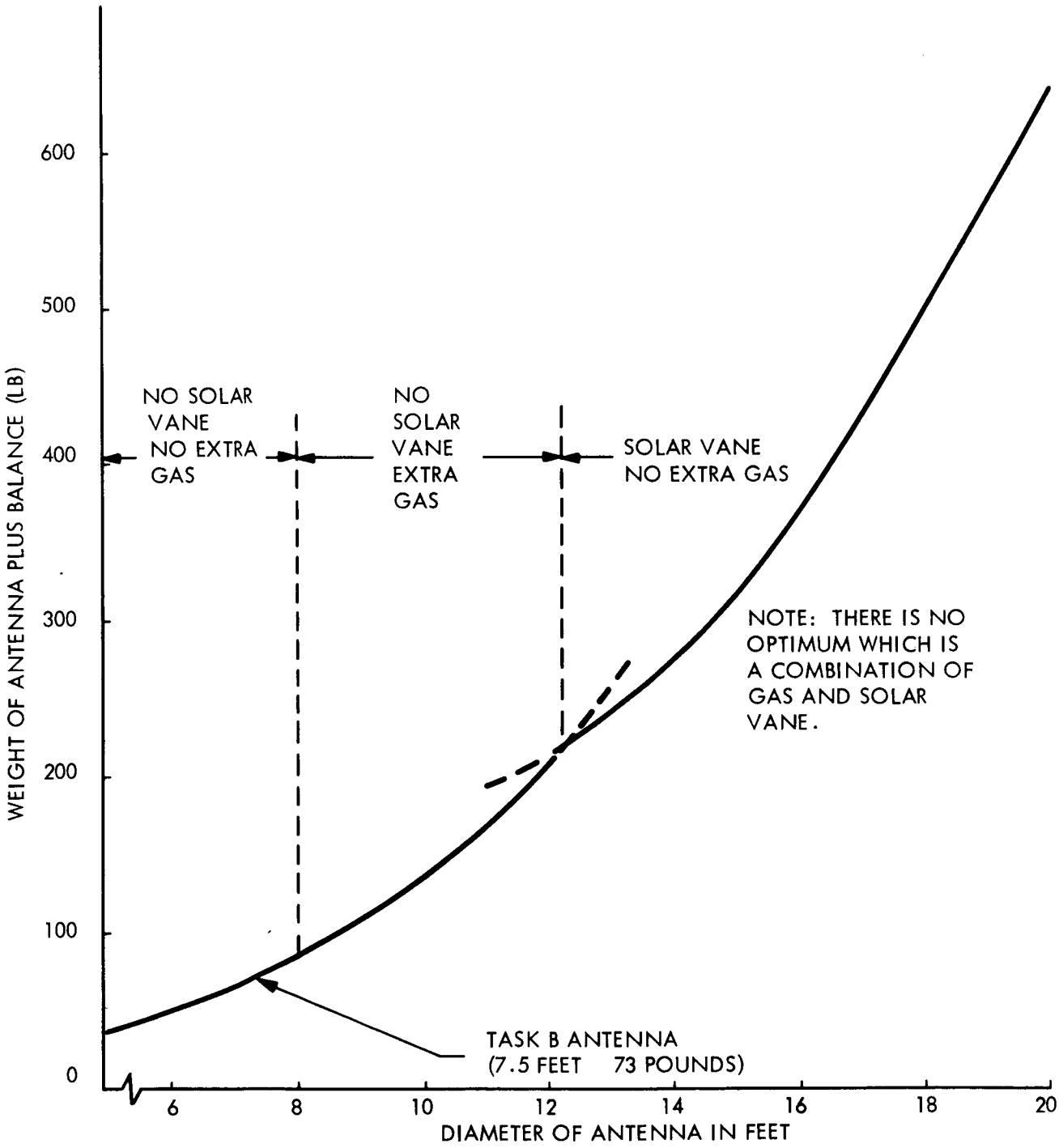

Figure 4. Optimum Assignment of Weight As A Function of Diameter of the Antenna

Figure 5 gives the result of the optimization. This curve was generated by applying weight to either the reduction of expected pointing error or to the increase in antenna diameter and balancing method. The size of the antenna and the expected pointing error are labeled on the optimum gain curve. As the antenna size increases, the expected pointing error must decrease for an optimum weight system.

3. TRANSMITTER POWER

3.1 RADIO SUBSYSTEM WEIGHT

In the power range of interest, 20 to 100 watts, only a 20-watt tube exists in a fully space-qualified form (Apollo development). Two other tube sizes, specifically 50 and 100 watts, have been built and operated at their respective levels. Table I gives an estimate of Radio Subsystem weight for the three transmitter power levels and assumes two power amps per system.

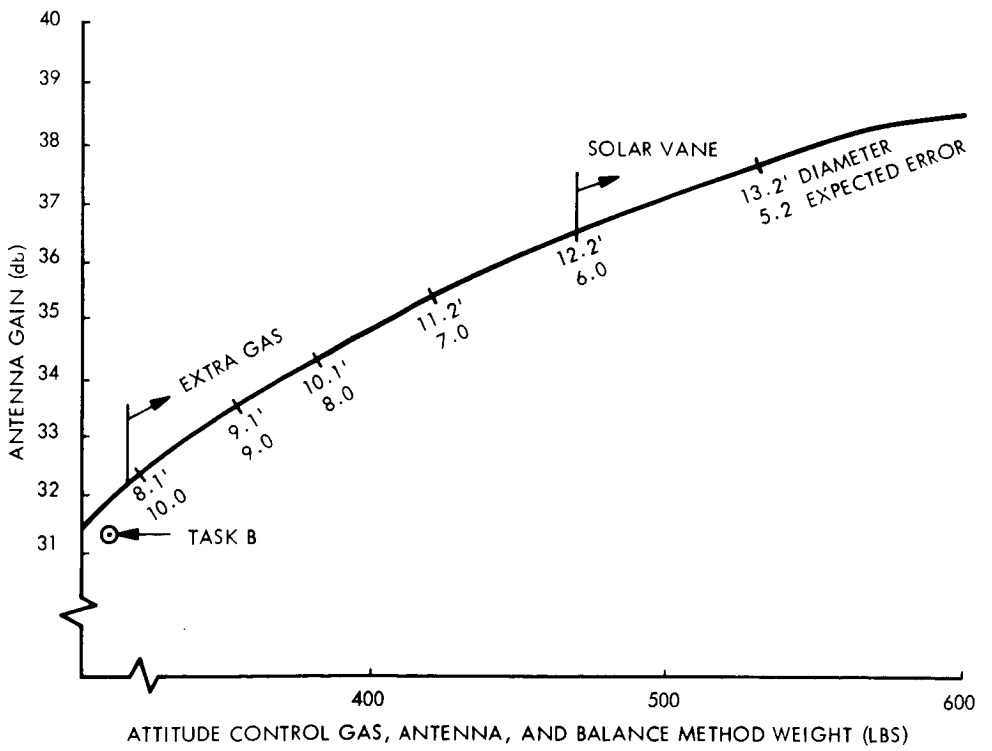

Figure 5. Optimum Gain Versus Weight

Table I. Radio Subsystem Weight Estimates

	20-watt	50-watt	100-watt
Power Amplifier	10 lb	15 lb	20 lb
Antenna and Deployment	73 lb	73 lb	73 lb
Radio Subsystem	182.3 lb	187.3 lb	192.3 lb

3.2 POWER SUBSYSTEM WEIGHT

The Power Subsystem was sized to supply unregulated dc power to the transmitter and estimated power requirements for all other purposes. The transmitter raw power level design points selected were 60, 150 and 300 watts corresponding to 20, 50 and 100 watts of transmitted power. Figure 6 presents the required solar array area as a function of transmitter power. Also shown in Figure 6 is the total Power Subsystem weight as a function of raw transmitter power.

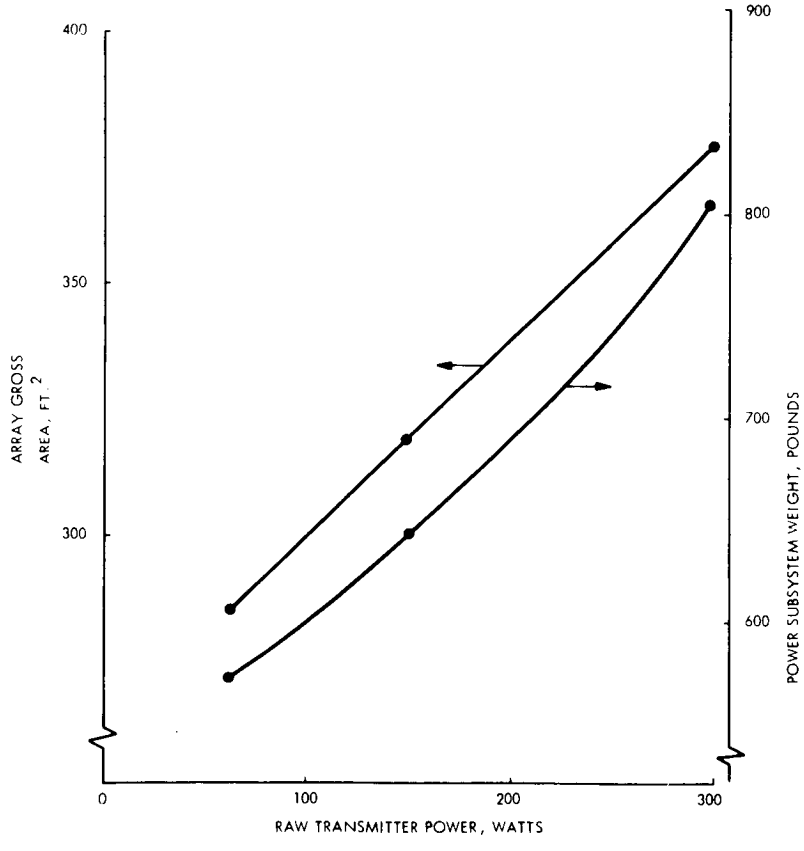

Figure 6. Solar Array Area And Power Subsystem Weight

Battery sizing was based on the use of nickel-cadmium batteries for orbital eclipse loads with silver-zinc batteries being used to provide the additional peak power required during orbit insertion and other high usage periods. Table II gives the weights of the batteries as a function of transmitted power.

Table II. Power Versus Weight (lb)

Power	Radio Subsystem	Power Subsystem				Remarks
		Battery	Power Cond.	Solar Array	Thermal Control	
20 Watts	110.3 (lb)	138	58	386.9	0.5	No change from Task B
50 Watts	115.3	148	58	440.5	11	2 deployable Solar panels
100 Watts	120.3	178	58	565.0	28	12 deployable Solar panels 9 in^2 base for tube

The weight for power conditioning equipment is assumed to be the same as for Task B design since only unregulated dc power is used for the power amplifier.

3.3 POWER AMPLIFIER THERMAL CONTROL

The thermal control of the power amplifier bay was investigated as a function of transmitted power. Particular emphasis was placed on the traveling wave tube (TWT) since it dissipates over 60 percent of the total power generated within the bay. Table II gives the radiator plate in pounds required by traveling wave tubes of 20, 50, and 100 watts. These weights are based upon a traveling wave tube base plate temperature of 140°F.

3.4 TOTAL WEIGHT VERSUS TRANSMITTED POWER

Figure 7 combines the above weights for power, radio, and thermal control as a function of transmitted power.

4. POWER-GAIN PRODUCT

Assuming that an unlimited power range of power amplifier tubes are available, the optimum power gain product as a function of affected elements is given in Figure 8. For the case of power amplifier tubes limited in size to 20, 50, and 100 watts output, the optimum power-gain product is shown in Figure 9.

These curves include the weight of the Radio Subsystem, solar vanes if used, the Attitude Control Subsystem, the Power Subsystem, and the power amplifier thermal control. A detailed breakdown of the radio, attitude control, and power subsystem characteristics for the optimum is given in Table III.

The configuration of the system update design limits the antenna diameter to 9.5 feet with the allowable system weight limiting the transmitted power to 50 watts. From the data of the report, other optimum system parameters for a 9.5 foot antenna and 50 watts transmitted are use of attitude control gas for solar pressure balancing, a 8 mrad attitude control dead-band, and an antenna pointing step of 3.3 mrad.

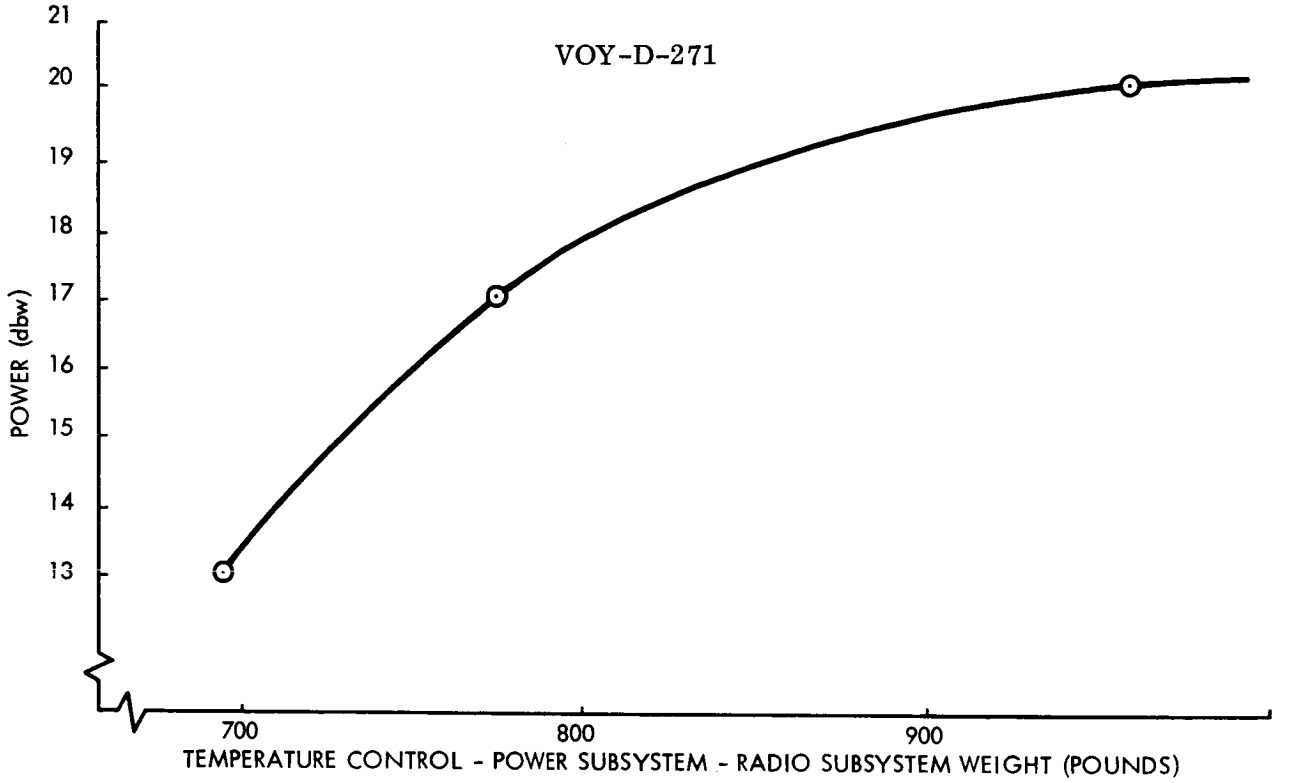

Figure 7. Power Versus Weight of the Solar Array, Radio Subsystem, And Temperature Control

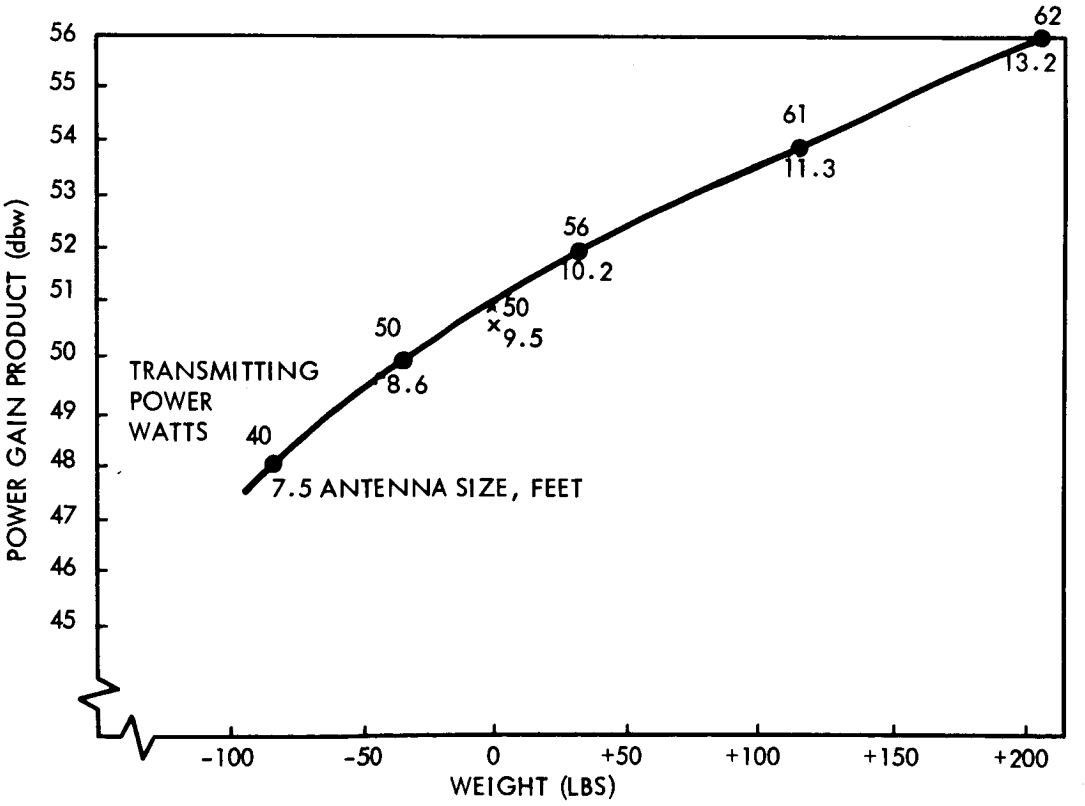

Figure 8. Power Gain Product Optimum Parameter Combination

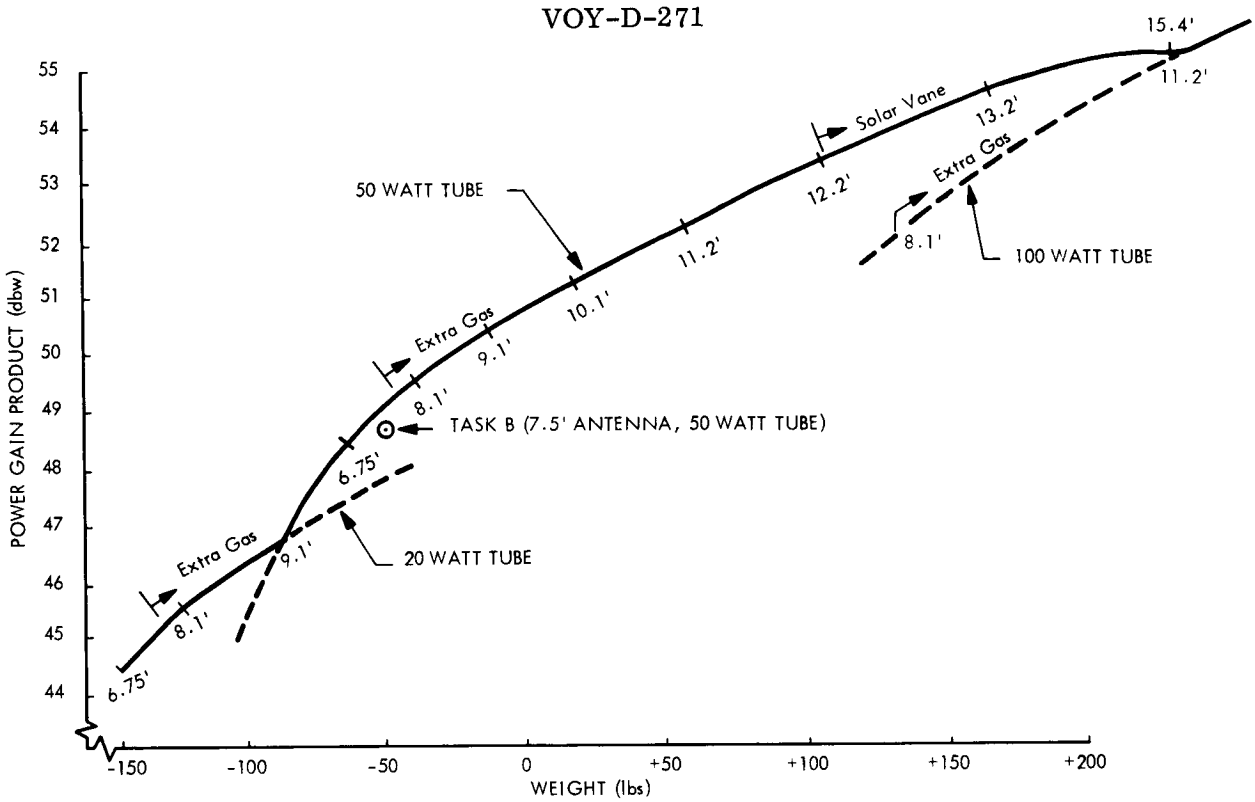

Figure 9. Power Gain Product As A Function of Weight

Table III. Solar Array and Antenna Size Summary

Weight* of Subsystems	Power Tube Output Watts	Radio Subsystem Weight	Attitude* Control Sys. Weight	Antenna* Wt. Plus Balance	Balance* Weight Gas/Vane	Solar Array Area	Power* Subsystem Weight	Attitude Control Deadband	Gimbal Stepsize (Degrees)	Antenna Size (Feet)	dbw
992	20	110.3	238	62	0/-	285	583	± 12.4	> 0.22°	6.75	44.4
1014	20	110.3	238	90	3/-	285	583	± 12.0	> 0.218°	8.1	45.6
1050	20	110.3	239	112	12-	285	583	± 11.0	> 0.20°	9.1	46.8
1075	50	115.3	238	62	0/-	319	646	± 12.4	> 0.22°	6.75	48.4
1100	50	115.3	238	90	3/-	319	646	± 12.0	> 0.218°	8.1	49.4
1125	50	115.3	239	112	12/-	319	646	± 11.0	0.20°	9.1	50.3
1156	50	115.3	242	144	18/-	319	646	± 10.0	0.188°	10.1	51.2
Above 10.2 feet, attitude control problem may exist due to interia coupling											
1195	50	115.3	245	176	31/-	319	646	± 7.4	0.14°	11.2	52.3
1243	50	115.3	250	218	40/-	319	646	± 6.2	0.125°	12.2	53.5
Above 12.2 feet, the C.G. shift becomes a limiting factor											
1303	50	115.3	259	246	-/46	319	646	± 5.0	0.107°	13.2	54.2
1356	50	115.3	264	340	-/54	319	646	± 4.5	0.10	15.4	55.5
Above 9.5 feet, the configuration limits the size											
1251.5	100	120.3	238	90	3/-	378	801	± 12.0	> 0.218	8.1	52
1276.5	100	120.3	239	112	12/-	378	801	± 11.0	> 0.20°	9.1	53.6
1301.5	100	120.3	242	144	18/-	378	801	± 10.0	0.188	10.1	54.4
Above 10.2 feet, attitude control problems may exist due to inertia											
1371	100	120.3	245	176	31/-	378	801	± 7.4	0.14°	11.2	55.9
1419	100	120.3	250	218	40/-	378	801	± 6.2	0.125°	12.2	56.2
Above 12.2 feet, the C.G. shift becomes a limiting factor											
1479	100	120.3	259	246	-/46	378	801	± 5.0	0.107°	13.2	57
1532	100	120.3	264	340	-/54	378	801	± 4.5	0.10°	15.4	58.3
1827	100	120.3	288	512	-/65	378	801	± 3.0	0.090°	18.3	59.9
1833	100	120.3	300	630	-/74	378	801	± 2.5	0.087°	20	60.1

* Weight estimates made before final spacecraft configuration selection and used in this study to indicate incremental effects of weight

VOY-D-272
SPACECRAFT PROPULSION FOURTH STAGING

1. INTRODUCTION

During the system update, a brief investigation was conducted to determine the advantages and disadvantages of using the Spacecraft propulsion system as a fourth stage to assist in heliocentric trajectory injection. Both Mars missions as well as more advanced Jupiter missions were considered.

2. 1977 MARS MISSION

As noted in VOY-D-210, two planetary vehicles with 7,000-pound capsules cannot be launched by the Saturn V in 1977 and maintain a 5,000 pound project contingency as well as a 20 day launch period. As discussed in that Section, one approach is to reduce the spacecraft provided velocity increment (hence propellant weight) to that required by the mission, rather than the specified velocity increment of 1.95 km/sec. A second approach is to use the spacecraft propulsion as a fourth stage for heliocentric trajectory injection. Even though the spacecraft propulsion has a lower specific impulse than the Saturn V, the difference in inert weights of the Saturn S-IV stage and the planetary vehicles could make a gain in the allowable planetary vehicle inert weight possible for the 1977 mission by the use of the spacecraft propulsion as a fourth stage.

If the fourth stage burn could occur immediately after the S-IV burnout, the effective increase in planetary vehicle dry weight would be as shown in Figure 1. The effective increase in dry weight is less than the actual dry weight by the increase in structure and tank weights necessary to support the propellant used in the fourth stage burn. Other factors used in the analysis were as noted below:

a. Effective $C_3 = 30.0\ km^2/sec^2$

(planetary vehicle weight for actual C_3 of 30 km^2/sec^2 equal to 22,400 pounds)

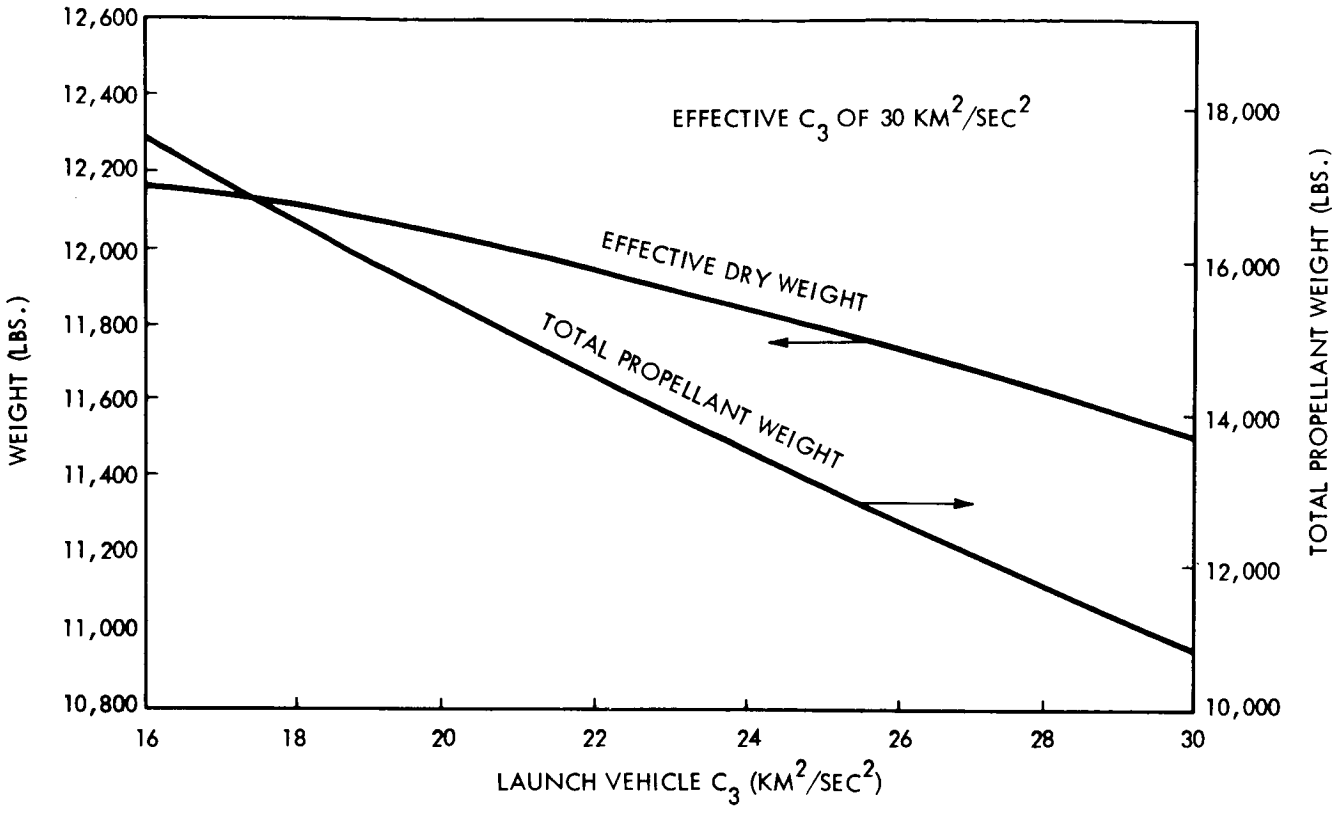

Figure 1. Fourth Staging for Mars Missions

b. LEMDE specific impulse = 300 sec.

c. Mission maneuver velocity requirement of 1.95 km/sec.

d. Increased tank and structure weight equal to 9.2 percent of propellant weight increase.

e. The fourth stage burn is impulsive and occurs immediately after heliocentric orbit injection.

From the curves of Figure 1, there is a potential increase in effective planetary vehicle weight of greater than 630 pounds by using the spacecraft propulsion as a fourth stage of the launch vehicle. However, the assumption that the fourth stage burn can occur immediately after the SIV-B burnout is not valid. The velocity penalty as a function of the delay between the two impulses is indicated by Figure 2 for a typical case. As noted on the figure, the effective C_3

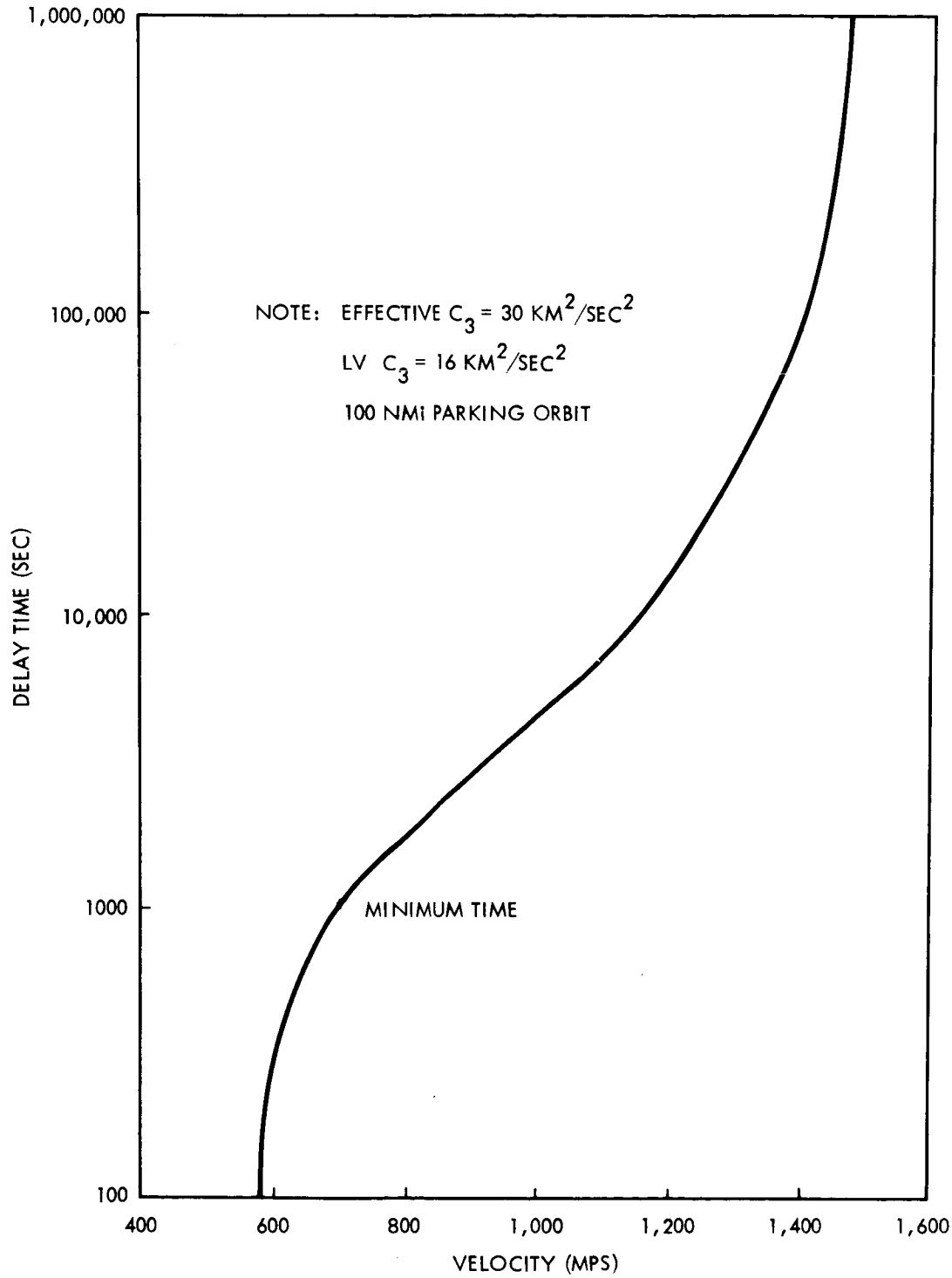

Figure 2. Fourth Stage Velocity Requirements

was maintained at 30 km^2/sec^2 and the actual launch vehicle supplied C_3 was 16 km^2/sec^2. On the basis of a preliminary investigation of the spacecraft operational problems (Section 4), the minimum tolerable delay between the two impulses is 15 minutes. A delay of 15 minutes results in a 20 percent increase in the required spacecraft supplied velocity for the case shown. This essentially eliminates any increase in effective weight.

An additional factor to be considered when investigating the fourth staging concept is the velocity increment necessary to change the time of flight of each planetary vehicle. This time of flight adjustment is necessary to provide a separation in the arrival of the vehicles at Mars as specified. The velocity increment required for time of flight adjustment varies approximately inversely with the delay in launch from the first day to the last day of the launch period. Since the required effective C_3 for injection into the transfer trajectory increases as the launch date is delayed, the required fourth stage velocity increment varies opposite to that required for time of flight adjustment. Thus, combining the time of flight maneuver with the fourth stage burn leads to some increase in effective payload weights.

3. JUPITER MISSIONS

The use of spacecraft provided fourth staging was also investigated for Jupiter missions. Differences in parameters as compared to those for Mars missions included a required effective C_3 of 96.5 km^2/sec^2, mission maneuver velocity for orbit insertion equal to 2.9 km/sec, zero time-of-flight adjustment velocity, and a spacecraft propulsion specific impulse of 305 seconds. For this analysis, the Saturn V capability was as given by Figure 3-11, TR 32-77, "Design Parameters for Ballistic Interplanetary Trajectories, Part II, One-Way Transfers to Mercury and Jupiter" issued by JPL and dated January 15, 1966. At the design point of C_3 equal to 96.5 km^2/sec^2, the Saturn V capability is 17,300 pounds of which 4,500 pounds is allocated to the shroud.

For Jupiter missions, the effective dry weight, fourth stage velocity requirements, and increased propellant weight are given by Figures 3 and 4. With zero delay between the S-IVB

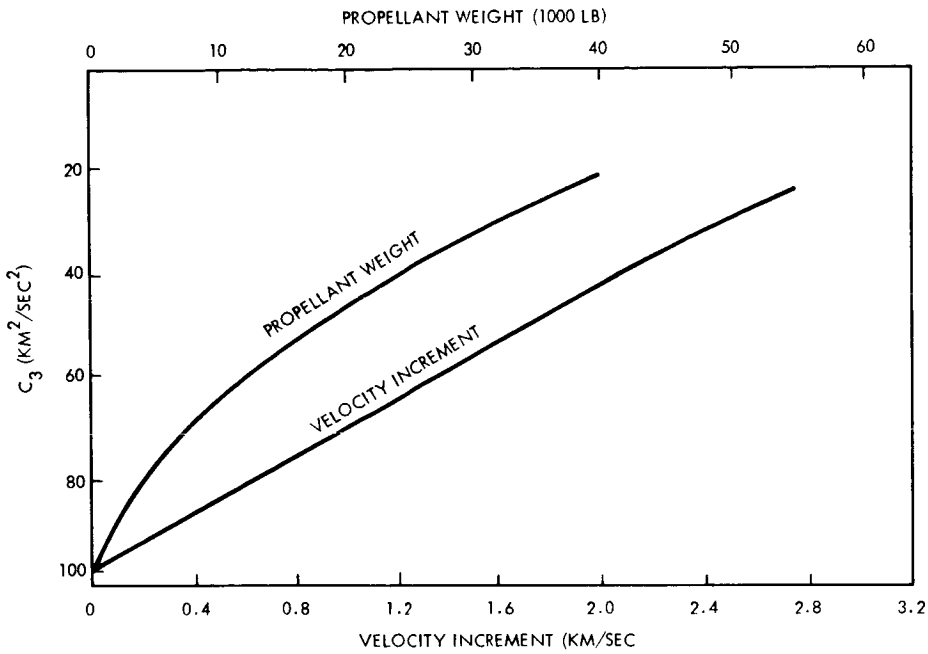

Figure 3. Jupiter Fourth Stage Requirements

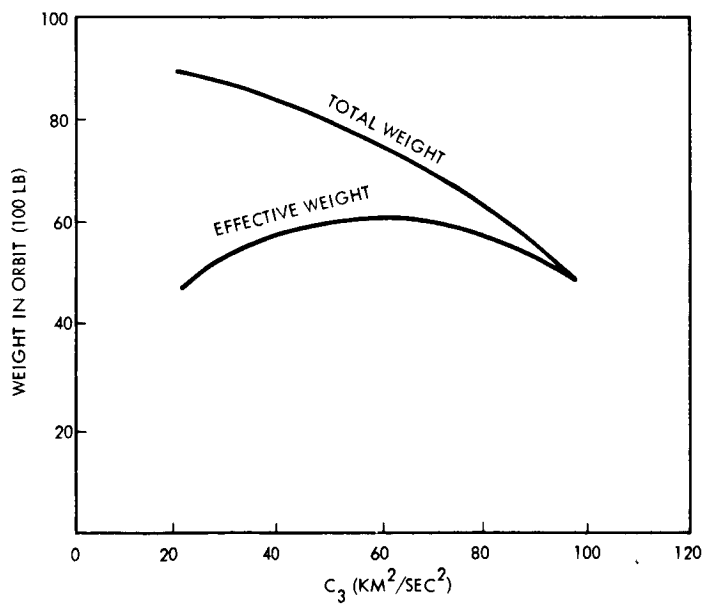

Figure 4. Jupiter Spacecraft Fourth Staging

stage burnout and fourth stage burn, the maximum increase in effective spacecraft weight is 1,250 pounds above the 4,850 pound capability without fourth staging. If a nominal delay of the fourth stage burn of 15 minutes is allowed, the increase in effective spacecraft weight will be approximately 600 pounds at the expense of an additional propellant weight of 15,420 pounds.

4. FOURTH STAGING OPERATIONAL CONSIDERATION

As noted in the previous sections, time must be allowed between the S-IVB stage cutoff and application of the fourth staging velocity increment in order to separate the planetary vehicles and orient them in the proper thrusting direction (to combine the separation date arrival time maneuver and the fourth staging velocity impulse addition). Two possible techniques could be utilized for orienting the planetary vehicles:

a. Orient each spacecraft with the S-IVB before separation.

b. Orient the vehicles after separation.

The latter approach was chosen to be the most feasible one to investigate. It was found to be marginally possible to separate, orient, and burn the LEMDE engines of both Planetary Vehicles in the typical 15 minute time allotment chosen in the previous section. If additional time is taken before adding the velocity increment, the value of doing it becomes marginal with a breakeven point for typical Mars missions of 1/2 to 3/4 of an hour after S-IVB engine cutoff. The time duration of the engine burn, as well as the possible exhaust plume impingment of one planetary vehicle with respect to the other, results in a difficult sequencing problem which would have to be investigated in detail before acceptance of the fourth staging concept.

The Guidance and Control Subsystem is currently capable of coping with S-IVB/PV tipoff rates of less than three degrees per second. However, to maintain the pre-separation attitude reference, the gyros must be operated in the position mode (in contrast to the rate mode used during normal celestial reference acquisition) and, even if the tipoff rates were reduced to

less than one degree per second, the gyros currently proposed for use would hit their stops and lose attitude reference. This problem does not seem insurmountable and could possibly be alleviated by utilizing different gyros as well as higher level thrust solenoids in the Cold Gas Jet Subystem. Additional investigation would be required concerning minimizing tipoff rates in conjunction with the proposed alterations in the Guidance and Control Subsystem.

5. CONCLUSIONS

The problems incurred and the injection accuracy obtainable by using fourth staging require further detailed investigation. As a result of these factors and because of the relatively small increase in effective payload as compared to the amount of additional propellant required, the use of spacecraft propulsion for fourth staging is not currently recommended. Increases in payload, particularly for Mars missions, comparable to that obtainable by fourth staging can be obtained by reducing the launch period by one to two days.

VOY-D-273
PLANETARY QUARANTINE

1. INTRODUCTION

The Planetary Quarantine Plan for the Voyager Project (Reference 1) states that the probability of contamination of Mars from a single spacecraft, its ejecta, or the launch vehicle, prior to calendar year 1985, shall not exceed 3×10^{-5}. The Plan further specifies that the probability of contamination from the sterilized landing capsule shall not exceed 1×10^{-6}. This latter allocation includes such items as the probability that the capsule is originally sterile, the probability of capsule sterility being breached by subsequent handling, and the probability of the capsule being recontaminated after the biobarrier is opened.

For the Voyager Mars missions, compliance with the National Planetary Quarantine Policy will be assured by: (1) enclosing the sterile landing capsule in an impermeable biological barrier to maintain its isolation from possible sources of microbial contaminations, and (2) identifying all other potential contamination mechanisms from non-sterile sources, and assuring that these mechanisms are adequately understood and controlled.

The General Electric Company recently completed a detailed Planetary Quarantine Study for the Jet Propulsion Laboratory (JPL) of the California Institute of Technology. Because of the direct application of this work to the system update, a summary of this Task C study is given in Paragraph 2 below with specific Planetary Quarantine mission and hardware restraints based on the study presented in Paragraph 3.

2. SUMMARY: TASK C PLANETARY QUARANTINE STUDY

The General Electric Company, Voyager Phase 1A, Task C, Planetary Quarantine Study program was conducted for the Jet Propulsion Laboratory under JPL Contract No. 951112. A thorough documentation of the program activities and results is presented in Reference 2. The following paragraphs briefly summarize the study.

The basic objective of the Planetary Quarantine Study was to perform analytical and experimental studies to define the potential sources of contamination and to assess the effects of the Planetary Quarantine requirements on the Voyager Program. Emphasis was placed on the possible ways of contaminating Mars via sources which had not previously been studied in depth, such as various ejecta leaving the unsterilized spacecraft and carrying viable organisms to Mars. The following areas were considered in evaluating the effects of the quarantine requirements:

a. The design of the orbiting spacecraft hardware elements.

b. The manufacturing and facilities requirements.

c. The operating mission.

A summary of the various possible sources of contamination, as defined in Reference 1, is shown in Figure 1. The potential sources of contamination within Categories 2 through 5 were investigated in the study program, although major emphasis was placed on Category 5 sources: Flight Spacecraft Ejecta/Efflux Impact. The Task C Study did not include the investigation of initial capsule sterility (Category 1).

The Task C Quarantine Study essentially included three activities, namely:

a. Development of the computerized analytical tools necessary to calculate the probability of contaminating Mars.

b. Experimental programs to develop the input information for the analytical tools,

c. Analytical studies to interpret the experimental results and to parameterize the potential contamination sources.

A mathematical model was developed to calculate the probability of contaminating Mars. The model, in effect, is a representation of the physical phenomena associated with the several contamination sources and describes the interactions between these sources and the lethality factors associated with interplanetary travel.

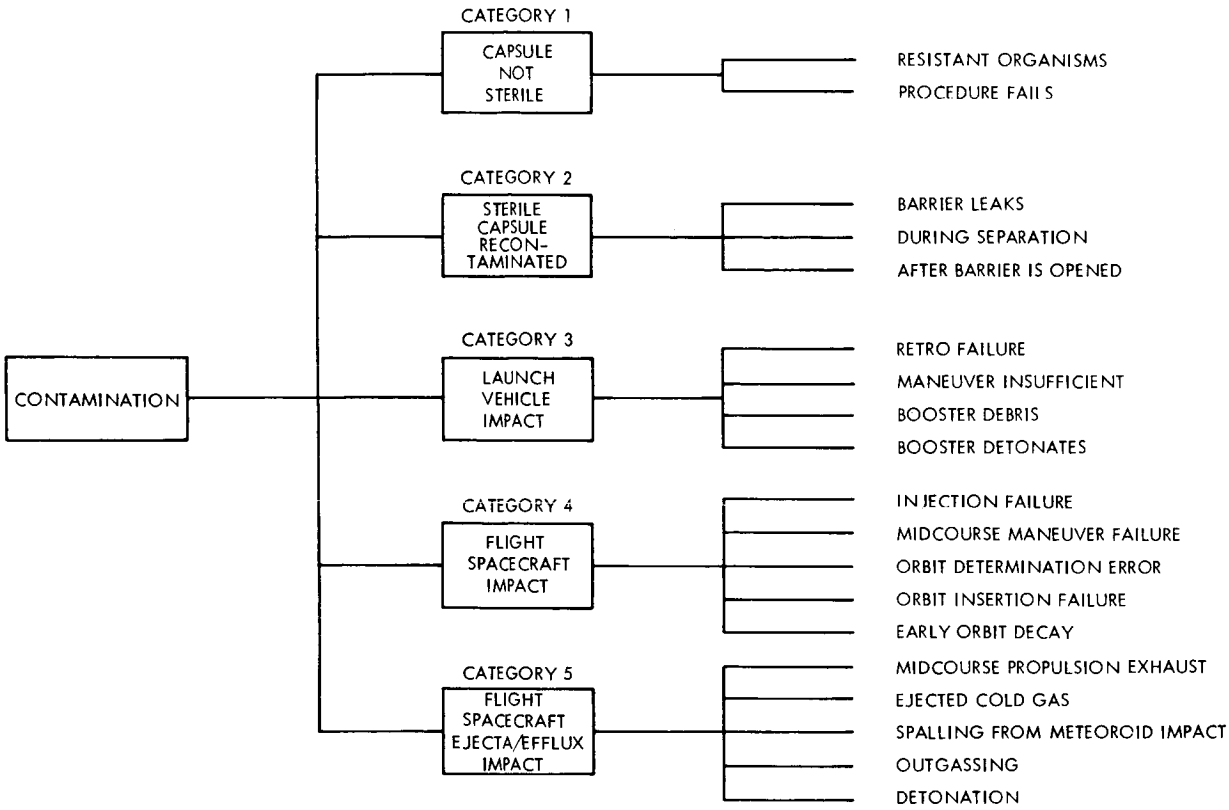

Figure 1. Sources of Contamination

Figure 2 is a matrix of the various elements in the mathematical model. The rows of the matrix represent the various potential sources of Mars contamination. The columns of the matrix describe how particles may find their way to the surface of Mars and the effects of the various lethal environments on these sources. For the purpose of this summarization, only four possible sources of contamination are indicated. A series of computer programs were developed which essentially perform the mathematical analysis represented by the matrix. Both the input and output information for the matrix is treated in the form of probability distributions, rather than simple average or worst-case values.

The analysis of the trajectories of microorganisms leaving the spacecraft is an integral part of the mathematical model. Particles coming off the Planetary Vehicle during the heliocentric trajectory phase, whose velocities are not sufficiently perturbed to cause a large separation from the spacecraft at encounter, may be captured by the planetary atmosphere. During the orbital phase, particles from the vehicle which are sufficiently perturbed from

SOURCE OF CONTAMINATION	1 INITIAL LOADING-V.O.	2 SURVIVE DURING TRIP	3 EJECTION PROCESS	4 TRANSPORT PROCESS	5 SURVIVE DIE-OFF	6 SURVIVE VACUUM	7 SURVIVE UV	8 SURVIVE OTHER SOLAR RADIATION	9 SURVIVE ENTRY HEATING	10 SURVIVE MARS ENVIRONMENT	11 NUMBER V.O.'s TO MARS SURFACE PRIOR TO TIME T
ATTITUDE CONTROL GAS SYSTEM											
ORBIT INSERTION ENGINE											
LOOSE PARTICLES											
MICROMETEOROID EJECTA											

Figure 2. Mathematical Model Format (Contamination Analysis Matrix)

the spacecraft orbit may enter the atmosphere before the end of the required quarantine period. For particles which do enter the atmosphere, the survivability is dependent on the entry time-temperature response of the microorganism. Based on free molecular flow, the time-temperature response was determined as a function of particle ballistic coefficient, emissivity, absorptivity, velocity, initial temperature, initial altitude, and entry angles; the probability of survival was determined as a function of particle temperature history.

Several experimental activities were conducted in support of the Quarantine Study. An experimental program was undertaken wherein small-scale rocket motors, inoculated with a known quantity of test spores, were fired into combination heat exchanger/collection chambers and the entrapped effluent biologically assayed to determine the effects of combustion environments on microorganism viability. A plastic mockup of the equipment used for these tests is depicted in Figure 3. Solid propellant, bipropellant and monopropellant propulsion systems were evaluated; the time-temperature profile of the experiment closely simulated the actual

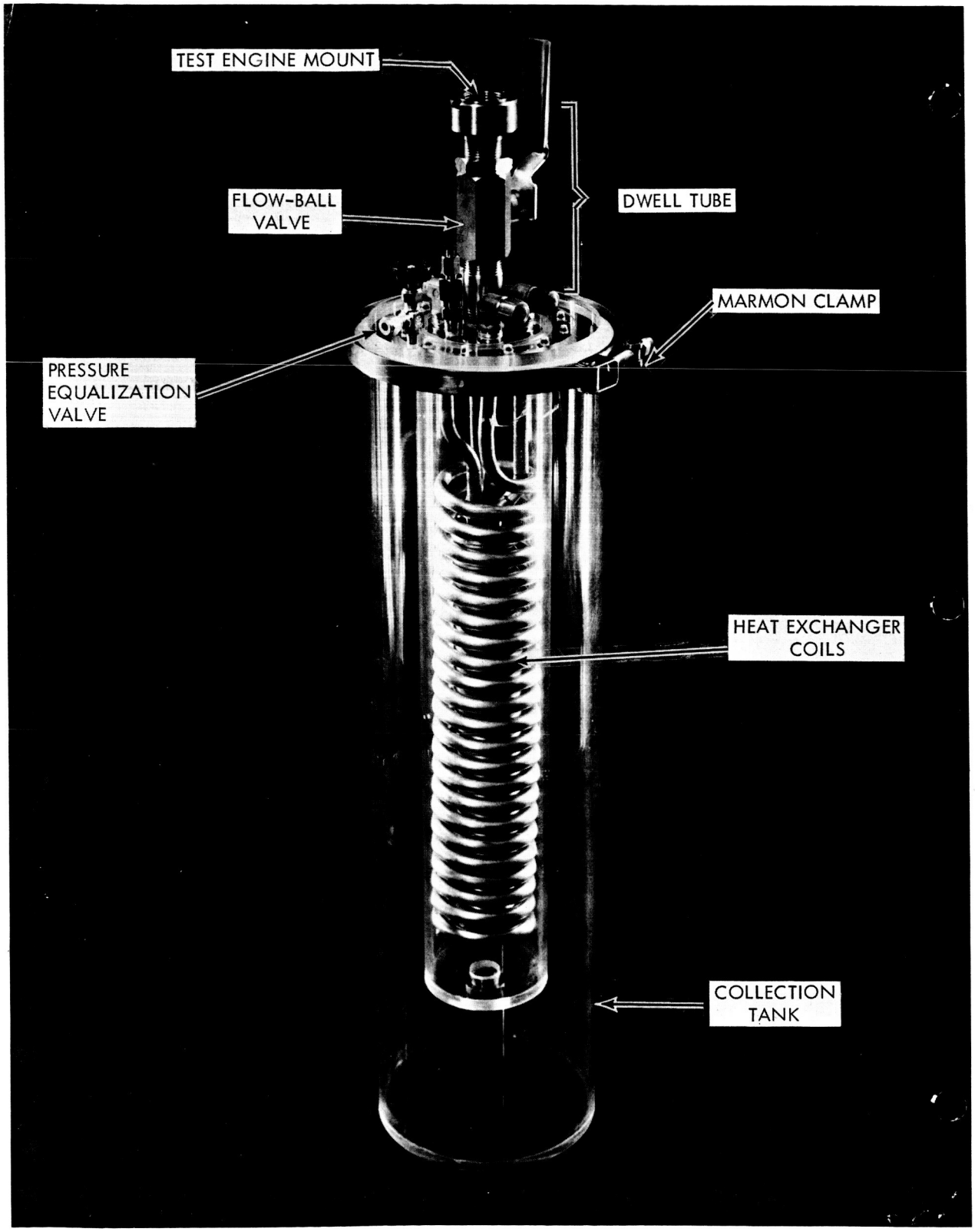

Figure 3. Rocket Firing Test Equipment Mock-Up

space time-temperature profile for each system. This experimental program is reported in detail in Reference 3.

High-velocity micrometeoroids impinging on an unsterile spacecraft surface may cause the ejection of viable and nonviable particles from the surface material. A study was undertaken to determine the mechanisms for particle ejection and to define the environment created by the impingement/ejection phenomena to determine the physical characteristics of the ejected particles and to determine the number of viable organisms surviving the impingement/ejection environment. Both experimental and analytical tasks were conducted. The experimental effort consisted of firing simulated micrometeoroids (five micron cast iron particles) at a velocity of 30,000 feet per second at targets which had been inoculated on the top and bottom with a known number of microorganisms and bioassaying the target ejecta. Figure 4 illustrates the micrometeoroid simulation test apparatus. The analytical effort involved activities such as extrapolation of velocities used in the experimental effort to cover the full range of the actual micrometeoroid environment and the compilation and analysis of related work by other investigators.

Other smaller, but meaningful experimental and assay activities performed during the Task C study included:

a. The collection and microbiological analysis of the gaseous effluent from attitude control gas systems during typical interplanetary mission duty cycles.

b. The experimental determination of the critical thermodynamic properties (solar absorptance and hemispherical emittance) of Bacillus subtillus var. niger spores.

c. Surface sampling of two GE spacecraft configurations to ascertain the particle contamination loading as a function of spacecraft cleaning.

Apart from the analytical work associated with the math model development, several specific studies and literature surveys were performed. Principal among these were (1) a survey of the existing data on spacecraft contamination and the generation of a Biological Burden

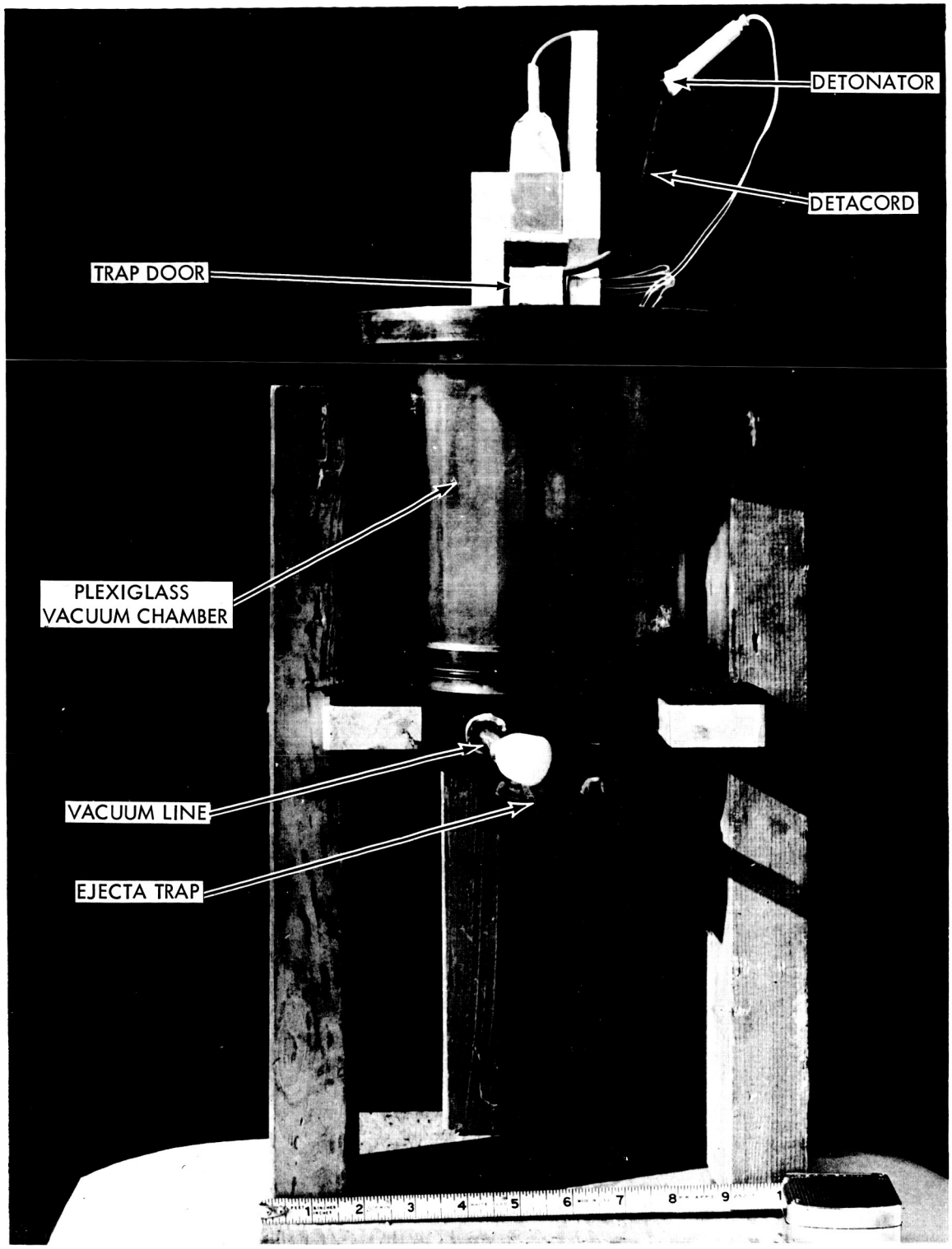

Figure 4. Photo of Micrometeorite Simulator Set-Up in Frame

Catalog (Reference 4) for various levels of cleanroom manufacture, and (2) an analysis to evaluate the potentially lethal effects of the several interplanetary environmental factors, chiefly the ultraviolet radiation and temperature.

The central problem in the study of lander recontamination was to evaluate potential mechanisms which could cause the transfer of viable organisms from an unsterile spacecraft to the uncovered lander. Figure 5 pictorially presents the several mechanisms identified. Experimental evidence and data concerning these transportation mechanisms are not available, and only the application of basic physical concepts and intuition is currently possible. A methodology for quantitatively evaluating the recontamination potential was developed, similar in design to the ejecta sources contamination matrix approach.

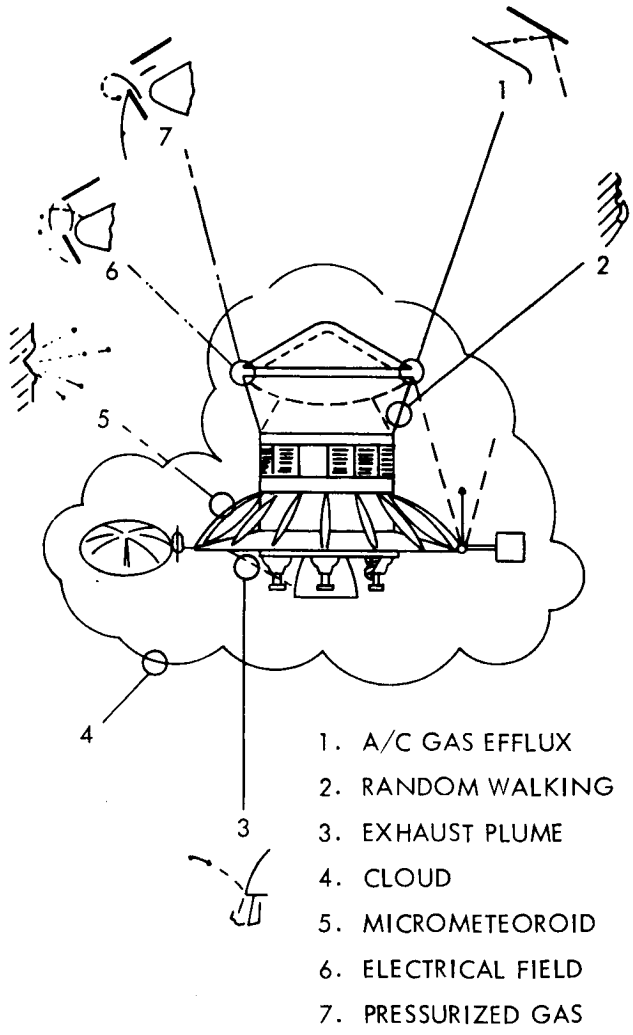

Figure 5. Several Potentially Important Lander Recontamination Mechanisms

Analytical studies were also performed to assess the probability of accidental impact of the launch vehicle, the spacecraft, or the biobarrier on Mars. Results of the studies indicate that:

a. The launch vehicle should be biased away from the final aim point to obtain an impact probability within the quarantine constraints.

b. Midcourse maneuver guidance policy must establish aim points sufficiently distant from Mars (prior to the final correction maneuver) to provide a sufficiently low probability of planetary vehicle impact.

c. Orbit insertion pointing and timing errors, if of moderate magnitude, need not result in planetary vehicle impact.

d. Mission and hardware solutions are available for maintaining the impact probability of the orbiting spacecraft or biobarrier within the quarantine constraints.

3. PLANETARY QUARANTINE DESIGN CONSIDERATIONS

As a result of the Task C Planetary Quarantine Study, significant conclusions and recommendations pertinent to mission and hardware design restraints have been developed. Based on this work, the following paragraphs specify the quarantine restraints and considerations which have been applied to the GE Voyager system update and which should be applied throughout the subsequent phases of the Voyager Program. It should be noted that, although the restraints are cited specifically, trade-off evaluations are generally implied. For example, the selection of orbital periapsis altitude is a function of the degree of spacecraft cleanliness. Where applicable, trade-off considerations applied to the system update are indicated in the subsequent paragraphs.

3.1. MISSION CONSIDERATIONS

The probability of impacting Mars with the S-IVB stage of the launch vehicle can be made to meet any reasonable planetary quarantine requirement. The launch trajectory and hardware accuracy and reliability are the major variables of concern in establishing this probability. Recognizing that quarantine is only one of several conflicting mission requirements affecting

these variables, the principal quarantine recommendation, pertinent to launch vehicle impact, is that the selected maneuver and hardware reliability result in impact probabilities within the contamination allocation for this source of 1×10^{-5} (Reference 1). Specifically:

a. S-IVB retrofire is not required.

b. Launch biasing away from the final aimpoint is required.

The potential Mars contamination sources, related to the transit phase of the Voyager mission, which have been studied are given below.

3.1.1. Planetary Vehicle Impact

Biasing of the Planetary Vehicle (PV) away from the final aimpoint and the use of three midcourse correction maneuvers will satisfy the quarantine requirements. As indicated in the Flight Sequence of Events, VOY-D-230, provision has been made for both PV aimpoint biasing and three midcourse maneuvers. Obviously, the maneuver reliability and design must support the probability calculation.

3.1.2. Planetary Vehicle Surface Ejecta

This class of ejecta consists of those viable organisms released from the vehicle surface, either independently or on carrier loose particles, due to vibrations, micrometeoroid impacts, or surface degradation. Task C study results, depicted in Figure 6, show that these low velocity ejecta, released prior to 30 days from encounter, have planetary miss distances in excess of 20,000 kilometers and, therefore, need no further study.

Indepth analyses of ejecta released within the last 30 days prior to encounter indicate that, if the spacecraft is manufactured within the guidelines presented later under Manufacturing Considerations, the probability of contamination from surface ejecta is within the quarantine allocations.

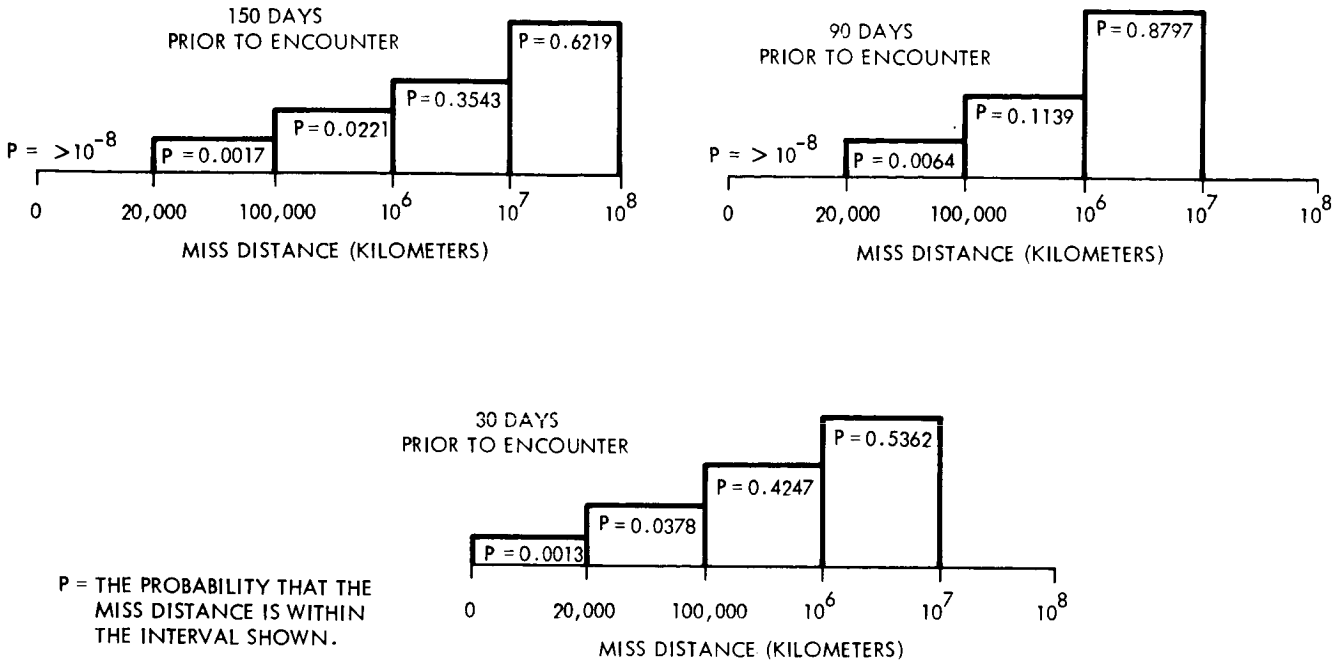

Figure 6. Low Velocity Ejecta Sources

3.1.3. Propulsion System Ejecta

The planetary quarantine analysis resulted in several hardware and propellant oriented conclusions pertinent to the bipropellant midcourse/orbit insertion engine and the attitude control gas system. These will be presented in a subsequent paragraph on hardware considerations.

The math model analysis indicated that, from the standpoint of ejecta from the nozzles, no contamination threat exists for any possible midcourse maneuver. Consequently, the recommendation is that, with regard to combustion exhaust ejecta, no planetary quarantine constraint be imposed on these maneuvers. The phrase, "with regard to ejecta," is important in that propulsion systems must be restrained by quarantine requirements as to the reliability of their operation and the consequent effects on spacecraft planetary impact probabilities.

Two specific orbit insertion maneuvers were examined to determine their effect on the probability of contaminating Mars. The maneuvers considered were insertion prior to hyperbolic periapsis and insertion after hyperbolic periapsis. For both cases, the contamination probability from the bipropellant engine ejecta was safely within the quarantine allocation. However, the specific insertion maneuver selected should be continuously subjected to rigorous quarantine analysis with particular emphasis on maneuver accuracy, pointing failure modes, and system reliability.

The selection of a nominal Mars orbit, as discussed in VOY-D-260, gave serious consideration to the quarantine restrictions. The contamination probability of orbits with 500 and 1000-km periapsis is shown in Figure 7. The contamination probability associated with any one periapsis is a function of the cleanliness level of the spacecraft itself. The figure depicts the cleanliness versus periapsis altitude trade-off based on data from two GE spacecraft programs, one with stringent contamination control requirements (clean) and one without

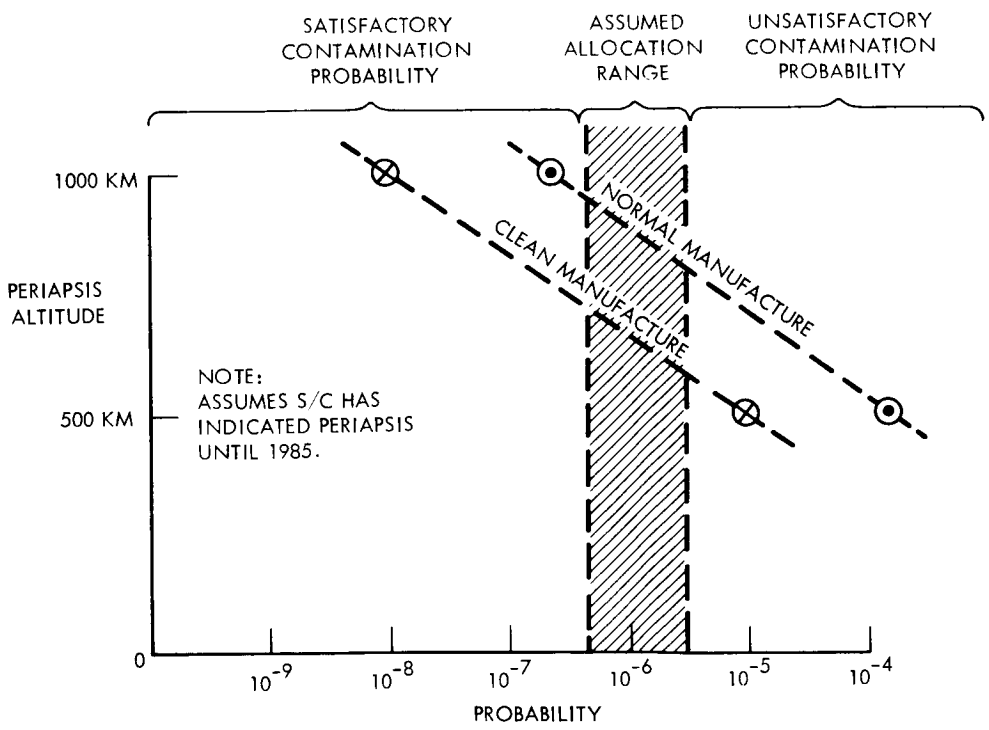

Figure 7. Probability of Contamination for Surface Related Sources

such requirements (normal). Based on such a trade-off, the contamination probability from ejecta sources in a 1000-km periapsis orbit was found to be within the quarantine requirements. With respect to the accidental impact on the surface of Mars of the orbiting spacecraft or biobarrier, periapsis altitudes of from 300 to 1000 km will be safe, depending on the atmosphere definition considered. However, guidance errors, which could be on the order of 300 km, must be considered when selecting the design orbit size. Therefore, although concern with accidental impact would permit considering lower altitudes than 1000 km, it does not appear overly conservative to accept a 1000-km periapsis as a nominal value.

For a worst case orbit trim maneuver (raising the vehicle orbit), the probability of contamination from the propulsion system combustion exhaust is within the quarantine requirements. No quarantine restraints should, therefore, be placed on orbit trim maneuvers from the ejecta standpoint. However, propellant pressurant gas may leave the system by intentional venting or leakage modes. Although not specifically studied, this gaseous ejecta source is quite similar to the attitude control gas system effluent and may be treated with the same hardware solutions recommended for that system (see Paragraph 3 below). It is recommended that the specific pressurization system selected be studied and, if necessary, these hardware solutions incorporated. An orbit trim maneuver which lowers the spacecraft orbit (periapsis) is potentially dangerous from a standpoint of failure of the engine to shut down. Again, system reliability becomes a quarantine consideration, and system selection, as well as maneuver selection, must receive continuous study from a quarantine viewpoint.

The separation of the capsule protective cover (biobarrier), presents several potential contamination sources; namely:

a. The orbit decay of the separated biobarrier.

b. The recontamination of the sterile lander during the separation event.

c. The generation of debris by the separation devices.

Evaluation of potential separation maneuvers and preliminary consideration of several potential barrier designs has fostered the development of recommendations which should be considered in the design of the maneuver and associated hardware:

a. The biobarrier, as presently conceived, with a M/C_dA of about 0.02 slugs/ft^2, can be safely released in a 1000 by 10000-kilometer orbit or greater.

b. The separating biobarrier should have the same electrical potential as the remainder of the vehicle during separation to eliminate the forming of an attractive electric field.

c. The biobarrier should be retained in place as long as possible to minimize the capsule exposure time, thus implying barrier separation in orbit.

d. The spacecraft attitude control gas system should be designed to prevent the reflection of effluent gases off the separating barrier onto the uncovered lander.

e. No direct line-of-sight should exist between the spacecraft and the exposed lander.

The Voyager system update, in applying these recommendations, incorporates (1) a 1000-km periapsis nominal orbit, (2) biobarrier separation in orbit only five minutes prior to capsule separation, and (3) a design which avoids any line-of-sight to the uncovered capsule.

3.2. HARDWARE DESIGN CONSIDERATIONS

Based on the current definition of contamination - one or more viable organisms on the planet surface - the attitude control gas system (ACGS) poses a contamination hazard and some degree of bioload reduction will be necessary. Several approaches to this bioload reduction are possible. Certainly heat sterilization would meet the requirements, although the magnitude of the hazard does not at all indicate the need for sterilization. Similarly, ethylene oxide (ETO) decontamination would more than meet the requirement. In fact, redefining contamination to be "two or more viable organisms on the surface" would negate the concern for the ACGS.

The use of an onboard filter, of 3 to 5-micron pore size, even if located between the storage tank and the pressure regulator, would maintain the probability of contamination from the ACGS source well within its allotment. The calculated probability using filters is 2.5×10^{-9}, versus an allocated probability of 1×10^{-6}. All the analyses assumed that the ACGS gaseous pressurant (nitrogen) was filtered through 0.45-micron filters during system loading, as for the Mariner and Ranger systems. The use of other pressurants, i.e., hydrazine, hydrogen peroxide, etc., has also been considered (see VOY-D-322) as to their sporicidal nature in reducing system bioloads.

A separate class of potential contamination sources was identified in the Task C Quarantine Study. These special sources include large pieces or chunks of hardware which can leave the spacecraft (the pieces being large with respect to previously considered ejecta, but small relative to the spacecraft). These items, in most cases, would be sufficiently large for a great number of organisms to be on or in them. Consequently, they do not readily lend themselves to a statistical type of analysis. In all cases, if these items exist it is because a failure or some undesired situation occurs. Examples of this class of potential sources are:

a. Debris due to a propellant explosion.

b. Pieces thrown off due to solar pressure spin-up of spacecraft (after end of active attitude control).

c. Debris from separation hardware.

d. Instrument covers.

e. Nozzle inserts and ablative liners.

Of the several examples considered, some indicate the necessity for analysis of specific hardware designs to assess the contamination potential (e.g., propellant explosions, spacecraft spin-up, nozzle throat inserts, and ablative liner materials). Other examples indicate potential sources of contamination which may be controlled more readily by general design guidelines than by detailed analysis (e.g., separation hardware and instrument covers).

This whole class of potential sources can only be controlled by continuously monitoring the spacecraft design, and the specific areas needing control can only be defined by evaluating fairly specific hardware design. Therefore, it is recommended that the following design guidelines be established:

a. Separation mechanisms, employed during or after 60 days prior to encounter, should be designed to minimize, and preferably to totally eliminate, loose debris of any size.

b. All spacecraft hardware should be designed to assure a low probability of accidental separation from the spacecraft proper.

In addition, it is recommended that as these special sources are specifically identified, detailed contamination analyses be performed leading to the establishment, if necessary, of more specific constraints.

3.3. MANUFACTURING CONSIDERATIONS

The cleanliness of the spacecraft must begin with the initial design. Inaccessible areas, small acute angles, sharp corners, and blind holes act as traps for living organisms and serve to defeat the intent of subsequent cleaning operations. The hardware design must avoid these conditions whenever possible.

Furthermore, the selection of spacecraft materials affects the cleanability and cleanliness of the final assembly. Surface finish is an important consideration; the contamination of prime concern is generally on the order of a few hundred microns in size and can readily be trapped in the irregularities of surfaces. The use of degradable materials or materials which outgas at high rates is also undesirable as the products of such degradation may act as carriers for the release of organisms from the spacecraft surface. In addition, the specification of manufacturing operations requiring abrasive processes is also undesirable for obvious reasons.

These above design considerations logically lead to the recommendations for permissible spacecraft biological and particulate loads. Based on the Task C Quarantine Study, it has been concluded that the planetary quarantine requirements, pertinent to surface related sources, can be met with an adequate safety margin if the maximum bioload is essentially as shown in Figure 8 and the maximum particulate load is as shown in Figure 9. The load restrictions are achievable, as demonstrated in a recent GE military space program, if the spacecraft manufacturing includes the three elements of: (1) good cleanroom facilities, (2) good cleanroom operating procedures, and (3) good hardware cleaning operations.

The specification of the cleanroom class, simply a measure of cleanroom air loading, is not sufficient to control nor predict the biological or particulate loading of the spacecraft. Both the personnel procedures and the cleaning operations are paramount in making any such determinations.

Procedures used to minimize the particulate load, e.g., flush cleaning, are effective in reducing the biological load as well. The loads recommended as limitations in Figures 8 and 9 are achievable within the present state of the art without the need for ethylene oxide decontamination or heat sterilization.

It should be noted that, as is well recognized by contamination control specialists, people are the greatest single source of manufacturing contamination. Consequently, through manufacture, assembly, test, and launch, personnel handling operations should be maintained at a minimum. This implies the minimization of required assembly and handling operations, the necessity for the exercise of great care during packaging and transportation, and limited access to the spacecraft by operational support and test personnel and equipment.

The system update spacecraft configuration, as described in VOY-D-220, has been designed to facilitate cleaning and to minimize personnel handling. The design provides a relatively open, easily accessible spacecraft and the modular subsystem approach reduces the number of personnel working in the vicinity of any module at any one time. Furthermore, the

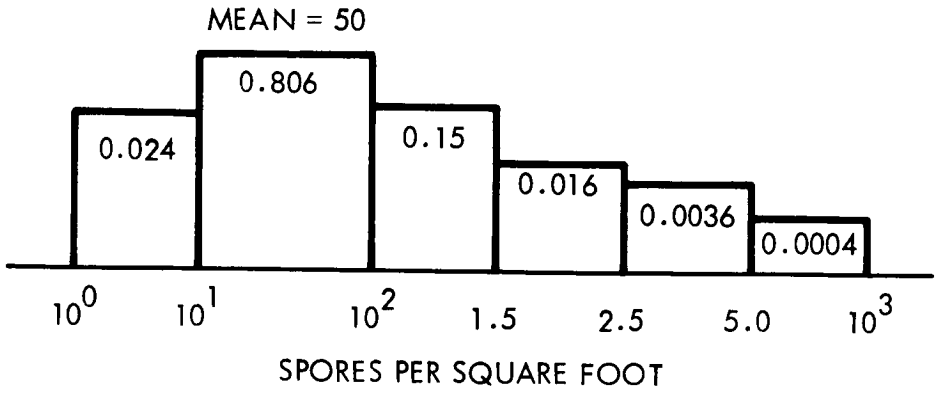

Figure 8. Recommended Maximum Biological Surface Load

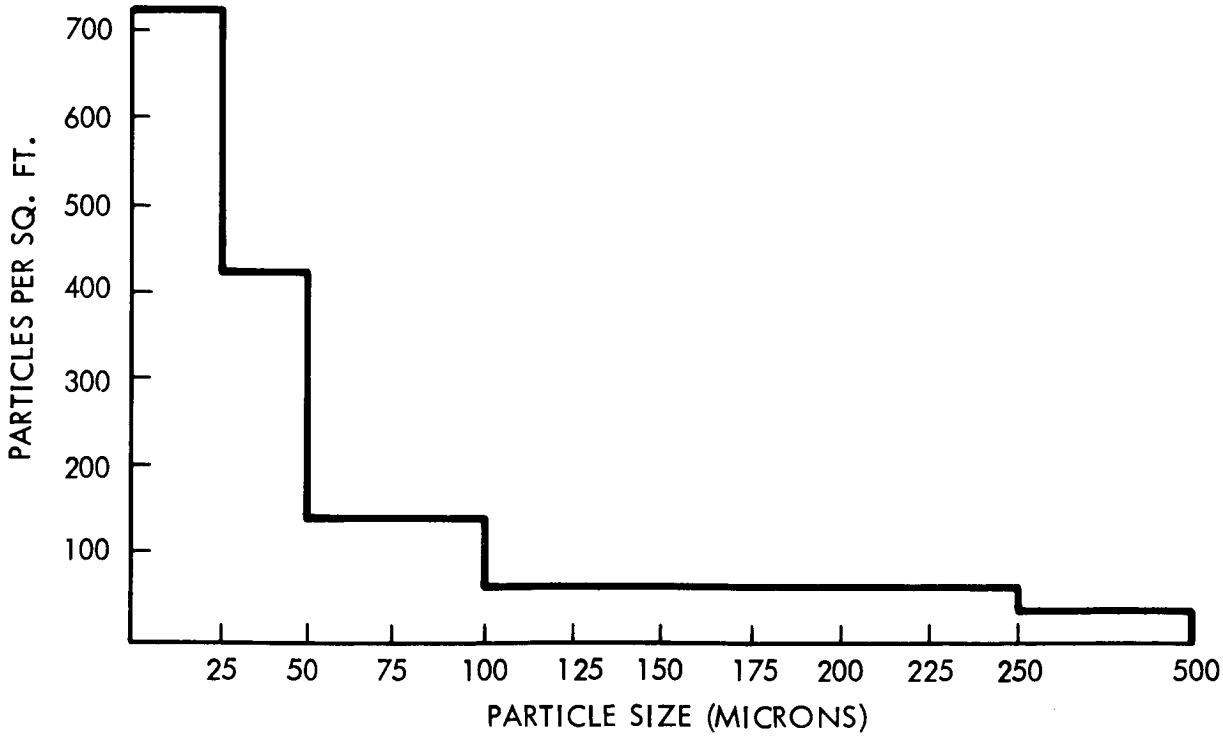

Figure 9. Recommended Maximum Particulate Surface Load

manufacturing, assembly, and test operations, as described in the Implementation Plan, Volume III, have been planned to reflect the incorporation of planetary quarantine restrictions.

4. REFERENCES

1. Planetary Quarantine Plan, Voyager Project, 15 March 1966, 3rd Revision, 1 June 1967 - 818-11-PQ0001.

2. General Electric Company, Document No. VOY-CO-FR, "Phase 1A Task C Final Report, Vol. 3, Planetary Quarantine Study".

3. General Electric Company, Document No. VOY-C2-TR14, "Voyager Mars Planetary Quarantine: Combustion Lethality Experiment, Final Report", 15 July 1967, A.F. Oberta, J.R. Gillis, M.J. Landry, F.X. McLaughlin.

4. General Electric Company, Document No. VOY-C2-TR10, "Microbiological Aspects of the Planetary Quarantine Program for Voyager", April 1967, M.G. Koesterer.

VOY-D-274
AUXILIARY THRUSTER CONSIDERATIONS

1. INTRODUCTION AND SUMMARY

A primary system trade-off which had to be made in the system update work consisted of determining the need for including auxiliary thrusters in the recommended spacecraft system design. Among the defined possible needs for auxiliary thrusters are:

a. Meeting the minimum impulse bit requirements for mid-course and orbit trim maneuvers.

b. Alleviating the problems of fluid motion (i.e. settling and migration).

c. Reduction of total propellant leakage through the main LEMDE engine control valves.

d. Handling of large center-of-mass offsets resulting from a possible deployed planet scan platform as well as loss in thrust vector control authority (as the C.G. moves toward the LEMDE engine gimbal) during Martian orbital mission phases.

e. Providing roll control during engine burn periods.

Detailed analyses located in the following paragraphs as well as in VOY-D-323 (Autopilot), VOY-D-363 (Mechanisms), and VOY-D-370 (Propulsion) of this report indicate that, although auxiliary thrusters might ease the capability of meeting the system requirements in some of the above areas, the main LEMDE engine is capable of performing all the propulsive functions of a Voyager Mars mission.

Among the numerous reasons for not incorporating auxiliary thrusters in the spacecraft design are:

a. The design of the propulsion subsystem is made more complex resulting in a reliability penalty; especially, if the auxiliary thrusters must be operated in a pulsed mode.

b. An over-all system weight increase of approximately 100 lbs. is incurred.

c. A more complex autopilot design with interfaces with both the LEMDE and auxiliary thruster systems.

d. Planetary vehicle configuration problems such as exhaust plume impingement.

e. Thermal adaptability.

Based upon the lack of a proven need for meeting performance requirements as well as the defined detrimental effects of incorporating auxiliary thrusters in the baseline design, it is concluded that a better design exists if the LEMDE engine is utilized to provide all propulsive requirements.

2. POSSIBLE MERITS OF AUXILIARY THRUSTERS

2.1. GUIDANCE REQUIREMENTS

The minimum impulse bit (MIB) requirements are dealt with in detail in General Electric Milestone Report "Propulsion Requirements," No. VOY-P-TM-13, dated August 11, 1967. In summary, this reference shows that the final midcourse correction is the significant maneuver with respect to propulsion impulse requirements. By incorporating a minor change in arrival time (approximately 6 minutes) with the trajectory correction, a MIB of 2,040 pound-seconds with a maximum uncertainty due to tail-off of 106 pound-seconds (3 sigma) will fulfill the guidance requirements. This corresponds to a minimum velocity increment of approximately 1 meter per second (mps), per the present NASA mission specification. According to published data, both the MIB and the tail-off impulse variations are within acceptable limits for the LEMDE thrust chamber. Thus, it can be concluded from trajectory and guidance accuracy studies that the LEMDE engine, operating by itself, can meet the minimum velocity and accuracy requirements for midcourse maneuvers.

The major criteria used in selecting a minimum velocity change for orbit trim is the orbit period as related to the surface mapping requirements. With the design orbit, 1000 x 11,727 km altitude, sensor view angle of 5.7 degrees, orbit inclination of 40 degrees, and a 10 percent overlap control of the ground swath at minimum spacecraft altitude, the period of the orbit must be controlled to 22.2 seconds. This corresponds to a velocity error or minimum impulse bit of 0.27 mps. For a minimum spacecraft weight (burn-out weight), this velocity corresponds to an impulse bit of 158 lb-sec which is approximately an order-of-magnitude less than the minimum impulse bit which can accurately be supplied, but greater than the uncertainty in impulse at the low thrust level for the LEMDE. From an over-all mission viewpoint, it is doubtful whether an orbit trim would be made to move the ground trace by only one-tenth of the swath width. If necessary, a slight change in other orbit parameters can be tolerated so as to increase the impulse to greater than the minimum capability of the LEMDE. Thus, the LEMDE engine, without auxiliary thrusters, can adequately perform the orbit trims.

2.2 AUTOPILOT AND ACTUATOR CONSIDERATIONS

Detailed analyses indicate that performing an orbit trim with the Planet Scan Platform (PSP) deployed is a marginal situation for the autopilot and LEMDE actuator to handle. For an after-capsule separation orbit trim with the PSP deployed, the nominal gimbal angle can approach seven degrees at the end of engine burn. The addition of auxiliary thrusters would ease the preceding thrust vector control problem as a result of the increased moment arms, etc. The trade-off of retracting the PSP versus adding auxiliary thrusters, increasing system complexity, leans in favor of retracting the PSP and eliminating the lateral center-of-gravity shift and thrust vector control problem during orbit trim maneuvers.

The question of whether the PSP should remain deployed during orbit trims was also examined from a structural and mechanisms viewpoint. The dynamic analysis performed assumed the following:

a. The planetary vehicle proper is a rigid body.

b. The PSP is rigid and connected to the spacecraft support module by a weightless elastic boom 60 inches long.

c. The LEMDE thrust is a step force of 1,050 pounds. The engine was also assumed to be oriented at a 6-degree angle with respect to the vehicle longitudinal axis.

d. The ignition transient is the most critical condition.

e. Motion is planar.

f. The planetary vehicle C.G. is radially offset by 3 inches.

g. Autopilot and fuel movements can be neglected.

The results of the analysis are presented in Table 1 and indicate that the PSP, if deployed during orbit trim maneuvers, should be designed to sustain a loading condition of 0.41 g's longitudinally combined with ±0.03 g's laterally. Negligible structural weight penalty is required with the preceding loads, but an additional 8 pounds as well as 20 watts gimbal locking

Table 1. Planet Scan Platform Limit Load Factors

	Longitudinal (Z) Load Factors (g)					Lateral (X) Load Factors (g)			
	Rigid body transl.	Rigid body rotation	Total rigid body	Dynamic load	Total combined load	Rigid body transl.	Rigid body rot.	Dynamic load	Total combined load
Planetary Vehicle Proper	0.18	-	0.18	0.003	0.19	0.02	-	-	0.02
Planet Scan Platform	0.18	0.09	0.27	0.14	0.41	0.02	0.01	-	0.03

power is required for the cone axis actuator. If the lower thrust level of auxiliary thrusters (total of 400 pounds versus 1,050 pounds for the LEMDE engine) were used, the mechanisms weight and power penalty would be negligible. It is concluded, however, that the small reliability penalty paid by retracting the PSP during orbit trims is negligible compared to the added system complexity of auxiliary engines and leaving the PSP deployed.

Preliminary results from a computerized simulation of thrust vector control for the autopilot and the LEMDE actuator during trajectory corrections, orbit insertion, and orbit trims are presented in VOY-D-323. A typical situation investigated consisted of the following conditions:

a. 30 degree propellant angle.

b. Rigid body C.G. offset angle of 2-1/2 degrees.

c. Orbit insertion LEMDE thrust level.

d. No capsule aboard.

e. System parameters as at middle of burn.

The results of this simulation indicated a maximum engine gimbal excursion of approximately 4 degrees; reducing the rigid body C.G. offset angle to 1.2 degrees, resulted in a maximum gimbal excursion of approximately 3 degrees. In summary, although only limited use has been made of the computer program developed, all results thus far indicate that the autopilot and LEMDE actuator are capable of handling the thrust vector control requirements providing that fluid motion control devices are included in the propellant tank design.

Another attitude control consideration is the control of the roll axis during engine burn in order to maintain the antenna pointing to earth. Auxiliary thrusters can perform this function; but preliminary analysis indicates that roll control to the required accuracy could be achieved utilizing the cold gas reaction control subsystem.

In summary, although the incorporation of auxiliary thrusters would ease the thrust vector control problem as faced by the autopilot and LEMDE actuator as well as allow the PSP to remain deployed during orbit trims, auxiliary thrusters are not required.

2.3. PROPELLANT LEAKAGE

The possibility of leakage through the main shutoff valves of the LEMDE is an area of concern. Milestone Report VOY-P-TM-20 dated August 15, 1967 and entitled "Auxiliary Thruster Requirements" discusses this subject in detail and reveals various schemes which might be utilized to provide propellant isolation and, in so doing, minimize leakage. However, the schemes proposed either suffer from a lack of available hardware or increase propulsion subsystem complexity and weight. Auxiliary thrusters utilized for trajectory corrections and orbit trims would allow the propellant to remain isolated from the LEMDE until orbit insertion and thus leakage could be minimized. As shown in Section 3, the addition of auxiliary thrusters has derogatory effects on the over-all system. Thus, this problem has been approached with the idea of determining the amount of leakage through the LEMDE main values that is detrimental to system performance.

Tests, using approximately 50 units of the current shutoff valve and performed by the LEMDE engine prime contractor, produced only one case of liquid leakage for 577 reactive firings and a total firing time of 50,152 seconds. In addition, valves have been repeatedly subjected to 30-day periods of pre-firing propellant exposure without adverse effects and the design is being upgraded to be qualified for 150 to 500 dry cycles in conjunction with a design goal of one year of continuous exposure to propellants in Earth environments.

Analyses which are presented in VOY-D-370 indicate that approximately 40 pounds of propellant per year could be lost at worst case leakage rates. In addition, leakage of either fuel or oxidizer alone would produce negligible disturbance forces on the planetary vehicle, and a combined leakage of fuel and oxidizer hypergolically ignited over a 250-day period would produce a ΔV of only 4.25 mps. On the basis of these data, it is concluded that propellant leakage is not a major problem.

3. EFFECTS ON VEHICLE DESIGN

The effects of adding auxiliary thrusters to the propulsion subsystem configuration are detailed in Milestone Report VOY-P-TM-20 ("Auxiliary Thruster Requirements"). In summary, the propulsion subsystem complexity is increased and the over-all weight of each planetary vehicle increases approximately 100 pounds with the addition of the auxiliary engines.

Auxiliary thrusters complicate integration of the spacecraft in the following ways:

a. Autopilot interface complexity is increased since an interface must be provided with two propulsion systems.

b. The auxiliary thrusters must be located at least several feet from the propellant supply. If they are mounted at the aft end of the vehicle, propellant lines could restrict accessibility to the equipment bays.

c. It is more difficult to modularize the entire propulsion subsystem.

d. Auxiliary thrusters provide field-of-view limitations for sensors, etc.

e. Micrometeoroid protection must be provided for the valving and active components of the thrust chamber assemblies.

4. CONCLUSIONS

A definite requirement for the incorporation of auxiliary thrusters into the spacecraft design has not been established. Time has allowed only a limited look at the autopilot - actuator adequacy with the LEMDE alone, but this investigation indicates that the non-auxiliary thruster configuration is adequate. In addition, the incorporation of auxiliary thrusters increases spacecraft system complexity as well as weight. As a result, it is currently recommended that the system design include only the LEMDE to accomplish all the propulsive functions of the Voyager missions.

VOY-D-275
RELIABILITY ANALYSES

1. INTRODUCTION AND BACKGROUND

During the Task C Study, an investigation was made of techniques for arriving at the most effective use of redundancy within the Voyager spacecraft. This study led to the successful development of methodology and associated computer programs for this purpose.* This method required that a simplex baseline or reference spacecraft be defined as well as possible redundant configurations. Redundancy was selected to maximize the index Mission Expected Worth (MEW) for a specified maximum spacecraft weight. The MEW is defined as the summation of worth over all mission outcomes, where the worth of each outcome is the product of the value of that particular mission outcome and the probability of obtaining the outcome.

This methodology was applied to Voyager, drawing heavily on the mission definition and design approaches resulting from the General Electric Phase 1A, Task B study. The results are reported in the Task C Final Report. Changes in the mission definition and spacecraft design approaches since that time led to the decision to update the inputs and re-determine the optimum application of redundancy as a function of weight. A two step approach was used. First, analysis of the Task C Study results was continued in order to determine where changes or additions to postulated redundant alternatives, not significantly affected by changing mission or system definitions, could most profitably be made. This also included discarding many of the earlier inferior alternatives. Second, the actual updating and remodeling was done in accordance with currently defined guidelines. These two steps are discussed in more detail in the following two sections.

* Task C Final Report, VOY-CO-FR, Volume 4, Section 3, Selection of Spacecraft Redundancy.

2. CONTINUED ANALYSIS OF TASK C RESULTS

The results of the optimization runs carried out during the Task C Study have shown that the typical curve of MEW versus weight has a fairly abrupt knee which occurs after the addition of the first 60 or 70 pounds, as seen in Figure 1. Analysis of the preferred configurations defined by the steep portion of the curve has shown that a relatively few of the spacecraft Independent Assemblies (I/A's) have accounted for the major portion of the increase in the attainable MEW. Note: An independent assembly is a grouping of hardware which can be replaced by an alternate mechanization without affecting the functional performance of other parts of the system. The saturation effect is due primarily to the intentional inclusion of marginal or inferior alternatives during the initial study.

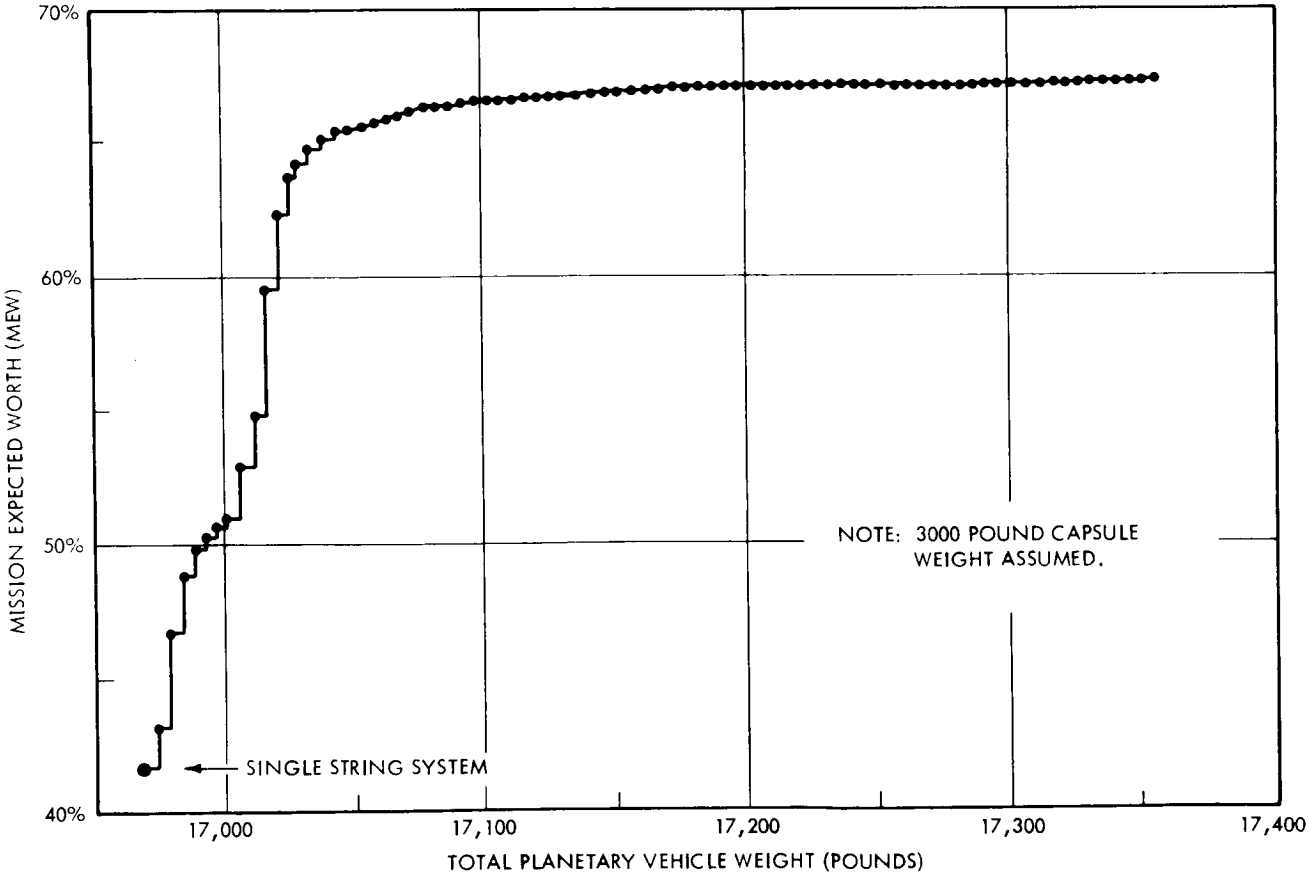

Figure 1. Optimum Configurations - Task C Study

The significance of the effect that an individual I/A has on the value of MEW can more easily be seen by calculating the "MEW Loss due to the I/A." This is determined by calculating the value of MEW when all I/A's, except the one under consideration, are assumed to be perfect (in a reliability sense) with the difference between maximum achievable value of MEW and this calculated value being the "MEW Loss." This number represents the maximum loss in MEW which can be attributed to that I/A.

The value of such a criticality factor is that it takes into account not only the degree of reliability of a given assembly, but also the degree to which the mission success depends upon that particular assembly. Figure 2 ranks the families of I/A's by MEW Loss for the single-string or simplex member of each family. It also shows the MEW Loss for the best alternate considered. The height of each bar of the single string "curve" is representative of the potential improvement that can be obtained in any family by the application of redundancy. The bar height between the single string and the best alternate is representative of the potential improvement in MEW obtainable with the given set of alternates. The cross-hatched area is representative of the potential improvement which could be obtained with increased reliability (redundancy).

Two points are immediately apparent from Figure 2. One, a large number of single string Independent Assemblies have only a very small effect upon the value of MEW. This due either to the fact that the reliability of the I/A is high or the assembly is not very critical to the achievement of mission value. Second, there are a few families such as the radio/command I/A as indicated by the cross-hatched areas where additional alternates should be sought.

The foregoing analysis was instrumental in focusing attention on the most critical areas during the system update study.

3. SYSTEM UPDATING

The major changes made to the redundancy optimization programs during this study are summarized in four sections, namely (1) mission definition, (2) system definition,

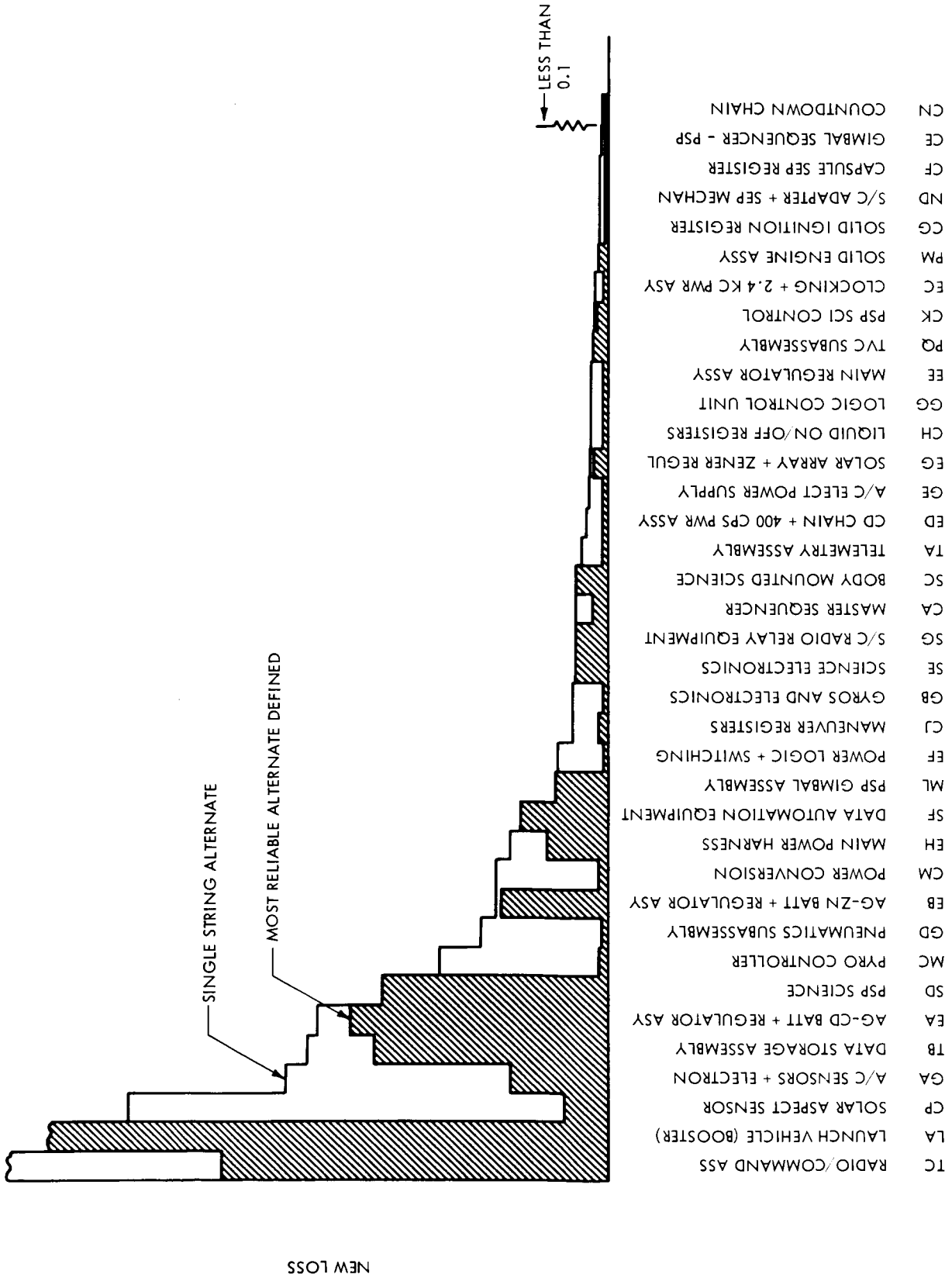

Figure 2. MEW Loss for Single String and "Best" Alternate in Each Family

No.	MISSION PHASE	TIME (hours)	ΔT	CUM VALUE	G	D1	D2	D3	E
0	PRELAUNCH	0.0			NA	NA	NA	NA	NA
1	LAUNCH	1.0	1.0	0.5	1	NA	NA	NA	0
2	INJECTION	1.2	0.2	2.5	1	NA	NA	NA	0
3	ACQUISITION	3.6	2.4	3.0	1	0	1	NA	0
4	INTERPLANETARY CRUISE	72.0	68.4	3.1	1	0.5	0.5	NA	0
5	ARRIVAL DATE SEP. MANEUVER	77.0	5.0	3.8	1	0	1	NA	0
6	INTERPLANETARY CRUISE	720.0	643.0	4.0	1	0.5	0.5	NA	0
7	INTERPLANETARY TRAJ. COR. MVR.	725.0	5.0	4.3	1	0	1	NA	0
8	INTERPLANETARY CRUISE	4776.0	4051.0	4.5	1	0.5	0.5	NA	0
9	INTERPLANETARY TRAJ. COR. MVR.	4781.0	5.0	4.7	1	0	1	NA	0
10	INTERPLANETARY CRUISE	4848.0	67.0	4.7	1	0.5	0.5	NA	0
11	P/V MARS ORBIT INSERT	5022.0	174.0	10.7	1	0	1	NA	0
12	PRESEP. ORBIT OPERATIONS	5112.0	90.0	15.0	1	0.333	0.667	NA	0
13	P/V ORBIT TRIM MVR.	5117.0	5.0	17.0	1	0	1	NA	0
14	PRESEP. ORBIT OPERATIONS	5184.0	67.0	27.0	1	0.333	0.667	NA	0
15	S/C - CAPSULE SEPARATION	5190.0	6.0	30.0	1	0	1	NA	0
16	CAPSULE SUPPORT	5215.0	25.0	45.0	1	1	0	NA	0
17	CAPSULE DE-ORBIT THRU LANDED OPS.	(5215.0)	(25.0)	75.0	1	1	1	NA	1
18	POST LANDED ORBITAL OPS.	5736.0	521.0	89.0	1	0.863	0.591	0.408	0
19	S/C ORBIT TRIM MVR.	5741.0	5.0	90.0	1	1	1	1	0
20	POST LANDED ORBITAL OPS.	9405.0	3664.0	100.0	1	0.769	0.308	0	0

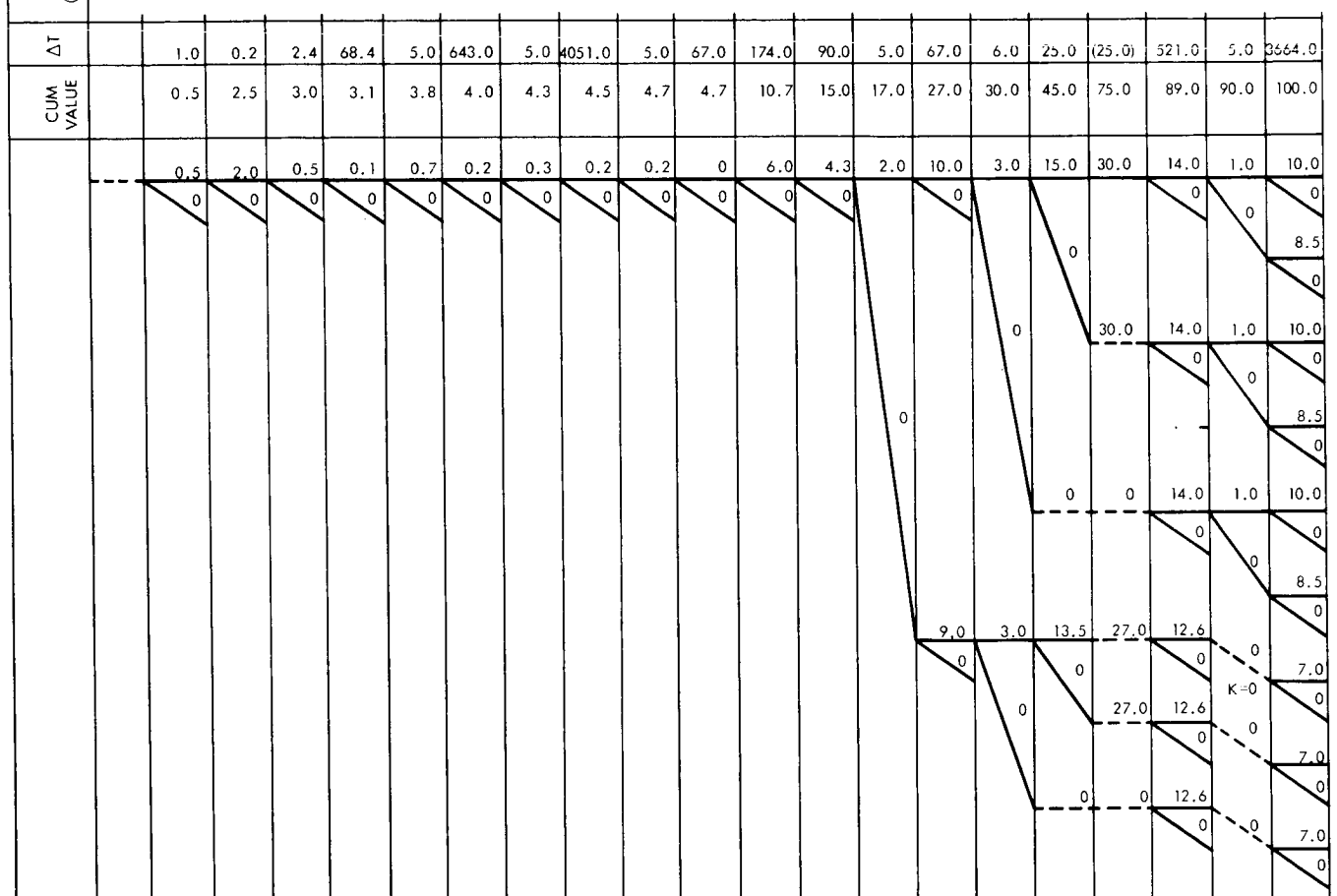

Figure 3. Mission Outcome Tree

(3) failure modes and effects analysis, and (4) configuration selection programs. The first three are primarily input data changes; the fourth involves computer programming modifications.

3.1. MISSION DEFINITION

The mission is defined via the mission outcome tree and time profile as shown in Figure 3. The purpose of the mission outcome tree is to denote the meaningful mission outcome along with the value obtained by each outcome and to define at what times in the mission that branching from the primary mission occurs. By denoting values allocated for each mission phase (fourth row) the value accumulated for all outcomes as a function of time can be obtained. The value obtained by successfully progressing from one mode to the next is noted on the diagram. A series of quality factors are also shown at the bottom of the figures (last five rows) with the use of these factors shown by the Map Matrix.

Since the completion of the Task C Study, changes have been made both to simplify the tree and to make it compatible with current mission guidelines. The significant changes in the mission outcome tree are as follows:

a. The mission phases used are those defined (with minor exceptions) in the JPL General Specification for the 1973 Voyager Mission, dated January 1, 1967.

b. Bio-barrier separation is combined with the capsule separation phase.

c. One orbit trim maneuver is assumed prior to capsule separation and one after capsule separation.

d. The tree is simplified by considering fewer branches (eliminating those having low probabilities of achievement and little value).

e. The capsule de-orbit, capsule orbital descent, capsule entry, capsule terminal deceleration, capsule landing, and landed operations phases are combined into a single phase (called capsule support phase) for the spacecraft system. The duration of this phase is assumed to be approximately one day.

The sensitivity analysis conducted during the Task C Study showed that small changes in the allocation of values to mission phases had little effect on the optimum configuration selection. Thus, the value assignments remain essentially unchanged except for being normalized with 100 being the maximum achievable value for a perfect mission.

3.2. SYSTEM DEFINITION

The spacecraft is subdivided into families for which a simplex and alternative redundant candidates are postulated. The Task C Study included 51 families with a total of 166 possible I/A's. Elimination of inferior alternates and redefining several families have reduced this to 39 families with 79 alternatives as defined in Table 1. Changes in family definitions primarily have been made either to combine closely related assemblies into a single assembly, or to break down complex families with many output states into more, less complex families. An example of the latter case includes segregating the radio/command family, with nine possible output states, into a radio family with three states and a command family with two states.

3.3. FAILURE MODES AND EFFECTS ANALYSIS

Failures within spacecraft assemblies are related to their effect on the mission in a two-step process. First, mathematical models are used to relate failures in hardware elements to the appropriate operating state of the assembly. Second, a map matrix is used to specify the operating states of the various families of assemblies which are required to complete the respective mission phases. Redefinitions of families, alternatives, the mission outcome tree, and the time profile have necessitated changes in the map matrix as well as many of the math models. The revised map matrix is shown in Table 2. The map matrix, although complex, is self-explanatory. A detailed explanation is given in the reference Task C Study Report.

Basic part failure data is used in the math models as the quantitative basis for determing the probabilities of assembly operating states. Table 3 shows this data base as updated for this

system study. The nature of the revisions made to the math models for the individual I/A's can be considered to be in the three following categories:

a. Essentially unchanged from previous model.

b. Minor refinements due to improvement in definition, parts, counts, etc.

c. Major remodeling for new alternatives, new families, etc.

About one-third of the 79 models used in this study were in each category.

3.4. CONFIGURATION SELECTION PROGRAMS

The computer programs used to determine the probability data and perform the configuration selection were revised in two respects: first, to simplify the computer-user interface, and second, to reduce the actual processing time. The first category includes improvements in formats, new control options, reduction and simplification of input data and improved operating procedures. In the second category, substantial improvements in operating time were achieved, ranging from better than a 50% reduction in the optimization program to a ten-to-one reduction in the probability calculator program.

4. STUDY RESULTS

Results from the redundancy optimization study are available in the form of probabilistic reliability (or MEW Loss) data at the assembly level as well as the final ordered listing of "best" configurations. The results in the former area have been useful in performing trade-offs within individual subsystem areas, and are discussed in more detail in other sections of this report. Table 4 is an example of these results for the Power Subsystem. This table briefly describes the alternatives postulated for each family of the power subsystem, shows the increase in weight and power required over a simplex design, indicates the probability of being "good" (fully performing its intended function) in the last mission phase in which it is required, and the loss in MEW that would be associated with that particular assembly if all other assemblies were perfect.

Table 4. Summary of Power Subsystem Results

Family	I/A Code	Redundancy Employed	Add'l Weight	Add'l Power	Last Mission Phase Req'd	P(Good) in Last Phase Req'd	MEW Loss
Ni-Cd Battery and Regulator	EAA*	Simplex	---	---	20	0.9361	0.691
	EAB	Multichannel cooperative (2 of 3)	82.0	28.0		0.9954	0.048
	EAC	Simplex (alternate arrangement)	7.0	1.0		0.9057	1.058
	EAD	Multichannel cooperative (3 of 4)	64.0	20.0		0.9920	0.136
Ag-Zn battery and Regulator	EBA*	Simplex	---	---	19	0.9760	2.003
	EBB	Multichannel cooperative (1 of 2)	46.5	1.0		0.9988	0.084
2.4 kHz Power and Clocking	ECA	Simplex	---	---	20	0.9925	0.434
	ECB	Simplex inverter, triplicated clocking	3.0	7.8		0.9937	0.364
	ECC	Dual inverters (standby-on) triplicated clocking	12.5	36.1		0.9974	0.147
	ECD	Dual inverters (standby-off), duplex or triplicated clocking.	10.75	6.1		0.9967	0.190
	ECE*	Dual inverters (standby-on), duplex or triplicated clocking.	11.50	33.1		0.9967	0.190
1-Phase 400 hz power and timing	EDA	Simplex	---	---	20	0.9962	0.067
	EDB*	Dual inverters (standby-off)	2.25	1.25		1.0000	0.001
3-Phase 400 hz power and timing	EEA	Simplex	---	---	19	0.9963	0.312
	EEB*	Dual inverters (standby-on)	5.5	10.1		0.9996	0.032
Main regulator	EFA	Simplex	---	---	20	0.9915	0.495
	EFB*	Dual regulators (standby-on)	21.5	33.4		0.9997	0.012
	EFC	Dual regulators (standby-off)	20.75	1.25		0.9999	0.002
Solar array and regulator	EGA*		---	---	20	1.0000	0.001

*Indiates change

Figure 4 and Table 5 show the results of the configuration selection. The former shows the MEW increase that can be obtained as system weight is allowed to grow. The elimination of the sharp "knee" characteristic of the results of the Task C Study is due both to the elimination of marginal alternatives previously considered as well as the consideration of new ones. (The fact that this is not a smooth continuous curve is indicative of the discrete alternatives considered.) The table shows a detailed tabulation of the configurations plotted graphically in Figure 4. Here the ordered listing of "best" configurations is given for increasing weights. At the top, the single-string configuration is listed followed by successively heavier configurations employing more redundancy. Only changes in the configurations are shown. Blanks indicate the "A" alternate is employed. In some subsystems, such as propulsion, only a single design was considered; thus, no alternates appear in the configuration.

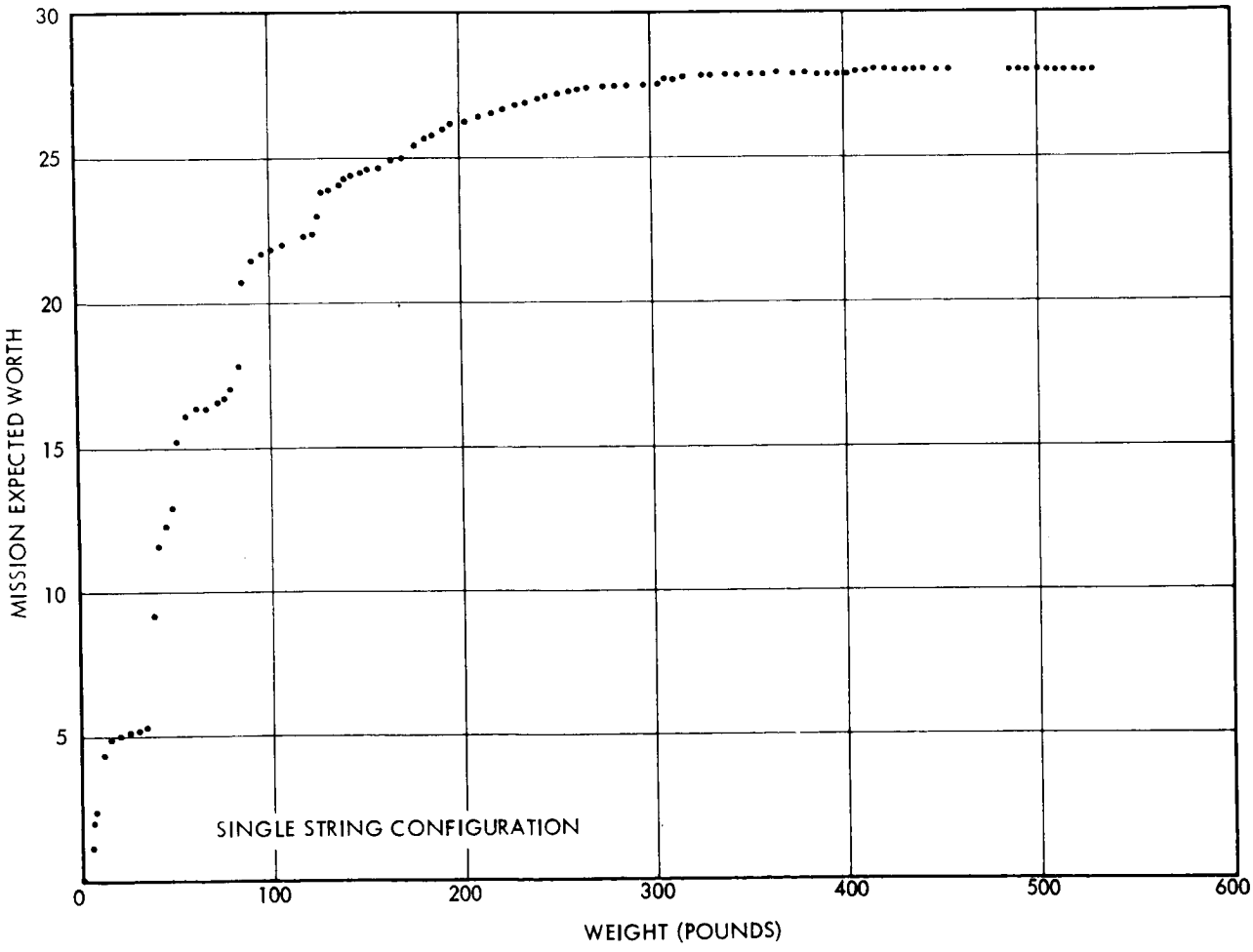

Figure 4. Optimum Configurations

Table 5. Ordered List of Configurations

C&S CCCCCC ABCDEF	POWER EEEEEEE ABCDEFG	G&C GGGGGGG ABCDEFG	VECH ENG MMMMMMMM ABCDEFGH	PROP PPP ABC	SCI SS AB	TELECOM TTTTTT ABCDEF	MISSION EXPECTED WORTH	DELTA WEIGHT
AAAAAA	AAAAAAA	AAAAAAA	AAAAAAAA	AAA	AA	AAAAAA	47.24	0.00
BB		D					48.86	3.46
BB		DB BB					49.80	6.60
BB		B					50.23	9.95
BBB		D B					52.62	13.76
BBBB		D BB					53.25	17.56
BCBB		DB BB					53.42	21.21
BCBB	B	DB BB					53.46	24.21
BCBB	B	DB BB					53.57	26.71
BCBBB	B	DB BB					53.69	31.71
BCBB	B	DBB BB					53.76	35.01
B		B B				B	58.10	38.80
BB		D BB				B	60.84	41.61
BBB		D BB				B	61.55	44.81
BB B						B	62.14	49.10
BBB		DB BB				B	64.82	52.51
BBBB		DB BB				B	65.57	55.71
BBBB	B	DB BB				B	65.62	58.71
BCBB	B	DB BB				B	65.79	63.26
BCBB		DBB BB				B	65.84	66.06
BCBBB	BB	DB BB				B	65.95	70.51
BCBB	BB	DBB BB				B	66.05	73.81
BCBBB	B	DBB BB				B	66.17	76.56
BCBBB	B B	DBB BB				B	66.21	79.56
BCBBB	BBB	DBBB BB				B	66.24	84.31
BBB		DB BB				BB	68.79	88.53
BBBB		DB BB				BB	69.60	91.73
BBBB	B	DB BB				BB	69.64	94.73
BBBB	B	DB BB				BB	69.79	97.23
BBBBB	B	DB BB				BB	69.94	102.23
BBBB	B	DBB BB				BB	70.05	105.53
BBBB	B B	DBB BB				BB	70.10	108.53
BCBBB	B	DBB BB				BB	70.24	112.58
BCBBB	B B	DBB BB				BB	70.28	115.58
BCBBB	BBB	DBBB BB				BB	70.32	120.33
BCBBB	B B	DBB BB				BB	70.40	124.08
BBB	B	DB BB				BBB	70.58	126.98
BCBB		DB BB				BBB	71.41	129.98
BCBB	B	DB BB				BBB	71.46	132.98
BCBB	BB	DB BB				BBB	71.64	137.73
BCBBB	B	DB BB				BBB	71.77	140.48
BBBB		DB BB				CBB	71.89	143.33
BBBB	B	DB BB				CBB	72.09	148.83
BBBB		DBB BB				CBB	72.18	151.63
BBBBBB	B	DB BB				CBB	72.25	155.88
BCBB	B	DBB BB				CBB	72.42	159.18
BCBB	B B	DBB BB				CBB	72.47	162.18
BCBBB	BB	DBB BB				CBB	72.61	166.43
BCBBB	BBB	DBB BB				CBB	72.66	169.43
BCBBB	BBB	DBBB BB				CBB	72.67	171.93
BCBB	B	DB BB				BBB	72.80	176.48
BCBB	BB	DB BB				BBB	72.85	179.48
BCBB	B BB	DB BB				BBB	73.03	184.23
BCBBB	B B	DB BB				BBB	73.16	186.98
BBBB	B	DB BB				CBB	73.29	189.83
BBBBB	BB	DB BB				CBB	73.34	194.88
BBBB	B	DBB BB				CBB	73.50	198.13
BBBBB	B B	DB BB				CBB	73.65	200.33
BBBBB	BBBB	DB BB				CBB	73.74	205.58
BCBB	BB B	DBB BB				CBB	73.87	208.68
BCBBB	B B	DBB BB				CBB	73.99	210.68
BCBBB	BBBB	DBB BB				CBB	74.07	215.93
BCBBB	BBBB	DBBB BB				CBB	74.08	218.43
BCBBB	BC B	DBB BB				CBB	74.19	223.18
BCBBB	BCBB	DBB BB				CBB	74.23	225.43
BCBBB	BBBB	DBB BB				BCBB	74.29	230.33
BCBBB	B BBC	DBB BB				CBB	74.37	233.68
BCBBB	BBBBC	DBB BB				CBB	74.42	236.68
BCBBB	BBBBC	DBBB BB				CBB	74.43	237.18
BCBBB	BC BC	DBB BB				CBB	74.54	243.93
BCBBB	B BBC	DBB BB				BCBB	74.59	248.08
BCBBB	BBBBC	DBB BB				BCBB	74.64	251.08
BCBBB	BBBBC	DBBB BB				BCBB	74.64	253.58
BCBBB	BC BC	DBB BB				BCBB	74.76	258.33
BCBBB	BCBBC	DBB BB				BCBB	74.79	260.58
BBCBBB	BCBBC	DBBB BB				BCBB	74.80	265.13
BCBBB	BCBBC	DBB BB	B			BCBB	74.87	268.58
BCBBB	BCBBC	DBBB BB	B			BCBB	74.87	271.08
BCBBB	BCBBC	DBB BB				BDBB	74.91	275.98
BCBBB	BCBBC	DBBB BB				BDBB	74.91	278.48
BCBBB	BCBBC	CBB BB				BDBB	74.93	281.78
BCBBB	BCBBC	DBBB BB	B			BDBB	74.96	286.48
BCBBB	BCBBC	CBB BB	B			BDBB	75.01	289.78
BCBBB	BCBBC	CBBB BB	B			BDBB	75.01	292.28
BCBBC	BCBBC	CBBB BB	B			BDBB	75.01	297.28
BBCBBC	BCBBC	CBBB BB	B			BDBB	75.01	299.33
CBCBBC	BCBBC	CBBB BB	B			BDBB	75.01	304.53
BCBBB	BC BC	DBB BC				BCBB	75.10	307.43
BBCBBB	BCBBC	DBB BC				BCBB	75.13	311.73
BCBBB	BC BC	DBB BC	B			BCBB	75.17	315.43
BCBBB	BCBBC	DBB BC	B			BCBB	75.21	317.68
BBCBBB	BCBBC	DBBB BC	B			BCBB	75.21	322.23
BCBBB	BCBBC	DBB BC				BDBB	75.25	325.08
BBCBBB	BCBBC	DBBB BC				BDBB	75.25	329.63
BCBBB	BCBBC	DBB BC	B			BDBB	75.32	333.08
BCBBB	BCBBC	DBBB BC	B			BDBB	75.33	335.58
BCBBB	BCBBC	CBB BC	B			BDBB	75.35	338.88
BBCBBB	BCBBC	CBBB BC	B			BDBB	75.35	343.43
BCBBC	BCBBC	CBBB BC	B			BDBB	75.35	346.38
BBCBBC	BCBBC	CBBB BC	B			BDBB	75.35	348.43
CBCBBC	BCBBC	CBBB BC	B			BDBB	75.35	353.63
BBCBBB	BCBBC	CBBB BC	C			BDBB	75.36	357.93
BCBBC	BCBBC	CBBB BC	C			BDBB	75.36	360.88
BBCBBC	BCBBC	CBBB BC	C			BDBB	75.36	362.93
CBCBBC	BCBBC	CBBB BC	C			BDBB	75.36	368.13
BBCBBB	DBCBBC	DBB BC				BCBB	75.37	376.73
BBCBBB	DBCBBC	DBBB BC				BCBB	75.37	379.23
BCBBB	BCBBC	DBB BC	B			BCBB	75.44	381.68
BBCBBB	DBCBBC	DBBB BC	B			BCBB	75.45	386.23
BCBBB	DBCBBC	DBB BC				BDBB	75.49	389.08
BCBBB	DBCBBC	DBBB BC				BDBB	75.49	391.58
BBCBBB	DBCBBC	CBB BC				BDBB	75.51	396.93
BCBBB	DBCBBC	CBBB BC	B			BDBB	75.57	399.58
BCBBB	DBCBBC	CBB BC	B			BDBB	75.59	402.88
BBCBBB	DBCBBC	CBBB BC	B			BDBB	75.59	407.43
BCBBC	DBCBBC	CBBB BC	B			BDBB	75.60	410.38
BBCBBC	DBCBBC	CBBB BC	B			BDBB	75.60	412.43
BCBBB	BBCBBC	CBBB BC	B			BDBB	75.62	417.58
BCBBB	BBCBBC	CBB BC	B			BDBB	75.64	420.88
BCBBB	BBCBBC	CBBB BC	B			BDBB	75.65	423.38
BCBBC	BBCBBC	CBBB BC	B			BDBB	75.65	428.38
BBCBBC	BBCBBC	CBBB BC	B			BDBB	75.65	430.43
CBCBBC	BBCBBC	CBBB BC	B			BDBB	75.65	435.63
BCBBB	BBCBBC	CBBB BC	C			BDBB	75.65	437.83
BCBBC	BBCBBC	CBBB BC	C			BDBB	75.65	442.83
BBCBBC	BBCBBC	CBBB BC	C			BDBB	75.65	444.88
CBCBBC	BBCBBC	CBBB BC	C			BDBB	75.65	450.08
BCBBB	BBCBBC	DBB BD	B			BDBB	75.67	495.98
BCBBB	BBCBBC	DBBB BD	B			BDBB	75.68	498.48
BCBBB	BBCBBC	CBB BD	B			BDBB	75.70	501.78
BBCBBB	BBCBBC	CBBB BD	B			BDBB	75.71	506.33
BCBBC	BBCBBC	CBBB BD	B			BDBB	75.71	509.28
BBCBBC	BBCBBC	CBBB BD	B			BDBB	75.71	511.33
CBCBBC	BBCBBC	CBBB BD	B			BDBB	75.71	516.53
BBCBBB	BBCBBC	CBBB BD	C			BDBB	75.71	520.93
BCBBC	BBCBBC	CBBB BD	C			BDBB	75.71	523.88
BBCBBC	BBCBBC	CBBB BD	C			BDBB	75.71	525.93
CBCBBC	BBCBBC	CBBB BD	C			BDBB	75.71	531.13

Examination of Figures 4 and Table 5 shows that the increase in MEW per pound is high for the first 150 pounds of additional spacecraft weight. Continued, but less rapid, improvement is realized over the next 150 to 200 pounds. Beyond this weight, for the alternative assemblies considered in this study, little improvement results. From the detailed configuration tabulation, it can be seen that these improvements are not concentrated in any one particular subsystem. In fact, with as little as 40 pounds devoted to redundancy, all subsystems (for which a substantial number of alternatives were considered during this study) employ one or more of the redundant designs.

The effect of the application of redundancy within the spacecraft to the mission phase probabilities of success if shown in Table 6. These probabilities are listed for both the single-string configuration and the configuration employing redundancy as recommended in the design described in this report. The improvement is significant, particularly in the later mission phases.

Table 6. Mission Phase Probabilities

Mission Phase		Probability of Completion	
No.	Name	Single-string Configuration	Redundant Configuration
1	Launch	0.9190	0.9190
2	Injection	0.8547	0.8547
3	Acquisition	0.8533	0.8547
4	Interplanetary Cruise	0.8525	0.8545
5	Arrival Date Sep. Maneuver	0.8441	0.8507
6	Interplanetary Cruise	0.8352	0.8491
7	Interplanetary Traj. Cor. Mvr.	0.7992	0.8449
8	Interplanetary Cruise	0.7474	0.8340
9	Interplanetary Traj. Cor. Mvr.	0.5861	0.8225
10	Interplanetary Cruise	0.5861	0.8225
11	P/V Mars Orbit Insert	0.5596	0.7987
12	Presep. Orbit Operations	0.5589	0.7984
13	P/V Orbit Trim Mvr.	0.5529	0.7947
14	Presep. Orbit Operations	0.5522	0.7945
15	S/C - Capsule Separation	0.5497	0.7943
16	Capsule Support	0.5495	0.7942
18	Post Landed Orbital Ops.	0.5441	0.7926
19	S/C Orbit Trim Mvr.	0.5338	0.7876
20	Post Landed Orbital Ops.	0.4591	0.7273